META-IODOBENZYLGUANIDINE: INVESTIGATIONS INTO A MECHANISM OF ACTION AND APPLICATION TO RESTENOSIS

BY

LORRAINE YAU

A Thesis

Submitted to the Faculty of Graduate Studies

in Partial Fulfillment of the Requirements

for the Degree of

DOCTOR OF PHILOSOPHY

Institute of Cardiovascular Sciences

Department of Physiology, Faculty of Medicine

University of Manitoba

Winnipeg, Manitoba

THE UNIVERSITY OF MANITOBA

FACULTY OF GRADUATE STUDIES

*****

COPYRIGHT PERMISSION PAGE

***Meta*-Iodobenzylguanidine: Investigations into a Mechanism of Action and Application to Restenosis**

BY

Lorraine Yau

A Thesis/Practicum submitted to the Faculty of Graduate Studies of The University of Manitoba in partial fulfillment of the requirements of the degree of

Doctor of Philosophy

This body of work is dedicated to:

My parents who have always believed in me and been my biggest fans;

My loving husband who has always been my pillar of strength;

My daughter/child(ren) who will always be my greatest joy;

My friends who never let me give up hope;

My Lord and Saviour, Jesus Christ, Who gave me a new life and purpose to go on.

The wise man accomplishes what must be done without dwelling on it.

- Lao Tzu

In the pursuit of learning, everyday something is acquired...

- Lao Tzu

There is a limit to our life, but there is no limit to knowledge.

- Chuang Tzu

TABLE OF CONTENTS

ACKNOWLEDGEMENTS

First, I would like to thank my supervisor, Dr. Peter Zahradka, for taking me on as a graduate student after that first and fateful summer at the University of Guelph. I would also like to thank him for his patience, support and guidance, and for still sticking by me after all these years. It's been quite the journey!

Second, I would like to thank my advisory committee members, Dr. Peter Cattini, Dr. Janice Dodd, Dr. David Litchfield and Dr. Barb Triggs-Raine for all their hard work and guidance that has helped me through this process.

Third, I would like to acknowledge all those whom I have had the opportunity and privilege to work with through the years, including Laura Saward (friend and comrade-in-arms), David Wilson, Mirei Nguyen, Michael Moon, Jeff Werner, Julieta Werner, Brenda Litchie, Jason Voldeng, Shawn Thomas, Shelly Buhay, Cameron Wong, Helena Lukes (in memorium) and many others. Thank you for all the discussion periods, superb technical assistance, advice and support, and most of all for making it fun along the way.

Fourth, I would like to thank my family and friends who have freely given of their love and support, especially my husband Nobby who has had to put up with everything, and my daughter Kendra who has grown up wonderfully despite it all.

Also, I would like to give praise and thanks to my God in Heaven and my Lord and Saviour, Jesus Christ, Who takes care of my life and Who was there every step of the way.

Finally, many thanks to the Medical Research Council of Canada and the St. Boniface Research Foundation for their funding support.

LIST OF FIGURES

LIST OF TABLES

LIST OF ABBREVIATIONS

3AB	3-aminobenzamide
α-MEM	α-modified minimal essential media
ACE	angiotensin converting enzyme
AngII	angiotensin II
arg	arginine
arg-mART	arginine-dependent mono(ADP-ribosyl)transferase
ART	ADP-ribosyltransferase
BCA	bicinchoninic acid
bFGF	basic fibroblast growth factor
BrdU	bromodeoxyuridine
BSA	bovine serum albumin
CABG	coronary artery bypass graft
CAD	coronary artery disease
CPK	creatine phosphokinase
CRE	cAMP responsive element
CREB	cAMP responsive element binding protein
Cy3	indocarbocyanine
D-MEM	Dulbecco's modified Eagle media
DTT	dithiothreitol
EC	endothelial cell
ECM	extracellular matrix
EDTA	ethylenediaminetetraacetic acid
EGTA	ethyleneglycol-bis(beta-aminoethyl ether)-N,N'-tetraacetic acid
ERK	extracellular signal-regulated kinase

FACS	Fluorescence-Activated Cell Sorting
FBS	fetal bovine serum
FITC	fluorescein isothiocyanate
GPI	glycosylphosphatidylinositol
HBS	Hepes buffered saline
HBSS	Hank's balanced salt solution
HMBA	hexamethylenebisacetamide
HRP	horse radish peroxidase
IGF-1	insulin-like growth factor-1
IL-1	interleukin-1
IL-6	interleukin-6
IRS-1	insulin receptor substrate-1
LAD	left anterior descending (coronary artery)
LAME	L-arginine methyl ester
LDH	lactate dehydrogenase
LNAME	L-nitro-arginine methyl ester
LY	LY294002
mART	mono(ADP-ribosyl)transferase
MAP kinase	mitogen activated protein kinase
MBP	myelin basic protein
MEF	myocyte-specific enhancer-binding factor
MEK	MAP/ERK kinase
MIBA	*meta*-iodobenzylamine
MIBG	*meta*-iodobenzylguanidine
MIHA	*meta*-idodohippuric acid

MRF	myogenic regulatory factor
MTT	3-(4,5-dimethyl-thiazol-2-yl)-2,5-diphenoltetrazolium bromide
NE	norepinephrine
NO	nitric oxide
NOS	nitric oxide sythase
ODN	oligodeoxynucleotide
PABA	para-aminobenzoic acid
PAGE	polyacrylamide gel electrophoresis
PAK	p21 activated serine/threonine kinase
PARP	poly(ADP-ribose) polymerase
PBS	phosphate buffered saline
PCD	programmed cell death
PCNA	proliferating cell nuclear antigen
PCR	polymerase chain reaction
PDGF	platelet derived growth factor
PEPCK	phosphoenolpyruvate carboxykinase
PG	prostaglandin
PGE_2	prostaglandin E_2
$PGF_{2\alpha}$	prostaglandin $F_{2\alpha}$
PGI_2	prostaglandin I_2/prostacyclin
PI	phosphatidylinositol
PI3-kinase	phosphatidylinositol 3-kinase
PIP	phosphatidylinositol 3-phosphate
PIP_2	phosphatidylinositol 4,5-bisphosphate
PIP_3	phosphatidylinositol 3,4,5-triphosphate

PMSF	phenylmethylsulfonylfluoride
PTCA	percutaneous transluminal coronary angioplasty
PVDF	poly(vinylidene difluoride)
RT-PCR	reverse transcription PCR
ROK	Rho-binding serine/threonine kinase
SDS	sodium dodecyl sulphate
SMC	smooth muscle cell
SRF	serum response factor
TBS	Tris buffered saline
TBS-T	Tris buffered saline + Tween-20
TCA	trichloroacetic acid
TGF-β	transforming growth factor-β
TLC	thin layer chromatography
TxA_2	thromboxane A_2
VEGF	vascular endothelium derived growth factor
WM	wortmannin

ABSTRACT

Failure of revascularization procedures for the treatment of coronary artery disease, such as balloon angioplasty, typically occurs as a result of restenosis, a renarrowing of the lumen at the site of intervention. Restenosis is characterized by the formation of a neointimal lesion, a process that involves migration of smooth muscle cells from the medial to intimal region of a blood vessel followed by cell proliferation and extracellular matrix deposition. No intervention to date has proven to be clinically significant with regards to efficacy. As a result, a unique compound, MIBG, that inhibits post-translational modification of proteins associated with signal transduction pathways that modulate cell migration, proliferation and differentiation was investigated. H4IIE hepatoma cells were used to establish that MIBG inhibited cell growth and proliferation. MIBG was also shown to prevent differentiation of L6 skeletal myoblasts into myotubes, an effect that was reversible on removal of the compound. The effect of MIBG on differentiation was found to be a consequence of its action on the expression of key elements in the myogenic program. Smooth muscle cells are the primary cell type involved in the events leading to restenotic lesion formation, and studies with MIBG demonstrated that this compound is capable of inhibiting both smooth muscle cell migration and proliferation in response to growth factors and other stimulating agents. Furthermore, there was an indication that the compound may affect several signaling pathways in smooth muscle cells, as demonstrated by MIBG-dependent inhibition of PGE_2-mediated c-*fos* gene expression. An organ culture model of balloon angioplasty was used to show that MIBG is capable of inhibiting restenosis under controlled experimental conditions. Finally, femoral angioplasty *in vivo* was used to confirm the data generated with the organ culture model in a physiologically relevant system. MIBG

significantly reduced neointimal formation in the injured regions of a porcine femoral artery when compared to arteries without MIBG treatment. These studies indicate that the inhibition of cell migration, proliferation and differentiation by MIBG may be beneficial in the treatment of restenosis post-angioplasty and therefore applicable to therapeutic intervention in a clinical setting.

1.0 Introduction

Coronary artery disease (CAD) is one of the leading causes of death in North America (49% of all cardiovascular disease deaths in the United States in 1997). With our aging population, the burden to the health care system associated with CAD will only get worse. Many medical, surgical and mechanical procedures are available to treat the symptoms of CAD, including percutaneous transluminal coronary angioplasty (PTCA), a common revascularization technique for the treatment for coronary artery disease. Unfortunately, late-stage procedural failure of this technique is prevalent (occurs in 30-50% of patients) due to the development of intimal hyperplasia at the site of angioplasty (Liu *et al.* 1989; McBride *et al.* 1988). The clinical consequences of restenosis, which include recurrence of angina, myocardial infarction and sudden death, typically necessitate the need for re-operation (Califf *et al.* 1991; McKenna *et al.* 1994).

Restenosis, defined as the loss of lumenal gain following revascularization of a lesion-filled vessel, represents the vascular response to arterial injury. The paradigm for restenosis post-angioplasty has three distinct but integrated phases: i) formation of a mural thrombus (involving both coagulation and inflammation), ii) migration and proliferation of cells, and iii) secretion of extracellular matrix (ECM) with subsequent remodeling (Glagov *et al.* 1987; Jackson & Schwartz 1992; Ross & Fuster 1996; Schwartz *et al.* 1992a; Schwartz *et al.* 1995a; Schwartz & Reidy 1996; Thyberg 1998). It is now clearly established that the (neo)intimal lesion forms as a result of smooth muscle cell (SMC) migration from the medial to intimal layer of the vessel, followed by proliferation of the cells and deposition of ECM (Schwartz *et al.* 1994; Schwartz *et al.* 1992a; Schwartz *et al.* 1995a). From this description, it would be assumed that an intervention that inhibits any of these SMC functions should have a significant impact on both the patient and the disease process. However, neither pharmacological nor

mechanical interventions targeted to these functions have been clinically effective to date (de Smet *et al.* 1997; Landzberg *et al.* 1997; Lefkovits & Topol 1997; Post *et al.* 1997). This would suggest that not all contributors to the complex process of restenosis have been defined, and that there may exist other targets that would be amenable to intervention.

Smooth muscle cells (SMCs) inhabit a unique position in the spectrum of cells that undergo differentiation. In comparison to skeletal and cardiac muscle cells that undergo terminal differentiation, SMCs do not appear to be terminally differentiated as demonstrated by their capacity to modulate between differentiated and de-differentiated states (Katoh & Periasamy 1996). As a result, the SMC is "phenotypically plastic", and retains the ability to proliferate and replicate in response to environmental cues and injury. However, much like skeletal and cardiac muscle cells, expression of phenotypic-specific genes in SMCs is regulated by distinct families of transcription factors (Owens 1995; Sartore *et al.* 1999; Sobue *et al.* 1998). The expression of these genes appears to provide the impetus for SMC activation and subsequent phenotype alteration in response to signals present in the immediate cellular environment.

The role and contribution of SMCs to restenotic lesion formation is significant (Bauters & Isner 1997; Glagov 1994; Schwartz *et al.* 1992a; Schwartz *et al.* 1995a). In response to vascular injury, activated SMCs undergo a change in phenotype from a quiescent, contractile state to a proliferative, synthetic state (i.e. de-differentiation) which is capable of repairing the damage (Sobue *et al.* 1999; Thyberg 1998). This change in function is characterized by an ability to migrate from the media to the intima (i.e. directional response), proliferate and secrete components of ECM (Majesky *et al.* 1992), and is accompanied by extensive structural re-organization (Thyberg 1998). The mechanism behind the shift in phenotype is still poorly understood, however, it is a

reversible process since the SMCs return to a contractile state after formation of the intimal plaque and completion of repair (Hedin *et al.* 1999b; Thyberg 1998). Interestingly, during normal wound healing, it has been suggested that remodeling continues indefinitely (Koopmann 1995; Kudravi & Reed 2000). Therefore, it is possible that SMCs do not truly return to their initial quiescent and contractile state, as seen *in vivo* in the normal media, but remain in an intermediary state that is capable of responding to certain stimuli (Gibbons & Dzau 1994; Owens *et al.* 1996; Thyberg 1996). In this scenario, it is then plausible that under certain circumstances, SMCs behave more like a transformed tumour cell capable of indefinitely responding to specific cues in its environment. Within the context of the vessel wall, this would constitute an exaggerated repair with resultant encroachment of the neointimal into the lumen, the hallmark of restenosis. Thus, the cellular events associated with de-differentiation, as defined by migration, proliferation and secretion of ECM proteins, ultimately precede restenotic lesion formation post-injury.

A variety of cell signaling molecules are coordinately regulated in the activated SMC, and these intracellular messengers have discrete functions with respect to the regulation of cell proliferation, migration, differentiation and secretion of ECM. The best characterized of the intracellular signal pathways involve either tyrosine phosphorylation cascades or the activation of GTP-binding proteins (including G protein-coupled receptors and small GTP-binding proteins). Examples of signal molecules involved with each type of signaling cascade include mitogen activated protein (MAP) kinase, phosphatidylinositol 3-kinase (PI3-kinase), and p21-Ras. These molecules have been associated with cellular processes such as cell proliferation, migration, differentiation, contraction and apoptosis (Adam *et al.* 1995; Cowley *et al.* 1994; Di Salvo *et al.* 1997; Force & Bonventre 1998; Inagami & Eguchi 2000; Khalil & Morgan 1993; Klemke *et al.*

1997; Mansour *et al.* 1994; Nelson *et al.* 1998; Pfitzer & Arner 1998; Soltoff *et al.* 1993; Varticovski *et al.* 1994). Many of these intracellular signaling cascades affect processes within the nucleus of the cell, including modulation of gene expression and regulation of cell cycle proteins (Cook *et al.* 2000; Marshall 1999; Treisman 1996; Zhang *et al.* 1993b). Also worth considering are novel intracellular regulatory modifications such as ADP-ribosylation which has been shown to occur endogenously in eucaryotic cells and has been demonstrated to influence a variety of cell functions (D'Amours *et al.* 1999; Okazaki & Moss 1996a; Okazaki & Moss 1996b; Zolkiewska *et al.* 1994). While this particular regulatory system is not as well characterized as traditional signal pathways, ADP-ribosylation of proteins by exogenous mono(ADP-ribosyl)transferases (mARTs) of bacterial origin has been shown to influence certain cell signaling cascades (Aktories 1994; Aktories 1997; Gierschik 1992; Moss 1987; Okazaki & Moss 1996b). Moreover, mART activity has been shown to increase following mitogen stimulation, and inhibition of this enzyme can prevent cell proliferation (Yau *et al.* 1998). Interestingly, the molecule at the centre of my studies, *meta*-iodobenzylguanidine (MIBG), is a known inhibitor of arginine-dependent mono(ADP-ribosyl)transferase (arg-mART) (Loesberg *et al.* 1990b; Smets *et al.* 1988a; Smets *et al.* 1988b; Smets *et al.* 1990b) and it may be this enzyme target that is central to the anti-proliferative effects of MIBG.

MIBG, an analog of norepinephrine (NE), is used clinically in the radio-iodinated form for the detection and therapy of neuroendocrine tumours. More recently, unlabelled MIBG has been used in the treatment of small bowel tumours (Akle *et al.* 1997) and has been tested for the therapy of neuroblastoma in experimental models and carcinoid syndrome clinically (Cornelissen *et al.* 1995a; Kuin *et al.* 1999; Ramage *et al.* 1995; Smets *et al.* 1988b; Taal *et al.* 1999; Taal *et al.* 1996; Zuetenhorst *et al.* 1999). Presently, its mechanism of action as a chemotherapeutic anti-tumour agent are not known,

although it appears to have both anti-proliferative and anti-metastatic properties (Cornelissen *et al.* 1997b; Cornelissen *et al.* 1995a; Prvulovich *et al.* 1998; Smets *et al.* 1988b). Furthermore, in experimental culture systems, MIBG has demonstrated an ability to inhibit both cellular proliferation and differentiation (Graves *et al.* 1997; Huang *et al.* 1996; Kharadia *et al.* 1992; Thyberg *et al.* 1995b). Interestingly, differentiated neuroblastoma cells exhibit an increased affinity for and uptake of MIBG (Iavarone *et al.* 1993; Montaldo *et al.* 1996). This information is highly suggestive that MIBG could be applied in the treatment of restenosis, since it affects not only cell proliferation but also cell migration and cell differentiation. This series of studies was designed to determine the efficacy of MIBG as an inhibitor of cell proliferation, migration and differentiation using a spectrum of cell types that encompass the various cellular properties representative of the target SMC population that contributes to restenosis. In addition, experiments were conducted to elucidate a mechanism of action for MIBG with respect to cell proliferation. Finally, models of vascular injury and (neo)intimal lesion formation were employed to examine the feasibility of using MIBG for the prevention of restenosis.

2.0 Review of Literature

2.1 Heart disease in North America

Cardiovascular disease is one of the leading causes of morbidity and mortality in North America. In 1997, it was estimated that close to 1,000,000 people died from a cardiovascular disorder in the United States. In Canada, although the number of deaths is not equivalent, a similar percentage of the population is affected (581/100,000 in US vs. 430/100,000 in Canada). Furthermore, it is estimated that the total cost of cardiovascular disease (and stroke) to the health care system was $286.5 billion (in 1999, and projected to be $326.6 billion in 2000) in the United States (AHA 1999) and $7.3 billion (in 1995) in Canada (Canada 1995). Moreover, because cardiovascular disease is primarily a disease of aging, the incidence of cardiovascular disease and the burden to the health care system is increasing, mainly due to an increase in the percentage of individuals over the age of 55. Although a variety of different conditions fall under the umbrella of cardiovascular disease, including hypertension, myocardial infarction, stroke, congestive heart failure and coronary artery disease (CAD) (atherosclerosis or arteriosclerosis), the majority of deaths are attributable to coronary artery disease (greater than 50%) and its sequelae (i.e. myocardial infarction, angina pectoris and congestive heart failure).

2.2 Coronary artery disease

2.2.1 Definition of coronary artery disease

CAD is defined as obstruction of the arteries that feed the heart. The obstruction is the result of arteriosclerosis, a group of diseases characterized by thickening, hardening, loss of elasticity and restructuring of arterial walls (Dorland 1988; Woolf 1982). There are three distinct forms of arteriosclerosis: 1) Monckeberg's arteriosclerosis, which involves calcification, hyalinization and necrosis in the media of the artery, 2)

arteriolosclerosis, which involves smaller arteries and 3) atherosclerosis, an extremely common form of arteriosclerosis in which deposits of yellowish plaques (atheromas) containing cholesterol, lipid material and foam cells (macrophage- and/or smooth muscle cell-derived) form within the intima and inner media of large (elastic arteries) and medium-sized (muscular) arteries (Dorland 1988). Although atherosclerosis develops over decades, it is nevertheless considered to be primarily a phenomena associated with the aging process. However, this may be a consequence of the mechanism and progression of atherosclerosis and the ability of the body to compensate for early stages of disease, since signs and symptoms of atherosclerosis arise during the more severe stages of disease when progressive deterioration is no longer tolerated by the body.

2.2.2 Classification of coronary artery disease

In the past, atherosclerosis was classified in purely descriptive terms. The classical nomenclature distinguished three stages of atherosclerotic plaque progression: 1) fatty streak, 2) fibrous plaque, and 3) complicated lesion (Grundy 1990; Yutani *et al.* 1999). More recently (past 10 years), these classifications have been revised according to information concerning the morphological and biochemical details of the processes involved in the progression of coronary atherosclerosis. Stary's classification, which separates lesion progression into five phases defined according to morphological characteristics established by the AHA committee on Vascular Lesions, is now universally accepted (Stary *et al.* 1992; Stary *et al.* 1995; Stary *et al.* 1994; and as reviewed in Yutani *et al.* 1999). Phase 1 represents the small lesion. These lesions progress slowly over a number of years, are commonly found in individuals under the age of 30 and are further subdivided into type I – III lesions. Type I lesions contain only macrophage-derived foam cells, while type II lesions contain both macrophages and smooth muscle cells, and type III lesions are made up largely of smooth muscle cells. At

this stage, all three lesion types contain lipid deposits. Phase 2 represents the plaque with a high lipid content. These plaques do not significantly reduce blood flow at this stage but are prone to rupture. Phase 2 plaques are classified as type IV or V. Type IV lesions are highly cellular and contain a large amount of lipid, while type V lesions are more fibrotic. Phase 3 lesions are considered to be complicated type VI lesions with the potential of initiating mural thrombus formation. These lesions may then progress to a fibrotic, non-occlusive phase 5 lesion or gradually evolve into an occlusive lesion. On the other hand, phase 4 lesions are complicated type VI lesions stemming from plaque rupture, thrombus formation and sudden occlusion. The occlusive thrombus may be fibrotic in phase 5. (Stary *et al.* 1992; Stary *et al.* 1995; Stary *et al.* 1994). In all cases, advanced atherosclerotic lesions (phases 2 to 5; types IV to VI) result in loss of local blood flow, tissue ischemia and possible episodes of angina pectoris (Gotlieb & Havenith 1991; Woolf 1982). Furthermore, the resulting occlusive lesion of advanced atherosclerosis (phase 3 to 5; types IV to VI) may lead to myocardial infarction, stroke or ischemic damage to other end organs (eg. kidney), with subsequent complications resulting in death (Gotlieb & Havenith 1991; Woolf 1982). Treatment options have included medical interventions, surgical interventions and, more recently, percutaneous revascularization techniques (Favaloro 1994; Frishman *et al.* 1998; Gruntzig *et al.* 1979).

2.2.3 Interventions for the treatment of coronary artery disease

The cost of atherosclerosis to the individual is high since its sequelae often include myocardial infarction, stroke, heart failure and other end organ failure, thereby limiting the quality of life and the range of activities for that individual. Furthermore, the mortality rate from this disease is estimated to be 50%, accounting for an estimated 520,189 deaths in North America in 1996 (44,065 Canada, 476,124 United States). As a result, both medical and surgical interventions have been developed to improve

symptoms and outcomes (i.e. morbidity and mortality), and as preventative measures for the onset of associated disease states. Medical interventions employ drug therapy to alleviate symptoms of angina pectoris, a consequence of ischemic CAD. These therapies include a host of vasodilating agents such as nitroglycerin, calcium channel blockers, angiotensin converting enzyme (ACE) inhibitors and, in some cases, beta-blocker therapy (Frishman *et al.* 1998; O'Neill 2000). Although these medical interventions are effective in improving the symptoms, thereby allowing patients to resume their normal daily activities, this treatment modality neither ameliorates the underlying atherosclerotic lesion, nor improves blood flow into the region that has been affected by the plaque, except on a somewhat cyclical, per treatment basis. Newer therapies based on prevention, including lipid-lowering agents (Siegel 1997) have had success, but only with subgroups of patients. Therefore, revascularization procedures have been developed as a means of restoring normal blood flow to the affected region of the heart. These procedures effectively reduce the mortality rate from myocardial infarction and heart failure resulting from coronary artery obstuction.

2.2.4 Surgical treatment of coronary artery disease

The primary surgical intervention for coronary artery obstruction is coronary artery bypass-grafting (CABG). In this procedure, a segment of saphenous vein is grafted from the aorta to the coronary artery, thereby circumventing the region of obstruction. While the autogenous vein graft still remains the standard conduit for all forms of revascularization because of its verasatility and ease of implantation, the use of arterial conduits, such as internal mammary and radial arteries, is gaining favour (Favaloro 1994; Green 1989). Arterial conduits, especially the internal mammary artery, are an advantage since they demonstrate excellent sustained patency (failure rate of 5 to 10% at 10 years), tending to fail much less frequently from the development of intimal hyperplasia

compared to vein grafts (failure rate of 50% at 10 years) (Galbut *et al.* 1990; Ivert *et al.* 1988; Loop *et al.* 1986; Lytle *et al.* 1985; Lytle *et al.* 1987; Zeff *et al.* 1988). This allows for longer-term survival of patients without the need for repeat revascularization procedures.

2.2.5 Non-surgical, non-medical treatments for coronary artery disease

While surgical intervention is considered to be the best treatment option for those with either multivessel disease or extensive atherosclerotic lesions, percutaneous transluminal coronary angioplasty (PTCA) is often preferred as the method of treatment in patient populations with atherosclerosis, since it is noninvasive and "non-surgical". For these reasons, recovery times are much shorter and the cost to the health care system is considerably less. Since the initial paper on PTCA by Gruntzig *et al.* (1979), the creation of newer methodologies based on similar principles of plaque "ablation" demonstrated by PTCA has flourished (Brown *et al.* 1996). Among the more popular options are directional atherectomy, coronary stenting and excimer laser angioplasty. While no method has proven better than any other, it does deserve mention that all of these techniques, including PTCA, have been improved upon over the last 20 years. There have not only been significant technical advances but there has also been an increase in operator experience and training, more refined patient selection criteria and improvement in angiographic selection criteria (Dangas & Fuster 1996; Fischman *et al.* 1994; Mudra *et al.* 1997). In addition, increased understanding of the primary post-operative complications has resulted in the development of adjunct drug therapy designed to decrease thrombus and clot formation. As an addendum, all the techniques discussed in previous sections and in the following sections for treatment of CAD can also be used to control peripheral vascular lesions and its sequelae.

2.2.5.1 Percutaneous transluminal coronary angioplasty

Since the introduction of PTCA in 1979 by Gruntzig *et al.* (1979), the procedure has gained widespread use and acceptance. In the United States alone, it is estimated that 447,000 PTCA procedures were performed in 1997, and this number is growing every year (greater than 5% annually). In Canada, an estimated 16,933 PTCA procedures were carried out in 1995. When Europe, Australia and Japan (and parts of SE Asia) are factored into the equation, close to 1,000,000 PTCA procedures are performed in any given year worldwide. PTCA involves positioning a catheter fitted with an inflatable balloon on its tip at the site of the obstruction, using the body's system of arteries as a conduit to the heart, and then inflating the balloon. Balloon inflation opens the arterial lumen which leads to restoration of blood flow (Brown *et al.* 1996; Lyon *et al.* 1987; Waller 1985). Although the precise mechanism by which PTCA increases lumen diameter is not defined, it is now accepted that plaque fracture, separation of the plaque from the underlying artery wall and stretching of the artery wall contribute to enlargement of the arterial lumen (Alexander *et al.* 1998; Lyon *et al.* 1987; Waller 1985; Yutani *et al.* 1999).

2.2.5.2 Coronary stenting

Coronary stenting is a method of revascularization that has been employed in the treatment of CAD for about the same period of time as balloon angioplasty. Stenting is really an adjunct of PTCA since it involves permanent placement of a metal coil into a vessel at the site of an atherosclerotic lesion while piggy-backed on a balloon catheter. Placement of the stent restores the luminal size and patency of the vessel by compressing the plaque in a radial fashion, which redistributes the plaque mass circumferentially without tissue removal (Laskey *et al.* 1993). The impressive and immediate angiographic

results with stent placement has made this the preferred method of treatment for CAD in the United States (Fischman *et al.* 1994; Serruys *et al.* 1994).

2.2.5.3 Atherectomy

Directional atherectomy involves insertion of a catheter fitted with small blades to the site of an atherosclerotic lesion and allowing the blades to either core out the lesion and remove the atheromatous tissue (Kimball *et al.* 1992; Lau & Sigwart 1995; Tenaglia *et al.* 1992) or pulverize the atheromatous plaques into small microparticles (Brogan *et al.* 1993; Lau & Sigwart 1992; Lau & Sigwart 1995). Laser (excimer laser) angioplasty works on the same principle, with the exception that the blades are replaced with a laser that burns away the atheromatous tissue (Litvack *et al.* 1994; Margolis & Mehta 1992; Reis *et al.* 1991; Spears *et al.* 1990). Both atherectomy and laser angioplasty debulk the obstructive lesion in an effort to restore the lumen diameter. These experimental revascularization procedures were popular for a period of time but demonstrated no advantage over PTCA (Adelman *et al.* 1993; Topol *et al.* 1993; Umans *et al.* 1993) with respect to restenosis.

2.3 Revascularization-induced restenosis

The long-term success for revascularization procedures of all types (CABG, balloon angioplasy, intracoronary stents, atherectomy, laser angioplasty, etc.) is limited by the development of restenosis within 6 to 10 months (Ellis *et al.* 1992; Kastrati *et al.* 1993; Lau & Sigwart 1995; Litvack *et al.* 1994; Liu *et al.* 1989; Lytle *et al.* 1987; McBride *et al.* 1988; Reis *et al.* 1991; Spears *et al.* 1990; Spray & Roberts 1977). It is well documented that 30-50% of patients undergoing revascularization procedures demonstrate clinical restenosis (defined by angiography) within 6 months, usually necessitating another revascularization procedure. Restenosis can be defined as the re-

appearance of luminal narrowing (i.e. renewed narrowing) in the region where a successful revascularization procedure had enlarged the lumen diameter. The initial stenosis (constriction or narrowing) is the result of an atheromatous lesion. The subsequent stenosis, or restenosis, is the end result of vascular repair processes (i.e. wound repair process or response to vascular injury) that are typified by not only a vascular proliferative response involving smooth muscle cells (and fibroblasts), but also a remodeling of the vessel (Andersen *et al.* 1996; Ellis & Muller 1992; Glagov *et al.* 1987; Lafont *et al.* 1995; Lau & Sigwart 1995; Liu *et al.* 1989; Mintz *et al.* 1996; Post *et al.* 1994; Schwartz *et al.* 1992a; Schwartz *et al.* 1995a). The proliferative response results in the development of a thickened neointima that encompasses and eclipses the primary atheromatous lesion (Ip *et al.* 1990; Schwartz *et al.* 1995a; Ueda *et al.* 1991). Deposition of extracellular matrix (ECM) is also a part of the sequelae of restenosis, as are the early events of thrombus formation and vascular recoil (Harker 1987; Lau & Sigwart 1995; Schwartz *et al.* 1992a; Schwartz *et al.* 1995a; Schwartz & Reidy 1996; Steele *et al.* 1985; Wilentz *et al.* 1987). Moreover, the vessel undergoes a remodeling, either adaptive or constrictive, over the time course of restenosis (Andersen *et al.* 1996; Glagov *et al.* 1987; Lafont *et al.* 1995; Mintz *et al.* 1996; Post *et al.* 1994). The resulting restenotic lesion, in comparison to the atheromatous lesion, is usually composed of smooth muscle cells (SMCs) in a matrix of connective tissue (as opposed to deposits of fat and foam cells) (Casscells 1992; Jackson & Schwartz 1992; Schwartz *et al.* 1995a). The cellularity or acellularity of this lesion is determined by not only biological variability, but possibly also by the elapsed time over which the lesion has progressed.

Restenosis is used as a broad term to describe the re-narrowing of a lumen after a procedure to create a patent, open lumen. However, in the clinical setting, multiple definitions for restenosis exist and, as a result, it is important to understand and consider

the definition that is being used within a specific context, especially when covering the literature. In general, clinical restenosis is the more important end point. Nonetheless, angiographic restenosis is the standard used to define the degree of restenosis (especially when the efficacy of a pharmacological intervention is being evaluated). Clinical restenosis is defined as recurrent ischemic symptoms within 6 months after a revascularization procedure (PTCA) (i.e. patient symptomology, exercise stress testing, need for repeat revascularization, myocardial infarction and death (Landzberg *et al.* 1997)). In contrast, angiographic restenosis is defined as: i) an increase in occlusive diameter from the immediate post-procedure stenosis on follow-up angiography of 30%, ii) a loss of 50% of the gain from the procedure (PTCA), or iii) a greater than 50% stenosis on follow-up angiography (Holmes *et al.* 1984; Landzberg *et al.* 1997). Therefore, a patient with angiographic restenosis could be living symptom free while having silent ischemia, whereas a patient with clinical restenosis may not have angiographically significant restenosis. Nevertheless, some degree of luminal narrowing occurs in all lesions after any catheter-based treatment or revascularization procedure (Kuntz & Baim 1993). Therefore, it may be desirable to view restenosis as not "simply an undesirable side effect that occurs in a minority of cases, but rather as a process that occurs to some extent in virtually all patients, following a gaussian distribution" (Landzberg *et al.* 1997; Rensing *et al.* 1992). Furthermore, since controlled injury to the arterial wall occurs in all coronary interventions, the vessel will repair itself and, thus, restenosis may be seen as an exaggerated healing response.

2.3.1 Pathogenesis of restenosis

The exact etiology of restenosis remains elusive, although it would not be argued that there are roles for vascular injury, platelet aggregation, inflammation, soluble factors, elastic recoil, hemodynamic factors, proliferation, migration and vascular remodeling.

There are many theories as to the pathophysiology of restenosis, including: 1) contribution of human cytomegalovirus infection (Landzberg *et al.* 1997; Speir *et al.* 1994), 2) restenosis as a remodeling process in which the critical factors are wall shear stress and wall tensile strength (Glagov 1994; Landzberg *et al.* 1997), 3) contribution of elastic recoil (Fischell *et al.* 1988; Landzberg *et al.* 1997), 4) restenosis as an autoimmune process (Eber *et al.* 1992; Landzberg *et al.* 1997), and 5) the wound healing theory of restenosis (Forrester *et al.* 1991; Landzberg *et al.* 1997). However, the possibility does exist that the complex nature of restenosis may encompass several of the above-mentioned processes during its progression. The wound healing theory of restenosis is most widely accepted in the literature and is reviewed by Landzberg *et al.* (1997) and will be dealt with here only briefly. Vascular and plaque injury after balloon angioplasty results in platelet aggregation at the surface of the injured vessel. Thromboxane A_2 (TxA_2) is then released from degranulated platelets, resulting in vascoconstriction and further platelet aggregation. Platelets, coronary endothelial cells, vascular smooth muscle cells and inflammatory cells (macrophages, leukocytes) then release a variety of soluble factors such as thrombin, platelet-derived growth factor (PDGF), basic fibroblast growth factor (bFGF), vascular endothelial growth factor (VEGF), angiotensin II (AngII), interleukin-1 (IL-1) and transforming growth factor-beta (TGF-β) into the local area. Since the endothelium is not present to secrete inhibitory factors such as nitric oxide (NO) and prostacyclin (PGI_2), stimulation of smooth muscle migration into the neointima, followed by proliferation and deposition of ECM occurs. The end result is the formation of a thickened neointima that decreases the lumen diameter of the vessel (i.e. occludes the vessel) (Landzberg *et al.* 1997; Schwartz *et al.* 1995a). Furthermore, in all animal models and in patients, it is suspected that the degree of injury influences the size of the restenotic lesion (Asada *et al.* 1996; Kimura *et al.*

1998; Schulz *et al.* 2000; Schwartz *et al.* 1992b). The processes of adaptive and/or constrictive (geometric) remodeling also contribute to progression of restenotic lesion formation. These events have been compared to an exaggerated wound healing response as is seen in an hypertrophied scar or keloid formation (Sherris *et al.* 1995; Tuan & Nichter 1998; Urioste *et al.* 1999).

2.3.2 Wound healing as the paradigm for restenosis

The vascular injury response follows the wound healing paradigm. Although both wound healing and restenosis are modeled and studied independently, the basic principles are the same. Wound healing is a dynamic, integrated, interactive process of three overlapping phases involving blood cells, ECM, soluble mediators and fibroblast/parenchymal cells: 1) an inflammatory phase in which there is coagulation, increased permeability of capillaries, and aggregation of platelets and leukocytes at the site of injury, 2) a proliferative phase which involves the movement of macrophages, fibroblasts and new blood vessels into the injured area, followed by proliferation of fibroblasts and deposition of ECM, and 3) a maturation phase which involves myofibroblasts, compaction of connective tissue and contraction of the wound followed by collagen remodeling and apoptosis (Hofstadter 1995; Koopmann 1995; Kudravi & Reed 2000; Mutsaers *et al.* 1997; Singer & Clark 1999). The corollary in restenosis also has three distinct but integrated phases: 1) formation of a mural thrombus (involving both coagulation and inflammation), 2) migration and proliferation of SMCs, and 3) secretion of ECM with subsequent remodeling (Schwartz 1994; Schwartz *et al.* 1995a; Schwartz & Reidy 1996; Thyberg 1998). While repair processes are clearly activated by revascularization procedures, their contribution to the development of the restenotic lesion remains to be clarified. Nevertheless, much has been learned about both repair

processes, and especially restenosis, from the study of animal models, particularly the rat (Libby & Tanaka 1997; Schwartz *et al.* 1995a).

2.3.3 Animal models of restenosis

Our understanding of the fundamental mechanisms of restenosis comes from studies carried out in animal models. Although much insight into the process of restenosis and the biology of the vascular response to injury has been derived from these models, either the model and/or the injury differs sufficiently from the human disease that translation of laboratory findings (with respect to mechanism and progression of restenosis and the application of pharmacological interventions for inhibiting the development of restenosis) to the level of the patient is rarely observed. However, for the sake of completeness and historical perspective, a review of animal models and restenosis is warranted.

2.3.3.1 Rat carotid injury model of restenosis

The rat carotid artery model, as reviewed by Schwartz *et al.* (1995a) and Libby & Tanaka (1997), is probably the most widely used and accepted experimental preparation for the study of restenosis. The rat carotid model gave rise to the multiwave model of restenosis. In this model, four phases or waves are observed after arterial injury The first wave consists of the replication of SMCs within the tunica media. A role for basic fibroblast growth factor (bFGF) in the stimulation of medial smooth muscle proliferation has been demonstrated (Libby & Tanaka 1997; Lindner *et al.* 1991; Lindner *et al.* 1990). The second wave involves migration of SMCs from the tunica media across the internal elastic lamina to the intima. Platelet-derived growth factor (PDGF) is required for this phenomena (Clowes *et al.* 1989; Libby & Tanaka 1997). Replication of smooth muscle cells in the intima constitutes the third wave, and, finally, the fourth wave is the increased responsiveness of the neointima to mitogens and other soluble factors (Schwartz *et al.*

1995a). Mural thrombus formation caused by the injury may additionally contribute cytokines, chemoattractants and growth factors that not only initiate but help to promote neointimal thickening. The final result is a space-occupying lesion that impinges on the arterial lumen. The problem with the rat carotid injury model is that it differs from angioplasty of diseased human vessels in many ways. First and foremost, an atheromatous lesion that may or may not already contain SMCs is not present in the rat carotid model. Secondly, the first and second waves of the arterial response to injury as mapped out in the rat carotid model (i.e. proliferation followed by migration) may not apply to the response of human vessels, at least not in the precise order observed with the rat model. Moreover, the actual rate of replication of SMCs in human coronary arteries (and rabbit or pig arteries (Carter *et al.* 1994; Clozel *et al.* 1991; Schwartz *et al.* 1992b)) is very low in comparison to experimental rat models (O'Brien *et al.* 2000; O'Brien *et al.* 1993; Schwartz *et al.* 1996). Thirdly, the vascular structure and responses of the rat are distinct from those of human vessels. A major difference is the lack of a subintimal layer in the rat vasculature prior to injury (Sims 1989). As well, rat arteries contain less medial elastin and do not have a vaso vasorum (Badimon *et al.* 1998; Sims 1989). Finally, the time course to experimental restenosis in animal models does not fit with the time course of restenosis seen in human patient populations, even when aging rates are factored in. As a result of these differences, successes in trials of pharmacological agents in experimental rat models have not translated to the clinical setting (Johnson *et al.* 1999). For example, the use of ACE inhibitor therapy in a rat carotid injury model proved to prevent restenosis (Fernandez-Alfonso *et al.* 1997; Powell *et al.* 1991). Based on these successful results, large human clinical trials of ACE inhibitors were initiated. Unfortunately, it was found that long-term ACE inhibition did not prevent intimal lesion formation (Desmet *et al.* 1994; MERCATOR 1992).

2.3.3.2 Larger animal models of restenosis

Other models of restenosis, employing larger animals such as rabbits, dogs and pigs, are now used more frequently since they fare slightly better in their ability to mimic the development of restenosis in humans. Rabbits are utilized for their similarity to humans in their response to cholesterol-loading (Barry *et al.* 1997; Fukuyama *et al.* 1996; Lawrence *et al.* 1995). Pigs are preferred for their ability to more closely model the human vasculature and the responses of the human vasculature to injury (Badimon *et al.* 1998; Ferrell *et al.* 1992; Fuster *et al.* 1991; Johnson *et al.* 1999; Karas *et al.* 1992; Muller *et al.* 1992a; Schwartz *et al.* 1992a; Schwartz *et al.* 1992b). Primate models have also been used, but to a lesser degree. Target vessels have included the rabbit iliac and rabbit carotid arteries, and pig coronary and pig femoral arteries. The rabbit arterial response to injury is similar to that of the rat, so a discussion of this model will not be necessary (Finking & Hanke 1997; Johnson *et al.* 1999). Ongoing cytokine expression and inflammatory responses may further contribute to lesion development in rabbits (Libby & Tanaka 1997; Tanaka *et al.* 1993). The porcine arterial injury model (coronary or femoral) has also been well studied, and use of this model is now more widespread due to the considerable similarities between pig and human responses (Badimon *et al.* 1998; Ferrell *et al.* 1992; Karas *et al.* 1992; Muller *et al.* 1992a). Three distinct phases have been identified in the porcine coronary artery after injury (Schwartz *et al.* 1992a). The immediate response to arterial injury involves formation of a thrombus (made up of aggregated platelets, fibrin and trapped erythrocytes). Cellular recruitment into the thrombus is then observed (macrophages and lymphocytes). Finally, SMCs migrate into the thrombus where they then proliferate and elaborate ECM. The ongoing involvement of inflammation and cytokine expression is also well documented in this model (Fuster *et al.* 1991). Nevertheless, although the pig model would seem better-suited for the study of

restenosis, the manageable size of the rabbit, the size of its vessels, and the potential for a more complex and intermediary response, makes the rabbit model favoured over the pig model. However, many limitations still exist with these models and data reported in the literature should be interpreted with great care prior to considering application to humans.

2.3.4 Benefits of animals models of restenosis

Regardless of the short-comings of animal models of restenosis, they have provided an insight into the biology, cell biology and molecular biology underlying the arterial response to injury (Johnson *et al.* 1999; Schwartz *et al.* 1992a; Schwartz *et al.* 1995a). Used appropriately, with an appreciation of the distinct features of natural or simulated disease in each species and the importance of proper design and execution of experiments, animals models can prove to be very valuable (Narayanaswamy *et al.* 2000). Animal models are relatively inexpensive (in comparison to human clinical trials) and allow for direct measurements of absolute intimal thickness and lumen/medial-intimal area ratios, which is not possible in humans unless at post-mortem (but results are less accurate). It would be ideal to study the development of restenosis in humans, but human samples are difficult to obtain and ethical considerations are a priority. However, there are now *in vitro* human models that are showing promise. For example, a recently developed human arterial organ culture model of post-angioplasty restenosis may offer a satisfactory intermediary model and adjunct for future studies of restenosis (Voisard *et al.* 1999).

2.4 Vascular injury and remodeling

A relatively new concept developed for restenosis is the idea of remodeling. Vascular remodeling, as viewed by Faxon *et al.* (1997), is a very important part of the restenosis process. Although once ignored, it is now known, with the advent of

intravascular ultrasound (IVUS), that vascular remodeling (or more accurately, geometric remodeling) contributes to the late lumen loss seen during restenosis (Mintz *et al.* 1996). In fact, its contribution may be more significant to the loss of lumen diameter than the increase in intimal mass, and the contribution of SMC migration and proliferation associated therein (Kakuta *et al.* 1994; Mintz *et al.* 1996; Post *et al.* 1994). However, it should be noted that bi-directional remodeling is observed after balloon angioplasty (i.e. early adaptive enlargement followed by late constrictive remodeling of the vessel) (Kimura *et al.* 1997; Mintz *et al.* 1996). Adaptive remodeling results in the preservation of lumen size and therefore blood flow in the face of a thickened neointima (i.e. the diameter of the vessel itself is enlarged). On the other hand, constrictive remodeling (i.e. decrease in the area of the vessel media) exacerbates the effect of a thickened neointima and the resulting decrease in lumen diameter greatly decreases blood flow. The resultant lumen diameter therefore represents a balance between the reparative response to injury that promotes neointimal formation and the contribution of shear-stress to expanding the lumen (Gibbons & Dzau 1994). More importantly, it is critical to understand that even relatively small changes in vessel diameter or area can lead to very major alterations in lumen diameter and blood flow (Faxon *et al.* 1997).

2.4.1 Remodeling and restenosis

The term remodeling refers to a change in size or structure and, in the cardiovascular field, this term has been applied to a variety of conditions (eg. ventricular remodeling and atrial remodeling). In the blood vessel, remodeling can refer to a chronic change in diameter or to an alteration in the components of the vessel wall with or without a change in size and/or shape (Faxon *et al.* 1997; Gibbons & Dzau 1994). Remodeling can also be good or bad (i.e. adaptive or maladaptive, compensatory or not). For example, during atherosclerosis, the vessel can enlarge and compensate for the loss

of lumen as a result of the encroaching atheromatous lesion (Glagov *et al.* 1987). However, the opposite is also seen during atherosclerosis, whereby the vessel decreases in size, exacerbating the loss of lumen and precipitating cardiovascular complications and events (Herity *et al.* 1999; Mintz *et al.* 1997; Pasterkamp *et al.* 1997). During restenosis, alterations in vessel size have the greatest impact, thus the term geometric remodeling has been coined to refer to changes in total vessel area (Faxon *et al.* 1997). Geometric remodeling can be defined as "lasting structural changes in the vessel wall in response to hemodynamic stimuli and is distinct from those acute variations in arterial tone that follow changes in blood pressure, flow and circulating vasoreactive substances" (Herity *et al.* 1999). This definition can be narrowed down to describing changes in cross-sectional area within the external elastic lamina (i.e. changes in medial area), thereby distinguishing it from the thickening of the vessel wall that is often associated with hypertension (Herity *et al.* 1999). Since vascular remodeling is ongoing, changes in at least four cellular processes are seen. These include: i) cell proliferation/growth; ii) cell migration; iii) apoptosis/cell death; and iv) synthesis/degradation of extracellular matix components. Dynamic interactions between a variety of factors (local generation of growth factors and soluble mediators, vasoreactive substances, hemodynamic stimuli) influence the relative contribution of these four processes to the eventual outcome of the remodeling process and its potential contribution to the restenotic lesion (Faxon *et al.* 1997; Gibbons & Dzau 1994; Herity *et al.* 1999). The concept of vascular remodeling, its mechanisms and its contribution to vascular restenosis are reviewed by Gibbons & Dzau (1994), Herity *et al.* (1999) and Faxon *et al.* (1997), and I refer you to these articles for the intricate details. Interestingly, the expansion of the paradigm of restenosis to include remodeling and its mechanisms has important implications to the therapeutic approaches used for treatment of restenosis.

2.5 Pharmacological approaches for the prevention of restenosis

A variety of pharmacological agents have been tested, both clinically and in animal models, for their ability to prevent restenosis. Unfortunately, to date, very few have been deemed successful. I refer you to reviews by Landzberg *et al.* (1997) and Lefkovits & Topol (1997) for a comprehensive discussion of the pharmacological agents already evaluated. Other approaches to control the development of restenosis include the use of stents, β-radiation and genetic therapies that include the local delivery of antisense oligodeoxynucleotides, dominant-negative mutants, suppressors of cell cycle and recombinant chimeric toxins (Landzberg *et al.* 1997; Lefkovits & Topol 1997). However, these approaches will not be discussed here and I refer you to recent reviews for further details (Chougule 2000; Kibbe *et al.* 2000; Kuntz & Baim 2000; Landzberg *et al.* 1997; Lau & Sigwart 1993; O'Brien & Simari 2000; Oesterle *et al.* 1998; Smith & Walsh 2000; Tio *et al.* 1998).

The process of restenosis can potentially be divided into three phases, thrombosus (thrombus formation and organization), granulation (proliferation and migration of SMCs followed by ECM deposition) and remodeling (organization of ECM), each amenable to pharmacological intervention. Pharmacological treatments have employed anti-platelet agents, anti-thrombotic/anti-coagulant agents, anti-inflammatory drugs, growth factor antagonists, vasodilators, anti-proliferative and anti-neoplastic agents, selective and non-selective AngII receptor antagonists, ACE inhibitors, lipid-lowering agents, and anti-oxidants (Landzberg *et al.* 1997; Lefkovits & Topol 1997). The bulk of these agents have shown little, if any, benefit. However, those agents that have reached clinical trial and thus far show potential include platelet glycoprotein IIb/IIIa receptor inhibitors (chimeric 7E3 monoclonal antibody or abciximab, Tirofiban, Integrilin), prostacyclin analogs such as Ciprostene (natural anti-platelet agent), non-steroidal anti-inflammatory agents such as

Ebselen and tranilast, specific growth factor antagonists such as trapidil (PDGF/TxA_2 receptor antagonist) and angiopeptin (somatostatin analog), vasodilators such as calcium channel antagonists (eg. verapamil), and nitric oxide donors (Landzberg *et al.* 1997; Lefkovits & Topol 1997). Other agents and approaches which have met with success in experimental animal models of restenosis include Taxol (an anti-microtubule agent), photochemotherapy with 8-methoxypsoralen (8MOP), antagonism of endothelial and leukocyte adhesion molecules, tissue plasminogen activator, anti-statin and $\alpha 1$ adrenergic blockers (Landzberg *et al.* 1997). Careful clinical testing will determine the suitability of these approaches in the arsenal against restenosis. Nevertheless, the intense study of the pharmacological prophylaxis of restenosis has led to improvements in patient mortality and morbidity. For example, the implementation of aspirin and heparin therapy has clearly reduced the acute complications of percutaneous revascularization procedures, although it has had little effect on restenosis itself (Landzberg *et al.* 1997).

Therapeutic approaches that focus on the inhibition of specific cellular processes, such as proliferation and/or migration, have the potential to fail because these therapies may not influence the contribution of vascular remodeling in its entirety. In the past, treatment strategies for controlling restenosis have focused primarily on cell proliferation and/or migration. Although cellular proliferation may be the initial event that activates the arterial remodeling process (in the rat), treatment strategies should encompass the contributions of cell proliferation, migration and arterial remodeling. Pharmacologic approaches that have attenuated arterial remodeling (when examined by IVUS) include probucol and PDGF antagonism (Cote *et al.* 1999; Maresta *et al.* 1994; Yokoi *et al.* 1997). Intravascular irradiation has also been demonstrated to have similar effects (King *et al.* 1998; Meerkin *et al.* 1998; Sabate *et al.* 1999). Stents have been deployed as a mechanical approach for the prevention of inward remodeling and restenosis (Lau &

Sigwart 1993; Lau & Sigwart 1995; Oesterle *et al.* 1998). However, the progression of restenosis with stent placement is characterized by increased neointimal thickening, which eventually obstructs the lumen diameter (Gershlick & Baron 1998; Mintz *et al.* 1998; Virmani & Farb 1999) and ironically reverts the problem of restenosis back to one of cellular proliferation and/or migration. As a result, it appears that combination therapy designed to inhibit all of the aforementioned cellular processes involved in restenosis, in a temporal manner, will have the most success with respect to treatment.

2.5.1 Perspectives on pharmacological treatment of restenosis

Although we are now at the stage where there are a variety of pharmacological agents that may prove beneficial for the treatment of restenosis, it is likely that no one therapeutic agent will be the 'magic bullet'. Likely, combination therapy and/or a combination of approaches will be required to control restenosis, since the progression of restenosis is multifactorial in nature and in part governed by independent risk factors such as diabetes and smoking. Furthermore, biological variation in the population may result in different pathogenetic mechanisms leading to restenosis in different individuals (Waller *et al.* 1991). Therefore, successful treatment of restenosis may lie with tailoring specific pharmacological approaches to specific patient populations. Moreover, elucidation of specific risk factors may identify and categorize patients into those who require and those who do not require prophylactic therapy, and those who should not undergo percutaneous revascularization procedures (Landzberg *et al.* 1997).

Why has the clinical success rate of pharmacological agents not been reflective of either the effort that has been put into the research and testing of compounds or the apparent success seen in experimental animal models? Firstly, the relative lack of success of pharmacological agents for the prevention of restenosis may lie with an incomplete understanding of its pathogenesis (Glagov 1994; Landzberg *et al.* 1997). For example, as

elaborated in section 2.4, the importance of vascular remodeling to restenosis complicates the scenario, making attempts to block a single event in the process untenable. Secondly, inadequate drug dosing in the clinical setting may arise due to toxicity limitations or an inability to deliver sufficient drug (Landzberg *et al.* 1997; Lincoff *et al.* 1994). As well, pretreatment periods necessary to reach therapeutic levels are often inadequate in clinical trials. Thirdly, the duration of treatment may not be long enough. Fourthly, results are often confounded due to concomitant administration of medications. Fifthly, follow-up periods and/or follow-up end-points are often of insufficient duration in the human population, and end-points are not consistent between animal and human studies, making evaluations difficult. Finally, interspecies differences in both vessel physiology, response to injury and baseline of the model make it difficult to translate findings from an animal model to the clinical setting. Although these deficiencies appear to be encompassing, advances in our understanding of the pathogenesis of restenosis, the more critical evaluation of experimental details, the generation of newer technologies and the use of more adequate animal models, will no doubt make translation of pharmacological agents and methodologies for the treatment of restenosis more dependable.

2.6 Vascular smooth muscle cells

2.6.1 Multifunctional nature of smooth muscle cells

The vessel wall is typically composed of three layers separated by an elastin matrix-containing lamina: an outer adventitial layer composed mainly of fibroblasts, an inner luminal layer composed of endothelial cells and, in between, a medial layer of smooth muscle cells (SMCs). SMCs are normally the only cell type found in the media of mammalian arteries. In this setting, under normal circumstances, the specialized function of the SMC is contraction for the purpose of maintaining blood pressure and flow

(Somlyo & Somlyo 1994a; Somlyo & Somlyo 1994b). However, the SMC is a remarkably plastic cell, and during the pathogenesis of certain vascular diseases and following injury the SMC can modulate its phenotype and perform a variety of functions as dictated by the environmental conditions set out by the pathology. Under these abnormal circumstances, as a result of environmental and/or autocrine/paracrine cues, the function of some medial SMCs will change from contraction to migration, proliferation and degradation/secretion of extracellular matrix (ECM). This modulation occurs in an effort to either adapt to local stresses or to repair portions of the vessel wall that have been damaged (Owens 1995; Schwartz *et al.* 1986; Schwartz & Ross 1984). This scenario is also applicable to normal developmental vasculogenesis, whereby proliferation, migration and ECM deposition are also required events (Owens 1995; Schwartz & Ross 1984). Since the processes involved in repairing vessels, specifically SMC proliferation, migration, differentiation and ECM synthesis, are similar to those active during new vessel formation, it has been suggested that SMCs involved in the vascular repair might re-express a fetal/neonatal phenotype (Kim *et al.* 1994; Majesky *et al.* 1992).

2.6.2 Smooth muscle cell phenotypic modulation

SMCs exist in two distinct differentiated states that were originally believed to be mutually exclusive, as postulated by Chamley-Campbell *et al.* (1979). The 'contractile' phenotype is observed in the normal mature media of the vessel wall, while the 'synthetic' phenotype is characteristic of the developing vessel wall and observed upon injury of the vessel wall (Chamley-Campbell *et al.* 1979; Schwartz *et al.* 1995a). The 'contractile' phenotype is characterized by a cell cytoplasm occupied by myofilaments. In contrast, the 'synthetic' phenotype is distinguished by a marked loss of myofilaments and an increase in organelles such as the endoplasmic reticulum and Golgi complex (Thyberg

1998; Thyberg *et al.* 1997). This classification is now known to be an oversimplification and that some degree of differentiation is compatible with proliferation in SMCs. For example, SMCs during vascular development express many proteins characteristic of a differentiated SMC even though these cells are rapidly proliferating and laying down ECM (Duband *et al.* 1993). Similarly, SMCs within intimal (atheroscleortic) lesions in human and experimental animal models continue to show an altered differentiated phenotype even when the proliferation rates have returned to normal levels (Clowes *et al.* 1988; Gordon *et al.* 1990; O'Brien *et al.* 1993). Since there has been little success in equating the appearance and disappearance of particular marker genes or proteins with a definitive phenotypic state, either 'contractile' or 'synthetic' SMCs may not typically exist (Owens 1998; Owens *et al.* 1996; Owens & Wise 1997). Rather, it has been proposed that medial SMCs consist of two or more subpopulations, each with distinct but overlapping properties (Bochaton-Piallat *et al.* 1994; Frid *et al.* 1994; Holycross *et al.* 1992; McNamara *et al.* 1993; Vernon *et al.* 1993). Support for this concept is provided by the detection of SMCs expressing these intermediary properties in vessels (Campbell & Campbell 1997; Shanahan & Weissberg 1998). Interestingly, it appears that SMC growth and differentiation can be dissociated in culture more completely. For example, individual growth factors for SMCs (eg. PDGF, thrombin and bFGF vs. serum) display very distinct effects on the expression of SMC differentiation marker proteins such as smooth muscle α-actin, smooth muscle myosin heavy chain and smooth muscle tropomyosin (Holycross *et al.* 1992; Kallmeier *et al.* 1995; McNamara *et al.* 1993; Vernon *et al.* 1993). Nevertheless, neither phenotype is a terminal event, as SMCs can revert back to a 'contractile' state after undergoing modulation from the 'contractile' to the 'synthetic' phenotype (Kocher *et al.* 1991).

2.6.3 Smooth muscle cell culture systems

Much of the information that has been gathered concerning SMC physiology, phenotypic modulation and SMC proliferation has come from studying isolated SMCs in culture (Chamley-Campbell *et al.* 1979; Owens 1995). SMCs have been isolated via explantation techniques (Jarmolych *et al.* 1968; Ross 1971) and enzymatic isolation techniques (Chamley *et al.* 1977), and several cell lines of supposed vascular SMC origin have been described in the literature (Kimes & Brandt 1976; Schubert *et al.* 1974). Each SMC culture model has its own unique advantages and disadvantages, and consideration of the age of the donor animals, the species of the donor animal and the inherent heterogeneity within the original cell populations is essential (Bochaton-Piallat *et al.* 1993; Lemire *et al.* 1994). Additionally, culture conditions will influence behaviour (Burke & Ross 1979; Carey 1991; Davies 1990; Davies & O'Connor 1990; Spahr & Piper 1990; Thyberg *et al.* 1990a; Thyberg *et al.* 1990b). In general, it has been noted that SMCs derived by enzymatic digestion retain their differentiated properties longer than explant-derived cells (Owens 1995). On the other hand, explant-derived cells may provide a model system that more suitably mimics the pathological state of SMCs within intimal lesions (Owens 1995). Taken together, these points would suggest that it is more important to keep in mind the experimental question that is being addressed when choosing a SMC culture method than it is to decide which experimental system is the most advantageous. Furthermore, it is critical to keep in mind that not all experimental systems will generate the same findings, since SMCs respond very differently depending on a multitude of environmental- and cell-related conditions.

2.6.4 Regulation of smooth muscle cell differentiation

The factors that influence SMC differentiation have long been topics of study. However, differentiation control genes equivalent to those present in other cell types (eg.

MyoD in skeletal muscle (Molkentin & Olson 1996a; Yun & Wold 1996), and Sox9 in chondrocytes (de Crombrugghe *et al.* 2000)) have not been identified in SMCs. Nevertheless, a number of genes expressed in SMCs contain regions that are highly homologous to homeobox genes coding for proteins that bind to specific promoter elements that either activate or inhibit the corresponding genes (Laughon 1991). Expression of three homeodomain-containing genes, Mhox (Blank *et al.* 1995; Cserjesi *et al.* 1992), Hox 1.11 (Patel *et al.* 1992) and Gax (Gorski *et al.* 1993) has been demonstrated in SMCs. Of these, Gax appears to be the favoured candidate for a vascular SMC differentiation control gene, since its expression is largely confined to the cardiovascular system of the adult (Gorski *et al.* 1993). Furthermore, Gax is rapidly downregulated during the G_0/G_1 transition in cultured SMCs, and it is suspected that this gene plays an important role in the control of SMC differentiation.

2.6.5 Factors controlling the phenotypic modulation of smooth muscle cells

The changes in SMC phenotype observed both in primary SMC culture and in the injured vessel wall are not only associated with functional and structural reorganization of the cells (i.e. differentiated SMCs), but also with alterations that can be brought about by ECM components and other physiologic factors (Owens 1995; Thyberg 1996; Thyberg 1998). These concepts are reviewed by Thyberg (1996 and 1998) and Owens (1995) and will not be covered here. However, the contribution of growth factors, cytokines, hormones and prostanoids to SMC phenotypic modulation, differentiation, proliferation and migration will be covered briefly.

2.6.6 Induction of smooth muscle cell proliferation (and migration)

Proliferation of SMCs is a phenotype- and mitogen-dependent process that is important in fetal life during the development of blood vessels and also in adult life during repair of injured blood vessels (Ross 1993). The regulation of SMC proliferation

is thus an important area of study and has been reviewed by many (Bobik & Campbell 1993; Nikol & Hofling 1995; Sanz-Gonzalez *et al.* 2000; Thyberg 1996). However, because of the many animal models used, the differences in disease status of the models, the differences in age of the animals, and the inherent heterogeneity of SMCs, the results are complicated and often difficult to interpret and apply to the general process of SMC proliferation (Berk & Alexander 1989; Bochaton-Piallat *et al.* 1993; Dartsch *et al.* 1990a; Gordon *et al.* 1986; Grunwald *et al.* 1987; Hadrava *et al.* 1989; Haudenschild & Grunwald 1985; Lemire *et al.* 1994; Orlandi *et al.* 1994a; Rosen *et al.* 1985; Saltis & Bobik 1992; Yoshida *et al.* 1988). Interestingly, the modulation of SMCs from a contractile to a synthetic phenotype precedes and is necessary but is not sufficient to initiate the proliferation of SMCs (Chamley *et al.* 1977; Chamley-Campbell *et al.* 1981; Fritz *et al.* 1970; Thyberg *et al.* 1983). Thus, SMCs appear to require serum or another source of mitogens in order for replication to begin (Dartsch *et al.* 1990b; Hoshi *et al.* 1988; Hwang *et al.* 1992; Ross *et al.* 1974; Ross *et al.* 1978; Thyberg 1996; Weinstein *et al.* 1981; Wren *et al.* 1986; Yamamoto *et al.* 1993b).

Migration of smooth muscle cells is also phenotype-dependent, but does not necessarily require a stimulus in the form of a chemoattractant factor since other matrix and physical cues can cause SMCs to become motile (Banai *et al.* 1990; Casscells 1992; Ingber & Folkman 1989). SMC migration is an important component of wound healing and the formation of hyperplastic lesions which contribute to restenosis post-angioplasty (Raines & Ross 1993; Ross *et al.* 1986). It is also known to occur during embryogenesis, tumour metastasis and angiogenesis (Casscells 1992). Cell migration involves regulated attachment/detachment to the ECM, contraction of non-muscle myosin and actin, cytoskeletal plasticity (i.e. re-organization of the cytoskeleton) and a requirement for oxygen and protein synthesis (Caterina & Devreotes 1991; Kelley *et al.* 1991; Madri *et*

al. 1991). How these events are coordinated and what intracellular signaling pathways are involved is at present not fully understood (Saxty *et al.* 1998b; Stossel 1993). Extracellular signals that regulate migration include physical forces (Ingber & Folkman 1989), soluble regulators (i.e. vasoactive hormones) (Bell & Madri 1989; Bell & Madri 1990), peptide growth factors (eg. PDGF) (Abedi *et al.* 1995; Abedi & Zachary 1995) and Ca^{2+}, Mg^{2+}, pH and oxygen tension (Banai *et al.* 1990; Casscells 1992).

It is reasonable to assume that SMCs must undergo a change in the cytoskeleton in order to migrate, so phenotypic modulation of SMCs with loss of contractile structures likely functions to activate cells for both proliferation and migration (Schwartz 1997; Schwartz *et al.* 1995a). A similar loss of contractile structure is observed in other muscle cells migrating into a wound, including skeletal muscle (Snow 1977a; Snow 1977b), and it is possible that migration of any differentiated cell into a wound requires de-differentiation. In SMCs, this de-differentiation may also be linked to an ability to enter the cell cycle (Schwartz *et al.* 1995a). On the other hand, migrating cells are not necessarily synthesizing DNA (Casscells 1992; Clowes & Reidy 1991). Another feature that distinguishes migration from proliferation is that migration is not affected by doses of radiation or drugs that inhibit cell division (Thorgeirsson *et al.* 1979). Typically, migration also precedes proliferation and the concentration of stimulus required (eg. PDGF) is much lower than that required for proliferation (Grotendorst *et al.* 1982).

2.6.7 Factors affecting smooth muscle proliferation (and migration)

Growth factors and cytokines have been detected in the immediate area of a vessel wall injury (Corson & Berk 1993; Libby *et al.* 1986; Loppnow & Libby 1992; Warner *et al.* 1987; Wilcox 1993). PDGF, bFGF and TGF-β1, for example, known stimulators of SMC migration and proliferation, originate from platelets, endothelial cells and SMCs immediately after injury (Bernstein *et al.* 1982; Blank & Owens 1990; Bowen-

Pope & Ross 1982; Bowen-Pope *et al.* 1985; Corjay *et al.* 1989; Corson & Berk 1993; Grotendorst *et al.* 1982; Grotendorst *et al.* 198 1; Janat & Liau 1992; Kocher & Madri 1989; Nilsson *et al.* 1983; Orlandi *et al.* 1994b; Raines *et al.* 1990; Ross 1993; Saltis & Bobik 1992; Saltis *et al.* 1995; van Neck *et al.* 1995; Weinstein *et al.* 1981; Wilcox 1993). Peptide mitogens that also have a positive effect on SMC replication include EGF, IGF-1, and thrombin (Banskota *et al.* 1989; Bar-Shavit *et al.* 1990; Clemmons 1984; Clemmons & Van Wyk 1985; Delafontaine *et al.* 1991; Gospodarowicz *et al.* 1981; Grainger *et al.* 1994; Hwang *et al.* 1992; McNamara *et al.* 1993; Pfeifle *et al.* 1987a; Pfeifle *et al.* 1987b; Saltis *et al.* 1995; Thyberg 1996; Weinstein *et al.* 1981). And finally, the effect of cytokines, such as IL-1 and TNF-α, on SMC migration and proliferation has been demonstrated (Bonin *et al.* 1989; Bourcier *et al.* 1995; Gay & Winkles 1991; Hajjar & Pomerantz 1992; Libby & Hansson 1991; Libby *et al.* 1988; Nilsson 1993; Raines *et al.* 1989; Sawada *et al.* 1990; Warner & Libby 1989).

2.6.7.1 Hormones

Hormones such as angiotensin II (AngII) and endothelin-1 have been shown to play an important role in the behaviour of SMCs, although their predominant effects are associated with the control of vascular tone (Levin 1995; Regoli *et al.* 1993). Nevertheless, these hormones and others (i.e. vasoactive peptides) have been demonstrated to promote migration and proliferation of SMCs (Battistini *et al.* 1993; Bobik *et al.* 1990; Dalsgaard *et al.* 1989; Hahn *et al.* 1991; Hahn *et al.* 1990; Hirata *et al.* 1989; Itoh *et al.* 1993; Janakidevi *et al.* 1992; Komuro *et al.* 1988; Naftilan *et al.* 1989; Newby & George 1993; Owens 1989; Stouffer & Owens 1992; Weber *et al.* 1994a; Weber *et al.* 1994b). On the other hand, their ability to modulate SMC phenotype appear to be distinct from those elicited by PDGF (Andrawis *et al.* 1993; Van Putten *et al.*

1994). For example, PDGF decreases α-actin whereas AngII increases α-actin, and yet both positively influence proliferation and migration.

2.6.7.2 Eicosanoids

Prostanoids (eg. $PGE_{1/2}$, PGI_2 and TxA_2) are arachidonic acid metabolites that modulate vascular tone. As well, they can modulate the SMC phenotype and consequently proliferation (Cornwell *et al.* 1979; Hara *et al.* 1995; Koh *et al.* 1993; Loesberg *et al.* 1985; Morinelli *et al.* 1994; Morisaki *et al.* 1988; Nilsson & Olsson 1984; Owen 1986; Pietila *et al.* 1980; Pomerantz & Hajjar 1989; Sachinidis *et al.* 1995; Thyberg *et al.* 1990a; Uehara *et al.* 1988). They are produced locally by endothelial cells, SMCs and macrophages in the vessel wall after injury. Release of TxA_2 has been shown to increase SMC growth (Morinelli *et al.* 1994) while prostacyclin has been found to have inhibitory effects (Hara *et al.* 1995; Isogaya *et al.* 1995; Koh *et al.* 1993; Schror & Weber 1997; Wu 1997). Interestingly, PGE_1 was found to increase the conversion of SMCs to the synthetic phenotype and stimulate DNA replication. However, as soon as the SMCs had entered a synthetic state, PGE_1 was demonstrated to have an inhibitory effect on SMC growth (Sjolund *et al.* 1984). Others have shown similar effects including Owen (1986), and recently Schror & Weber (1997) postulated a dual role for PGs during vascular injury and repair.

2.6.8 Cell signaling systems involved in injury and the response of SMCs

Arterial injury typically results in damage to SMCs and the exposure of medial layer SMCs and possibly adventitial layer fibroblasts to multiple blood borne and inflammatory factors, with ensuing phenotypic modulation and activation of the SMCs. These factors, including growth factors such as PDGF, bFGF and TGF-β1, cytokines such as TNFα, IL-1 and IL-6, hormones such as AngII and endothelin-1, and prostanoids such as TxA_2 and $PGE_{1/2}$, bind to specific cell surface receptors on SMCs and thereby

activate multiple effector proteins. The cell surface receptors on binding of the ligand, undergo a conformational change that allows for subsequent activation of signaling cascades. Although the initial events are different for each receptor, it would appear that a common set of signal molecules must be activated for proliferation (and/or migration) to occur and these prominent signal moieties include PI3-kinase, p21-Ras and MAP kinase. All three have the potential to influence nuclear activation of immediate-early growth response genes such as c-*fos*, c-*jun* and c-*myc* (Bravo 1990; Marshall 1999). It is presumed that activation of these genes, since they encode transcription factors, regulates the subsequent activation and entry of the cell into the cell cycle. Interestingly, the magnitude of the vascular response to all of these growth factors and hormones must be coordinated by the cell, since it is unlikely that any of these factors acts individually.

2.6.8.1 Phosphatidylinositol 3-kinase

PI3-kinase is a lipid kinase that is activated by a number of growth factors and is an integral component in the cascade of signal transduction events involved in cell growth and transformation (Soltoff *et al.* 1993). It is a heterodimeric protein composed of p85 and p110 subunits that catalyzes the synthesis of 3-phosphorylated phosphoinositides. It is considered to be a key component in receptor-mediated mitogenesis (Varticovski *et al.* 1994). PI3-kinase links the autophosphorylated and activated receptor to adapter proteins such as IRS-1 and Shc for recruitment to Grb/mSOS complexes, with subsequent activation of Ras/Raf and the MAP kinase cascade (Kapeller & Cantley 1994; Sun *et al.* 1993). The 3-phosphorylated modified lipids generated by PI3-kinase can also serve as intermediates for specific downstream signal events that will eventually determine the cellular response to a particular growth stimulus (Li *et al.* 1995; Rameh *et al.* 1995; Saward & Zahradka 1997a; Shepherd *et al.* 1996). Inhibition of PI3-kinase by specific inhibitors (i.e. LY294002) has demonstrated

the importance of this enzyme for the activation of DNA synthesis, MAP kinase, p70 ribosomal S6 kinase, protein synthesis and glucose uptake (Cheatham *et al.* 1994; Ferby *et al.* 1994; Petritsch *et al.* 1995; Sanchez-Margalet *et al.* 1994), thereby being an important aspect of the intracellular signaling cascades that are generated by growth factor receptors with intrinsic tyrosine kinase activity. PI3-kinase is also demonstrated to be an important component of G protein-coupled receptor activation of MAP kinase and growth related pathways, since it can be activated by $G_{\beta\gamma}$ subunit of G proteins and behaves as the tyrosine kinase pathway intermediate that links G proteins to kinase signaling pathways (Della Rocca *et al.* 1997; Force & Bonventre 1998; Lopez-Ilasaca *et al.* 1997).

2.6.8.2 p21-Ras

p21-Ras is a guanine nucleotide binding protein that sits at the threshold of the MAP kinase cascade and is considered to be important for cell growth and proliferation, since constitutive activation of Ras leads to a "transformed" phenotype (Bos 1995; Mansour *et al.* 1994; Maruta & Burgess 1994; Seuwen *et al.* 1988) and dominant-negative mutants of Ras inhibit MAP kinase activition and cell proliferation (Bos 1995; de Vries-Smits *et al.* 1992; Mansour *et al.* 1994; Maruta & Burgess 1994; Robbins *et al.* 1992; Seuwen *et al.* 1988; Thomas *et al.* 1992; Wood *et al.* 1992). The Ras proteins function as signal transducers in the GTP-bound state and are inactive in the GDP-bound state. Although activation of MAP kinase is not necessarily dependent on the activation of this protein, a direct link between Ras/Raf and MAP kinase activation has been established (Bos 1995; de Vries-Smits *et al.* 1992; Force & Bonventre 1998; Mansour *et al.* 1994; Maruta & Burgess 1994; Robbins *et al.* 1992; Seuwen *et al.* 1988; Thomas *et al.* 1992; Wood *et al.* 1992). The Ras pathway has also been associated with activation of signals other than MAP kinase (Olson & Marais 2000). These effectors include p21-

activated serine/threonine kinase (PAK) and the Rho-binding serine/threonine kinase (ROK) (Lim *et al.* 1996; Marshall 1996). Activation of p21-Ras is also involved in Rho directed cytoskeletal rearrangement which potentially influences cell migration (Hall 1993; Lim *et al.* 1996; Marshall 1996).

2.6.8.3 MAP kinase

Of the three MAP kinase cascades that have been characterized in mammalian cells, the best understood is the ERK (extracellular signal-regulated protein kinase) cascade. This particular pathway is activated by treatment of SMCs with growth factors that induce cell proliferation, and is also a critical component of cellular differentiation, contractility and cell migration processes (Adam *et al.* 1995; Force & Bonventre 1998; Khalil & Morgan 1993; Klemke *et al.* 1997; Nelson *et al.* 1998). The importance of the ERK pathway in cell growth and proliferation is demonstrated by the ability of constitutively active forms of MEK-1 to activate mitogenesis in fibroblasts (Cowley *et al.* 1994; Mansour *et al.* 1994) and the ability of dominant-negative mutants of Ras, Raf or MEK-1 to block growth factor-induced mitogenesis. Moreover, sustained ERK activation seems to be required for cells to pass through the G_1/S restriction point (Marshall 1995; Pages *et al.* 1993). The importance of the ERK pathway in SMC migration vs. proliferation was reported by Nelson *et al.* (1998) who demonstrated that distinct phases of MAP kinase activation were required to stimulate these two discrete cellular events (i.e. MAP kinase activity within the first 15 minutes was required for SMC migration, whereas MAP kinase activity between 1 and 4 hours was required for SMC proliferation). The other two MAP kinase cascades, the SAPK/JNK/p54 MAP kinase pathway and the p38 MAP kinase pathway, are induced by cellular stress. Activation of all three MAP kinase cascades results in the stimulation of transcription factors, and modulation of these

transcription factors regulates the induction of genes that will determine the biological response of the cell (Cook *et al.* 2000).

The MAP kinases, ERK1 (p42) and ERK2 (p44), are activated by stimulation of SMCs with PDGF (Graves *et al.* 1993; Rakhit *et al.* 2000), AngII (Mii *et al.* 1994; Sadoshima *et al.* 1995), TxA_2 (Morinelli *et al.* 1994), endothelin (Malarkey *et al.* 1995; Wang *et al.* 1992) and thrombin (Papkoff *et al.* 1994). Subsequently, MAP kinase translocates to the nucleus and activates transcription factors c-*myc* and Elk-1 (Seger & Krebs 1995; Treisman 1995; Treisman 1996; Zhang *et al.* 1993b). Elk-1 is a ternary complex factor which, along with other ternary complex factors (i.e. SAP-1, SAP-2), binds to the promoter of genes like c-*fos* that contain serum response elements (Gille *et al.* 1992). ERKs also activate other serine/threonine kinases such as $p90^{rsk}$, PLA_2 and the EGF receptor (Lin *et al.* 1993; Nemenoff *et al.* 1993; Sturgill *et al.* 1988; Takishima *et al.* 1991; Zhao *et al.* 1995). c-*fos* is an immediate early gene, and its activation by signaling cascades such as MAP kinase, has been linked to the stimulation of both SMC proliferation and migration (Law *et al.* 1996; Miano *et al.* 1993; Suggs *et al.* 1999). Interestingly, both c-*fos* and c-*jun* are elevated after vascular injury and Fos and Jun proteins have been localized in the nuclei of SMCs at the luminal border (Miano *et al.* 1993). Moreover, antisense oligonucleotides to c-*fos* and c-*jun* have been shown to inhibit intimal lesion formation after vascular injury (Suggs *et al.* 1999).

2.6.9 New frontiers in cell signaling: Regulation by non-traditional signal molecules

The traditional signaling systems linking cell surface receptors to cell migration and proliferation involve the three pathways discussed above. In general, activation of a receptor leads to PI3-kinase activation which results in p21-Ras activation with subsequent activation of MAP kinase leading to stimulation of cellular events involved in

cell migratory and proliferative processes, including activation of c-*fos*. However, other essential pathways may also participate, but these have not been mapped to the same degree. Examples would include: 1) integrins and ECM, both of which alter cytoskeletal components and regulate c-*fos* (Brizzi *et al.* 1999; Dike & Ingber 1996; Lee *et al.* 2000; Li & Xu 2000); 2) Rho, which is independently required for activation of c-*fos* via SRF (i.e. other ternary complex factors are required to activate c-*fos*) (Montaner *et al.* 1999; Poser *et al.* 2000; Sun *et al.* 1999; Wang *et al.* 1998); and 3) mono(ADP-ribosyl)transferase (i.e. ADP-ribosylation reactions), which has been demonstrated to be an important endogenous component of many cell activities, including differentiation and cell communication (Brune *et al.* 1994; Hilz 1997; Kharadia *et al.* 1992; Zolkiewska *et al.* 1992). All have been shown to be active in SMCs (Li & Xu 2000; Li *et al.* 1999; Thyberg *et al.* 1995b; Yamakawa *et al.* 2000). The latter pathway is of particular interest because of its involvement in SMC differentiation and the regulation of G protein receptors. In SMCs, the relative importance of this signal pathway has already been documented by Thyberg et al. who showed the potential importance of a mART in the differentiation status of rat aortic primary SMCs (Thyberg *et al.* 1995b). And more recently, Li *et al.* (1999) demonstrated that an endogenous mono(ADP-ribosyl)transferase was present in bovine coronary artery SMCs, and that it may mediate intracellular signal transduction and play a role in activating K^+ channels in response to 11,12-epoxyeicosatrienoic acid (11,12-EET) . In other muscle cell types, the importance of this signal molecule has also been documented, although a precise biological function, mode of action and associated signaling has not yet been identified (Kharadia *et al.* 1992; Zolkiewska & Moss 1993).

2.7 ADP-ribosylation

ADP-ribosylation is a post-translational modification of proteins that involves the transfer of an ADP-ribose moiety from NAD^+ to an acceptor amino acid. ADP-ribosylation reactions can be divided into 2 distinct classes: mono(ADP-ribosyl)ation and poly(ADP-ribosyl)ation. Both are considered important for a variety of cellular functions including cell signaling, cell differentiation, cell growth, cell proliferation, cell death and DNA repair. However, mono(ADP-ribosyl)ation controls enzymatic activity directly while poly(ADP-ribosyl)ation modulates the binding of proteins to nucleic acids.

2.7.1 Poly(ADP-ribosyl)ation reactions

Poly(ADP-ribosyl)ation is catalyzed by the enzyme poly(ADP-ribose) polymerase (PARP, EC 2.4.2.30), which transfers ADP-ribose to nuclear acceptor proteins. This reaction is thought to be ubiquitous in eukaryotic cells, with possibly the exception being yeast. Interestingly, a correlation exists between PARP activity in mononuclear leukocytes of mammals and species-specific life span (Burkle *et al.* 1994; Grube & Burkle 1992; Lagueux *et al.* 1994). Poly(ADP-ribosyl)ation is associated with a variety of DNA-related processes including chromatin condensation, replication, recombination, DNA repair, gene expression, cellular differentiation, growth and transformation (D'Amours *et al.* 1999; de Murcia *et al.* 1994; Lagueux *et al.* 1994; Shall 1994) and, more recently, the phenomena of apoptosis (Negri *et al.* 1997; Pieper *et al.* 1999; Rosenthal *et al.* 1997; Scovassi & Poirier 1999). ADP-ribosylation is a mechanism for the alteration of chromatin structure and this property may be the foundation of its effects on several cellular functions (Hayaishi & Ueda 1977; Kleczkowska & Althaus 1996; Purnell *et al.* 1980). A shuttle mechanism that links the synthesis and degradation (i.e. ADP-ribosylation cycle) of poly(ADP-ribose) polymers with changes in PARP activity and DNA binding (de Murcia *et al.* 1983; Ferro & Olivera 1984; Zahradka & Ebisuzaki

1982) also accounts for the contribution of PARP to various nuclear processes (Lindahl *et al.* 1995). Furthermore, the ADP-ribosylation cycle has been described in a variety of cell types including lymphocytes (Schraufstatter *et al.* 1986), endothelial cells (Kirkland 1991; Thies & Autor 1991), fibroblasts (Yamamoto *et al.* 1993a), SMCs (Szabo *et al.* 1997) and hepatocytes (Bowes *et al.* 1998; Stubberfield & Cohen 1988). Degradation of poly(ADP-ribose) polymers is carried out by the enzyme poly(ADP-ribose) glycohydrolase (Lagueux *et al.* 1994). The apparently constitutive activation of this enzyme accounts for the short half-life of poly(ADP-ribose) polymers within the cell nucleus. Poly(ADP-ribose) glycohydrolase has been reviewed in the past (Desnoyers *et al.* 1995; Lagueux *et al.* 1994) and will not be discussed within the body of this work.

2.7.1.1 Poly(ADP-ribose) polymerase (PARP)

PARP is a nuclear enzyme of MW 116,000 that consists of 1014 amino acids. The gene encoding PARP is located on chromosome 1q, the same as that for the proto-oncogene *trk* and for the cytokine TGF-β (Smulson 1994). From biochemical and genetic studies, three functional domains have been identified: i) an N-terminal 46-kDa DNA binding domain that contains two Zn^{2+} finger structures, a nuclear localization signal and the newly described 24-kDa apoptotic domain (which is generated after cleavage of PARP by caspase-3 (Smulson *et al.* 1998)); ii) a 22-kDa automodification domain, and iii) a 54-kDa NAD^+ binding domain at the C-terminus (Alvarez-Gonzalez *et al.* 1994). Within this protein, two functional modules have been identified: the N-terminus, which acts as the sensor for DNA nicks, and the C-terminus which synthesizes the poly(ADP-ribose) polymers. Within each of these domains, there are strongly conserved regions (eg. Zn^{2+} fingers, NAD^+ binding domain, DNA binding domain, β-sheet structures, Rossman fold structure), and homology of this enzyme is greater than 90% among mammals (with 61% similarity and 43% identity to Drosophila) (Alvarez-Gonzalez *et al.* 1994). It is

interesting that PARP is so highly conserved in eukaryotes despite the high energy cost associated with the ADP-ribosylation cycle, which points to an important role for this enzyme in cellular function.

2.7.1.2 Enzymology of PARP

PARP is a multifunctional enzyme having the capacity to catalyze 3 separate reactions: i) initiation (1 reaction per acceptor site), ii) elongation (greater than 200 reactions per site), and iii) branching (5-7 reactions per site) (Alvarez-Gonzalez & Jacobson 1987; Alvarez-Gonzalez *et al.* 1994; Kiehlbauch *et al.* 1993). Polymers of greater than 100 units in length have been detected. Using NAD^- as a substrate, PARP catalyzes a reaction that involves the transfer and subsequent synthesis of ADP-ribose polymers, either linear or branched, on nuclear proteins. Furthermore, PARP is a catalytic dimer with an intermolecular automodification reaction (Bauer *et al.* 1990; Mendoza-Alvarez & Alvarez-Gonzalez 1993). Experiments utilizing purine-base substituted NAD^+ analogs have conclusively demonstrated that the presence of an amino group within the purine base at a specific position is important for efficient catalysis (Oei *et al.* 1996). Furthermore, PARP is dependent on the presence of DNA strand breaks for its full enzymatic activity and PARP is an important component of efficient DNA excision repair (Satoh & Lindahl 1992; Shall 1994).

2.7.1.3 PARP substrates

Over the years, more than 30 nuclear proteins have been proposed as targets for poly(ADP-ribosyl)ation, including histones (H1, H2B) (Boulikas 1988; Boulikas 1990; Huletsky *et al.* 1985), DNA polymerase-α (Simbulan *et al.* 1993; Yoshida & Simbulan 1994), endonucleases (Tanaka *et al.* 1984), topoisomerase I (Ferro & Olivera 1984; Kasid *et al.* 1989), DNA ligase II (Creissen & Shall 1982), HMG proteins (Tanuma & Johnson 1983; Tanuma *et al.* 1985), RNA polymerases (Furneaux & Pearson 1980;

Taniguchi *et al.* 1985), Fos (Amstad *et al.* 1992), p53 (Malanga *et al.* 1998; Pleschke *et al.* 2000; Simbulan-Rosenthal *et al.* 1999) and PARP itself (i.e. automodification) (Adamietz 1987; Kawaichi *et al.* 1981; Kreimeyer *et al.* 1984; Yoshida & Simbulan 1994; Yoshihara *et al.* 1977). However, whether these proteins are true endogenous substrates of PARP should be considered carefully since many of the experimental procedures employed for the identification of these acceptor proteins involved the use of permeabilized cells and nuclear extracts from cells. These procedures in and of themselves would have resulted in cellular, nuclear and DNA damage, and thus PARP activation, with the consequence of having artifactually induced ADP-ribosylation of protein.

2.7.1.4 Function of PARP within cells

PARP is a critical regulatory component of the cellular response to stress, including DNA damage. PARP is expressed constitutively and usually found bound to chromatin and requires the presence of DNA nicks or strand breaks (single or double stranded) for activation (Shall 1994). It participates in DNA repair by associating with strand breaks, and the subsequent elaboration of poly(ADP-ribose) polymers then signals the cell to switch off DNA synthesis temporarily (Satoh & Lindahl 1992). This serves as a mechanism to ensure that lesions are not replicated before DNA repair can be completed and may indicate that PARP is a survival factor that plays an essential and positive role during DNA damage recovery (de Murcia *et al.* 1997). Interestingly, PARP has also been shown to play a role in apoptosis or programmed cell death (PCD) (Scovassi & Poirier 1999). The mechanism behind this action is postulated to involve a decrease in a cell's energy pools (i.e. NAD^+) upon massive activation of PARP (by DNA damage/strand breaks) (Berger 1985; Carson *et al.* 1986; Tanizawa *et al.* 1989; Wintersberger & Wintersberger 1985). Since the degree of PARP activation is dependent

on the amount of DNA damage, this may be the signal that determines whether the cell either repairs the damage or, if the damage is too great, induces PCD. Activation of the apoptotic program involves cleavage of PARP by proteases such as protease resembling ICE (interleukin-β converting enzyme) (prICE) or caspase-3 (Lazebnik *et al.* 1994; Scovassi *et al.* 1998; Smulson *et al.* 1998) and, ultimately, PARP cleavage may represent a critical juncture at which point a cell must decide whether it is able to recover or undergo PCD or necrotic cell death. The role of PARP in apoptosis was confirmed by observations that 3-aminobenzamide (3AB), an inhibitor of PARP, could rescue cells from undergoing PCD (Kuo *et al.* 1996; Malorni *et al.* 1995; Scovassi & Poirier 1999; Yamamoto *et al.* 1993a). Furthermore, PARP has been reported to modify p53, a tumour suppressor protein that is associated with activation of apoptosis (Beneke *et al.* 2000; Kapasi & Singhal 1999; Simbulan-Rosenthal *et al.* 1999).

Increased PARP activity has also been found in proliferating cells (Simbulan-Rosenthal *et al.* 1998; Yoshida & Simbulan 1994) and the transcription of PARP has been detected before the onset of DNA synthesis early in the cell cycle (Lagueux *et al.* 1994). Moreover, activation of PARP may contribute to regulation of gene activity as has been observed with phosphoenolpyruvate carboxykinase (PEPCK) and procollagen gene expression (Ghani *et al.* 1992; Leverence *et al.* 1988; Zahradka & Yau 1994). Furthermore, PARP has been reported to exist associated with the nuclear matrix in rat testis (Quesada *et al.* 1994). Interestingly, activation of PARP in this system involves both automodification and heteromodification reactions at the nuclear matrix level with both histones and nuclear matrix acting as acceptors (Quesada *et al.* 2000). Finally, NF-κB expression may be regulated by PARP (Hassa & Hottiger 1999; Kameoka *et al.* 2000; Oliver *et al.* 1999), having repercussions in the sequelae of both apoptosis and inflammatory processes (Pero *et al.* 1999).

2.7.1.5 PARP in the cardiovascular system

In the cardiovascular system, inhibition of PARP by 3AB has been shown to attenuate cell death associated with oxidant stress in isolated cardiac myoblast preparations and in experimental models of cardiac ischemia (Bowes *et al.* 1999; Thiemermann *et al.* 1997). As a result, inhibition of PARP may be therapeutic for myocardial infarction due to a prevention in the decline of high energy phosphates during ischemia/reperfusion (Bowes *et al.* 1999; Bowes *et al.* 1998). Conversely, activation of PARP may contribute to the pathophysiology of reperfusion injury via the PARP suicide hypothesis (Thiemermann *et al.* 1997). It is suspected that ischemia/reperfusion results in DNA damage and therefore activates PARP which then depletes energy pools (both NAD^+ and ATP) and results in activation of the cell death program (i.e. PARP suicide hypothesis) (Berger 1985; Carson *et al.* 1986; Tanizawa *et al.* 1989; Thiemermann *et al.* 1997; Wintersberger & Wintersberger 1985). In the vasculature, PARP may play a role in the pathogenesis of endothelial dysfunction, having a role in peroxynitrite-induced cytotoxicity (Szabo *et al.* 1997). Development of endothelial dysfunction in this model has been demonstrated to improve with 3AB treatment (Szabo *et al.* 1997).

2.7.1.6 Lessons learned from PARP knockout mice

The preparation of $PARP^{-/-}$ knockout mice (KO-1: (Wang *et al.* 1995), KO-2: (Trucco *et al.* 1998), KO-3: (Masutani *et al.* 1999)) has permitted the detection of additional PARP isoforms within the cell, since $PARP^{-/-}$ is not a developmentally lethal phenotype (Wang *et al.* 1995), and poly(ADP-ribose) polymers are present in $PARP^{-/-}$ mice. Furthermore, cells and cell lines derived from neuronal cells and fibroblast cells of $PARP^{-/-}$ mice are able to undergo DNA repair after exposure to reactive oxygen species (Shieh *et al.* 1998). Nevertheless, cells derived from the KO-1 mouse had a marginally slower rate of proliferation and skin hyperplasia was observed in about 1/3 of older mice

(Wang *et al.* 1995). Interestingly, $PARP^{-/-}$ mice are resistant to drug-induced inflammation (Wang *et al.* 1995) and this may be related to a requirement for PARP in the activation of NF-κB-dependent target genes (Hassa & Hottiger 1999). Recently, both PARP-2 and PARP-3 have been identified and cloned (Ame *et al.* 1999; Johansson 1999), and PARP-2, a 62-kDa protein that is also DNA damage-dependent, may account for the residual poly(ADP-ribose) synthesis observed in PARP-1 deficient cells exposed to DNA damaging agents (Shall & de Murcia 2000). Taken together, it may be concluded that PARP is dispensible during embryogenesis and that its DNA repair function is sufficiently important for genome protection to warrant a redundant enzyme activity. Alternatively, PARP-2 may play a more significant role in DNA repair, since, interestingly, the generation of knockout mice has indicated that PARP (or PARP-1 as it should now be referred to or identified) may play a critical role in cell death and in various inflammatory processes (Shall & de Murcia 2000). The presence of a PARP gene family may suggest that specific PARP enzymes have specific cellular functions and provide the cell with an additional regulatory mechanism for distinct cell processes.

2.7.2 Mono(ADP-ribosyl)ation reactions

Mono(ADP-ribosyl)ation reactions are catalyzed by a family of mono(ADP-ribosyl)transferases (mART) found in viruses, bacteria and eucaryotic cells (Moss *et al.* 1997; Okazaki & Moss 1996a; Zolkiewska *et al.* 1994). This is a reversible post-translational modification of proteins in eucaryotic and prokaryotic cells that involves the transfer of an ADP-ribose moiety from NAD^+ to an acceptor amino acid (Figure 1). The reaction catalyzed by mART's is distinct from that catalyzed by PARP in several ways. Most notably, the chain length of ADP-ribose units is shorter (one compared to 100-200), but the chemical nature of the glycosidic linkage, the character of the enzymes involved and the site of reaction are also distinct (Soman & Graves 1988; Zolkiewska *et al.* 1994).

FIGURE 1*: Arginine-dependent Mono(ADP-ribosyl)ation*

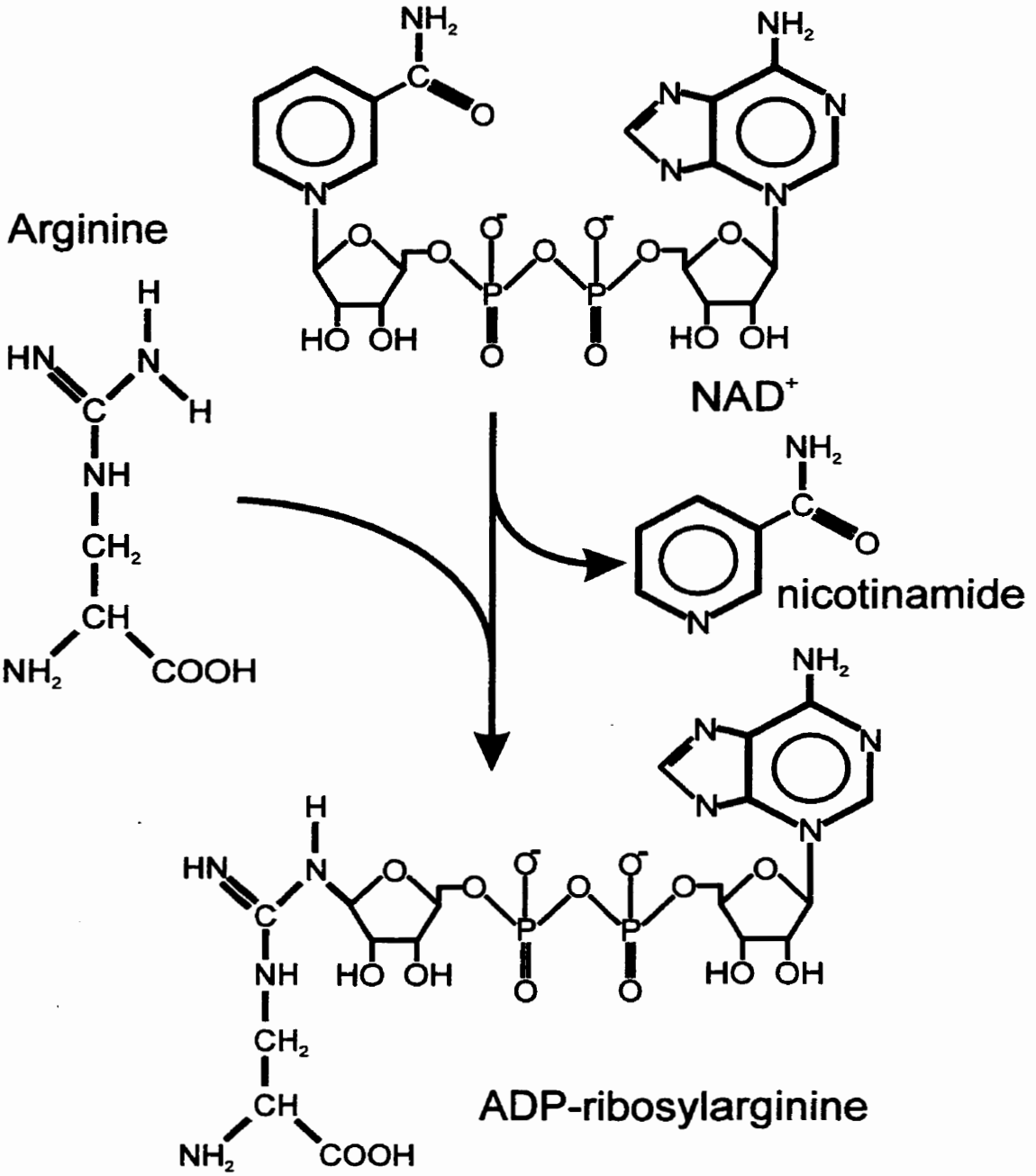
Arginine
NAD+
nicotinamide
ADP-ribosylarginine

The role of mono(ADP-ribosyl)ation in cell function is related to cellular metabolism and has been associated with cellular differentiation (Kharadia *et al.* 1992), cellular proliferation (Thyberg *et al.* 1995b), cell migration (Norgauer *et al.* 1988; Saxty *et al.* 1998a; Saxty *et al.* 1998b; Stasia *et al.* 1991) and both intra- and extra-cellular communication, (Brune *et al.* 1994; Hilz 1997; Zolkiewska & Moss 1993; Zolkiewska *et al.* 1992).

Catabolism of mono(ADP-ribose) is catalyzed by ADP-ribosyl(amino acid)transferase hydrolases (EC 3.2.2.19). The end result is the regeneration of free, unmodified amino acid (arginine, cysteine, diphthamide or asparagine). Hydrolases have been identified in bacterial, avian and mammalian systems, appearing to be ubiquitous in eukaryotic tissues, and thus supporting the premise that ADP-ribosylation reactions are important mediators of cellular regulation. The best characterized of the hydrolases is the ADP-ribosylarginine hydrolase in eucaryotic cells (Moss *et al.* 1997; Takada *et al.* 1994; Williamson & Moss 1990). This hydrolase activity was detected in the soluble fraction of turkey erythrocytes (Moss *et al.* 1988), cultured mouse cells (Smith *et al.* 1985), rat skeletal muscle (Chang *et al.* 1986) and rat brain (Moss *et al.* 1992). Thus a eucaryotic ADP-ribosylation cycle is hypothesized based on the reversible modification of proteins by transferases and hydrolases (Moss *et al.* 1997; Williamson & Moss 1990), much like the reversible phosphorylation modification of proteins by kinases and phosphatases (Graves & Krebs 1999). Additionally, ADP-ribose can be processed by phosphodiesterases and phosphatases as seen with the GPI-anchored skeletal muscle mART, generating a phosphoribosyl-integrin and 5'AMP, although the physiological consequences of this structure have yet to be examined (Okazaki & Moss 1999; Zolkiewska & Moss 1997).

2.7.2.1 Mono(ADP-ribosyl)transferase (mART)

The discovery of eucaryotic protein ADP-ribosylation (Gill & Meren 1978; Honjo *et al.* 1968; Moss & Vaughan 1977) resulted in the identification of mARTs. Bacterial toxins such as cholera toxin, pertussis toxin, diphtheria toxin and botulinum C3 endotoxin ADP-ribosylate a variety of eucaryotic and prokaryotic acceptor proteins, and modulate their associated cellular functions (Aktories 1994; Aktories 1997; Gierschik 1992; Lerm *et al.* 2000; Moss 1987; Okazaki & Moss 1996b; Popoff 1998). A variety of animal tissue and organs are also now known to contain mART and mART activity (Soman & Graves 1988). Vertebrate mART activity was first detected in turkey erythrocytes (Moss & Stanley 1981b; Moss *et al.* 1980), rat liver homogenates (Moss & Stanley 1981a) and Xenopus tissues (Godeau *et al.* 1984; Okazaki & Moss 1999; Tsuchiya & Shimoyama 1994). Presently, 6 avian mARTs (4 turkey erythrocyte ARTs: A, B, C and A', and chicken ARTs from hen liver and heterophil granules) and more than 13 mammalian mARTs (eg. ART 1-5, ART I-IV from rat brain, and 4 mARTs from rat adrenal medulla) have now been purified and/or cloned and characterized (Fujita *et al.* 1995; Matsuyama & Tsuyama 1991; Okazaki & Moss 1999). This subject has been reviewed recently by Okazaki & Moss (1999), and I refer you to this article for more details.

Of the mammalian mARTs, expression was initially identified in cardiac and skeletal muscle, leukocytes/lymphocytes, brain and testis (Duman *et al.* 1991; Hara *et al.* 1987; Kharadia *et al.* 1992; Obara *et al.* 1989; Obara *et al.* 1991; Peterson *et al.* 1990; Piron & McMahon 1990; Soman & Graves 1988; Soman *et al.* 1991; Soman *et al.* 1984a; Soman *et al.* 1983; Yamashita *et al.* 1991). Subsequently, mART expression was demonstrated in hepatoma cells (Ledford & Leno 1994; Leno & Ledford 1989), SMCs

(Li *et al.* 1999) and endothelial cells where these enzymes participated in signal transduction and prostacyclin production (Halldorsson *et al.* 1992).

Vertebrate mARTs (eg. NAD:arginine(ADP-ribosyl)transferases (EC 2.4.2.31)) are a family of enzymes ranging in molecular weight from approximately 25- to 36-kDa and 66- and 69-kDa (4 distinct ART's from rat brain – I to IV and rat adrenal medulla) (Okazaki & Moss 1999). Despite a lack of overall similarity in the amino acid sequences (i.e. lack of conservation among sequences), there appear to be 3 regions (regions I, II, III) of sequence homology that make up the catalytic site. A precise configuration of these regions is required for the ADP-ribose transfer reaction (Domenighini & Rappuoli 1996; Okazaki & Moss 1999; Takada *et al.* 1995). Conserved regions house an NAD-binding cleft composed of an α-helix bent over a β-strand, along with an arginine or histidine residue and an active-site glutamate which are critical for enzymatic activity (Domenighini & Rappuoli 1996; Okazaki & Moss 1999). Furthermore, 2 separate groups of enzymes can be defined by the presence of either arginine (cholera and pertussis toxin-like) or histidine (diphtheria toxin-like) in region I. Region II contains a specific amino acid motif (aromatic-hydrophobic-Ser-X-Ser-hydrophobic) and region III contains the active-site glutamate. For more details, please refer to the review by Okazaki & Moss (1999). Interestingly, several of the mammalian mARTs have regions of homology to glycosylphosphatidylinositol (GPI)-anchored proteins, and thus may be membrane bound with an extracellular orientation (Ferguson & Williams 1988; Low 1989; Zolkiewska *et al.* 1994). Secretory and intracellular counterparts also exist and there may therefore be 3 discreet families of transferases (Okazaki & Moss 1998).

2.7.2.2 Enzymology of mART

A common mechanism of substrate binding and catalysis apparently exists between and among both bacterial and eucaryotic mARTs. Mammalian and bacterial

mARTs are believed to act via an SN2-like mechanism in which nucleophilic attack on NAD^+ is followed by displacement of the nicotinamide and inversion of configuration (Takada *et al.* 1995). In this enzymatic reaction, a single ADP-ribose moiety is transferred to the acceptor substrate. Amino acid-specific acceptors for mARTs include arginine, cysteine, diphthamide, histidine and asparagine of which arginine-mARTs are the best characterized thus far (Zolkiewska *et al.* 1994). Mechanisms for regulating mARTs have not been described since little research has been done in this area, however, Weng *et al.* (1999) did recently report on the auto(ADP-ribosyl)ation of ART5 as a mechanism for regulation of mART activity.

2.7.2.3 mART substrates

Vertebrate mARTs are typically species- and tissue-specific with respect to acceptor proteins (Taniguchi *et al.* 1993). Although a large variety of proteins are ADP-ribosylated, the majority of mARTs are arginine-specific (and can also modify other simple guanidino derivatives) and a variety of potential substrates have been described (Huang *et al.* 1993; Okazaki & Moss 1999; Wang *et al.* 1996; Zolkiewska & Moss 1993). Acceptors of ADP-ribose in these mammalian (*in vitro*) systems include casein, ovalbumin and simple guanidino compounds such as arginine and agmatine (Zolkiewska *et al.* 1994). Additional target proteins include Ha-ras-p21, transducin, protein kinases (with subsequent reduction in activity), and skeletal Ca^{2+}-ATPase (with subsequent decrease in activity) (Okazaki & Moss 1996a; Tsuchiya & Shimoyama 1994). Finally, endogenous arginine-dependent ADP-ribosylation of G proteins (i.e. G_s, G_i and G_o) is well documented in mammalian cells and tissues (Donnelly *et al.* 1992; Duman *et al.* 1991; Jacquemin *et al.* 1986; Molina y Vedia *et al.* 1989; Obara *et al.* 1991).

Endogenous vertebrate ADP-ribosylation of cysteine residues is less common, but has been observed in human and bovine erythrocytes via the actions of a cysteine-specific

mART purified from erythrocyte and platelet membranes. This cys-mART is also reported to modify $G_i\alpha$ (Okazaki & Moss 1999; Saxty & van Heyningen 1995; Tanuma *et al.* 1988). Interestingly, ADP-ribosyl-cysteine linkages can occur as the result of a nonenzymatic reaction involving ADP-ribose and NAD^+ glycohydrolases. In this case, an ADP-ribosyl-thiazolidine linkage is generated in place of the thioglycoside ADP-ribosyl-cysteine linkage, the type normally observed with pertussis toxin catalyzed reactions (McDonald *et al.* 1992; Okazaki & Moss 1999).

2.7.2.4 Function of mART within cells

Bacterial mARTs have a variety of biological consequences and functions within eucaryotic cells and organisms. For example, cholera toxin ADP-ribosylates an arginine residue of $G_s\alpha$, the stimulatory α-subunit of the heterotrimeric GTP-binding (G) proteins, and irreversibly inhibits its GTPase activity. The result is activation of adenylyl cyclase and a subsequent increase in cellular cAMP levels (Cassel & Pfeuffer 1978; Gill & Meren 1978; Moss & Vaughan 1977). On the other hand, pertussis toxin ADP-ribosylates a cysteine residue in the α-subunit of G_i and G_o which blocks the inhibitory effect of the α_i-subunit on adenylyl cyclase and results in activation of the cAMP cascade and/or uncoupling of the G protein from its receptor (Takada *et al.* 1994; Ui & Katada 1990). Nevertheless, both modifications result in abnormalities in cellular electrolyte flux and fluid secretion in the small intestines (Field 1976; Moss & Vaughan 1988; Sharp 1973). Diphtheria toxin (and *Pseudomonas aeruginosa* exotoxin A) ADP-ribosylates a diphthamide (i.e. a modified histidine) residue in elongation factor-2 (EF-2) resulting in the inactivation of EF-2. This disrupts the regulatory mechanism for translocation of elongating proteins across the endoplasmic reticulum membrane and results in inhibition of protein synthesis (Collier 1967; Collier 1975; Iglewski 1994; Wick *et al.* 1990). Interestingly, a fusion protein of IL-2 and diphtheria toxin has been successfully applied

for the treatment of neoplastic diseases. This fusion protein targets cells with IL-2 receptors and the resultant ADP-ribosylation of EF-2 inhibits cell proliferation (vanderSpek *et al.* 1994). Finally, exotoxin C2 and C3 both modify components of the cytoskeletal network. Botulinum C2 exotoxin ADP-ribosylation of an arginine causes inhibition of (non-muscle) actin polymerization and subsequent degradation of the microfilament/cytoskeletal network in cells (Aktories 1994). Botulinum C3 exotoxin ADP-ribosylation of an asparagine residue on the small GTP-binding protein Rho results in the inactivation and attenuation of Rho-associated signaling pathways (Kumagai *et al.* 1993). The resultant decrease in tyrosine phosphorylation and subsequent phosphatidylinositol 3-kinase (PI3-kinase) activation has the potential for modulating cell proliferation and differentiation as a result of altered GTP-binding protein interactions with the cytoskeletal system and a disturbance in the organization of the actin cytoskeleton (Aktories 1994; Kishi *et al.* 1993; Maehama *et al.* 1994; Nishiki *et al.* 1990; Paterson *et al.* 1990; Ridley & Hall 1992; Ridley *et al.* 1992).

As mentioned previously, eucaryotic mARTs are involved in a variety of cell functions, including cell differentiation, proliferation, migration and cellular communication (Brune *et al.* 1994; Hilz 1997; Kharadia *et al.* 1992; Norgauer *et al.* 1988; Saxty *et al.* 1998a; Saxty *et al.* 1998b; Stasia *et al.* 1991; Thyberg *et al.* 1995b; Zolkiewska & Moss 1993; Zolkiewska *et al.* 1992). Specific modification of certain cytoskeletal/intermediate filament proteins would result in the alteration of the above-mentioned cell functions. For example, desmin is ADP-ribosylated by an endogenous arg-mART in skeletal muscle (Graves *et al.* 1997; Huang *et al.* 1996; Yuan *et al.* 1999). This modification results in desmin disassembly (Yuan *et al.* 1999), with consequences related to cell differentiation, migration, proliferation and intracellular communication (Huang *et al.* 1993). ADP-ribosylation of desmin is an important regulatory mechanism

in differentiating muscle cells, with mART activity increasing dramatically after myoblast fusion (Kharadia *et al.* 1992). In addition, desmin from SMCs has been shown to react with an antibody specific for ADP-ribosylated-arginine (Graves & Krebs 1999). A second example would be the modification of actin filaments. ADP-ribosylation of actin in human neutrophils is associated with inhibition of neutrophil chemotaxis (Stasia *et al.* 1991). Additionally, non-muscle β/γ-actin, skeletal muscle α-actin and smooth muscle γ-actin are ADP-ribosylated *in vitro* with resultant inhibition of actin polymerization (Terashima *et al.* 1992). Furthermore, endogenous ADP-ribosylation of heterophil non-muscle actin was proposed as a mechanism for regulating heterophil phagocytosis, secretion and chemotaxis (functions dependent on actin de/polymerization) (Terashima *et al.* 1992). The final example is the ADP-ribosylation of integrin α7, the receptor for the extracellular protein laminin, on skeletal muscle cells by mART. This modification may modulate cell-cell or cell-matrix interactions, with effects on cellular differentiation and/or proliferation (Zolkiewska & Moss 1993; Zolkiewska & Moss 1997; Zolkiewska *et al.* 1998).

Other eucaryotic cell functions that may be altered by mART include neuronal transmission (in the brain, ADP-ribosylation of G proteins may modify neuronal signal transmission) (Duman *et al.* 1991; Matsuyama & Tsuyama 1991), and regulation of T-cell proliferation and cytolytic activity (ADP-ribosylation of a $p56^{lck}$-associated protein) (Wang *et al.* 1996). More recently, Lupi *et al.* (2000) have reported the modification of the β-subunit of $G_{\beta\gamma}$ by arg-mART as a novel mechanism of regulating G protein-mediated signal transduction. This modification prevented the inhibition of calmodulin-stimulated type I adenylyl cyclase. Finally, modification of MARCKS and tubulin by mART has been demonstrated to lead to changes in cytoskeletal and microtubular assembly/organization (Aktories & Wegner 1992; Chao *et al.* 1994; Scaife *et al.* 1992),

as well as alterations in the ability of MARCKS to bind calmodulin and interact with the plasma membrane (Chao *et al.* 1994).

From a more clinical point of view, in experimental diabetic neuropathy, mART activity has been associated with a reduction of substance P axonal transport and subsequent onset of diabetic peripheral neuropathy (Donadoni *et al.* 1995). It was observed that exogenous ADP-ribosylation reactions were reduced in extracts from diabetic retinas, suggesting increased cytosolic endogenous ADP-ribosylation activity. Treatment with an inhibitor of ADP-ribosylation (silybin) increased the extent of exogenous ADP-ribosylation (Donadoni *et al.* 1995).

2.7.2.5 Mono(ADP-ribosyl)ation in the cardiovascular system

In the cardiovascular system, arg-mART has been found in relatively high levels in neonatal and adult rat hearts (Piron & McMahon 1990). In cardiac muscle, ADP-ribosylation reactions have been associated with developmental regulation (Piron & McMahon 1990). Furthermore, Jones and Baird (Jones & Baird 1997) have shown that bFGF, a growth factor intimately associated with the cardiovascular system, angiogenesis and the musculoskeletal system, is ADP-ribosylated on the surface of adult bovine arch endothelial cells (and in human hepatoma cells). This modification may represent an additional regulatory mechanism, in conjunction with phosphorylation, for this potent mitogen. In the past, bFGF has been found to be both phosphorylated and ADP-ribosylated *in vitro* (Boulle *et al.* 1995; Feige & Baird 1989; Vilgrain & Baird 1991; Vilgrain *et al.* 1993).

Nitric oxide (NO) is a second messenger produced by NO synthase (NOS) in response to a variety of signals that is able to stimulate endogenous ADP-ribosylation *in vitro*. Moreover, NO, acting as a free radical molecule, can activate ADP-ribosylation of several proteins *in vivo* (Brune & Lapetina 1989; Schuman *et al.* 1994; Zhang & Snyder

1992) and result in cellular damage (Parrado *et al.* 1999). In the vasculature, NO-dependent ADP-ribosylation of G proteins by an endogenous ART in smooth muscle increases the activity of adenylyl cyclase and results in vasodilatation via a decrease in the activation of phospholipase C (Kanagy *et al.* 1995). As a result, it is postulated that hypertension-associated decreases in eNOS expression and activity would decrease the amount of NO produced, thereby leading to decreased ADP-ribosylation of G proteins and, consequently, increased vessel constriction since activation of G proteins by agonists is unopposed (Kanagy *et al.* 1995). Moreover, ADP-ribosylation was discovered in SMCs derived from bovine coronary artery (Li *et al.* 1999). Here, this modification was found to modulate $G_s\alpha$ and thereby play a role in activating K^+ channels as induced by 11,12-EET. Taken together, these studies suggest that ADP-ribosylation may constitute a novel participant in the cardiovascular system and vasculature, playing a role in regulation of cellular processes such as development, differentiation, proliferation and SMC contractility (i.e. vasoactivity).

2.8 Inhibitors of mART and PARP

Over the years, numerous inhibitors of mART and PARP have been discovered and used successfully (and primarily) to study the biological function of these enzymes. A number of compounds have been shown to inhibit mART, however, specificity is typically lacking because of the similarity of the mART and PARP catalyzed reactions (reviewed in Banasik *et al.* (1992), Banasik & Ueda (1994) and Rankin *et al.* (1989). This ambiguity has impacted on our understanding of ADP-ribosylation, since data interpretation can be biased if it is based on an inhibitor that is not selective for either mART or PARP. For example, many of the cellular functions of PARP were identified by extensive use of 3-aminobenzamide (3AB) (Sims *et al.* 1982). However, the fact that this

compound also inhibits mART suggests a re-examination of the conclusions should be made (Banasik *et al.* 1992; Milam & Cleaver 1984; Rankin *et al.* 1989; Zahradka & Yau 1994). Other examples of PARP inhibitors include benzamide and nicotinamide. A more complete listing of inhibitors is provided in articles that have reviewed this topic in detail (Banasik *et al.* 1992; Banasik & Ueda 1994; Rankin *et al.* 1989). Examples of arg-mART inhibitors include benzamide, napthalimide, novobiocin, and vitamin K. Although more PARP and mART inhibitors have since been identified, few are selective for arginine-dependent mART. The best examples are silymarin/silybin and *meta*-iodobenzylguanidine (MIBG) (Donadoni *et al.* 1995; Loesberg *et al.* 1990b; Smets *et al.* 1990b), and I will be concentrating on the latter compound, MIBG, since it is the focus of this thesis.

2.8.1 MIBG

MIBG was synthesized as a norepinephrine analogue, and is structurally similar to guanidines such as the antihypertensive drug guanethidine (Montaldo *et al.* 1996; Short & Darby 1967). Its discovery was brought on by the search for agents that could be used for the visualization of the adrenal medulla and possibly other related neoplasms (Wafelman *et al.* 1994b). MIBG is a ring-substituted alkylguanethidine and this family of agents and its potency was first reported by Short & Darby (1967) as a series of aralkylguanidines with high sympathetic nerve blocking capacity (Wafelman *et al.* 1994b). The evaluation of radioiodinated forms of the aralkylguanidines as adrenal medulla visualizing agents then followed and, in 1980, Wieland *et al.* (1980) investigated and reported on the effects of radiolabelled *o*, *m* and *p* position iodine-substituted-benzylguanidine. The investigators found that the *m* form was more resistant to *in vivo* deiodination and, for this reason, radiolabelled MIBG was selected for further investigations which led to its widespread use today (Wieland *et al.* 1980). Presently,

MIBG in its radiolabelled form (^{123}I- or ^{131}I-labelled) is used for both diagnostic and therapeutic purposes. Due to its selective uptake, radiolabelled MIBG enables the detection and localization of neuroendocrine tumours and adrenergic tumours (i.e. adrenal medullary hyperplasia). Typically, the radiolabelled MIBG is used for diagnostic scintigraphy of neural crest-derived tumours (Hoefnagel 1994; Hoefnagel *et al.* 1991; Smets *et al.* 1988b) and also for the scintigraphic assessment of cardiac sympathetic neuronal integrity (i.e. detection of cardiac sympathetic dysinnervation) in a variety of disease states that include ischemia and diabetes (Nakata *et al.* 1996; Schnell *et al.* 1996; Valdes Olmos *et al.* 1993). Although targeted radiotherapy of neuronal (neuroendocrine) tumours by radiolabelled MIBG is practical and beneficial, non-radioactive forms of MIBG have been tested for the treatment of carcinoid tumours and their metastases (Cornelissen *et al.* 1995a; Kuin *et al.* 1999; Smets *et al.* 1988b; Taal *et al.* 1999; Taal *et al.* 1996; Zuetenhorst *et al.* 1999). Furthermore, MIBG can be used for the detection, diagnosis and therapy of smooth muscle tumours of the small bowel (Akle *et al.* 1997). Finally, MIBG is a known inhibitor of arg-mART reactions (Loesberg *et al.* 1990b; Smets *et al.* 1990b) and has been used as a tool for the study of ADP-ribosylation reactions and their biological functions (Richter 1990). Its utility in this capacity is based on its structure, which contains a guanidino group that mimics the acceptor portion of an arginine moiety, and permits it to act as a pseudosubstrate (high affinity substrate) for arg-mART and thereby inhibit its activity.

2.8.1.1 Biodistribution and pharmacokinetics of MIBG

After intravenous administration, radiolabelled MIBG is distributed from the vascular compartment within 1 hour and then is slowly redistributed from the perpiheral compartment to the central compartment (Wafelman *et al.* 1994a). Interestingly, the initial uptake of MIBG involves both neuronal and nonneuronal organs, and early

clearance (less than 4 hours) occurs from the nonneuronal sites (Wafelman *et al.* 1994a). Within 24 hours, MIBG is observed mainly in the liver and to a lesser extent in the lungs, heart, spleen salivary glands and urinary bladder (Wafelman *et al.* 1994a). Uptake in the normal adrenal glands is very low, but hyperplastic adrenals, and tumours such as pheochromocytoma and neuroblastoma, along with other tumours that have neurosecretory granules, have increased rates of uptake (Wafelman *et al.* 1994a). Significant clearance of radiolabelled MIBG from the liver and spleen occurs within 72 hours (Wafelman *et al.* 1994a). The biodistribution of MIBG can be altered by interaction with other drugs, especially agents that act in, and interfere with, the sympathetic nervous sytem (eg. labetalol, reserpine and cocaine) (Wafelman *et al.* 1994a).

2.8.1.2 Cellular uptake and retention of MIBG

MIBG shares the same mechanism of transport and storage as norepinephrine (NE) (Jaques *et al.* 1984; Tobes *et al.* 1985; Wieland *et al.* 1980). In general, there are two mechanisms of uptake by which MIBG enters the cell (eg. adrenomedullary cells). The first route is an active uptake system at the cell membrane specific to catecholamines (Uptake-1) and the second is a non-specific uptake system, which is presumed to be passive diffusion (Jaques *et al.* 1984; Tobes *et al.* 1985). MIBG has specific affinity for uptake-1 mechanism of catecholamines and serotonin transporter (Jaques *et al.* 1987; Rutgers *et al.* 1993; Smets *et al.* 1991). The NE transporter/Uptake-1 is a neuron-specific, ATPase-dependent catecholamine-Na^+ symport that is driven by a Na^+ gradient generated by Na^+/K^+-ATPase (Gasnier *et al.* 1986; Jaques *et al.* 1984; Tobes *et al.* 1985). Uptake-1 is also temperature-dependent, high-affinity, low-capacity, saturable, oubain- (inhibitor of Na^+/K^+-ATPase) sensitive, imipramine- or cocaine-sensitive and energy-dependent (i.e. decreased uptake when glucose is low in the medium) (Jaques *et al.* 1984; Tobes *et al.* 1985). At relatively high concentrations of MIBG (i.e. 10^{-6} M), non-specific uptake (i.e.

passive diffusion) dominates over active uptake as the transporter becomes saturated (Jaques *et al.* 1987; Lashford *et al.* 1991). The non-specific uptake system is also temperature-dependent, but is not energy-dependent, oubain-sensitive or saturable (Jaques *et al.* 1984; Tobes *et al.* 1985). Although passive diffusion is assumed to characterize this non-specific uptake system, some *in vivo* studies have now indicated that nonspecific membrane binding of MIBG provides the explanation for non-specific uptake as opposed to simply passive diffusion through the plasma cell membrane (Glowniak *et al.* 1993). Although MIBG is highly protonated (pK of about 13 *in vivo* (Wieland *et al.* 1984)), it lacks polar hydroxyl groups that decrease the lipophilicity of the phenyl ring. Thus, MIBG may be able to associate with the cell membrane. It has also been suggested that this high positive charge results in accumulation of MIBG in cells and mitochondria via an electro-chemical gradient (Smets *et al.* 1990b). In cells that have active uptake (eg. neuroblastoma), the typical time frame for maximal intracellular MIBG concentration is 1-2 hours incubation (Iavarone *et al.* 1993; Smets *et al.* 1989). In cells that do not contain active uptake mechanisms (eg. L1210, a murine lymphoblastic leukemia cell line), saturation of the cell with MIBG will take about 3 hours (Smets *et al.* 1990b).

Within cells, MIBG is stored in intracellular storage vesicles (Montaldo *et al.* 1991) and as freely diffusable cytoplasmic molecules, and is not associated with macromolecular complexes (Smets *et al.* 1990a). However, the process of MIBG retention is also considered to involve dynamic uptake, release and re-uptake processes. Mechanisms of release are three-fold: exocytosis, carrier-mediated efflux and passive diffusion, and the contribution of each will vary depending on environmental conditions (Servidei *et al.* 1995). This uptake/release mechanism allows for the rapid homogeneous distribution of MIBG within a cell or tissue (Smets *et al.* 1989). For example, in

neuroblastoma cells, MIBG is stored mainly in the cytoplasm and only to a small extent in the chromophilic granules. Coupled with the dynamic process of MIBG retention mentioned above, this mechanism of storage facilitates the homogeneous distribution of MIBG within a tumour (Servidei *et al.* 1995; Weber *et al.* 1996) and allows for efficient visualization and treatment. Interestingly, if MIBG is ADP-ribosylated by arg-mART, the modified molecule, which will contain an ADP-ribose moiety, will likely not move out of the cell by the aforementioned mechanisms, and should increase the cellular retention of MIBG. The modified MIBG should stay within the cell until the reverse enzyme reaction (i.e. via arg-mART hydrolase) occurs. However, since the modification with ADP-ribose is typically reversible, this possibility should not influence the cellular retention and re/uptake of MIBG.

2.8.1.3 Metabolism of MIBG

Within the body, MIBG is not metabolized by monoamine oxidase (MAO) nor by catchol-o-methyltransferase, but is rapidly excreted in urine (Iversen *et al.* 1971; Mangner *et al.* 1986; Schnell *et al.* 1996; Sisson *et al.* 1987; Tobes *et al.* 1985). MIBG is primarily excreted by the kidneys and, within 24 hours, 60% of the dose is eliminated (Kuin *et al.* 1998). As a result, MIBG has been documented to cause stress-related symptoms associated with the release of bioamines, thereby affecting renal perfusion (Kuin *et al.* 1994).

2.8.1.4 Excretion/Elimination of MIBG

The rate of MIBG excretion is similar for either a diagnostic or a therapeutic dose (Mangner *et al.* 1986). MIBG is eliminated from the body via the renal pathway, mostly in the unaltered form, and glomerular filtration rate has a major influence on MIBG kinetics (Blake *et al.* 1989). Within 24 hours, 40-50% is eliminated, and by 72-96 hours, 70-90% is excreted, primarily as unchanged drug (Mangner *et al.* 1986). The importance

of renal excretion is confirmed by fecal recovery of the drug that is usually less than 2% within 0-24 hours and less than 2% at 0-4 days (Kline *et al.* 1981; Mangner *et al.* 1986; Shulkin *et al.* 1986). The primary metabolites of MIBG are *meta*-iodohippuric acid (MIHA) (2-16%), iodine (2-6%) (typically in the radiolabelled form and thus likely to affect the thyroid gland), *meta*-iodobenzoic acid (less than 0.5%) and *para*-hydroxy-*meta*-iodobenzylguanidine (less than 0.5%) (Mangner *et al.* 1986). Since most of the metabolic studies with MIBG have used the radiolabelled forms, metabolism has been easy to follow. As well, sensitive HPLC techniques have been developed for detection in plasma and urine (Mangner *et al.* 1986).

2.8.1.5 Toxicity of MIBG

MIBG has been shown to have cytotoxic effects in the unlabelled form (Slosman *et al.* 1988; Smets *et al.* 1988b; Wieland *et al.* 1981). Within the cell, cytotoxicity may be related to its ability to inhibit mitochondrial activity (Loesberg *et al.* 1990b; Smets *et al.* 1990b). MIBG is selectively accumulated by cells, and it is predominantly the mitochondria that actively accumulate MIBG (Gaze *et al.* 1991). The uptake of MIBG into mitochondria is passive, since mitochondria do not possess uptake I (Cornelissen *et al.* 1995a). Specifically, MIBG can inhibit both complex I and complex III of the mitochondrial respiratory chain (Cornelissen *et al.* 1995b; Loesberg *et al.* 1990a; Loesberg *et al.* 1991; Slosman *et al.* 1993). Increased glycolytic flux is observed 2.5 hours after exposure to 31 μM MIBG and this has been interpreted as a compensatory mechanism to the inhibition of mitochondrial respiration. This increased glycolytic flux is accompanied by an increase in lactate production and leads to intracellular acidification (Loesberg *et al.* 1990a). An interesting benefit to this cytotoxic effect is that MIBG can potentiate the anti-neoplastic actions of certain cancer drugs that require a lower intracellular pH for maximal function (Kuin *et al.* 1999; Kuin *et al.* 1994). The possibility

also exists that the cytotoxic effects of MIBG may be related to the inhibition of arg-mART, since 3 classes of ADP-ribose acceptors have been identified in mitochondria (Althaus & Richter 1987). However, the contribution of mARTs to mitochondrial function has not yet been documented or studied in detail (Kuin *et al.* 1998).

At the tissue level, the MIBG toxicity primarily involves the renal system (Kuin *et al.* 1998). MIBG at a dose of 40 mg/kg results in decreased renal blood perfusion and the induction of reversible kidney damage (i.e. decrease in EDTA clearance and histological damage in the distal tubules). Although the onset of renal toxicity would be assumed to be associated with inhibition of mitochondrial respiration, interestingly, benzylguanidine (de-iodinated form of MIBG) does not affect renal clearance even though benzylguanidine also decreases mitochondrial respiration. As a result, it is likely that decreased mitochondrial respiration is not the main mechanism of MIBG-induced renal damage (Kuin *et al.* 1998). Recent work has shed some light on this matter. MIBG inhibits all three forms of human NOS (Kuin *et al.* 1998) and it is suspected that MIBG at 100 μM causes the inhibition of NOS (nitric oxide synthase). It is this inhibitory act that may thus contribute to the decrease in renal clearance that is observed (Kuin *et al.* 1998).

2.8.1.6 Clinical application of MIBG

Because of its high affinity for the norepinephrine (NE) transporter, MIBG is used mostly as an adrenal imaging agent via scintigraphic visualization of tumours and metastases (Montaldo *et al.* 1996). Clinically, MIBG labelled with radioactive iodine (^{123}I or ^{131}I) is used for scintigraphy of neuroendocrine tumours such as pheochromocytoma, neuroblastoma, medullary thyroidoma and tumours of the APUD (amine precursor uptake and decarboxylation) series (Smets *et al.* 1990a). Since MIBG is taken up by neuroendocrine tumours, radioiodinated MIBG has been used for treatment of these very same tumours (Smets *et al.* 1990a). After uptake of radiolabelled MIBG into the tumour,

the cancerous cells are slowly ablated by the effects of β/γ-radiation release. Unfortunately, one of the consequences of radiolabelled MIBG treatment for cancer is thrombocytopenia resulting from the uptake of MIBG via the serotonin transporter into platelets and megakaryocytes with subsequent death of the platelets by radiation (Lode *et al.* 1995; Tytgat *et al.* 1995).

Unlabelled MIBG is also cytostatic, and even cytotoxic in various cell lines (Smets *et al.* 1988b). For example, MIBG has been shown to almost completely inhibit the proliferation of a neuroblastoma cell line (SK-N-BE(2c)), and also decreases the ATP/ADP ratio in this cell line (Cornelissen *et al.* 1995a). As a result, MIBG has now been tested in its unlabelled form for the palliation of cardinoid syndromes and has shown some success (Taal *et al.* 1999; Taal *et al.* 1996; Zuetenhorst *et al.* 1999). In its unlabelled form, 60 mg/kg is the tolerated dose by oral administration with a bioavailability of 59%. The only evident toxicity is a decrease in renal function that correlates with histologically detectable changes in the distal tubule (occurs at 40 mg/kg) (Kuin *et al.* 1998). At these levels, however, the damage is entirely reversible (Kuin *et al.* 1999). Moreover, there appear to be no histological abnormalities in the kidney, intestines, liver, heart, lungs, thymus, salivary glands and testes. As a result, repeated oral administration of MIBG is a promising alternative for the long-term palliation of the carcinoid syndrome without the need for hospitalization (Kuin *et al.* 1999) and without the requirement for radiation therapy.

It is interesting to note that MIBG uptake increases on differentiation of human neuroblastoma cells and the intracellular half-life is correspondingly increased (Montaldo *et al.* 1996). This is mainly due to greater uptake capabilities of the differentiated cells and does not reflect an increase in the storage capacity (Montaldo *et al.* 1996). A correlation also exists between cell maturity and the ability of MIBG to accumulate

within those cells (Montaldo *et al.* 1996). Within certain neuroblastoma cell populations, MIBG resistance is observed. This is likely due an inability to take up the MIBG and corresponds to the presence of a very immature cell subpopulation (Montaldo *et al.* 1996).

2.8.1.7 Clinical application of MIBG in the cardiovascular system

In the cardiovascular system, MIBG scintigraphy has been used for the assessment of cardiac dysinnervation (i.e. cardiac sympathetic dysfunction) (Schnell *et al.* 1996). In this application, the affinity of MIBG for post-ganglionic sympathetic nerve endings permits a direct assessment of sympathetic nervous activity in cardiac tissue. This method has become a relatively reliable method for detection of cardiac dysinnervation and is effective at identifying changes that occur even before the onset of ECG-based abnormalities (Schnell *et al.* 1996). For example, MIBG scintigraphy can be used to assess the extent of myocardial damage after infarction since sympathethic nerve fibres are damaged throughout the infarct zone. It has also been used to evaluate the cardiac autonomic nervous system defects at the onset of IDDM where a decrease in global uptake is observed (Turpeinen *et al.* 1996).

The diagnostic efficiency for MIBG tomography for the detection of coronary artery disease (CAD) is limited due to nonspecific reductions in MIBG uptake in the inferior and postlateral regions of the heart (Nakata *et al.* 1996). Interestingly, the cardiac sympathetic nerves travel with coronary arteries, and congenital defects in coronary anatomy can also result in regional sympathetic denervation (Wichter *et al.* 1994)]. Nevertheless, the severity of coronary stenosis can be correlated with MIBG uptake defect (Hartikainen *et al.* 1997). In CAD, the extent of denervation is related to the local severity of ischemia and not related to the size of myocardium with impaired perfusion defect (Hartikainen *et al.* 1997; Nakata *et al.* 1996). It has also been noted that cardiac

adrenergic tissue is very sensitive to ischemia and regional cardiac sympathetic denervation can occur in patients with stable CAD without previous MI. Interestingly, 3-4 months after a coronary angioplasty, there is recovery of MIBG uptake if the residual stenosis after angioplasty is less than 40% of the lumen diameter (Guertner *et al.* 1993).

The sympathetic nervous system also plays an important role in the development and progression of heart failure, since it has been documented that myocardial NE content falls with the progression of heart failure (Takeishi *et al.* 1997). Impairment of both neuronal uptake and vesicular storage function is apparent in the failing heart (Seto *et al.* 1996) and there is a correlation between cardiac MIBG uptake and myocardial NE content (Schofer *et al.* 1988). Moreover, myocardial MIBG uptake can reflect the effect of treatments and therapies for cardiomyopathy (eg. ACE inhibitors, verapamil improve uptake), in addition to the progression of cardiomyopathy (Somsen *et al.* 1996; Wakabayashi *et al.* 1997). For example, ACE inhibitors act not only on systemic vasodilation but also directly to inhibit the release of NE from sympathetic nerve terminals and as a result improve myocardial fibrosis (i.e. ACE inhibitor suppression of neurohormonal system may contribute to some of the beneficial effects) (Somsen *et al.* 1996; Wakabayashi *et al.* 1997). Furthermore, AngII prevents the neuronal uptake of NE which then in turn leads to a decrease in β-adrenoceptors during heart failure (Somsen *et al.* 1996).

2.8.1.8 Mode of action of MIBG

In many cell lines, the anti-proliferative effect of MIBG is suggested to result from inhibition of complexes I and III of the mitochondrial respiratory chain, as stated previously. However, a complete proliferation arrest is observed at concentrations of MIBG much higher than those required for the complete inhibition of mitochondrial ATP synthesis (Cornelissen *et al.* 1995a; Cornelissen *et al.* 1995b). The maximum inhibition

for ATP synthesis was seen at 10 μM while the optimum concentration for inhibition of cell proliferation was observed at concentrations greater than 25 μM. Therefore, inhibition of mitochondrial respiratory chain activity is not entirely responsible for the cell proliferative inhibition properties of MIBG, and MIBG must influence cellular processes apart from mitochondrial ATP synthesis (Cornelissen *et al.* 1997b; Cornelissen *et al.* 1995a).

Initially it was suggested that the differential inhibition of cell proliferation and mitochondrial activity may be due to generation of superoxide and lipid peroxidation of the mitochondrial inner membrane (via inhibition of complex I), since increasing MIBG concentrations increase the levels of malondialdehyde (MDA) which defines the extent of lipid peroxidation (Cornelissen *et al.* 1997a). When MIBG was used to inhibit complex I, superoxide formation occurred maximally at concentrations of MIBG seven times higher than those required for optimal inhibition of mitochondrial ATP synthesis (Cornelissen *et al.* 1997b). Interestingly, the authors could use either vitamin E or GSH to scavenge free radical formation and, as a result, there was little or no MDA formed with increasing concentrations of MIBG (0 — 25 μM; 25 μM produced the maximal concentration of MDA) incubated with cells overnight. However, despite the protective effect of the scavengers on MIBG-induced increase in MDA levels, no increase in the cell proliferation rate was observed when cells were cultured for 5 days in the presence of MIBG with vitamin E (Cornelissen *et al.* 1997b). This would suggest that still other cellular mechanisms are being influenced by MIBG in its anti-proliferative effect. One possibility is that MIBG is inhibiting an arg-mART enzyme activity. Thus, the mitochondrial proteins that have been shown to be mono(ADP-ribosyl)ated could mediate the disruption of mitochondrial function by MIBG (Althaus & Richter 1987).

2.8.1.9 MIBG as an inhibitor of arg-mART

Smets and colleagues demonstrated that MIBG was an inhibitor of arg-mART (Loesberg *et al.* 1990b; Smets *et al.* 1988a; Smets *et al.* 1988b; Smets *et al.* 1990b). Their initial studies revealed that non-radiolabelled MIBG had several cellular effects, including cytotoxicity, which they ascribed to interference with cellular mARTs (Smets *et al.* 1988a; Smets *et al.* 1988b). The reasons for this assumption were two-fold: i) MIBG could potentiate the leukemolytic actions of glucocorticoid hormones similar to inhibitors of ADP-ribosylation such as nicotinamide and 3AB (Smets *et al.* 1988a), and ii) MIBG was structurally similar to arginine and guanyltyramine, two known substrates for N-linked mART activity of cholera toxin (Althaus & Richter 1987). Upon further investigation, they found that MIBG could serve as an acceptor for the mART activity of not only cholera toxin, but also of an endogenous mART activity from erythrocyte membranes (Loesberg *et al.* 1990b), and MIBG could compete with intracellular acceptors of arg-mART enzymes (Smets *et al.* 1990b). Moreover, this activity was dependent on the presence of the guanidino-group, since MIBA (*meta*-iodobenzylamine), the related monoamine precursor, had no effect (Loesberg *et al.* 1990b). This would suggest that MIBG competes effectively with endogenous acceptors via its guanidino-group, making it a valuable tool for the study of the physiological functions of cellular mARTs.

Armed with the knowledge that MIBG is an anti-tumour agent and that it also inhibits arg-mART enzyme activity (Cornelissen *et al.* 1995a; Loesberg *et al.* 1990b; Taal *et al.* 1996), it is conceivable that the anti-tumour activity of MIBG may be linked with its ability to inhibit mono(ADP-ribosyl)ation reactions. Studies in this laboratory have demonstrated that arg-mART activity increases following mitogen stimulation, and that inhibition of this enzyme activity prevents cell proliferation (Yau *et al.* 1998). These

studies certainly support the contention that the anti-proliferative actions are mediated through inhibition of arg-mART and that cell proliferative processes may be associated with activation of this enzyme. Furthermore, the ability of MIBG to inhibit an arg-mART which is linked to cell proliferation would emphasize the findings of Cornelissen *et al.* (1997b and 1995a) that a differential inhibition of mitochondrial respiration and cell proliferation was observed, with the latter requiring much higher concentrations of MIBG. Taken together, these data would suggest that MIBG must influence cellular processes apart from mitochondrial ATP synthesis with respect to its ability to inhibit cell proliferation, and a likely candidate is N-linked mono(ADP-ribosyl)ation of endogenous acceptor proteins.

2.9 General Perspectives

The preceding literature review demonstrates that considerable knowledge exists concerning restenosis, its pathogenesis and the involvement of vascular remodeling and SMCs, as well as the cellular processes activated within the SMC population of the restenotic lesion. However, even with this understanding, and the extensive amount of research that is still ongoing, the pharmacological therapies and mechanical strategies that have been implemented to date have not brought about a significant reduction in the incidence of restenosis after revascularization procedures. Thus, it is still of paramount importance to continue defining the temporal sequence of events that take place during and after vascular injury. In particular, the cellular systems associated with the repair processes that bring about the fibroproliferative and remodeling events characteristic of restenosis must be defined, since there is a lack of continuity of information regarding the progression of the entire disease process. Novel players may yet still be discovered and characterized. Interestingly, many of the cellular processes activated in vascular repair

and restenosis are similar to those seen during tumour progression and metastases. Although many chemotherapeutic agents, especially those that inhibit cell proliferative processes, have been tested without much success, the spectrum of agents has not been exhausted. Nevertheless, more details concerning the progression of restenosis will improve the likelihood that a successful therapeutic modality will be found. Armed with the knowledge that restenosis is in part a disorder of activated vascular (smooth muscle) cells and in part a consequence of vascular remodeling, it is evident that combination therapy will be required. Alternatively, a single compound that will interfere with multiple processes within the restenotic program must be identified. Thus, the investigation of novel compounds for the treatment of restenosis is still a burgeoning field. It is the potential for MIBG to inhibit cell proliferation, cell migration and cell differentiation, and the ability of MIBG to influence a novel cell regulatory mechanism potentially related to cell proliferation, migration and differentiation that brought me to investigate this molecule in a variety of cellular systems, and finally apply MIBG to the treatment of restenosis post-angioplasty.

3.0 Statement of the Problem: Hypothesis and Objectives

The information summarized in the introduction (section 1.0) allowed the formation of a general hypothesis under which studies reported in this thesis were carried out. To review briefly, the incidence of restenosis after revascularization procedures is close to 50%. The clinical consequences of restenosis include angina, myocardial infarction and sudden death. A variety of pharmacological agents have been tested as therapeutic agents for the inhibition of restenosis, none of which has had measurable clinical success. MIBG, synthesized as a norepinephrine analog, is used clinically for the detection of neuroendocrine tumours and cardiac sympathetic dysinnervation. When tagged with radioactive iodine, MIBG has been successfully used as therapy for neuroendocrine tumours (i.e. neuroblastoma). More recently, favourable results have been found for non-radiolabelled MIBG as a chemotherapeutic agent for neuroblastoma and as therapy for small bowel tumours, since it effectively abrogates tumour growth and metastases. This information would infer that MIBG has the potential to prevent neointimal formation, and thus be employed clinically to suppress restenosis post-angioplasty.

GENERAL HYPOTHESIS -- *Meta*-iodobenzylguanidine (MIBG), an inhibitor of mono(ADP-ribosyl)transferase (mART), will effectively reduce restenosis (neointimal lesion formation) post-balloon angioplasty by interfering with the cellular processes that mediate proliferation, migration and differentiation. As a corollary to the hypothesis, MIBG is an inhibitor of mART, and therefore, mART activity may be essential for cell proliferation, cell migration and cell differentiation.

Within the context of the stated General Hypothesis, two objectives were advanced:

GENERAL OBJECTIVES –

1) To characterize the response of cells to MIBG and to identify its mechanism of action.

2) To evaluate MIBG as an inhibitor of restenosis.

It is anticipated that the information provided by these studies will lead to a novel therapeutic application for MIBG that will benefit patients who require revascularization procedures each year. Furthermore, it is expected that these studies will generate renewed interest in the basic cellular mechanisms that contribute to the restenotic process.

4.0 Experimental Procedures/Materials and Methods

4.1 Materials

All media, antibiotics, sera and other reagents used for cell culture experiments were obtained from Gibco/BRL - Life Technologies (Burlington, ON), unless otherwise noted. Reagents for the SMC serum-free defined supplement (pyruvate, ascorbate, holo-transferrin, selenium and insulin) were obtained from Sigma Chemicals (St. Louis, MO). Nunc plastic tissue culture plates were from Gibco/BRL – Life Technologies (Burlington, ON), while Linbro plastic multiwell tissue culture dishes were acquired from ICN/Flow Technologies (Costa Mesa, CA).

Individual growth promoting agents were acquired from a variety of commercial sources. Insulin used for the H4IIE experiments was purchased either from Sigma Chemicals (St. Louis, MO) or from Eli Lilly Company (Scarborough, ON). IGF-1 and PDGF were obtained from Peprotech Incorporated (Rockyhill, NJ). Angiotensin II (AngII) was purchased from Sigma Chemicals (St. Louis, MO), Peninsula Laboratories (Belmont, CA) or Calbiochem (Cedarlane Laboratories Ltd.; Hornby, ON). PGE_2, PGI_2, $PGF_{2\alpha}$ and $cTxA_2$ were obtained from Cayman Chemicals (Ann Arbor, MI). Thrombin was acquired from Sigma Chemicals (St. Louis, MO). Inhibitors used throughout the studies were also procured from a variety of commercial sources. MIBG, MIBA, 3AB and PABA were purchased from Sigma Chemicals (St. Louis, MO). PD128763 was a generous gift of Parke-Davis (Ann Arbor, MI). PD98059, SC-51322 and LY294002 were from BioMol Research Laboratories Inc. (Plymouth Meeting, PA), while wortmannin was obtained from Sigma Chemicals (St. Louis, MO).

Radiolabelled compounds ([methyl-^{3}H]thymidine, [5,6-^{3}H]uridine, [γ-^{32}P]ATP, D-[6-^{3}H(N)]glucose, [^{32}P]orthophosphate, [^{3}H]PGE_2, [^{32}P]dCTP, [2,8-^{3}H]adenosine, [^{32}P]NAD^+, [^{3}H]NAD^+) and Aquasol were purchased from Dupont-NEN/Mandel-NEN

(Guelph, ON), while Cytoscint ES was acquired from ICN/Flow Technologies (Costa Mesa, CA). Trichloroacetic acid (TCA) was supplied by Fisher Scientific (Nepean, ON). Cell Lifters manufactured by CoStar were obtained from Fisher Scientific (Nepean, ON). Whatman GF/A glass fibre filters, GF/C glass fibre filters, DE-81 filters, polyethylenimine-cellulose (PEI-cellulose) chromatography plates, and silica gel TLC plates were acquired through Fisher Scientific (Nepean, ON). Ionex-25 SA-Na plates were purchased from Machery-Nagel (Easton, PA). ADP-ribose, NAD^+, L-arginine methyl ester and L-nitro-arginine methyl ester were obtained from Sigma Chemicals (St. Louis, MO) or Boehringer-Mannheim/Roche Diagnostics (Laval, QC).

Immobilon-P poly(vinylidene difluoride) (PVDF) membranes used for Western blot analysis were from Millipore as purchased through Fisher Scientific (Nepean, ON). The ECL chemiluminescent detection system was provided by Amersham Life Sciences (Oakville, ON) both in the regular format and in the super sensitive format. Reflection film and Kodak X-OMAT high sensitivity film were from Dupont-NEN/Mandel-NEN (Guelph, ON) and VWR Scientific (Edmonton, AB), respectively. Kodak film and developing reagents were purchased from Don's Camera (Winnipeg, MB). Myelin basic protein (MBP) was supplied by Sigma Chemicals (St. Louis, MO) while bovine serum albumin (BSA) (fraction V) was purchased from Boehringer-Mannheim/Roche Diagnostics (Laval, QC). Protein G Sepharose and immunoprecipitin was from Amersham Pharmacia Biotech (Baie d'Urfe, QC). The bicinchoninic acid (BCA) protein assay kit was supplied by Pierce through BioLynx Inc. (Brockville, ON). Protease inhibitors (phenylmethylsulfonylfluoride (PMSF), sodium orthovanadate, sodium fluoride, aprotinin, leupeptin, etc.) were from Sigma Chemicals (St. Louis, MO). The LDH cytotoxicity assay kit was purchased from Boehringer-Mannheim/Roche

Diagnostics (Laval, QC). The T4 DNA polymerase labeling kit was obtained from Gibco/BRL - Life Technologies (Burlington, ON).

Balloon angioplasty catheters (different sizes) were acquired from Boston Scientific/SciMed (Maple Grove, MN) or Cook Inc. (Stouffville, ON). Suture was from Ethicon (Johnson & Johnson, Somerville, NJ). Tisseel™ was supplied by Baxter, Canada (Mississauga, ON). OCT/Tissue Tek was obtained from Ted Pella Inc (Redding, CA). Superfrost Plus glass slides and paraformaldehyde used for immunological staining were purchased from Fisher Scientific (Nepean, ON) and TAAB Laboratories Equipment Ltd. (Reading, Berks, England), respectively. Streck tissue fixative was obtained from Streck Laboraties (Omaha, NE). CrystalMount anti-fade mounting media was supplied by Biomeda (Foster City, CA). JB-4 embedding resin was purchased from Polysciences Inc. (Warrington, PA).

TRIzol reagent for RNA extraction was obtained from Gibco/BRL – Life Technologies (Burlington, ON). Reverse Transcriptase-Polymerase Chain Reaction (RT-PCR) kits were purchased from Perkin-Elmer/Cetus Corporation (Ville St. Laurent, QC), while extra nucleotides were supplied by Boehringer-Mannheim/Roche Diagnostics (Laval, QC). SYBR Green I was purchased from Molecular Probes (Eugene, OR).

Primary antibodies were obtained from Sigma Chemicals (St. Louis, MO) [anti-(smooth muscle α-actin), anti-(smooth muscle myosin)], Transduction Laboratories (San Diego, CA) [anti-(phosphotyrosine PY20) IgG coupled to horseradish peroxidase (HRP), anti-(p21-Ras)], New England Biolabs (Mississauga, ON) [anti-(de/phosphoMEK1/2), anti-(de/phosphoMAP kinase)], Promega through Fisher Scientific (Nepean, ON) [anti-(phosphoMAP kinase)], Santa Cruz Biotechnologies (Santa Cruz, CA) [anti-(MyoD), anti-(myogenin), anti-($p21^{CIP1}$), anti-(MEF2)], Boehringer Mannheim/Roche Diagnostics (Laval, QC) [anti-(bromodeoxyuridine)], DAKO (Mississauga, ON) [anti-(proliferating

cell nuclear antigen – PCNA)], Trevigen (Gaithersburg, MD) [anti-(poly-(ADP-ribose))], and Upstate Biotechnologies (Lake Placid, NY) [anti-(p85)]. Secondary antibodies were obtained from Bio-Rad (Mississauga, ON) [HRP-coupled anti-(rabbit IgG), HRP-coupled anti-(mouse IgG)], Jackson ImmunoResearch Laboratories (BioCan Scientific, Mississauga, ON) [Cy-3 conjugated anti-(rabbit IgG), Cy-3 conjugated anti-(mouse IgG), Cy-3 conjugated anti-(goat IgG), Cy-3 conjugated anti-(rat IgG)]. Hoescht No. 33342 nuclear stain was acquired from Sigma Chemicals (St. Louis, MO). Fluorescein (FITC)-conjugated mouse, monoclonal anti-BrdU antibody was purchased from Becton Dickinson (San Jose, CA). Propidium iodide and DNAse I globular actin stain was purchased from Molecular Probes (Eugene, OR). Bromodeoxyuridine (BrdU) was acquired from Boehringer-Mannheim/Roche Diagnostics (Laval, QC).

General laboratory chemicals were purchased from either Sigma Chemicals (St. Louis, MO) or Fisher Scientific (Nepean, ON) unless otherwise noted. Ultrapure chemicals (Tris, glycine, SDs, acrylamide, glycerol, Tween 20, Triton X-100 etc.) were supplied by Gibco-BRL – Life Technologies (Burlington, ON), Bio-Rad (Mississauga, ON) or Boehringer-Mannheim/Roche Diagnostics (Laval, QC). 3-(4,5-dimethyl-thiazol-2-yl)-2,5-dipheoltetrazolium bromide (MTT) was purchased from Sigma Chemicals (St. Louis, MO).

4.2 Experimental Systems

4.2.1 H4IIE cell culture

Rat H4IIE hepatoma cells (American Type Culture Collection, CRL 1548) were grown in 150-mm culture dishes in α-modified minimal essential media (α-MEM) containing 10% fetal bovine serum (FBS), 2 mM glutamine, 50 μg/mL streptomycin and 50 μg/mL penicillin. The cells were passaged every second day at a 1:6 dilution. Cells

were placed into serum-free α-MEM for 72 h prior to the start of experimentation to ensure entry into a quiescent state (Yau *et al.* 1998).

4.2.2 L6 myoblast/tube cell culture

Rat L6 skeletal myoblast cells (obtained from Dr. Ted Lo, University of Western Ontario) were grown in 150-mm culture dishes in α-MEM containing 10% FBS, 2 mM glutamine, 50 μg/mL streptomycin and 50 μg/mL penicillin. The cells were passaged every second day at a 1:3 dilution. Confluency was maintained at less than 70% to ensure that the cells did not begin to differentiate spontaneously. To induce differentiation, cells were placed into α-MEM containing 2.5% horse serum for 96 h at which point myotube formation was essentially complete (Zahradka *et al.* 1989).

4.2.3 Primary smooth muscle cell culture

Primary cultures of porcine coronary artery smooth muscle cells (SMCs) were generated from the left anterior descending coronary artery (LAD) by an explant organ culture method (Saward & Zahradka 1997b). The LAD was dissected free of the heart, cut into segments of 2-5 mm, placed into Dulbecco's modified Eagle media (D-MEM) containing 20% FBS, 2 mM glutamine, 50 μg/mL streptomycin, 50 μg/mL penicillin and 10× antibiotic/antimycotic (™Fungizone, Gibco-BRL), and incubated at 37°C in 5% CO_2. After approximately 2-3 weeks in culture, SMCs migrating from the free-floating explants populated the tissue culture dish and were ready for passaging. SMCs were propagated in D-MEM containing 20% FBS, 2 mM glutamine, 50 μg/mL streptomycin, 50 μg/mL penicillin and 1× antibiotic/antimycotic. Cells were used only after the second passage to maintain consistency between cultures. To obtain a quiescent cell population, SMCs were grown to 70% confluence, rinsed with phosphate-buffered saline (PBS) and incubated in serum-free D-MEM supplemented with 11 μg/mL pyruvate, 5 μg/mL transferrin, 10^{-9} M selenium, 2×10^{-4} M ascorbate and 10^{-8} M insulin for 5 days.

4.2.4 *In vivo* pig model of femoral angioplasty

Male castrated pigs, 30-35 kg, were obtained locally and kept in quarantine for a week. Prior to the procedure, the pigs were sedated (zolazepam). The pigs were then anaesthetized (tiletamine, xylazine), intubated and maintained on isofluorane gas anaesthesia according to University of Manitoba Use Protocol 97-060 until the surgery was completed. The animal protocol was approved by the University of Manitoba Animal Care committee, and the procedure carried out in accordance to the guidelines set out by the protocol and the Canadian Council on Animal Care. With the pig in the supine position, an incision was made to expose the left femoral artery extending from the bifurcation of the femoral and superficial femoral arteries to the point of femoral artery insertion into the groin area. Once the tissue planes were cleared and the area was exposed, a 1:1 mixture of nitroglycerine:papaverine (1.0 mL of 5 mg/mL nitroglycerine and 1.0 mL 8.125 mg/mL papaverine) was applied to the femoral artery. The right femoral artery was then exposed and treated in the same manner. Exposed tissue was kept moist with a saline-soaked sponge. Once the femoral artery was vasodilated, atraumatic vascular clamps were placed at the proximal site (groin area) and at the distal site, just past the bifurcation of the femoral. A #11 scalpel was then used to create an arteriotomy at the site of bifurcation. An appropriately sized balloon (typically 6.0 × 20 mm – in a few cases 5.0 × 20 mm – based on intravascular ultrasound measurements of the femoral artery diameter of test pigs and a balloon:artery diameter ratio of 1.2 to 1.4) was inserted through the arteriotomy in a retrograde manner and the proximal vascular clamp removed. Once the balloon was in place, 20-mm from the point of insertion, the balloon was inflated to 6 atm for 1 min. The balloon was then deflated and removed, and the proximal vascular clamp reapplied. The arteriotomy was then closed with 6.0 Prolene suture. If required, Tisseel (1.0 mL) was applied along the length of the femoral artery

from the arteriotomy to the proximal region of the vessel, encompassing the site of balloon injury. The incision, including the deep fascia, was then closed with 3.0 Vicryl or 3.0 Dexon suture, and the skin stapled to close the wound. Pigs were given antibiotics (amoxicillin) for 5 days following the procedure in accordance to Manitoba Animal Care committee guidelines. The pigs were euthanized 14 days after the angioplasty procedure, and the femoral arteries harvested. The femorals were divided into 4 regions (arteriotomy, distal, balloon and proximal) and each region cut into 2 sections. All sections were placed into OCT/Tissue Tek, blocked, flash frozen in a dry ice/ethanol bath and stored at -80°C.

4.2.4.1 Femoral angiography

Femoral artery angiograms were conducted prior to euthanization of the pigs. The pigs were sedated, intubated endotracheally, anaesthetized and maintained on isofluorane anaesthesia for the duration of the procedure. With the pigs in supine position, exposure of the left main carotid artery was conducted using a combination of sharp and blunt dissection. Upon exposure, silk loops were placed to secure the carotid artery. Hemostatic clamps were placed proximally and distally to gain vascular control and allow an arteriotomy in the vessel. A 6 French (6F) cannula was placed into the carotid artery and secured in place with silk ligature. A 6F angiocatheter was advanced under fluoroscopic guidance into the aorta and then the left common iliac artery. The pigs were identified using radio-opaque numbers, and the letter "L" to denote the left side. Fluoroscopic imaging and the use of radio-opaque dye confirmed the field of view. Once satisfactory, 60 mL of radio-opaque dye was injected while the image was being recorded onto a VCR tape. The same procedure was repeated for the right common iliac artery/femoral. The right side was identified on VCR tape by the letter "O" to represent the right side.

Following the completion of the angiogram, the pigs were euthanized to harvest the femoral arteries.

In those instances where the carotid approach was unsuccessful, angiography was initiated at the most proximal portion of the femoral artery. Briefly, with the pig in supine position, the femoral artery was carefully exposed, as proximally as possible. Silk loops were placed to secure the femoral artery. Hemostatic clamps were placed proximally and distally to gain vascular control to allow an arteriotomy. A 6F cannula was placed into the femoral artery and secured with silk ligature. Fluoroscopic imaging and the use of radio-opaque dye confirmed the appropriate field of view. A pair of hemostat clamps identified the entry point of the catheter and a second pair was placed distally to identify the positioning of the leg joint. When the field of view was satisfactory, 60 mL of radio-opaque dye was injected while the image was being recorded onto a VCR tape. Upon completion of the angiogram, the femoral arteries were harvested for histologic processing.

4.3 Cell growth and viability assays

4.3.1 Radiotracer incorporation for measurements of DNA and RNA synthesis

Cells (H4IIE, SMC, L6) were plated in 24-well multiwell dishes and allowed to grow over 2 days. Quiescent cells were prepared with the serum-free conditions described in 4.2.1, 4.2.2 and 4.2.3, and stimulated by direct addition of the indicated compounds without replacing the media. When inhibitors were used, they were added 10-15 min prior to addition of stimulating agents. To measure RNA synthesis, cells were incubated with 2 μCi [^{3}H]uridine for 6 h after addition of stimulating agents. Similarly, DNA synthesis was measured by incubating the H4IIE cells with 2 μCi [^{3}H]thymidine for 24 h. For SMC cultures, the [^{3}H]thymidine was added 24 h after the initial stimulation,

and the incubation continued for 48 h. The cells were subsequently lysed with 1.0 mL lysis buffer containing 10 mM Tris-HCl (pH 7.4), 100 mM NaCl, 1 mM EDTA and 0.5% SDS, and the nucleic acids precipitated with an equal volume of ice-cold 20% trichloroacetic acid (TCA). The precipitate was collected on Whatman GF/A glass fiber filters, which were washed 4 times with 5% TCA, once with ethanol and then allowed to air-dry. Radioactivity was determined by liquid scintillation counting using a Beckman LS6500 Multipurpose Scintillation Counter.

4.3.2 Radiotracer incorporation for measurement of cell cycle re-entry

Cells (H4IIE and SMC) were plated in 24-well multiwell dishes and allowed to grow over 2 days. Quiescent cells were prepared with the serum-free conditions described in 4.2.1 and 4.2.3. To evaluate the time required to re-enter the cell cycle, DNA synthetic activity was measured by pulse-labeling cultures with 2 μCi [^{3}H]thymidine for 30 min at varying times after mitogen stimulation. Cells were then lysed and analyzed as described in section 4.3.1.

4.3.3 Cell Number I

Cells (H4IIE and SMC) prepared in 96-well multiwell culture dishes (Nunc, 200 μL volume) were either maintained for 96 h in serum-free/serum-free supplemented media containing varying concentrations of inhibitor, or were stimulated with a variety of agents ± inhibitors over 96 hours without replacing the media. If inhibitors were used, they were added 15 min prior to addition of stimulating agents. Cell number (i.e. mitochondrial density) was measured after a 4 h incubation with MTT according to Shi *et al.* (1993). Colour development was quantified using a Molecular Devices ThermoMAX plate reader with a 550-nm filter. A decline in cell numbers may be observed under conditions that promote cell death. For this reason, the MTT assay can also be employed to measure cytotoxicity (Denizot & Lang 1986; Mossman 1983).

4.3.4 Cell number II

Cultures of quiescent cells (H4IIE and SMC) in either 12- or 24-well culture dishes were stimulated by direct addition of the indicated compounds without replacing the media. When inhibitors were used, they were added 15 min prior to addition of stimulating agents. At the selected times (24, 48, 72 or 96 h), cells were trypsinized in 200 μL and neutralized with 200 μL of media containing FBS. The cells were then added to vials containing 9.0 mL of filtered PBS. Each well was then washed twice with 300 μL of PBS and each wash added to the vials. Cell number was determined with a Coulter Counter set to count 500 μL volumes. Each condition was conducted in triplicate and each vial was counted three times.

4.3.5 Bromodeoxyuridine (BrdU) cell labeling

Cells (H4IIE and SMC) were grown on Superfrost Plus glass slides and made quiescent by incubating in serum-free media (with or without supplement, depending on cell type). Quiescent cells were then stimulated by direct addition of agents without replacing the media. BrdU (50 μM) was added for 2-24 h before harvest of the slides at the selected times (24, 48, 72 or 96 h). Control slides were incubated with BrdU over the same time period in the absence of stimulating agent. Additional controls were generated in the absence of BrdU. Slides were washed in PBS and fixed by placing in ice-cold methanol for 5 min. The slides were allowed to air-dry and were subsequently rehydrated in PBS (3 changes, 5 min each). The slides were incubated for 1 h at 37°C in 2 N HCl and neutralized with 3 changes of 0.1 M borate (5 min each). After 3 washes with PBS, the slides were incubated for 1 h at room temperature with monoclonal anti-BrdU antibody (diluted 1:200) in 1% bovine serum albumin (BSA) in TBS-T containing 10 mM Tris-HCl (pH 7.5), 100 mM NaCl and 0.1% Tween 20. The slides were then washed in PBS and anti-mouse secondary antibody conjugated to Cy-3 (diluted 1:400) in 1%

BSA/TBS-T was applied for 1 h at room temperature. The slides were washed in PBS and allowed to dry slightly before mounting with an antifade agent (CrystalMount or VectaShield). The slides were then viewed with an epifluorescence microscope and the number of nuclei showing BrdU staining recorded.

4.3.6 FACS analysis

$1 \times 10^6 - 2.5 \times 10^6$ cells (H4IIE) were prepared in 6-well multiwell culture dishes. The cells were then treated with agonist or inhibitor for 48 h, and 50 μM BrdU/50 μM 5-fluoro-2'-deoxyuridine (BrdU Labeling Solution, Amersham Life Sciences, Oakville, ON; Catalogue number RPN 201) was added 2 h prior to cell harvest. The cells were then trypsinized and transferred to 10 mL conical tubes and centrifuged for 5 min at 2400×g. The cell pellet was washed in PBS/1% BSA/0.5% Tween/20 mM EDTA, transferred to microfuge tubes and centrifuged for 5 min at 2400×g. The supernatant was removed and the cell pellet resuspended in 1 mL ice-cold 0.9% saline. The cells were then fixed by adding the resuspended cells dropwise to 5 mL of 70% ethanol while vortexing. The tube was rinsed in 100 μL saline and the cells incubated for 30 min on ice or stored at -20°C for a maximum of 5 days. The cells were centrifuged for 5 min at 3000×g. The supernatant was removed, the cell pellet vortexed vigorously and the cells resuspended in 0.5 mL PBS/20 mM EDTA/0.5% Tween. The cells were passed through a 26 gauge needle to break up clumps and transferred to a glass tube. 1 mL of 4 M HCl/1% Triton was added while vortexing. The cells were then incubated at room temperature for 30 min and centrifuged at 3000×g for 5 min. The acid was neutralized with 1.5 mL of 0.1 M borate (pH 8.5) and the cells vortexed vigorously. The cells were collected by centrifugation for 5 min at 3000×g and resuspended in 100 μL of PBS/1% BSA/0.5% Tween/20 mM EDTA. After adding 20 μL of FITC-mouse anti-BrdU, the sample was mixed for 2 h in the dark at room temperature before washing in PBS/20 mM

EDTA/0.5% Tween. The cells were pelleted and 500 μL of propidium iodide stain solution (15 μg/mL) was added and the cell suspension mixed for an additional 2 h in the dark, before FACS analysis.

Immunofluorescence was quantified with an EPICS Model 753 Fluorescence Activated Cell Sorter (Coulter Electronics, Hialeah, FL) equipped with a 488-nm (500 mW) line from an argon laser. To enable the detection of FITC fluorescence (emission peak of 520-nm), a 540-nm band pass filter was used. Propidium iodide fluorescence (emission peak of 620-nm) was determined with a 610-nm long pass filter. Data collection and analysis was conducted by Dr. Ed Rector (Department of Immunology).

4.3.7 LDH assay

The LDH cytotoxicity assay was carried out according to the method provided with the kit purchased from Boehringer-Mannheim/Roche Diagnostics (Laval, QC). Briefly, cells (H4IIE) were plated in 96-well multiwell tissue culture plates. Growing or serum-deprived H4IIE cells were then treated with varying concentrations of compound and, 24 h later, a 20 μL aliquot of media was mixed with 80 μL of PBS and transferred to a new 96-well plate. Reaction mixture (100 μL of a mixture of catalyst, diaphorase/NAD^+, dye solution, iodotetrazolium chloride and sodium lactate) was then added to each well and the plates incubated at room temperature for 30 min. Conversion of the dye by released LDH was measured colorimetrically by absorbance at 490-nm with a ThermoMAX plate reader.

4.3.8 [^{3}H]glucose uptake assay

Quiescent cells (H4IIE) were prepared in 24-well culture dishes. The media was replaced with glucose-free buffer (137 mM NaCl, 4.7 mM KCl, 10 mM sodium phosphate (pH 7.4), 0.5 mM $MgCl_2$, 1 mM $CaCl_2$, 0.2% (w/v) BSA), and the cells were subsequently stimulated with insulin or IGF-1. After 10 min, 10 mM [^{3}H]glucose (0.5

μCi) was added to each well and the incubation continued for a further 10 min (Kato *et al.* 1993). The cells were then washed three times with ice-cold PBS and solubilized with 1 M NaOH. The lysate was neutralized with acetic acid, mixed with 5 mL Aquasol, and the radioactivity monitored by liquid-scintillation counting on a Beckman LS6500 Multipurpose Scintillation Counter.

4.4 Cell differentiation

L6 skeletal myoblasts were grown in 6-well culture dishes and switched into a 2.5% horse serum media as described in 4.2.2. The media was refreshed after 48 h. Cell fusion was routinely monitored by phase/contrast microscopy. To quantify differentiation, cells were fixed in methanol, stained with Wright's-Giemsa stain, rinsed in water and 70% ethanol and the number of nuclei in fused myotubes quantified by counting. If agents or inhibitors were added to assess their effect on L6 myoblast differentiation, they were added directly to the wells after the growth media had been replaced with differentiation media.

4.5 Cell migration (Boyden chamber)

SMCs were prepared in a standard 48-well Boyden chamber (supplied by Neuroprobe). In the lower chamber, 30 μL of serum-free D-MEM ± chemotactic factors was placed into each of the 48 wells. A membrane with pore size of 5 μm was then placed over the top of the wells and the upper plate fitted over the membrane. SMCs (1.5×10^3 cells) were then loaded into the wells of the top chamber in 35 μL of serum-free D-MEM. If inhibitors were added, they were added to the top chamber. The Boyden chamber was then incubated at 37°C in 5% CO_2 for 48 h. The membrane was subsequently removed from between the two plates and the cells fixed by immersion in

methanol for 5 min. Cells that adhered to the upper surface of the membrane were scraped off. The underside of the membrane was then rinsed in ddH_2O and the cells stained with Giemsa stain for 60 min. The membrane was then cut into sections and the membrane mounted on glass slides. The number of cells present in each well area was then counted under light microscopy (n = 6 per condition).

4.6 Fibrin glue preparation

Fibrin glue (Tisseel) was prepared according to the manufacturer's instructions. All components were premeasured and used completely unless otherwise specified. Briefly, the vials containing lyophilized fibrin and thrombin were warmed to 37°C in the apparatus provided. Aprotinin was then added to the fibrin vial and the contents allowed to mix for 10 min and kept at 37°C until use. A $CaCl_2$ (40 mM) solution was then added to the thrombin 500 vial (quick setting), mixed and kept at 37°C until used. For application of Tisseel, equal amounts of fibrin and thrombin were drawn up in the syringes provided and the syringes placed into the specially designed Duploject clip for simultaneous ejection and mixing of the components. The Tisseel was then applied as described in 4.2.4. If application of MIBG was being tested in the Tisseel, the inhibitor was dissolved in $CaCl_2$ solution and filter-sterilized before addition into the vial of thrombin 500. The final concentration of inhibitor upon application was 25 mM. In control pigs, right and left femoral arteries were randomly treated with either Tisseel or no Tisseel. In experimental pigs, femoral arteries were treated with either Tisseel alone or Tisseel plus inhibitor in a random double-blind manner. Blinding of the experiment was not revealed until all tissue samples had been processed and neointimal index quantified.

4.7 Histology

4.7.1 Paraformaldehyde preparation

A solution consisting of 40 mL water, 10 mL 9.0% NaCl and 3-4 drops NaOH was heated to 55°C, after which 4 g of paraformaldehyde was added. Once dissolved, the solution was removed from the heat and 20 mL of 0.5 M $NaPO_4$ (pH 7.4) added before allowing to cool to room temperature. The pH of the solution was adjusted to 7.4 and the volume increased to 100 mL with ddH_2O before filtration. The 4% paraformaldehyde solution was kept at 4°C until used (maximum 24 h).

4.7.2 Histology of tissue sections

Tissue frozen in OCT was cryosectioned (6-7 μm thickness), placed onto Superfrost Plus glass slides and stored at –80°C. Slides were allowed to warm to room temperature for processing. The sections were then treated with Streck tissue fixative for 10 min at room temperature, rinsed 3× with TBS (20 mM Tris-HCl (pH 7.5), 150 mM NaCl) and stained for 1 min with Lee's methylene blue (0.026% methylene blue, 0.026% basic fuchsin, 25% ethanol in PBS) for identification of internal elastic lamina, nuclei and muscular tissue. The slides were then rinsed sequentially with distilled water, 70% ethanol and distilled water, and allowed to air-dry before viewing by light microscopy. The images were captured with a DAGE-MTI CCD camera and associated software.

4.7.3 Immunocytochemistry

Cells (H4IIE, SMC) grown on Superfrost Plus glass slides and washed 3× with TBS were fixed prior to antibody treatment. Fixatives included 4% paraformaldehyde, Streck tissue fixative, methanol, methanol:acetone (1:1) or acetone for 5-15 min at either 4°C or room temperature depending on the antibody being used. If the slides were fixed with an organic solvent (methanol, acetone), the slides were air-dried before rehydration in TBS or PBS and treatment of the slides with blocking buffer (3% bovine serum

albumin (BSA) in TBS-T containing 20 mM Tris-HCl (pH 7.5), 150 mM NaCl, and 0.1% Tween 20) for 60 min at room temperature. If the slides were fixed with a cross-linking agent, the slides were washed 3× in TBS or PBS before incubation with 0.1% Triton X-100 (in TBS or PBS) for 15 min to permeabilize the cells. After 3 washes in TBS or PBS, the slides were treated with blocking buffer for 60 min at room temperature. After treatment with blocking buffer, the slides were rinsed with TBS and incubated with primary antibody (diluted with 1% BSA/TBS-T) for 60 min at room temperature. After washing in TBS, the primary antibody was detected with a Cy3-, Cy2- or Oregon Green-coupled secondary antibody (diluted with 1% BSA/TBS-T). The slides were then washed in TBS and Hoescht No. 33342 (0.5 mg/mL diluted 1:4000 in TBS), a nuclear stain, was applied for 1 min before washing extensively with TBS. Photographs were taken with an Olympus BH-2 RFCA microscope fitted with a 35-mm camera using Fuji Provia400 slide film or Tri-X Pan black and white 400 ASA film. Alternatively, images were captured with a DAGE-MTI CCD camera and associated software.

4.7.4 Photography

Cells (SMC, L6) prepared in 6-, 12-, or 24-well culture dishes were photographed with an Olympus CK-2 inverted phase-contrast microscope fitted with a 35-mm camera containing Tri-X Pan black and white 400 ASA film.

4.8 Protein analysis techniques

4.8.1 BCA protein assay

Protein assays were based on the instructions provided by Pierce, supplier of the BCA protein assay kit, for the standard protocol. The method was modified to a 96-well format in conjunction with a Molecular Devices ThermoMAX plate reader fitted with a 550-nm filter. Briefly, 10 µL of cell lysate (or an appropriate dilution) was added to each

well (each condition was measured in triplicate) followed by addition of 200 µL BCA solution (1:50 mixture). The plate was then incubated at 37°C for 30 min. After colour development, the plate was allowed to cool and the absorbance read at 550-nm. BSA standards were prepared in triplicate and the standard curve produced by the standards was used to quantitate the amount of protein in the cell lysates.

4.8.2 Immunoprecipitation

Cell lysates were prepared from 6-well or 100-mm culture dishes by addition of 0.5 mL or 1.0 mL lysis buffer, respectively, containing 1% NP-40, 20 mM Tris-HCl (pH 7.5), 10% glycerol, 137 mM NaCl, 1 mM $MgCl_2$, 1 mM PMSF, 0.4 mM orthovanadate and 1 mM NaF. The plates were scraped and the lysates cleared by centrifugation (10 min at 12,000×g at 4°C). Protein concentrations were measured and aliquots of 100 µg protein were mixed for 2 h at 4°C with Protein G Sepharose. Protein G Sepharose was subsequently removed by centrifugation at 12,000×g for 5 min at 4°C. Each aliquot was then mixed over 2.5 – 4 h at 4°C with 2-5 µg of antibody. Protein G Sepharose was added for an additional 0.5 - 2 h and the Protein G Sepharose beads collected by centrifugation (12,000×g for 5 min at 4°C). The Protein G Sepharose was washed 4 times with 1.0 mL lysis buffer. The beads were then either resuspended directly in 50 µL of 2× SDS/gel loading buffer (1× buffer contains 62.5 mM Tris-HCl (pH 6.8), 1% SDS, 10% glycerol, 0.005% bromophenol blue and 5% β-mercaptoethanol) for Western blot analysis or further manipulated before measurement of PI3-kinase activity (see section 4.9.4).

4.8.3 Immunoblotting (Western blotting)

Immunoprecipitates or aliquots of cell lysates prepared by detergent lysis (cells treated with agents and then lysed in 2× SDS/gel loading buffer minus bromophenol blue and β-mercaptoethanol) containing equal protein concentration were mixed with an equal volume of 2× SDS/gel loading buffer and heated for 5 min at 95°C. Samples were then

loaded onto 7.5% or 10% polyacrylamide gels. Following electrophoresis (BioRad Mini-Protean II) at 20 mA constant current for 1 h, protein was transferred to PVDF membrane at 90 V (0.5 A) over 60 min in 15-20% methanol, 25 mM Tris and 130 mM glycine. Membranes were treated for 60 min at room temperature with blocking buffer (3% BSA/TBS-T). Primary antibody (diluted with 1% BSA/TBS-T) was added and incubated for 60 min at room temperature. The membranes were then washed 3× with TBS-T over 15 min and horse-radish-peroxidase-(HRP)-conjugated-secondary antibody (1:10,000 diluted) applied in 1% BSA/TBS-T for 60 min at room temperature. After 3 washes in TBS-T, the HRP was detected using the ECL chemiluminescent system. Intensity of bands appearing on the autoradiographs was quantified by scanning densitometry using a BioRad Model-670 Imaging Densitometer and Molecular Analyst software.

4.8.4 Subcellular fractionation

Cells (H4IIE, SMC and L6), prepared in 150-mm diameter tissue culture dishes (Nunc), were washed twice in PBS following treatment, harvested by scraping in 3.0 mL of PBS and collected by centifugation (Varifuge, 5 min at 3,000×g at 4°C). The cells were disrupted in 2.5 cell pellet volumes of homogenization buffer (0.25 M sucrose, 5 mM Tris-HCl (pH 8.0), 3 mM $CaCl_2$, 1 mM EDTA, 0.5 mM EGTA, 0.2 mM PMSF, 25 kU/mL aprotinin, 25% glycerol) using a Pro200 homogenizer (Pro Scientific Inc.) fitted with a 5-mm generator. Nuclei were removed by centrifugation (10 min at 8,000×g at 4°C) and the supernatant further centifuged to separate the membrane and cytoplasmic fractions (70,000×g for 60 min at 4°C). The microsomal pellet was resuspended in 200 µL homogenization buffer. Additionally, the nuclear pellet was extracted with 3 volumes of 175 mM K_2HPO_4, 0.1 mM EDTA and the debris removed by centrifugation (3000×g for 10 min).

4.8.5 Ligand binding assay

Quiescent SMC cultures prepared in 12-well multiwell tissue culture dishes were washed twice in PBS and 0.5 mL binding buffer was added to each well. The binding buffer was essentially a Hepes buffered salt solution with the following composition: 10 mM Hepes (pH 7.4), 2 mM glutamine, 1.25 mM $CaCl_2$, 0.5 mM $MgCl_2$, 0.45 mM $MgSO_4$ and 150 mM NaCl. 10 μM of competing "cold" PGE_2 was added just prior to the addition of radiolabelled [^{3}H]PGE_2 (0, 20, 50, 100, 200, 300 nM) to create a competition dose response curve. The plates were then incubated at room temperature for 30 min with rotation, followed by three washes with ice-cold binding buffer. The cells were lysed in 0.25 mL of 1 N NaOH for 30 min with rotation and neutralized with 0.25 mL 1/10 diluted glacial acetic acid for 30 min with rotation. The material was then transferred to scintillation vials and 4 mL of Aquasol added to each vial. The vials were vortexed vigorously, allowed to sit overnight and vortexed again before liquid scintillation counting with a Beckman LS6500 Multipurpose Scintillation Counter.

4.8.6 Nuclear extract preparation

L6 cells prepared in 150-mm culture dishes were washed three times in TBS, and 2.5 mL of lysis buffer (20 mM Hepes (pH 7.6), 20% glycerol, 10 mM NaCl, 1.5 mM $MgCl_2$, 0.2 mM EDTA, 0.1% Triton X-100, 1 mM DTT, 1 mM PMSF, 10 μg/mL pepstatin, 100 μg/mL aprotinin) was added to each plate. Cells were scraped and collected by centrifugation at 4°C (5 min at 2000 rpm). Nuclei were suspended in 2.5 volumes of nuclear extraction buffer (lysis buffer with 500 mM NaCl), gently rocked for 1 h at 4°C and centrifuged for 10 min at 10,000 rpm. The supernatant was collected, aliquoted and stored at -80°C until use.

4.8.7 UV-crosslinking

Oligodeoxynucleotides (ODNs) containing the myogenin binding site of MEF2 (see 4.10.1) were labeled with [^{32}P]dCTP (800 Ci/mmol) using a T4 DNA polymerase labeling kit. 0.5 – 5 μL of nuclear extracts (see section 4.8.6) and labelled ODN (5000 cpm) were incubated for 15 min at 37°C in 15 μL of solution containing 110 mM KCl, 12.5 mM Hepes (pH 7.9), 5 mM $MgCl_2$ and 10% glycerol, in addition to 0.1 mg/mL poly[d(I-C)]. Samples were then subjected to UV-irradiation (1200 × 100 μJ/cm^2) over 10 min (samples were maintained on ice), loaded onto 10% SDS/polyacrylamide gels and protein-ODN complexes were visualized by autoradiography at -80°C with one intensifying screen.

4.9 Enzyme Assays

4.9.1 Activity gel MAP kinase assay

Cells (H4IIE, SMC) prepared in 6-well multiwell or 100-mm culture dishes were treated, rinsed twice with ice-cold PBS and samples prepared by detergent lysis (50 mM β-glycerphosphate (pH 7.4), 0.5% (v/v) Triton X-100, 25% (v/v) glycerol, 2 mM EGTA, 1 mM orthovanadate, 1 mM dithiothreitol, 0.5 mM PMSF, 0.1 mM bacitracin and 20 μg/mL aprotinin) followed by homogenization or sonication (5 sec at 60 Hz.). After centrifugation (10 min at 12,000×g at 4°C), aliquots of the lysate were mixed with 3× SDS/gel loading buffer and loaded (without heating) onto a 10% polyacrylamide gel containing 0.5 mg/mL myelin basic protein. Following electrophoresis (20 mA for 1 h), SDS was removed from the gels by washing twice in 20% isopropanol/50 mM Tris-HCl (pH 8.0) and once in 50 mM Tris-HCl (pH 8.0)/5 mM β-mercaptoethanol for 1 h each at room temperature. Proteins were then denatured by treating the gel with 6 M guanidine/HCl in 50 mM Tris-HCl (pH 8.0)/5 mM β-mercaptoethanol for 1 h at room

temperature, and renatured in 50 mM Tris-HCl (pH 8.0) containing 0.04% Tween 40 and 5 mM β-mercaptoethanol with 5 changes over 16 hours at 4°C. Phosphorylation of myelin basic protein was assayed by incubating the gel with 25 μCi [γ-^{32}P]ATP in 50 mM Tris-HCl (pH 8.0), 2 mM DTT, 0.1 mM EGTA, 5 mM $MgCl_2$ and 100 μM ATP for 1 h at room temperature. Unincorporated label was removed by washing 5× in 1% sodium pyrophosphate/5% trichloroacetic acid. The gel was then dried and exposed to Reflection film (Dupont) at –80°C with one intensifying screen. Intensity of bands appearing on the autoradiographs was quantified by scanning densitometry with a BioRad Model-670 Imaging Densitometer and Molecular Analyst software.

4.9.2 *In vitro* MAP kinase assay

Cleared cell lysates (4 μL), prepared as described in 4.9.1, were incubated at 30°C for 5 min in a final volume of 24 μL with 0.25 mg/mL myelin basic protein and 2 μCi [γ-^{32}P]ATP in kinase reaction buffer (50 mM β-glycerphosphate (pH 7.4), 1 mM DTT, 1.5 mM EGTA, 10 mM MgOAc and 100 μM ATP). The reaction was terminated by addition of 8 μL 4× SDS/gel loading buffer. Samples were heated for 5 min at 95°C, loaded onto a 12% polyacrylamide gel and electrophoresed at 20 mA for 1 h. The gel was dried onto Whatman 3MM paper using a BioRad gel dryer (80°C stepped cycle for 1.5 h) and subjected to autoradiography at –80°C. Intensity of bands appearing on the autoradiographs was quantified by scanning densitometry with a BioRad Model-670 Imaging Densitometer and Molecular Analyst software.

4.9.3 Phosphatidylinositol 3-kinase (PI3-kinase) assay, *in vivo*

To metabolically label phosphatidylinositol pools *in vivo*, quiescent cells (SMCs prepared in 4-well culture dishes containing 0.8 mL media) were incubated with 200 μCi/mL [^{32}P]orthophosphate for 4 h in phosphate-free media after preincubation for 1 h in phosphate-free serum-free D-MEM. Cells were then stimulated with agonist for 15

min. Inhibitors were added 10 min prior to addition of agonists. After incubation, the media was removed and replaced with ice-cold 5% perchloric acid and kept on ice for 20 min. The material on the plate was removed by scraping, transferred to 15 mL conical tubes, and the precipitate collected by centrifugation (10 min at 3,000×g at 4°C). Phosphatidylinositides were extracted from the precipitate (pellet) with methanol:chloroform (1:1) and analyzed by TLC. Silica G plates (pre-run with 1.2% potassium oxalate in methanol:water (2:3) and heated at 110°C for 20 min) were developed in chloroform:acetone:methanol:acetic acid:water (80:30:26:24:14) and product separation was visualized by autoradiography at –80°C. Intensity of spots appearing on the autoradiographs was quantified by scanning densitometry with a BioRad Model-670 Imaging Densitometer and Molecular Analyst software.

4.9.4 PI3-kinase assay, *in vitro*

PI3-kinase was assayed *in vitro* after immunoprecipitation of the p85 subunit from cell lysates (refer to section 4.8.2). Protein G Sepharose beads were washed 3× with assay buffer (20 mM Tris-HCl (pH 7.6), 10 mM $MgCl_2$, and 100 mM NaCl) and resuspended in 90 µL assay buffer containing 20 µM [^{32}P]ATP. The reaction was initiated by adding 10 µL of a phosphoinositide mixture (equal volumes of phosphatidylserine, phosphatidylinositol, and $PI(4,5)P_2$ prepared in assay buffer, final concentration of 200 µg/mL). After a 20 min incubation at 37°C, the reaction was terminated by the addition of 200 µL 1 M HCl:methanol (1:1) and the samples extracted twice with 200 µL chloroform. The lipids, recovered from the combined organic phases by evaporation, were resuspended in 10 µL chloroform and analyzed by TLC as described in section 4.9.3.

4.9.5 p21-Ras activity assay

Quiescent cells (H4IIE and SMC prepared in 4-well culture dishes) were treated with agonist for 15 min after incubation with 200 mCi/L [^{32}P]orthophosphate as described in section 4.9.3. Inhibitors were added 10 –15 min prior to addition of agonists. The cells were then washed once in ice-cold PBS and lysed in 0.5 mL lysis buffer (50 mM Tris/HCl, pH 7.5, 150 mM NaCl, 5 mM $MgCl_2$, 1 mM $NaVO_4$, 1 mM PMSF, 1 mM DTT, 10 μg/mL aprotinin, 10 μg/mL leupeptin, 1% Triton X-100) for 20 min - 1 h on ice. The wells were then scraped and the lysate collected and centrifuged for 2 min at 12,000×g. The supernatant was then removed and aliquoted before storage at -80°C if not used immediately. A 0.5 mL aliquot of supernatant was cleared by rotating with Protein G Sepharose (25 μL) and/or 10% activated charcoal (100 μL) for 1 h at 4°C. The samples were then centrifuged for 5 min at 5000 rpm and the supernatant transferred to fresh tubes. Radioactivity in a 2 μL aliquot was then measured by liquid scintillation counting to ensure all comparisons were based on an equal level of radioactivity in each sample. The Ras immunoprecipitation protocol is identical to the procedure described in 4.8.2. Briefly, 15 μL of anti-Ras antibody was added to tubes containing $0.5 - 5 \times 10^7$ cpm and mixed for 2.5 h at 4°C. Protein G Sepharose (25 μL) was added for an additional 30 min while mixing and the beads collected by centrifugation (13,000 rpm for 1 min) in a fixed angle rotor. The Protein G Sepharose beads were then washed three times with 0.5 mL lysis buffer and twice with 0.5 mL PBS. The beads were then resuspended in 30 μL of 0.75 M KH_2PO_4 (pH 3.4), and boiled for 5 min. The beads were collected by centrifugation (13,000 rpm for 1 min) and, with care not to disturb the beads, the supernatant was spotted onto PEI-cellulose plates, 10 μL at a time (20 μL total supernatant spotted onto plates). The PEI-cellulose plates had been pre-treated with methanol and pre-spotted with 10 mM GDP and 10 mM GTP. The plates were then

developed in 0.75 M KH_2PO_4 (pH 3.4). When the running front was 2 cm from the top of the plate, the plate was removed from the developing chamber, allowed to air dry and autoradiography carried out at -80°C with one intensifying screen. Prior to this, the position of the GDP and GTP were marked onto the plates with pencil. A hand-held UV light source was used to illuminate the nucleotide phosphates. Once the autoradiographs were developed, the regions on the PEI-cellulose plate corresponding to the spots and the initial marked regions, were cut out and the radioactivity quantified by liquid scintillation counting.

4.9.6 Poly(ADP-ribose) polymerase (PARP) assay

Poly(ADP-ribose) polymerase activity was measured according to Zahradka & Ebisuzaki (1982) without inclusion of histone in the reaction. To each tube was added 110 µL of the reaction mix (0.1 M Tris/HCl (pH 8.0), 10 mM $MgCl_2$, 1.4 mM DTT, 0.1 mM NAD^+, 0.25 µCi [^{3}H]NAD^+ and 10% glycerol), 20 µL calf thymus DNA and 20 µL of the prepared nuclear extract (section 4.8.4). The mixture was then vortexed and placed into a 30°C water bath for 5 min. The enzyme reaction was stopped by placing the tube on ice and adding 1 mL of 20% TCA to the reaction mixture. The sample was then filtered onto GF/C glass fibre filters, washed extensively with 5% TCA and the radioactivity remaining on the filter quantified by liquid scintillation counting using a Beckman LS6500 Multipurpose Scintillation Counter.

4.9.7 Mono(ADP-ribosyl)transferase (mART) assay

The cytosolic and microsomal fractions obtained in section 4.8.4 were assayed for mono(ADP-ribosyl)transferase activity. Inhibitors of mART were first added to the designated tubes. To each tube was then added 70 µL of the reaction mix (70 mM Tris/HCl (pH 7.5), 0.1 mM NAD^+, 0.25 µCi [^{32}P]NAD^+, 0.1 mM PMSF), 10 µL acceptor protein (2 mg/mL polyarginine or 1 mg/mL histone H1) and 20 µL of cytosolic or

microsomal extract. The mixture was then vortexed, and incubated for 30 min at 30°C. The enzyme reaction was stopped by placing the tube on ice and adding 1 mL of 20% TCA. The sample was then filtered onto GF/C glass fibre filters or DE-81 filter paper, washed extensively with 5% TCA and the remaining radioactivity on the filter quantified by liquid scintillation counting using a Beckman LS6500 Multipurpose Scintillation Counter.

Alternatively, arginine-dependent mART activity was assayed in a total volume of 50 µL (50 mM Tris-HCl (pH 7.5), 100 µM [^{3}H]NAD$^+$) using 75 mM arginine methylester as the acceptor substrate (Tanigawa *et al.* 1984). A 30 µL aliquot was analyzed by TLC on Ionex-25 SA-Na plates (Machery-Nagel) with water as the developing solution. Since the position of ADP-ribosylated arginine-methylester could not be routinely visualized, the entire lane was cut into 1 cm sections and the radioactivity of each square quantified by liquid scintillation counting using a Beckman LS6500 Multipurpose Scintillation Counter.

4.9.8 Metabolic labeling of mono(ADP-ribosyl)ated proteins

Quiescent cells (H4IIE) were incubated in 12-well tissue culture dishes with 20 µCi [2,8-^{3}H]adenosine for 16 hours (Aboul-Ela *et al.* 1988). Following treatment with insulin, the cells were harvested by two possible methods. In method A, the cells were washed once with ice-cold PBS, and solubilized directly with 150 µL 2× SDS/gel loading buffer. The sample was then clarified by centrifugation (12,000×g, 10 min) and an aliquot of 25 µL was subsequently loaded onto a 10% polyacrylamide gel. In method B, the cells were scraped from the wells into 0.5 mL PBS using Cell Lifters (CoStar), collected by centrifugation (3,000×g, 5 min) and extracted with 25 µL lysis buffer (1% Nonidet P-40, 20 mM Tris/HCl, pH 7.5, 10% glycerol, 137 mM NaCl, 1 mM $MgCl_2$). Aliquots containing equivalent amounts of protein (25 µg), as determined by BCA protein assay,

were then mixed with an equal volume of 2× SDS/gel loading buffer and subjected to SDS/PAGE using a 10% polyacrylamide gel. The radioactivity present in the gels was detected by salicylate-enhanced fluorography (Zahradka & Ebisuzaki 1982), with Reflection film and one intensifying screen.

4.9.9 *In situ* gel assay for mART

This method was based on the MAP kinase in gel activity assay method of 4.9.1. Microsomal fractions prepared according to 4.8.4 were mixed with 3× sample buffer without β-mercaptoethanol (20 µL sample + 10 µL sample buffer), allowed to sit for 5 min at room temperature, and loaded onto a 10% polyacrylamide gel containing 0.2 mg/mL polyarginine. Following electrophoresis at 4°C for 1 h at 200 V, the gels were washed twice for 30 min in 2.5% Triton X-100 and once for 30 min in ice-cold ddH_20. The gels were then incubated for 1 h at 37°C in 10 mL of incubation buffer (50 mM Tris/HCl (pH 8.0), 5 mM DTT, 10 µM ADP-ribose, 10 µM NAD^+ and 25 µCi [^{32}P]NAD^+) followed by extensive washing in 5% TCA/1% sodium pyrophosphate (5 washes). The gels were dried onto 3MM Whatman paper and autoradiography carried out at -80°C with one intensifying screen.

4.9.10 *In situ* labelling of intact cells for detection of an extracellular mART

Cells (L6) were prepared in 6-well tissue culture dishes as described previously (section 4.2.2). The cells were rinsed in PBS and then incubated for 1 h at 37°C in 1 mL incubation buffer (PBS with 1 mM ADP-ribose, 5 µM NAD^+ and 25 µCi [^{32}P]NAD^+) with or without prior addition of ADP-ribosylation inhibitors (i.e. 3AB, PABA, MIBG, MIBA or PD128763). The cells were then washed twice in PBS and disrupted in 0.5 mL lysis buffer (3% SDS, 0.1 M NaOAc (pH 6.8) and 5 mM EDTA), followed by boiling for 10 min. An equal volume of 20% TCA was then added to the samples which were then placed on ice for 10 min. The samples were centrifuged (12,000 rpm for 10 min) and the

pellet washed twice with acetone and once with 70% ethanol. The pellet was dried and resuspended in 40 μL of 3× sample buffer containing 5% β-mercaptoethanol. The samples were run on a 10% polyacrylamide gel which was dried onto Whatman 3 MM paper and subjected to autoradiography at -80°C with two intensifying screens.

4.10 Nucleic acid manipulations

4.10.1 Oligodeoxynucleotide preparation

Oligodeoxynucleotides (ODNs) were prepared using an Oligo1000 DNA Synthesizer (Beckman) according to the manufacturer's recommended procedure. ODNs were synthesized for RT-PCR or UV-crosslinking.

ODNs generated:

1) GAPDH (s) 5'-CGGTGTGAACGGATTTGGCCGTAT-3'

   GAPDH (as) 5'-AGCCTTCTCCATGGTGGTGAAGAC-3',

2) c-*fos* (s) 5'-GAATAAGATGGCTGCAGCCAAGTGC-3'

   c-*fos* (as) 5'-AAGGAAGACGTGTAAGCAGTGCAGC-3'

3) MEF2 (s) 5'-CGTTGGCTATATTTATCTCT-3'

   MEF2 (as) 5'-AGAGATAAATATAGCCAACG-3'

4.10.2 RNA preparation

Total RNA was isolated from cells (SMC) prepared in 6-well culture dishes using TRIzol. After treatment, cells were rinsed twice in PBS and 1.0 mL TRIzol was added to each well. Lysates were transferred to microfuge tubes, extracted with 500 μL chloroform and centrifuged for 10 min at 11,000×g. The aqueous phase was transferred to fresh microfuge tubes and precipitated with an equal volume of isopropanol. Precipitated RNA was collected (10 min at 11,000×g) and the pellets washed and stored in 70% ethanol at –20°C.

4.10.3 RT-PCR

RNA stored in 70% ethanol was collected by centrifugation (10 min at 11,000×g) and allowed to air dry. The RNA was resuspended in 25 µL RNase-free water containing 25 IU/L of RNase inhibitor, and concentration determined by spectrophotometic absorbance at 260-nm. Reverse transcription of 1 µg of RNA was conducted according to the protocol recommended for the GeneAmp kit from Perkin Elmer-Cetus using oligo-dT as the primer and 1 IU of reverse transcriptase enzyme (MuLV Reverse Transcriptase). For PCR, 25 ng sense and antisense primers and 1.25 IU Amplitaq *Taq* DNA polymerase (GeneAmp kit) were added to each RT-reaction (50 µL final volume). Amplification was conducted over 35 cycles using a three-step program (1 min at 95°C, 1 min at 55°C, 1 min at 72°C; annealing and elongation temperatures were varied slightly depending on the primers being used) that was concluded with 7 min at 72°C. Samples were analyzed by electrophoresis in 1.7% agarose gels and visualized with SYBR Green I (Molecular Probes). Photographs were then taken using a Polaroid DS34 Direct Screen Instant Camera fitted with an EP-H6 0.8× hood and green filter and Polaroid 667 black and white instant film. Band intensity on the photographs was quantified by scanning densitometry with a BioRad Model-670 Imaging Densitometer and Molecular Analyst software. Control reactions (minus RNA, minus RT and minus primers) were used to demonstrate the specificity of the PCR reaction.

4.11 Data measurement and statistical analysis

Radiotracer incorporation, cell number and morphometric data were quantified and presented as means ± SEM of individual experiments conducted in triplicate. Student's t-test (paired and unpaired) was used to compare treatment means versus controls. Statistical significance was set at $p < 0.05$.

Quantification of data obtained on film or autoradiographs was accomplished with a BioRad Model-670 Imaging Densitometer under non-saturating conditions. Background subtraction was achieved by reading the absorbance of an equal sized region directly adjacent (above, below or beside) to the band. Although multiple exposures were acquired to ensure the absence of film saturation, the experimental figures typically show longer exposures selected specifically for visual presentation and not used for data analysis.

5.0 H4IIE rat hepatoma cells as a model of cell proliferation

5.1 Introduction

Historically, interest in the mammalian hepatic cell began when the unique function that the cell serves in governing the relationship of the external environment to the internal "milieu" was recognized (Pitot *et al.* 1964). The metabolic flexibility of hepatic cells was identified by early workers who studied the effect of dietary intake and composition on the enzymatic content of the liver (Knox *et al.* 1956). It was found that specific small molecules controlled the alteration in liver enzymes (Civen & Knox 1960; Feigelson & Greengard 1961; Knox 1951; Lee 1956). Moreover, hepatic cells respond to environmental cues that influence enzyme levels and modulate the metabolic plasticity of these cells (Pitot *et al.* 1964). Of note, biologic alterations such as regeneration and cirrhosis do not alter the response to environmental stimuli (Pitot 1959; Thomson & Moss 1955).

The neoplastic hepatic cell, or hepatoma, has mainly been studied in relation to enzymatic differences with normal hepatic cells. It was hoped that perhaps a "simple" alteration in the biochemistry of the cell would account for its malignant phenotype. On the contrary, it was found that different types of hepatic carcinomas contained vastly different modifications with respect to cellular metabolism and function. Moreover, some hepatic carcinomas exhibited little similarity to the hepatocyte while others very closely resembled liver, and each type of tumour differed in terms of its morphology and behaviour (Novikoff 1961; Pitot 1962; Pitot *et al.* 1964). As a result, it became of interest to study these cellular systems in isolation, to define the absolute characteristics and enzymatic responses in the absence of other environmental cues (Murray & Kopech 1953).

The H4IIE hepatoma cell line is an experimental (solid) tumour cell line originating from the Reuber H-35 hepatoma, a well-differentiated hepatocellular carcinoma induced by a chemical carcinogen (Morse *et al.* 1961; Pitot *et al.* 1964; Reuber 1961). These cells have been in culture since 1961, and are used primarily for biochemical and cytogenetic investigations (DeLuca *et al.* 1972; Haggerty *et al.* 1975; Kovacs *et al.* 1977; Miller *et al.* 1972; Potter *et al.* 1967; Reel & Kenney 1968). The generation of this particular line was an attempt to achieve a virtually pure culture of a serially propagated cell line that could be used for determining the levels of metabolic enzymes in comparison to liver and other hepatomas (Pitot *et al.* 1964). It was hoped that the biochemical properties of normal and malignant liver growing *in vitro* could be rationally compared, even though at the time a "normal liver" equivalent of the hepatoma was not available. Furthermore, the H4IIE tumour cell system provides an opportunity to investigate quantitatively several general areas of both solid tumour therapy and of radiobiological principles in neoplastic cells, along with the ability to study tumour growth and cell proliferation and to monitor the clonogenic potential of tumour cells following therapy (Evans & Kovacs 1977).

The H4IIE cell line can be maintained and studied either in cell culture or as a transplantable solid tumour in ACI male rats (Evans & Kovacs 1977). In addition, it allows for the *in vitro* assay of cell survival following treatment of animal tumours *in situ* (i.e. clonogenicity of primary tumour to treatment efficacy) (Evans & Kovacs 1977). H4IIE hepatoma cells are considered to be a poorly differentiated hepatoma, with loss of connective tissue and an increased growth rate (Evans & Kovacs 1977). H4IIE cells form rather typical epithelial colonies, and the morphology *in vivo* is almost identical to its original parent line, the H-35 (Pitot *et al.* 1964). The cell line retains the ability to cause neoplasms that are almost indistinguishable biochemically and morphologically from the

original explanted hepatocellular carcinoma tissue (Pitot *et al.* 1964). Interestingly, several enzymes present in the liver and in H-35 cells are absent from the H4IIE, including tryptophan pyrrolase, glucose-6-phosphate dehydrogenase and proline oxidase. However, the hepatic marker enzymes histidase, ornithine transaminase, tyrosine transaminase, thymine reductase and glucokinase are present at measurable levels (Pitot *et al.* 1964).

In this laboratory, interest in H4IIE cells came from earlier work aimed at defining the regulation of the phosphoenolpyruvate carboxykinase gene (PEPCK) by insulin (Yau and Zahradka, unpublished observations; Yau *et al.* 1998). The function and regulation of this enzyme was of interest due to its strategic positioning in the glycolytic/gluconeogenic pathway, which is of primary importance in liver cells, and the expression of this gene is acutely regulated by several different hormones including insulin and glucagon (Beale *et al.* 1984; Christ *et al.* 1988). H4IIE cells provided a convenient cell culture system that, although phenotypically different from primary hepatocytes in many ways, was similar enough with respect to the metabolic pathways of glucose storage and release that the system was feasible to work with.

As the work evolved, it became clear that H4IIE hepatoma cells would provide a good model of cell proliferation with the ability of this cell line to proliferate in response to a single growth factor, insulin. Moreover, with insulin being a key factor in both proliferation and metabolic regulation, interactions between the two events could be monitored (especially with respect to the possibility of neoplasia and malignancy). Furthermore, because this hepatoma cell line was considered to be less differentiated than other hepatoma cell lines, especially in comparison to hepatocytes, the potential to examine the spectrum between differentiation and proliferation was available. As a result, when studies dealing with MIBG were first proposed, it was with respect to ADP-

ribosylation and its control of metabolic events in H4IIE cells (i.e. PEPCK gene expression via insulin). As the growth inhibitory properties of MIBG came to light, the utility of the H4IIE model as a model of cell proliferation became apparent. H4IIE cells were abundant, easy to culture and responded to insulin by initiating growth events. Thus, the initial studies with MIBG were carried out in this cell line.

Based on this information, a specific hypothesis was proposed: *Insulin-mediated growth and proliferation of H4IIE hepatoma cells will be inhibited by MIBG through inhibition of a specific cellular signaling pathway that will involve an ADP-ribosylation reaction.*

This goal was achieved by i) defining the cellular system, ii) testing the efficacy of the inhibitor in the system, and iii) examining the signaling components that might be involved.

5.2 Mitogenic actions of insulin and IGF-1

5.2.1 Background and rationale

The liver plays a central role in glucose metabolism and is one of the major targets for insulin. Glycolysis, glycogenolysis and gluconeogenesis are among the processes controlled by insulin in response to nutritional status. For example, the elevation of blood glucose levels leads to insulin release from the pancreas, which results in increased glucose uptake by the liver, stimulation of glycogen synthesis and inhibition of both gluconeogenesis and glycogenolysis. Although regulation of liver metabolism is the major function for insulin, insulin also promotes liver regeneration following hepatectomy (Bucher & Swaffield 1975). Since liver regeneration involves hepatocyte growth and proliferation, insulin must function as a growth factor for certain cell types, much like IGF-1 (Gressner *et al.* 1995). However, it is unclear whether the hepatic

growth response to insulin is mediated solely by the insulin receptor and its affiliated signaling systems or if participation of IGF-1 is also required.

While insulin, IGF-1 and their respective receptors share a high degree of homology, the cellular response to each peptide is well defined. In mammals, insulin is the primary regulator of glucose metabolism influencing both glucose uptake and utilization. These effects occur as a result of changes in both protein activity, as mediated by post-translational modification, and *de novo* protein synthesis (Czech 1977). In contrast, the effect of IGF-1 on the metabolic pathways associated with glucose utilization is limited (Cohick & Clemmons 1993), although it has been shown to modulate certain aspects of hepatic glucose metabolism (Freemark *et al.* 1985; Heaton *et al.* 1980; Verspohl *et al.* 1984). Nevertheless, IGF-1 cannot fully substitute for insulin in mice lacking the insulin receptor (Di Cola *et al.* 1997). For these reasons, IGF-1 is primarily considered a growth factor that influences cell proliferation by directly stimulating transit through the cell cycle. Support for this function has been provided by the identification of IGF-1 as a critical factor for G_1 progression (Baserga *et al.* 1994), and by its mitogenic actions on skeletal muscle, NIH-3T3 cells and fibroblasts (Coolican *et al.* 1997; Knebel *et al.* 1997; Scrimgeour *et al.* 1997; Takata *et al.* 1996). Although the functions of insulin and IGF-1 differ, the structural similarity of both the peptides and their receptors results in heterologous binding. Sufficient specificity exists, however, that these heterologous interactions occur with an approximately 100-fold reduced affinity (Massague & Czech 1982).

Insulin and IGF-1 receptors are $\alpha_2\beta_2$ heterotetramers. The α subunit present on the external surface of the cell contains the ligand-binding domain. Signals from the α subunit are conducted into the cell by the β subunit, a transmembrane polypeptide with an intrinsic tyrosine kinase activity (De Meyts *et al.* 1994; White & Kahn 1994).

Activation of the kinase results in the stimulation of an intracellular phosphorylation cascade which influences various processes associated with cell growth and metabolism Although the cellular response to insulin and IGF-1 is usually distinct, a similar set of intracellular mediators participate in both signal-transduction systems. For example, insulin receptor substrate-1 (IRS-1), phosphatidylinositol 3-kinase (PI3-kinase) and Syp interact directly with insulin and IGF-1 receptors (Seely *et al.* 1995). Ligand-binding to the receptor also triggers p21-Ras and leads to activation and translocation of MAP kinase to the nucleus where it mediates the phosphorylation of specific transcription factors (Karin 1996). MAP kinase is therefore important for the propagation of signals from cell surface receptors into the nucleus.

The stimulation of H4IIE hepatoma cell growth and glucose metabolic pathways by insulin makes this cell line an ideal model for characterizing the role of both insulin-dependent and insulin-independent signaling systems (Lauris *et al.* 1986; Mohn *et al.* 1991; Taub *et al.* 1987). This laboratory also recently found that H4IIE cells also express IGF-1 receptors (Zahradka *et al.* 1998). The present study was thus initiated to compare the effect of insulin and IGF-1 on cell proliferation and metabolism, with an emphasis on the signaling pathways that mediate these cellular processes.

5.2.2 Specific aims

1. To establish the growth and metabolic response of H4IIE cells to insulin and IGF-1.
2. To identify the signaling pathways stimulated in H4IIE cells in response to insulin and IGF-1 administration.
3. To determine the relative importance of MAP kinase activation for the activation of H4IIE cellular growth by insulin.

5.2.3 Experimental design

H4IIE cells were cultured according to standard conditions as suggested by ATCC (section 4.2.1). Cells were passaged every second day and maintained in 10% FBS/α-MEM. For most experiments, H4IIE cells were employed when quiescent, a state obtained by incubating cells in serum free α-MEM for 72 h. Growth of cells in culture was measured by [^{3}H]thymidine and [^{3}H]uridine incorporation, and cell number was measured with the MTT (mitochondrial reduction of tetrazolium compound) assay after administration of both insulin and IGF-1. Western blot analysis was used to monitor changes in protein phosphorylation and activation of specific protein kinases and adapter proteins participating in the receptor-mediated signal transduction pathways that contribute to insulin and IGF-1 stimulated growth of H4IIE cells. An inhibitor of the MAP kinase pathway, PD98059, which is specific for MEK (MAP kinase kinase), was included to determine the relative importance of this signaling pathway to insulin-mediated H4IIE cell growth.

5.2.4 Results

5.2.4.1 Growth characteristics of H4IIE cells in response to insulin

The response of H4IIE cells to serum withdrawal and insulin addition was monitored over set periods of time. Subconfluent H4IIE cells were placed into serum-free α-MEM and the rate of DNA synthesis at specific time points measured by pulse-labeling with [^{3}H]thymidine over a 30 min period. Over 140 h, the rate of DNA synthesis declined considerably in comparison to growing cells (Figure 2A). By approximately 72 h in serum free α-MEM, a low, steady-state level of DNA synthesis indicative of quiescence was achieved (i.e. the cells have stopped progressing through and possibly have exited from the cell cycle). Although cell viability assays were not conducted, there was no

evidence of cell death by microscopic examination (data not shown), and the ability of quiescent H4IIE cells to re-enter the cell cycle was assumed to indicate that the cells remained healthy and viable (Figure 2B). As a result of this experiment, H4IIE cells were subjected to a 72 h incubation in serum free α-MEM before initiation of most experiments.

Although the ability of insulin to function as a mitogen in H4IIE cells has already been described previously by our laboratory (Yau *et al.* 1998; Zahradka & Yau 1994), synchronous re-entry of quiescent H4IIE cells into the cell cycle was established by measuring the rates of both DNA and RNA synthesis over a period of 24 h after stimulating the cells with insulin (10^{-6} M). Insulin was able to stimulate the H4IIE cells to re-enter the cell cycle as indicated by the onset of DNA synthesis at approximately 6-8 h after treatment. This experiment also showed that S phase peaked at approximately 14 h (Figure 2B). In addition, insulin was able to stimulate the incorporation of [^{3}H]uridine which was linear for a period of more than 10 h (Figure 2C) indicating an increase in cellular activity. This RNA synthesis experiment provided the time frame (6 h) for all subsequent studies that employed [^{3}H]uridine incorporation as a measure of cellular activity and growth.

To determine whether insulin was required for the entire period of a growth assay, an insulin washout study was carried out, monitoring both the rates of RNA and DNA synthesis. It was observed that a 5 min exposure to insulin was sufficient to maximally stimulate both RNA and DNA synthesis (Figure 3). These data indicate that insulin works rapidly and "early" as a growth factor in this particular cell type, and that the intracellular signals generated by the binding of insulin to its receptor are sufficient to initiate the cascade of events required for enhanced growth.

FIGURE 2: ***Response of H4IIE Cells to Insulin Withdrawal and Addition.***

(A) Subconfluent H4IIE cells were placed into serum-free α-MEM and the DNA synthetic rate monitored at specific time points by addition of 2 μCi [^{3}H]thymidine for 30 min. The cells were subsequently lysed and the incorporation of radiolabel into DNA measured as described in Materials and Methods (section 4.3.1). No loss of cell viability was evident after 5 days under serum-free conditions. (B) DNA synthesis was measured according to section 4.3.2 after addition of insulin (10^{-6} M) to quiescent H4IIE cells that had been maintained under serum-free conditions for 72 h. The cells were pulse-labelled with [^{3}H]thymidine for 30 min at the specified time points. (C) Measurement of RNA synthesis was conducted as described in section 4.3.1 after addition of insulin (10^{-6} M) to quiescent H4IIE cells that had been maintained under serum-free conditions for 72 h. The cells were pulse-labelled with [^{3}H]uridine for 30 min at the specified time points. The data are presented as the mean ± SE of at least three separate experiments conducted in triplicate.

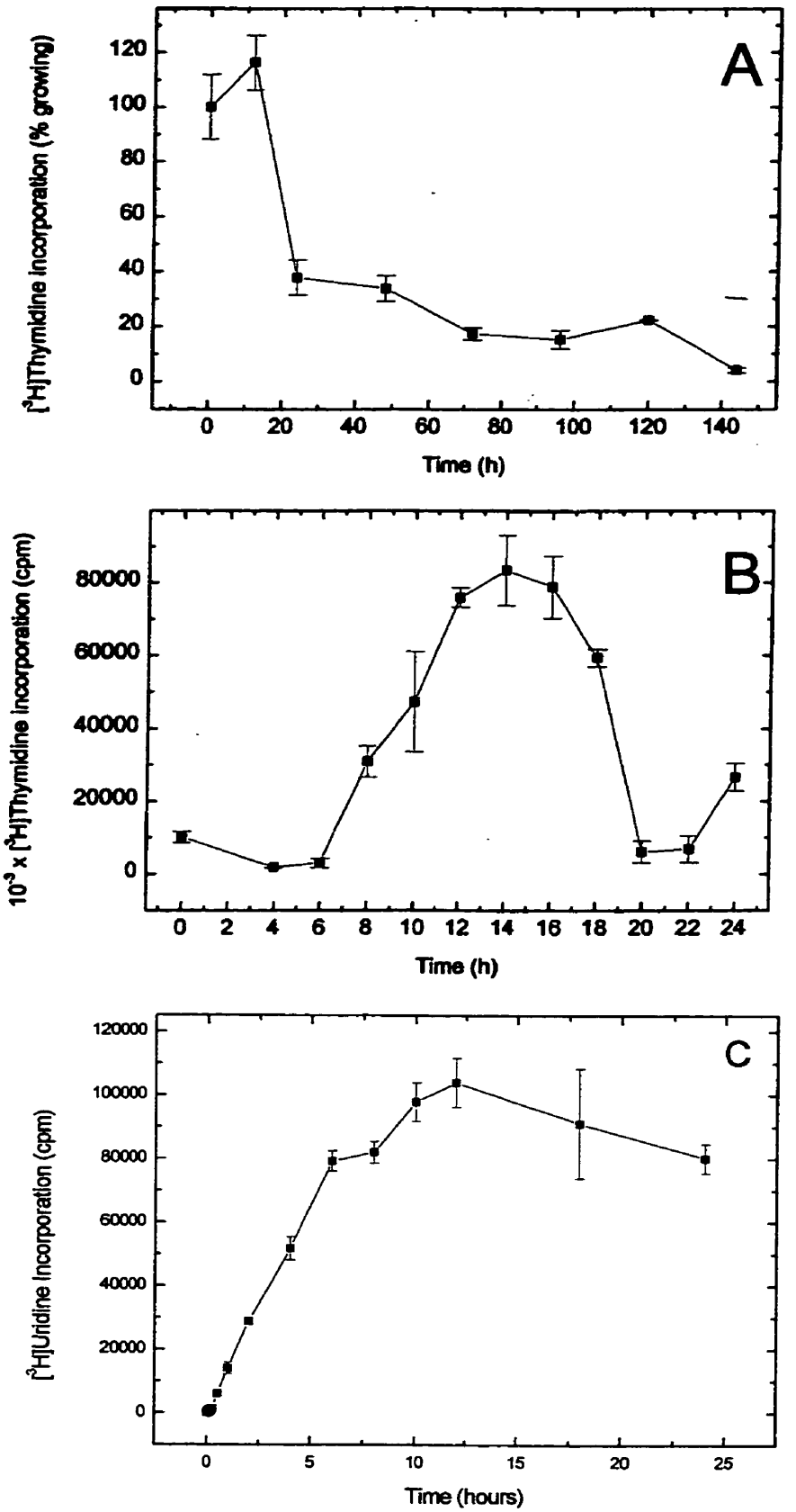
A
[³H]Thymidine Incorporation (% growing)
120
100
80
60
40
20
0
0
20
40
60
80
100
120
140
Time (h)
B
10⁻³ x [³H]Thymidine Incorporation (cpm)
80000
60000
40000
20000
0
0
2
4
6
8
10
12
14
16
18
20
22
24
Time (h)
C
[³H]Uridine Incorporation (cpm)
120000
100000
80000
60000
40000
20000
0
0
5
10
15
20
25
Time (hours)

FIGURE 3: ***Effect of Insulin Exposure on Cell Growth Response.***

The rate of DNA synthesis (A) and the rate of RNA synthesis (B) were measured by incorporation of [^{3}H]thymidine and [^{3}H]uridine, respectively, after addition of insulin (10^{-6} M) to quiescent H4IIE cells. At the time points indicated (min to h), the insulin was removed from the cells and the media replaced with serum-free α-MEM for the remainder of the assay period. The radiolabel was present for the duration of the assay. No insulin was added to the cells at the zero time point, while insulin was present for the entire period in the 6 h time point. The data are presented as the mean ± SE of at least three separate experiments conducted in triplicate.

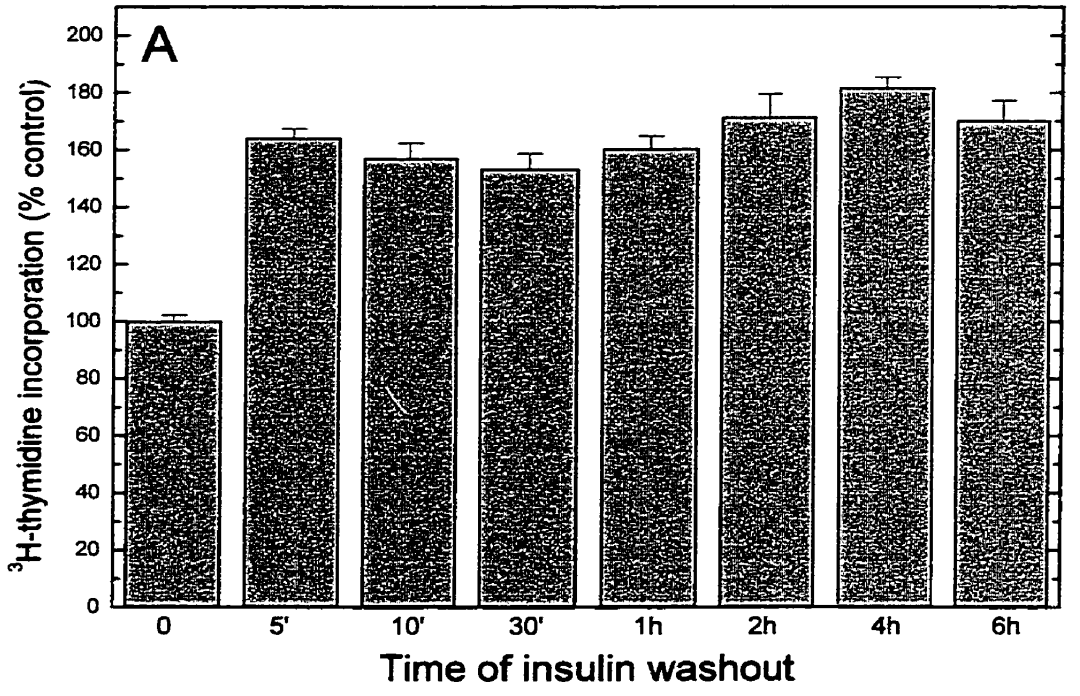
A
^{3}H-thymidine incorporation (% control)
200
180
160
140
120
100
80
60
40
20
0
0
5'
10'
30'
1h
2h
4h
6h
Time of insulin washout

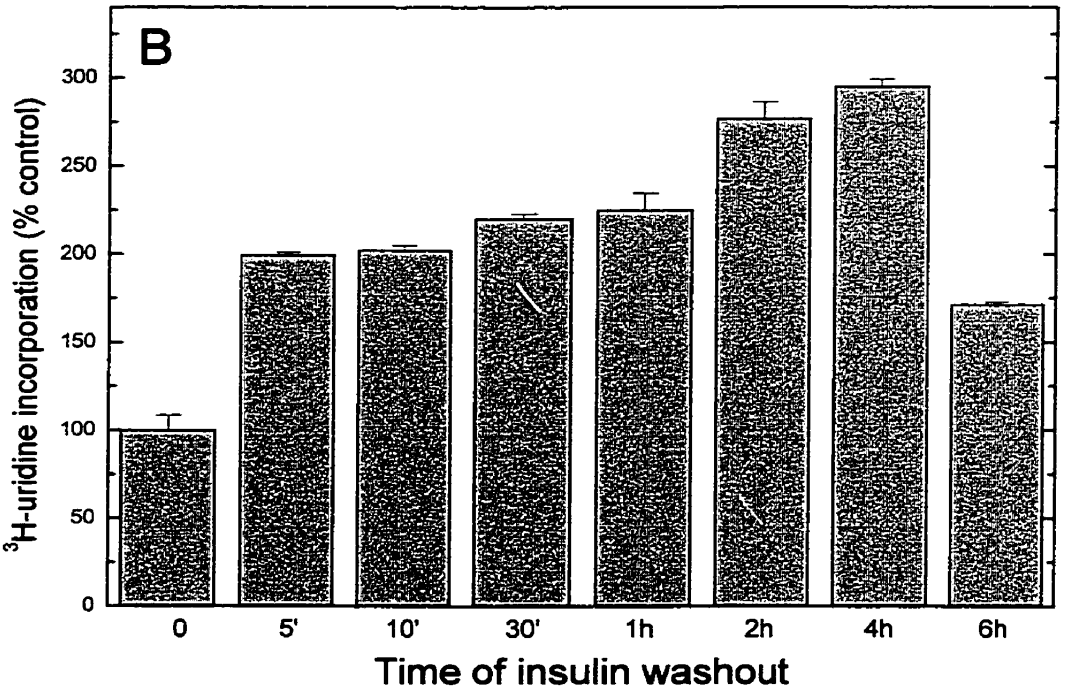
B
^{3}H-uridine incorporation (% control)
300
250
200
150
100
50
0
0
5'
10'
30'
1h
2h
4h
6h
Time of insulin washout

5.2.4.2 Growth and metabolic response of H4IIE cells to insulin and IGF-1

In many cell systems, IGF-1 is considered to be a potent stimulator of growth and is classified as a progression factor with respect to cell cycle kinetics (Baserga *et al.* 1994). Based on the studies in section 5.2.4.1, it could not be ruled out that IGF-1 and/or its receptor participate in the process of insulin-mediated H4IIE growth. As a result it was of interest to determine if H4IIE cells, which are reported to be responsive to insulin alone (Figure 2; Yau *et al.* 1998), are also influenced by IGF-1. Both insulin and IGF-1 were able to significantly stimulate RNA and DNA synthesis (Figure 4A,B) in a concentration-dependent manner (10^{-12} to 10^{-7} M), reaching a maximum effect at 10^{-7} M. However, insulin was able to stimulate a greater response than IGF-1 at a concentration two orders of magnitude lower (10^{-9} M compared to 10^{-7} M, respectively) (Figure 4A,B). Furthermore, although increased DNA synthesis is a good indicator that cell proliferative processes have been triggered, it does not guarantee that cell division will occur. Therefore, the effect of insulin and IGF-1 on cell number was monitored 72 h after addition of the peptides to quiescent H4IIE cells (Figure 4C). As observed with the growth assays, insulin increased cell number at 10^{-9} M while 10^{-7} M IGF-1 was required before an equivalent increase in cell number was obtained. Taken together, these results indicate that insulin is a significantly stronger mitogen than IGF-1 in this cell type. Moreover, the difference in effective concentrations of insulin and IGF-1 eliminates the possibility that the growth response occurs as a result of insulin cross-reacting with IGF-1 receptors. Furthermore, since the relative affinity of IGF-1 for the insulin receptor is 100-fold less than that for insulin (Massague & Czech 1982) the converse is also unlikely. The results obtained with this experiment thus indicate that mitogenesis is mediated by the insulin receptor of H4IIE cells.

FIGURE 4: ***Comparison of Mitogenic Effects of Insulin and IGF-1 on Quiescent H4IIE Hepatoma Cells.***

RNA and DNA synthesis were monitored after treatment of quiescent H4IIE cells with varying concentrations (10^{-12} to 10^{-7} M) of insulin and IGF-1. The incorporation of [^{3}H]uridine (6 h incubation) and [^{3}H]thymidine (24 h incubation) into trichloroacetate-precipitable material after addition of insulin of IGF-1 was used as an indication of RNA (A) or DNA (B) synthetic activity. The incorporation rate of untreated cells was set to 100%. (C) Cell number was measured using the conversion of MTT at 550-nm as described in Materials and Methods (section 4.3.3). The assay was conducted 72 h after addition of insulin or IGF-1 (10^{-12} to 10^{-7} M). The data are presented as the mean ± SE of at least three separate experiments conducted in triplicate.

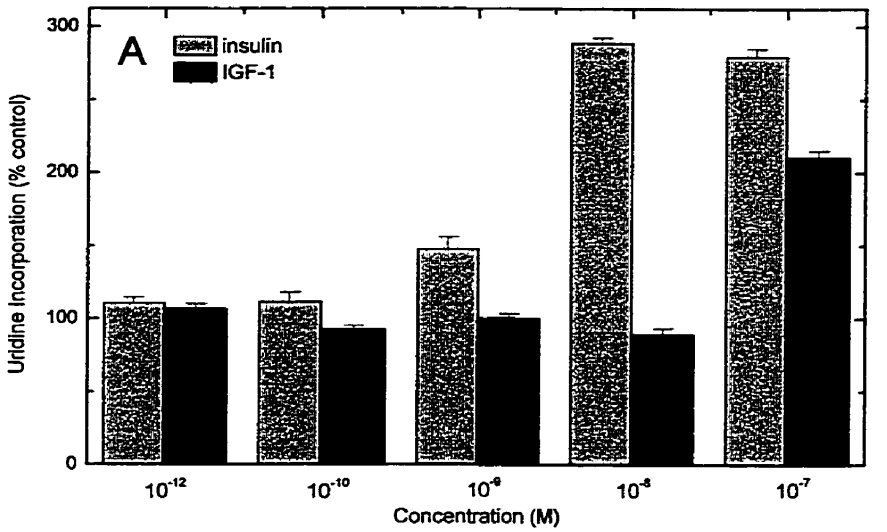
A
insulin
IGF-1
Uridine Incorporation (% control)
300
200
100
0
10^{-12}
10^{-10}
10^{-9}
10^{-8}
10^{-7}
Concentration (M)

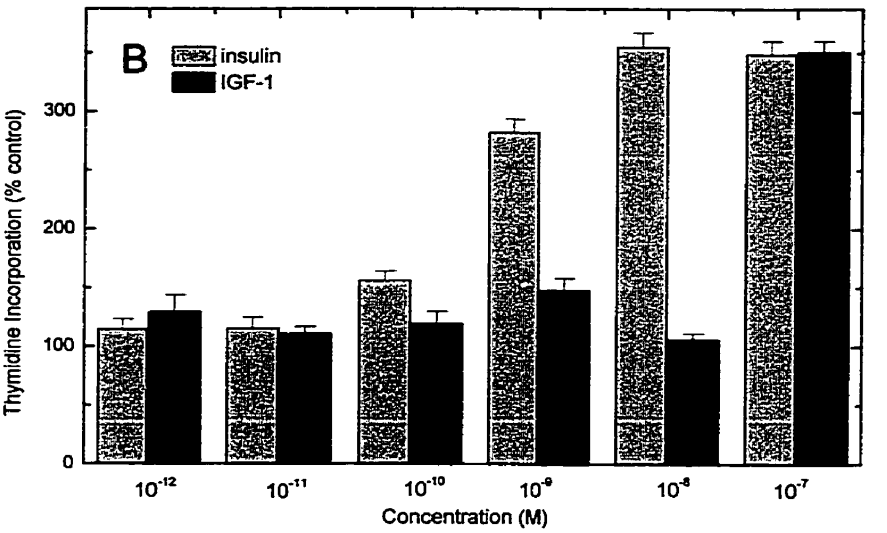
B
insulin
IGF-1
Thymidine Incorporation (% control)
300
200
100
0
10^{-12}
10^{-11}
10^{-10}
10^{-9}
10^{-8}
10^{-7}
Concentration (M)

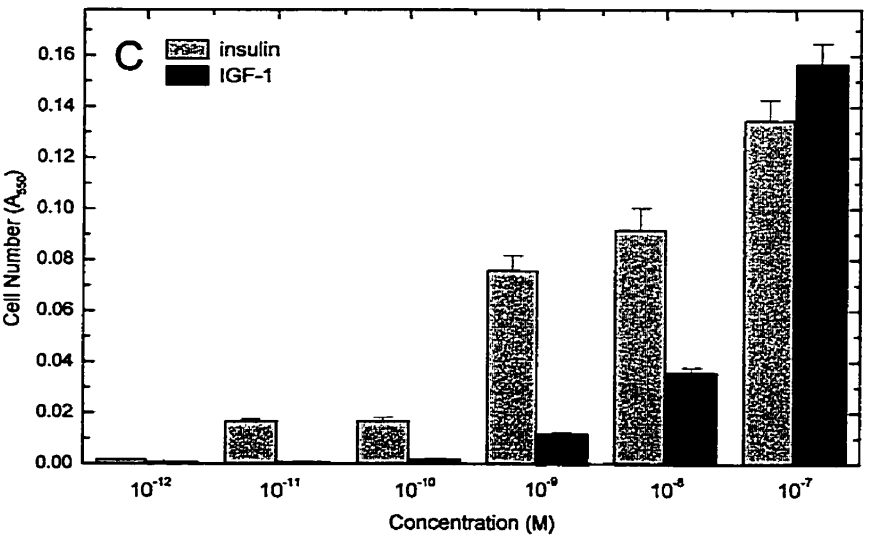
C
insulin
IGF-1
Cell Number (A_{550})
0.16
0.14
0.12
0.10
0.08
0.06
0.04
0.02
0.00
10^{-12}
10^{-11}
10^{-10}
10^{-9}
10^{-8}
10^{-7}
Concentration (M)

Insulin in most cell systems (eg. skeletal muscle and liver) is a metabolic activator and regulator of events such as glucose uptake and usage (Czech 1977). For example, insulin controls glucose utilization by the liver, influencing glucose uptake, glycogen synthesis, glycolysis and gluconeogenesis. Under the experimental conditions established, H4IIE cells responded to insulin (10^{-9} M) by taking glucose up into the cell as would be expected in physiologically relevant systems such as the liver (Figure 5). In contrast, IGF-1 was unable to enhance glucose uptake over a small concentration range (10^{-9} to 10^{-7} M). Serum (2% v/v FBS), which contains insulin and many other growth factors, was used as the positive control for comparing the increased glucose uptake generated by either insulin or IGF-1 (Figure 5). These results clearly demonstrate that the IGF-1 receptor does not modulate glucose metabolism in H4IIE cells.

5.2.4.3 Signaling components of the H4IIE response to insulin and IGF-1

Binding of insulin to its receptor initiates an intracellular signaling cascade that involves protein tyrosine phosphorylation (Frattali *et al.* 1992; Wilden *et al.* 1992). Although IGF-1 activates a similar cascade in most systems responsive to this peptide (Kato *et al.* 1993; LeRoith *et al.* 1995), it remains unclear how the IGF-1 signaling system produces a response that is different from insulin. To address this issue, a study of the relationship between protein tyrosine phosphorylation events and insulin or IGF-1 ligand binding was conducted. Treatment of H4IIE cells with insulin (10^{-9} M) resulted in a rapid phosphorylation of proteins with molecular mass 60-, 95-, 125- and 180-kDa, as detected with an antibody specific for phosphotyrosine (Figure 6A), although the change in the 125-kDa protein (assumed to be $p125^{FAK}$) was much less obvious. These proteins remained phosphorylated over the 120 min time course of the experiment. In contrast, phosphorylation of these same proteins was considerably less when the cells were treated with 10^{-9} M IGF-1. A concentration curve of insulin and IGF-1 indicated that IGF-1 was

FIGURE 5: ***Comparative Metabolic Effects of Insulin and IGF-1 on Quiescent H4IIE Hepatoma Cells.***

The incorporation of [^{3}H]glucose was measured as described in Materials and Methods (section 4.3.8) after addition of serum (2% v/v FBS), insulin (10^{-9} M) or IGF-1 (10^{-9} to 10^{-7} M) to quiescent H4IIE cells. The rate of uptake in untreated cells was set to 100%. Each data point represents the mean ± SE of at least three individual experiments conducted in triplicate.

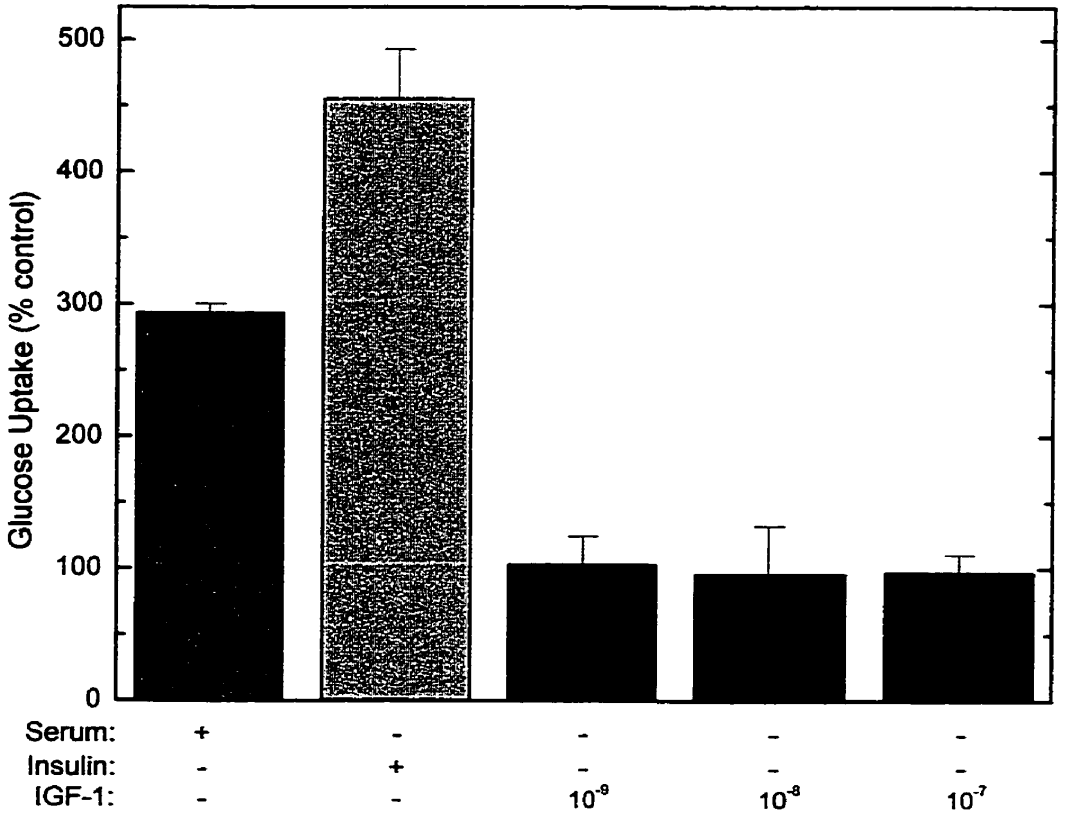
Glucose Uptake (% control)
500
400
300
200
100
0
Serum: + - - - -
Insulin: - + - - -
IGF-1: - - 10-9 10-8 10-7

able to stimulate a level of p180 and p95 phosphorylation that was approximately equivalent to that obtained with 10^{-8} M insulin, but only when IGF-1 was applied at a concentration of 10^{-6} M (Figure 6B). p95 was identified as either the insulin or IGF-1 receptor β-subunit (Zahradka *et al.* 1998). However, to distinguish between the receptors for insulin and IGF-1 in terms of their phosphorylation state, cell extracts were immunoprecipitated with receptor-specific antibody after treatments and subsequently examined for tyrosine phosphorylation (Figure 6C). The insulin receptor was modified after addition of insulin (10^{-8} M)but not IGF-1 (10^{-8} M). The IGF-1 receptor was not modified under any treatment condition. Measurement of receptor kinase activity revealed that the insulin receptor kinase was activated by insulin treatment while the IGF-1 receptor kinase was not activated by IGF-1 treatment (data not shown; refer to Yau *et al.* 1999). The lack of detectable tyrosine phosphorylation after IGF-1 treatment may suggest that the IGF-1 receptor kinase is inactive as a result of either a mutation in the receptor or a defect in the kinase, since H4IIE cells have been shown to express IGF-1 receptors capable of binding IGF-1 (Zahradka *et al.* 1998).

The phosphoprotein at 180-kDa is presumed to be IRS-1, however, several other proteins of similar molecular mass may be targets for receptor-mediated phorphorylation as well. As a result, the degree of IRS-1 phosphorylation was assessed using extracts prepared from cell that had been treated with insulin or IGF-1 (both at 10^{-8} M) for 10 min. The samples were immunoprecipitated with an antibody to phosphotyrosine and the IRS-1 content determined by Western blot analysis (Figure 6D). This experiment indicated that IRS-1 is minimally phosphorylated in quiescent H4IIE cells and that only treatment with insulin increases the level of IRS-1 phosphorylation. These data suggest that the limited tyrosine phosphorylation of a 180-kDa protein following IGF-1 treatment

FIGURE 6: ***Tyrosine Phosphorylation of H4IIE Proteins after Treatment with Insulin and IGF-1.***

(A) Quiescent H4IIE cells, prepared in 12-well culture dishes containing 1 mL media, were treated with 10^{-8} M insulin or 10^{-8} M IGF-1 and harvested by direct addition of SDS/gel loading buffer (as described in Materials and Methods, section 4.8.3) at the indicated time points. Samples were subjected to SDS/PAGE (7.5% gel), transferred to PVDF membrane and immunostained with PY20 anti-phosphotyrosine monoclonal antibody (diluted 1:5000). The antibody was visualized with HRP-coupled anti-mouse IgG and the ECL chemiluminescent detection system. Pre-stained molecular mass markers were run in parallel with the samples and were used to identify the bands. Identical results were obtained in two independent experiments of which one representative blot is shown. (B) Cells were harvested for Western blot analysis 5 min after addition of insulin or IGF-1 (10^{-11} to 10^{-6} M). After SDS/PAGE and transfer to PVDF membrane, PY20 antibody was used to monitor tyrosine phosphorylation. Pre-stained molecular mass markers were run in parallel with the samples and were used to identify the bands. Identical results were obtained in three independent experiments of which one representative blot is shown. (C) Cells were lysed for immunoprecipitation (IP) as described in Materials and Methods (section 4.8.2) 5 min after addition of insulin or IGF-1 (10^{-8} M). The protein content of each sample was measured by BCA protein assay, and equal 100 μg protein aliquots were incubated with antibody (3 μg) to either the insulin receptor β-subunit (insulin-R) or the IGF-1 receptor β-subunit (IGF1-R). The antibody-antigen complexes were collected with protein G Sepharose, solubilized by heating in SDS/gel loading buffer and subjected to SDS/PAGE. After transfer of the proteins to PVDF membrane, tyrosine phosphorylation was detected with PY20 antibody (diluted 1:5000). Pre-stained molecular mass markers were run in parallel with the samples and were used to identify the bands. Comparable results were obtained in two independent experiments. (D) Proteins were resolved by SDS/PAGE after immunoprecipitation with anti-phosphotyrosine antibody (3 μg). The membrane was subsequently probed for IRS-1 using an IRS-1 specific antibody (diluted 1:1000). The cells were untreated (lane C) or treated with 10^{-8} M insulin (lane Ins) or 10^{-8} M IGF-1 (lane IGF) for 5 min before cell lysis. Comparable results were obtained in three independent experiments.

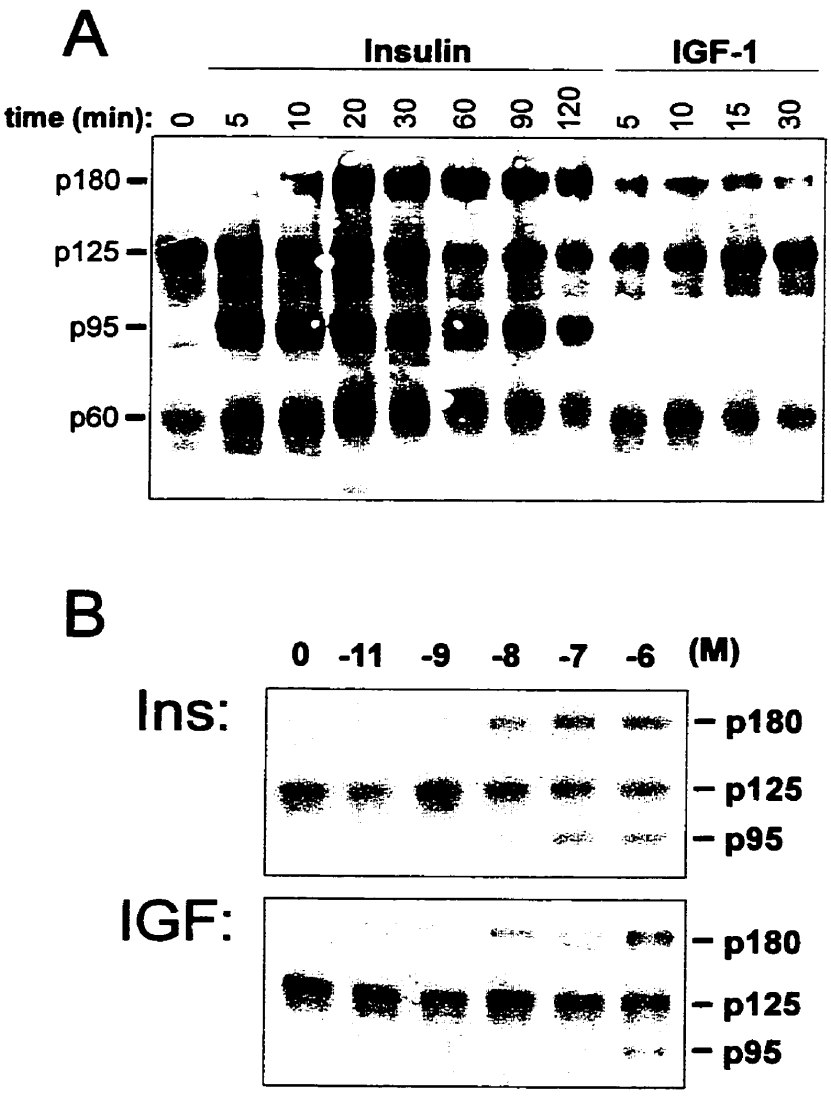
A
Insulin
IGF-1
time (min): 0 5 10 20 30 60 90 120 5 10 15 30
p180
p125
p95
p60
B
0 -11 -9 -8 -7 -6 (M)
Ins:
IGF:
p180
p125
p95
p180
p125
p95

C

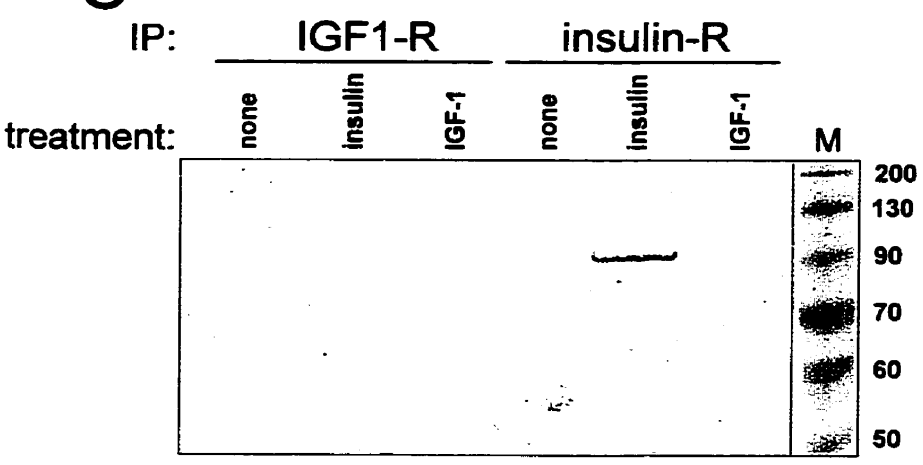
IP:
IGF1-R
insulin-R
treatment:
none
insulin
IGF-1
none
insulin
IGF-1
M
200
130
90
70
60
50

D

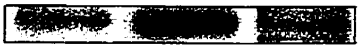
C
Ins
IGF

(Figure 6A) does not represent modification of IRS-1, but that of another protein with similar molecular mass, possibly IRS-2.

Mitogen activated protein (MAP) kinase is considered to be an essential signaling component for the growth of a variety of cell types (Adam *et al.* 1995; Force & Bonventre 1998; Khalil & Morgan 1993; Klemke *et al.* 1997; Nelson *et al.* 1998). The activation of p42 (ERK1) and p44 (ERK2) MAP kinase is an early event in the signaling cascades activated by both insulin and IGF-1 (Kim & Kahn 1997). As a result, MAP kinase is considered to be a required intermediate in the cellular response to these peptides. The stimulation and activation of MAP kinase involves the phosphorylation of both tyrosine and threonine residues by MAP kinase kinase (MEK) (Payne *et al.* 1991). In this study, the activation of MAP kinase was monitored by Western blot analysis, using an antibody specific for the phosphorylated form of this protein (Xu *et al.* 1996; Yau & Zahradka 1997). Insulin and IGF-1 induced a similar transient increase in p42/p44 MAP kinase phosphorylation at 10^{-8} M (Figure 7A) with a peak at 10 min and a return to basal levels after 20 min. To verify that MAP kinase phosphorylation correlated with an increase in activity, an *in situ* polyacrylamide gel assay was used to measure MAP kinase activity. This method was chosen for its ability to distinguish the myelin basic protein phosphorylated by p42 vs. p44 MAP kinase (Yau & Zahradka 1997). Increased modification of myelin basic protein was observed with increasing concentrations of insulin and IGF-1 (10^{-11} to 10^{-8} M) with maximal phosphorylation observed at 10^{-8} M for both peptides (Figure 7B). The results indicate that both peptide ligands are equally effective at activating MAP kinase, which is in contrast to the tyrosine phosphorylation data presented above (Figure 6). Although it was observed that several other proteins are capable of phosphorylating myelin basic protein (most notably proteins of molecular

FIGURE 7: ***Stimulation of MAP Kinase by Insulin and IGF-1.***

(A) H4IIE cells were treated with 10^{-8} M insulin of 10^{-8} M IGF-1 for various time periods (0 to 20 min) and harvested for Western blot analysis by direct addition of SDS/gel loading buffer. The proteins were resolved on SDS/PAGE (10% gels), transferred to PVDF membrane and visualized with an antibody specific for phosphorylated MAP kinase (diluted 1:1000). The results were confirmed in two independent experiments. (B) Extracts were prepared 6 min after treatment with varying concentrations of insulin or IGF-1 (10^{-11} to 10^{-8} M) and MAP kinase activity was measured by activity gel assay. Specific phosphorylation of myelin basic protein by $p42^{MAPK}$ and $p44^{MAPK}$ is shown. Identical results were obtained in three independent experiments.

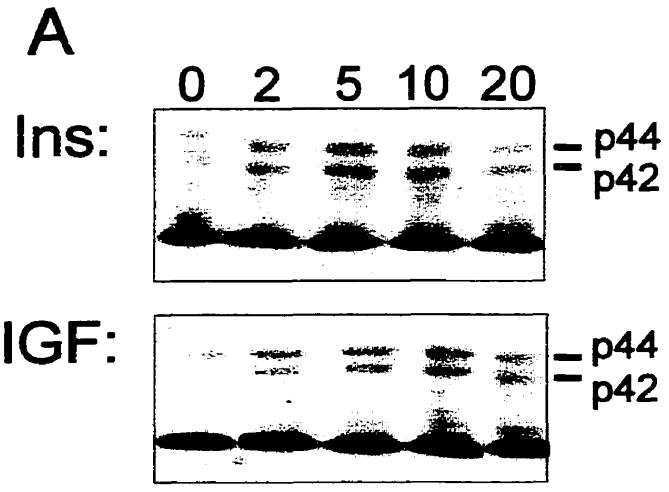
A
0 2 5 10 20
Ins:
p44
p42
IGF:
p44
p42

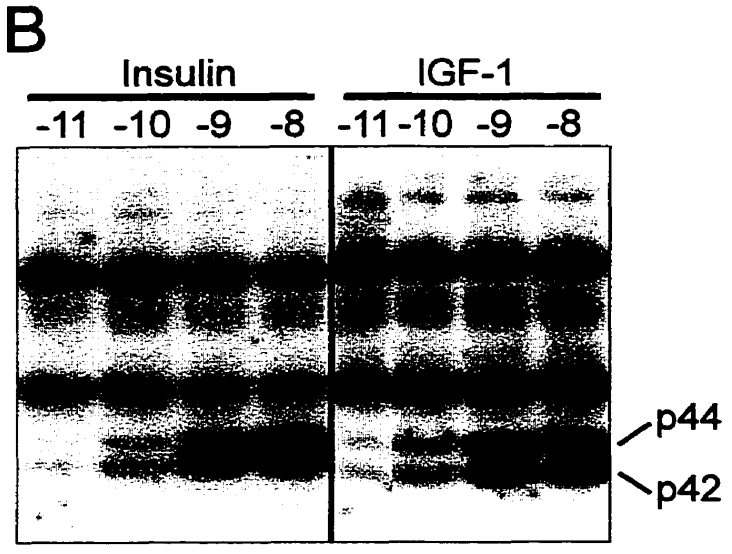
B
Insulin
IGF-1
-11 -10 -9 -8 -11 -10 -9 -8
p44
p42

mass 58- and 112-kDa), these proteins were constitutively active and did not respond to mitogen stimulation (Figure 7B).

To verify that MAP kinase activation correlated with nuclear translocation, the subcellular distribution of phosphorylated MAP kinase was monitored by immunocytochemical staining. Phosphorylated MAP kinase was at the lower limits of detection in quiescent H4IIE cells, and no nuclear staining was evident (Figure 8A). After treatment with both insulin and IGF-1 (10^{-8} M), nuclear translocation of phosphorylated MAP kinase was evident (Figure 8B,C). Since equimolar concentrations of insulin and IGF-1 activated MAP kinase, these data suggest that IGF-1-dependent induction of MAP kinase signaling is mediated through the IGF-1 receptor.

To confirm that the signaling system responsible for MAP kinase activation is triggered by both insulin and IGF-1, the phosphorylation status of MEK, the kinase that phosphorylates MAP kinase (Payne *et al.* 1991), was monitored. Western blot analysis, with antibodies specific to de/phosphorylated MEK1/2 kinase, showed that MEK phosphorylation was increased by both insulin and IGF-1 in a concentration-dependent manner (10^{-10} to 10^{-7} M), with maximal stimulation observed at 10^{-8} M (Figure 9A). The ratio of phosphorylated MEK and total MEK band intensities (Xu *et al.* 1996) was similar over the entire concentration range (Figure 9B), thus confirming that IGF-1-mediated MEK phosphorylation results from stimulation of the IGF-1 receptor.

5.2.4.4 Effect of an inhibitor of MEK (PD98059) on insulin-mediated H4IIE growth

As mentioned previously, MAP kinase is an essential signaling molecule in the activation and growth of a variety of cell types. Therefore, the importance of the MAP kinase cascade in mediating insulin-stimulated growth events in H4IIE cells was assessed using PD98059, a specific inhibitor of MEK (Alessi *et al.* 1995; Dudley *et al.* 1995). By inhibiting MEK1/2, PD98059 prevents the phosphorylation and subsequent activation of

FIGURE 8: ***Nuclear Translocation of MAP Kinase in Response to Insulin and IGF-1.***

Epifluorescence microscopy was used to monitor the subcellular localization of phosphorylated MAP kinase. Quiescent H4IIE cells (A), cells treated with 10^{-8} M insulin (B) and cells treated with 10^{-8} M IGF-1 (C) were used in these experiments. Magnification: 120×.

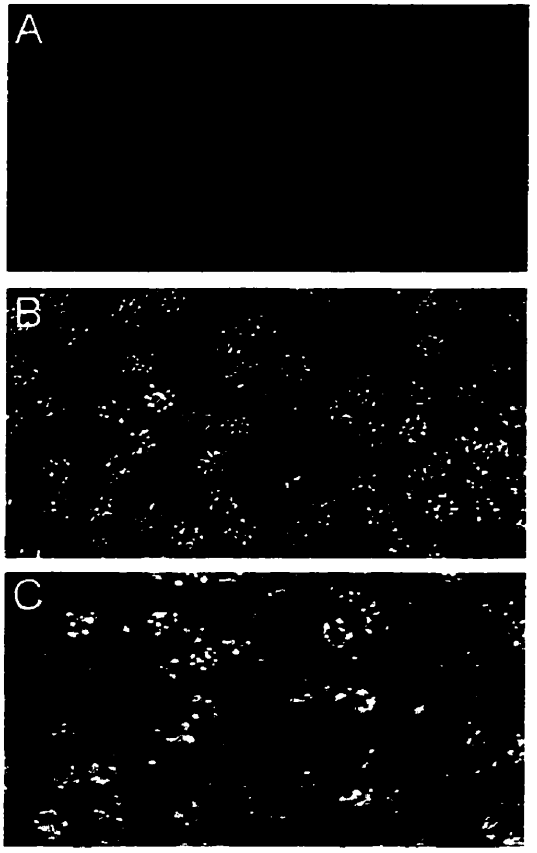
A
B
C

FIGURE 9: ***Insulin- and IGF-1-dependent Phosphorylation of MEK.***

(A) MEK phosphorylation in response to various concentrations of insulin or IGF-1 (10^{-10} to 10^{-7} M) was assessed by Western blot analysis using antibodies (diluted 1:1000) specific to either the phosphorylated (pMEK) or all forms of MEK. One of three independent experiments is presented, all of which exhibited the same response. (B) The ratio of pMEK/MEK was calculated by combining densitometric values obtained from three separate blots for each condition. This ratio provides a control for variation in protein loading.

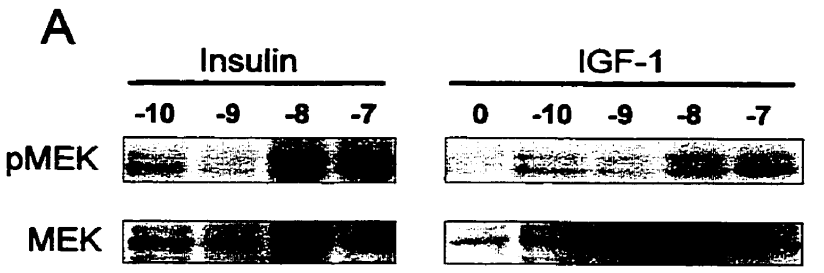
A
Insulin
IGF-1
-10 -9 -8 -7
0 -10 -9 -8 -7
pMEK
MEK

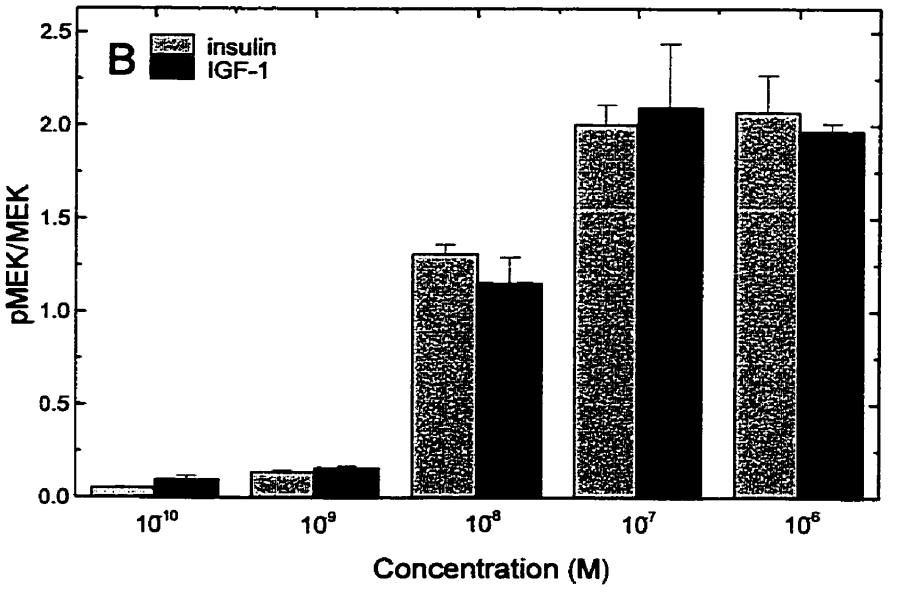
B
insulin
IGF-1
pMEK/MEK
2.5
2.0
1.5
1.0
0.5
0.0
10^-10
10^-9
10^-8
10^-7
10^-6
Concentration (M)

MAP kinase. This event was verified in H4IIE cells by pretreating H4IIE cells with PD98059 for 10 min before stimulation with insulin (10^{-8} M). PD98059 significantly decreased the phosphorylation of MAP kinase in a concentration-dependent manner (10^{-8} to 10^{-4} M) (Figure 10A). Quantification of these data indicated that PD98059 at 10^{-4} M inhibited MAP kinase phosphorylation (both p42 and p44 MAP kinase) by 90% (Figure 10B). PD98059 also had a marked effect on the growth response of H4IIE cells. This inhibitor reduced insulin (10^{-8} M)-mediated RNA and DNA synthesis, with 10^{-4} M PD98059 decreasing RNA and DNA synthesis by 52% and 88%, respectively (Figure 10C,D). These data clearly establish that MAP kinase activation is necessary for the growth and proliferation of H4IIE cells.

5.2.5 Discussion

Insulin elicits a variety of biological responses in the liver relating predominantly to glucose metabolism. As well, this hormone is noted for its influence on cell growth during liver regeneration. The response of H4IIE hepatoma cells to insulin also includes modification of their glucose metabolic pathways and initiation of cell growth (Mohn *et al.* 1991; Taub *et al.* 1987). We have confirmed that both DNA and RNA synthesis are increased upon insulin stimulation (Yau *et al.* 1998; Zahradka & Yau 1994) and have extended this to demonstrate that H4IIE cells traverse the entire cell cycle and complete cell division (Figure 4). These findings establish that insulin is a potent mitogen for H4IIE cells, especially considering the ineffectiveness of so-called strong mitogens such as platelet-derived growth factor (PDGF) and epidermal growth factor (EGF) in this system (P. Zahradka, unpublished observations). In contrast, IGF-1, an agent more noted for its growth stimulatory effects, does not trigger cell growth unless high concentrations are used (Figure 4). The 100-fold or greater concentration difference indicates the

FIGURE 10: ***Inhibition of MAP Kinase Phosphorylation and Cell Proliferation by the MEK Inhibitor PD98059.***

(A) Quiescent H4IIE cells were treated with 10^{-8} M insulin in the presence of various concentrations (10^{-8} to 10^{-4} M) of PD98059. Samples were run on SDS/PAGE (10% gel) and phosphorylation of MAP kinase was monitored by Western blot analysis using an antibody specific for phosphorylated MAP kinase (diluted 1:1000). The response produced by PD98059 alone (10^{-4} M) is shown in the last lane. The relative positions of the molecular mass markers (in kDa) is shown. This experiment was conducted in duplicate for treatment with both 10^{-8} M and 10^{-7} M insulin; one representative gel depicting the effect with 10^{-8} M insulin is shown. Similar results were obtained for both experiments. (B) Band densities were determined by densitometry and the data plotted for both the 42- and 44-kDa bands. (C, D) Insulin (10^{-8} M)-stimulated RNA (C) and DNA (D) synthesis was measured in the presence of varying concentrations of the MEK inhibitor PD98059 (10^{-8} to 10^{-4} M). Each data point represents the mean ± SE of at least three individual experiments conducted in triplicate. Values are presented relative to a non-insulin-treated control which was set to 100%.

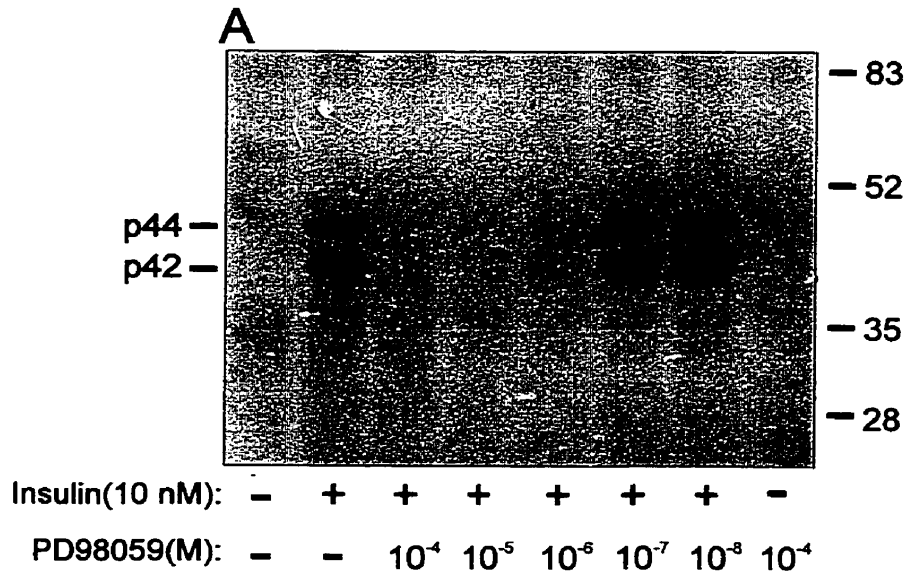
A
83
52
35
28
p44
p42
Insulin(10 nM): - + + + + + + -
PD98059(M): - - 10^{-4} 10^{-5} 10^{-6} 10^{-7} 10^{-8} 10^{-4}

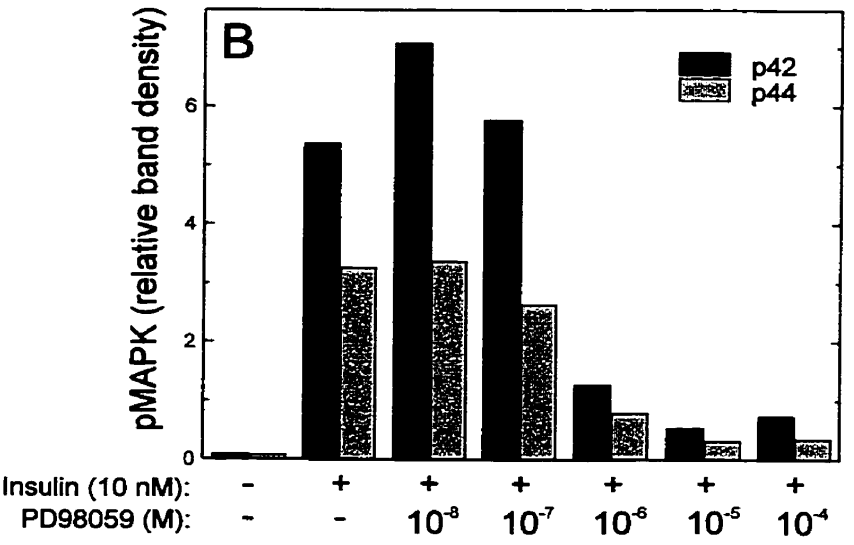
B
pMAPK (relative band density)
0
2
4
6
p42
p44
Insulin (10 nM): - + + + + + +
PD98059 (M): - - 10^{-8} 10^{-7} 10^{-6} 10^{-5} 10^{-4}

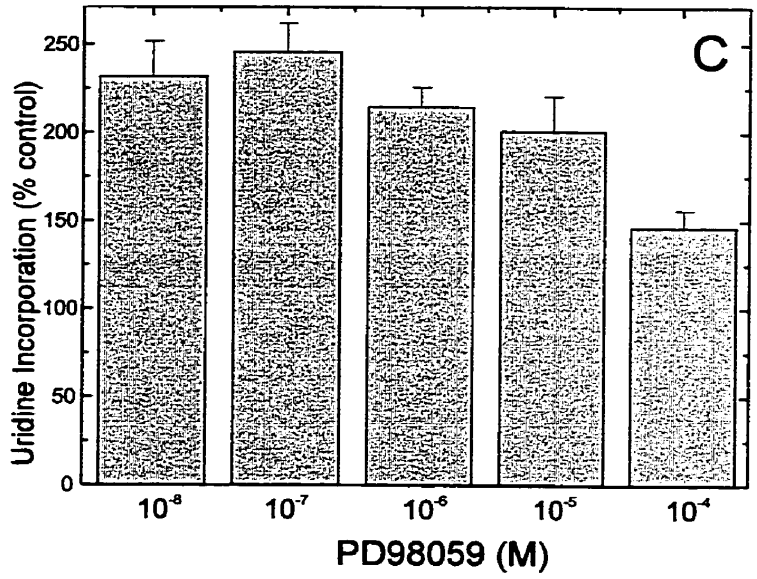
C
Uridine Incorporation (% control)
250
200
150
100
50
0
10-8
10-7
10-6
10-5
10-4
PD98059 (M)

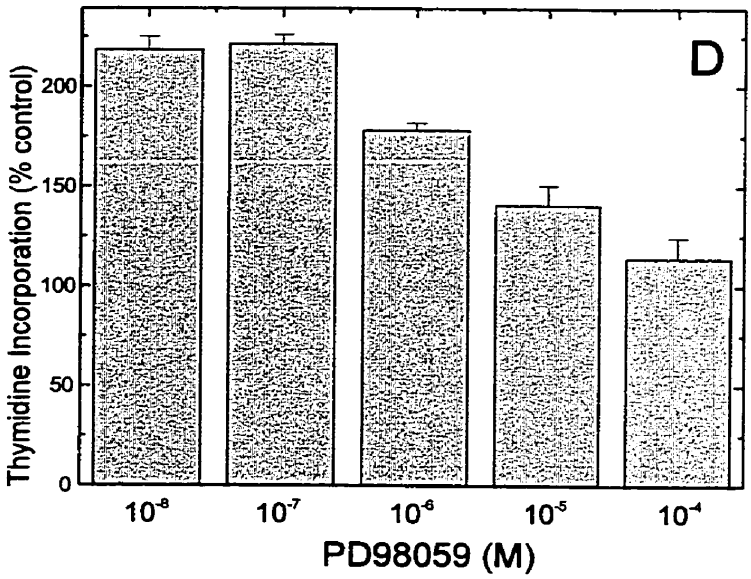
D
Thymidine Incorporation (% control)
200
150
100
50
0
10-8
10-7
10-6
10-5
10-4
PD98059 (M)

stimulation of H4IIE cell growth by IGF-1 is likely mediated by the insulin receptor rather than the IGF-1 receptor (Koontz 1984; Massague & Czech 1982). An examination of the effects of insulin and IGF-1 on glucose metabolic systems revealed a similar pattern, since IGF-1 did not increase glucose uptake at a concentration below 10^{-6} M (Figure 5). While the inability to detect glucose uptake with IGF-1 at 10^{-7} M cannot be explained, although it was observed at 10^{-6} M (data not shown), it is plausible that at this concentration IGF-1 does not stimulate glucose uptake beyond 10 min, and uptake has therefore ceased before addition of the radiolabelled substrate. These data, nevertheless, confirm that IGF-1 does not influence the regulatory systems responsible for mediating the metabolic changes associated with insulin in this cell type. Nevertheless, H4IIE cells express receptors capable of binding IGF-1 (Zahradka *et al.* 1998) and it is generally accepted that common elements exist in the respective signaling pathways of IGF-1 and insulin (Kadowaki *et al.* 1996; Prager & Melmed 1993; Sasaoka *et al.* 1996).

Experiments utilizing kinase-defective insulin receptor mutants have demonstrated that induction of the β subunit tyrosine kinase activity is essential for both mitogenesis and changes in glucose metabolism (McClain *et al.* 1990). The insulin receptor kinase stimulates various cytoplasmic signaling cascades through IRS-1 (Kadowaki *et al.* 1996; Myers *et al.* 1994a; Myers *et al.* 1994b), an intermediary protein that recruits proteins vital for further signal transmission. In general, the phosphorylation of IRS-1 results in the binding of proteins with SH2 domains, such as p85, Syp and Grb2, that have been linked to the production of phosphatidylinositol 3-phosphates, tyrosine dephosphorylation and p21-Ras/MAP kinase activation, respectively (Myers *et al.* 1994b; White & Kahn 1994). IRS-1 has an equivalent role in the signaling system for IGF-1 (De Meyts *et al.* 1994; Frattali *et al.* 1992; Myers *et al.* 1994a) and an inability to initiate IRS-1 phosphorylation (Figure 6D) could therefore account for the lack of effect by IGF-1 on

H4IIE cell growth and metabolism. Since these cells obviously have functional IGF-1 receptors, as demonstrated by the stimulation of both MEK phosphorylation and MAP kinase activity with 10^{-8} M IGF-1 (Figures 7, 9), the defect could potentially exist in the receptor kinase. This assumption was confirmed by directly measuring receptor kinase activity where it was observed that insulin, but not IGF-1, could elicit tyrosine phosphorylation of the respective β subunit (data not shown; refer to Yau *et al.* 1999). This detail explains the lack of IGF-1 receptor autophosphorylation (Figure 6C) and the absence of IRS-1 tyrosine phosphorylation (Figure 6D) when H4IIE cells are treated with IGF-1.

The lack of correlation between IRS-1 phosphorylation and MAP kinase activation has been previously observed in cells expressing mutated insulin receptors deficient in tyrosine kinase activity (Krook *et al.* 1996; Takata *et al.* 1996). Interestingly, these reports noted that IRS-1 tyrosine phosphorylation still occurred following insulin treatment, yet MAP kinase activation was suppressed. In conjunction with the data presented in this report, support for the premise that IRS-1 is not a component of the MAP kinase cascade becomes apparent. Although it has been well established that IRS-1 directs certain elements of the signaling cascade leading from both insulin and IGF-1 receptors (Waters *et al.* 1993), it has also become evident that alternative pathways for regulating specific intracellular processes exist.

These data confirm that MAP kinase (p42/p44) is an essential intracellular mediator of the proliferative response to insulin (Figure 10C, D), and it is most likely that MAP kinase promotes cell proliferation by stimulating gene expression and protein synthesis. On the other hand, it has been shown that activation of MAP kinase alone is insufficient for these events (Scrimgeour *et al.* 1997). Mechanistically, MAP kinase is presumed to operate by stimulating gene expression, particularly of key proto-oncogenes

such as c-*fos* and c-*jun* (Karin 1996). It has become evident, however, that modulation of transcription factors can occur independent of MAP kinase (Kim & Kahn 1997). Similar findings relate to specific metabolic processes that are controlled by insulin. For instance, MAP kinase does not participate in the stimulation of gluconeogenesis (Sutherland *et al.* 1998). As well, there is consensus in the literature that the physiological role of MAP kinase does not encompass the metabolic effects of insulin (Combettes-Souverain & Issad 1998; Lazar *et al.* 1995). Unfortunately, a relevant model of intracellular signaling that defines the role of MAP kinase in cell proliferation and cell metabolism has not been elucidated, presumably because the inter-relationships between various signal transduction pathways, including the MAP kinase cascade, have yet to be clarified. Nevertheless, it has been recently suggested that MAP kinase activation by IGF-1 requires the participation of G proteins through their βγ subunits (Luttrell *et al.* 1995; van Biesen *et al.* 1995). It has generally been assumed, however, that tyrosine phosphorylation events must precede G protein activation. These results, on the other hand, support a paradigm wherein activation of MAP kinase by IGF-1 occurs in the absence of receptor-mediated tyrosine phosphorylation events. These characteristics are emphasized by three critical points: 1) IGF-1 does not trigger tyrosine phosphorylation of either IRS-1 or the IGF-1 receptor (Figure 6), 2) the H4IIE IGF-1 receptor apparently lacks tyrosine kinase activity (data not shown; Yau *et al.* 1999), and 3) MAP kinase activation occurs at IGF-1 concentrations that are below the threshold necessary for insulin receptor stimulation (Figures 7, 9). It is therefore credible that the lack of tyrosine kinase activity displayed by the IGF-1 receptor of H4IIE cells (data not shown, Yau *et al.* 1999) may be irrelevant with respect to the MAP kinase cascade. Evidence that G protein activation is an essential component for intracellular signalling by insulin (Rizzo & Romero 1998; Uehara *et al.* 1999) thereby provides a mechanism by which receptor

tyrosine kinase-independent events may by implemented. Further exploration of these alternative pathways is clearly warranted, and H4IIE hepatomas represent an excellent system for defining the divergent signaling pathways associated with IGF -1 receptor function.

5.3 Contribution of ADP-ribosylation to H4IIE cell proliferation

5.3.1 Background and rationale

ADP-ribosylation reactions can be divided into two groups. Those involving PARP occur in the cell nucleus and those involving mARTs are not similarly restricted to a specific cellular compartment (D'Amours *et al.* 1999; Moss *et al.* 1997; Okazaki & Moss 1996a; Shall 1994; Zolkiewska *et al.* 1994). Both of these reactions have been implicated in cell proliferation. One of the known functions of PARP is participation in DNA repair and replication (Cesarone *et al.* 1990), while mARTs have been demonstrated to be direct or indirect regulatory factors in the growth processes of a variety of cell types (Kharadia *et al.* 1992; Loesberg *et al.* 1990b; Smets *et al.* 1990b; Thyberg *et al.* 1995a).

ADP-ribosylation is characterized by the transfer of ADP-ribose from NAD^+ to an acceptor protein (Moss & Vaughan 1988; Ueda & Hayaishi 1985). O-linked polymers of ADP-ribose are produced by the enzyme poly(ADP-ribose) polymerase. Each molecule of poly(ADP-ribose) is anchored via the terminal ADP-ribose moiety to the acceptor protein by an ester linkage to a glutamate residue. Polymerization is achieved through the formation of glycosidic bonds which couple adjacent ADP-ribose units. Due to the specific cellular location of poly(ADP-ribose) polymerase, poly(ADP-ribosyl)ation occurs only in the nucleus. Since the principal acceptors for poly(ADP-ribose) are DNA-binding proteins, and attachment of poly(ADP-ribose) reduces their affinity for DNA (de Murcia *et al.* 1983;

Zahradka & Ebisuzaki 1982), changes in gene expression may be coupled to the modification of specific transcription factors that regulate either gene activation or repression. Alternatively, gene transcription could be controlled indirectly by poly(ADP-ribosyl)ation of histones, a process that modulates chromatin condensation (de Murcia *et al.* 1988).

N-linked mono(ADP-ribosyl)ation occurs in the nuclear, cytosolic and membrane fractions of a cell (Moss & Vaughan 1988; Ueda & Hayaishi 1985). Arginine-dependent mono(ADP-ribosyl)transferases (arg-mART) couple a single ADP-ribose to the guanidino moiety of arginine. Transferases that catalyze the ADP-ribosylation of cysteine, serine, lysine, asparagine and histidine residues have also been detected (Zolkiewska *et al.* 1994). It has become apparent that mono(ADP-ribosyl)ation can modulate numerous enzymatic processes, especially those associated with GTP-hydrolysis. For example, G protein function is stimulated by ADP-ribosylation of the G_s α-subunit at the same arginine that is modified by cholera toxin (Jacquemin *et al.* 1986). At this point, however, there is no indication that mono(ADP-ribosyl)ation participates directly in the regulation of gene expression.

In the liver, the ribosylation of proteins has been associated with both regenerating liver (Cesarone *et al.* 1990), the onset of hepatocellular carcinoma (McKillop *et al.* 1998) and inhibition of hepatocyte growth via nitric oxide (Dalmau *et al.* 1996). Moreover the actions of insulin have been linked to the increased expression of G_i proteins (Livingstone *et al.* 1994; Sanchez-Margalet *et al.* 1999) and expression is altered by exogenous pertussis toxin ribosylation events (Sanchez-Margalet *et al.* 1999). Furthermore, in diabetes, G_i expression is decreased (Gawler *et al.* 1987). As a result, the question of whether ADP-ribosylation events are linked to and with insulin-mediated H4IIE cell growth becomes an extremely relevant question and this study is the first to

directly examine this cellular phenomena and its participation in specific cellular processes.

This section describes the results of experiments designed to clarify the relevance of ADP-ribosylation to insulin-mediated cell growth. Furthermore, it describes attempts to differentiate between the class of ribosylation reaction contributing to cell growth through the use of different inhibitors of the ribosylation process. A potential role for protein modification with mono(ADP-ribose) rather than poly(ADP-ribose) in the regulation of growth by insulin in H4IIE cells was identified.

5.3.2 Specific aims

1. To determine the contribution of ADP-ribosylation reactions to H4IIE cell growth and proliferation.
2. To identify the class of ADP-ribosylation reaction involved in H4IIE cell growth and proliferation through the use of specific ADP-ribosylation inhibitors.

5.3.3 Experimental design

H4IIE cells prepared as described in section 4.2.1, will be stimulated with insulin and the extent of ADP-ribosylation activity correlated with the activation state as it relates to cell proliferation. The experiments in this section are based on two previous publications. The first report found that insulin-dependent inhibition of the gluconeogenic pathway was prevented by inhibitors of ADP-ribosylation, specifically 3-aminobenzamide (3AB) and PD128763. Furthermore, these inhibitors of ADP-ribosylation could themselves induce PEPCK gene expression (Yau *et al.* 1998). It was postulated in this paper that control of PEPCK gene expression, a key component of the

gluconeogenic pathway, may involve a mART enzyme rather PARP. The second publication established that 3AB was an effective inhibitor of H4IIE cell growth (Zahradka & Yau 1994). The class of ADP-ribosylation reaction associated with insulin stimulation of H4IIE cells will be identified through the use of specific inhibitors of either arg-mART or PARP. At this point, it should be noted that 3AB has been shown to inhibit both PARP and arg-mART activities depending on the concentrations that are being used, with lower concentrations more specific to PARP and higher concentrations influencing arg-mART activity as well (Banasik *et al.* 1992; Milam & Cleaver 1984; Rankin *et al.* 1989). PD128763, on the other hand, is reported to be a specific inhibitor of PARP activity (Arundel-Suto *et al.* 1991; Burkart *et al.* 1999; Yau *et al.* 1998).

5.3.4 Results

5.3.4.1 Insulin stimulates ADP-ribosylation

Based on a previous publication that demonstrated 3AB and PD128763 both had unique effects on the expression of PEPCK mRNA (Yau *et al.* 1998), two scenarios were generated: i) ADP-ribosylation participates in the insulin-mediated control of PEPCK gene activity, or ii) ADP-ribosylation is responsive to insulin treatment. To define these events, the activities of both PARP and arg-mART were measured in extracts from quiescent and insulin-stimulated H4IIE cells. Significant stimulation of PARP was not detected in the nuclear fraction of H4IIE cells prepared without and with a 30 min insulin treatment (10^{-6} M) (Table 1). On the other hand, the microsomal fraction demonstrated a profound increase in arg-mART activity after stimulation with insulin (10^{-6} M) compared to without insulin treatment (Table 1). A panel of ADP-ribosylation inhibitors was then tested in conjunction with both PARP and arg-mART assays *in vitro*. This not only helped to establish the specificity of the ADP-ribosylation events occuring in the

Table 1: ***Responsiveness of ADP-Ribosylation to Insulin Stimulation in H4IIE Hepatomas.***

Microsomal and nuclear fractions were prepared from quiescent H4IIE cells before and after a 30 min treatment with 10^{-6} M insulin. The activity of poly(ADP-ribose) polymerase and arginine-dependent mono(ADP-ribosyl)transferase was quantified as described in Materials and Methods (sections 4.9.6 and 4.9.7). The values represent the mean ± SE of assays conducted in triplicate. The entire experiment was conducted in duplicate.

Treatment	Enzyme Activity	
	Poly(ADP-ribose) Polymerase	Mono(ADP-ribosyl)transferase
	nmol min^{-1}mg $protein^{-1}$	
None	4.93 ± 0.51	1.72 ± 0.29
Insulin	4.91 ± 0.23	6.91 ± 0.17

nuclear and microsomal fractions of growing H4IIE cells, but also validated the selectivity of the inhibitors for use in future assays. ADP-ribosylation inhibitors assessed included: i) PD128763, a specific PARP inhibitor (Arundel-Suto *et al.* 1991), ii) 3AB, a dual inhibitor of PARP and mART (Banasik *et al.* 1992; Milam & Cleaver 1984; Rankin *et al.* 1989), and iii) MIBG, a specific arg-mART inhibitor (Loesberg *et al.* 1990b; Smets *et al.* 1990b). It was observed that growing H4IIE cells have a relatively high basal level of ADP-ribosylation activities (Table 2). 3AB (2 mM) was able to inhibit both PARP activity of nuclear fractions and arg-mART activity of microsomal fractions, confirming its dual inhibitory role (Table 2). PD128763 (10 μM), on the other hand, was only capable of inhibiting the PARP activity of nuclear fractions, thereby confirming its specificity for PARP (Table 2). Finally, MIBG (50 μM) inhibited arg-mART activity without significantly reducing PARP activity, thereby validating its specificity for arg-mART. Taken together, these data support the specificity of the ADP-ribosylation reactions that are being observed in H4IIE cells *in vitro* (Table 1). Similar magnitudes of inhibition were observed using extracts from insulin-stimulated H4IIE cells (data not shown).

To confirm the results of PARP enzyme activity measurements *in vitro*, which are not always representative of changes in activity *in vivo* (Lautier *et al.* 1993), an alternative approach was utilized. Western blot analysis with an antibody specific to poly(ADP-ribose) was used to identify proteins modified with poly(ADP-ribose). Numerous proteins were detected, including proteins of molecular mass 110-, 74-, 62-, 52-, 46-, 31-, 29-, 27-, and 25-kDa (Figure 11). The prominent bands between 15- and 30-kDa presumably represent various histone proteins that are known acceptors of poly(ADP-ribose) (Figure 11). The lack of detectable variation in the 116-kDa PARP band, which undergoes automodification in response to cell damage (Kawaichi *et al.*

TABLE 2: ***Sensitivity of Poly(ADP-ribose) Polymerase and Mono(ADP-ribosyl)transferase to Inhibition by 3-aminobenzamide, PD128763 and MIBG.***

The nuclear and microsomal fractions of growing H4IIE cells were prepared as described (section 4.8.4) and the efficacy of specific inhibitors of poly(ADP-ribosyl)ation and mono(ADP-ribosyl)ation assessed with both fractions. 3-aminobenzamide (2 mM), PD128763 (10 μM) and MIBG (50 μM) were added as indicated. Each value represents the mean ± SE of three individual experiments. Similar magnitudes of inhibition were also observed with extracts from quiescent and insulin-treated cells.

Treatment	Enzyme Activity	
	Poly(ADP-ribose) Polymerase	Mono(ADP-ribosyl)transferase
	nmol min^{-1}mg $protein^{-1}$ (% control)	
None	4.93 ±0.51 (100)	3.14 ± 0.48 (100)
3-Aminobenzamide	0.28±0.02 (5.7)	0.37±0.06 (11.8)
PD128763	0.31±0.03 (6.3)	2.85±0.14 (90.8)
MIBG	4.34±0.12 (88.0)	0.30±0.02 (9.6)

FIGURE 11: ***Protein Poly(ADP-ribosyl)ation in H4IIE Hepatoma Cells in vivo.***

H4IIE cells maintained for 30 h in serum-free α-MEM media were harvested at various time points after addition of insulin (10^{-6} M) and the protein modification monitored by Western blot analysis using polyclonal α-pADP anti-poly (ADP-ribose) serum (diluted 1:1000). Positions of molecular mass markers are indicated. Antibody binding was shown to be specific using an auto-modified poly(ADP-ribose) polymerase control. Similar results were obtained with the monoclonal 10H antibody.

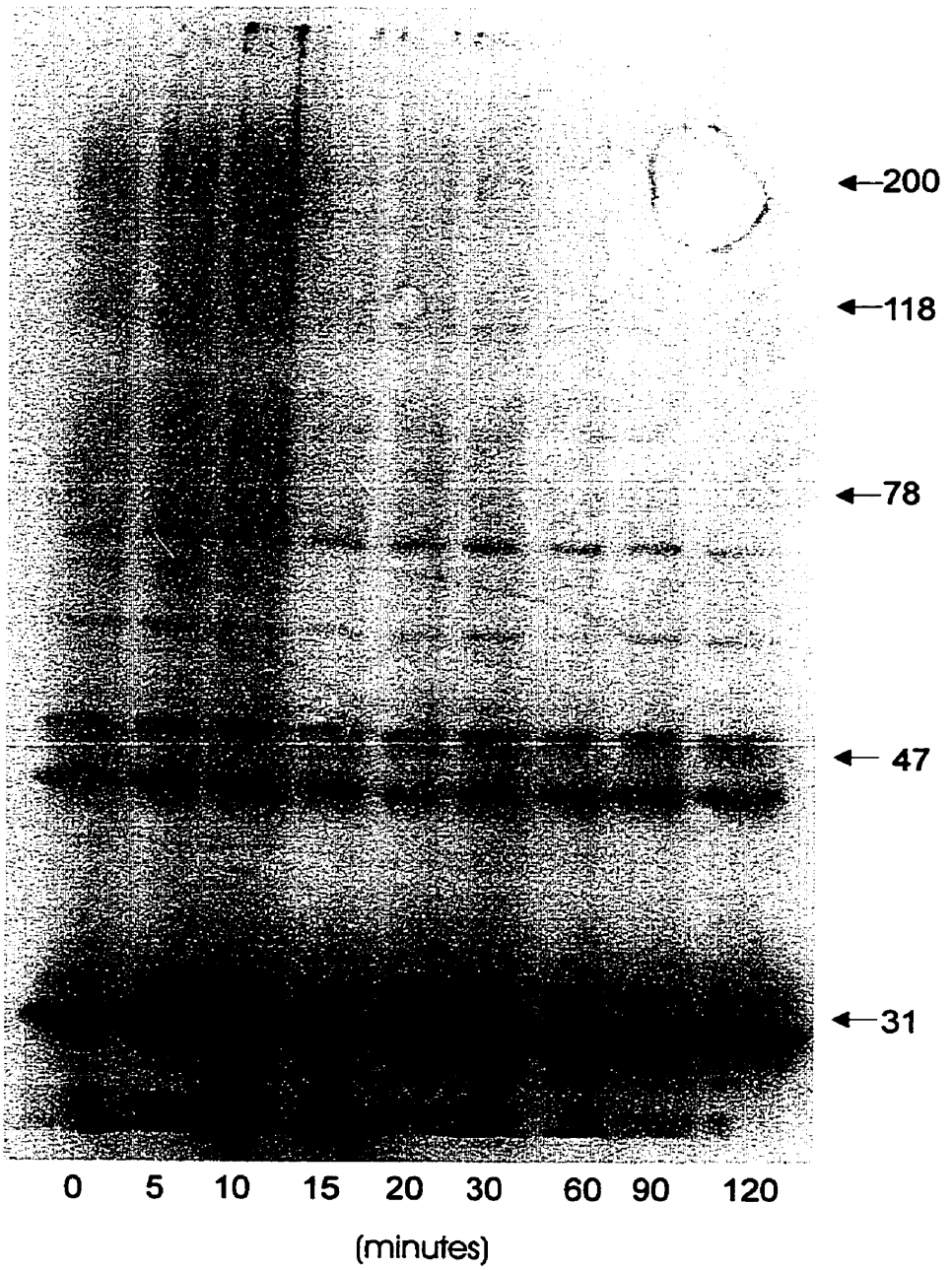
200
118
78
47
31
0
5
10
15
20
30
60
90
120
(minutes)

1981; Schraufstatter *et al.* 1986), indicates that cellular repair systems were not activated (Figure 11). Over a time course of insulin treatment (10^{-6} M), significant changes in the pattern of poly(ADP-ribosyl)ation were not observed, thus supporting the enzyme activity data shown in Table 1.

A more cellular and less invasive approach was also used to monitor mono(ADP-ribosyl)ation in H4IIE cells in order to confirm the results in Table 1. H4IIE cells were labeled with [^{3}H]adenosine for 16 h prior to insulin addition and the modified proteins were then visualized by fluorography after separation of the proteins by SDS/PAGE. This analysis showed that modification of a 53-kDa band was increased following insulin treatment (Figure 12A). Furthermore, modification of this protein was slightly decreased in the presence of 3AB, but not PD128763 (Figure 12B). To verify that radiolabeling under these experimental conditions represented ADP-ribosylation, the samples were treated with 1 M NaOH or 1 M hydroxylamine, agents which disrupt the argininyl-ADP-ribose bond (Figure 12B) (Jacobson *et al.* 1994). The loss of protein-associated radiolabel with these two treatments confirms that the 53-kDa protein is mono(ADP-ribosyl)ated on an arginine residue (Figure 12B). The correlation between insulin-dependent mono(ADP-ribosyl)ation (Figure 12A) and insulin-stimulated arg-mART activity (Table 1) suggests that this process, and not poly(ADP-ribosyl)ation is activated upon insulin stimulation of H4IIE cells and may be involved in insulin-mediated H4IIE cell growth and proliferation.

Cellular arg-mART activity has been detected in several cell fractions. For example, Zolkiewska and Moss (Zolkiewska & Moss 1993; Zolkiewska *et al.* 1992) have demonstrated a mART associated with the external plasma membrane of chick skeletal muscle cells, and Graves and colleagues (Huang *et al.* 1996; Kharadia *et al.* 1992) have shown a microsomal arg-mART activity in chick muscle cells. For this reason, arg-mART assays were employed to determine which cell fractions contained the arg-mART

FIGURE 12: ***Stimulation of Mono(ADP-ribosyl)ation in H4IIE Cells by Insulin.***

Quiescent H4IIE cells (30 h in serum-free α-MEM media) were incubated with [^{3}H]adenosine for 16 h and subsequently stimulated with insulin (10^{-6} M). The cells were harvested directly in 2× SDS/gel loading buffer (method A) after treatment with insulin for 0, 10 or 60 min. The radiolabelled proteins were then analyzed by fluorography after SDS/PAGE. The position of molecular mass markers is indicated. (B) Cell extracts were prepared according to the alternative method (method B) 60 min after addition of 10^{-6} M insulin. Addition of either 3-aminobenzamide (5 mM) or PD128763 (1 μM) preceded the insulin treatment by 10 min. The extracts were mixed with an equal volume of 2× SDS/gel loading buffer and separated by SDS/PAGE. To verify the presence of an ADP-ribose linkage, aliquots of the insulin-treated extract were incubated on ice with 1 M hydroxylamine (NH_2OH) (pH 7.0), or 1 M NaOH for 60 min prior to addition of the SDS/gel loading buffer. The samples were subsequently analyzed by SDS/PAGE. The NaOH sample was neutralized with HCl before loading onto the gel. Both (A) and (B) present the results of one of two independent experiments, both of which exhibited a similar response.

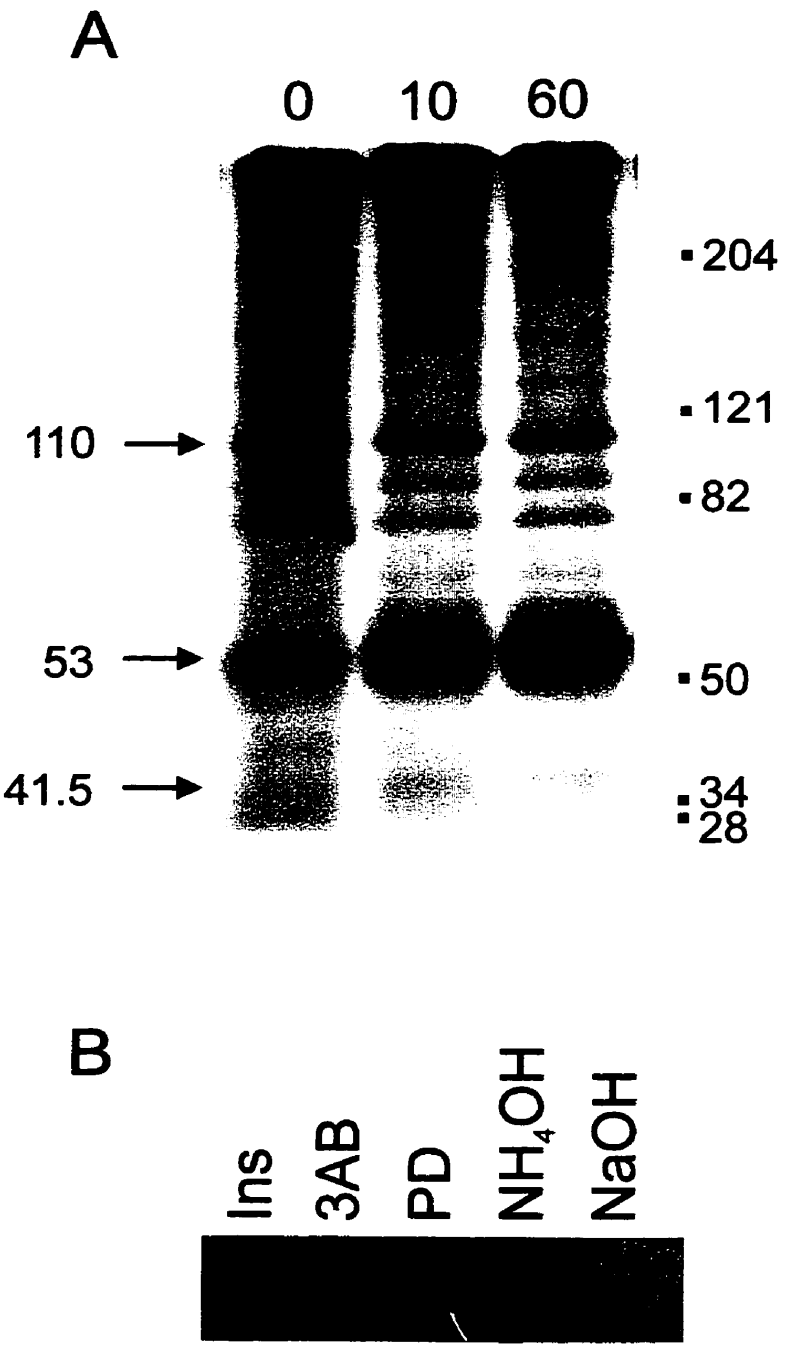
A
0
10
60
204
121
82
110
53
50
41.5
34
28
B
Ins
3AB
PD
NH4OH
NaOH

activity that increased after insulin stimulation. An *in situ* ADP-ribosyltransferase activity assay indicated arg-mART activity was increased in the microsomal fraction over a 3 h period after insulin stimulation (10^{-6} M) (Figure 13), while the cytosolic fraction had no detectable activity by this method (data not shown). *In vitro* arg-mART activity assays were then conducted with both cytosolic and microsomal fractions of H4IIE cell extracts that had been treated over a 2 h time course with insulin (10^{-6} M). The microsomal fraction showed significantly more arg-mART activity in comparison to the cytosolic fraction even in the basal state (Figure 14A), and the microsomal fraction demonstrated an increase in arg-mART activity in response to insulin stimulation. Since peak activity was observed at 1 h, a separate *in vitro* assay was carried out with subcellular fractions prepared from H4IIE cells 1 h after insulin treatment. This assay showed that insulin increased microsomal arg-mART activity by 1.5-fold over basal levels (Figure 14B). The change in arg-mART activity of the cytosolic fraction was not more than 1.15-fold (Figure 14B). These data confirm the observation that insulin is able to stimulate arg-mART activity in H4IIE cells (Table 1, Figure 13), and that the activation of this enzyme may be linked to insulin-mediated cell growth and proliferation.

To verify the specificity of the microsomal arg-mART activity stimulated by insulin (Table 1, Figure 14), an *in vitro* arg-mART activity assay was carried out in which selective ADP-ribosylation inhibitors were included during the incubation time of the assay. 3AB (5 mM) or MIBG (50 μM) was added exogenously to the microsomal fraction of 1 h insulin-stimulated H4IIE cells and compared to microsomal extracts from quiescent H4IIE cells. As seen previously (Figure 14), insulin treatment increased the arg-mART activity from basal levels in quiescent cells (Figure 15). Both 3AB and MIBG were able to decrease the arg-mART activities to control, untreated levels (Figure 15),

FIGURE 13: ***Effect of Insulin on Mono(ADP-ribosyl)ation in H4IIE Cells.***

Quiescent H4IIE cells were treated with insulin (10^{-6} M) and harvested by subcellular fractionation over a 3 h period as described in Materials and Methods (section 4.8.4). The microsomal fraction was then separated by SDS/PAGE on a 10% gel containing 0.2 mg/mL polyarginine. The gel was incubated with 25 μCi [^{32}P]NAD^+ as described in Materials and Methods (section 4.9.9) and, following extensive washing, dried. Autoradiography was carried out at –80°C with one intensifying screen. One of two independent experiments is shown, both of which exhibited the same response.

.

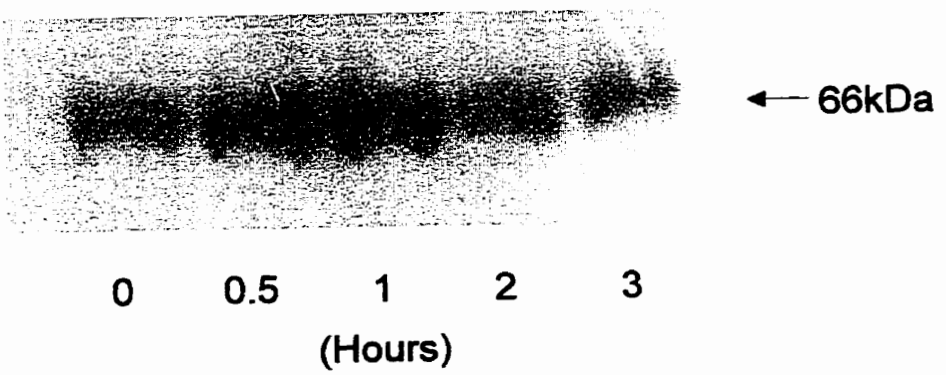
66kDa
0
0.5
1
2
3
(Hours)

FIGURE 14: ***In vitro Mono(ADP-ribosyl)transferase Activity in Insulin-treated H4IIE Cells.***

Quiescent H4IIE cells were treated with insulin (10^{-6} M) and subcellular fractions were harvested at various times (0 – 120 min) as described in Materials and Methods (section 4.8.4). (A) An *in vitro* mono(ADP-ribosyl)ation assay was used to measure transfer of ADP-ribose in both the microsomal (membrane) and cytosolic (cytosol) fractions over a 120 min time course as described in Materials and Methods (section 4.9.7). Polyarginine (2 mg/mL) was used as the acceptor protein for the assay. Each data point represents the pooled data from two independent experiments. (B) An *in vitro* mono(ADP-ribosyl)ation assay was carried out using both the microsomal (membrane) and cytosolic (cytosol) fractions, and the changes in mono(ADP-ribosyl)transferase activity compared in insulin-treated (1 h stimulation) and untreated cells. Polyarginine (2 mg/mL) was used as the acceptor protein for the assay. The activity present in untreated cells was set to 1.0 for comparison. These data represent one of two independent experiments, both of which exhibited the same response.

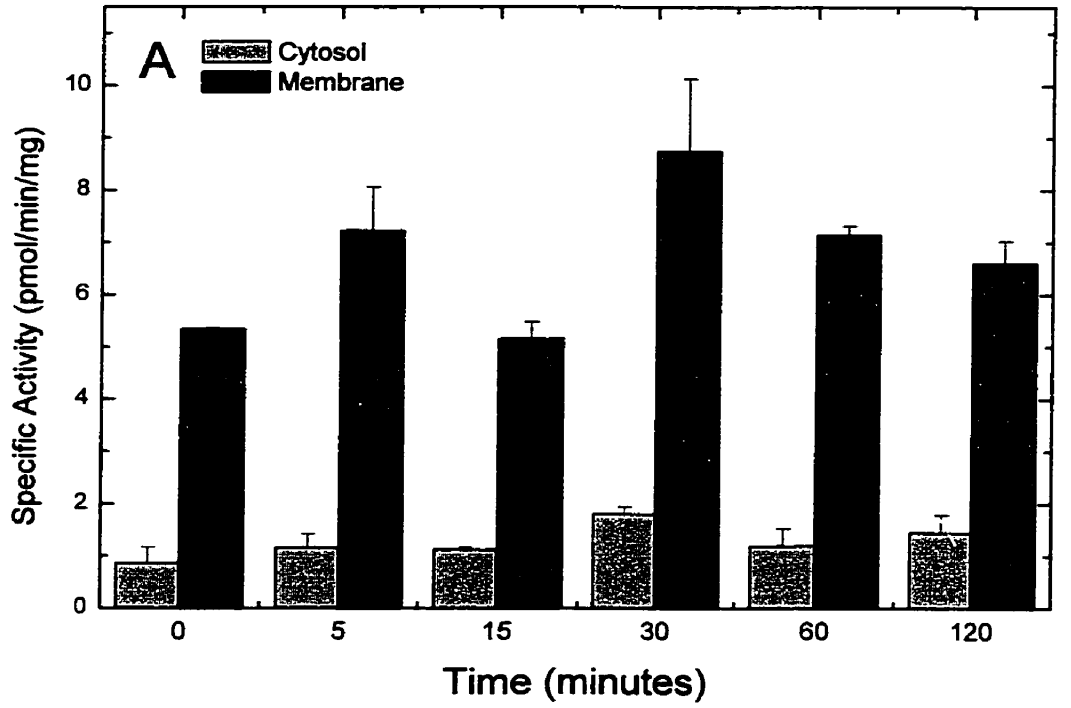
A
Cytosol
Membrane
Specific Activity (pmol/min/mg)
0
2
4
6
8
10
0
5
15
30
60
120
Time (minutes)

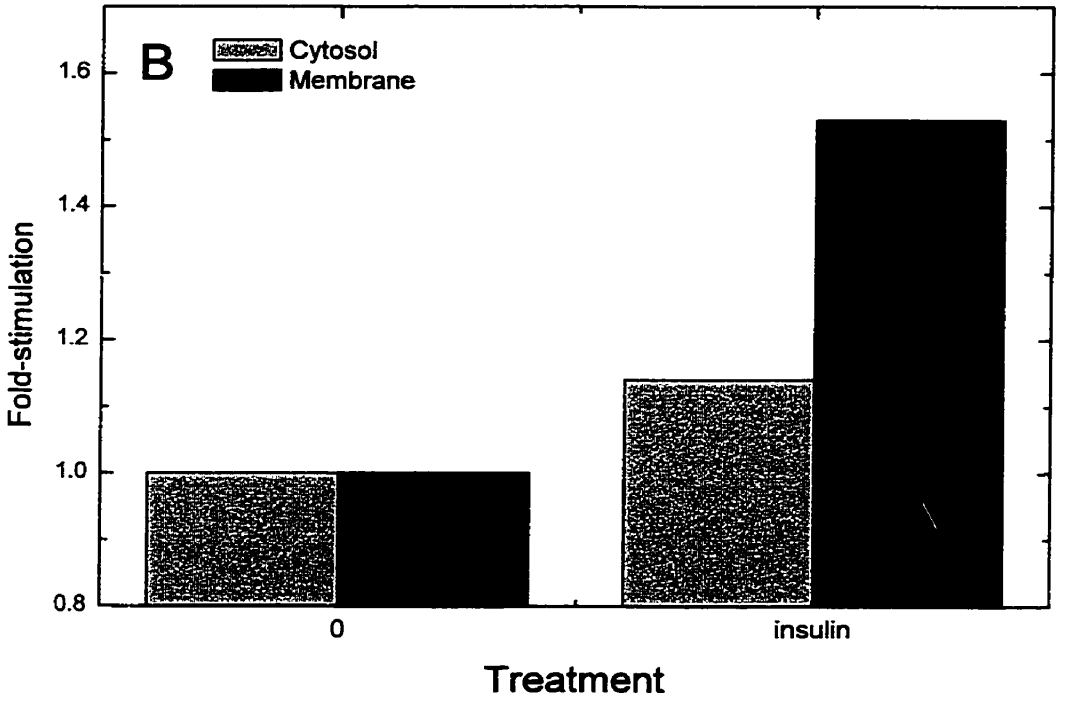
B
Cytosol
Membrane
Fold-stimulation
0.8
1.0
1.2
1.4
1.6
0
insulin
Treatment

FIGURE 15: ***Sensitivity of Mono(ADP-ribosyl)transferase to Inhibition.***

Quiescent H4IIE cells were treated with insulin (10^{-6} M) and harvested after 1 h by subcellular fractionation as described (section 4.8.4). mART activity in the microsomal fraction was assayed in the presence of 3-aminobenzamide (5 mM) or MIBG (50 μM). Polyarginine (2 mg/mL) was used as the acceptor protein for the assay. Data represent one of two independent experiments, both of which exhibited the same response.

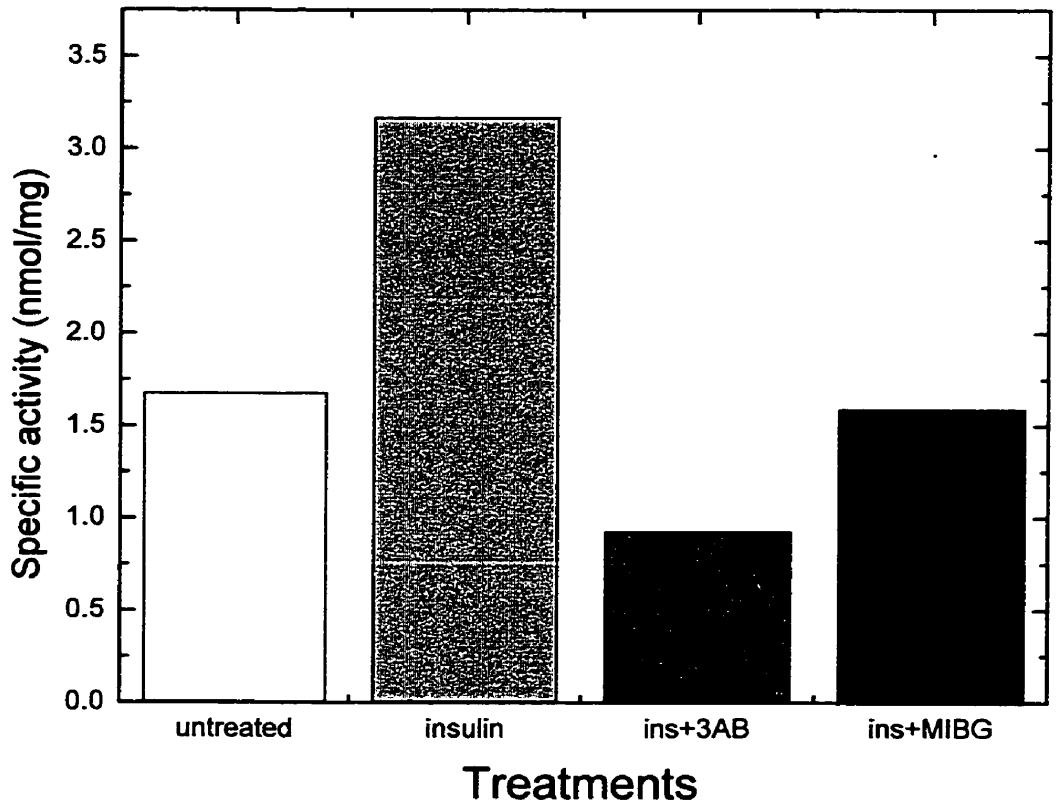
Specific activity (nmol/mg)
3.5
3.0
2.5
2.0
1.5
1.0
0.5
0.0
untreated
insulin
ins+3AB
ins+MIBG
Treatments

demonstrating specificity of the cellular ADP-ribosylation response after insulin treatment.

5.3.5 Discussion

Several cytosolic and microsomal monotransferases have been identified (Tsuchiya & Shimoyama 1994; Zolkiewska *et al.* 1994), however, none have been linked to a specific regulatory process. The purpose of this study was to clarify the role of ADP-ribosylation and ADP-ribosyltransferases in the signal transduction processes associated with the regulation of H4IIE cell growth by insulin. A previously published paper (Yau *et al.* 1998) had examined the participation of ADP-ribosylation in the regulation of gene expression by insulin. In that paper, expression of the PEPCK gene as controlled by insulin was examined in conjunction with the ADP-ribosylation inhibitor 3-aminobenzamide (3AB). It was noted here that the activity of PARP was not significantly changed between insulin-stimulated and control cells. In contrast, both mART activity and protein mono(ADP-ribosyl)ation were elevated in cells treated with insulin, the first indication that mono(ADP-ribosyl)ation events are responsive to growth factors such as insulin. Moreover, this activity could be inhibited by 3AB. Although these findings did not confirm a role for mART activity in insulin-mediated changes in gene expression, the data did emphasize that mART may have a role in mediating insulin-dependent signaling systems.

In the previous section, it was demonstrated that insulin alone was able to act as a growth factor for H4IIE cells and that certain signaling pathways such as MAP kinase played a critical role in the insulin-mediated cell growth and proliferation. The data generated in this section suggested a mono(ADP-ribosyl)transferase participates in the cell growth effects mediated by insulin in H4IIE cells. The data showed that nuclear

PARP activity was not increased on cell stimulation with insulin and that there was no change in the pattern of poly(ADP-ribosyl)ation following insulin stimulation (Table 1). In contrast, an increase in arg-mART activity was observed and this was consistent with the increase in ADP-ribosylation of the 53-kDa protein (Figure 12). Although the identity of this protein was not clarified, a band at 53-kDa has been observed in other cell systems (Graves *et al.* 1997). PARP is typically associated with cell growth and replicative events. Its activity is increased in liver regeneration (Cesarone *et al.* 1990), and upregulation occurs in many tissues and cell types during proliferation. On the other hand, PARP can also be activated during cell senescence, apoptosis and by negative growth regulatory factors such as nitric oxide (Dalmau *et al.* 1996; Pieper *et al.* 1999; Scovassi & Poirier 1999). Nevertheless, in our cell system, PARP does not appear to play a significant role in the cell growth processes mediated by insulin.

Arg-mART reactions on the other hand participate directly in cellular events in the cytoplasm. In this scenario, ADP-ribosylation behaves as a post-translational modification much like phosphorylation that signals cells to undergo a particular event. In several different cell systems, including smooth muscle and skeletal muscle, arg-mART has been shown to participate in the cellular events leading to cell proliferation and differentiation (Kharadia *et al.* 1992; Thyberg *et al.* 1995a). Moreover, the success of MIBG therapy for the treatment of neuroblastoma, carcinoid tumours and metastases suggests that perhaps an arg-mART event may be involved in tumour progression, which involves cell proliferation (Cornelissen *et al.* 1995a; Hoefnagel *et al.* 1991; Smets *et al.* 1988b; Smets *et al.* 1989). In H4IIE cells, it was demonstrated that particular cellular fractions exhibited elevated arg-mART activity after insulin stimulation (Figures 13, 14). The microsomal fraction was shown by both *in situ* ADP-ribosyltransferase labeling (Figure 13) and with an *in vitro* assay (Figure 14), that insulin was able to increase the

arg-mART activity in that particular cell fraction. The stimulation was approximately 1.5-fold (Figure 14B). On the other hand, the cytosolic fraction did not appear to contain arg-mART detectable with the *in situ* ADP-ribosyltransferase labeling assay (data not shown), and insulin was only able to marginally increase the activity measurable with the *in vitro* biochemical assay (Figure 14). These results suggest that the arg-mART activity is associated with the cell membranes and that its compartmentalization within the cell is via membranous components. This finding is in support of the findings of Zolkiewska and colleagues (Zolkiewska & Moss 1993; Zolkiewska *et al.* 1992) and Kharadia *et al.* (1992) who have also found that the arg-mART activity is more prominent in the microsomal fraction. With respect to the ability to transmit signals, having the arg-mART within the membrane fraction indicates that the activity is likely localized to one place and that the enzyme does not shuttle between compartments. Considering that G proteins and small GTP-binding proteins are such good targets for ADP-ribosylation reactions, and that G proteins and GTP-binding proteins are mostly associated with the membrane (Milligan & Grassie 1997; Rodbell 1997; Willard & Crouch 2000), the membrane-bound nature of mART likely places it at an advantage for modulating G protein reactions.

With respect to the specificity of the reaction, the initial findings that mART activity, but not PARP, was increased upon insulin stimulation (Table 1) led to the use of specific inhibitors of both enzymes in order to confirm this finding. PD128763, a reportedly specific inhibitor of PARP, only inhibited PARP activity, while MIBG only inhibited arg-mART activity. 3AB on the other hand, inhibited both PARP and mART activities (Table 2, Figure 15), confirming the dual inhibitory capabilities of this compound. Furthermore, at the concentrations used in these studies ($\geq$ 2 mM), 3AB will inhibit mART activity (Banasik *et al.* 1992; Milam & Cleaver 1984; Rankin *et al.* 1989). Thus, these data further validate the contention that insulin is stimulating an arg-mART

and that activation of this mART is a key mediator of insulin-dependent H4IIE cell growth and proliferation. Although the studies in this section do not necessarily establish that mART is a component of insulin-mediated H4IIE growth, the fact that insulin stimulates this enzyme and that insulin correspondingly stimulates H4IIE cell growth suggests that a link exists between these events. The studies described in the next section were designed to establish that link and confirm the requirement of mART activation for H4IIE hepatoma cell proliferation in response to insulin.

5.4 Modulation of cell proliferation by inhibitors of mART

5.4.1 Background and rationale

Mono(ADP-ribosyl)transferase is an enzyme present in the nuclear, cytosolic or microsomal fractions of cells and is involved in the post-translational modification of proteins (Moss & Vaughan 1988; Ueda & Hayaishi 1985; Zolkiewska *et al.* 1994). This enzyme transfers a single ADP-ribose moiety from NAD^+ to acceptor proteins that usually contain an arginine, cysteine or diphthamide moiety (Zolkiewska *et al.* 1994). This modification, much like phosphorylation, is reversible and is a component of modulating signaling processes and cellular events (coordinating the processes within a cell) (Williamson & Moss 1990; Zolkiewska *et al.* 1994). The most studied and commonly modified proteins are those associated with G proteins and proteins that undergo GTP binding and hydrolysis, such as $G_{s\alpha}$, G_i and small GTP-binding proteins such as Rho and Ras (Ali & Agrawal 1994; Di Girolamo *et al.* 1997; Gierschik 1992; Kanagy *et al.* 1995; Lerm *et al.* 2000; Schmidt & Aktories 1998; Tsuchiya & Shimoyama 1994).

Inhibitors of mART come in many forms. The most popular of those employed for biochemical studies of this protein include novobiocin, benzamide, naphthalimide,

hydroxyisoquinoline, silybin (silymarin) and *meta*-iodobenzylguanidine (MIBG). Many of these compounds inhibit the action of the enzyme directly. However, others such as MIBG (and other compounds containing guanidino groups or guanylhydrazones) act as a decoy substrate, mimicking the arginine present on the acceptor protein of the regular substrates. Although MIBG does not directly inhibit the action of arg-mART, by preventing the modification of the actual acceptor protein the potency of the mART enzyme is lost.

MIBG was first recognized as a diagnostic molecule for the identification and radiotherapy of adrenal tumours and other neuroendocrine tumours in its radioiodinated form (Hoefnagel 1994; Hoefnagel *et al.* 1987; Lode *et al.* 1995; Smets *et al.* 1990a; Wafelman *et al.* 1994b; Wieland *et al.* 1980). Subsequently, the non-radiolabelled compound was shown to decrease tumour progression (Kuin *et al.* 1999; Smets *et al.* 1988b; Taal *et al.* 1999; Taal *et al.* 1996; Zuetenhorst *et al.* 1999). Although the mechanism of action for the anti-tumour activity of MIBG without the radiolabel is not presently known, it has been postulated to involve inhibition of mitochondrial respiration (Cornelissen *et al.* 1995b; Loesberg *et al.* 1990a; Loesberg *et al.* 1991; Smets *et al.* 1990b). However, the arg-mART inhibitory activity of MIBG may also explain its anti-neoplastic properties (Loesberg *et al.* 1990b; Smets *et al.* 1990b). Since these issues have not been adequately addressed, an understanding of how ADP-ribosylation contributes to cell proliferation will help to clarify these points.

5.4.2 Specific Aims

1. To examine the effect of inhibitors of ADP-ribosylation on insulin-mediated H4IIE cell growth and proliferation.

2. To confirm the link between ADP-ribosylation and insulin-mediated H4IIE cell growth and proliferation.
3. To clarify the adverse effects of MIBG on H4IIE cells.
4. To identify a potential mechanism of action for MIBG by determining the effects of MIBG on two signaling intermediates stimulated by insulin: MAP kinase and p21-Ras.

5.4.3 Experimental design

H4IIE cells, prepared as described in section 4.2.1, will be pretreated for 10 min with inhibitors of ADP-ribosylation (eg. 3AB, MIBG, precursor analog MIBA, etc.), stimulated with insulin, and monitored for growth according to parameters such as RNA and DNA synthesis. The exposure time required for MIBG to exert an inhibitory effect will also be defined, along with an assessment of inhibitor reversibility. The relative toxicity of MIBG will also be examined using an MTT cytotoxicity assay, an LDH formation assay and FACS analysis of MIBG-treated H4IIE cells. Finally, potential mechanisms of MIBG action on insulin-stimulated H4IIE cells will be defined using assays to detect activation of two prominent signaling enzymes: MAP kinase and p21-Ras.

5.4.4 Results

5.4.4.1 Effects of ADP-ribosylation inhibitors on cell growth: involvement of mART in H4IIE cell growth and proliferation

In the previous section (section 5.3), it was established that insulin activates an arg-mART. Based on the findings presented in section 5.2 regarding insulin-mediated H4IIE cell growth and proliferation, it was speculated that stimulation of arg-mART

might be a component of the signaling systems that influence H4IIE cell growth post-insulin treatment. As a result, to further define the system and to confirm the participation of this protein modification in H4IIE cell growth and proliferation mediated by insulin, inhibitors of ADP-ribosylation were tested for their ability to affect incorporation of [^{3}H]uridine and [^{3}H]thymidine. H4IIE cells were pretreated for 10 min with the inhibitors before the addition of insulin. The dual PARP/mART inhibitor, 3AB, showed a modest inhibition of insulin-stimulated RNA synthesis (Figure 16A), while it did not affect insulin-stimulated DNA synthesis (Figure 16B). Interestingly, at the high concentrations (2 to10 mM) of 3AB required for modest inhibition of RNA synthesis, 3AB inhibits both mART and PARP activity (Table 2, Figure15). The analog of 3AB that lacks inhibitory action, *para*-aminobenzoic acid (PABA), also did not affect DNA synthesis (data not shown). Furthermore, neither agent was toxic to H4IIE cells as confirmed by lactate dehydrogenase (LDH) release assay after 72 h incubation with varying concentrations (0.1 to 10 mM) of 3AB or PABA (data not shown). These data suggest that 3AB is working via mART to inhibit insulin-mediated RNA synthesis, and that perhaps mART may not participate in the events leading to DNA synthesis.

The evidence that 3AB influenced the cellular response to insulin by inhibiting mART activity led to experiments with selective inhibitors of arg-mART. Several different ADP-ribose acceptors (i.e. pseudosubstrates) for arg-mART catalyzed reactions were tested including MIBG, L-arginine methylester (LAME) and L-nitro-arginine methylester (LNAME). The common feature of these compounds is the presence of an argininyl moiety, the group to which the ADP-ribose is transferred. In addition, norepinephrine (NE) was tested in these experiments since NE is a physiological analog of MIBG. MIBG was capable of significantly decreasing insulin- and FBS-mediated H4IIE cell growth (Figure 17). The other agents were unable to inhibit RNA synthesis in

FIGURE 16: ***Sensitivity of Insulin-mediated Cell Growth in H4IIE Cells to 3-Aminobenzamide.***

Quiescent H4IIE cells were pretreated with 3-aminobenzamide (0.5 to 10 mM) for 10 min prior to addition of insulin (10^{-6} M). The incorporation of [^{3}H]uridine (6 h incubation) and [^{3}H]thymidine (24 h incubation) into trichloroacetate-precipitable material after addition of insulin was used as an indication of RNA (A) or DNA (B) synthetic activity in the presence and absence of the inhibitor. For DNA synthetic activity (B), a single dose of 3-aminobenzamide (5 mM) was tested. The incorporation rate of untreated cells was set to 100%. The data are presented as the mean ± SE of at least three individual experiments conducted in triplicate. Comparisons were made between insulin ± 3-aminobenzamide treated cells using Student's t-test (*, $p < 0.05$).

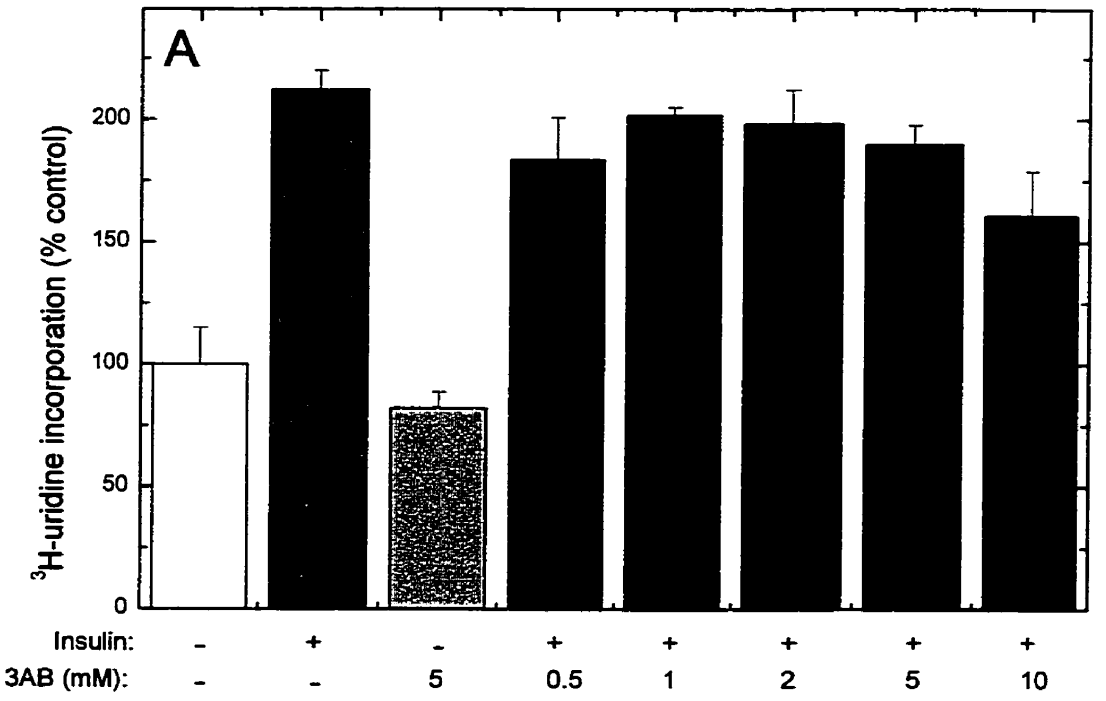
A
^{3}H-uridine incorporation (% control)
0
50
100
150
200
Insulin: - + - + + + + +
3AB (mM): - - 5 0.5 1 2 5 10

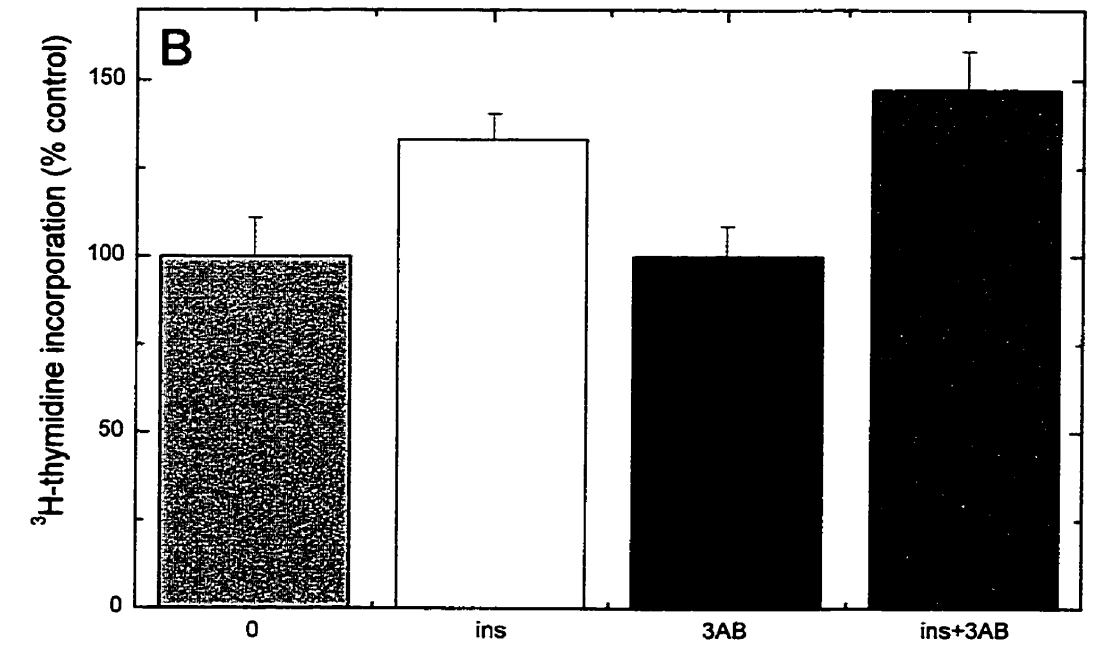
B
^{3}H-thymidine incorporation (% control)
0
50
100
150
0
ins
3AB
ins+3AB

FIGURE 17: ***Sensitivity of Insulin-mediated RNA Synthesis to Inhibitors of Mono(ADP-ribosyl)ation Reactions.***

Quiescent H4IIE cells were pretreated with a variety of inhibitors for 10 min prior to addition of insulin (10^{-6} M) or FBS (10% v/v). Inhibitors tested included: MIBG (50 μM), 3-aminobenzamide (3AB, 10 mM), L-arginine methylester (LAME, 1 μM), L-nitro-arginine methylester (LNAME, 1 μM) and norepinephrine (NE, 1 μM). The incorporation of [^{3}H]uridine (6 h incubation) into trichloroacetate-precipitable material after addition of insulin or FBS was used as an indication of RNA synthetic activity in the presence and absence of the inhibitors. The incorporation rate of untreated cells was set to 100%. The data are presented as the mean ± SE of at least three separate experiments conducted in triplicate. Comparisons were made between growth factor treated and growth factor + each inhibitor treatment with the Student's t-test (*, $p < 0.05$).

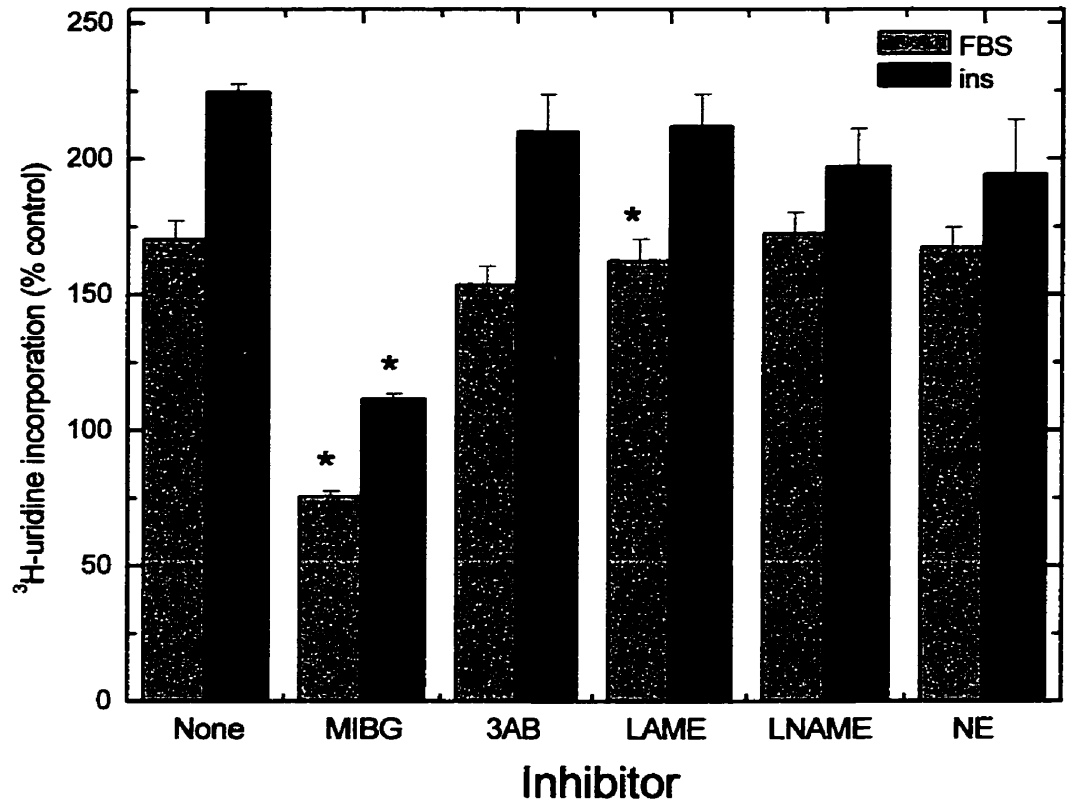
250
200
150
100
50
0
FBS
ins
*
*
*
^{3}H-uridine incorporation (% control)
None
MIBG
3AB
LAME
LNAME
NE
Inhibitor

either insulin- or FBS-treated H4IIE cells (Figure 17), although LAME had a slight and statistically significant effect on the FBS-treated cells. These data validate the premise that insulin-stimulated H4IIE cell growth may be mediated by an arg-mART-dependent pathway. Moreover, these data are suggestive of a requirement for not only structural similarity (i.e. arginine-like guanidino group), but also for physicochemical compatability.

The effect of MIBG on insulin-mediated H4IIE cell growth and proliferation was then examined in greater detail. MIBA was included as a control since the body of the molecule is identical to MIBG, but it lacks the argininyl (guanidino) moiety. MIBG inhibited insulin-stimulated RNA synthesis in a concentration-dependent manner (2.5 to 50 μM) (Figure 18A). In contrast, MIBA did not appreciably inhibit insulin-stimulated RNA synthesis at any concentration (Figure 18A). Similarly, MIBG inhibited insulin-stimulated DNA synthesis in a concentration-dependent manner to below basal levels, while MIBA had little effect (Figure 18B). Since MIBG is a specific inhibitor of arg-mART, these data further support the premise that an arg-mART may be part of the cell growth pathway stimulated by insulin. The lack of effect of MIBA to inhibit insulin-mediated cell growth suggests that the argininyl (guanidino) moiety is the critical portion of the molecule for the inhibitory effect and confirms that MIBG may be inhibiting arg-mART activity by acting as a pseudosubstrate.

To determine when MIBG exerts its inhibitory effects as cells progress from the initial stimulus to beginning DNA synthesis, MIBG (50 μM) was added at specific time points after insulin addition to H4IIE cells, and both [^{3}H]uridine and [^{3}H]thymidine incorporation monitored. Over the 6 h period of an RNA synthesis assay, it was observed MIBG reduced insulin-mediated uridine incorporation at every point of addition (Figure 19A). Most significant is the fact that MIBG does not reduce incorporation to basal

FIGURE 18: ***Sensitivity of Insulin-mediated Cell Growth in H4IIE Cells to MIBG and its Analog MIBA.***

Quiescent H4IIE hepatoma cells were pretreated with MIBG or MIBA (2.5 to 50 μM) for 10 min prior to addition of insulin (10^{-6} M). The incorporation of [^{3}H]uridine (6 h incubation) and [^{3}H]thymidine (24 h incubation) into trichloroacetate-precipitable material after addition of insulin was used as an indication of RNA (A) or DNA (B) synthetic activity in the presence and absence of the inhibitor. For RNA synthesis (A), the control analog MIBA was only tested at the highest concentration (50 μM) with insulin (10^{-6} M). The incorporation rate of untreated cells was set to 100%. The data are presented as the mean ± SE of at least three separate experiments conducted in triplicate.

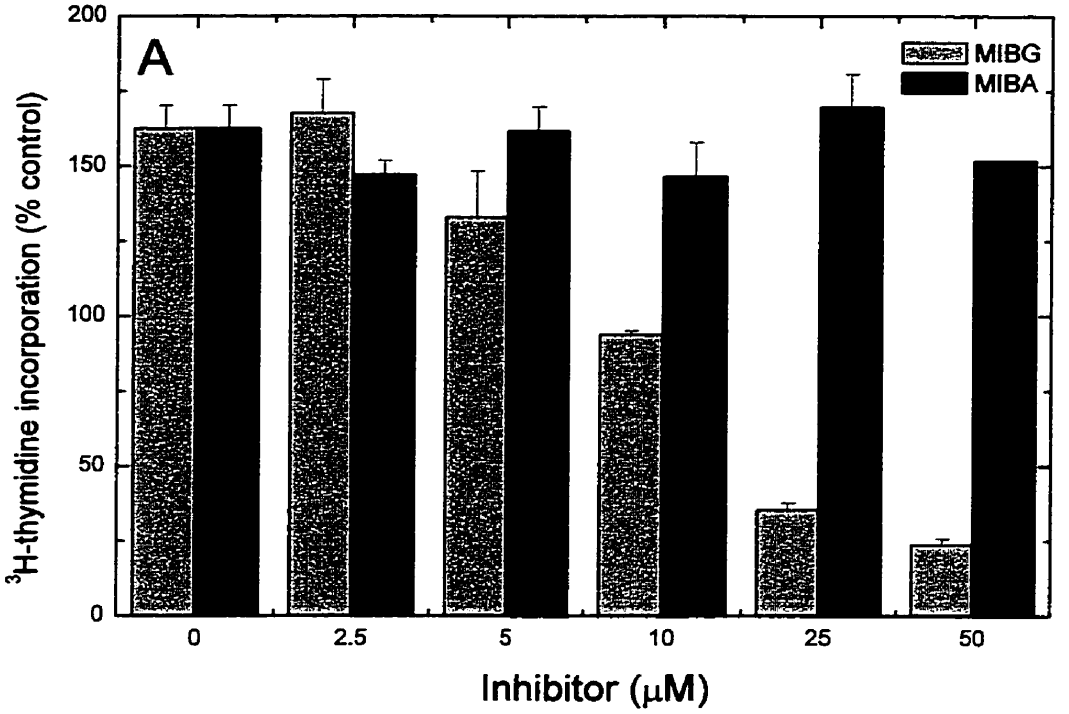
A
MIBG
MIBA
^{3}H-thymidine incorporation (% control)
200
150
100
50
0
0
2.5
5
10
25
50
Inhibitor (μM)

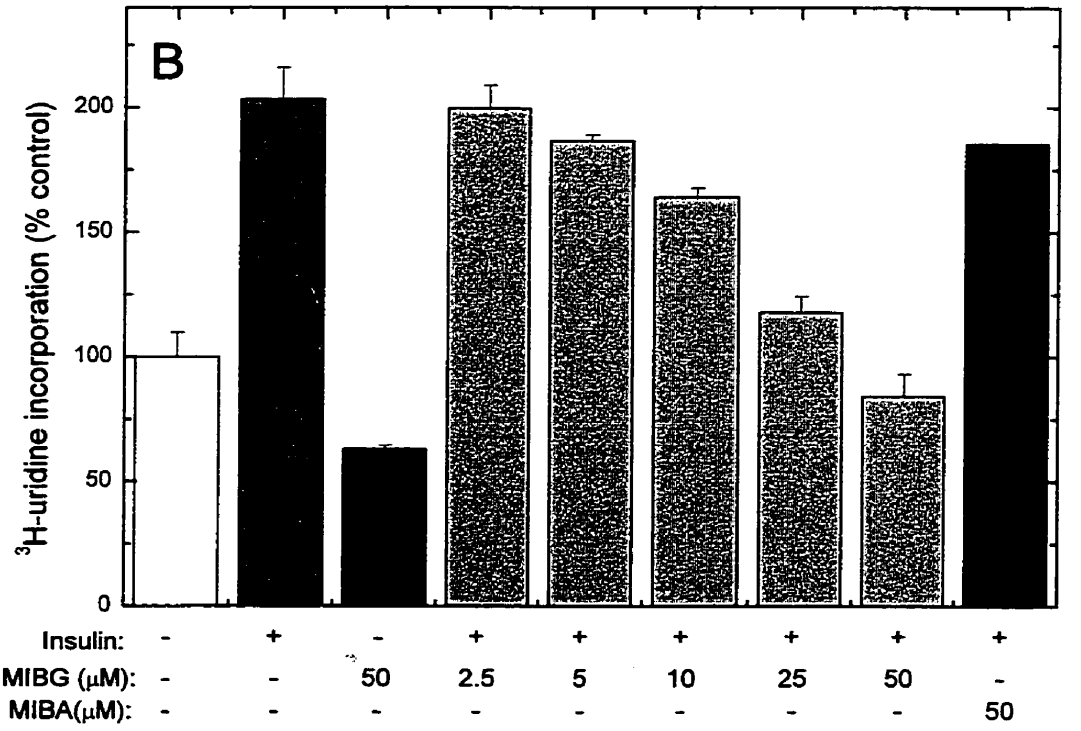
B
^{3}H-uridine incorporation (% control)
200
150
100
50
0
Insulin: - + - + + + + + +
MIBG (μM): - - 50 2.5 5 10 25 50 -
MIBA(μM): - - - - - - - - 50

levels, but produces an inhibition that linearly correlates with the time remaining in the assay. These data suggest that MIBG must be present throughout the assay to completely suppress RNA synthesis. Moreover, this relationship indicates that there is no single point at which the inhibitor is effective and implies that mART activity is required continuously for this process. On the other hand, it was shown that addition of MIBG up to 3 h after insulin administration effectively reduced insulin-stimulated DNA synthesis to baseline levels, with addition of MIBG at the earlier time points being more effective (Figure 19B). Addition of MIBG at 5 h or later did not produce an appreciable decrease in DNA synthesis, which suggests that the inhibition by MIBG as it pertains to DNA synthesis contributes to an early event and is no longer required after 3-5 h. For this reason, MIBG has no effect on insulin-mediated cell growth beyond this time period.

To confirm the above findings, MIBG washout assays were conducted in which H4IIE cells were treated with MIBG, stimulated with insulin and then the media containing MIBG and insulin removed and replaced with media containing insulin only. These experiments were devised to determine the length of time that the cells must be exposed to MIBG in order for an effect to be seen. For the RNA synthesis assay, it was demonstrated that the length of MIBG exposure correlated with the degree of inhibition (Figure 20A), with the levels of RNA synthesis returning to baseline after 4 h treatment with MIBG and declining even more by the end of the 6 h assay. These findings are consistent with the previous data (Figure 19A) and suggest that MIBG may either inhibit multiple steps in the RNA synthesis program or that the target is required throughout. In contrast, inhibition of DNA synthesis was only observed if MIBG was present for the first 6 h of the assay or longer (Figure 20B) (i.e. 24-48 h). Removal of MIBG prior to 4 h prevented inhibition. While these data apparently do not agree with the result of the MIBG addition experiment (Figure 19), it is worth noting that insulin need only be

FIGURE 19: ***Time Course of MIBG Addition to Insulin-stimulated H4IIE Cells.***

Quiescent H4IIE hepatoma cells were treated with insulin (10^{-6} M). At the indicated times, MIBG (50 μM) was added to the cells. [^{3}H]uridine and [^{3}H]thymidine were present throughout the incubation period. The incorporation of [^{3}H]uridine (6 h incubation) and [^{3}H]thymidine (24 h incubation) into trichloroacetate-precipitable material after addition of insulin was used as an indication of RNA (A) or DNA (B) synthetic activity. The incorporation rate of insulin treated cells was set to 100%. The 6 h (A) and 24 h (B) time points had insulin addition but no MIBG addition. 'None' indicates untreated H4IIE cells. The data are presented as the mean ± SE of at least three separate experiments conducted in triplicate. Comparisons were made between insulin only and insulin + MIBG treated cells at each addition time point using the Student's t-test (*, $p < 0.05$).

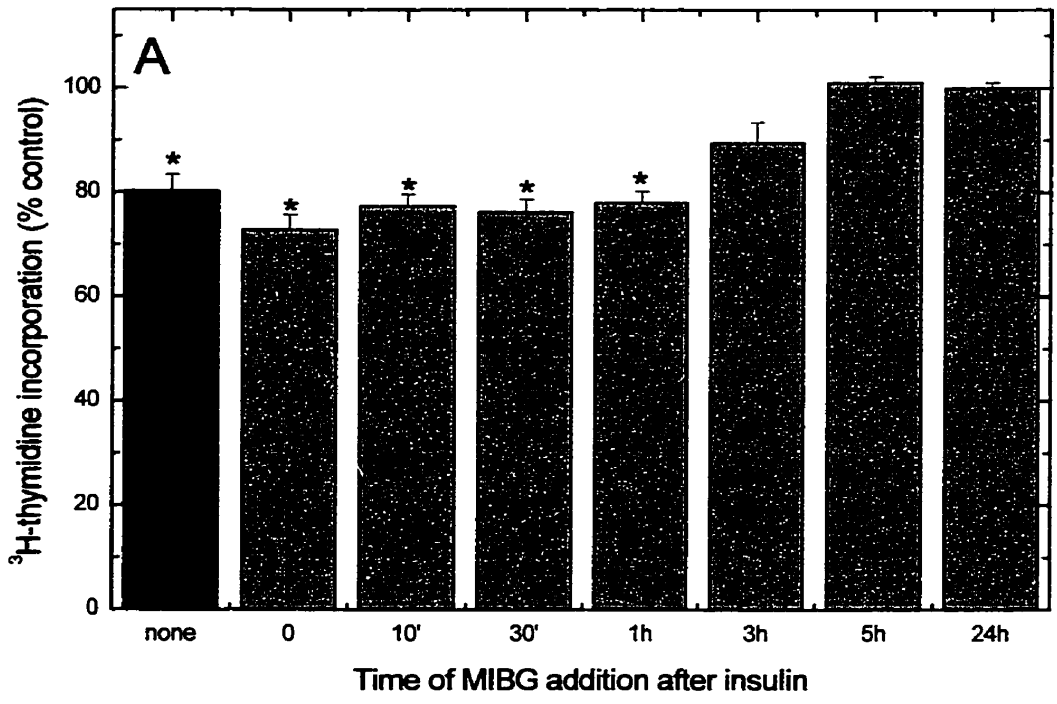
A
^{3}H-thymidine incorporation (% control)
0
20
40
60
80
100
none
0
10'
30'
1h
3h
5h
24h
Time of MIBG addition after insulin

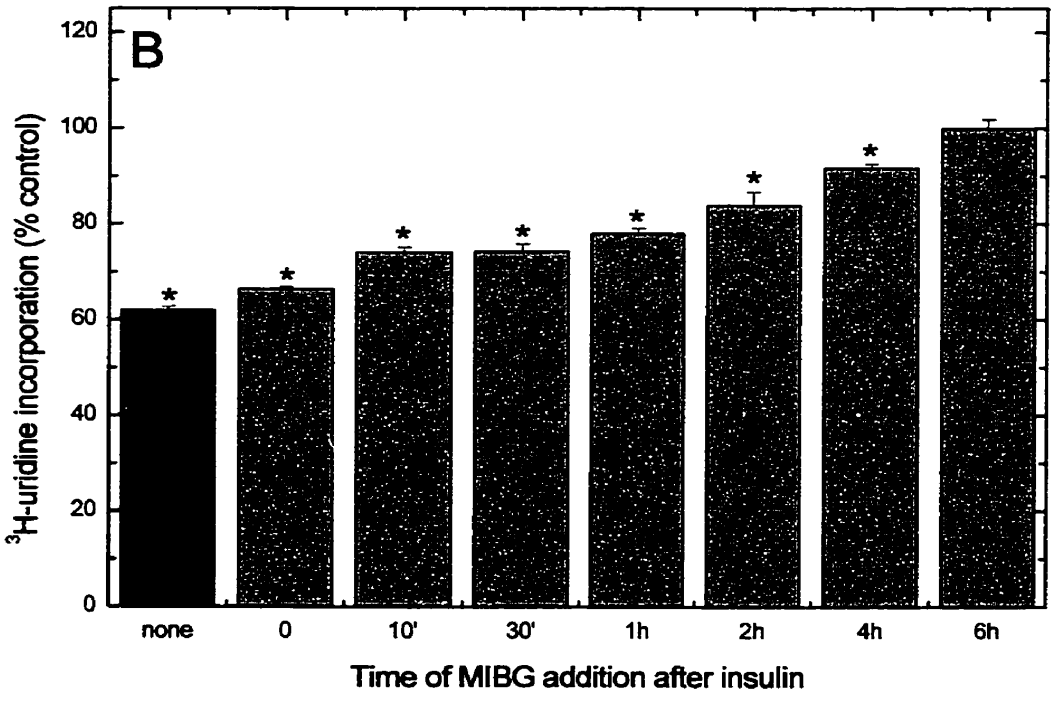
B
^{3}H-uridine incorporation (% control)
0
20
40
60
80
100
120
none
0
10'
30'
1h
2h
4h
6h
Time of MIBG addition after insulin

FIGURE 20: ***Time Course of MIBG Washout After Addition to Insulin-treated H4IIE Cells. Effect on Insulin-mediated Cell Growth.***

Quiescent H4IIE hepatoma cells were pretreated with MIBG (50 μM) for 10 min and insulin (10^{-6} M) was added. At the indicated times, the media containing MIBG was replaced with media containing insulin (10^{-6} M) and either 2 μCi of [^{3}H]uridine or 2 μCi of [^{3}H]thymidine. The incorporation of [^{3}H]uridine (6 h incubation) and [^{3}H]thymidine (24 h incubation) into trichloroacetate-precipitable material after addition of insulin was used to measure RNA (A) and DNA (B) synthetic activity. The incorporation rate of untreated cells (0) was set to 100%. For the 6 h time point, MIBG was not removed from the cells. The data are presented as the mean ± SE of at least three separate experiments conducted in triplicate. Comparisons were made between untreated cells and insulin treated cells that had MIBG removed at the indicated times using the Student's t-test (*, $p < 0.05$).

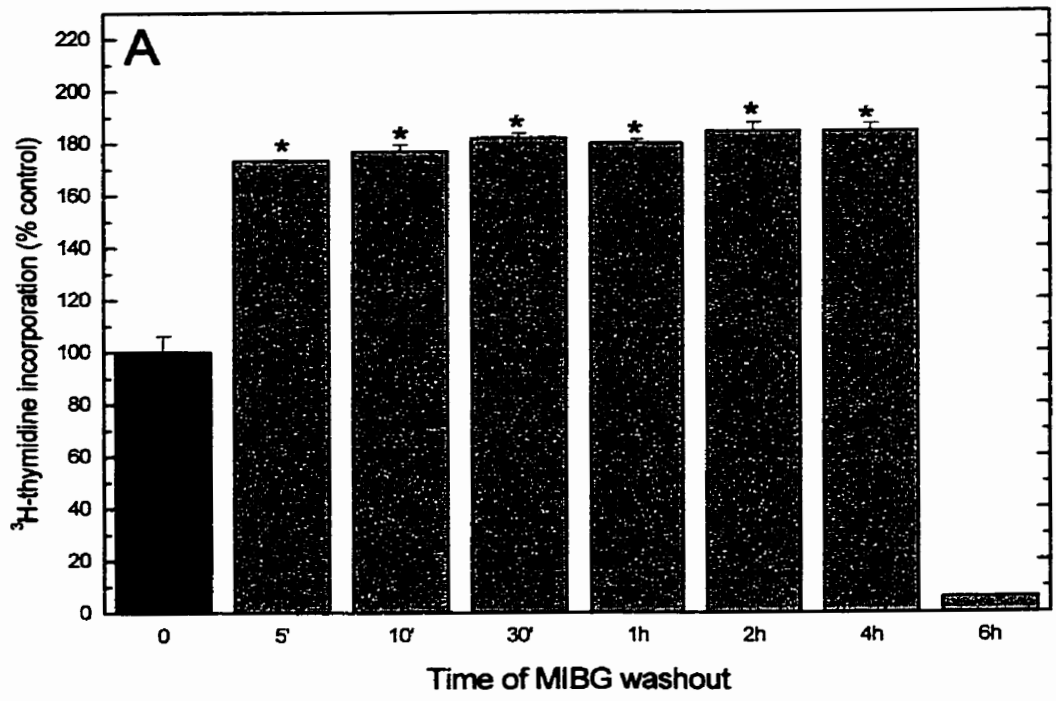
A
^{3}H-thymidine incorporation (% control)
0
20
40
60
80
100
120
140
160
180
200
220
0
5'
10'
30'
1h
2h
4h
6h
Time of MIBG washout

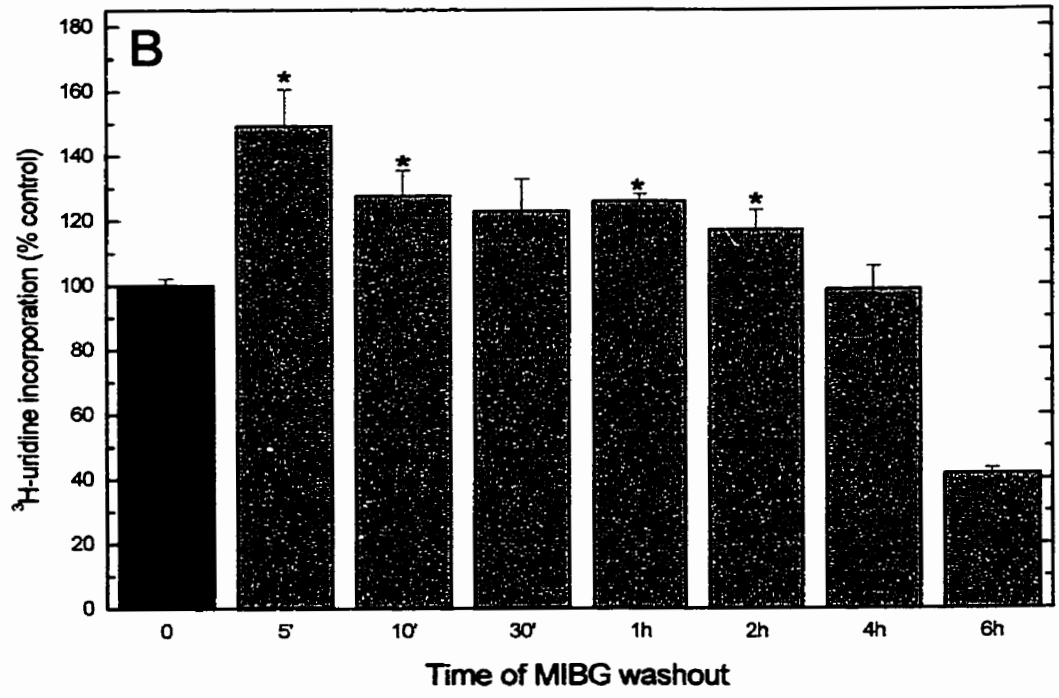
B
^{3}H-uridine incorporation (% control)
0
20
40
60
80
100
120
140
160
180
0
5'
10'
30'
1h
2h
4h
6h
Time of MIBG washout

present for 5 min to induce cell proliferation (Figure 3). Therefore, addition of MIBG at 10 min may have missed the critical MIBG-sensitive event activated by insulin. Nevertheless, these results, as well as those of the addition study (Figure 19), indicate that MIBG also inhibits a specific event occurring 3 to 6 h following insulin stimulation.

5.4.4.2 Toxicity of MIBG

As a result of the findings in section 5.4.4.1, where MIBG completely inhibited DNA synthesis, it was of interest to ascertain if the inhibition of H4IIE cell growth by MIBG was the result of a direct effect on cell cycle re-entry or the result of cellular toxicity. MTT cytotoxicity assays (i.e. mitochondrial reduction of a tetrazolium dye) employed a concentration range of both MIBA and MIBG (0-200 μM), and data were collected (i.e. cells lysed) at both 48 and 96 h after addition of the compounds. Growing, quiescent H4IIE cells and insulin-stimulated H4IIE cells were used to cover the entire growth spectrum for this assay. In growing and quiescent H4IIE cells, MIBA had little effect on MTT conversion after either 48 or 96 h of incubation, although quiescent cells appeared to be more sensitive to the MIBA (Figure 21A,C). The significance of the extra-sensitivity of the quiescent state may reflect the altered metabolic rate in quiescent cells. Taken together, these data suggest that MIBA is not cytotoxic to the cells and is minimally affecting the mitochondria of the cells. On the other hand, MIBG treatment decreased MTT conversion by both growing and quiescent H4IIE cells, with increasing concentrations of MIBG having a significantly greater effect (Figure 21B,D). This effect was time-dependent as well, with 96 h of incubation having a greater effect than 48 h (Figure 21B,D). Most importantly, these experiments identified the dose, 20 μM, at which MIBG (mitochondrial) toxicity may affect the cells. Moreover, H4IIE cells treated with insulin (data not shown) responded similarly to both treatments as growing and quiescent H4IIE cells. These data would indicate that MIBG is cytotoxic to the cells at

FIGURE 21: ***Effect of MIBG and MIBA on Growing and Quiescent H4IIE Cells.***

MTT Assay as a Measure of Cell Cytotoxicity.

Growing (A, B) and quiescent (C, D) H4IIE hepatoma cells were treated with varying concentrations (0 to 200 μM) of MIBA (A, C) or MIBG (B, D) for 48 and 96 h. MTT was then added to the cells for an additional 4 h, and colour development in the 96-well microtitre plates monitored at OD_{550}. The data are presented as the mean ± SE of at least three separate experiments conducted in quadruplicate.

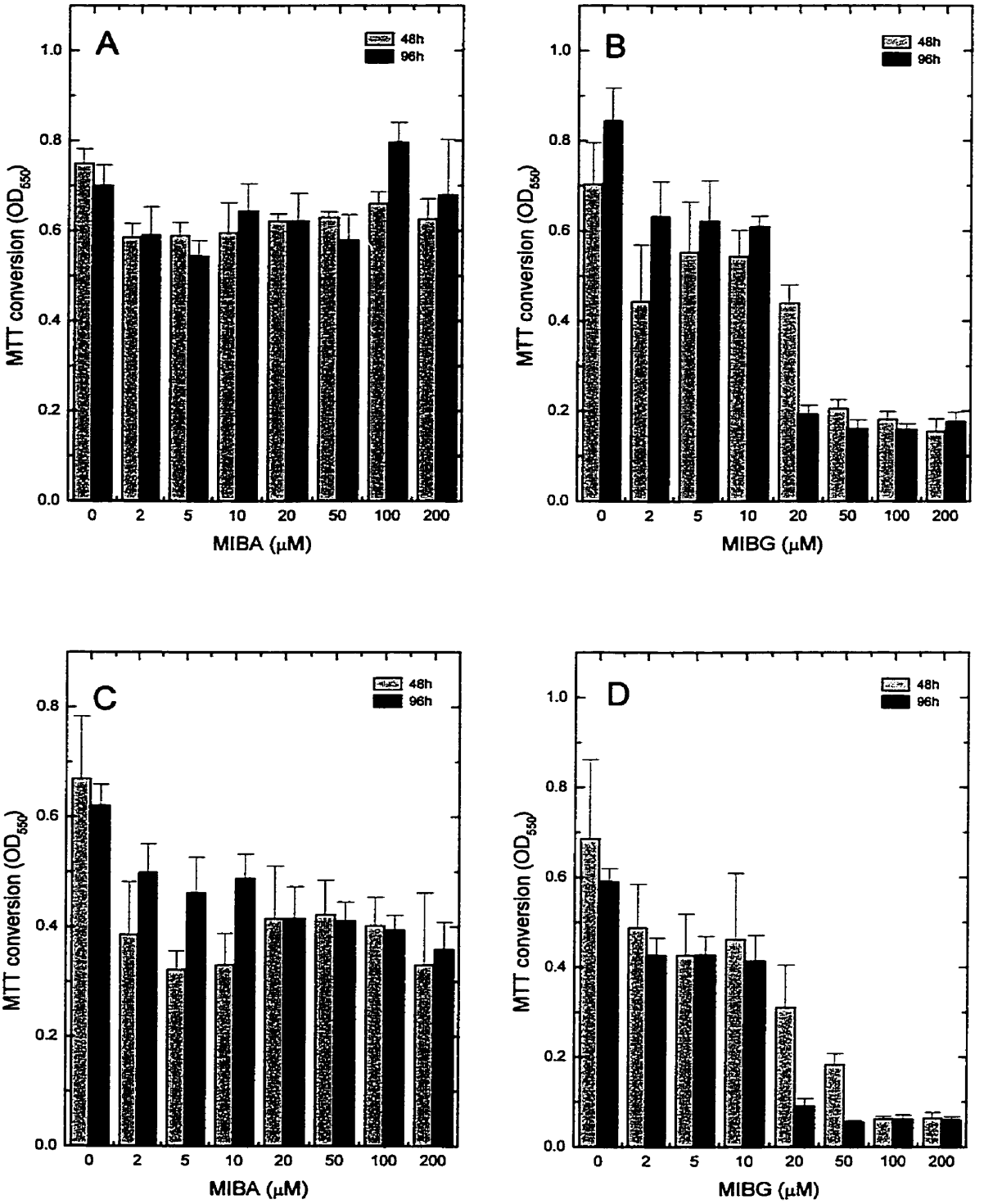
A
48h
96h
MTT conversion (OD_{550})
1.0
0.8
0.6
0.4
0.2
0.0
0
2
5
10
20
50
100
200
MIBA (μM)
B
48h
96h
MTT conversion (OD_{550})
MIBG (μM)
C
48h
96h
MTT conversion (OD_{550})
MIBA (μM)
D
48h
96h
MTT conversion (OD_{550})
MIBG (μM)

the higher concentrations and/or is having a detrimental effect on mitochondrial function, as previously reported (Loesberg *et al.* 1990a; Smets *et al.* 1990b). It should be noted however, that the MTT assay is limited in its ability to detect cell death. Since conversion of MTT is mitochondrial dependent, non-lethal effects on mitochondrial activity would also be observed with this assay.

To distinguish between cytotoxicity and mitochondrial activity inhibition by MIBG, a second assay was employed. LDH release from cells has been used as a measure of cytotoxicity and cellular membrane integrity. H4IIE cells were exposed to both MIBA and MIBG (0-200 μM) for 24 and 72 h, and LDH activity in the media was measured. After 24 h, MIBA did not increase LDH levels (Figure 22A). On the other hand, a 24 h treatment with MIBG increased LDH levels, but only at concentrations greater than 50 μM (Figure 22B). At 72 h, only the highest MIBA concentration increased LDH levels (Figure 22A), while LDH release was obtained with 20 μM or more MIBG (Figure 22B). These data support the MTT findings and imply that MIBG is having a cytotoxic effect. However, this interpretation must also take into account the effects of MIBG on mitochondrial respiration. MIBG (and analogs such as benzylguanidine) are proven inhibitors of complex I/III of the mitochondrial respiratory chain (Cornelissen *et al.* 1995a; Cornelissen *et al.* 1995b; Loesberg *et al.* 1990a; Loesberg *et al.* 1991; Smets *et al.* 1990b). If mitochondrial respiration is inhibited, a cell must obtain energy from the anaerobic glycolytic pathway which increases the lactate content of a cell. This increase in lactate content would be expected to induce LDH, and it may be this increase in LDH levels that is being detected with this assay. Although the LDH released may not have been the result of cytotoxicity, nevertheless, membrane integrity must have been compromised since LDH activity was detectable in the media.

FIGURE 22: ***Effect of MIBG and MIBA on Growing H4IIE Cells. LDH Release as a Measure of Cell Cytotoxicity.***

Growing H4IIE hepatoma cells were treated with varying concentrations (0 to 200 μM) of MIBA (A) or MIBG (B) for 24 and 72 h. Media were harvested and the LDH content measured with the LDH Cytotoxicity Assay kit from Boehringer-Mannheim. Colour development in the 96-well microtitre plates was monitored at OD_{490}. The data are presented as the mean ± SE of at least three separate experiments conducted in quadruplicate.

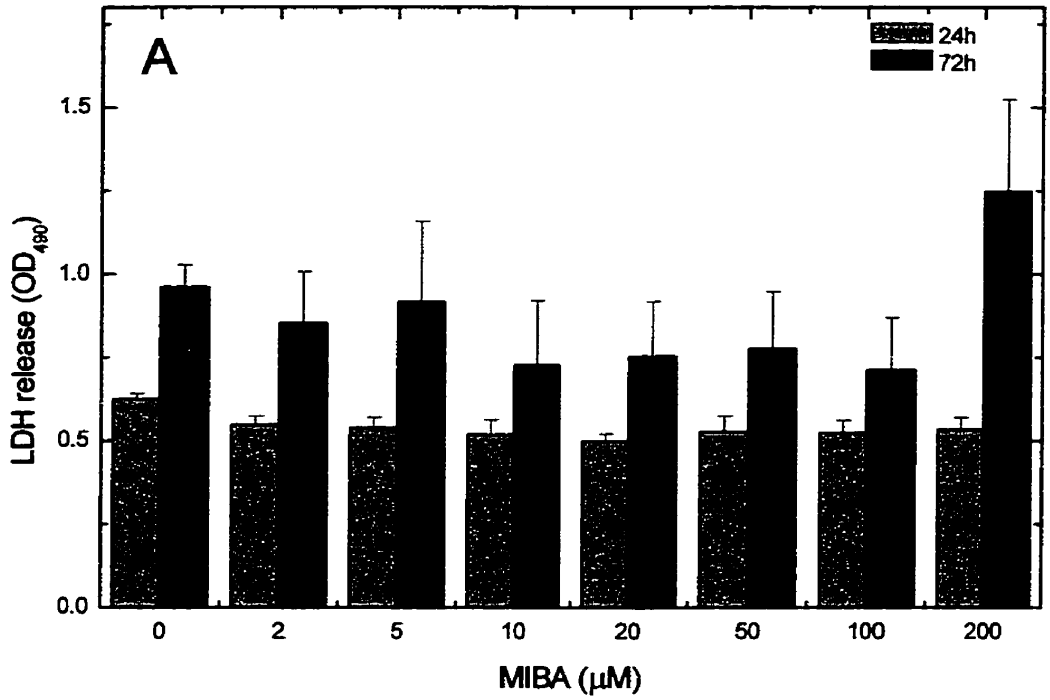
A
24h
72h
LDH release (OD490)
1.5
1.0
0.5
0.0
0
2
5
10
20
50
100
200
MIBA (μM)

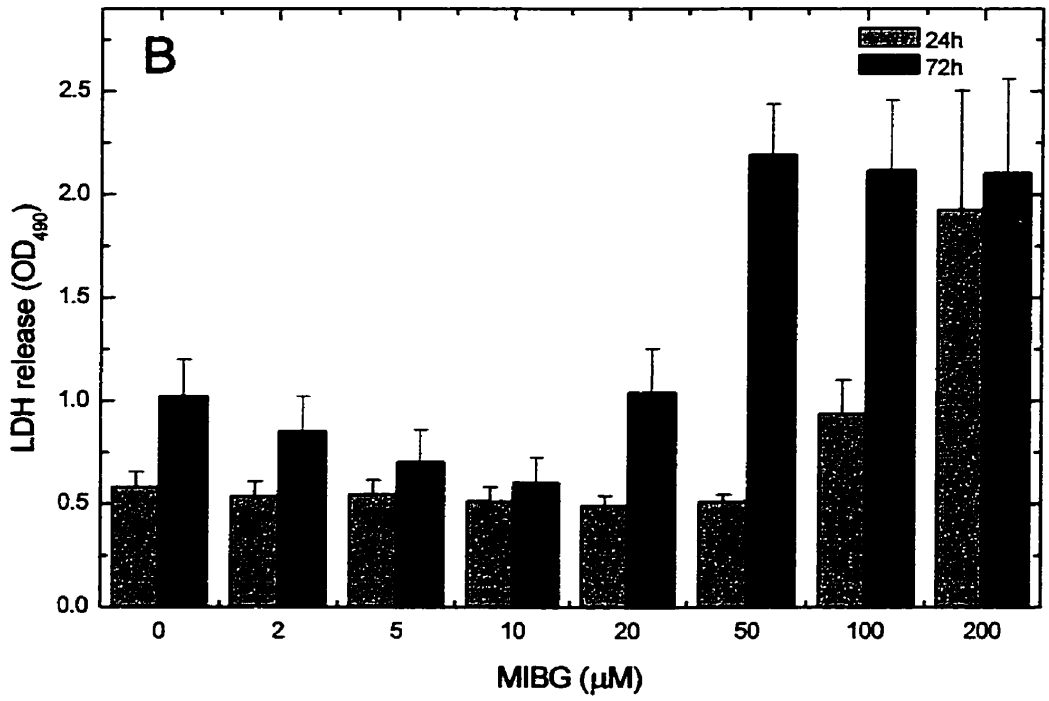
B
24h
72h
LDH release (OD490)
2.5
2.0
1.5
1.0
0.5
0.0
0
2
5
10
20
50
100
200
MIBG (μM)

The uncertainty in detecting MIBG cytotoxicity with the MTT and LDH assays led to the inclusion of a third assay in this study. FACS analysis was used to determine the extent of cellular damage produced by MIBG, to determine whether cell death was occurring and to determine how MIBG affects progression of H4IIE cells through the cell cycle. Untreated, growing H4IIE cells demonstrated the typical distribution of cells in various stages of the cell cycle, with a broad band of cells in the S phase of the cell cycle (Figure 23). After 48 h in the presence of MIBG (50 μM), H4IIE cells were primarily distributed in the G_1 phase of the cell cycle, with a noticeable absence of S phase cells (Figure 23). Interestingly, the cells were distributed in a pattern suggestive of cells that were viable, but not undergoing replication. Moreover, distribution of cells by size on the axes indicated that the cells had not fragmented or undergone lysis, since the size of MIBG treated cells was comparable to that of untreated cells (Figure 23). These particular data would suggest that MIBG is not exerting cytotoxic effects on H4IIE cells, which contrasts with the previous assays (Figures 21, 22), and rather that MIBG is having a cytostatic effect.

To further clarify whether MIBG has adverse effects on H4IIE cells, H4IIE cell number was measured after 48 and 96 h of MIBG and MIBA treatment (0-1000 μM). MIBG significantly decreased cell number in both growing and quiescent H4IIE cells, with the higher concentrations demonstrating an almost complete loss of cells (Figure 24C,D). However, cell losses were not detected at concentrations below 20-50 μM. In contrast, MIBA did not significantly affect cell number unless very high concentrations (greater than 200 μM) were used (Figure 24A,B). These data would suggest and support the earlier results (Figures 21, 22) that indicate MIBG is cytotoxic. Further studies, not contained within the body of this work, are attempting to clearly establish whether MIBG

FIGURE 23: ***Effect of MIBG on Cell Cycle.***

Growing H4IIE hepatoma cells were treated with MIBG (50 μM) for 48 h prior to manipulation of cells for FACS analysis (B). Untreated growing H4IIE cells were used for comparison (A). Two hours prior to harvest, cells were pulse-labelled with 50 μM BrdU. Incorporation of BrdU into DNA-synthesizing cells and cell cycle distribution was assessed by FACS using a monoclonal FITC-anti-BrdU antibody and propidium iodide staining to measure cellular DNA content, respectively. Shown are dot plots of the cell cycle distribution. DNA content is represented by propidium iodide fluorescence along the *x*-axis while BrdU incorporation is represented by the log of FITC fluorescence on the *y*-axis. The box depicts those cells in S phase, both early and late. One of three independent experiments is shown, all of which exhibited a similar response.

.

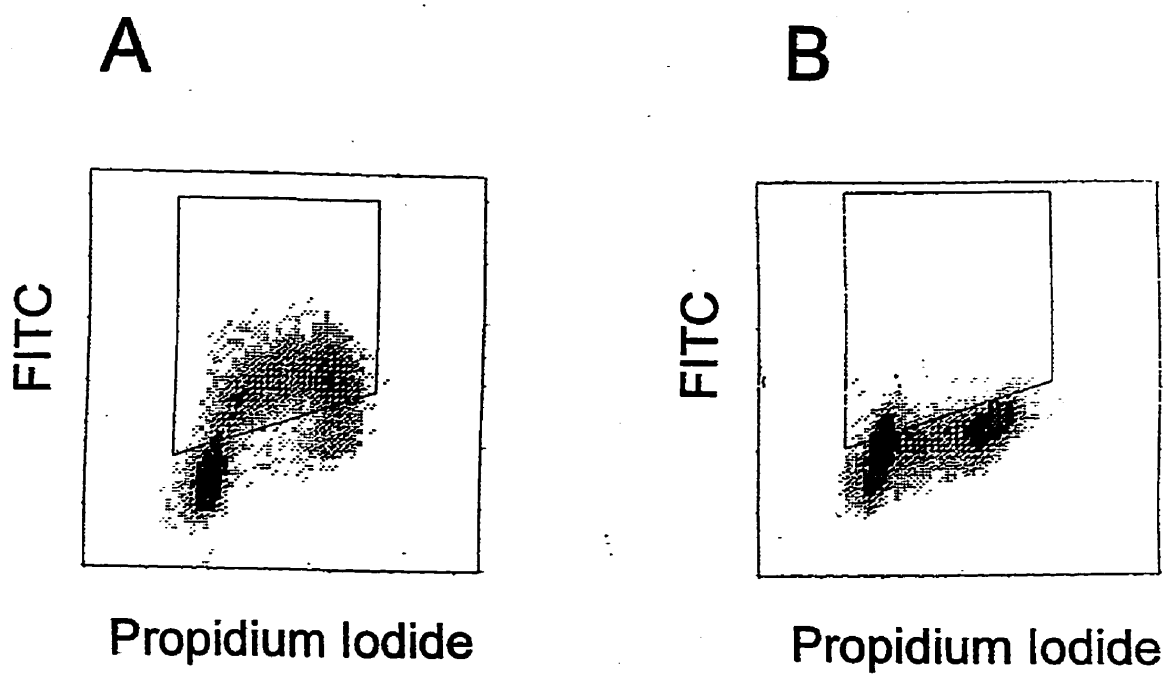
A
FITC
Propidium Iodide
B
FITC
Propidium Iodide

FIGURE 24: ***Effect of MIBG and MIBA on Cell Viability. Coulter Counting as a Method for Determining Cell Cytotoxicity.***

Growing (A, C) and quiescent (B, D) H4IIE hepatoma cells were treated with MIBG (C, D) or MIBA (A, B) (0-1000 μM) for 96 h. The wells were then rinsed, the cells released by trypsinization and cell number assessed with a Coulter Counter. One of two experiments is shown, both of which exhibited a similar response. Each data point was counted in triplicate from samples prepared in duplicate.

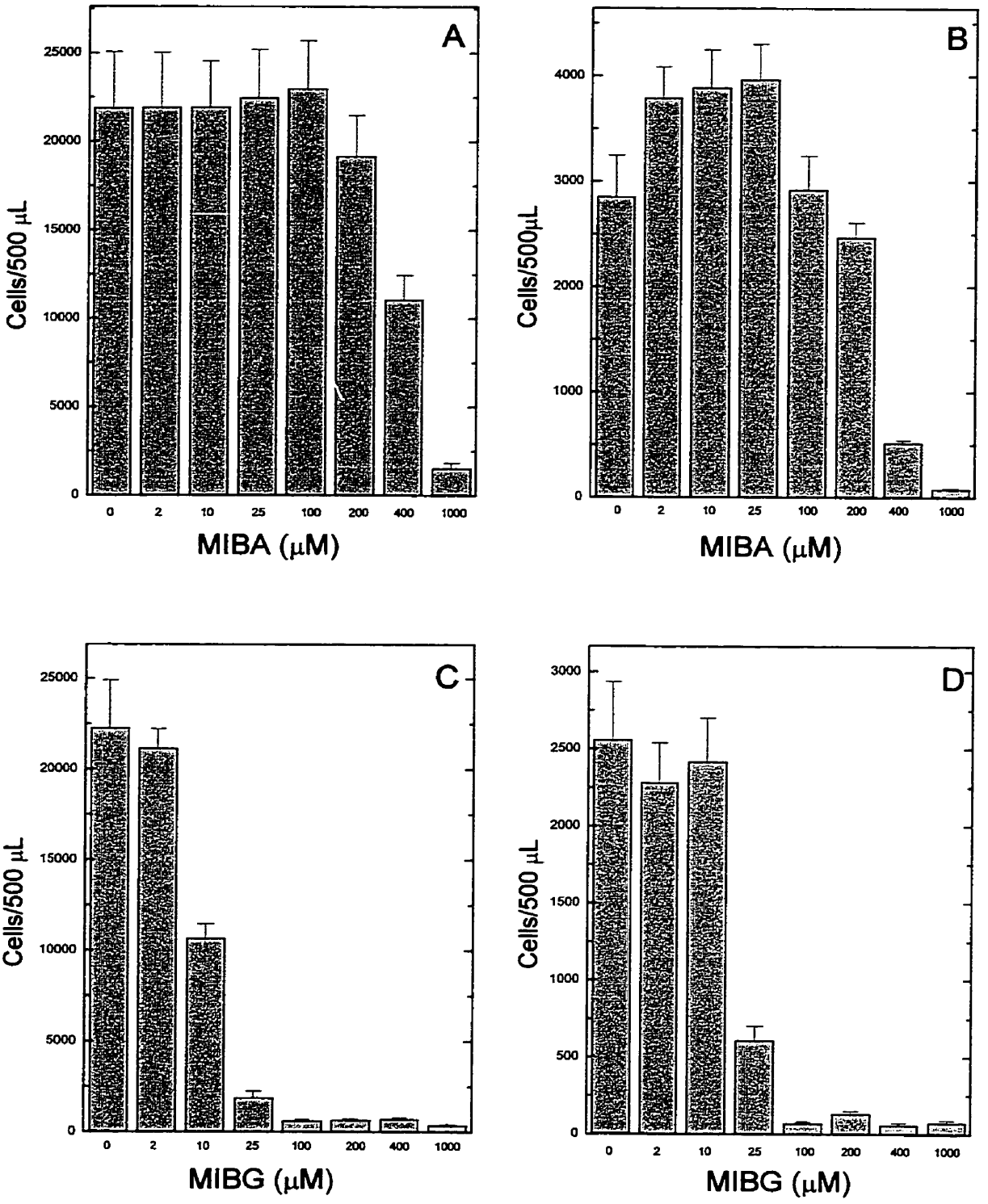
A
Cells/500 µL
25000
20000
15000
10000
5000
0
0 2 10 25 100 200 400 1000
MIBA (µM)
B
Cells/500µL
4000
3000
2000
1000
0
0 2 10 25 100 200 400 1000
MIBA (µM)
C
Cells/500 µL
25000
20000
15000
10000
5000
0
0 2 10 25 100 200 400 1000
MIBG (µM)
D
Cells/500 µL
3000
2500
2000
1500
1000
500
0
0 2 10 25 100 200 400 1000
MIBG (µM)

is cytotoxic or cytostatic and to identify the mechanism by which cell cycle and S phase progression are inhibited.

Finally, to determine if MIBG has an effect on the metabolism of H4IIE cells, glucose uptake was measured after stimulation with insulin in the presence and absence of MIBG (10-100 μM). It was observed that MIBG significantly reduced the amount of insulin-mediated [^{3}H]glucose uptake by H4IIE cells (Figure 25) in a concentration–dependent manner. These data support the contention that MIBG may be having a metabolic effect and may also suggest a second mechanism by which it affects cell growth and proliferation.

5.4.4.3 Mechanism of action of MIBG

MIBG has a potent inhibitory effect on cell growth induced by insulin stimulation. As a result, it was of interest to identify growth-associated signaling pathways activated by insulin that are inhibited by the actions of MIBG. Two signaling systems were identified as possible candidates: MAP kinase, which is generally activated in a variety of cell types that undergo growth, and p21-Ras which is upstream of MAP kinase, but also participates in signaling events independent of MAP kinase (Hall 1993; Lim *et al.* 1996; Marshall 1996; Olson & Marais 2000).

Insulin stimulated the activation of MAP kinase as measured by an in gel activity assay. Activity was transiently increased over a time course of 20 min, with peak activation occurring at 2 to 5 min (Figure 26 and Figure 7 from section 5.2.4.3). Pretreatment of H4IIE cells with 3AB (5 mM) for 10 min before insulin addition resulted in a diminution of the MAP kinase response (Figure 26). In contrast, pretreatment with MIBG (50 μM) for 10 min before insulin addition resulted in an apparent enhancement of MAP kinase activity (Figure 26). The importance of MAP kinase in the insulin-mediated growth response is already documented (Figure 10). Therefore, these findings suggest

FIGURE 25: ***Effect of MIBG on Glucose Uptake in H4IIE Cells.***

The incorporation of [^{3}H]glucose was measured as described in Materials and Methods (section 4.3.8) after addition of insulin (10^{-9} M) to quiescent H4IIE cells subsequent to pretreatment with varying concentrations (10 to 100 μM) of MIBG. The rate of uptake in untreated cells was set to 100%. FBS (2% v/v) was used as a negative control. Each data point represents the mean ± SE of two experiments conducted in triplicate.

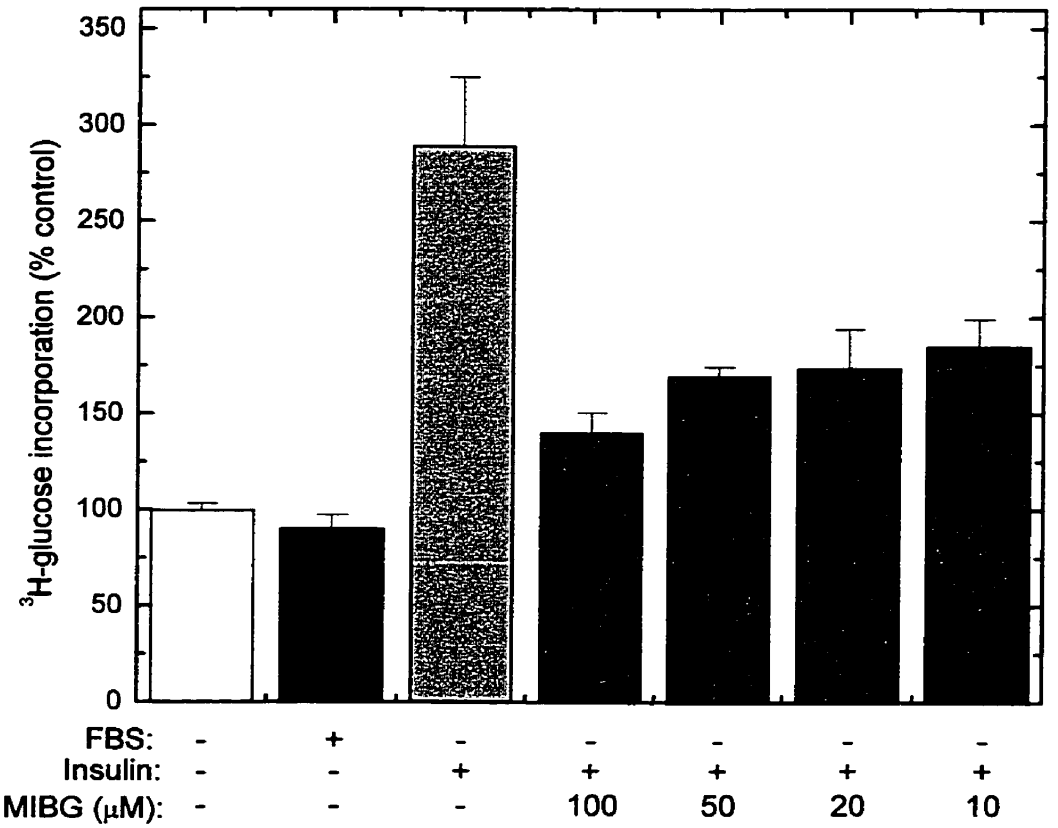
350
300
250
200
150
100
50
0
^{3}H-glucose incorporation (% control)
FBS: - + - - - - -
Insulin: - - + + + + +
MIBG (μM): - - - 100 50 20 10

FIGURE 26: ***Effect of Inhibitors of ADP-ribosylation, 3-Aminobenzamide and MIBG, on MAP Kinase Activation by Insulin in H4IIE Cells.***

MAP kinase activity was measured over 20 min by activity gel assay. Cells were stimulated with insulin (10^{-6} M) and pretreatment with either 3-aminobenzamide (5 mM) or MIBG (50 μM) occurred 10 min prior to insulin addition. Cells were harvested at the indicated time points. Densitometry of the $p42^{MAPK}$/$p44^{MAPK}$ bands is plotted from one experiment. Three independent experiments were conducted, all of which exhibited a similar response.

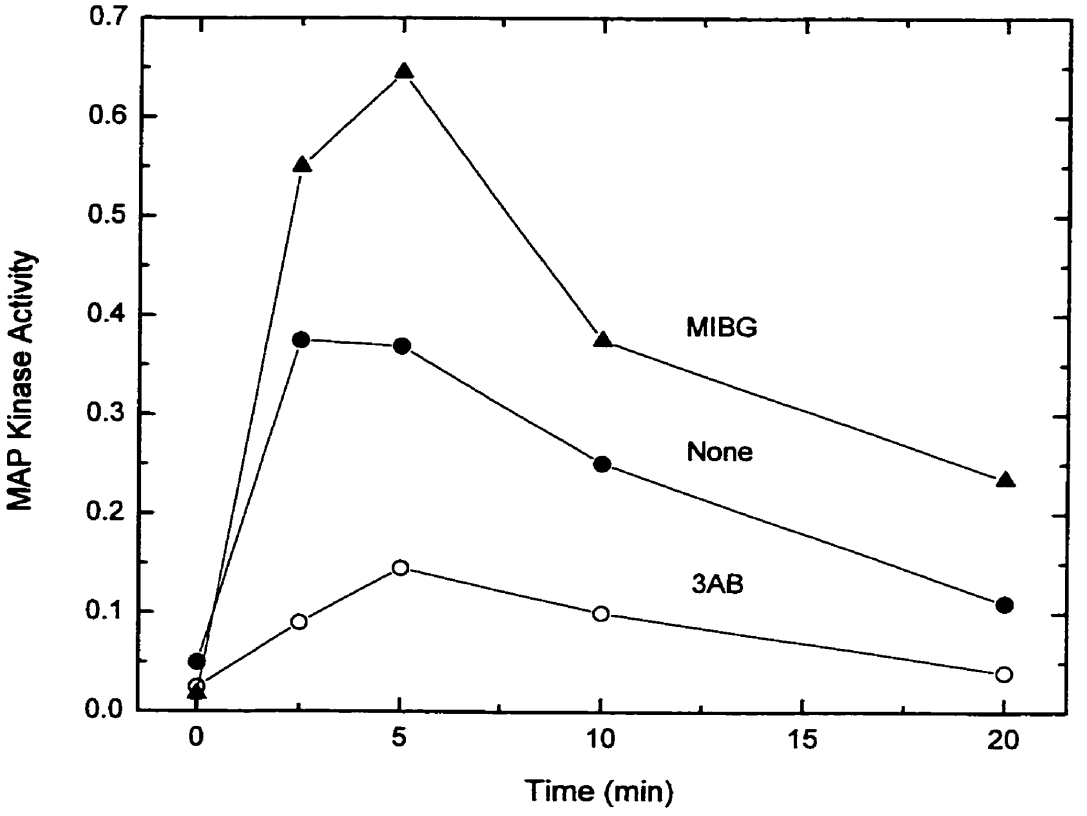
MAP Kinase Activity
0.0
0.1
0.2
0.3
0.4
0.5
0.6
0.7
0
5
10
15
20
Time (min)
MIBG
None
3AB

that the inhibition of cell growth and proliferation by MIBG is not the result of inhibition of MAP kinase activity.

p21-Ras was investigated because it is frequently activated in growing cells (de Vries-Smits *et al.* 1992; Mansour *et al.* 1994) and, because as a small GTP-binding protein, the possibility that it might be ADP-ribosylated is quite high (Lerm *et al.* 2000; Schmidt & Aktories 1998; Tsuchiya & Shimoyama 1994). Ras activation was detected by measuring the ratio of GTP and GDP bound Ras. This assay involved [^{32}P]orthophosphate labeling of cellular phosphate pools followed by immunoprecipitation with a specific anti-Ras antibody and subsequent separation of GTP/GDP pools by TLC (section 4.9.5). Addition of insulin (10^{-6} M) to quiescent H4IIE cells for 10 min resulted in a significant increase in GTP:GDP ratio in the cells (Figure 27). This activation could not be blocked by either pretreatment with 3AB (5 mM) or MIBG (50 μM), which would suggest that p21-Ras is not the target for MIBG action.

5.4.5 Discussion

The initial studies in this section, dealing with a variety of different inhibitors of ADP-ribosylation reactions, indicated that only the specific inhibitor of arg-mART, MIBG, was capable of inhibiting insulin-stimulated cell growth and proliferation in H4IIE cells (Figures 16, 17, 18). The dual ADP-ribosyltransferase inhibitor 3AB, had only a modest effect on RNA synthesis and no effect on DNA synthesis (Figures 16, 17). Structural analogues of MIBG, that should behave as pseudosubstrates for arg-mART, did not have apparent inhibitory effects on H4IIE cell growth or proliferation (Figure 17). Specifically, based on structure, it was assumed that LAME and LNAME would behave in a similar fashion to MIBG if arg-mART was indeed the target of inhibition. However, physicochemical constraints were noted that could have prevented these compounds from

FIGURE 27: ***Effect of Inhibitors of ADP-ribosylation, 3-Aminobenzamide and MIBG, on p21-Ras Activation by Insulin in H4IIE Cells.***

p21-Ras activity was measured in quiescent H4IIE cells after stimulation with insulin or IGF-1 (10^{-6} and 10^{-7} M, respectively) following a 10 min pretreatment with 3-aminobenzamide (5 mM) or MIBG (50 μM). [^{32}P]Orthophosphate labeling of cellular phosphate pools allowed the separation of Ras-activated GTP/GDP pools by TLC analysis (section 4.9.5). Data pooled from three independent experiments is represented graphically. Untreated controls were set to 100%. Data are presented as means ± SE. Comparisons were made between control and insulin treated cells, and insulin treated cells and insulin + inhibitors cells using the Student's t-test (*, $p < 0.05$).

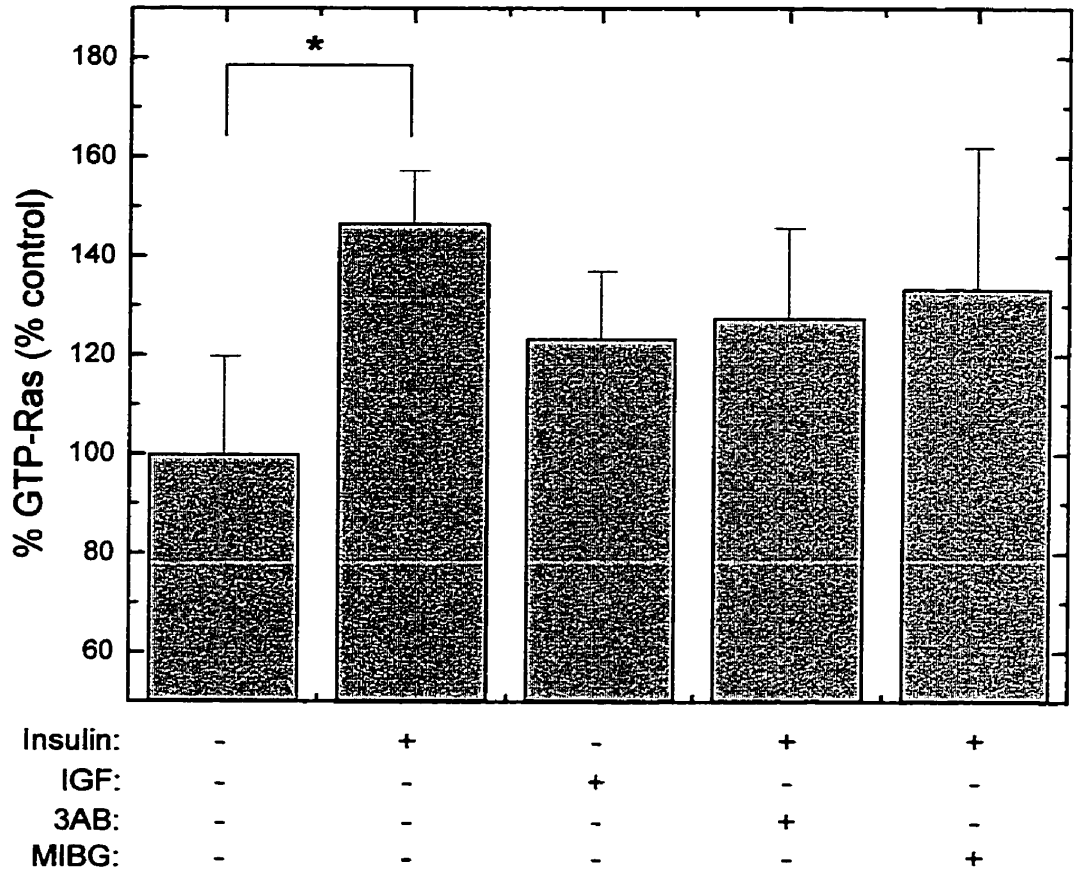
*
180
160
140
120
100
80
60
% GTP-Ras (% control)
Insulin: - + - + +
IGF: - - + - -
3AB: - - - + -
MIBG: - - - - +

behaving as pseudosubstrates for arg-mART. In particular, LNAME may not behave as a pseudosubstrate due to steric hindrance from the presence of a nitro group on the guanidino moiety. On the other hand, LAME is highly positively charged, and the presence of the charges would reduce cell entry via passive diffusion (although the charges may allow the molecule to be more attractive to the cell membrane). As a result, although LAME is a substrate for arg-mART *in vitro*, it may not be able to reach its point of action *in vivo*. Thus, lack of inhibitory effect of these compounds (LAME and LNAME) does not necessarily imply that MIBG is not effectively inhibiting an arg-mART. In fact, these studies support the concept that an arg-mART is involved in the cell proliferative processes activated by insulin and that MIBG is inhibiting this enzyme activity. Since MIBG was able to inhibit the activation of an arg-mART *in vitro* (section 5.3.4.1), it may be assumed that inhibition of cell growth by MIBG involves the inhibition of an arg-mART that regulates a process that is critical for the cell proliferative program. Moreover, the steps that may be affected are related to progression of the cells from quiescence into the cell cycle. MIBG may be behaving as a cytostatic agent through the blockade of events required for the entry of cells into the cell cycle, or transition from the G_1 to S phase. Although studies were not carried out to delineate in more detail the mechanism of action of MIBG and how it relates to inhibition of the cell cycle, these studies are planned. It is also possible that MIBG could just be inhibiting the mechanism for the uptake of the radiolabelled agents and thus the appearance of inhibition of cell proliferation would be observed. However, this scenario does not appear to be borne out by the FACS analysis, where it was shown that MIBG could specifically inhibit S phase entry (Figure 23). It is possible that the absence of cells in S phase could indicate cell death, but the presence of cells in other phases of the cell cycle would not support this conclusion. Furthermore, the cells did not appear to be dead or dying, or undergoing

necrosis, since cell fragmentation was not apparent, and a downshift of the curve was not observed. Moreover, if uptake of BrdU was being prevented, the height of the curve would have shifted to reflect this.

It is generally accepted that mitogenic stimulation initiates a cascade of events that are temporally ordered to ensure regulated progression through the cell cycle. As part of this process, the cell is required to provide the necessary macromolecular components for each step of the mitogenic program, as well as supply energy in the form of ATP. While MIBG could inhibit cell growth by either mechanism, there is strong evidence in the literature to support interference with mitochondrial function as the primary route by which MIBG operates (Loesberg *et al.* 1990a; Smets *et al.* 1991; Van den Berg *et al.* 1997). Additional support for this concept is provided by the MTT and LDH release experiments (Figures 21, 22), since the FACS analysis (Figure 23) indicates the cells exposed to MIBG are not actually dying. The results of both MTT and LDH studies can be explained by the known inhibitory effects of MIBG on mitochondrial respiration (Cornelissen *et al.* 1995a; Cornelissen *et al.* 1995b; Loesberg *et al.* 1990a; Smets *et al.* 1991). Inhibition of mitochondrial respiration would prevent the conversion of the tetrazolium dye by the mitochondria, since this process requires electron transfer. Similarly, inhibition of mitochondrial respiration leads to an elevated rate of glycolysis in order to maintain ATP levels. During anaerobic respiration, the amount of lactate generated by the cell would increase. Concomitantly, LDH levels would rise. Thus, inhibition of mitochondrial function does not necessarily lead to cell death, but could interfere with cell functions essential for growth and proliferation. On the other hand, an analog of MIBG, benzylguanidine, has been shown to also inhibit mitochondrial respiration (Van den Berg *et al.* 1997). However, this compound was not able to inhibit insulin-mediated H4IIE cell proliferation (Bernardin, Litchie & Zahradka, unpublished

observations), which would definitely suggest that mitochondrial inhibition is not linked to the anti-proliferative effects of MIBG. This latter point would support the participation of a mART in the cell proliferative processes mediated by insulin in H4IIE cells, and a role for MIBG in preventing cell proliferation via an arg-mART. Moreover, Cornelissen *et al.* (1995a; 1995b) have observed a differential concentration of MIBG required for complete inhibition of mitochondrial ATP synthesis in comparison to inhibition of cell proliferation (10 μM vs. 25 μM, respectively). Thus, the inhibition of mitochondrial respiration is not entirely responsible for the cell proliferative inhibitory properties of MIBG, and MIBG must influence cellular processes apart from mitochondrial ATP synthesis (Cornelissen *et al.* 1997b; Cornelissen *et al.* 1995a), lending further support for the participation of a mART.

The possibility also exists that MIBG may be inhibiting cell growth via a non-ADP-ribosyltransferase pathway. Since MIBG resembles arginine, which is a donor for nitric oxide (NO) synthesis, it is possible that MIBG also behaves as a donor for NO synthesis, and NO is a known inhibitor of cell proliferation (Cornwell *et al.* 1994; Kolpakov *et al.* 1995; Nakaki *et al.* 1990). However, Kuin et al. (Kuin *et al.* 1998) demonstrated that MIBG (100 μM) inhibits all three forms of nitric oxide synthase, which would prevent NO synthesis and the inhibitory effects typically associated with NO. If the converse were true, that inhibition of NO synthesis is required for inhibition of cell proliferation, then it would have been expected that LNAME, an inhibitor of nitric oxide synthase, would have been able to inhibit cell growth and proliferation in this cell system (Figure 16). Thus, the participation of NO in these events is unlikely, and lends further credence to the participation of an arg-mART in H4IIE cell growth and proliferation that is inhibitable by MIBG.

In addition to inhibiting cell growth processes, MIBG decreased glucose uptake in response to insulin (Figure 25). Glucose is transported into cells via the GLUT-2/4 transporter and MIBG could potentially be having a direct effect on the transporter (Czech 1995; Fletcher & Tavare 1999; Kahn 1996; Mueckler 1994; Olson & Pessin 1996; Thorens 1992). Alternatively, MIBG might reduce the cellular energy pools (via its effects on the mitochondria) and indirectly halt this energy-dependent transporter process. Ironically, a cell with inhibited mitochondrial respiration relies more heavily on glucose and the glycolytic pathway for the generation of ATP. Thus, while it would be more advantageous for the cell to increase glucose uptake for the glycolytic pathway, if the cell does not, disruption of a wide variety of energy-dependent process and, subsequently, cell death may instead ensue. This may be part of the mechanism of inhibition of cell growth for MIBG.

H4IIE cells may be more sensitive to the effects of MIBG because hepatocytes and hepatomas have a high metabolic rate and would therefore rely heavily on their mitochondria for metabolism, including cell growth and proliferation. On the other hand, exclusion of a direct effect on the mitogenic program by MIBG is not possible on the basis of the delayed addition and washout studies. The effect of MIBG on DNA synthesis, in particular, would suggest that the target is a specific process required for progression to S phase that occurs within the first 3 to 6 h after treatment with insulin (Figures 19, 20). Thus, the first 5 to 6 h are the most critical for the inhibitory action to be evident, although MIBG should be present over the entire time period to produce the most profound effect. In contrast, MIBG was required to be present for the entire length of the assay in order to be effective at reducing RNA synthesis (Figures 19, 20). These results may suggest that MIBG is affecting this process on a more global level or that

constitutive activation of a single target is required for the insulin-dependent increase in RNA synthesis.

Since the mechanism by which MIBG inhibits cell growth could not be consistently and conclusively linked to an inhibition of mitochondrial respiration, the effect of MIBG on certain signaling pathways was examined. MAP kinase, which was established as being critical for insulin-stimulated H4IIE cell proliferation (Figure 10), was not inhibited by MIBG (Figure 26). This may indicate that inhibition of cell proliferation by MIBG occurs downstream of MAP kinase or involves a separate but parallel pathway. Similarly, MIBG did not decrease the GTP:GDP ratio of p21-Ras stimulated by insulin addition (Figure 27). The latter molecule was chosen because of the importance of p21-Ras in growth regulatory signaling pathways, and also because it is a small GTP-binding protein that may be modified by ADP-ribosylation (Tsuchiya & Shimoyama 1994). These results would indicate that the action of MIBG lies after both of these signaling steps have occurred, possibly in the nucleus.

5.5 Summary

H4IIE hepatoma cells, used primarily for the study of the biochemical and metabolic changes in the liver during malignancy, have also been used for the study insulin-dependent cell proliferation. To define the proliferative response to insulin in our cell system, and to identify the signaling molecules associated with the cell proliferative responses, the responses of H4IIE cells to insulin and IGF-1 were studied. In this series of studies it was observed that insulin, but not IGF-1 is capable of stimulating both mitogenesis and glucose utilization in H4IIE hepatoma cells. The distinct response to insulin and IGF-1 exhibited by H4IIE cells made it possible to examine the early signaling events triggered by these ligands. The data suggest that phosphorylation of IRS-

1 via the receptor tyrosine kinase is required for both cell growth and metabolism, but it does not necessarily participate in the pathways leading to MAP kinase activation. Furthermore, MAP kinase activation appears to play an important role in the cell growth and proliferation events activated by insulin in H4IIE cells. However, it is recognized that distinct and independent pathways other than MAP kinase also contribute to cell growth and proliferation.

The activation of cell growth in H4IIE cells appears to be linked to the activation of an arg-mART, since insulin increases the activity present in the microsomal fraction of H4IIE cells. Enhanced nuclear PARP activity was not observed and inhibition of this enzyme did not prevent cell growth. In contrast, inhibitors of arg-mART were able to abrogate the insulin-stimulated RNA and DNA synthesis in H4IIE cells. Although the precise mechanism of action of MIBG to prevent cell growth is still not clear, despite the numerous attempts made to clarify this issue, it can be concluded that the insulin-mediated H4IIE cell growth is sensitive to MIBG and not to its analog MIBA. This conclusion speaks of the importance of the argininyl (guanidino) moiety for the inhibitory activity of these compounds. Two distinct mechanisms of action were considered: i) MIBG is acting at specific points within the cell to inhibit cell growth and proliferation, and ii) MIBG is affecting cell growth processes indirectly through its ability to inhibit mitochondrial activation. Experiments to define the latter mechanism were inconclusive while experiments targeted to the former mechanism revealed that MIBG must be affecting signal molecules downstream to MAP kinase, or an unrelated but parallel signal pathway that is also critical for cell growth and proliferation. At this point, regardless of its mechanism of action, it is sufficient to mention that MIBG is an effective inhibitor of cell growth. Future studies will need to clarify these issues and to further define the

cytotoxic effects of MIBG. Direction for these additional studies will be based on the results presented in section 7.4.

6.0 L6 skeletal myoblasts as a model of differentiation

6.1 Introduction

The development of skeletal muscle is controlled by a highly synchronized series of events. In this process, called myogenesis, cells that have no specialized characteristics are converted into muscle fibres which permit body movement. Various signals from outside and inside the cell regulate the switch from unspecialized to muscle cell.

The conversion of multipotential mesodermal stem cells present in the ventral somites into muscle fibres occurs through a multistep process directed by the sequential expression and activation of specific transcription factors (Sassoon 1993; Venuti & Cserjesi 1996). Two distinct stages are involved in the establishment of the skeletal muscle phenotype (Ludolph & Konieczny 1995). The first, termed commitment or determination, requires the synthesis of a single myogenic factor (either MyoD or myf5) and establishes the cell's ability to eventually express the skeletal muscle phenotype. The ensuing second stage, which governs the actual differentiation process, requires the sequential expression of myogenin and $p21^{CIP1}$, and is characterized by expression of muscle-specific contractile proteins (eg. myosin heavy chain), fusion of the individual myoblasts into multinucleated myotubes and cessation of cell division (Dias *et al.* 1994; Walsh 1997). Expression of $p21^{CIP1}$ is required for withdrawal of cells from the cell cycle. Both stages of the myogenic program are temporally distinct and independently regulated (Lassar & Munsterberg 1994).

The myogenic lineage is established once mesodermal stem cells, which have the potential to differentiate into either chondroblasts, adipoblasts or myoblasts, express either MyoD or myf5. MyoD was first identified when Davis *et al.* (1987), showed that expression of a single gene was sufficient to convert a fibroblast into a myoblast. Similar experimental approaches were used to isolate myf5, myogenin and MRF4, and their

importance for skeletal muscle formation was confirmed by their ability to direct myogenesis when ectopically expressed in non-myogenic cells (Weintraub *et al.* 1991). Expression studies of these myogenic regulatory factors (MRFs) during embryonic development revealed that all four proteins are synthesized within the somites in a temporally ordered pattern (Smith *et al.* 1993; Yun & Wold 1996). It was further demonstrated that both MyoD and myf5 are expressed in proliferating myogenic cells (myoblasts) prior to their differentiation into myotubes (Rudnicki *et al.* 1993). The correlation between these factors and commitment to a myogenic lineage was also evident in myogenic cell lines where MyoD or myf5 are expressed in the myoblast. Moreover, recently generated knockout mice for MyoD and myf5 suggest that absence of one of these MRFs does not abrogate the myogenic program while the absence of both results in mice with no skeletal muscle (Rudnicki *et al.* 1993; Valdez *et al.* 2000).

MyoD, myf5, myogenin and MRF4 belong to the bHLH family of proteins. These proteins contain two functional domains, a helix-loop-helix (HLH) motif that mediates protein dimerization and a basic region that facilitates DNA binding. The DNA binding activity of these bHLH proteins is triggered once they form heterodimers with a distinct class of bHLH proteins, the E proteins E12/E47, constitutively present in most cells (Lassar *et al.* 1991). The resultant MRF/E protein complex binds to a *cis*-element termed the E-box, present in the promoter regions of most skeletal muscle-specific genes. Although the bHLH MRFs have an important role in myogenesis, the E-box is absent from several key skeletal muscle-specific genes such as myosin heavy chain and α-actin (Takeda *et al.* 1995). A novel DNA-binding protein was found to bind to a distinct sequence present in the promoter of these and other genes. This myocyte-specific enhancer-binding factor (MEF2), while not uniquely present in cells of skeletal muscle lineage, is expressed at an early point in somite development (Olson *et al.* 1995) and

mutation of the MEF2 site severely reduces gene expression (Kaushal *et al.* 1994). Thus, a ternary complex between MRF, E-protein and MEF2 has been proposed as the functional unit required for expression of skeletal muscle-specific genes during differentiation (Molkentin & Olson 1996a; Molkentin & Olson 1996b; Yun & Wold 1996). This ability to interact constitutes one of the principal mechanisms by which the differentiation of skeletal muscle precursors can be controlled.

Skeletal muscle differentiation is driven by the ordered expression of specific transcription factors that control the synthesis of muscle-specific contractile proteins and concomitant fusion of mononucleated myoblasts into multinucleated myotubes. The function of these transcription factors is modulated through their interaction with either positive (eg. E12/E47) or negative (eg. Id and Twist) regulatory proteins that determine their ability to bind to specific promoter elements (eg. E-box). Two mechanisms govern the balance between positive and negative components, protein abundance and post-translational modification, and these are regulated in turn by intracellular signaling systems (eg. PKC) that respond to extracellular cues (eg. bFGF, IGF and TGF-β) (Hardy *et al.* 1993; Lim *et al.* 1995; Miles & Wagner 2000; Zappelli *et al.* 1996).

Skeletal muscle comprises one of the best systems to study terminal differentiation. Myogenic differentiation involves the withdrawal of proliferating myoblasts from the cell cycle and the coordinated activation and expression of muscle specific genes, giving rise to the myogenic phenotype which is characterized by the fusion of mononucleic myoblasts into multinucleated myotubes. Although molecular studies to define the temporal recruitment and coordination of muscle specific genes are ongoing in other laboratories, very little is known about the cellular signals that cause myoblasts to exit from the cell cycle and initiate the terminal differentiation program. To this end, the signals that activate the recruitment and coordinated expression of muscle

specific genes during myogenesis are best studied using an isolated system, and L6 myoblasts, a well established myogenic system (Yaffe 1968), provide a good model.

L6 skeletal myoblast cells, an established cell line originally derived from rat skeletal hindlimb muscle, are a committed skeletal muscle precursor which can be induced to differentiate into multinucleated, terminally differentiated myotubes. The L6 cell line has theoretically also been transformed by the carcinogen methylcholanthrene in an effort to maintain the cultures by serial passage (Yaffe 1968). This cell line can also be kept in a frozen state (at –80°C) for extended periods of time without loss of viability and without loss of differentiation properties. The conditions for differentiation involved the removal of growth media (10% FBS/α-MEM) and replacement with mitogen-poor differentiation media (2.5% horse serum/α-MEM). Upon differentiation, the immature skeletal myotubes enter a quiescent state and are unable to re-enter the cell cycle. Terminal differentiation is accompanied by a change in cell morphology (fusion of myoblasts into myotubes), the synthesis of contractile muscle proteins and the organization of muscle bundle filaments (Zahradka *et al.* 1989). Interestingly, L6 cells constitutively express MyoD, suggesting that these cells are firmly committed to the myogenic lineage (Lognonne & Wahrmann 1986). However, the spectrum of MRF activation and association thereafter thereby controls the final outcome. Since relatively little is known about the mechanisms that determine how myogenesis is modulated by external factors and intracellular signaling systems, the role of mART in this cellular program will be examined. Several published reports have already indicated that inhibitors of mART, including MIBG, are capable of preventing the differentiation of skeletal myoblasts into myotubes.

Based on this information, a specific hypothesis was proposed: *MIBG will inhibit the differentiation of L6 skeletal myoblasts into myotubes by interfering with the expression of one or more MRFs essential for myogenesis.*

6.2 Contribution of mono(ADP-ribosyl)transferase to myogenesis

6.2.1 Background/rationale

Based on the studies of Kharadia *et al.* (1992) and Huang *et al.* (1996), inhibition of ADP-ribosyltransferase activity results in the inhibition of myoblast fusion. A glycosylphosphatidylinositol (GPI)-linked arginine-specific mono(ADP-ribosyl)-transferase is expressed in skeletal muscle tissue and myotubes but not in myoblasts (Zolkiewska *et al.* 1992). This enzyme, which is located on the external surface of the cell, has been shown to modify α7 integrin (Zolkiewska & Moss 1995) and desmin (Huang *et al.* 1996). While this evidence for increased ADP-ribosylation during differentiation is intriguing, a more direct association between ADP-ribosylation and myogenesis was indicated by the ability of MIBG, an inhibitor of arg-mART, to prevent myoblasts fusion (Kharadia *et al.* 1992). In addressing this point, a detailed analysis of which cellular processes are inhibited by MIBG has not been reported.

The ubiquitous presence of ADP-ribosyltransferases in all cell types suggests that they are crucial elements in normal cell function. Given the broad range of action attributed to the various ADP-ribosyltransferases that have been identified (Zolkiewska *et al.* 1994), the assumption that there is a direct connection between the GPI-linked ADP-ribosyltransferase and myoblast differentiation (Huang *et al.* 1996; Kharadia *et al.* 1992) may be incorrect. A more comprehensive examination of the role of ADP-ribosyltransferases in myogensis is therefore necessary to clarify this issue.

6.2.2 Specific Aims

1. To document the effect of ADP-ribosylation inhibitors on the myogenic program of L6 skeletal myoblasts.
2. To identify the myogenic markers that are affected by inhibitors of ADP-ribosylation.
3. To determine if ADP-ribosylation is a part of the myogenic program of L6 cells.

6.2.3 Experimental Design

L6 rat skeletal muscle myoblasts undergo differentiation into myotubes upon removal of fetal bovine serum and replacement with horse serum. Over a 4 day period, differentiation will be assessed by monitoring cell morphology. Inhibitors of ADP-ribosylation and appropriate analogs will be tested to determine if they are capable of interfering with the myogenic program and preventing myoblast differentiation. A quantitative measure of differentiation (fusion index) will be employed in parallel. Time of addition, reversibility and cell viability studies will be carried out with MIBG. Finally, Western blot analysis will be used to examine the effect of MIBG on the expression of specific myogenic factors and correlate these observations with changes in myoblast differentiation. Immunoprecipitation studies and a UV-cross-linking assay will also be conducted to confirm some of the results obtained with the Western blot analysis.

6.2.4 Results

6.2.4.1 Differentiation of L6 skeletal myoblasts into myotubes

The time course of L6 skeletal myoblast differentiation into myotubes has been well documented (Zahradka *et al.* 1989). After removal of serum and replacement with a

differentiation media, L6 myoblasts differentiate into myotubes over a period of 4 days as demonstrated by the loss of individual cells and the fusion of individual myoblasts into multinucleated myotubes (Figure 28). Note that two distinct stages can be distinguished: 1) the cells line up once confluence is reached, and 2) individual myoblasts fuse with adjoining cells and nuclei cluster in the central region. These same events are visible in phase contrast micrographs (Figure 29, untreated column).

6.2.4.2 ADP-ribosylation inhibitors and their effect on L6 skeletal myoblast differentiation

As demonstrated in chapter 5, inhibitors of ADP-ribosylation are capable of regulating cell growth and proliferation. It was therefore of interest to determine if ADP-ribosylation inhibitors might also influence cell differentiation, since cessation of proliferation in some cell types is often a requirement for differentiation (Myster & Duronio 2000; Zavitz & Zipursky 1997). Thus, in L6 cells, if proliferation was inhibited, it might be expected that stimulation of differentiation would be observed (Lassar *et al.* 1994; Molkentin & Olson 1996b). An inhibitor of PARP (PD128763), the dual PARP/mART inhibitor (3AB) and an arg-mART inhibitor (MIBG), along with appropriate controls (PABA and MIBA), were added to L6 cells prior to inducing differentiation. At day 4, the degree of cell fusion was assessed. Untreated L6 cells showed extensive myotube formation, as did cells treated with PD128763 (10 μM), 3AB (5 mM), PABA (5 mM) and MIBA (50 μM) (Figure 30). In contrast, treatment with MIBG (50 μM) prevented myotube formation (Figure 30). These cells, at day 4, resembled untreated myoblasts at the day 1 and 2 stage of the myoblast to myotube transformation (Figures 28, 29) with the cells having reached confluence and lined up, but not having yet fused. These inhibitor data would suggest that poly(ADP-ribosyl)ation

FIGURE 28: ***Nomarsky micrography of L6 Differentiation: Transition from Myoblast to Myotube.***

L6 skeletal myoblasts were placed into low-serum α-MEM and differentiation to myotubes monitored over 4 days. Nomarsky micrographs were taken at daily intervals to record the morphology of the cells as they fuse to form myotubes. (A) growing myoblasts, (B) 1 day myotube, (C) 2 day myotube, (D) 3 day myotube, and (E) 4 day myotube. Magnification: 132×. The figures are representative photomicrographs of three individual experiments, all of which exhibited the same response.

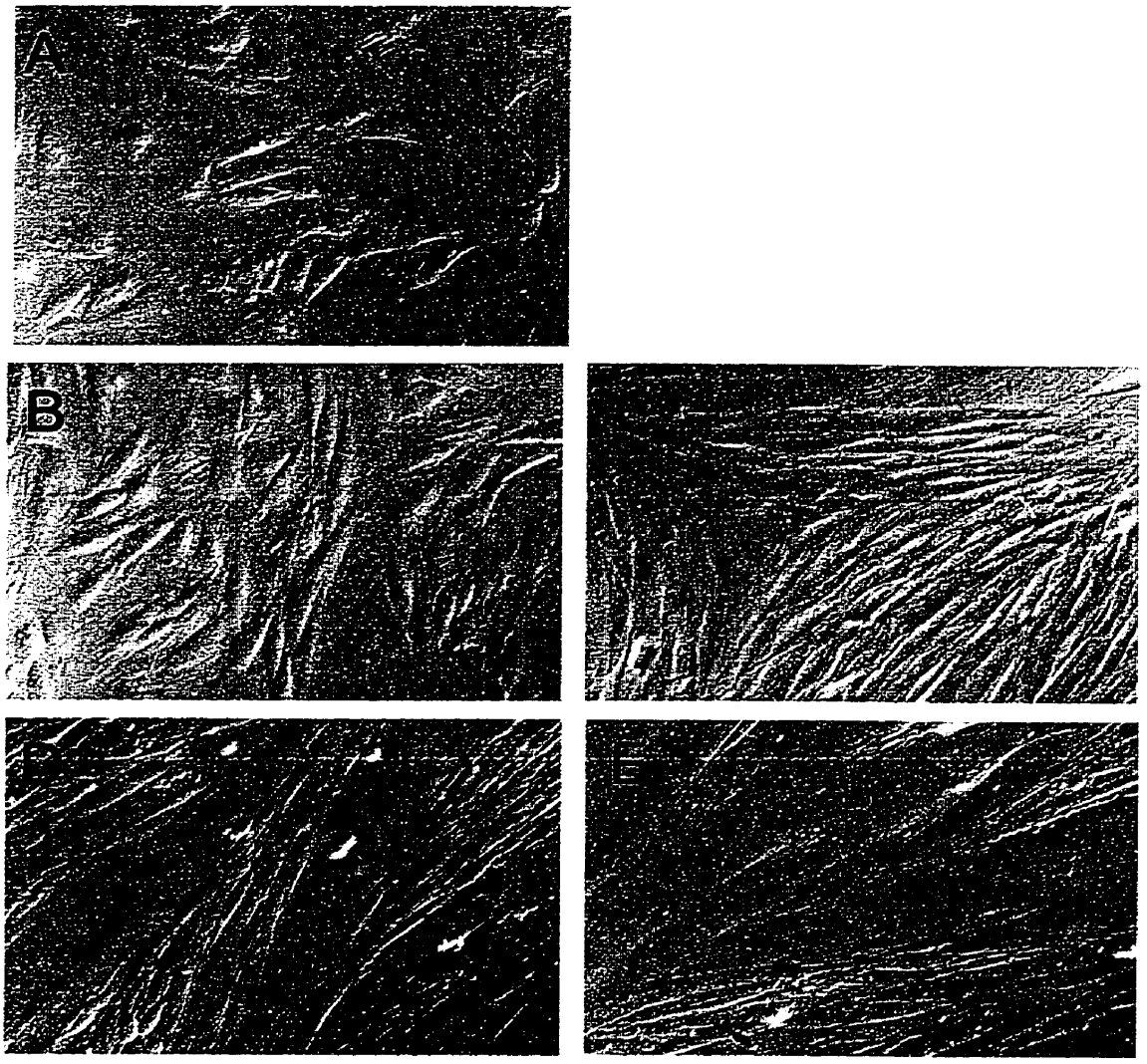
A
B

FIGURE 29: ***L6 Differentiation: Effect of MIBG.***

L6 skeletal myoblasts were placed into low-serum α-MEM and differentiation to myotubes monitored over 4 days in the presence or absence of MIBG (50 μM). Phase-contrast micrographs were used to record the morphology of the cells. Magnification: 105×. The figures are representative photomicrographs of three individual experiments, all of which exhibited the same response.

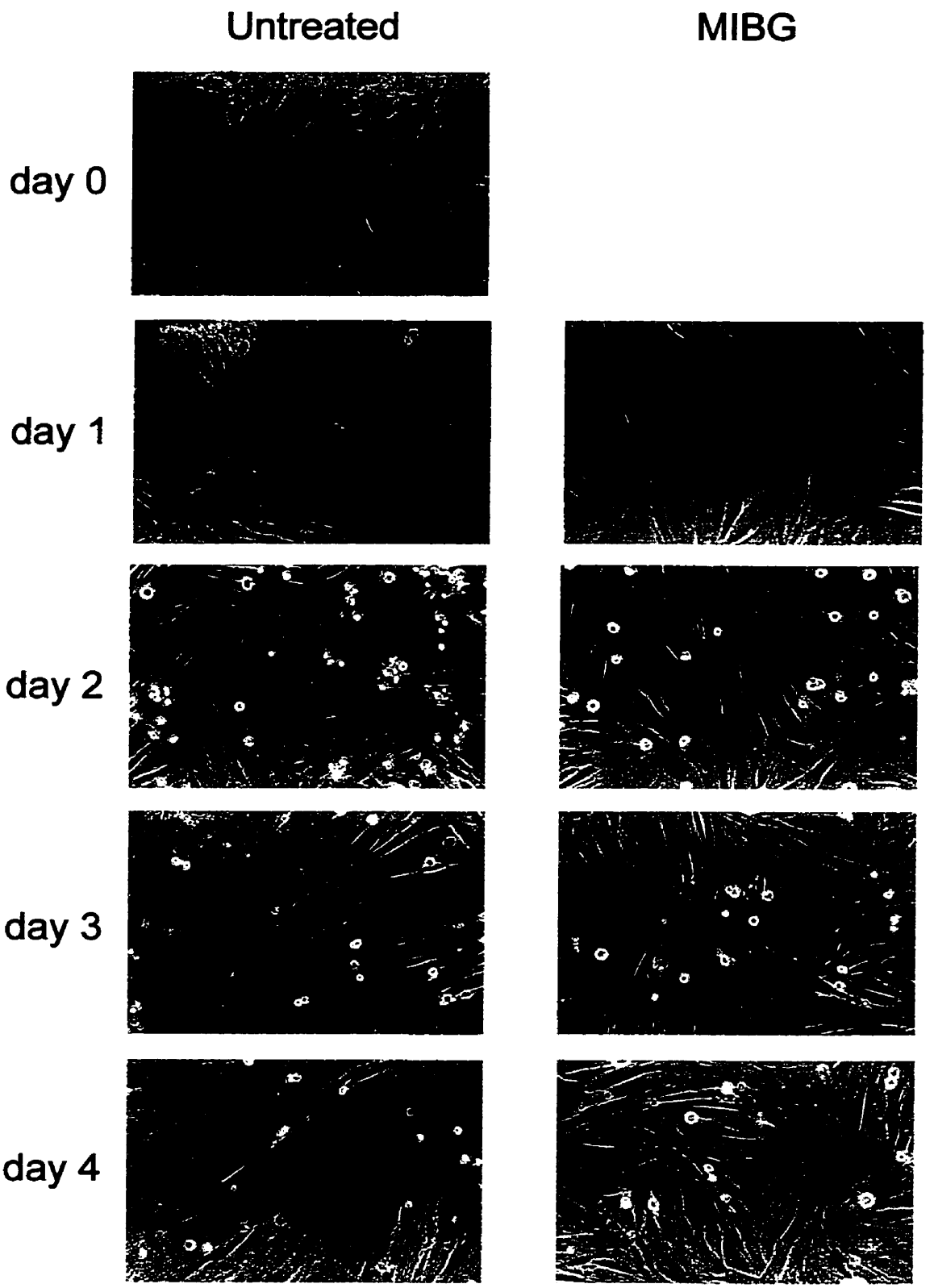
Untreated
MIBG
day 0
day 1
day 2
day 3
day 4

FIGURE 30: ***Effect of ADP-ribosylation Inhibitors on L6 Differentiation.***

L6 skeletal myoblasts were placed into low-serum α-MEM and differentiation to myotubes monitored over 4 days in the absence and presence of a variety of ADP-ribosylation inhibitors. Inhibitors tested include: PD128763 (10 μM), 3-aminobenzamide (3-AB) (5 mM), para-aminobenzoic acid (PABA) (5 mM), MIBG (50 μM) and MIBA (50 μM). Phase-contrast micrographs were taken at the 4 day mark to record the morphology of the cells. Note that all comparisons should be made versus the 4 day untreated panel. Magnification: 138×. The figures are representative photomicrographs of two individual experiments, both of which exhibited a similar response.

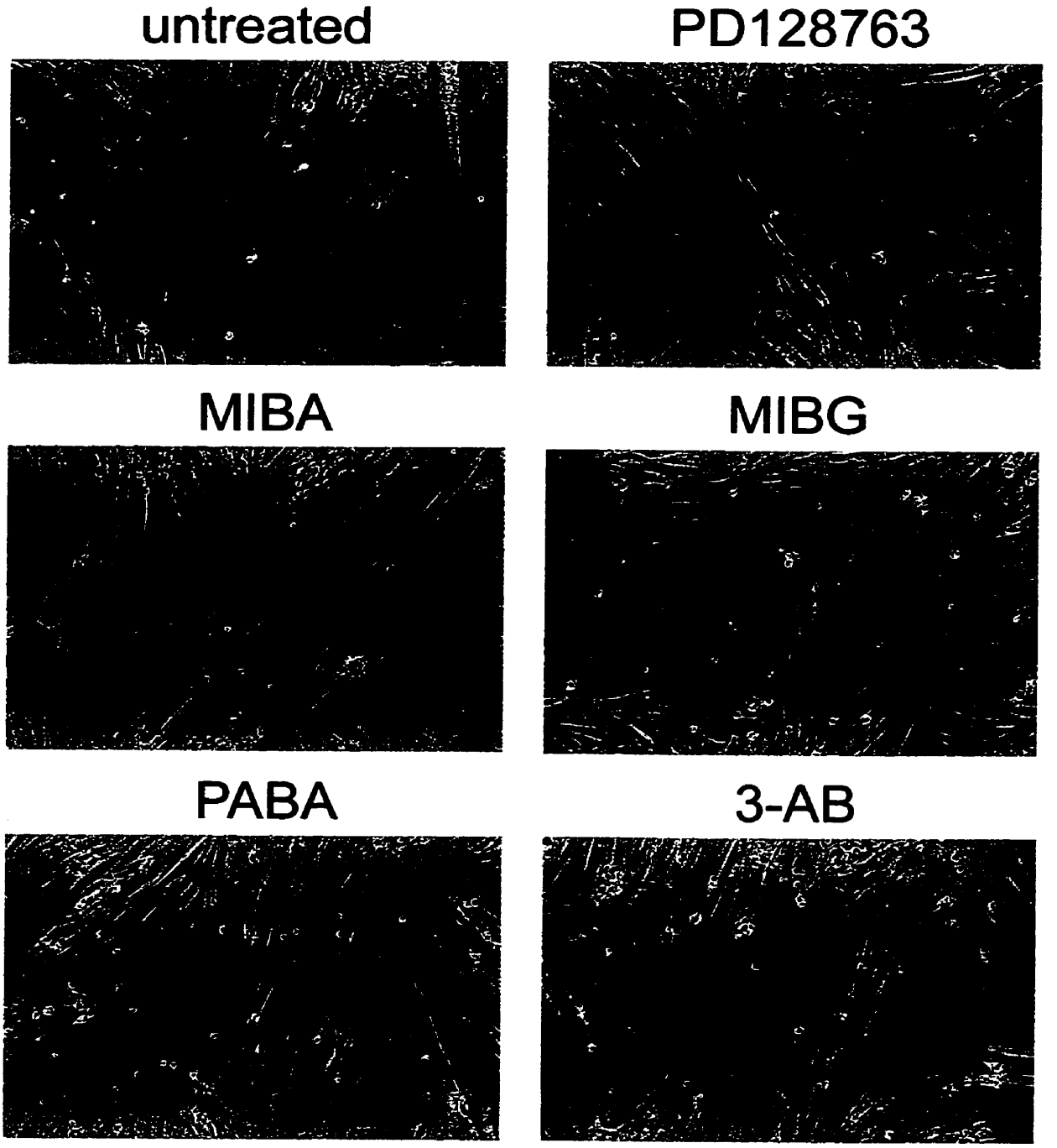
untreated
PD128763
MIBA
MIBG
PABA
3-AB

events are not required for differentiation, but that mono(ADP-ribosyl)ation events may play a role in regulating the differentiation process.

Since MIBG inhibited the differentiation of L6 myoblasts, further studies were conducted to examine the effect of this arg-mART inhibitor on L6 myoblast differentiation. To determine how MIBG influences the morphological changes associated with differentiation, cells were viewed at daily intervals. This study clearly established that MIBG inhibited the differentiation of these cells (Figure 29, MIBG column). Interestingly, MIBG may have slowed the growth of these cells, since a day-by-day comparison between untreated and MIBG treated L6 cells showed fewer cells were present on both day 1 and day 2. The cells also appeared to be larger, possibly indicating a block in cell division, which would cause hypertrophy after a round of DNA synthesis. Furthermore, the myoblasts appeared to be less organized at day 2, and at day 4 loss of cell borders and fusion of the cells was not observed (Figure 29). Since there was no fusion, clustering of the nuclei was not seen.

To establish the minimum concentration at which MIBG was inhibiting L6 skeletal myoblast differentiation, a concentration-response study was conducted (Figure 31). Quantitation of myotube formation was also conducted in parallel, using Giemsa stain to visualize the cell nuclei. This stain permits the counting and subsequent quantification of nuclei in fused and unfused L6 cells (Figure 32A,B). These values were then used to calculate the fusion index (number nuclei in fused cells/total number of nuclei), a numerical transformation that allows a direct comparison of the various treatments (Figure 32C). MIBG (0.5 to 50 μM) was added to the differentiation media and myotube formation monitored after 4 days. MIBG at concentrations from 0.5 to 10 μM did not significantly inhibit myotube formation (Figures 31, 32C). Only the highest concentrations were effective (20 and 50 μM), with 50 μM having the greatest effect

FIGURE 31: ***Effect of MIBG Concentration on Inhibition of L6 Differentiation.***

L6 skeletal myoblasts were placed into low-serum α-MEM and differentiation to myotubes monitored over 4 days in the presence of varying concentrations of MIBG (0.5 to 50 μM). Phase-contrast micrographs were taken on day 4 to record morphology of the cells. MIBG concentrations used in each panel are: (A) 0.5 μM, (B) 2 μM, (C) 5 μM, (D) 10 μM, (E) 20 μM and (F) 50 μM. Magnification: 132×. The figures are representative photomicrographs of two experiments, both of which exhibited the same response.

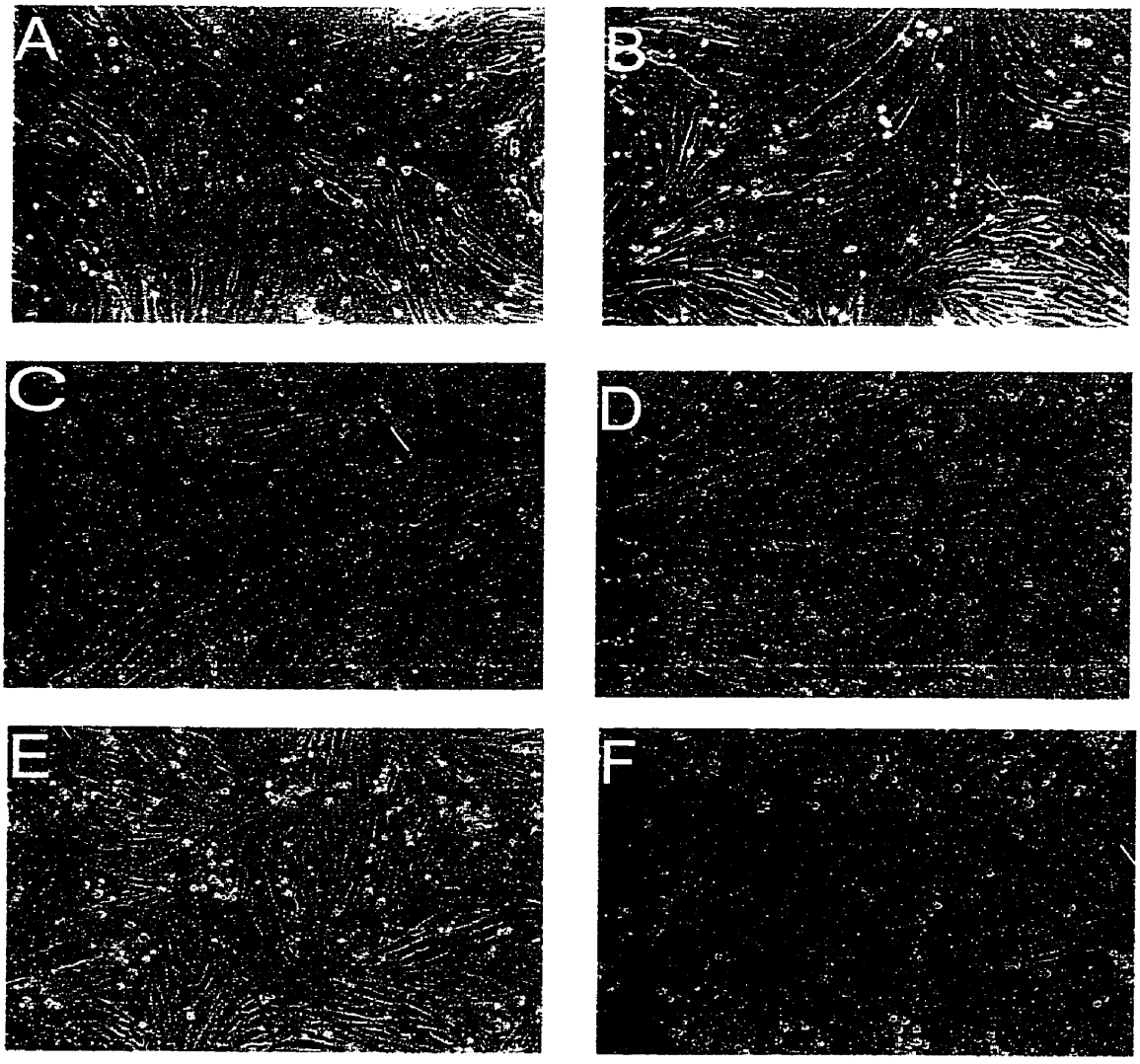
A
B
C
D
E
F

FIGURE 32: ***Effect of MIBG Concentration on Inhibition of L6 Differentiation.***

Quantification of L6 Myotube Formation.

Representative photomicrographs of Giemsa stained L6 cells that were untreated (A) or treated with 50 μM MIBG (B) over 4 days of differentiation. Magnification: 63×. (C) The number of nuclei present in fused and unfused L6 cells was determined after addition of MIBG (5 to 50 μM) for 4 days and presented as the fusion index (fused/total nuclei). Data are presented as mean ± SE from one of two experiments.

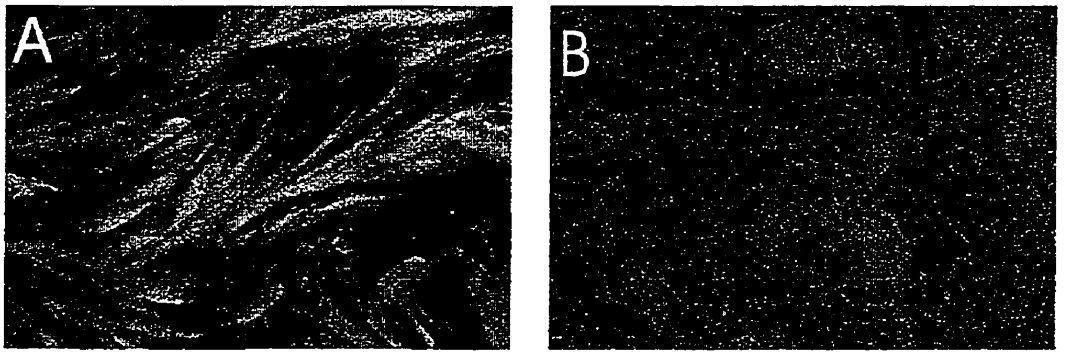
A
B

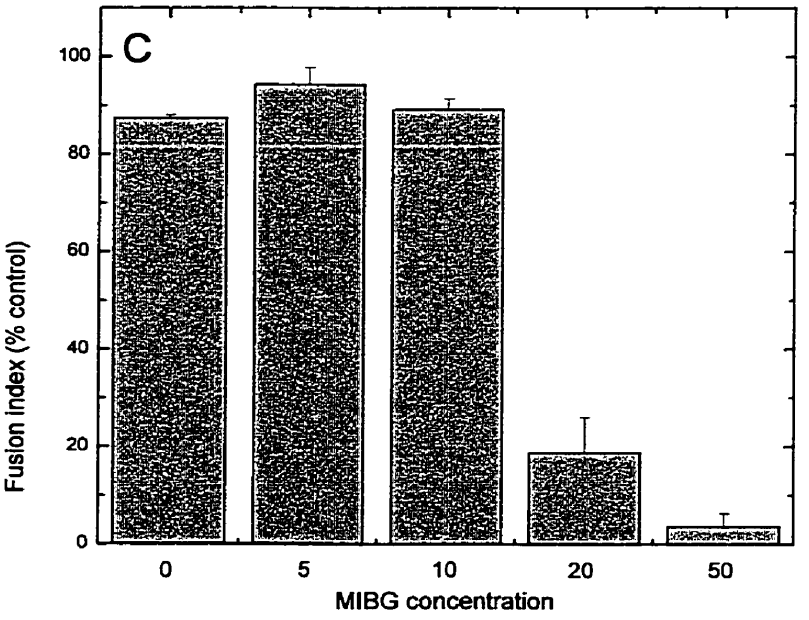
C
100
80
60
40
20
0
Fusion index (% control)
0
5
10
20
50
MIBG concentration

(Figure 32C). Thus, 50 μM MIBG was used in all subsequent experiments. This was also the concentration used in the initial studies (Figures 28, 29, 30). Interestingly, this is also the most effective concentration for inhibiting cell growth and proliferation (chapter 5).

To quantify myotube formation, L6 cells were treated, allowed to differentiate and visualized with Giemsa stain. Exposure to 3AB (5 mM) decreased the number of fused cells while treatment with MIBG (50 μM) significantly decreased the number of fused cells (Figure 33A,B). The fusion index for control, untreated L6 cells was approximately 85%, while 3AB treatment decreased the fusion index to approximately 50% (Figure 33B). Treatment with MIBG reduced the fusion index to less than 5% demonstrating very effective inhibition of differentiation (Figure 33B). In this experiment, a decrease in the total number of nuclei was observed after MIBG treatment, possibly indicative of an inhibition of cell growth (Figure 33A). As a result, a limited [^{3}H]thymidine incorporation experiment was conducted in which growing L6 cells were treated with MIBG (50 μM) or MIBA (100 μM) over 36 h and incorporation of [^{3}H]thymidine used as a measure of cell proliferation (Figure 33C). MIBG decreased DNA synthesis in L6 cells, while MIBA did not, suggesting that MIBG may be inhibiting events associated with cell proliferation in addition to differentiation-specific events in L6 myoblasts.

To identify the time period during which MIBG inhibits differentiation, a delayed addition experiment was conducted. In this study, MIBG (50 μM) was added to cells at varying times (0 to 48 h) after placing the myoblasts into differentiation media. Cell morphology was examined on day 4. Administration of MIBG up to 12 h after the switching to differentiation media completely blocked differentiation into myotubes (Figure 34). Even addition of MIBG at 24 and 48 h was able to inhibit the differentiation event, although the morphology indicated the cells had progressed to the point at which

FIGURE 33: ***Effect of 3-aminobenzamide and MIBG on L6 Differentiation.***

Quantification of L6 Myotube Formation: Fusion Index.

L6 skeletal myoblasts were placed into low-serum α-MEM and differentiation to myotubes monitored on day 4 in the absence or presence of 3-aminobenzamide (3AB, 5 mM) and MIBG (50 μM). Experiments were carried out in duplicate. (A) The number of nuclei present in fused and unfused L6 cells and the total number of nuclei in each treatment was determined and presented as the fusion index (fused/total nuclei) (B). Data are presented as mean ± SE from one of two individual experiments. (C) Growing L6 skeletal myoblasts were treated with MIBG (50 μM) or MIBA (100 μM) and incorporation of [^{3}H]thymidine over 36 h used as a measure of DNA synthesis. The data are presented as the mean ± SE of experiments conducted in triplicate.

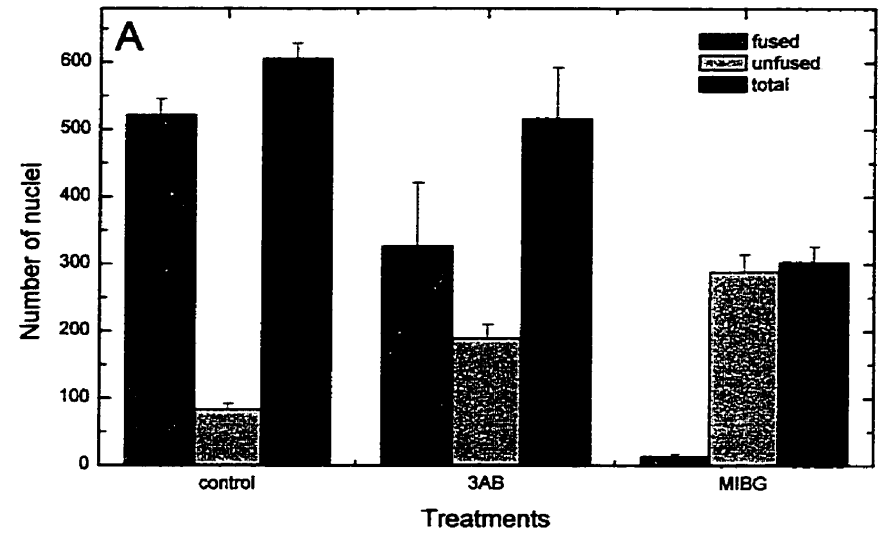
A
fused
unfused
total
Number of nuclei
0
100
200
300
400
500
600
control
3AB
MIBG
Treatments

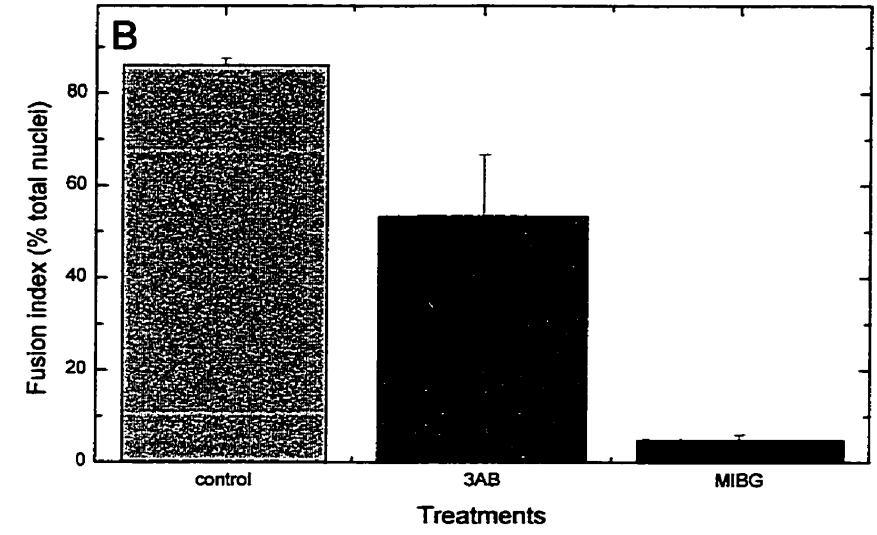
B
Fusion index (% total nuclei)
0
20
40
60
80
control
3AB
MIBG
Treatments

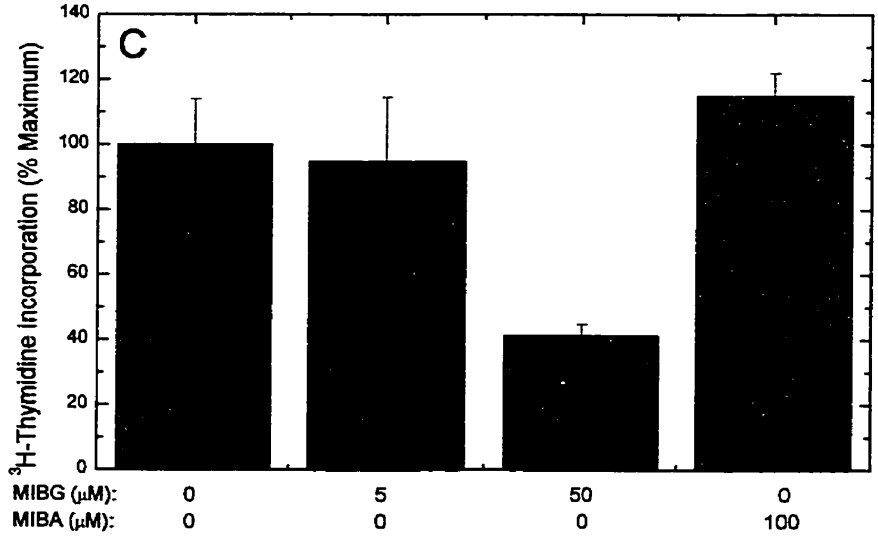
C
^{3}H-Thymidine incorporation (% Maximum)
0
20
40
60
80
100
120
140
MIBG (μM): 0 5 50 0
MIBA (μM): 0 0 0 100

FIGURE 34: ***Effect of Delayed Addition of MIBG on L6 Differentiation.***

L6 skeletal myoblasts were placed into low-serum α-MEM and differentiation to myotubes monitored on day 4 (A). MIBG (50 μM) was added at different time points (0 to 48 h) after the switch to differentiation media. The time points at which MIBG was added were: (B) 0 h, (C) 3 h, (D) 6 h, (E) 12 h, (F) 24 h and (G) 48 h. Phase-contrast micrographs were taken on day 4 to record the cell morphology. Magnification: 132×. The figures are representative photomicrographs of two individual experiments, both of which exhibited a similar response.

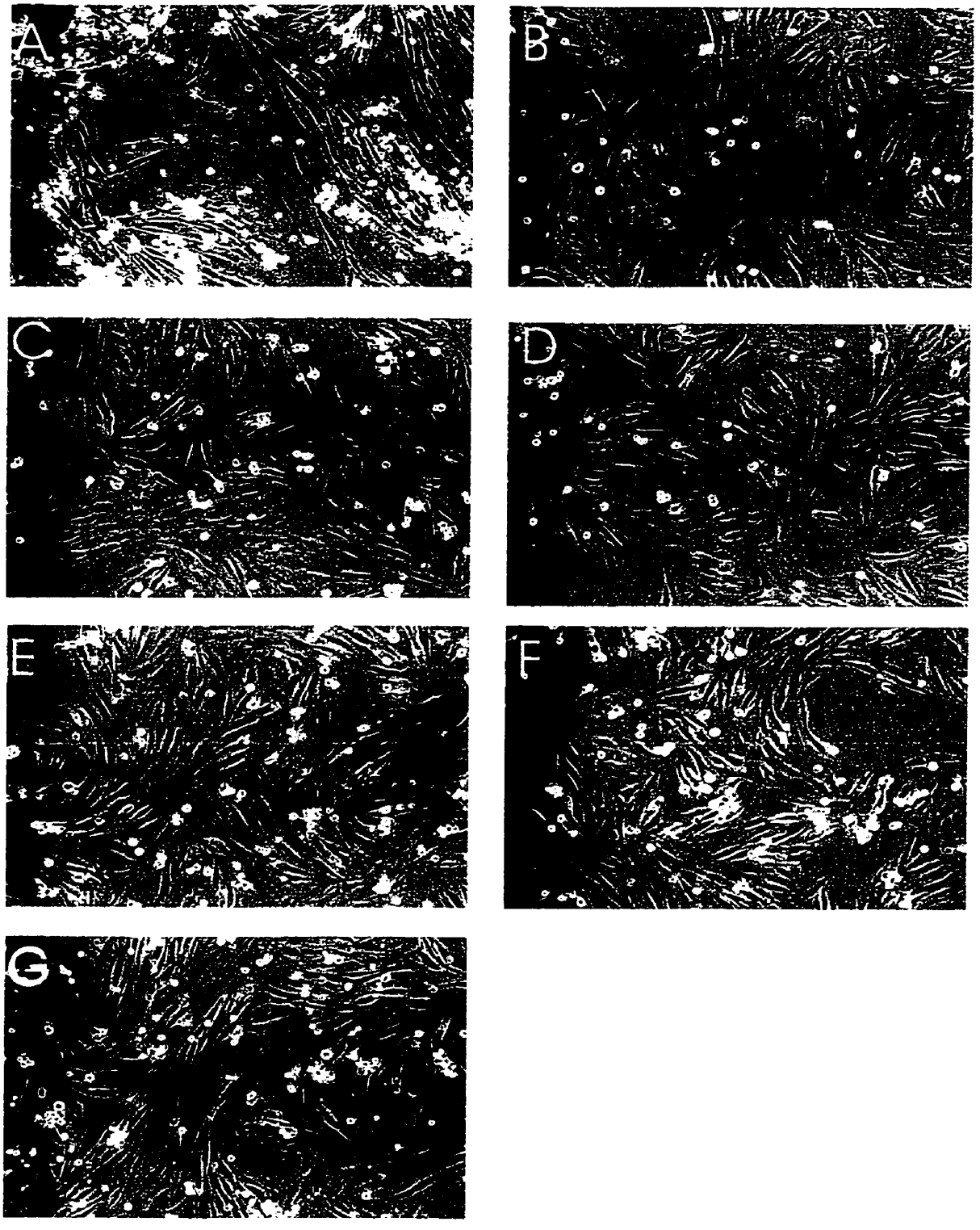
A
B
C
D
E
F
G

they were lined up and the cell borders had become less distinct (Figure 34). These data indicate MIBG is likely inhibiting a late event in the myogenic program, one that is not activated until 24 to 48 h after onset of myogenesis (possibly cell fusion). Since L6 myoblasts do not initiate the actual fusion process until after 48 h, these data are in good agreement with the earlier findings in untreated myoblasts (Figures 28, 29). Alternatively, since MIBG prevents both cell organization and cell fusion events (depending on the time of addition), MIBG may influence myogenesis at multiple points.

To complement the delayed addition experiment, an MIBG removal experiment was conducted. In this study, MIBG (50 μM) was added with the differentiation media and then removed at specific time points (30 min to 48 h). The cells were then maintained in differentiation media without MIBG for the remainder of the 4 day period. These experiments were expected to more closely identify the critical time points at which MIBG exerts its inhibitory effects on differentiation. Both cell morphology (data not shown) and the fusion index depicted a noticeable decrease in myotube formation after approximately 24 h with MIBG treatment (Figure 35). More dramatic differences were noted when MIBG was present for 48 and 96 h (Figure 35). Quantification of cell fusion demonstrated a significant decrease in myotube formation had occurred as a result of a 4 h exposure to MIBG (Figure 35). Longer treatments with MIBG result in significantly greater inhibition of cell fusion (Figure 35). These data suggest that the full inhibitory effect of MIBG requires its presence throughout the entire 4 day period. However, MIBG may be affecting myogenesis at a point as early as 4 h after the media change. Taken together, these findings would indicate the MIBG is inhibiting multiple points in the myogenic program.

To determine the reversibility of the inhibition cause by MIBG, a differentiation rescue study was conducted. This experiment was designed to also examine whether

FIGURE 35: ***Effect of Transient MIBG Treatment on L6 Differentiation.***

L6 skeletal myoblasts were placed into low-serum α-MEM in the presence of MIBG (50 μM) and the degree of differentiation monitored on day 4. MIBG was removed from the cells at the indicated times: 0 h, 30 min, 1 h, 2 h, 4 h, 12 h, 24 h, 48 h and 96 h. Control cells were not exposed to MIBG, while at 96 h MIBG was not removed. The number of nuclei present in fused and unfused L6 cells was determined after Giemsa staining of the cells (A), and used to calculate the fusion index (fused/total nuclei) (B). Data are presented as mean ± SE. The results were confirmed in two independent experiments.

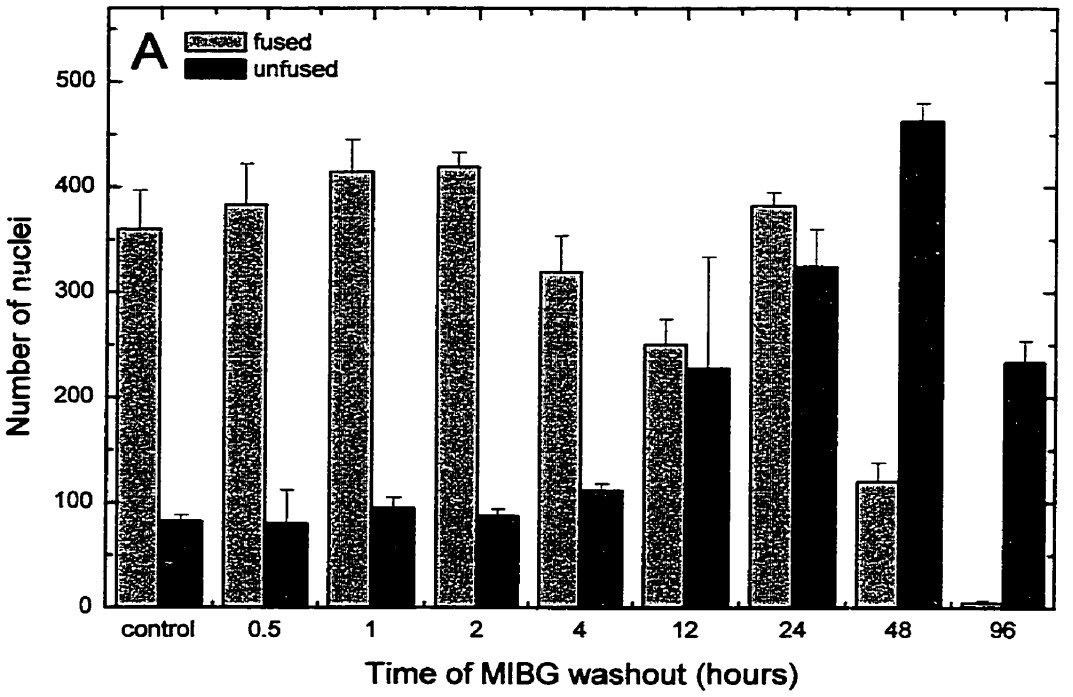
A
fused
unfused
Number of nuclei
0
100
200
300
400
500
control
0.5
1
2
4
12
24
48
96
Time of MIBG washout (hours)

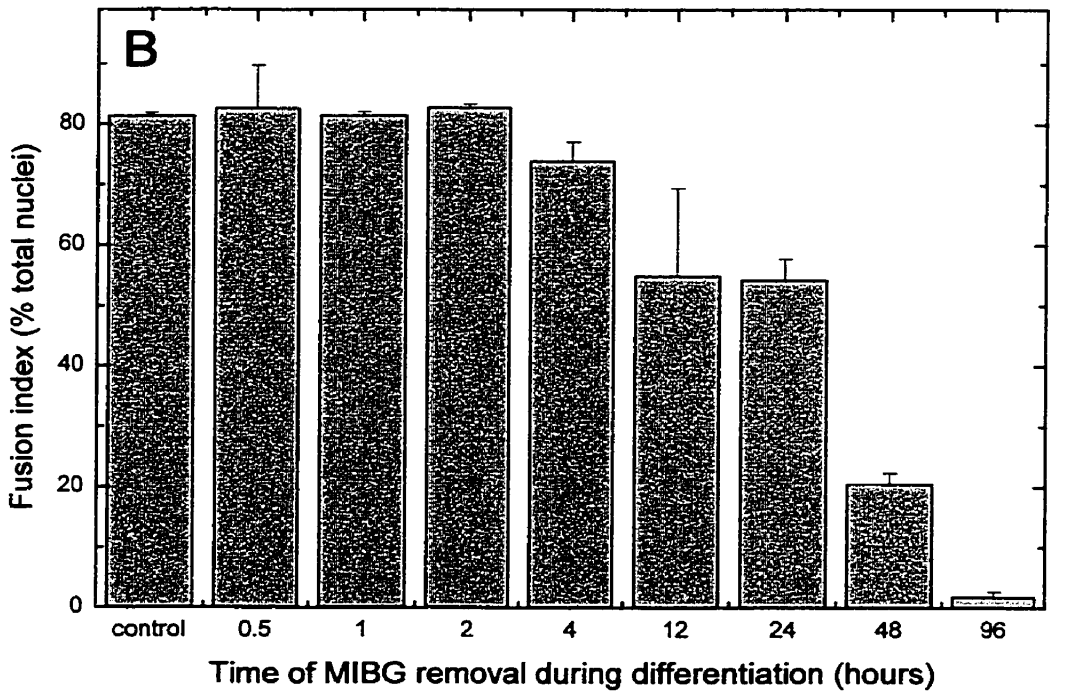
B
Fusion index (% total nuclei)
0
20
40
60
80
control
0.5
1
2
4
12
24
48
96
Time of MIBG removal during differentiation (hours)

MIBG was toxic to L6 cells or was 'cytostatic' with respect to differentiation. L6 myoblasts were treated with MIBG (50 μM) over 4 days. On the fourth day, the media was removed and replaced with differentiation media without MIBG. The cells were then incubated for an additional 4 days and differentiation monitored on day 8. Cell fusion was observed on day 8 whether the cell had been treated with MIBG or not. In fact, myotube formation was comparable to those of day 4 untreated cells (Figure 36). Nevertheless, all day 8 cells had begun to show signs of necrosis (Figure 36), especially the untreated cells, since under higher power magnification granulation was observed within the cells. These data demonstrate that MIBG is not toxic to L6 cells, since the cells remained capable of initiating differentiation after removal of the MIBG. These data further suggest that MIBG blocks a specific event in the myogenic program and that this inhibition is reversible.

6.2.4.3 Expression of myogenic proteins affected by MIBG

Since it was observed that MIBG was capable of inhibiting L6 cell differentiation in a reversible manner, it was of interest to identify specific events in the myogenic program sensitive to inhibition by MIBG. A variety of proteins of the myogenic program (muscle regulatory factors) are expressed during the transition from myoblast to myotube. Many of these form complexes that then interact with other proteins to regulate progression to the differentiated state. MyoD is the first major myogenic protein expressed during differentiation and operates in a complex in association E-proteins and MEF2 (Lassar *et al.* 1991). MEF2 then binds to specific promoter elements of other muscle regulatory factors and muscle-specific genes (Kaushal *et al.* 1994; Olson *et al.* 1995; Takeda *et al.* 1995) to enhance their expression. As a result, it was of interest to determine whether MIBG influenced either of these processes. Immunoprecipitation of E12/47 proteins followed by Western blot analysis for MyoD was carried out to

FIGURE 36: ***Effect of MIBG on L6 Cell Survival: Test of MIBG Cytotoxicity.***

L6 skeletal myoblasts were placed into low-serum α-MEM in the absence or presence of MIBG (50 μM) for 4 days. On day 4, the differentiation media ± MIBG was removed and replaced with differentiation media without MIBG. Four days later (day 8), phase-contrast micrographs were used to record cell morphology. Magnification: 128×. The figures are representative photomicrographs of two experiments, both of which exhibited the same response. Conditions shown: (A) 4 days without MIBG, (B) 4 days with MIBG, (C) 8 days without MIBG, (D) 4 days with MIBG + 4 days without MIBG.

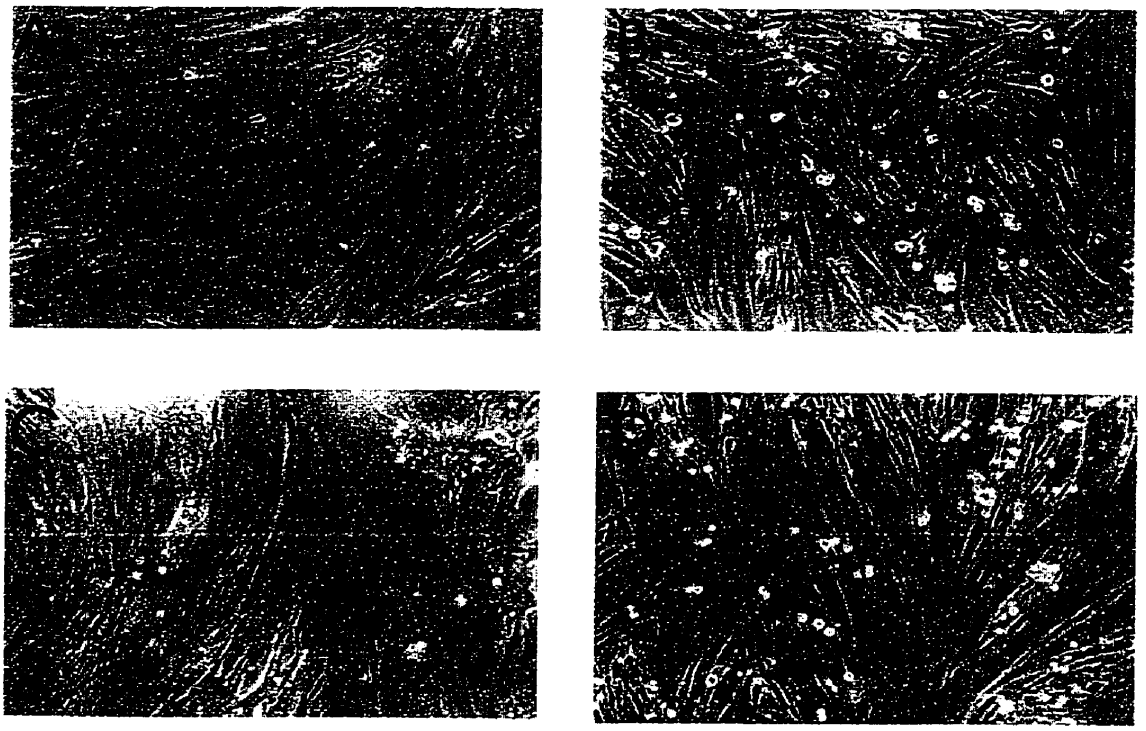

determine if MyoD had associated with E12/47 proteins and to determine if MIBG was inhibiting formation of this complex. This particular step in the myogenic program occurs before the formation of the MyoD/MEF2 complex (Lassar *et al.* 1991). Myoblasts did not contain a prominent MyoD/E12/47 complex (Figure 37). In contrast, increased expression of the complex was observed in myotubes. Treatment with MIBG did not alter the formation of this complex (Figure 37). These data indicate that the formation of the MyoD/E12/47 complex is not the event affected by MIBG and that MIBG is inhibiting a downstream event in the differentiation process.

To assess the downstream myogenic event affected by MIBG, extracts of L6 myoblasts/myotubes were prepared at daily intervals over 4 days and Western blot analysis was used to monitor myogenin, MEF2 and $p21^{CIP1}$ expression. Control, untreated L6 cells showed gradual increase in the levels of myogenin and $p21^{CIP1}$ protein over the 4 day time course (Figure 38). MEF2 expression was also increased in untreated cells, however, expression decreased after day 2, reaching near basal levels by day 4 (Figure 38). In contrast, L6 myoblasts treated with MIBG did not express myogenin or $p21^{CIP1}$ (Figure 38). Interestingly, the pattern of MEF2 expression was similar to that of untreated cells, becoming even more prominent on day 2, and remaining elevated on day 3 (Figure 38). These data would suggest that myogenin and $p21^{CIP1}$ expression is prevented by MIBG and that this inhibition blocks progression of the myogenic program to the fusion stage.

The distinct effects of MIBG on MEF2 expression relative to myogenin and $p21^{CIP1}$ suggested differential regulation of these genes. Since MEF2 has been reported to modulate myogenin, an alteration in MEF2 binding to DNA could produce the observed results (i.e. decreased myogenin expression with concomitant decrease in $p21^{CIP1}$ expression, Figure 38). Nuclear extracts were incubated with radiolabelled

FIGURE 37: ***Association of E12/47 with MyoD in L6 Skeletal Myotubes.***

MyoD was immunoprecipitated from L6 cell extracts and the presence of E12/47 proteins complexed with MyoD was determined by Western blot analysis using an antibody specific to E12/47 proteins. Extracts from myoblasts (B), myotubes (T) and MIBG-treated (50 μM) myotubes (M) were used for this experiment. Similar results were obtained in two independent experiments.

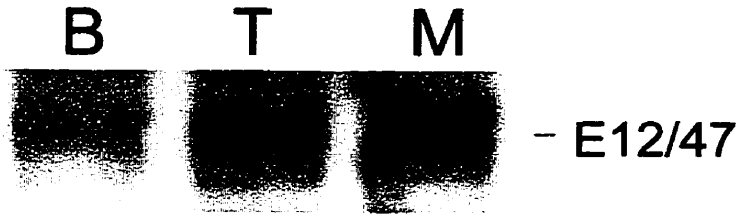
B
T
M
E12/47

FIGURE 38: ***Effect of MIBG on Protein Markers of L6 Cell Differentiation.***

L6 cell extracts were prepared at specific time points after transfer of cells to low serum α-MEM ± MIBG (50 μM). The samples were subjected to SDS/PAGE (10% gels) and Western blot analysis with antibodies for myogenin (diluted 1:1000), MEF2 (diluted 1:1000) and p21 (diluted 1:1000). Proteins were visualized with the ECL chemiluminescent detection system. MB denotes myoblast, while 1, 2, 3, 4 denote the days of differentiation. Specific antibodies are identified on the left of the figure (myogenin, MEF2 and p21). One of two independent experiments is shown, both of which exhibited the same response.

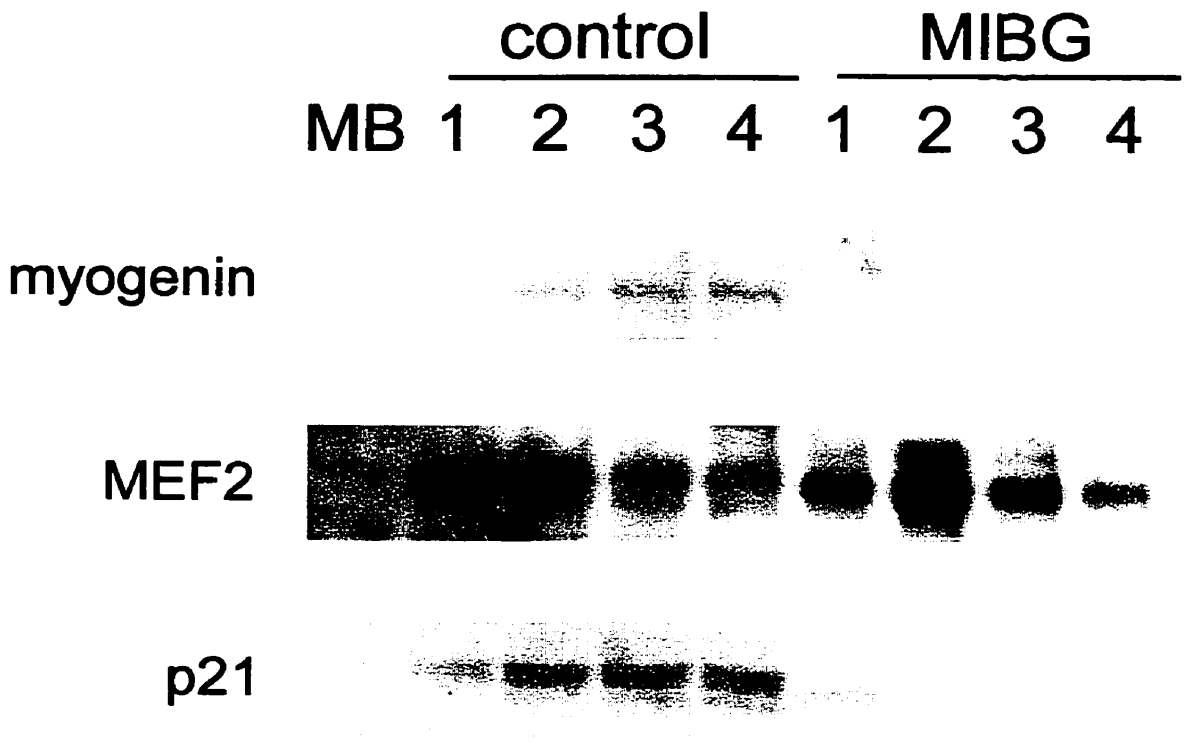
control
MIBG
MB 1 2 3 4 1 2 3 4
myogenin
MEF2
p21

oligonucleotides containing the MEF2 element, subjected to UV light and the proteins separated by SDS/PAGE. The proteins crosslinked to the labelled oligonucleotides were then visualized by autoradiography. Three bands between the 50- and 84-kDa molecular mass markers were prominently labelled in the myotube extract (Figure 39). The myoblast extract displayed two labelled bands. Interestingly, the MIBG treated extracts showed the same banding pattern as the myoblast extract, and were missing the third labelled band of 50- to 53-kDa present in the myotube extracts (Figure 39). These data suggest that a protein capable of binding to the MEF2 element is either not activated or not expressed with MIBG treatment. Furthermore, it may be speculated that expression of this protein is crucial for full expression of the myogenic program.

6.2.4.4 ADP-ribosylation and differentiation

To date, two mART activities (extracellular and intracellular) have been reported in myoblasts/myotubes (Huang *et al.* 1993; Huang *et al.* 1996; Kharadia *et al.* 1992; Soman & Graves 1988; Soman *et al.* 1984a; Zolkiewska & Moss 1993; Zolkiewska *et al.* 1992). Of these activities, the extracellular mART has been associated with α7 integrin and desmin (Huang *et al.* 1996; Zolkiewska & Moss 1995). Both proteins have been associated with skeletal muscle function and cell communication. To determine if the extracellular enzyme was the target for MIBG action, its activity was evaluated over the myotube differentiation process and then in the presence of MIBG. ADP-ribosylation of a surface protein by mART was monitored by incubating cells with [^{32}P]NAD^{+}. Labeling of a single band was detected on days 2 and 3 of the differentiation period of untreated myoblasts (Figure 40A). Since the presence of labelled bands was not greatly altered by treatment with MIBG or other inhibitors of ADP-ribosylation (Figure 40B), a role for an extracellular (or GPI-linked) arg-mART in the differentiation process is not indicated.

FIGURE 39: ***Effect of MIBG on Protein Binding to the MEF2 Element.***

Nuclear extracts from L6 myoblast (B), L6 myotube (T) and MIBG-treated (50 μM) L6 cells (M) were incubated with radiolabelled oligonucleotide, cross-linked by UV-irradiation (see Materials and Methods section 4.8.7) and subjected to SDS/PAGE (7.5% gel). Molecular mass markers used to identify the proteins by size are shown on the right hand side. The labelled proteins are indicated on the left-hand side by numerical notation. One of two independent experiments is shown, both of which exhibited the same response.

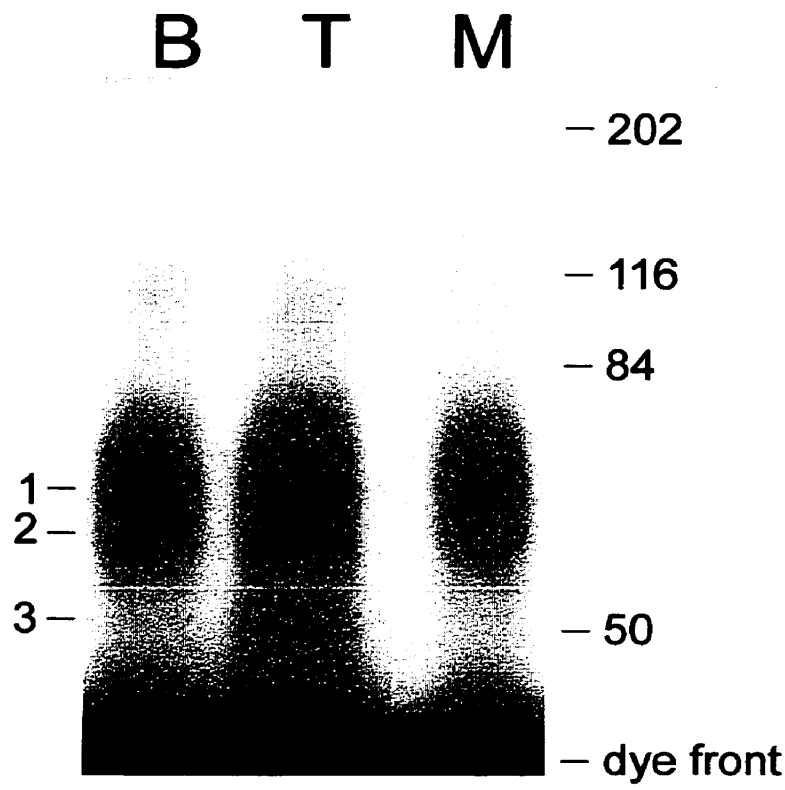
B T M
202
116
84
1
2
3
50
dye front

FIGURE 40: ***ADP-ribosylation and L6 Differentiation. In situ ADP-ribosylation of Extracellular Proteins.***

L6 myoblasts were placed into differentiation media and ART-dependent modification of extracellular proteins monitored on a daily basis. Cells were exposed to [^{32}P]NAD^{+} and transfer of label to specific proteins examined by autoradiography after SDS/PAGE (7.5% gel). (A) Separate lanes from autoradiographs of untreated L6 cells allowed to differentiate over 4 days are shown. MB denotes myoblast, while 1, 2, 3 and 4 denote the days of differentiation. (B) Autoradiograph of L6 cells on day 3 that were untreated (0) or treated with different inhibitors of ADP-ribosylation: *para*-aminobenzoic acid (PABA, 5 mM), 3-aminobenzamide (3AB, 5 mM), PD128763 (PD, 1 μM), MIBA (50 μM) or MIBG (50 μM) during the incubation period with [^{32}P]NAD^{+}. One of two independent experiments is shown, both of which exhibited a similar response. Arrows point to the most prominent bands detected in these experiments.

.

A

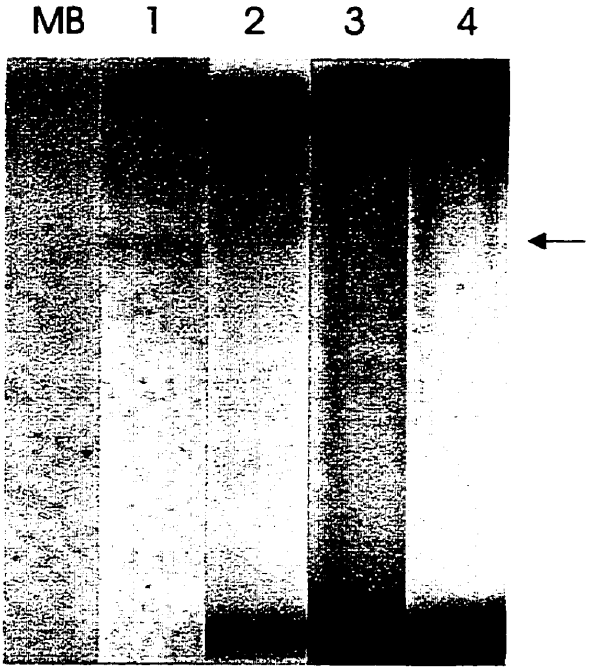

B

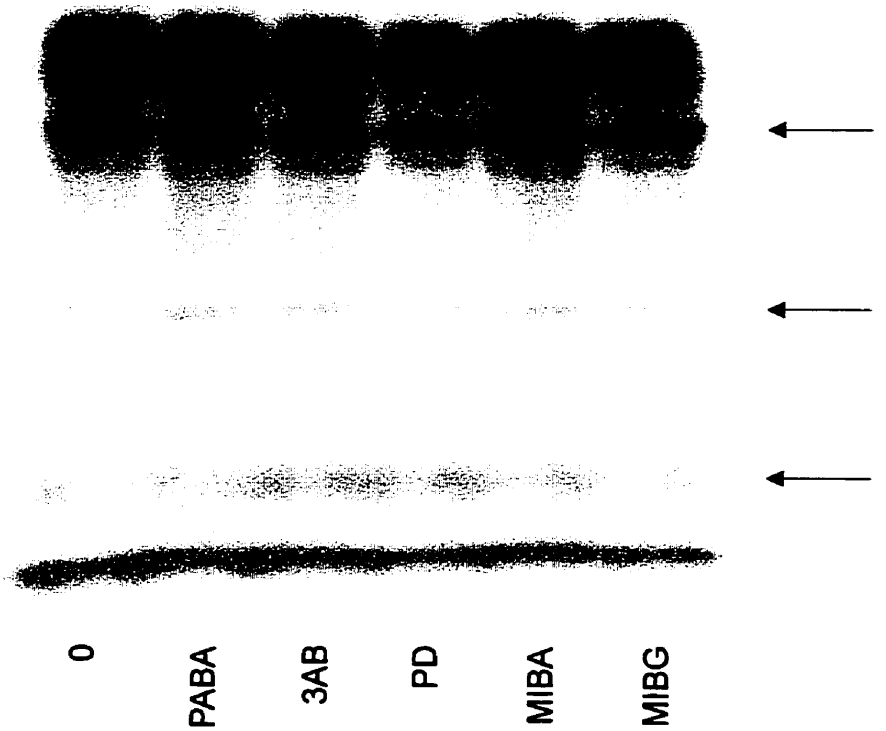

6.2.5 Discussion

The results of this study clearly demonstrated that MIBG is a reversible inhibitor of myoblast differentiation and theoretically of myoblast cell proliferation in L6 skeletal muscle myoblast cell line. This work is in very good agreement of the studies carried out by Kharadia *et al.* (1992) and not only confirms their findings, but also extends their work with respect to identifying the step in the myogenic differentiation program which MIBG, and presumably an arg-mART, may be influencing.

The initial survey of ADP-ribosylation inhibitors (Figures 30, 33) was in quite good agreement with the previous work of Shall and associates (Farzaneh *et al.* 1982), who demonstrated that the poly(ADP-ribosyl)ation inhibitor 3AB was able to reversibly inhibit the fusion of myoblasts from primary cultures of chick myogenic cells. These authors suggested that PARP was involved in the regulation of myoblast differentiation. However, as correctly pointed out in the paper by Kharadia *et al.* (1992), at the concentrations of 3AB that were used for those experiments, both PARP and mART activities would have been inhibited (Banasik *et al.* 1992; Duncan *et al.* 1988; Milam & Cleaver 1984; Rankin *et al.* 1989). Although a significant inhibition of differentiation (Figure 30), was not apparent upon visual examination, in contrast to the observations of Shall and associates (Farzaneh *et al.* 1982), the quantitative studies demonstrated 3AB caused a 40% reduction in the fusion index (Figure 33). On the other hand, the reduction in myotube fusion achieved with 3AB was significantly less than the effects obtained with MIBG treatment (Figures 29, 33, 35). The effective concentrations of MIBG were between 20 and 50 μM, within the concentration range defined by Kharadia *et al.* (1992) and, also interestingly, in agreement with the concentrations that were able to inhibit cell proliferation of H4IIE cells (and the systems described in chapters 7 and 8). In the studies of L6 cells, growth inhibition was indicated by a reduction in cell number (Figures 28,

29, 33, 35), and the decrease in [^{3}H]thymidine incorporation of growing L6 cells treated with MIBG (50 μM) (Figure 33C). Furthermore, the cells appear larger, somewhat suggestive of a block in cell proliferation at the G_2/M stage (i.e. blocked cell division). Since L6 myoblasts constitutively express MyoD (Lognonne & Wahrmann 1986), MIBG must affect progression through the differentiation process as opposed to determination or commitment to the muscle lineage.

As discussed in the previous chapter, MIBG could interfere with L6 myoblast differentiation directly or indirectly. For instance, lack of cell fusion could result from changes in membrane properties independent of myogenic-specific events. As stated by Kharadia *et al.* (1992), the effect of MIBG appears to be on the entire differentiation program, and not just simply the process of cell fusion, since both creatine phosphokinase (CPK) activity and protein accumulation were blocked by MIBG. However, previous studies have shown that muscle-specific proteins are expressed either in myogenic cell cultures in which fusion has been blocked or in fusion-deficient cell lines (Devlin & Konigsberg 1983; Nguyen *et al.* 1983). Thus, if only fusion, but not differentiation, was affected by MIBG treatment, increases in muscle-specific marker proteins such as CPK activity would be expected. Although neither CPK activity nor other markers of differentiated muscle were examined in this study, the fact that MIBG-dependent effects could be seen with only 4 to 12 h exposure early in the differentiation process supports that fact that MIBG is not just affecting the fusion step. Furthermore, the effect of MIBG is reversible (Figures 35, 36) and thus the short treatment time with MIBG should not be able to inhibit fusion, a process that occurs 48 to 72 h later. On the other hand, the MIBG delayed addition studies would suggest that the presence of MIBG may be required at multiple, temporally separated steps. Alternatively, the time frame for expression of muscle-specific genes during differentiation is a longer process over the initial time

period. Finally, Western blot analysis showed that the expression of muscle-specific proteins is blocked, which supports the contention that MIBG is affecting specific events required for differentiation (Figure 38). Nevertheless, an effect on the fusion and multinucleation processes cannot be ruled out.

According to the findings of this study and information in the literature, the step at which differentiation is blocked occurs after determination, since L6 skeletal myoblasts are already committed myogenic precursor cells (Yaffe 1968). MIBG blocked the expression of not only myogenin but also $p21^{CIP1}$ (Figure 38). It is well established that the absence of these proteins prevents myoblast differentiation and fusion into multinucleated myotubes (Dias *et al.* 1994; Walsh 1997). Myogenin has been shown to mediate the differentiation process (Walsh 1997), since it is a marker of myoblast commitment to the differentiation pathway. Subsequently, the expression of $p21^{CIP1}$ is increased and $p21^{CIP1}$ is a cyclin-dependent kinase inhibitor (Walsh 1997). Presumably it is the increased expression of this protein that irreversibly withdraws the skeletal myoblasts from the cell cycle and results in terminal differentiation. Interestingly, with MIBG treatment, since the expression of $p21^{CIP1}$ is decreased, it would suggest that the myoblasts are still capable of proliferating. On the other hand, MIBG inhibits cell proliferation (see chapter 5, Figure 33C and Kharadia *et al.* 1992). Based on this information, and the requirement for withdrawal from the cell cycle for progression of differentiation (Lassar *et al.* 1994; Molkentin & Olson 1996b), it might have been expected that MIBG treatment would stimulate differentiation. The ability of MIBG to abrogate differentiation of L6 cells, in addition to possibly proliferation, suggests that a separate mechanism during differentiation may be inhibited. In these studies, although detailed growth measurements were not conducted, it was observed that the number of myoblasts in the MIBG samples was reduced (Figures 28, 29) and that there was a

decrease in total number of nuclei (Figures 33, 35). This was confirmed by [^{3}H]thymidine incorporation studies where it was observed that uptake of [^{3}H]thymidine was decreased with MIBG treatment (Figure 33C).

Since L6 skeletal myoblasts are already commited to the myogenic lineage, MIBG may delay differentiation by affecting one crucial step. However, the activation or expression of this one protein may be required for multiple steps in the cascade. MIBG could also be toxic to the cells, however, the washout studies would suggest otherwise, as would the rescue study that was conducted (Figures 35, 36). These findings are in agreement with those of Kharadia *et al.* (1992), who also suggested that the inhibition of differentiation by MIBG was not due to the inhibition of cell division (i.e. proliferation of myoblasts was blocked before a necessary terminal mitosis during differentiation). The inhibitory effects of MIBG were immediate with respect to cell fusion (Figures 35, 36), and removal of MIBG resulted in a rapid increase in cell fusion (Figure 36), which might not have been expected if mitosis was required to initiate the differentiation step (Kharadia *et al.* 1992). The requirement for mitosis was also ruled out by Kharadia *et al.* (1992) through the addition of cytosine arabinoside to the refed cultures. If an additional round of mitosis was required for recovery from the MIBG treatment, blockade of cell proliferation with the cytosine arabinoside would have inhibited the differentiation process, and this was not observed.

The immunoprecipitation studies found that MIBG did not prevent the association between MyoD and E12/47 proteins (Figure 37). On the other hand, with the cross-linking studies, it was found that an oligonucleotide containing the MEF2 element associated with a protein in myotube nuclear extracts that was missing in nuclear extracts from myoblasts and MIBG treated-myotubes (Figure 39). This protein has a molecular mass of approximately 40-kDa (band size of 53-kDa minus the 13-kDa oligonucleotide).

Interestingly, the size of this protein does not correlate with the predominant protein that binds to this sequence, MEF2 (which is 72-kDa), which is required to transcriptionally activate numerous muscle-specific genes including creatine kinase, myosin heavy chain, desmin and certain MRFs (Ludolph & Konieczny 1995). For this reason, it is unclear whether the 40-kDa protein has a role in the induction of myogenesis-specific genes. If this protein is MEF2 (possibly a breakdown product or novel variant), an impairment in DNA binding is indicated. This conclusion can be reached because MEF2 expression is unaffected by MIBG (Figure 38). Furthermore, MIBG may influence the phosphorylation state of MEF2 which modulates both DNA binding and protein-protein interactions (Ferrari *et al.* 1997; Molkentin *et al.* 1996). Alternatively, the 40-kDa protein is unrelated to MEF2, but it is critical for the expression of muscle-specific genes via the MEF2 element. One such candidate protein may be SRF (serum response factor) which is also a part of the MADS box family of transcription factors (Black & Olson 1998; Brand-Saberi & Christ 1999; Shore & Sharrocks 1995). Of note, it is entirely possible that the MEF2 oligonucleotide, which was based on a MADS box consensus sequence, could bind other MADS box family transcription factors. For example, SRF is a 62-kDa protein and splice variants have been found in smooth and skeletal muscle of approximately 67-, 60-, 57- and 50-kDa (Kemp & Metcalfe 2000). There is mounting evidence to suggest that muscle specific transcription may require functional interactions of muscle-specific bHLH factors with other regulatory proteins such as SRF (Duprey & Lesens 1994; Hautmann *et al.* 1998; Hautmann *et al.* 1997; Solway *et al.* 1995). Moreover, MEF2 DNA binding sites are typically positioned within close proximity to MRF binding sites (i.e. E-boxes) in the regulatory regions of many muscle genes. These sites are required for the transcriptional activation of myogenin, MRF4 and MyoD (Cheng *et al.* 1993; Naidu *et al.* 1995; Wong *et al.* 1994). The MEF2-binding site, but not the E-box, is necessary for cell

type-specific expression and activation of the myogenin gene by MyoD in tissue culture cells (Buchberger *et al.* 1994). Thus, an effect by MIBG on the expression of myogenin via the MEF2 site (or a similar MADS box site) would prevent differentiation. Further study is necessary to determine the exact target through which MIBG has its effect. Interestingly, if the target protein is SRF, then regulation by MIBG may occur through Rho (Montaner *et al.* 1999; Poser *et al.* 2000) which is modulated by ADP-ribosylation (Aktories 1997; Lerm *et al.* 2000).

The ability of MIBG to inhibit L6 skeletal myoblast differentiation suggests that an arginine-dependent mART may be involved in one or more of the steps leading to differentiation of myoblasts into myotubes. Both intracellular and extracelluar arg-mARTs have been identified in skeletal muscle cells from a variety of species (Okazaki & Moss 1998; Soman & Graves 1988; Zolkiewska & Moss 1993; Zolkiewska *et al.* 1992). An extracellular GPI-linked arg-mART was first demonstrated by Zolkiewska and Moss (Zolkiewska & Moss 1993) who originally had cloned a rabbit skeletal muscle NAD:arginine ADP-ribosyltransferase (Zolkiewska *et al.* 1992), and then subsequently found that it was able to modify integrin α7 of differentiated mouse C2C12 and L8 cells. Intracellular arg-mARTs have been identified in the membrane fraction of rabbit skeletal muscle (Peterson *et al.* 1990; Soman & Graves 1988; Soman *et al.* 1984a). The extracellular arg-mART was not involved in modulating differentiation since incubation with MIBG did not alter the labeling with [^{32}P]NAD^{+} (Figure 40). Kharadia *et al.* (1992) had provided evidence that an intracellular arg-mART was inhibited by MIBG. Furthermore, they concluded that this was the reason for the inhibitory effect of MIBG on myogenic cell differentiation and proliferation. Their studies demonstrated that a specific transferase activity was detectable in their primary embryonic chick skeletal muscle cultures and that the ADP-ribosylated form of MIBG could be detected in homogenates

of cultures treated with MIBG (Kharadia *et al.* 1992). Secondary evidence provided by these authors include studies showing that MIBG is capable of inhibiting the purified skeletal muscle arg-mART (Kharadia *et al.* 1992). Interestingly, the authors also provide evidence for the specificity of the MIBG effect through its guanidino group, since MIBA which lacks the guanidino group was unable to inhibit differentiation. The studies presented in this chapter also show that MIBA does not inhibit fusion of myotubes (Figure 30).

To this point, the only identified mechanism by which ADP-ribosylation might influence the differentiation process is the modification of desmin, an intermediate filament. ADP-ribosylation results in the inhibition of desmin assembly, and de-ADP-ribosylation results in assembly (Huang *et al.* 1993; Zhou *et al.* 1996). Furthermore, desmin is one of the earliest myogenic markers and one of the first muscle-specific proteins to appear during mammalian embryonic development (Babai *et al.* 1990; Choi *et al.* 1990; Furst *et al.* 1989; Lin *et al.* 1994; Mayo *et al.* 1992). Thus, interfering with desmin intermediate filament assembly-disassembly by mono(ADP-ribosyl)ation (Yuan *et al.* 1999) may be a possible regulatory mechanism for myogenesis involving fusion and myofibril organization. However, the block in myogenin and $p21^{CIP1}$ expression is more applicable to the early stages of myogenesis (although desmin is expressed in pre-fusion myoblasts (Babai *et al.* 1990)). Nevertheless, inhibition of desmin organization could be a part of the regulatory process for differentiation and a part of the multiple steps that MIBG may be inhibiting. Further investigation of these events and their regulation by mARTs will be necessary.

6.2.6 Summary

MIBG inhibits the differentiation of L6 skeletal myoblasts into myotubes and the mechanism is likely mediated by a membrane-associated intracellular arg-mART. The expression of two key proteins, myogenin and $p21^{CIP1}$, for the myogenic lineage appear to be inhibited by MIBG. Myogenin is an MRF that is critical for the subsequent expression of other muscle-specific proteins, while expression of $p21^{CIP1}$ is crucial for the irreversible withdrawal of the cells from the cell cycle. Furthermore, MIBG also appears to influence binding of a protein, possibly MEF2, to the MEF2 element, which may further explain the lack of myogenin protein expression and the abrogation of the myogenic fusion program.

7.0 SMC as a model of de-differentiation, proliferation and migration

7.1 Introduction

Within the normal vessel wall, SMCs are found in the medial layer, and SMCs within this layer have been shown to express a range of phenotypes that exist between two extreme states traditionally referred to as 'contractile' and 'synthetic' (Campbell *et al.* 1987; Chamley-Campbell *et al.* 1979). Contractile SMCs are characterized by the presence of myofilaments and smooth muscle specific genes that encode contractile proteins and proteins that regulate contraction (Campbell *et al.* 1987; Shanahan *et al.* 1993). On the other hand, synthetic SMCs have a limited myofilament presence and an abundance of organelles (especially rough endoplasmic reticulum and Golgi apparatus) for the processing of newly synthesized proteins (Campbell *et al.* 1987). This concept of SMC heterogeneity was first identified in cell culture studies (Chamley-Campbell *et al.* 1979) and since that time SMC heterogeneity has been found not only in experimental animals (Bochaton-Piallat *et al.* 1996; Orlandi *et al.* 1994a; Pauletto *et al.* 1994; Schwartz *et al.* 1995b; Villaschi *et al.* 1994; Wohrley *et al.* 1995), but also in the human population (Glukhova *et al.* 1991). The relevance of heterogeneity to vascular fibroproliferative diseases lies with the question of the identification of the SMCs that are responding in a pathological manner. Were these cells originally heterogeneous and thus only a certain population was responding? Is there a spatiotemporal heterogeneity in the expression of differentiation markers? Or, do SMCs modulate their phenotype and differentiation status in response to environmental factors? To add to this complexity, evidence is mounting that committed and differentiated cells can transdifferentiate into another cell type (Arciniegas *et al.* 2000; Gressner 1996; Lipton *et al.* 1991; Smith *et al.* 1999). With the application of cell and molecular biological techniques for the study of development, differentiation and the pathophysiology of vascular proliferative disorders, distinct

cellular phenotypes involved with SMC myogensis and proliferative and fibrotic responses of SMCs in diseased arteries has been identified (McHugh 1995; Owens 1995; Ross 1993; Sartore *et al.* 1994; Schwartz *et al.* 1986).

To define the response of SMCs to various stimuli and growth factors in an isolated system *in vitro*, various SMC culture systems have been developed (Chamley-Campbell *et al.* 1979). The most commonly studied SMCs are derived from either rabbit or rat arteries (Birukov *et al.* 1993; Bochaton-Piallat *et al.* 1992; Campbell *et al.* 1989; Kocher & Gabbiani 1986; Schwartz *et al.* 1986; Schwartz *et al.* 1995a; Skalli *et al.* 1986; Thyberg *et al.* 1990b). In these culture systems, the biological features of SMCs have been systematically studied, and the identification of distinct SMC phenotypes and responses to environmental and exogenous stimuli have been described (Birukov *et al.* 1993; Bochaton-Piallat *et al.* 1992; Campbell *et al.* 1987; Campbell *et al.* 1989; Chamley-Campbell *et al.* 1979; Kocher & Gabbiani 1986; Owens 1995; Schwartz *et al.* 1995a; Skalli *et al.* 1986; Thyberg *et al.* 1990b). However, in these SMC culture systems, limitations to their use have arisen due to species-specific differences observed in the response to injury, both *in vivo* and *in vitro*, as well as environmental factors (Schwartz *et al.* 1995b). As a result, many larger animal models of restenosis and SMC tissue culture models derived from these larger animals have been developed. Among the most popular have been models of restenosis/intimal thickening employing porcine arteries (Gal *et al.* 1990; Grinstead *et al.* 1994; Schwartz *et al.* 1993; Zalewski & Shi 1997). With these models, both pig aortic and coronary SMCs have been studied (Christen *et al.* 1999; Gotlieb & Boden 1984; Koo & Gotlieb 1989; Koo & Gotlieb 1991; Koo & Gotlieb 1992; Saward & Zahradka 1997b; Wilson *et al.* 1999). Porcine coronary artery SMCs have been shown to maintain a high level of differentiation marker expression, including smoothelin (Christen *et al.* 1999) and, since they behave differently *in vitro* from the

majority of SMCs previously studied, they may thus represent a better model for the study of agents influencing SMC behaviour *in vitro* and *in vivo* (Christen *et al.* 1999). Furthermore, porcine SMCs appear to exhibit features that are more similar to those observed in human arterial SMCs in culture (Christen *et al.* 1999; Kocan *et al.* 1980).

One of the most commonly employed methods for the establishment of primary SMC cultures involves the use of enzymatic dispersion of vessels (Gimbrone & Cotran 1975). However, separation of the different cell types present within the vessel wall is much more difficult after a generalized digestion. Additionally, the potential for damage to cellular membranes and protein receptors bound to the membrane is increased with time of digestion, thereby affecting the responses of the SMCs to stress, growth stimuli and other environmental factors. Alternatively, microdissection of the vessel wall to remove only the smooth muscle containing medial layer which can then be cultured by an explant method has been used to establish primary SMC cultures (Ross 1971). This approach selects for SMCs but the size of the vessel limits the species and vessel type that can be used. A primary culture system employing SMCs derived from porcine coronary artery explants was developed in this laboratory by a fellow student (Saward & Zahradka 1997b). Due to numerous advantages afforded by this system, including ease of preparation and homogeneity of the cell population, this well characterized system was employed for the studies described in this chapter.

Using this primary porcine SMC culture system and based on findings from the previous chapters, a specific hypothesis was proposed: *Growth factor-mediated growth and proliferation of porcine SMCs will be inhibited by MIBG through inhibition of a specific cellular signaling pathway that will involve an ADP-ribosylation reaction.*

This goal was achieved by i) defining the cellular system, ii) testing the efficacy of the inhibitor in the system, and iii) examining the signaling components that might be involved.

7.2 Mitogenic response of SMC's to growth factors: role of PGE_2

7.2.1 Background/rationale

Abnormal and/or excessive proliferation of SMCs is believed to play a key role in the pathogenesis of atherosclerosis and restenosis after revascularization (Ross 1995; Schwartz *et al.* 1986; Schwartz & Reidy 1996). Upon injury or exposure to increasing environmental stress, SMCs within the vessel wall become activated and respond to secreted growth factors and other stimuli by increasing their growth potential. The factors controling SMC growth in both normal and disease states have therefore become the subject of intensive investigations over the past 10 years. Both positive and negative stimuli exist for SMCs and small alterations in the balance of these factors can have profound effects on SMCs and their growth responsiveness (Liu *et al.* 1989). Mitogens such as platelet-derived growth factor (PDGF), angiotensin II (AngII), thrombin and fibroblast growth factor (bFGF) have been shown to be released by platelets, damaged endothelial cells and SMCs after injury, and have been demonstrated to influence the growth and migration of SMCs during the formation of a neointimal thickening (Davies & Hagen 1994; Neville & Sidawy 1998; Schwartz *et al.* 1995c). On the other hand, inhibitors of SMC growth, such as heparin and prostaglandins of the E family, are also released by cells after the injury (Schror & Weber 1997; Scott-Burden & Vanhoutte 1994).

The role of prostaglandins of the E family in the modulation of SMC proliferative status has been examined in a variety of venues, however, the results remain

controversial. PGE_1 and PGE_2 have been shown to operate as both positive and negative regulators of SMC growth (Owen 1986; Pasricha *et al.* 1992; See *et al.* 1987; Shechter *et al.* 1997). For example, Shechter *et al.* (1997) and Umemura *et al.* (1997) have shown PGE_1 is effective during angioplasty as preventative therapy for coronary restenosis, and Fan and associates, and others (Fan *et al.* 1997; Loesberg *et al.* 1985; Nilsson & Olsson 1984) have shown that PGE_1 inhibits vascular SMC growth. PGE_1 has antiplatelet aggregation and deposition characteristics, as well as anti-spasm, vasodilation and cytoprotective effects (Siegel *et al.* 1984), and is derived from macrophages that may be populating the injured region. Furthermore, exogenously added PGE_2 has an antiproliferative effect on cultured guinea pig tracheal and human airway SMCs (Florio *et al.* 1994; Johnson *et al.* 1995) and rabbit aortic SMCs (Lei & Deng 1989). On the other hand, Pasricha *et al.* (1992) have demonstrated that PGE_1 and PGE_2 stimulate the proliferation of pulmonary artery SMCs. It is possible that the effect of $PGE_{1/2}$ on the proliferation of SMCs is dependent on the vascular bed. However, Owen (1986) demonstrated that the effect of PGE_1 on SMCs is dependent on the phase of the cell cycle when it is added. If PGE_1 was added to a quiescent cell population, DNA synthesis was enhanced. If PGE_1 was added to asynchronous cycling cells, it functioned as an anti-proliferative agent. Moreover, Sjolund *et al.* (1984) have described a phenotype modulatory action of PGE_1 in primary cultures of arterial SMCs. It was thus suggested by Schror & Weber (1997) that endogenous prostaglandins may serve a dual purpose in SMCs: maintenance of the differentiated, contractile state and control of proliferation in the presence of growth factors (Pomerantz & Hajjar 1989). Thus, PGs could stimulate SMCs to enter the cell cycle and to divide in response to tissue injury in order to facilitate tissue repair while also preventing uncontrolled growth of SMCs by interfering with the synthetic phase of the cell cycle (i.e. inhibition of proliferation of SMC after stimulation

with growth factors) (Asada *et al.* 1994; Koh *et al.* 1993; Owen 1986; Pasricha *et al.* 1992; Schror & Weber 1997; Shirotani *et al.* 1991).

Recently, Inagami and colleagues (Ohnaka *et al.* 2000) demonstrated that AngII induced the expression of cyclooxygenase-2 in cultured rat vascular SMCs with subsequent PGE_2 production. It has also been demonstrated by others that AngII stimulates the release of PGs in a variety of cellular systems, including SMCs through the activation of PLA_2 (Alexander & Gimbrone 1976; Catalioto *et al.* 1996; Gimbrone & Alexander 1975; Schlondorff *et al.* 1987; Vallotton *et al.* 1989). This laboratory has also demonstrated a link between AngII and PG release in porcine SMCs, that was associated with a positive growth response (Saward, Yau, Thomas & Zahradka, unpublished observations). This particular study was therefore initiated to examine the effect of PGE_2 on SMC growth and proliferation in relation to SMC growth status.

7.2.2 Specific Aims

1. To compare the growth response of SMCs to a variety of growth factors.
2. To define the contribution of PGE_2 to SMC growth.
3. To determine the signaling pathways activated by PGE_2 that are related to the growth response.

7.2.3 Experimental Design

Primary cultures of porcine SMCs, generated by the explant culture technique, were incubated in serum-free supplemented media for 5 days before experimentation. This was to ensure that the SMCs were in a quiescent, differentiated, contractile state that is reminiscent of SMCs in the vessel wall. The time required for the SMCs to re-enter the cell cycle was monitored by [^{3}H]thymidine incorporation. The rates of RNA and DNA

synthesis were then measured in response to serum and growth factor (eg. AngII) stimulation. A broad spectrum of growth factors were assessed for their ability to stimulate DNA synthesis. Growth assays were carried out to monitor the specific effect of PGE_2, a novel stimulator of SMC growth (Owen 1986; Pasricha *et al.* 1992). These assays included [^{3}H]uridine and [^{3}H]thymidine incorporation, MTT assay, immunocytochemistry for PCNA expression and incorporation of bromodeoxyuridine (BrdU), and RT-PCR analysis of c-*fos* gene expression. Moreover, the signaling pathways associated with PGE_2-stimulated growth were assessed by Western blot analysis. The activation of p21-Ras and MAP kinase was also examined separately. Finally, the contribution of the PI3-kinase pathway was examined with respect to PGE_2-stimulated SMC growth.

7.2.4 Results

7.2.4.1 Growth characteristics of SMCs in response to serum and other growth factors

The response of primary porcine coronary artery SMCs to serum withdrawal was monitored over preset periods of time. Subconfluent SMCs were placed into serum-free supplemented D-MEM and the rate of DNA synthesis monitored at specific time points with 30 min pulses of [^{3}H]thymidine. Over a period of 168 h (7 days), the rate of DNA synthesis declined considerably, with a basal steady-state level of DNA synthesis being reached at approximately 48 h (Figure 41A). This is similar to the findings of Saward & Zahradka (1997b), who first characterized this particular model. It was observed that the cells, even after 7 days under serum-free conditions, did not appear to be dying (data not shown; Figure 41A). Although cell viability assays were not conducted, the ability of the quiescent SMCs to re-enter the cell cycle was taken as evidence that the cells were still

healthy (Figures 41B and 50). Based on this experiment and the findings of Saward & Zahradka (1997b), SMCs were consistently prepared by incubating them in a serum-free supplemented D-MEM for 120 h (5 days) before initiation of experimentation. The prolonged starve down period ensured that the SMCs had exited the cell cycle and expressed a contractile phenotype. To characterize the differentiated state of these SMCs, immunocytochemistry with specific antibodies was conducted to assess the expression of the smooth muscle specific markers α-actin and SM-myosin (Figure 42). Hoescht nuclear stain was applied to identify the location of all cells. After 5 days in serum-free supplemented D-MEM, SMCs displayed both α-actin and SM-myosin filamentous staining (Figure 42A, B). Moreover, staining with α-actin antibody and a stain specific for globular actin showed that filamentous actin was present in the cytoplasm of the cell, and that the localization of globular actin was mainly within the nucleus of the cell (Figure 42C). These findings are consistent with the expression of a quiescent, contractile phenotype for the SMCs.

The ability of quiescent SMCs to synchronously re-enter the cell cycle after 120 h in serum-free supplemented media was demonstrated by stimulating the SMCs with FBS (20% v/v) and measuring the rate of DNA synthesis with pulse additions of [^{3}H]thymidine (Figure 41B). Addition of the supplement was conducted in parallel as the negative control (Figure 41B). It was essential to establish that cell growth was growth factor-dependent and did not result from manipulation of the cells. FBS was able to stimulate SMC re-entry into the cell cycle with a lag period of approximately 8-10 h before the onset of S phase (DNA synthesis) (Figure 41B). These data indicate that even after a prolonged period of serum starvation, SMCs are responsive to growth factor stimulation, and certainly indicative of cell viability. Furthermore, micrographs of serum-

FIGURE 41: ***Response of SMCs to Serum Withdrawal and Addition.***

(A) Subconfluent SMCs were placed into serum-free supplemented D-MEM media and the DNA synthetic rate was monitored at specific time points by addition of 2 μCi [^{3}H]thymidine for 30 min. The cells were subsequently lysed and the incorporation of radiolabel into DNA measured as described in Materials and Methods (section 4.3.1). No loss of cell viability was evident after 7 days under serum-free supplemented conditions. (B) Quiescent SMCs were prepared by placing cells into serum-free supplemented D-MEM for 120 h (5 days). The cells were pulse-labelled with 2 μCi [^{3}H]thymidine for 30 min at specific time points after addition of serum (20% v/v FBS). Addition of the serum-free supplemented D-MEM media was used as a negative control. Incorporation of radiolabel into DNA was measured as described in section 4.3.1. The data are presented as the mean ± SE of experiments conducted in triplicate. These results were confirmed in three independent experiments using different SMC isolations.

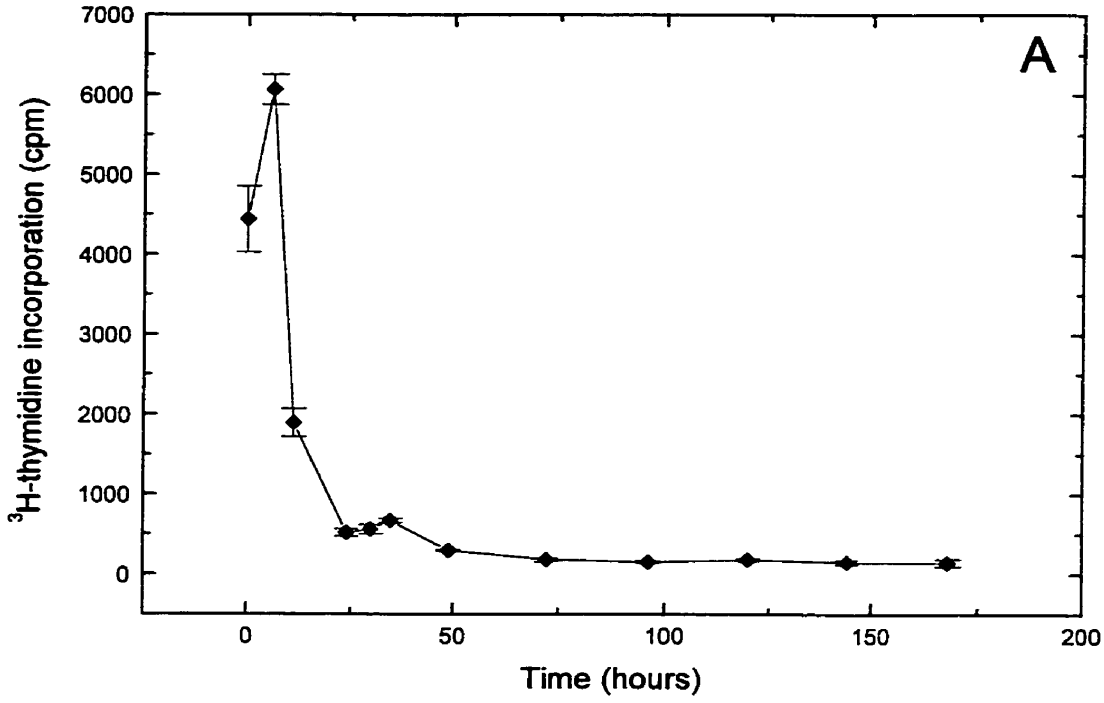
A
^{3}H-thymidine incorporation (cpm)
7000
6000
5000
4000
3000
2000
1000
0
0
50
100
150
200
Time (hours)

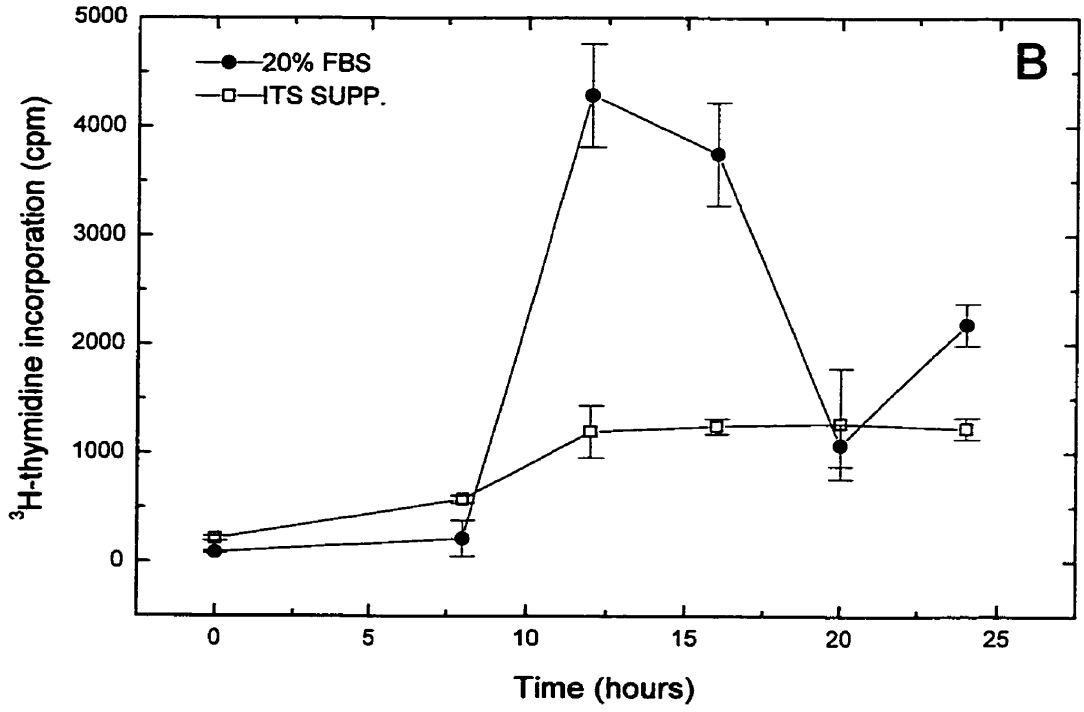
B
20% FBS
ITS SUPP.
^{3}H-thymidine incorporation (cpm)
5000
4000
3000
2000
1000
0
0
5
10
15
20
25
Time (hours)

FIGURE 42: ***Immunocytochemistry of Smooth Muscle Cells.***

SMCs prepared on Superfrost Plus glass slides were maintained in serum-free supplemented D-MEM for 5-7 days and markers of SMC differentiation assessed. (A) Cells were stained with SM α-actin and Hoescht No. 33342. (B) Cells were stained with SM-myosin and Hoescht No. 33342. (C) Cells were stained with SM α-actin and DNAse I. Magnification: 286×. Representative immunofluorescence micrographs are shown.

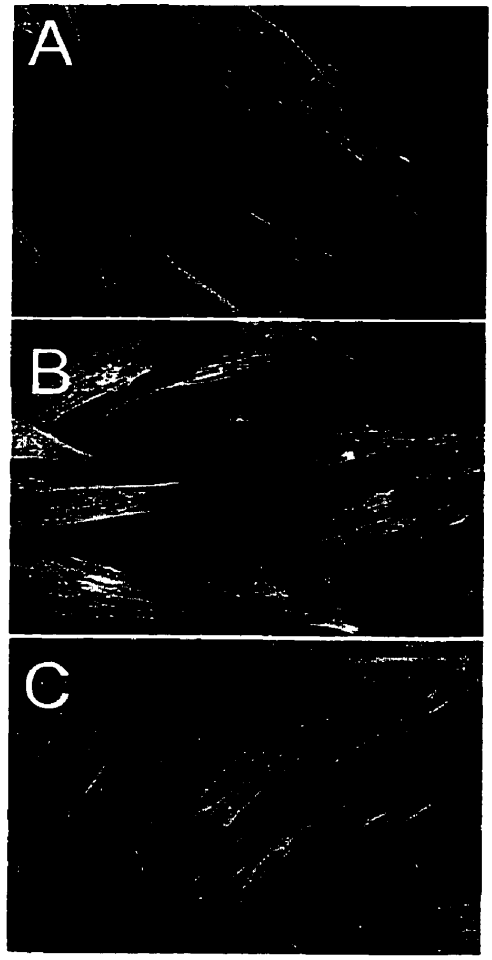
A
B
C

stimulated (5% v/v FBS) cells (Figure 43) demonstrated a change in the morphology of the SMCs as they responded to serum and re-entered the cell cycle.

To determine the responsiveness of SMCs to individual growth factors, both RNA and DNA synthesis studies were carried out with AngII (10^{-12} to 10^{-5} M) and FBS (0.5 to 20% v/v). AngII significantly increased the rate of both RNA and DNA synthesis in porcine SMCs (Figure 44B,D), although the magnitude of activation was considerably less than the increase in RNA and DNA synthesis observed with FBS stimulation (Figure 44A,C). Interestingly, increasing concentrations of AngII continued to augment the response (Figure 44B,D), while higher concentrations of FBS (greater than 5%) appeared to have an inhibitory effect on RNA synthesis (Figure 44A). This may be attributed to increasing concentrations of inhibitory molecules within the FBS. Finally, other growth factors and stimulating agents were tested for their ability to stimulate DNA synthesis in porcine SMCs. Relative to FBS administration, IGF-1 and PGE_2 had moderate but significant effects on [^{3}H]thymidine incorporation, while thrombin had positive but not significant effects (Figure 45). These results demonstrate that porcine SMCs are responsive to a broad range of growth factors, and that individual growth factors have distinct efficacy with respect to SMC growth. The potential exists, therefore, for a synchronous additive effect on SMC growth between growth factors if the appropriate combination or conditions is achieved.

7.2.4.2 Growth response of SMCs to PGE_2

Of the growth factors and stimulating agents tested above, one of the more interesting and somewhat surprising findings was that an eicosanoid was able to increase DNA synthesis (Figure 45). In a variety of cell systems, eicosanoids/prostanoids, in particular PGE_2 and TxA_2, have exhibited both inhibitory and stimulatory effects on cell growth and proliferation (Florio *et al.* 1994; Johnson *et al.* 1995; Lei & Deng 1989;

FIGURE 43: ***Response of SMCs to Serum and Growth Factor Stimulation.***

SMCs were maintained in serum-free supplemented D-MEM for 5-7 days and the morphology of the SMCs recorded on photomicrographs. (A) SMCs in their differentiated, contractile phenotype. Photomicrographs were used to record cell morphology after the quiescent SMCs had been stimulated with serum (20% v/v FBS) for 24 h (B), 48 h (C) and 96 h (D). Representative micrographs are shown from one of three independent experiments conducted using different SMC isolations. Magnification: 132×.


A


B

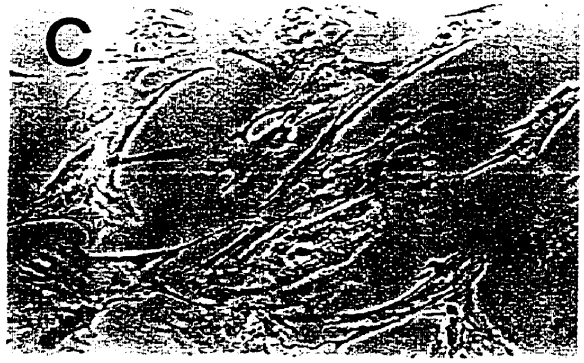
C

FIGURE 44: ***Response of SMCs to Serum and Angiotensin II.***

SMCs maintained in serum-free supplemented D-MEM for 5 days were treated with either serum (0.5 to 20 % v/v FBS) (A, C) or angiotensin II (AngII) (10^{-12} to 10^{-5} M) (B, D) and the growth response monitored. The incorporation of [^{3}H]uridine (6 h incubation) and [^{3}H]thymidine (48 h incubation) into trichloroacetate-precipitable material after addition of serum or AngII was used as an indication of RNA (A, B) or DNA (C, D) synthetic activity. The incorporation rate of untreated cells was set to 100%. The data are presented as the mean ± SE of experiments conducted in triplicate. These results were confirmed in three independent experiments using different SMC isolations.

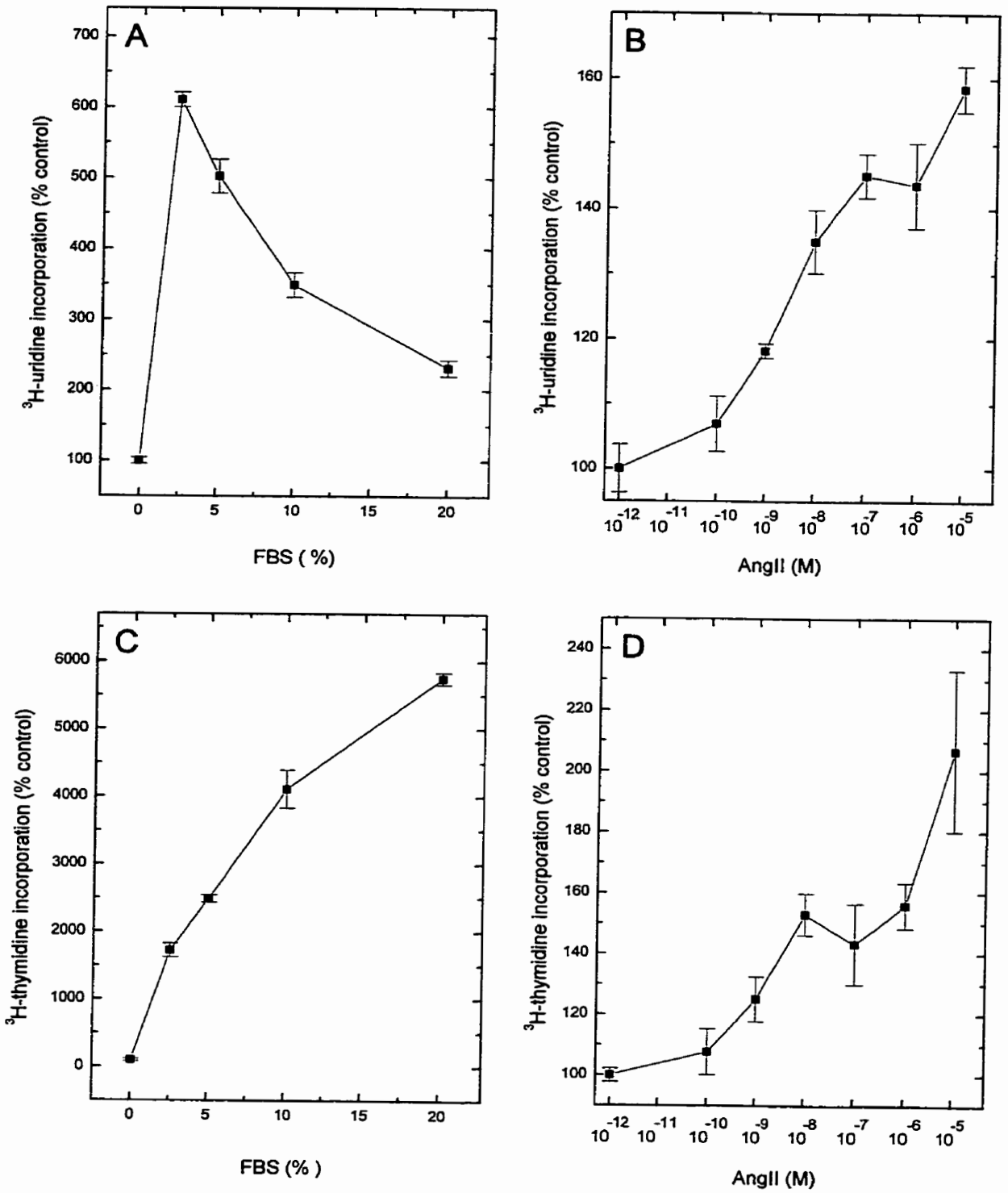
A
^{3}H-uridine incorporation (% control)
FBS (%)
B
^{3}H-uridine incorporation (% control)
AngII (M)
C
^{3}H-thymidine incorporation (% control)
FBS (%)
D
^{3}H-thymidine incorporation (% control)
AngII (M)

FIGURE 45: ***Response of SMCs to a Spectrum of Growth Factors and Growth Stimulating Agents.***

SMCs maintained in serum-free supplemented D-MEM for 5 days were treated with a variety of mitogenic agents and the growth response monitored. The incorporation of [^{3}H]thymidine (48 h incubation) into trichloroacetate-precipitable material after addition of serum (5% v/v FBS), IGF-1 (10^{-7} M), thrombin (10^{-6} M) or PGE_2 (10^{-6} M), was used as an indication of DNA synthetic activity. The incorporation rate of untreated cells was set to 100%. The data are presented as the mean ± SE of experiments conducted in triplicate. These results were confirmed in two independent experiments using different SMC isolations. Comparisons were made between untreated SMCs and SMCs treated with growth stimulating agents using the Student's t-test (*, $p < 0.05$).

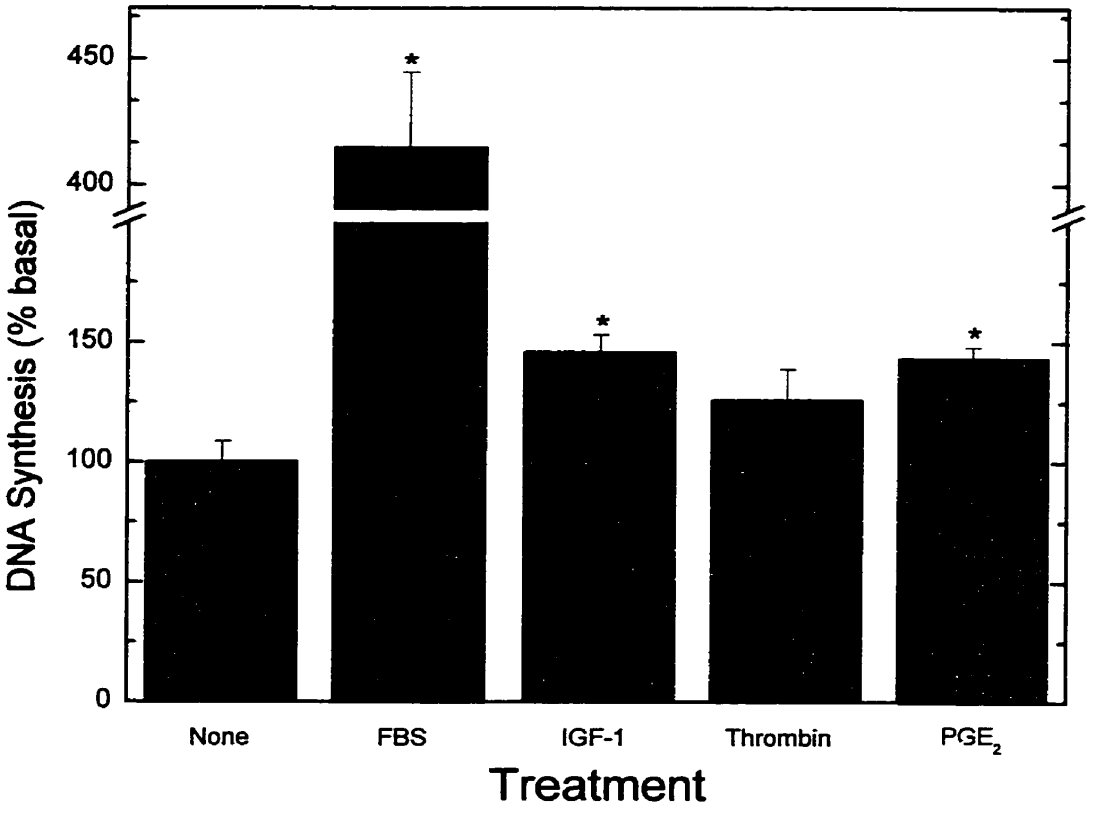
450
400
150
100
50
0
DNA Synthesis (% basal)
*
*
*
None
FBS
IGF-1
Thrombin
PGE2
Treatment

Morinelli *et al.* 1994; Owen 1986; Pasricha *et al.* 1992; Sachinidis *et al.* 1995; Sjolund *et al.* 1984). For example, TxA_2 has positive growth effects in SMCs (Morinelli *et al.* 1994; Sachinidis *et al.* 1995), while PGE_2 has had both stimulatory and inhibitory effects in SMCs (Owen 1986; Pasricha *et al.* 1992; Sjolund *et al.* 1984). It was of interest then to further define the response of SMCs to PGE_2 considering that previous work in the laboratory had established that PGs were a part of the growth stimulatory pathway of AngII (Saward 2000).

To confirm that SMCs were capable of responding to PGE_2, PGE_2 (10^{-10} to 10^{-5} M) was administered to SMCs and the rates of RNA and DNA synthesis monitored at 6 h and 48 h, respectively. A second PG species, PGI_2, was employed in parallel as a negative control for the growth response. Increasing concentrations of PGE_2 were able to significantly stimulate the SMC uptake of [^{3}H]uridine and [^{3}H]thymidine (Figure 46A,B), with a more abrupt concentration response observed in the DNA synthesis study. In contrast, if PGE_2 was administered concurrently with low dose FBS (1% v/v), a decrease in the growth response was observed (Figure 46C). These data indicate that the growth state of the SMCs is very important in determining the response of the cells to PGE_2. These findings were in agreement of the studies done by Owen (1986) and the hypothesis put forth by Schror & Weber (1997).

To verify that the SMC response to PGE_2 was due to a specific association with PGE_2 receptors, ligand binding was assessed (Figure 47). Unlabelled PGE_2 was used to compete for [^{3}H]PGE_2. This assay demonstrated that increasing concentrations of PGE_2 resulted in increased numbers of PGE_2 molecules bound to the receptor (Figure 47). Furthermore, competition with a different PG species (eg. PGI_2, $PGF_{2\alpha}$) did not decrease PGE_2 binding (data not shown). Additionally, a specific receptor antagonist for the EP_1 receptor (SC51322) was used to determine whether the growth response of SMCs to

FIGURE 46: ***Response of SMCs to Prostaglandin E_2.***

Quiescent SMCs were treated with prostaglandin E_2 (PGE_2) or prostacyclin/prostaglandin I_2 (PGI_2) and the growth response monitored. The incorporation of [^{3}H]uridine (6 h incubation) and [^{3}H]thymidine (48 h incubation) into trichloroacetate-precipitable material after addition of PGE_2 and PGI_2 (10^{-10} to 10^{-5} M) was used as an indication of RNA (A) or DNA (B) synthetic activity. (C) The incorporation of [^{3}H]thymidine (48 h incubation) into trichloroacetate-precipitable material after addition 1 % (v/v) FBS and PGE_2 simultaneously over a concentration range (10^{-10} to 10^{-5} M) was used as an indication of DNA synthetic activity. The incorporation rate of untreated cells was set to 100%. The data are presented as the mean ± SE of experiments conducted in triplicate. These results were confirmed in three independent experiments using different SMC isolations. In (C), comparisons were made relative to FBS treated cells (*, $p < 0.05$) using the Student's t-test.

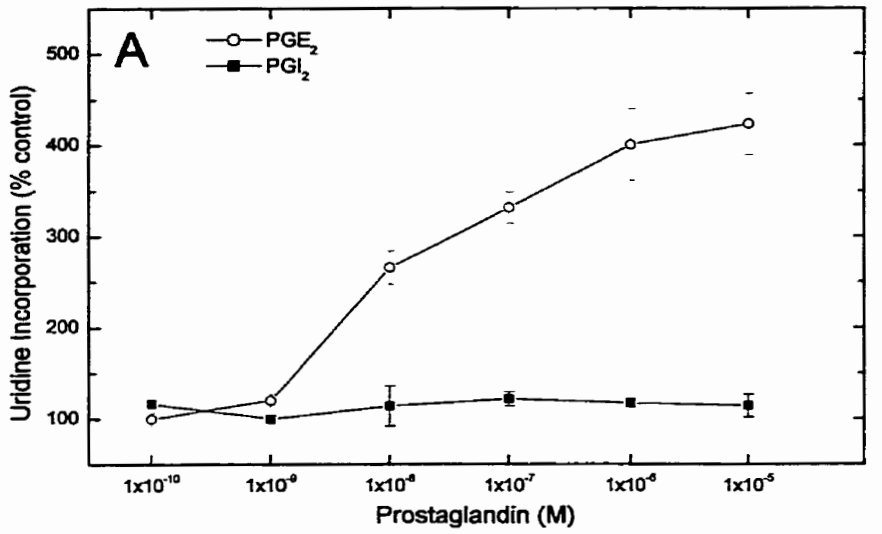
A
PGE2
PGI2
Uridine Incorporation (% control)
500
400
300
200
100
1x10-10
1x10-9
1x10-8
1x10-7
1x10-6
1x10-5
Prostaglandin (M)

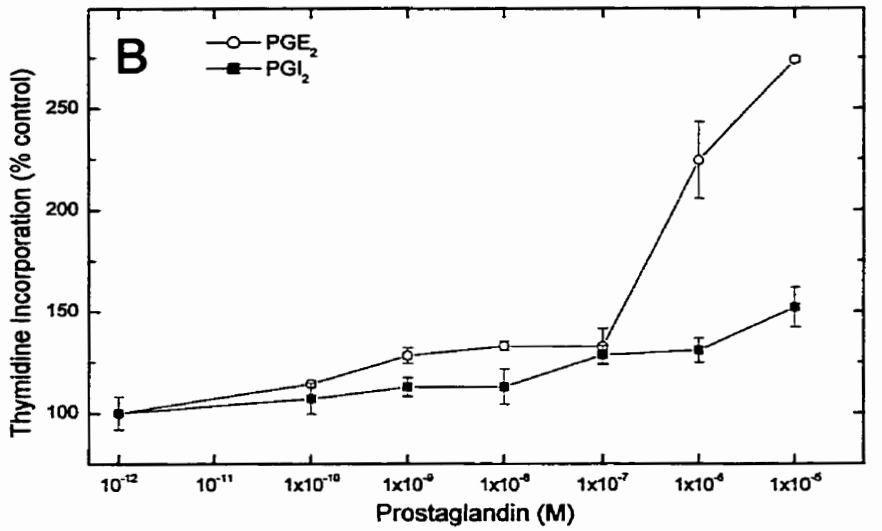
B
PGE2
PGI2
Thymidine Incorporation (% control)
250
200
150
100
10-12
10-11
1x10-10
1x10-9
1x10-8
1x10-7
1x10-6
1x10-5
Prostaglandin (M)

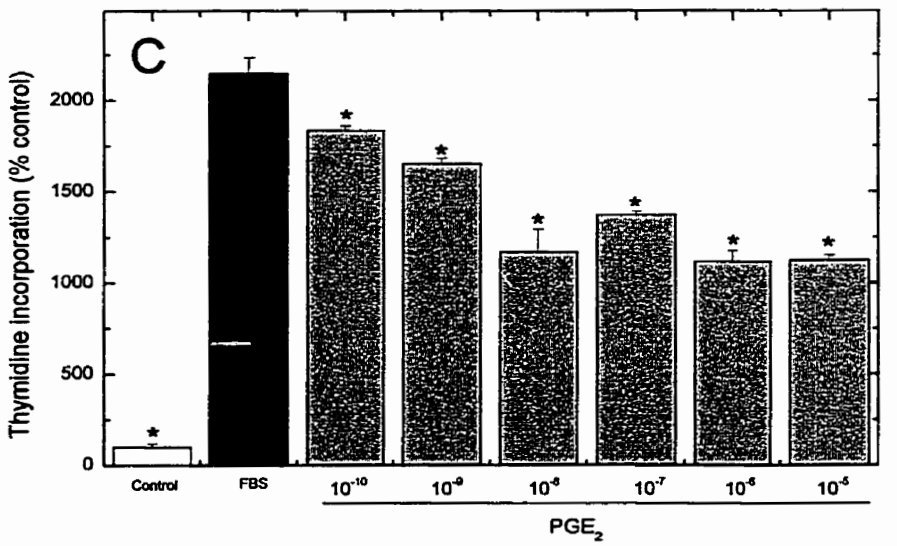
C
Thymidine Incorporation (% control)
2000
1500
1000
500
0
Control
FBS
10-10
10-9
10-8
10-7
10-6
10-5
PGE2

FIGURE 47: ***Prostaglandin E_2 Specificity for its own Receptor During the Growth Response.***

Labelled PGE_2 (0 to 300 nM) was added to quiescent SMCs and subsequently incubated at room temperature for 20 – 30 min. Non-specific ligand binding was assessed in a parallel experiment in the presence of 10^{-6} M unlabelled PGE_2. Bound PGE_2 was then plotted vs. concentration. The results were confirmed in three independent experiments.

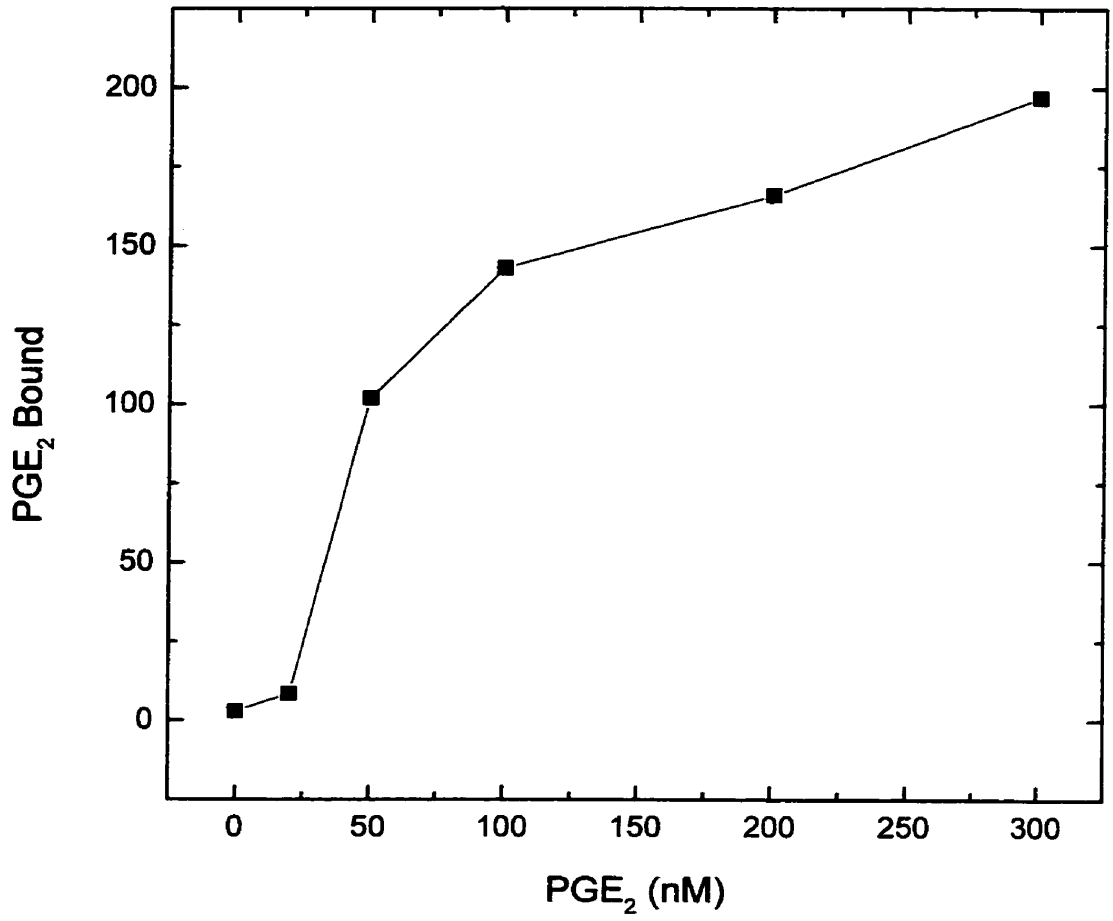
200
150
100
50
0
PGE2 Bound
0
50
100
150
200
250
300
PGE2 (nM)

PGE_2 was mediated by that receptor subtype. RNA and DNA synthesis assays were used to monitor the response to PGE_2 in the presence of SC51322 which was administered to the SMCs 10 min prior to PGE_2. Only the highest concentration of SC51322 tested (10^{-5} M) was able to decrease PGE_2-dependent RNA synthesis (Figure 48A,B), suggesting that this receptor subtype is not likely involved in the PGE_2 growth response in SMCs.

The MTT assay was used to confirm that PGE_2 activated the growth response of SMCs. FBS was used as a positive control for growth stimulation and other PG species were used as negative controls. Over 96 h, with assays conducted every 24 h, FBS significantly increased the conversion of MTT by SMC mitochondria (Figure 49A). PGE_2 also stimulated increasing conversion of MTT, but to a lesser extent (Figure 49A). Neither PGI_2 nor $PGF_{2\alpha}$ had a stimulatory effect, even after 96 h of incubation. The one limitation of the MTT assay is that it cannot distinguish between hypertrophic and hyperplastic growth. As a result, cell number was also quantified by Coulter counting after treatment with PGE_2 (10^{-6} M) and FBS (10% v/v). The number of SMCs was only increased significantly after 96 h incubation with PGE_2 compared to the increase seen at 48 h with the FBS stimulation of SMCs (Figure 49B). The time frame of the PGE_2 response is similar to that observed for the MTT conversion assay.

Other parameters of cell growth were used to confirm the findings of the RNA and DNA synthesis experiments. Immunostaining of SMC monolayers treated with PGE_2 revealed increased PCNA expression at 48 h (Figure 50C). Interestingly, not all PGE_2-treated cells expressed PCNA, unlike the data obtained after administration of FBS (10% v/v) (Figure 50B). Immunostaining for BrdU incorporation at 72 h revealed a similar distribution of activated cells between PGE_2-treated and FBS-treated SMCs (Figure 50D-F). These results confirm that PGE_2 is capable of eliciting a growth response in SMCs, but also indicate that only a subset of cells are responsive to this agent.

FIGURE 48: ***Involvement of a Specific Prostaglandin E_2 Receptor Subtype in Prostaglandin-mediated SMC Growth.***

Quiescent SMCs were treated with PGE_2 (10^{-6} M) in the presence or absence of SC51322 (10^{-9} to 10^{-5} M). The incorporation of [^{3}H]uridine (6 h incubation) and [^{3}H]thymidine (48 h incubation) into trichloroacetate-precipitable material after addition of both agents was used as an indication of RNA (A) or DNA (B) synthetic activity. The incorporation rate of DMSO treated cells was set to 100%. The data are presented as the mean ± SE of experiments conducted in triplicate. These results were confirmed in three independent experiments using different SMC isolations. Comparisons were made relative to PGE_2 treated SMCs using the Student's t-test (*, $p < 0.05$).

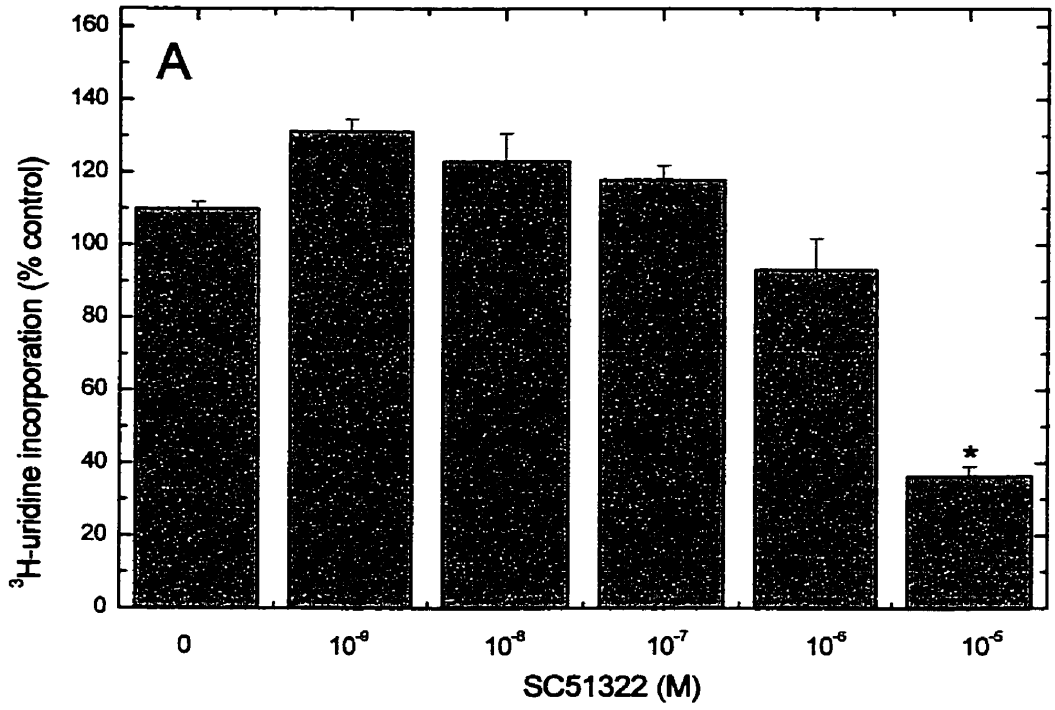
A
^{3}H-uridine incorporation (% control)
160
140
120
100
80
60
40
20
0
*
0
10^{-9}
10^{-8}
10^{-7}
10^{-6}
10^{-5}
SC51322 (M)

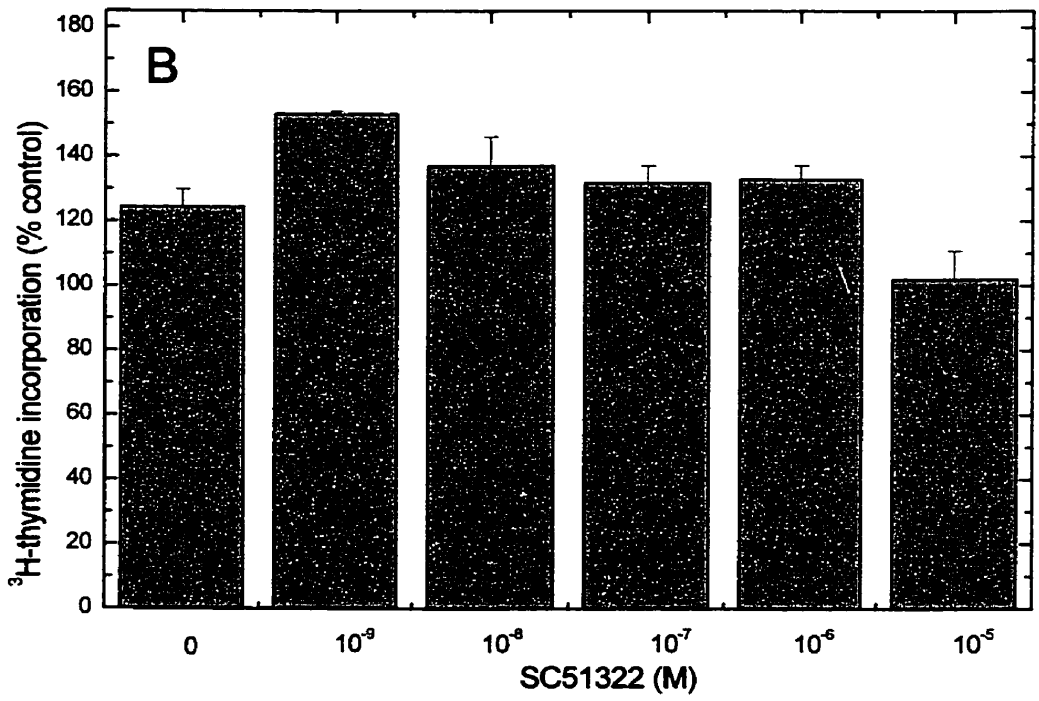
B
^{3}H-thymidine incorporation (% control)
180
160
140
120
100
80
60
40
20
0
0
10^{-9}
10^{-8}
10^{-7}
10^{-6}
10^{-5}
SC51322 (M)

FIGURE 49: ***Response of SMCs to Serum and Prostaglandins: Hypertrophic vs. Hyperplastic Growth.***

(A) Cell growth was measured using the MTT asaay as described in Materials and Methods (section 4.3.3). The assay was conducted every 24 h over 4 days after addition of serum (10% v/v FBS) or prostaglandins (PGE_2, PGI_2 and $PGF_{2\alpha}$) (10^{-6} M) to quiescent SMCs. The data are presented as the mean ± SE of at least three separate experiments conducted in triplicate. (B) Cell number was assessed using a Coulter Counter. Quiescent SMCs were stimulated with serum (10 % v/v FBS) or PGE_2 (10^{-6} M), and cell number quantified 48 h and 96 h after treatment as described in section 4.3.4. One of two experiments is shown, both of which exhibited a similar response. Each data point was counted in triplicate from samples prepared in duplicate. Comparisons were made relative to untreated cells using the Student's t-test (*, $p < 0.05$).

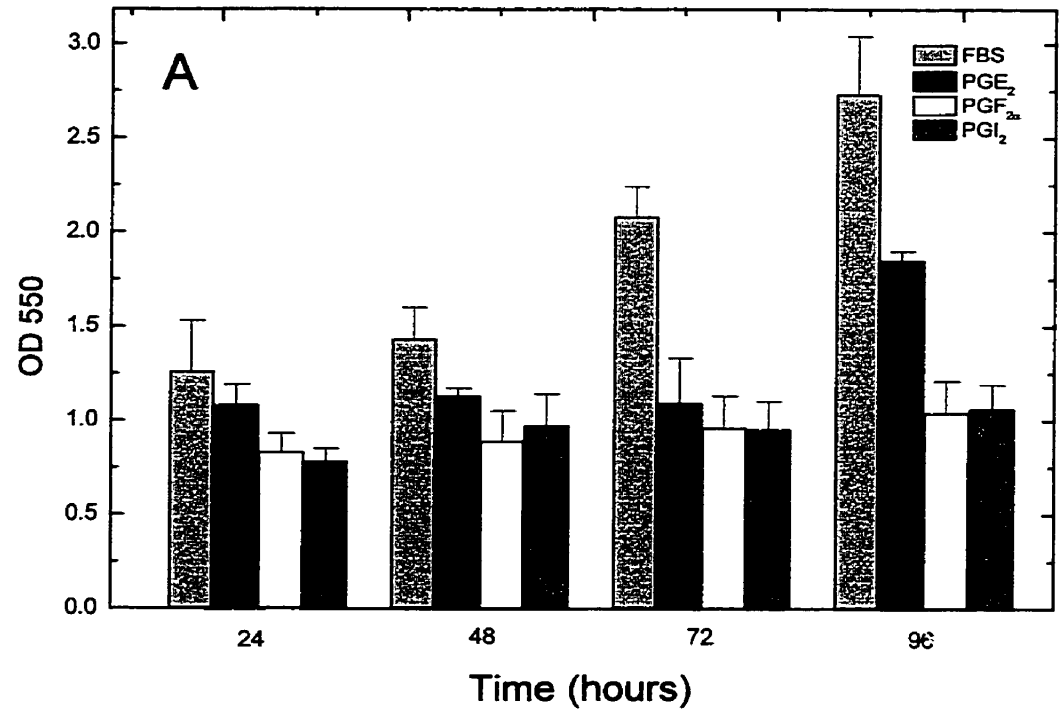
A
FBS
PGE2
PGF2α
PGI2
OD 550
3.0
2.5
2.0
1.5
1.0
0.5
0.0
24
48
72
96
Time (hours)

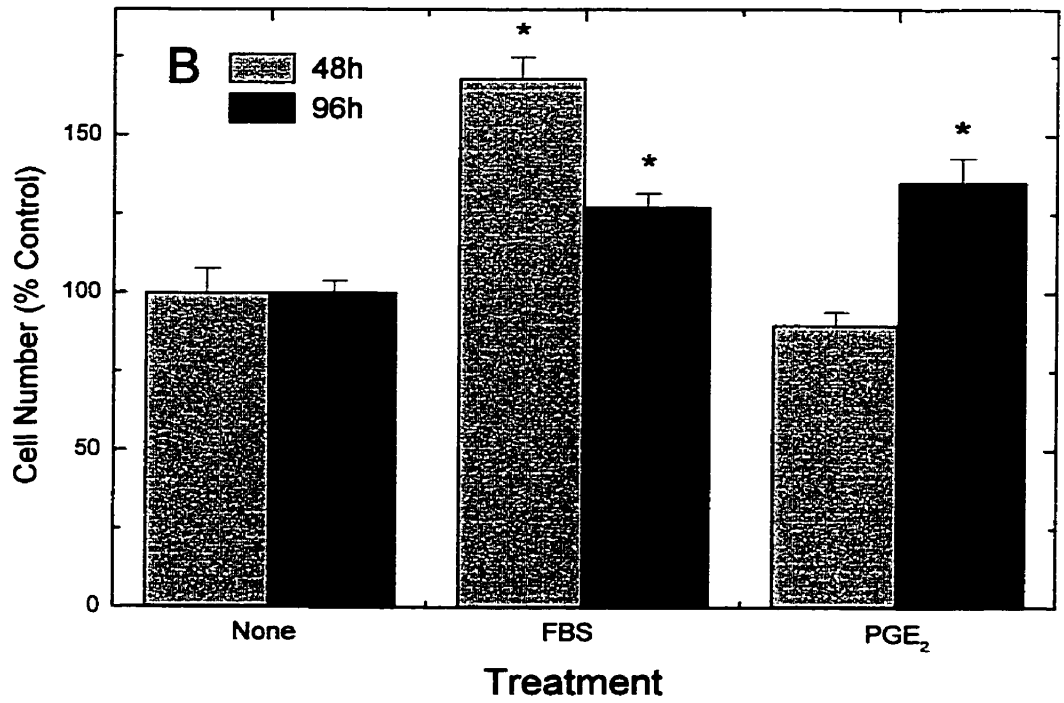
B
48h
96h
Cell Number (% Control)
150
100
50
0
*
*
*
None
FBS
PGE2
Treatment

FIGURE 50: ***Response of SMCs to Serum and Prostaglandins: Other Growth Parameters.***

(A to C) Quiescent SMCs were treated with either serum (10 % v/v FBS) or PGE_2 (10^{-6} M) for 48 h. Immunocytochemistry was used to monitor PCNA (proliferating cell nuclear antigen) expression as described in section 4.7.3. (A) no treatment, (B) 48 h FBS treatment and (C) 48 h PGE_2 treatment. Representative micrographs are shown. Magnification: 140×. (D to F) Quiescent SMCs were treated for 72 h with either serum (10 % v/v FBS) or PGE_2 (10^{-6} M). Before harvest, cells were pulse-labelled for 2 h with 50 μM BrdU. Immunocytochemistry was employed to visualize BrdU incorporation as described in section 4.7.3. (D) no treatment, (E) 72 h FBS treatment and (F) 72 h PGE_2 treatment. Representative micrographs are shown. Magnification: 140×. These results were confirmed in two and three independent experiments, respectively, using different SMC isolations, all of which exhibited similar patterns of response.

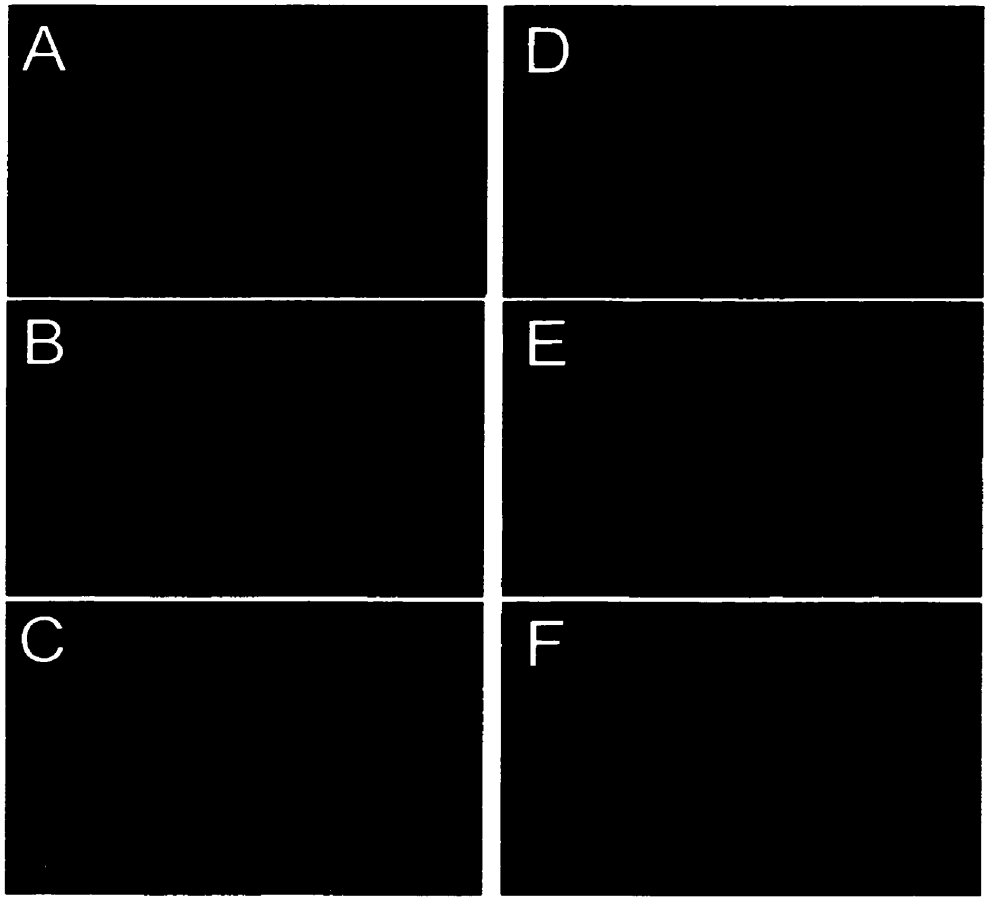
A
D
B
E
C
F

Immediate early genes (eg. c-*fos*) are activated upon stimulation of cells with growth promoting agents (Rivera & Greenberg 1990; Woodgett 1989). To determine whether PGE_2 could induce c-*fos* gene expression, RT-PCR analysis of c-*fos* mRNA levels was examined over a time course of 2 h. Addition of PGE_2 to SMCs resulted in a rapid rise in c-*fos* mRNA levels that peaked at 30 min and returned to basal levels by 2 h (Figure 51). These data support the contention that PGE_2 is a positive modulator of SMC growth.

7.2.4.3 Activation of MAP kinase and p21-Ras by PGE_2

Many intracellular signaling pathways are activated upon stimulation by growth factors and tyrosine phosphorylation cascades are commonly involved (Ahn *et al.* 1992). As such, the tyrosine phosphorylation of proteins was examined after PGE_2 (10^{-6} M) stimulation. Over a time course of 8 h, PGE_2 was able to stimulate the phosphorylation of a variety of proteins, most noticeably, proteins of 125-, 85- and 42/44-kDa (Figure 52A). Moreover, immunocytochemistry revealed that after 15 min of PGE_2 (10^{-6} M) treatment there was an alteration of the pattern of tyrosine phosphorylated proteins with a greater number of membrane localized associations (Figure 52B,C). Since one of the tyrosine phosphorylated bands observed in Figure 52A correlated with the molecular mass of MAP kinase, it was of interest to determine whether MAP kinase was activated by PGE_2. Moreover, MAP kinase is one of the signaling molecules associated with growth events (Adam *et al.* 1995; Cowley *et al.* 1994; Force & Bonventre 1998; Khalil & Morgan 1993; Klemke *et al.* 1997; Mansour *et al.* 1994; Nelson *et al.* 1998). With an in gel MAP kinase activity assay, it was observed that PGE_2 transiently stimulates MAP kinase over a time course of 20 min, with peak activation occurring between 5-10 min (Figure 53A). A parallel study was conducted using FBS as the stimulus, and a similar pattern of MAP kinase activation was observed (Figure 53B), although the magnitude of activation was

FIGURE 51: ***RT-PCR Analysis of PGE_2-mediated c-fos Gene Expression.***

Quiescent SMCs were treated with PGE_2 (10^{-6} M). RNA was extracted at 0, 15, 30, 60 and 120 min after PGE_2 addition and c-*fos* mRNA levels monitored by RT-PCR. GAPDH expression was assessed simultaneously and served to control for RNA loading. Molecular mass markers (φX174 and DNA marker VI) were used to confirm the size of the PCR products. One representative agarose gel is shown. These results were reproduced in three independent experiments using different SMC isolations. Appropriate control reactions were run independently (refer to section 4.10.3).

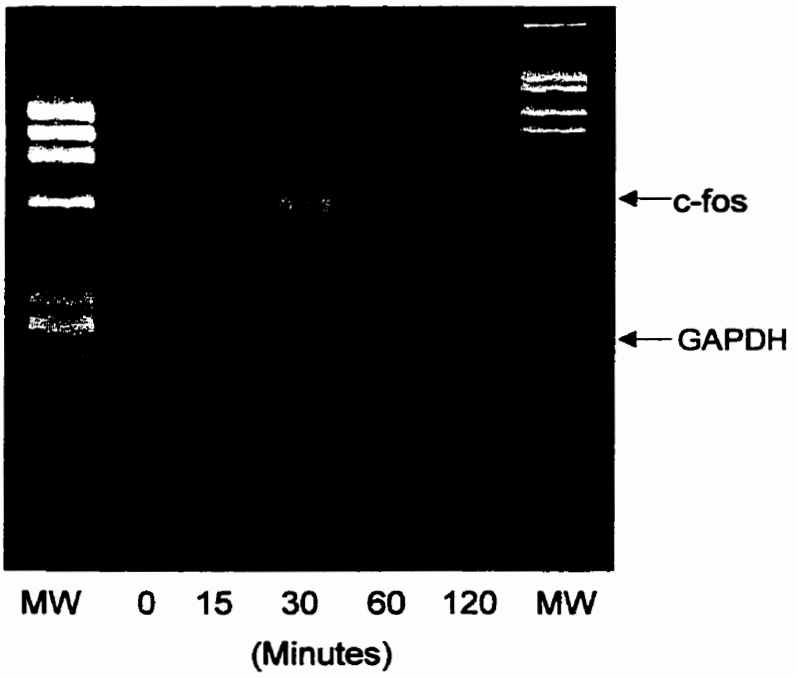
c-fos
GAPDH
MW
0
15
30
60
120
MW
(Minutes)

FIGURE 52: ***Tyrosine Phosphorylation Stimulated by Prostaglandin E_2.***

(A) Quiescent SMCs were treated with PGE_2 (10^{-6} M) over a time course of 8 h, and extracts prepared according to section 4.8.3. The samples were subjected to SDS/PAGE and Western blot analysis with an antibody specific for phosphorylated tyrosine (PY20) (diluted 1:1000). Proteins were visualized with the ECL chemiluminescent detection system. Molecular mass markers used to identify the proteins are shown. The results were reproduced in three independent experiments using different SMC isolations. (B, C) Quiescent SMCs were treated for PGE_2 (10^{-6} M) for 15 min, and immunocytochemistry was used to monitor SM α-actin (red) (diluted 1:400) and PY20 (green) (diluted 1:100) localization. (B) control SMCs with no treatment, (C) SMCs with PGE_2 treatment . Representative fluorescence micrographs are shown. Magnification: 122×.

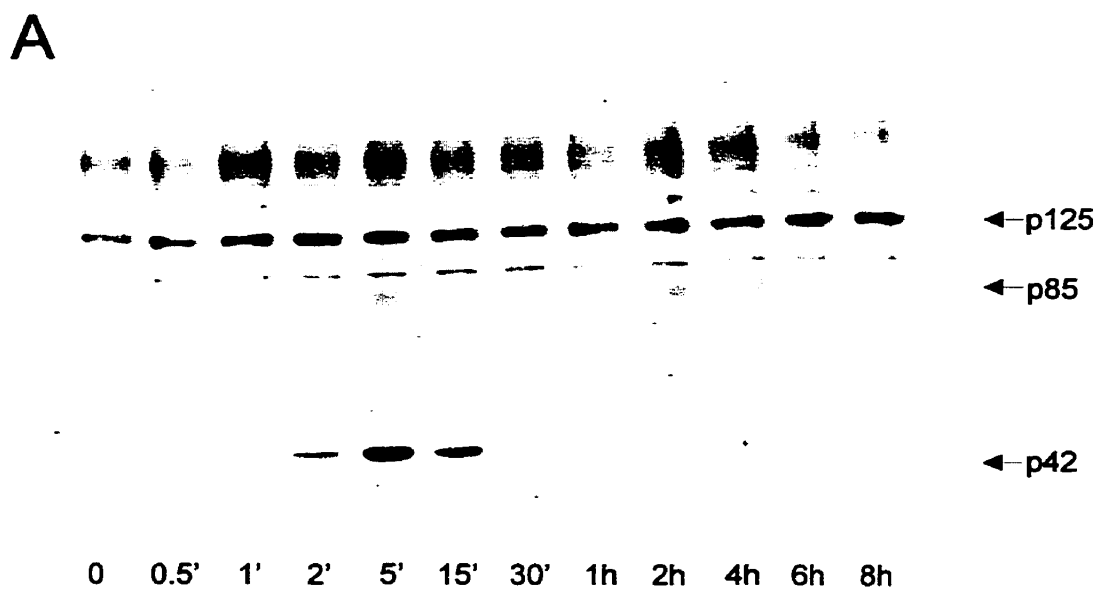
A
p125
p85
p42
0
0.5'
1'
2'
5'
15'
30'
1h
2h
4h
6h
8h

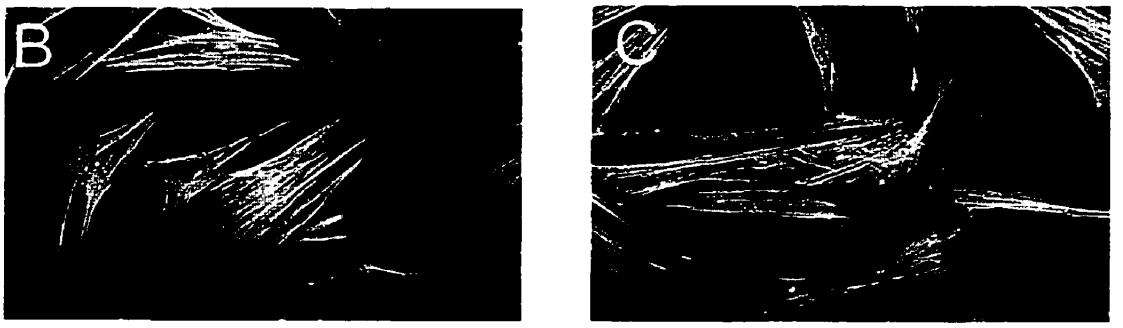
B
C

FIGURE 53: ***Activation of MAP Kinase by Prostaglandins and Serum.***

MAP kinase activity was measured by activity gel assay over a 20 min period after treatment with PGE_2 (10^{-6} M) (A) or serum (10% v/v FBS) (B). Specific phosphorylation of myelin basic protein by $p42^{MAPK}$ and $p44^{MAPK}$ is shown. One of three independent experiments (each employing a different SMC preparation) is presented, all of which exhibited a similar response. (C) MAP kinase activity was measured by activity gel assay in cell extracts prepared 6 min after stimulation with FBS (10% v/v), PGI_2, $PGF_{2\alpha}$ or PGE_2 (10^{-6} M). Band intensity was determined by densitometry and the data plotted for the 42-kDa band. Similar results were obtained in three independent experiments.

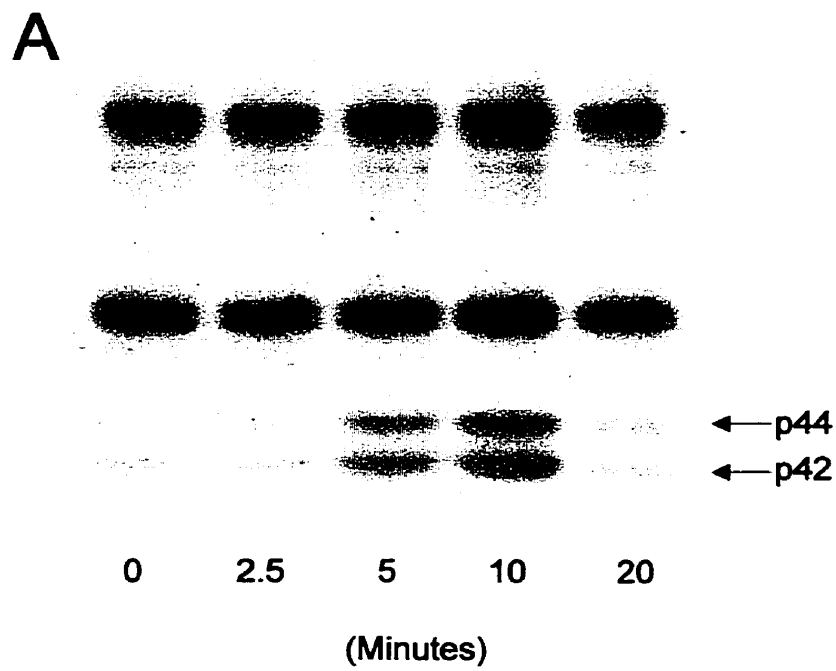
A
p44
p42
0
2.5
5
10
20
(Minutes)

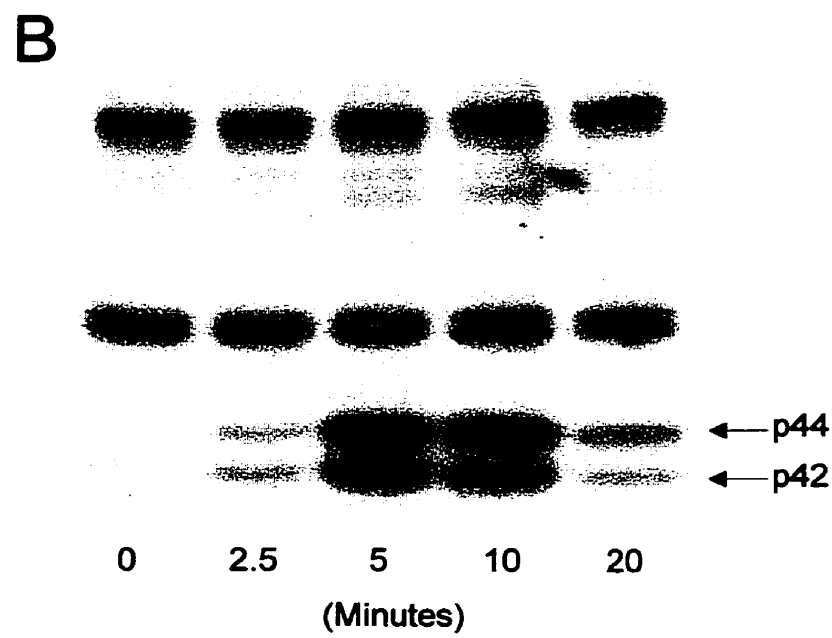
B
p44
p42
0
2.5
5
10
20
(Minutes)

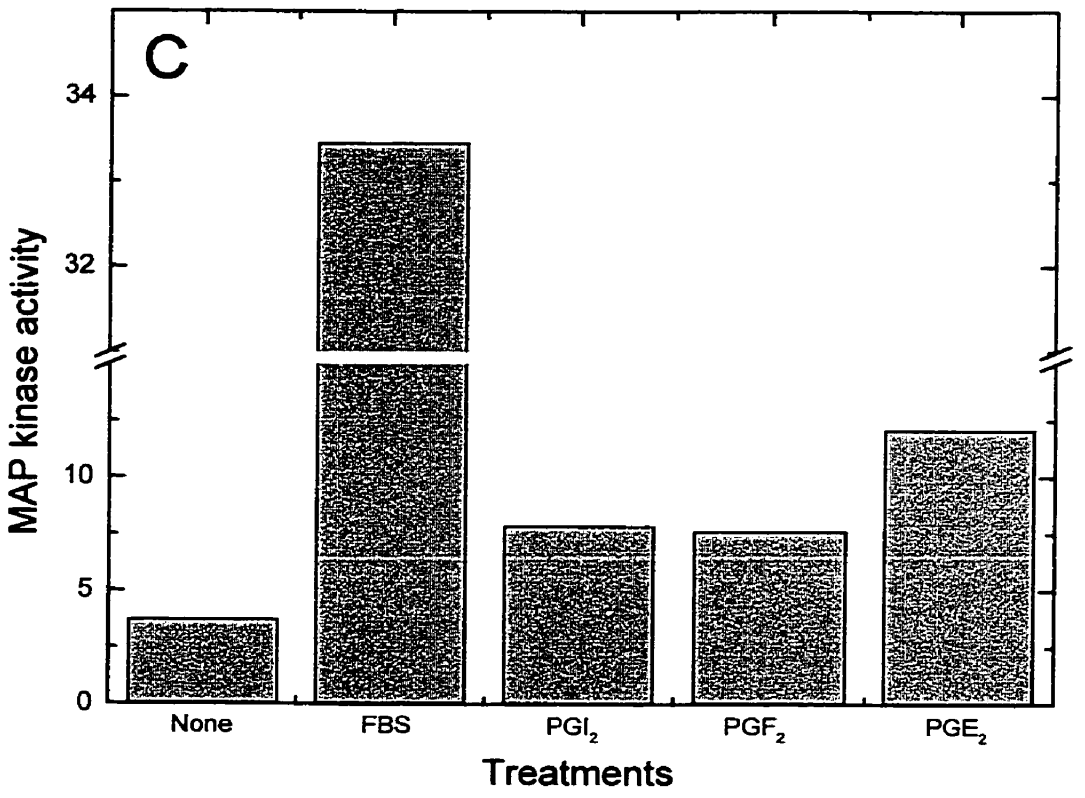
C
34
32
10
5
0
MAP kinase activity
None
FBS
PGI2
PGF2
PGE2
Treatments

more intense. Interestingly, other PG species tested with respect to MAP kinase activation, PGI_2 and $PGF_{2\alpha}$, were also capable of stimulating MAP kinase activation (Figure 53C), and yet neither of these PGs was capable of significantly increasing either RNA or DNA synthesis (Figure 46 and data not shown). These data would suggest that MAP kinase activation, although potentially linked to growth in the case of PGE_2, does not necessarily lead to growth. This is not surprising since activation of MAP kinase is also required for other events, such as stress and contractility, that are independent of cell growth (Adam *et al.* 1995; Force & Bonventre 1998; Khalil & Morgan 1993; Klemke *et al.* 1997; Nelson *et al.* 1998; Watts 1998).

As a result of the above data, it was necessary to determine if the PGE_2-stimulated MAP kinase activation correlated with SMC growth. An inhibitor of MEK (MAP kinase kinase), PD98059, was added to SMCs 10 min prior to PGE_2 stimulation. PD98059 (10^{-6} M) decreased PGE_2-mediated cell growth as measured by RNA and DNA synthesis (Figure 54). These results confirm the supposition that MAP kinase activation is essential for PGE_2-mediated SMC growth.

A second mediator of intracellular signaling that is relevant to growth of a variety of cell types is p21-Ras (Bos 1995; Maruta & Burgess 1994). This cytosolic GTP-binding protein was also of interest considering the link to mono(ADP-ribosyl)ation. The contribution of p21-Ras to SMC growth was defined by correlating p21-Ras activation, specifically an increase in bound GTP, with mitogen stimulation. [^{32}P]Orthophosphate labelled SMCs were stimulated with PGE_2 (10^{-6} M), PGI_2 (10^{-6} M) and TxA_2 (10^{-7} M), and cell lysates were immunoprecipitated with a specific antibody to Ras. The ratio of GTP:GDP in the immunoprecipitates was calculated after TLC separation. The results of this assay are presented in Table 3, and show that p21-Ras is not activated upon PGE_2 stimulation, and neither is it activated by the other prostanoids PGI_2 or TxA_2. These data

FIGURE 54: ***Inhibition of Cell Proliferation by the MEK Inhibitor PD98059.***

PGE_2 (10^{-6} M)-stimulated RNA ([^{3}H]uridine) and DNA ([^{3}H]thymidine) synthesis were measured in the presence of the MEK inhibitor PD98059 (10^{-6} M). Each data point represents the mean ± SE of at least three individual experiments conducted in triplicate. Values are presented relative to an untreated control which was set to 100%. These results were confirmed in two independent experiments using different SMC isolations.

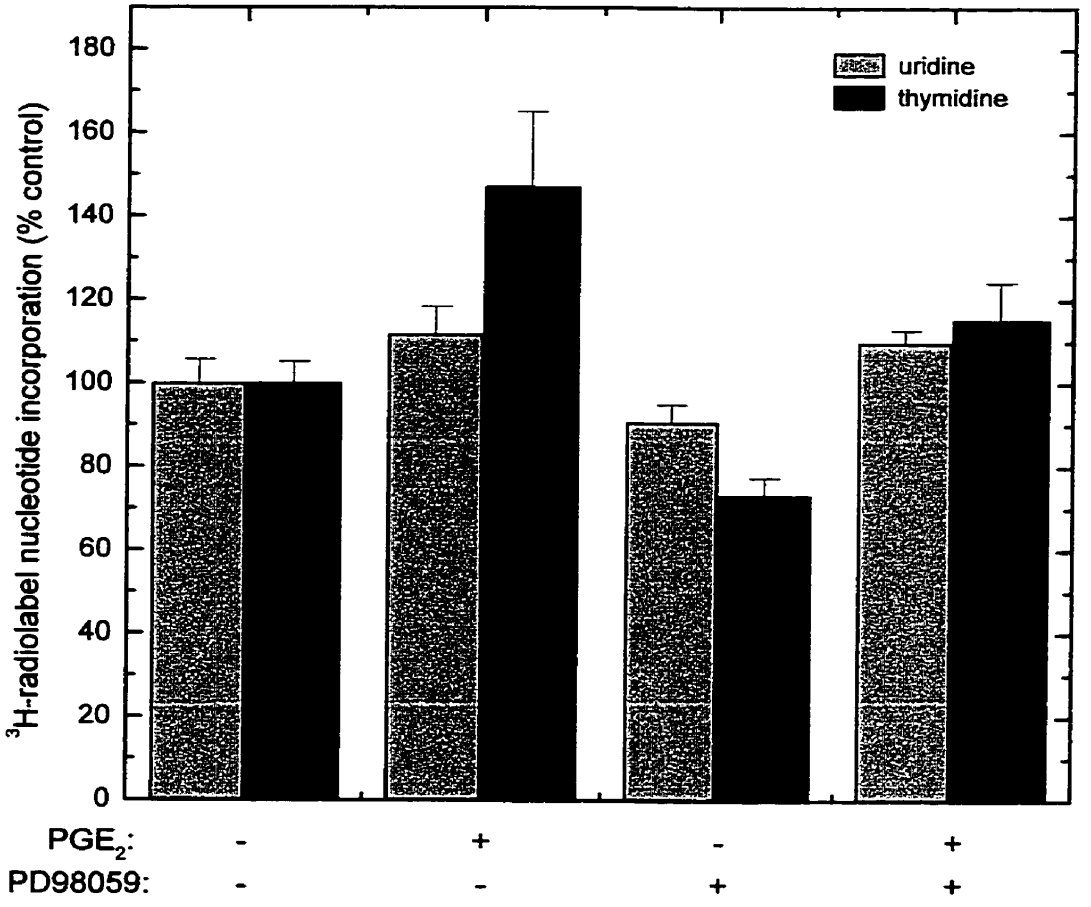
uridine
thymidine
^{3}H-radiolabel nucleotide incorporation (% control)
0
20
40
60
80
100
120
140
160
180
PGE$_2$: - + - +
PD98059: - - + +

TABLE 3: ***Modulation of p21-Ras Activity in SMCs by Prostaglandins.***

p21-Ras activity was measured in quiescent SMCs cells after PGE_2 (10^{-6} M), PGI_2, (10^{-6} M) and TxA_2 (10^{-7} M) stimulation, and MIBG (50 μM for 15 min) pretreatment followed by PGE_2 (10^{-6} M) stimulation. Cellular phosphate pools were labelled with [^{32}P]orthophosphate, treated for 15 min with prostaglandin and p21-Ras bound GTP and GDP pools assessed by TLC analysis after immunoprecipitation as described in section 4.9.5. Radiolabelled GTP and GDP were cut out from each lane and quantified by liquid scintillation counting. Data from one independent experiment are presented.

Treatment	GDP	GTP	% GTP
		cpm	
Control	38.25	44.24	53.6
PGE_2	38.81	46.02	54.2
TxA_2	47.87	44.11	48.0
PGI_2	64.06	91.04	58.7
MIBG+PGE_2	35.7	41.98	54.0

indicate that p21-Ras may not be an important component of PGE_2-mediated SMC growth.

7.2.4.4 Involvement of PI3-kinase in PGE_2-dependent SMC growth

The final transducer of intracellular signaling that was examined in relation to PGE_2-mediated SMC growth was PI3-kinase. This enzyme has been established as an important component of AngII-mediated SMC growth (Saward & Zahradka 1997a). Since PGs may be important mediators of AngII-dependent cell growth (Saward 2000), exploration of the PI3-kinase pathway was considered relevant. Furthermore, the membrane receptor system for AngII and PGs is similar (i.e. G protein-coupled), and both compounds are able to elicit cell growth responses in SMCs. In addition, PI3-kinase is an important component of G protein-coupled receptor activation of MAP kinase (Della Rocca *et al.* 1997; Force & Bonventre 1998; Lopez-Ilasaca *et al.* 1997). An examination of the importance of this signal molecule was initiated by monitoring RNA and DNA synthesis after a 10 min pretreatment of SMCs with specific inhibitors of PI3-kinase, LY294002 (LY) and wortmannin (WM), followed by addition of PGE_2. Both LY and WM (10^{-10} to 10^{-5} M) inhibited RNA and DNA synthesis stimulated by PGE_2, with increasing concentrations of LY and WM having a significantly greater inhibitory effect (Figure 55A,B). These data suggest that PI3-kinase is important for PGE_2-mediated SMC growth.

To establish that PI3-kinase is indeed activated in SMCs by PGE_2, PI3-kinase assays were carried out, both *in vivo* and *in vitro*. The *in vivo* assay involved monitoring PIP pools after [^{32}P]orthophosphate labeling of SMCs and subsequent stimulation with PG compounds. A spectrum of PGs were assessed in this manner and included PGE_2 (10^{-6} M), TxA_2 (10^{-7} M), PGI_2 (10^{-6} M) and $PGF_{2\alpha}$ (10^{-6} M). All of the PGs tested were capable of increasing PIP_3 production compared to control, untreated cells extracts

FIGURE 55: ***Involvement of PI3-Kinase in PGE_2-mediated SMC Growth.***

PGE_2 (10^{-6} M)-stimulated RNA (A) and DNA (B) synthesis was measured in the presence of varying concentrations of the PI3-kinase inhibitors wortmannin (WM) and LY294002 (LY) (10^{-10} to 10^{-5} M). The incorporation of [^{3}H]uridine (6 h incubation) and [^{3}H]thymidine (48 h incubation) into trichloroacetate-precipitable material after addition of both agents was measured as described in section 4.3.1. Values are presented relative to maximal stimulation with PGE_2 (set to 100%). The data are presented as the mean ± SE of experiments conducted in triplicate. These results were confirmed in three independent experiments using different SMC isolations.

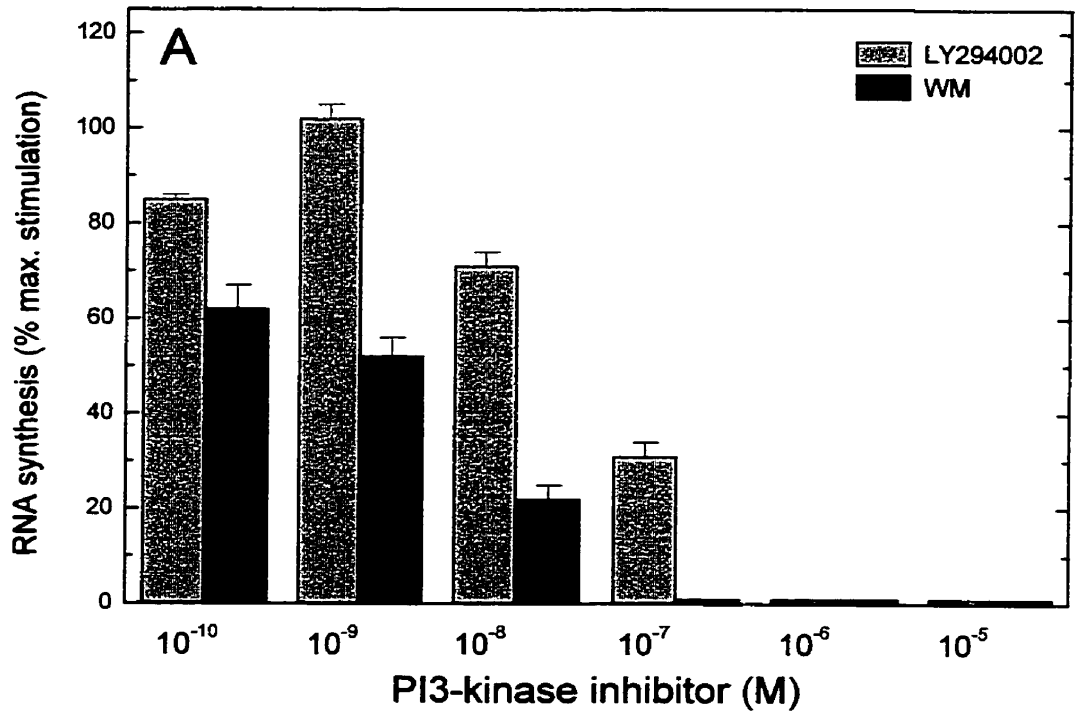
A
LY294002
WM
RNA synthesis (% max. stimulation)
120
100
80
60
40
20
0
10-10
10-9
10-8
10-7
10-6
10-5
PI3-kinase inhibitor (M)

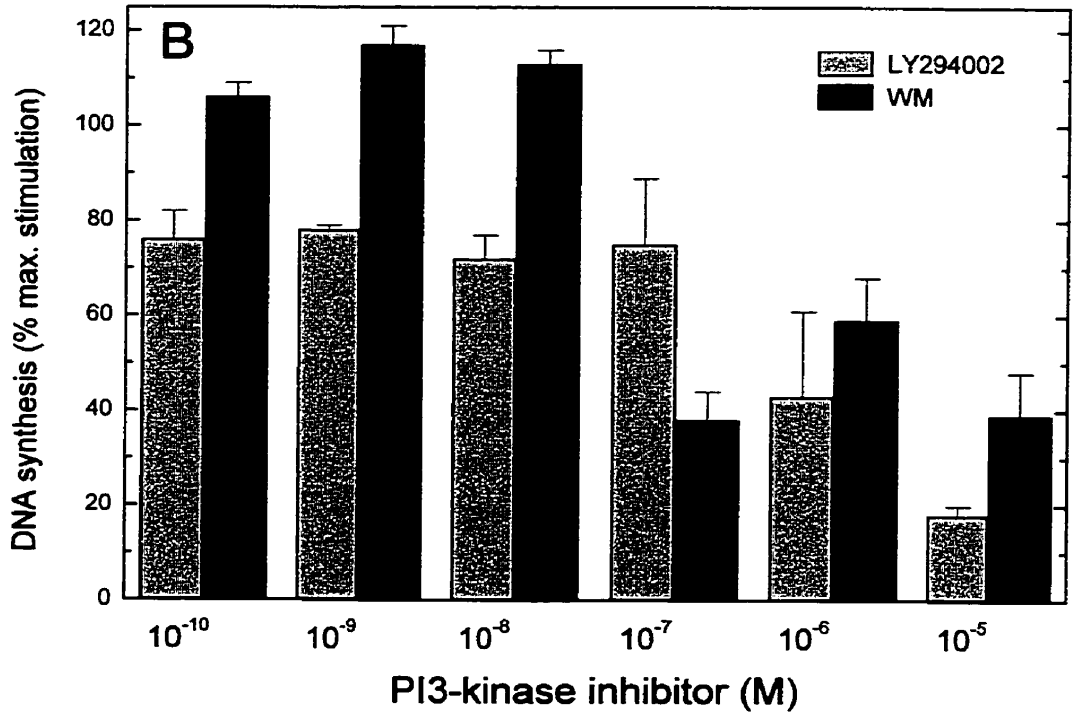
B
LY294002
WM
DNA synthesis (% max. stimulation)
120
100
80
60
40
20
0
10-10
10-9
10-8
10-7
10-6
10-5
PI3-kinase inhibitor (M)

(Figure 56A). To assess the specificity of the PI3-kinase response and to verify that wortmannin was indeed inhibiting PI3-kinase, the activation of PI3-kinase by PGE_2 was tested in the presence of wortmannin (Figure 56B). It was observed that wortmannin inhibited PIP_3 generation induced by PGE_2 (Figure 56B). LY294002 had a similar effect (data not shown). An *in vitro* PI3-kinase assay was then employed to confirm the activation of PI3-kinase by PGs. In this assay the PI3-kinase complex was immunoprecipitated with a specific antibody to p85, the regulatory subunit of PI3-kinase and phosphorylation of PI and PIP_2 was identified by TLC. This experiment demonstrated that PGE_2 (10^{-6} M), TxA_2 (10^{-7} M), and $PGF_{2\alpha}$ (10^{-6} M) increased the production of PIP_3 (Figure 57), albeit to different degrees, and that PGE_2 (10^{-10} to 10^{-6} M) increased the production of PIP_3 with higher concentrations having the greatest effect (Figure 58). These data clearly established that PI3-kinase is activated by PGE_2.

The temporal and spatial positioning of PI3-kinase with respect to other signaling molecules and endpoints activated by PGE_2 in SMCs was evaluated with the PI3-kinase inhibitors, LY294002 and wortmannin. Activation of MAP kinase by PGE_2 was diminished by either LY294002 or wortmannin, indicating that PI3-kinase activation is an event that occurs before MAP kinase (Figure 59). Furthermore, RT-PCR analysis of c-*fos* mRNA levels revealed that both LY294002 and wortmannin abrogated PGE_2-mediated c-*fos* expression (Figure 60), suggesting that activation of PI3-kinase is an important step in the expression of early growth response genes. Overall, these data confirm that PI3-kinase is an important element in PGE_2-mediated SMC growth.

7.2.5 Discussion

This study has demonstrated that PGE_2 has growth stimulatory effects in porcine SMCs. PGE_2 was chosen for study because it is released on stimulation or damage of

FIGURE 56: ***Activation of PI3-Kinase by Prostaglandins: In vivo Assay.***

Phosphate pools in quiescent SMCs were labelled with 200 μCi [^{32}P]orthophosphate for 4 h prior to stimulation for 15 min with various prostaglandins (PGE_2, PGI_2, $PGF_{2\alpha}$ at 10^{-6} M and TxA_2 at 10^{-7} M) and PGE_2 ± wortmannin (10^{-5} M). Phosphoinositides were extracted from the cells and the phosphorylated forms of phosphoinositol were resolved by thin layer chromatography (TLC) as described in Materials and Methods (section 4.9.3). (A) A representative autoradiogram of a TLC plate is shown from an experiment examining the effect of prostaglandins on PI3-kinase activation. PIP, PIP_2 and PIP_3 are indicated. These results were confirmed in three independent experiments. (B) Densitometric analysis of an autoradiogram from separate experiments employing PGE_2 ± wortmannin treatment was used to provide a graphical representation of PIP_3 formation. One of two independent experiments is shown, both of which exhibited a similar response.

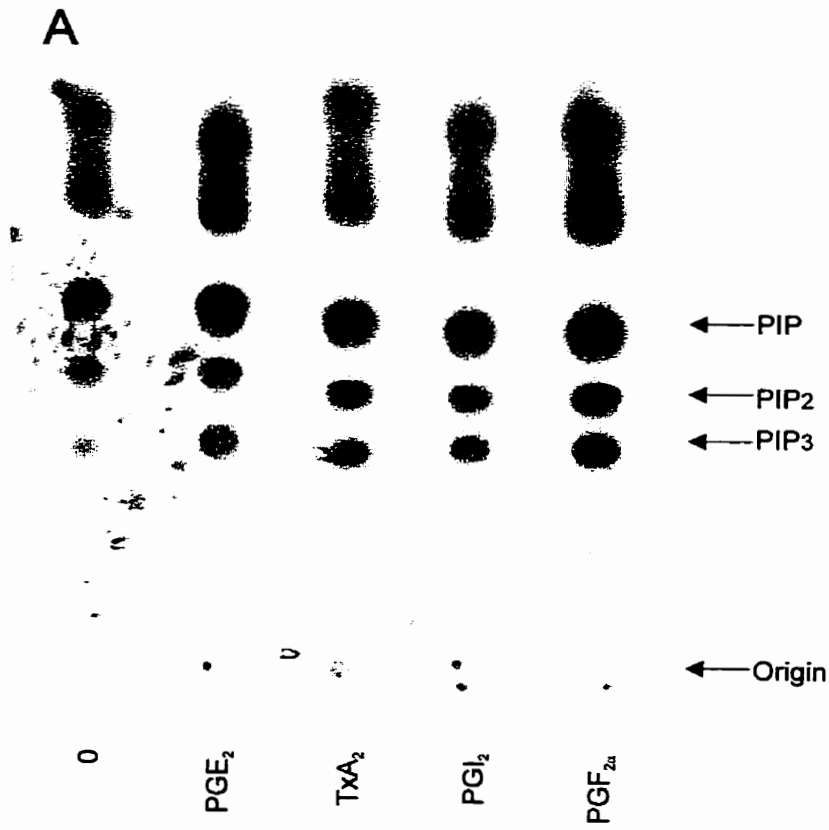
A
PIP
PIP2
PIP3
Origin
0
PGE2
TxA2
PGI2
PGF2a

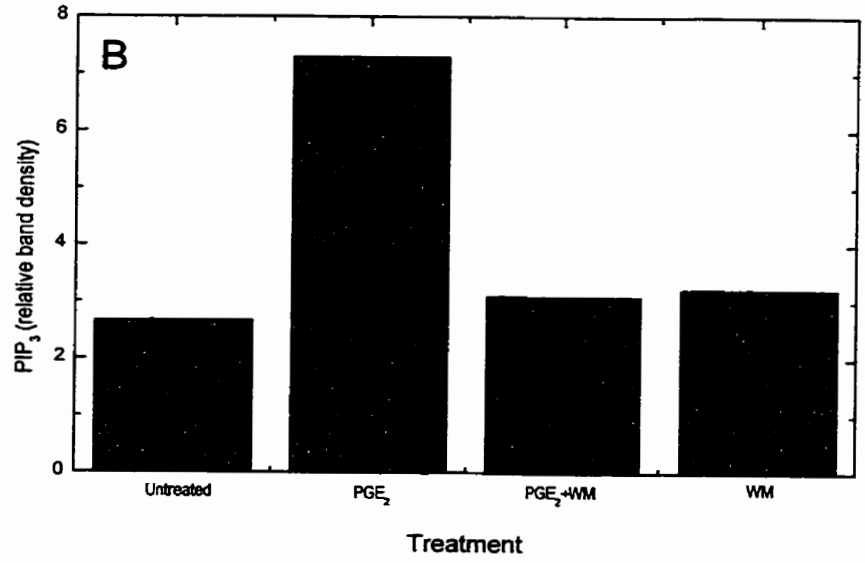
B
PIP3 (relative band density)
0
2
4
6
8
Untreated
PGE2
PGE2+WM
WM
Treatment

FIGURE 57: ***Activation of PI3-Kinase by Prostaglandins: In vitro Assay.***

Analysis of PI3-kinase activity *in vitro* following immunoprecipitation. Lysates of SMCs were prepared following prostaglandin treatment and were immunoprecipitated with anti-p85 antibody and assayed for PI3-kinase-dependent phosphorylation of PI and PIP_2 as described in Materials and Methods (section 4.9.4). Treatments included PGE_2 (10^{-6} M), $PGF_{2\alpha}$ (10^{-6} M), PGI_2 (10^{-6} M) and TxA_2 (10^{-7} M). (A) A representative autoradiogram of a TLC plate is shown. Positions of PIP and PIP_3 are indicated. These results were confirmed in two independent experiments. (B) Graphical representation of PIP_3 formation observed in (A) after densitometric analysis of the autoradiogram.

A

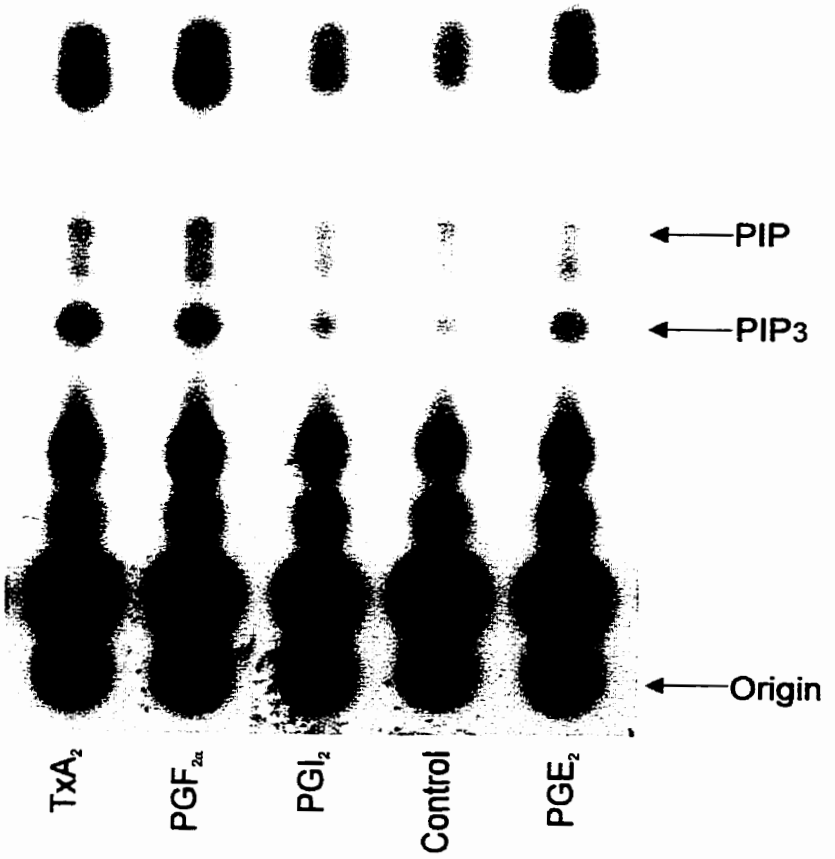
PIP
PIP3
Origin
TxA2
PGF2α
PGI2
Control
PGE2

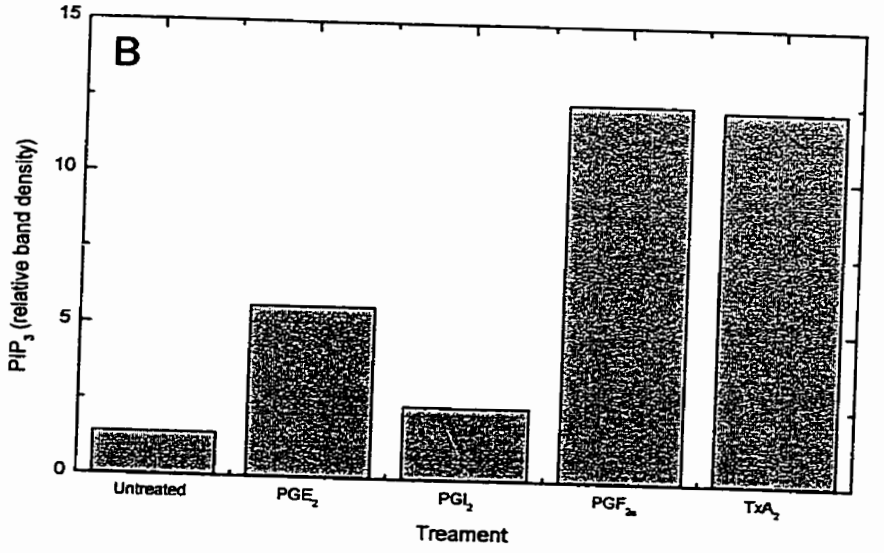
B
15
10
5
0
PIP3 (relative band density)
Untreated
PGE2
PGI2
PGF2α
TxA2
Treament

FIGURE 58: ***Activation of PI3-Kinase by Prostaglandins: Concentration Effect of Prostaglandin E_2.***

Analysis of PI3-kinase activity *in vitro* following immunoprecipitation. Lysates of SMCs prepared following prostaglandin treatment were immunoprecipitated with anti-p85 antibody and assayed for PI3-kinase-dependent phosphorylation of PI and PIP_2 as described in Materials and Methods (section 4.9.4). Treatment was PGE_2 (10^{-10} to 10^{-6} M). (A) A representative autoradiogram of a TLC plate is shown. Positions of PIP and PIP_3 are indicated. These results were confirmed in two independent experiments. (B) Graphical representation of PIP_3 formation observed in (A) after densitometric analysis of the autoradiogram.

A

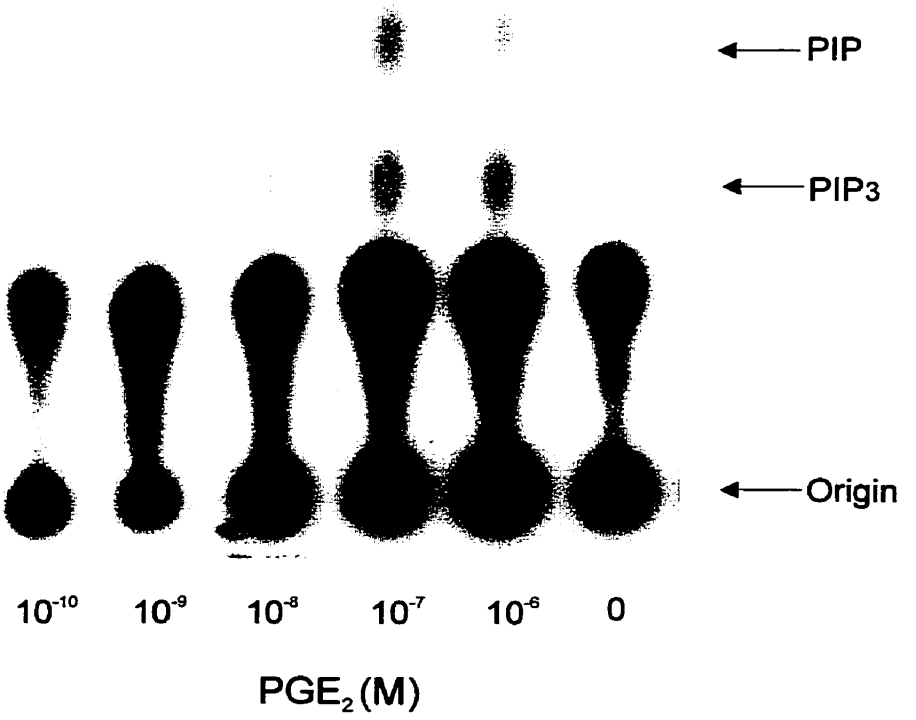
PIP
PIP3
Origin
10-10
10-9
10-8
10-7
10-6
0
PGE2 (M)

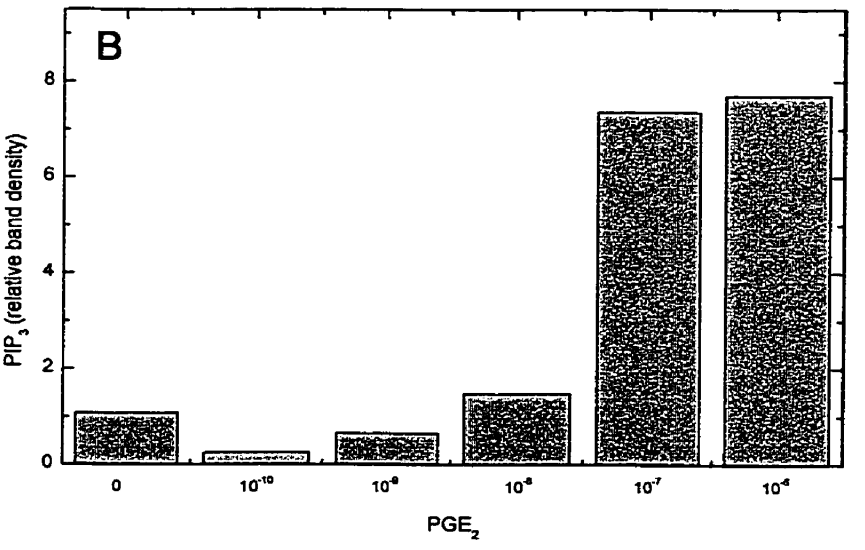
B
PIP3 (relative band density)
0
2
4
6
8
0
10-10
10-9
10-8
10-7
10-6
PGE2

FIGURE 59: ***Effect of PI3-Kinase Inhibitors on PGE_2-mediated Activation of MAP Kinase.***

MAP kinase activity was measured by activity gel assay after 6 min of stimulation with PGE_2 (10^{-6} M) and prior pretreatment (10 min) with PI3-kinase inhibitors wortmannin (WM) (10^{-5} M) or LY294002 (LY) (10^{-5} M). (A) An example of the activity gel is shown with the specific phosphorylation of myelin basic protein by $p42^{MAPK}$ and $p44^{MAPK}$ identified. (B) Band intensity was determined by densitometry and the data plotted for the combination of 42- and 44-kDa bands. One of three independent experiments is presented from different SMC isolations, all of which exhibited the same response.

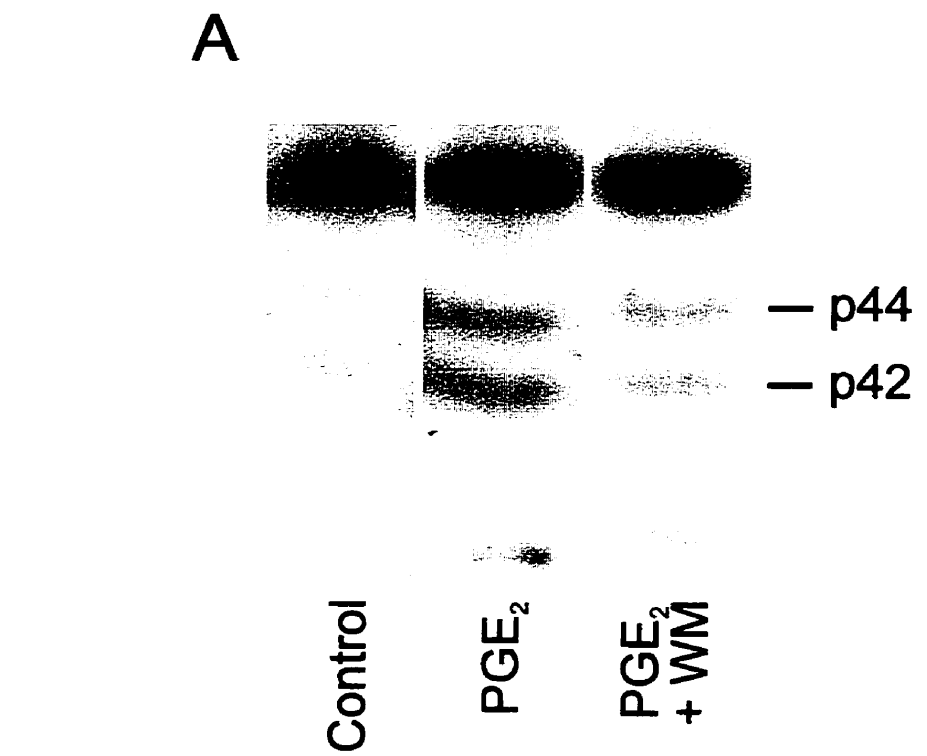
A
— p44
— p42
Control
PGE2
PGE2 + WM

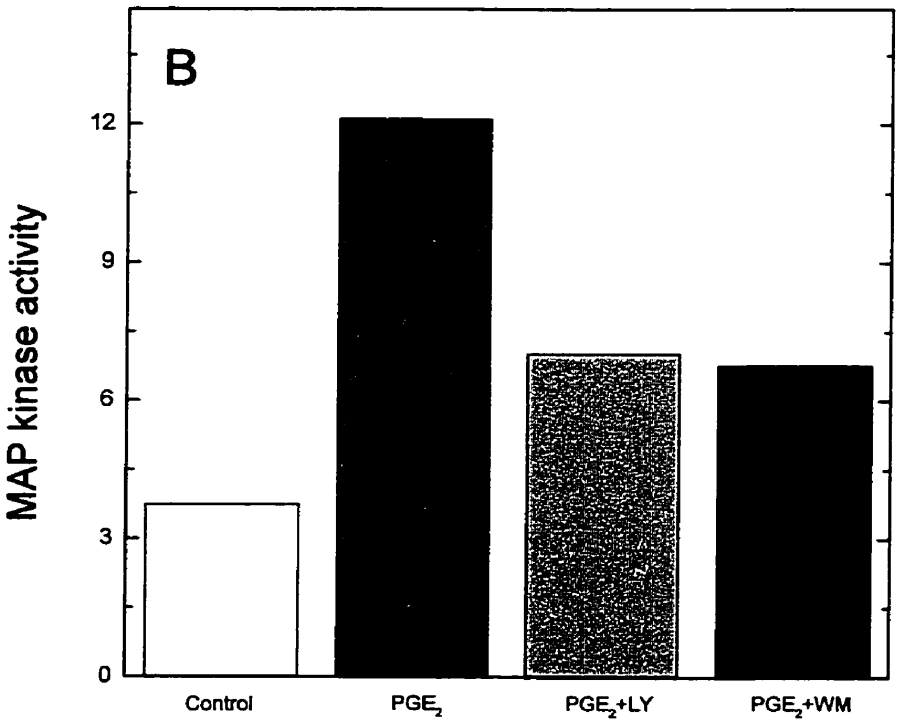
B
MAP kinase activity
0
3
6
9
12
Control
PGE2
PGE2+LY
PGE2+WM

FIGURE 60: ***Effect of PI3-Kinase Inhibitors on PGE_2-mediated Expression of c-fos.***

(A) Quiescent SMCs were pretreated for 10 min with the PI3-kinase inhibitor wortmannin (WM) (10^{-5} M) and subsequently treated with PGE_2 (10^{-6} M) for 15 min. RNA was extracted and c-*fos* gene expression assessed by RT-PCR. Molecular mass markers (φX174 and DNA Marker VI) were used to confirm the size of the PCR products. One representative agarose gel is shown. These results were confirmed in two independent experiments using different SMC isolations. (B) Band intensities from a separate experiment using the PI3-kinase inhibitor LY294002 (LY) (10^{-5} M) were quantified by densitometry and the data plotted to show the intensity of the c-*fos* band relative to treatment. One of two independent experiments is shown, both of which exhibited a similar response.

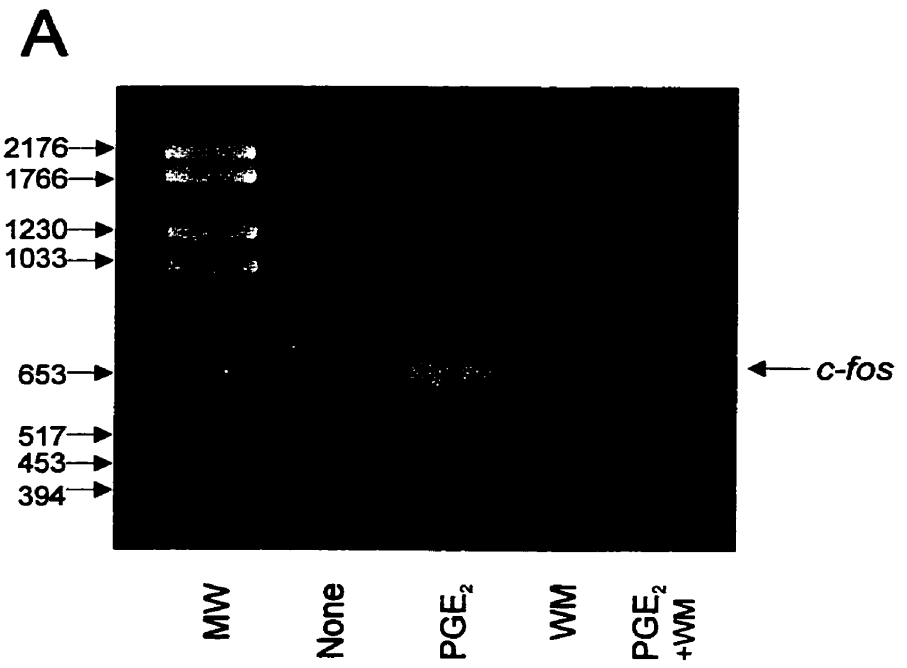
A
2176
1766
1230
1033
653
517
453
394
c-fos
MW
None
PGE2
WM
PGE2 +WM

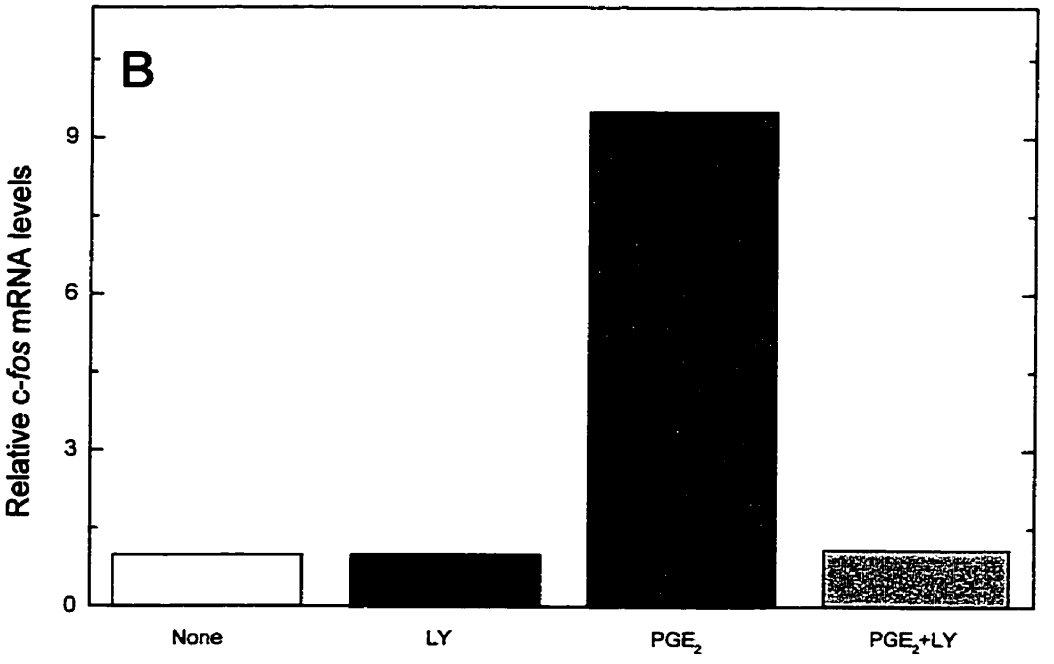
B
Relative c-fos mRNA levels
0
3
6
9
None
LY
PGE2
PGE2+LY

endothelial cells, vascular SMCs and tissue macrophages, and can accumulate during the inflammatory responses that occur following injury to the vasculature (Kennedy *et al.* 1982; Leslie & Watkins 1985; Revtyak *et al.* 1987; Wendling & Harakal 1991). Furthermore, this laboratory and others have demonstrated that PGE_2 levels are increased after stimulation of SMCs and other cells with AngII (Ohnaka *et al.* 2000; unpublished observations from Saward, Yau, Thomas & Zahradka; Saward *et al.* submitted) and PDGF (Graves *et al.* 1996; Weksler 1987), both of which have known migratory and proliferative effects on SMCs, and both of which have been implicated in the formation of a neointimal lesion after vascular injury (Casterella & Teirstein 1999; Cercek *et al.* 1991; Liu *et al.* 1989; Wilson *et al.* 1999).

Prostanoids are potentially important mediators of normal vascular healing or abnormal vascular responses following vascular damage (i.e. neointimal thickening following to balloon injury). Schror & Weber (1997) have postulated that some species of PGs are bimodal in nature, having both the ability to stimulate SMCs to enter the cell cycle and divide in response to tissue injury in order to facilitate tissue repair, and the ability to prevent uncontrolled growth of SMCs by interfering with the progression of cells through the cell cycle, especially in S phase. This hypothesis is certainly borne out by the work of Owen (1986) who demonstrated that the effect of PGE_1 on SMCs is dependent on the phase of the cell cycle when it is added. In quiescent cells, PGE_1 enhanced DNA synthesis, while in growing cells PGE_1 inhibited cell proliferation (DNA synthesis). That particular study suggested that in growth-arrested SMCs (such as would be found in the normal vasculature), PGE_1 may have the ability to stimulate DNA synthesis (eg. during a possible repair procedure after injury), whereas in growing vascular SMCs (as would be seen under conditions of atherosclerotic plaque formation or after activation of SMCs by injury) PGE_1 can function as an inhibitor of DNA synthesis.

The studies reported here show PGE_2 also exhibits growth state-dependent effects on SMCs, thus supporting and extending the hypothesis postulated by Schror & Weber (1997). When PGE_2 was added to SMCs primed with 1% FBS, PGE_2 was able to inhibit the uptake of [^{3}H]thymidine, an indicator of the rate of DNA synthesis (Figure 46C). In contrast, PGE_2 added alone to quiescent SMCs stimulated RNA and DNA synthesis (Figure 46A,B). To support the above finding related to DNA synthesis, PGE_2 was also capable of stimulating PCNA expression, BrdU incorporation, increased c-*fos* mRNA levels and increases in cell number (Figures 49, 50, 51), all indications of cells undergoing proliferation. However, only a subpopulation of SMCs appeared to respond to PGE_2 based on the observations from BrdU incorporation and PCNA immunostaining (Figure 50). This would certainly account for the restricted mitogenic potential of PGE_2 in comparison to FBS (Figure 49). Whether the SMCs responsive to PGE_2 represents a distinct subpopulation of SMCs remains to be determined. In light of the contrasting reports in the literature concerning the mode of regulation of SMC proliferation by PGs of the E family, it is interesting to note that the majority who reported an inhibitory effect employed $PGE_{1/2}$ in conjunction with a stimulator of growth (Fan *et al.* 1997; Florio *et al.* 1994; Hayashi *et al.* 1992; Johnson *et al.* 1995; Loesberg *et al.* 1985; Nilsson & Olsson 1984), while those who saw a stimulatory effect, added $PGE_{1/2}$ alone (Owen 1986; Pasricha *et al.* 1992). Only one publication has to this point examined SMCs in both growth states (Owen 1986). Thus, although much of the work appears to be contradictory and somewhat controversial, the findings observed here support evidence for a bimodal effect by PG's of the E family that is dependent on SMC growth status. The relevance of PGE_2 to intimal lesion formation may therefore be two-fold: i) during the course of intimal lesion formation, PGE_2 will act first to stimulate tissue repair, and ii) following activation of SMCs and/or completion of repair, PGE_2 inhibits cell cycle re-entry. Thus,

restenosis may occur in those individuals where PGE_2 does not inhibit SMC proliferation and consequently a much thickened neointima will form. Alternatively, the bifunctional effects of PGE_2 could be the result of the differential expression and function of PGE_2 receptors that may be found on populations and subpopulation of SMCs. This possibility remains to be explored.

PGE_2 receptors belong to the class of G protein-coupled receptors, and 4 isotypes (EP_{1-4}) have been identified. EP receptors mediate a wide range of biological actions including contraction and relaxation of SMC, induction and inhibition of neurotransmitter release and inhibition of inflammatory mediator release. (Coleman *et al.* 1987; Coleman *et al.* 1994). Each receptor subtype is associated with a particular cellular response and the activation of unique signaling molecules and mediators (Coleman *et al.* 1987; Coleman *et al.* 1994). The EP_1 receptor is predominant in smooth muscle of the trachea, gastrointestinal tract, uterus and bladder where it mediates smooth muscle contraction (Coleman *et al.* 1987; Coleman *et al.* 1994). The EP_2 receptor is more widespread and the response more varied, however, in smooth muscle it also mediates relaxation (Coleman *et al.* 1987; Coleman *et al.* 1994). The most ubiquitous of the subtypes is the EP_3 receptor which is present in smooth muscle of gastrointestinal, uterine and vascular origin where it mediates contraction (Coleman *et al.* 1987; Coleman *et al.* 1994). EP_4 receptors appear to primarily have a vascular distribution (Coleman *et al.* 1987; Coleman *et al.* 1994; Lawrence & Jones 1992; Lydford *et al.* 1996). The signaling pathways associated with each of the receptor subtypes is varied and includes: calcium, adenylate cyclase stimulation and cAMP generation (Coleman *et al.* 1994; Creese & Denborough 1981; Hardcastle *et al.* 1982; Jumblatt & Paterson 1991; Reimer *et al.* 1992; Sonnenburg & Smith 1988). In this study, an EP_1 receptor antagonist was used to assess the specificity of the PGE_2-mediated growth response. This receptor antagonist was apparently

incapable of inhibiting PGE_2-stimulated growth (Figure 48), implying that this receptor subtype is not involved. Unfortunately, receptor antagonists for the other EP receptor isotypes were either not available, or not specific at the time that these studies were carried out. The advent of newer generations of receptor antagonists and antibodies to the receptors should help to clarify this issue.

The mechanism by which PGE_2 exerts its biological effects is likely through the activation of adenylate cyclase with elevation of cAMP levels, as shown previously by Owen (1986) for PGE_1. Transient increases in cAMP are required to initiate cell cycle (Franks *et al.* 1984), but increased cAMP during S phase has the opposite effect, thus inhibiting DNA synthesis (Franks *et al.* 1984; Owen 1986). Although activation of adenylate cyclase and levels of cAMP were not investigated in this study, the association of this signaling molecule with PGE_2 receptors (Coleman *et al.* 1994; Hardcastle *et al.* 1982; Jumblatt & Paterson 1991; Reimer *et al.* 1992; Sonnenburg & Smith 1988), and the dual nature of cAMP with respect to the cell cycle (much like $PGE_{1/2}$), strongly suggests that this may be the case. Interestingly, cAMP has been reported to inhibit SMC proliferation in response to mitogenic stimulation (Giasson *et al.* 1997), and agents that stimulate adenylate cyclase are therefore considered anti-proliferatives. However, unlike skeletal myogenesis where the dual contribution of cAMP to commitment and differentiation has been clarified (Ball *et al.* 1979; Ball & Sanwal 1980; Ball *et al.* 1980; Kovala *et al.* 1994), more in depth studies will be required to similarly characterize the role of cAMP in SMCs and the relationship to different growth stimulating agents.

Mitogenic stimulation by growth factors (eg. PDGF and AngII) results in the activation of signaling systems commonly associated with cell proliferation events. The best characterized of these signaling pathways include the Ras/MAP kinase cascade and PI3-kinase. MAP kinase is one component of a signaling pathway that encompasses a

multistep phosphorylation cascade responsible for transmiting cellular signals from cell surface receptors to specific targets in the nucleus (Seger & Krebs 1995). Interestingly, MAP kinase has been shown to be activated for smooth muscle contraction (Adam *et al.* 1995), cell differentiation (Traverse *et al.* 1992), cell attachment (Chen *et al.* 1994) and protein synthesis (Servant *et al.* 1996), and also the inhibition of cell growth/proliferation (Bornfeldt *et al.* 1997), depending on the cell type and cell status.

The studies reported here show that MAP kinase can be activated by PGE_2 (Figure 53) which, in our experimental system, is required for cell proliferation as demonstrated by use of the MEK inhibitor, PD98059 (Figure 54). This inhibitor has been used in the past to specifically inhibit the MAP kinase response in other studies involving prostanoids (Bornfeldt *et al.* 1997) and has been shown to inhibit proliferation and reverse the transformed phenotype induced by p21-Ras in specific cell lines (Dudley *et al.* 1995). Interestingly, other PGs (i.e. PGI_2, $PGF_{2\alpha}$) were also capable of eliciting an increased MAP kinase activation even though these PGs did not enhance SMC growth. This result is not surprising, however, since MAP kinase activation alone is insufficient for the proliferative response (Gire *et al.* 2000; Gire *et al.* 1999; Myers *et al.* 1994c).

MAP kinase can be activated by both Ras-dependent and Ras-independent pathways (de Vries-Smits *et al.* 1992; Thomas *et al.* 1992). Ras-dependent pathways leading to MAP kinase activation are usually mediated via activation of tyrosine kinase receptors (Egan *et al.* 1993; Seger & Krebs 1995; Treisman 1995; Treisman 1996; Zhang *et al.* 1993b). In contrast, Ras-independent pathways of MAP kinase activation are usually associated with G protein-coupled receptors (Arai & Escobedo 1996; Hedin *et al.* 1999a; Ueda *et al.* 1996; van Biesen *et al.* 1996). In either case, tyrosine phosphorylation events are activated in response to receptor ligands that activate MAP kinase pathways. Thus, a rapid elevation in tyrosine phosphorylation in response to PGE_2 is not surprising

(Figure 52). In contrast, the importance of p21-Ras to PGE_2-mediated cell proliferation cannot be predicted. Although intuitively PGE_2 should not be able to activate Ras since PGE_2 activates a G protein-coupled receptor, new evidence linking G protein-coupled receptors to MAP kinase may indicate that this signal molecule (i.e. p21-Ras) does function in some cell types (Lopez-Ilasaca 1998; Luttrell *et al.* 1995; Sugden & Clerk 1997; van Biesen *et al.* 1995; Zou *et al.* 1998). In this study, it was found that Ras was not activated by PGE_2 or any of the other prostanoids (Table 3). In this case, PKA-dependent Raf-1 activation is a plausible alternative (Wan & Huang 1998), as is PKC activation of Raf-1 (Takeda *et al.* 1999). However, neither Raf-1 nor PKC was explored in these experiments.

In addition to p21-Ras, PI3-kinase has also been linked to MAP kinase activation by G protein-coupled receptors (Hawes *et al.* 1996; Touhara *et al.* 1995). PI3-kinase is a heterodimeric protein composed of two subunits, p85 and p110, that catalyzes the synthesis of 3-phosphorylated phosphoinositides and is a key intermediate in receptor-mediated cell proliferation (Varticovski *et al.* 1994). The regulatory p85 subunit of PI3-kinase has no catalytic activity but is charged with forming complexes with activated growth factor receptors as well as signal pathway adaptor proteins such as IRS-1 and Shc (Kapeller & Cantley 1994; Sun *et al.* 1993). The catalytic p110 subunit is translocated to a membrane-associated fraction (Kelly & Ruderman 1993) and thus PI(3)P, $PI(3,4)P_2$ and $PI(3,4,5)P_3$ are formed. These lipids subsequently serve as intermediates for specific downstream signaling events that determine the cellular response to particular growth factors. One key target for $PI(3,4,5)P_3$ is PDK, a serine/threonine kinase that controls Akt phosphorylation, which in turn, regulates $p70^{S6K}$ and thus protein synthesis.

Experimental compounds that inhibit PI3-kinase include LY294002 and wortmannin (Powis *et al.* 1994; Sanchez-Margalet *et al.* 1994; Vlahos *et al.* 1994; Yano

et al. 1995). LY294002 exhibits greater specificity for PI3-kinase (Sanchez-Margalet *et al.* 1994; Vlahos *et al.* 1994; Yano *et al.* 1995), since wortmannin has also been shown to have inhibitory effects on unrelated kinases such as myosin light chain kinase (Arcaro & Wymann 1993) and phospholipases C, D and A_2 (Bonser *et al.* 1991; Cross *et al.* 1995). These compounds were therefore utilized in this study to determine not only the specificity of the PI3-kinase response to PGE_2 but also to determine the importance of this signal molecule in PGE_2-mediated SMC growth.

To evaluate the role of PI3-kinase in PGE_2-mediated SMC growth, inhibitors of PI3-kinase were first tested in relation to their ability to inhibit the increase in DNA and RNA synthesis mediated by PGE_2. Both LY294002 and wortmannin were capable of decreasing RNA and DNA synthesis in a concentration-dependent manner (Figure 55), confirming the importance of PI3-kinase in the PGE_2-mediated SMC growth effect. To verify that these compounds were indeed inhibiting PI3-kinase, the activation of PI3-kinase by PGE_2 was monitored in the presence of wortmannin (Figure 56B). The *in vivo* assay, where [^{32}P]orthophosphate-labelled lipid pools were separated by TLC analysis, demonstrated that PGE_2 and other PGs were capable of increasing the PIP_3 production compared to control cells in SMCs (Figure 56A). Inclusion of wortmannin suggested that these inhibitor compounds were inhibiting PI3-kinase (Figure 56B). *In vitro* assays were carried out to establish the specificity of the increased PIP_3 production observed with the *in vivo* assay relative to activation of PI3-kinase and demonstrated that PGE_2 was capable of increasing the production of PIP_3 above basal levels in a concentration-dependent manner (Figures 57, 58), and that other prostanoids were also capable of eliciting increased PIP_3 production, although in smaller quantities (Figure 57). These data suggest that PI3-kinase is an important component of PGE_2-mediated SMC growth.

PI3-kinase has already been demonstrated to be an important component of AngII-mediated SMC growth (Saward & Zahradka 1997a). It is also known to link other G protein-coupled receptors to MAP kinase. To determine whether PI3-kinase operated similarly in this particular cell system, the PI3-kinase inhibitors were tested for their ability to abrogate the activation of MAP kinase by PGE_2. Addition of either LY294002 or wortmannin inhibited the activation of MAP kinase (Figure 59). The expression of c-*fos* in response to PGE_2 was also prevented (Figure 60). These findings verify the placement of the PI3-kinase pathway before the MAP kinase pathway (Lopez-Ilasaca 1998; Luttrell *et al.* 1997; Sugden & Clerk 1997; Zou *et al.* 1998) and also confirm the importance of this pathway in regulating cellular growth, since activation of c-*fos* is considered a hallmark of cell proliferation (Rivera & Greenberg 1990; Woodgett 1989). Interestingly, based on the lack of p21-Ras activation by PGE_2, the signal molecule that links PI3-kinase to MAP kinase may be an isoform of PKC (Takeda *et al.* 1999).

In conclusion, this study demonstrates that PGE_2 is a positive modulator of SMC growth, since it can stimulate not only RNA and DNA synthesis, but other markers of cell growth and proliferation, such as PCNA expression, BrdU incorporation and expression of c-*fos* mRNA. Moreover, PGE_2 positively modulates intracellular signaling pathways associated with cell growth including MAP kinase and PI3-kinase. These studies also suggest that PI3-kinase is activated by PGE_2 prior to MAP kinase activation, but that the activation of MAP kinase is via a Ras-independent mechanism, possibly via PKA or PKC (Takeda *et al.* 1999; Wan & Huang 1998). This might suggest an alternative regulatory pathway for linking PI3-kinase to MAP kinase, and it would be interesting to investigate the potential for differential involvement of adenylate cyclase and cAMP levels, especially in relation to the dual role for PGE_2, both as a stimulator and inhibitor of SMC growth.

7.3 ADP-ribosylation and SMC proliferation

7.3.1 Background/rationale

The role of ADP-ribosylation in regulating cell differentiation and growth is becoming increasingly more apparent (Grainger *et al.* 1992; Kharadia *et al.* 1992; Miwa & Sugimura 1990; Thyberg *et al.* 1995b). For example, as described in previous chapters (chapters 5 and 6), ADP-ribosylation reactions are involved in differentiation of skeletal myoblasts into myotubes and the proliferation of H4IIE cells. ADP-ribosylation may also be involved in tumour cell growth, since MIBG, a specific inhibitor of arg-mART, is capable of inhibiting neuroblastoma tumour progression and metastases (Kuin *et al.* 1999; Smets *et al.* 1988b; Taal *et al.* 1996). Furthermore, a link between ADP-ribosylation reactions and SMC growth and differentiation has been documented by Thyberg *et al.* (1995b) and Grainger *et al.* (1992) who showed that inhibitors of ADP-ribosylation inhibit the proliferation (and/or phenotypic modulation) of rat (and human) SMCs.

The participtation of SMCs in the formation of a neointimal lesion after vascular injury is clearly established (Davies & Hagen 1994; Ellis & Muller 1992; Liu *et al.* 1989; Schwartz *et al.* 1995a; Schwartz & Ross 1984). The SMCs located in these vascular lesions express a modulated phenotype compared to the SMCs in the media of the normal vessel wall (Owens 1995; Schwartz *et al.* 1986). However, phenotypic modulation is fully reversible both *in vitro* and *in vivo* under the appropriate conditions (Kocher *et al.* 1991; Owens 1995; Thyberg 1998; Thyberg *et al.* 1997). Considering the possible participation of ADP-ribosylation in the control of cell differentiation and growth, a contribution to the modulation of SMC differentiation status may be postulated. This has already been indicated by the findings of Thyberg *et al.* (1995b). Thus, an examination of ADP-ribosylation in the regulation of SMC growth was carried out in a primary SMC

culture system with MIBG. The activation of arg-mART was also examined in SMCs after treatment with two growth stimulatory molecules, AngII and PGE_2.

7.3.2 Specific Aims

1. To determine if arg-mART activity is increased following growth factor-stimulation of SMCs by AngII and PGE_2.
2. To assess the efficacy of the mono(ADP-ribosyl)ation inhibitor, MIBG, to inhibit SMC proliferation.

7.3.3 Experimental Design

Primary cultures of porcine SMCs will be utilized for all experiments after 5 days in serum-free supplemented D-MEM. To assess the participation of arg-mART in SMC growth and proliferation, mitogenic activation of mART will be measured in both cytosolic and microsomal extracts of AngII- and PGE_2-stimulated SMCs. Subsequently, the contribution of arg-mART to SMC growth and proliferation will be assessed with MIBG, an inhibitor of arg-mART. Specifically, RNA and DNA synthesis and cell number will be monitored after growth factor stimulation of SMCs. The precursor analog, MIBA, will be included in the majority of these assays. Finally, specific assays will be used to ascertain the role of mitochondria in the cytostatic actions of MIBG.

7.3.4 Results

7.3.4.1 Activation of an arg-mART in porcine SMCs

To determine if ADP-ribosylation events are responsive to growth factor treatment of SMCs, arg-mART activity was measured in extracts from SMCs that had been treated with AngII (10^{-6} M). It was observed that a cytosolic arg-mART activity was

transiently increased, exhibiting a peak at 15 min. In contrast, only a minimal increase in microsomal arg-mART activity was detected (Figure 61A). Although this appears to be the converse of the findings with H4IIE cells, it is possible that the arg-mART activity that is stimulated in SMCs arises from a different intracellular source, or that the arg-mART activity observed with AngII is specific to AngII activation only. On the other hand, when stimulation of SMCs by AngII and PGE_2 was compared, it was found that AngII provoked a much larger arg-mART activation in both cytosolic and microsomal fractions when compared to PGE_2 (Figure 61B), but that the degree of stimulation in both fractions was equivalent. Interestingly, although the overall magnitude of the arg-mART activity stimulated by PGE_2 was smaller than with AngII, the microsomal fraction demonstrated a stronger activation than the cytosolic fraction (Figure 61B). These data indicate that arg-mART is activated in response to AngII and PGE_2, and suggests the possibility that specific growth factors have a defined but distinct arg-mART response.

7.3.4.2 Effect of MIBG on SMC proliferation/growth

From the previous sections, it was evident that SMCs are responsive to mitogens (eg. AngII, FBS and PGE_2), and that two of these compounds, AngII and PGE_2, can activate arg-mART. Based on these findings and those from chapter 5, it was postulated that growth factor stimulation of SMC arg-mART might be involved in the signaling and/or activation of SMC growth. Therefore, the arg-mART inhibitor, MIBG, was used to further define this relationship, and to confirm mART participation in SMC growth and proliferation. Increased SMC growth was monitored via incorporation of [^{3}H]uridine and [^{3}H]thymidine. SMCs were pretreated with MIBG for 10 min prior to addition of the growth stimulating agents (2% v/v FBS, 10^{-6} M AngII or 10^{-6} M PGE_2). MIBG (2.5 to 50 μM) inhibited both RNA and DNA synthesis in AngII-stimulated SMCs in a concentration-dependent manner (Figure 62A,B). Similarly, MIBG inhibited both RNA

FIGURE 61: ***Activation of Mono(ADP-ribosyl)transferase by Angiotensin II and Prostaglandin E_2.***

Quiescent SMCs were treated with angiotensin II (AngII) (10^{-6} M) or PGE_2 (10^{-6} M) over 120 min and subcellular fractions prepared as described in Materials and Methods (section 4.8.4) at the specified times. (A) Microsomal (membrane) and cytosolic (cytosol) fractions of AngII-stimulated SMCs were assayed for arg-mART activity as described in Materials and Methods (section 4.9.8). Polyarginine (2 mg/mL) was used as the acceptor protein for the assay. One of two independent experiments is shown, both of which exhibited a similar response. (B) An *in vitro* mono(ADP-ribosyl)ation assay was carried out using both the microsomal (membrane) and cytosolic (cytosol) fractions, and the changes in arg-mART activity compared in AngII-treated (30 min stimulation), PGE_2-treated (30 min stimulation) and untreated cells. Polyarginine (2 mg/mL) was used as the acceptor protein for the assay. Untreated cell activity was set to 1.0. Data represent one of two independent experiments, both of which exhibited a similar response.

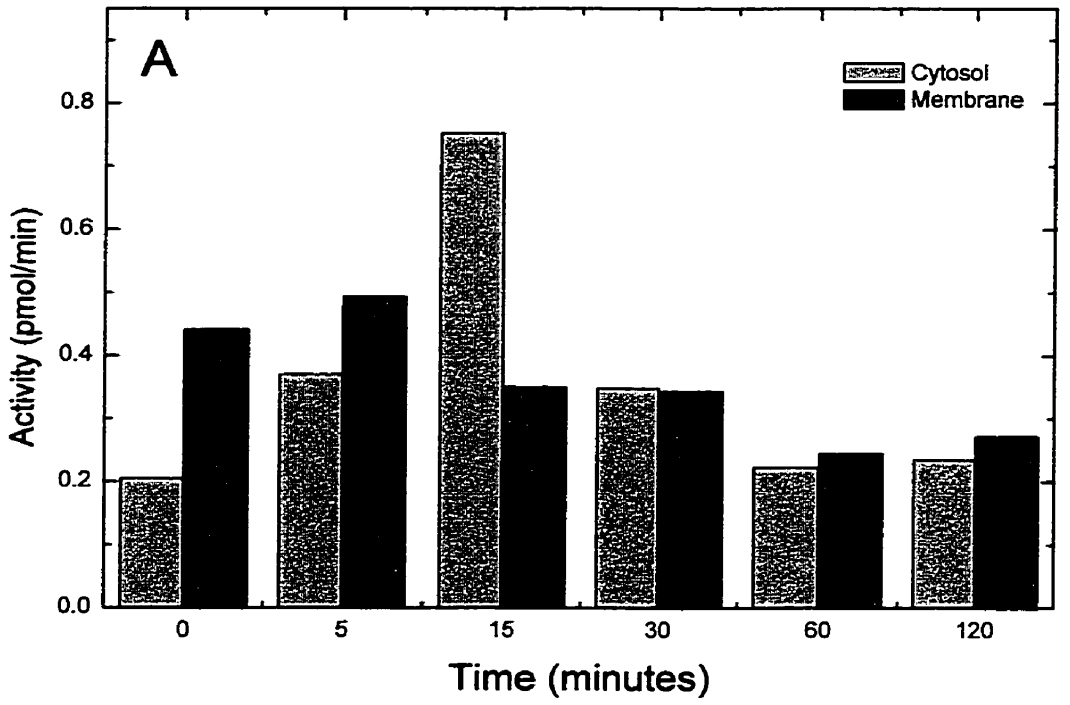
A
Cytosol
Membrane
Activity (pmol/min)
0.0
0.2
0.4
0.6
0.8
0
5
15
30
60
120
Time (minutes)

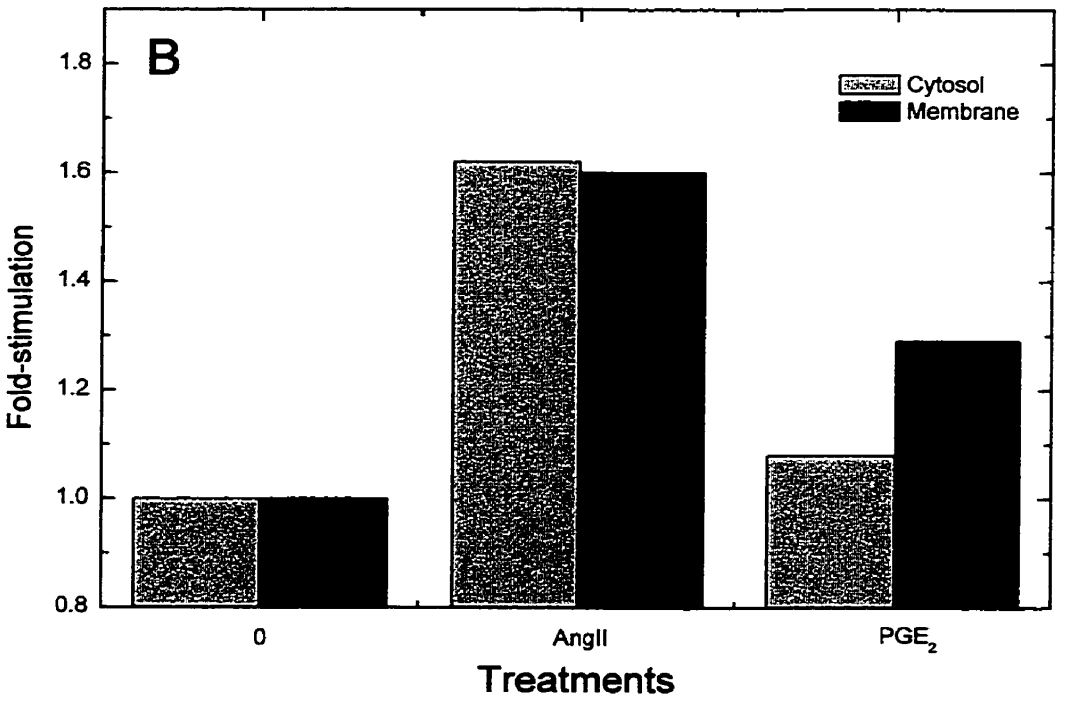
B
Cytosol
Membrane
Fold-stimulation
0.8
1.0
1.2
1.4
1.6
1.8
0
AngII
PGE2
Treatments

FIGURE 62: ***Sensitivity of Mitogen-stimulated SMC Growth to MIBG.***

Quiescent SMCs were pretreated with MIBG (2.5 to 50 μM) for 10 min prior to addition of angiotensin II (AngII) (10^{-6} M) (A, B) or serum (2% v/v FBS) (C, D). The incorporation of [^{3}H]uridine (6 h incubation) or [^{3}H]thymidine (48 h incubation) into trichloroacetate-precipitable material after addition of AngII and FBS was used as an indication of RNA (A, C) and DNA (B, D), respectively. The incorporation rate of untreated cells was set to 100%. The data are presented as the mean ± SE of at least three separate experiments conducted in triplicate using different SMC isolations. Comparisons were made relative to growth factor treated SMCs with the Student's t-test (*, $p < 0.05$).

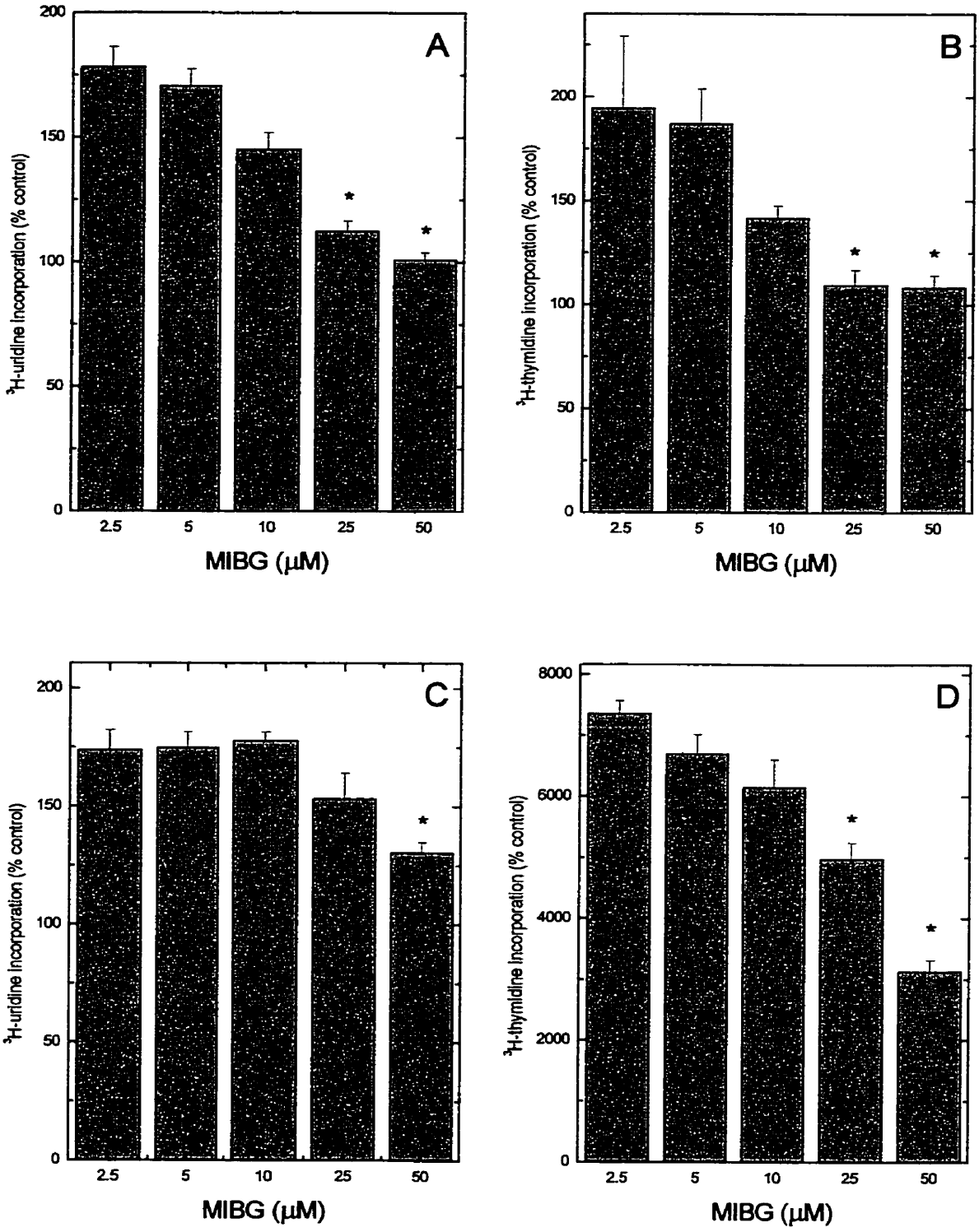
A
B
C
D
^{3}H-uridine incorporation (% control)
^{3}H-thymidine incorporation (% control)
MIBG (μM)
2.5
5
10
25
50
0
50
100
150
200
2000
4000
6000
8000
*

and DNA synthesis in FBS-stimulated SMCs (Figure 62C,D), although the response was not returned to basal levels as seen with the AngII (Figure 62A,B). This is likely due to the magnitude of the SMC growth response elicited by FBS as a result of the multiple growth stimulating agents present in FBS. When MIBG was tested with PGE_2-stimulated SMCs, MIBG (2.5 to 50 μM) decreased both RNA and DNA synthesis in a concentration-dependent manner (Figure 63A,B), and the inhibition was comparable to that seen with AngII (Figure 62A,B). Moreover, MIBG inhibition of DNA synthesis was also observed in human SMCs stimulated with FBS (data not shown). To confirm the specificity of MIBG, the actions of MIBA (2.5 to 50 μM) were also tested in FBS-treated SMCs. MIBA was ineffective at inhibiting FBS-mediated stimulation of DNA synthesis (Figure 64), even at the highest concentration.

Cell number was quantified to determine if MIBG (20 μM) prevented the increase in SMC cell number induced by FBS addition. FBS (2% v/v) essentially doubled cell number over a 72 h period (Figure 65). This increase in cell number was only modestly inhibited by MIBG (20 μM), and not at all by the analog, MIBA (20 μM) (Figure 65). MIBG and MIBA treatment of SMCs in the absence of mitogen did not alter cell number relative to untreated control SMCs. These data suggest that MIBG inhibits SMC proliferation. The small degree of inhibition observed in this experiment may be due to the concentration of MIBG (20 μM) used in the study relative to the strength of the mitogen being used (i.e. FBS vs. a single mitogen such as AngII). Furthermore, because the treatment of SMCs with MIBG or MIBA alone did not decrease the cell number, as was observed with H4IIE cells (chapter 5), it is possible that MIBG is less toxic to SMCs. Cytotoxicity studies were therefore conducted to assess this parameter.

FIGURE 63: ***Sensitivity of Prostaglandin E_2-mediated Cell Growth in SMCs to MIBG.*** Quiescent SMCs were pretreated with MIBG (2.5 to 50 μM) for 10 min prior to addition of prostaglandin E_2 (PGE_2) (10^{-6} M). The incorporation of [^{3}H]uridine (6 h incubation) or [^{3}H]thymidine (48 h incubation) into trichloroacetate-precipitable material after addition of PGE_2 was used as an indication of RNA (A) and DNA (B) synthetic activity, respectively. The incorporation rate of untreated cells was set to 100 %. The data are presented as the mean ± SE of at least three separate experiments conducted in triplicate using different SMC isolations.

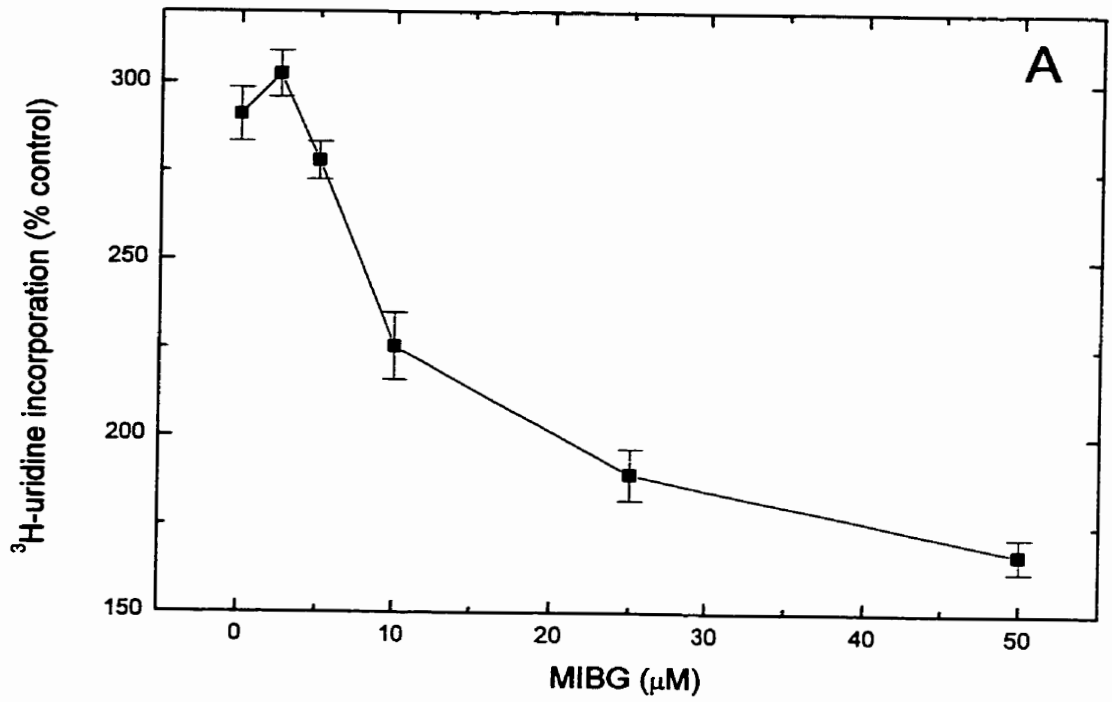
A
^{3}H-uridine incorporation (% control)
300
250
200
150
0
10
20
30
40
50
MIBG (μM)

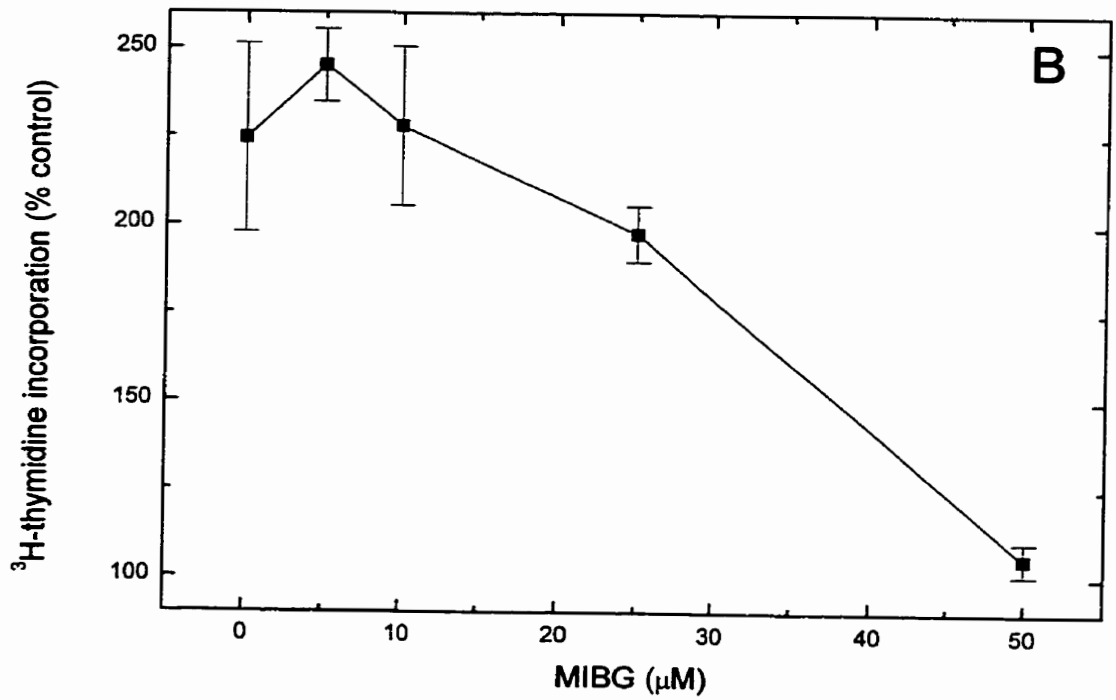
B
^{3}H-thymidine incorporation (% control)
250
200
150
100
0
10
20
30
40
50
MIBG (μM)

FIGURE 64: ***Sensitivity of Serum-mediated Cell Growth in SMCs to MIBA.***

Quiescent SMCs were pretreated with MIBA (2.5 to 50 μM) for 10 min prior to addition of serum (2% v/v FBS). The incorporation of [^{3}H]thymidine (48 h incubation) into trichloroacetate-precipitable material after addition of FBS was used as an indication of DNA synthetic activity. The incorporation rate of serum-treated cells was set to 100%. The data are presented as the mean ± SE of three separate experiments conducted in triplicate using different SMC isolations.

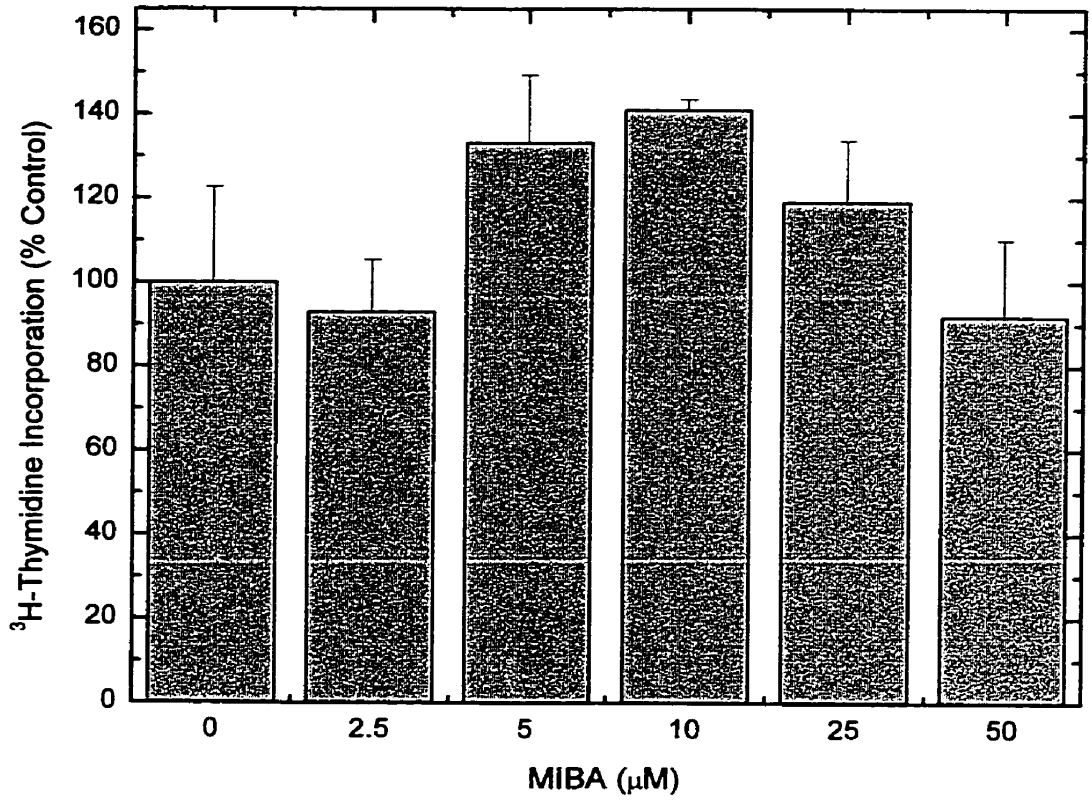
160
140
120
100
80
60
40
20
0
^{3}H-Thymidine Incorporation (% Control)
0
2.5
5
10
25
50
MIBA (μM)

FIGURE 65: ***Effect of MIBG and MIBA on Serum-stimulated SMC Proliferation.***

Quiescent SMCs were pretreated with MIBG or MIBA (20 μM) for 10 min prior to addition of serum (2% v/v FBS). The cells were incubated for 72 h and the cell number quantified using a Coulter Counter. Similar results were obtained in two independent experiments. Each data point was counted in triplicate from samples prepared in duplicate. Data is presented as mean ± SE. Comparisons were made relative to serum-treated cells with the Student's t-test (*, $p < 0.05$).

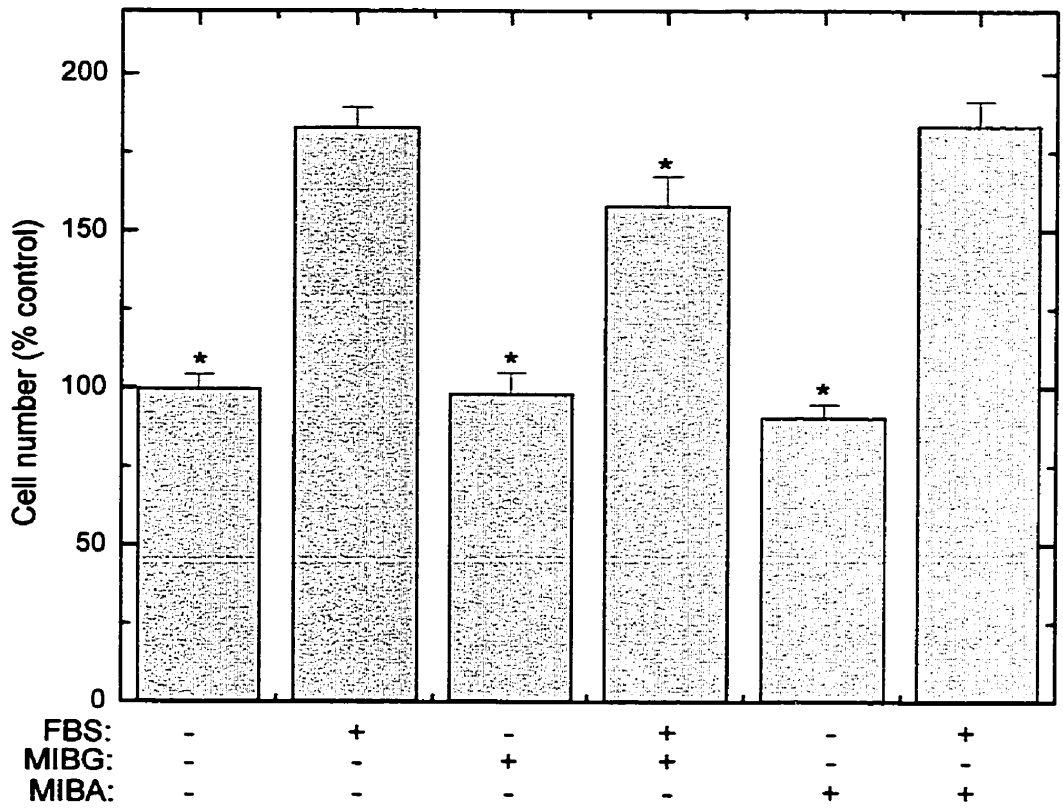
Cell number (% control)
200
150
100
50
0
*
*
*
*
FBS: - + - + - +
MIBG: - - + + - -
MIBA: - - - - + +

7.3.4.3 Cytotoxic effects of MIBG on SMCs

As observed in chapter 5, H4IIE cells are quite sensitive to the addition of MIBG. On the other hand, L6 skeletal myoblasts, as observed in chapter 6, are not adversely affected by MIBG. Studies of SMCs (Figure 65) suggest that the sensitivity of SMCs to MIBG has greater similarity to myoblasts than hepatomas. An MTT assay that assesses mitochondrial function was used to obtain information regarding the cellular toxicity of MIBG. Over a concentration range from 0 to 100 μM, MIBG, even after 72 h, did not appreciably decrease MTT conversion in quiescent SMCs (Figure 66). These data would suggest that MIBG is not toxic to SMCs, which is in marked contrast to the results with H4IIE cells. Moreover, a comparison of the effect of MIBA and MIBG (0 to 500 μM) on SMC morphology, after incubation with the compounds for 72 h, demonstrated that only at the highest concentration was MIBG toxic (i.e. 500 μM) (Figure 67). Only in panel I was it observed that SMCs had rounded up and lifted off the plate. At the concentration that effectively inhibited DNA and RNA synthesis and differentiation in the previous studies (50 μM), no change in cell morphology was observed. MIBA did not appear to exert toxic effects at any of the concentrations tested (Figure 67). Therefore, SMCs may resemble L6 skeletal myoblast cells in their sensitivity and response to MIBG.

7.3.5 Discussion

The results of this study indicate that an arg-mART is activated upon stimulation of SMCs with growth factors such as AngII and PGE_2, and that MIBG, a specific inhibitor of arg-mART activity, is capable of inhibiting SMC growth and proliferation resulting from growth factor stimulation. These findings would therefore suggest that an ADP-ribosylation event is important for SMC proliferation and that inhibition of this enzyme prevents growth. These findings imply that an arg-mART is important for the

FIGURE 66: ***Effect of MIBG on Quiescent SMCs. MTT Assay as a Measure of Cell Cytotoxicity.***

Quiescent SMCs were treated with MIBG (0 to 100 μM) for 72 h. MTT was then added for 4 h, and colour intensity quantified at OD_{550}. The data are presented as the mean ± SE of three separate experiments conducted in quadruplicate using different SMC isolations. Comparisons were made relative to control (0) using Student's t-test (*, $p < 0.05$).

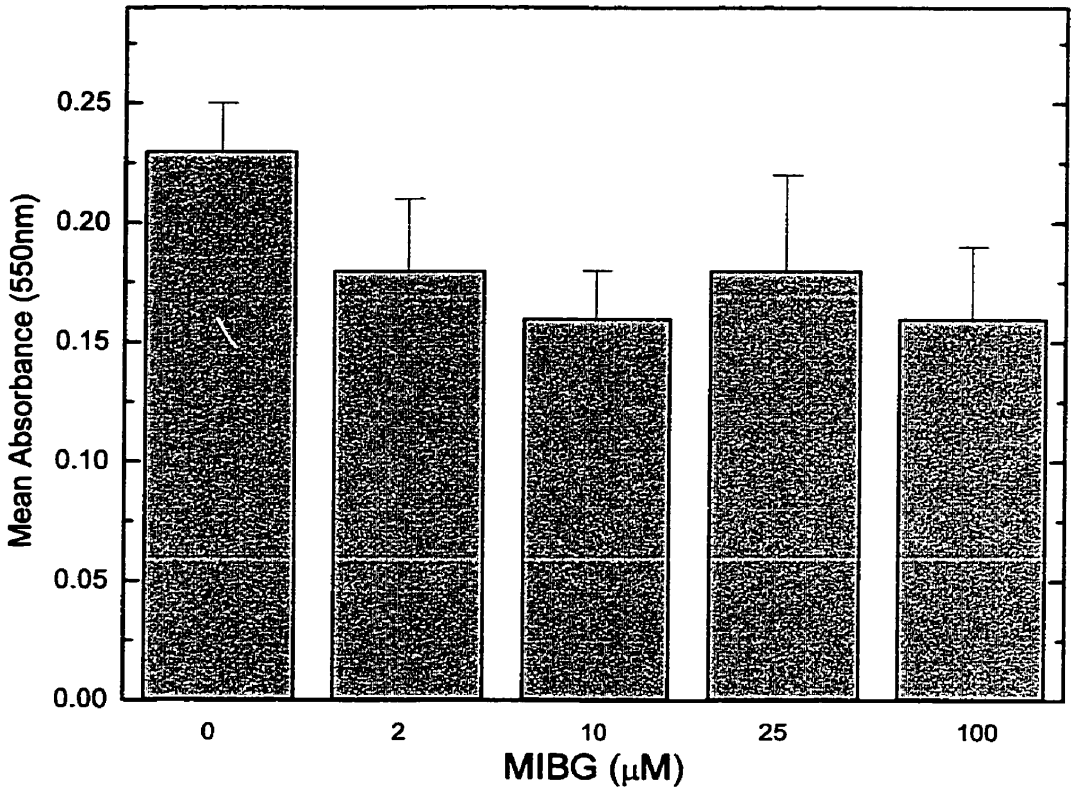
Mean Absorbance (550nm)
0.25
0.20
0.15
0.10
0.05
0.00
0
2
10
25
100
MIBG (μM)

FIGURE 67: ***Effect of MIBG and MIBA on the Morphology of Quisecent SMCs.***

Quiescent SMCs were treated with MIBG or MIBA (0 to 500 μM) for 72 h. Photomicrographs were used to record cell morphology. Representative micrographs are shown for untreated SMCs. Specific treatments are: control (A), 50 μM MIBA (B) and MIBG (C), 100 μM MIBA (D) and MIBG (E), 200 μM MIBA (F) and MIBG (G), and 500 μM MIBA (H) and MIBG (I). Magnification: 128×.

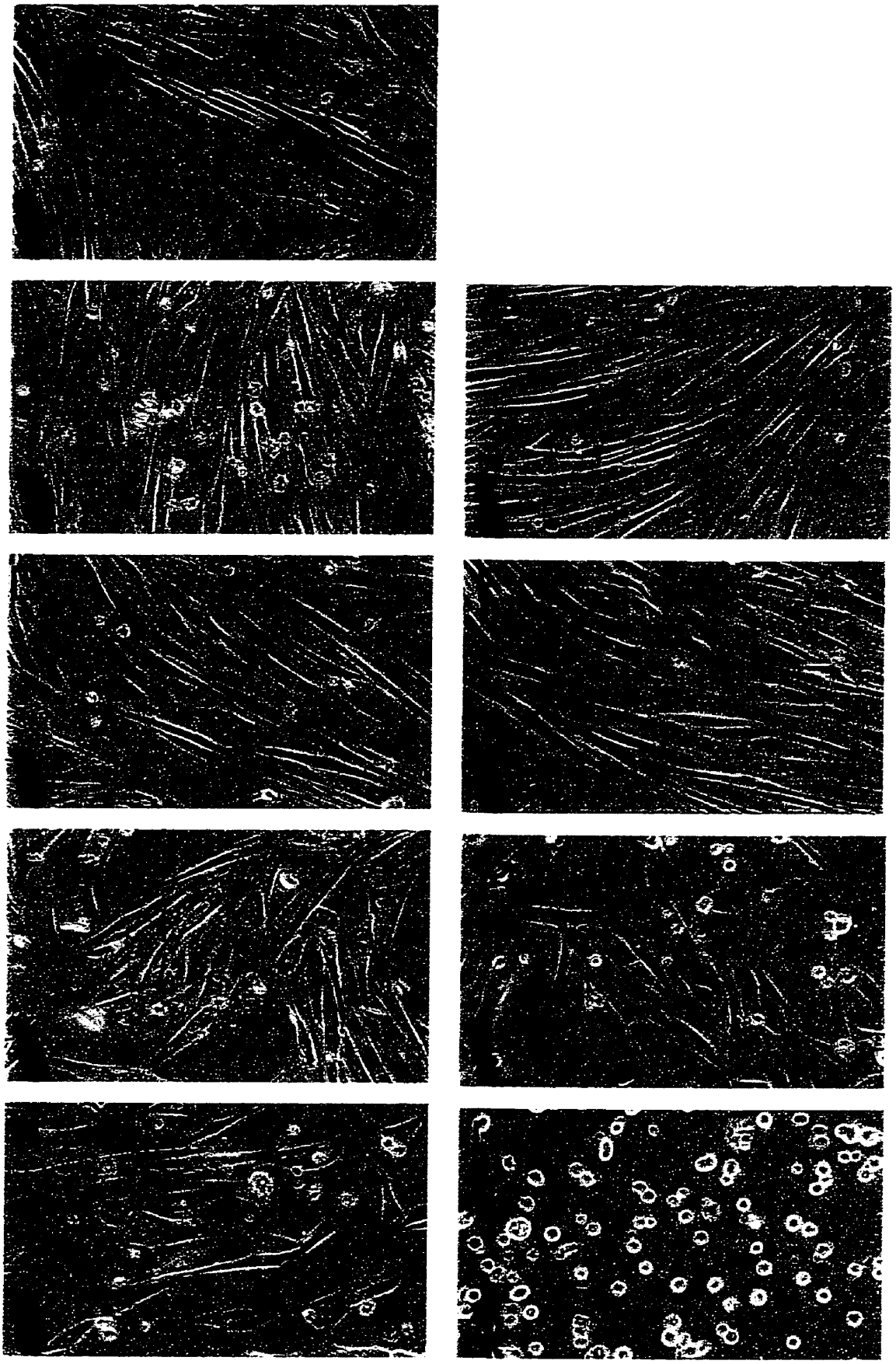

transduction of signals that regulate cell proliferation. MTT and cytotoxicity experiments eliminated the possibility that the inhibitory actions of MIBG were mediated by a general effect on mitochondrial activity. Furthermore, MIBG was not toxic to SMCs as seen with the H4IIE cells, thus showing greater similarity to myoblasts.

Thyberg *et al.* (1995b) demonstrated that inhibitors of ADP-ribosylation were able to suppress the phenotypic modulation and the proliferation of SMCs isolated from rat aorta. Their studies detail that two different inhibitors of ADP-ribosylation events, HMBA (hexamethylenebisacetamide, a PARP inhibitor) and MIBG (arg-mART inhibitor) could inhibit the transition of rat aortic SMCs from a contractile to a synthetic phenotype (Thyberg *et al.* 1995b). However, these compounds were not able to stimulate a return from the synthetic to a contractile phenotype. Nevertheless, both compounds were capable of inhibiting cell proliferation in a reversible manner independent of the status of the cells (i.e. independent of phenotypic state at start of treatment). Studies to establish whether an ADP-ribosylation enzyme was activated in any of these cell states, however, were not pursued. The results reported here expand upon and extend the findings of Thyberg *et al.* (1995b) by establishing that an ADP-ribosylation activity is stimulated in response to growth factor treatment. In this study, both AngII and PGE_2 were able to increase the activity of an arg-mART differentially depending on the cell fraction in which the activity was being measured (Figure 61). AngII significantly increased the activity of a cytosolic arg-mART within 15 min, while only modestly increasing the activity of a microsomal arg-mART (Figure 61A). When the arg-mART activity was measured following a 30 min stimulation with either AngII or PGE_2, it was observed that AngII activated both cytosolic and microsomal arg-mARTs equivalently, whereas with PGE_2 the microsomal arg-mART activity was greater than the cytosolic activity (Figure 61B). The magnitude of response between AngII and PGE_2 was also

different with AngII eliciting a larger arg-mART activation. Based on these results, it may be possible to suggest that specific growth stimulating agents operate through distinct arg-mART enzymes. The number of responsive cells and the magnitude of the response may govern the final effect of the growth factor. For example, it is possible that a growth factor that elicits a hyperplastic growth response requires the activation of both a cytosolic and microsomal arg-mART, whereas a growth factor that elicits a hypertrophic growth may response may only require the activation of a microsomal arg-mART, or vice versa. It is also possible that the arg-mARTs that have been activated are specific to a cellular event (i.e. proliferation vs. migration vs. contractility). Regardless, although a specific divergence of signaling pathways between the hypertrophic and hyperplastic growth response has not been identified in SMCs, the dependency of the system on the activation of both systems could be postulated. Furthermore, it is more than likely that if several arg-mARTs were activated as part of the cell proliferative response, MIBG could inhibit one or all of the steps.

To confirm that an ADP-ribosylation reaction was involved in the growth of SMCs, the arg-mART inhibitor MIBG was tested for its ability to inhibit RNA and DNA synthesis and increases in cell number (Figures 62, 63, 65). MIBG completely inhibited the cell growth response of SMCs to AngII and PGE_2 as measured by [^{3}H]thymidine and [^{3}H]uridine incorporation studies (Figures 62, 63), while only partially inhibiting the SMC proliferative response to serum (2% v/v FBS) (Figures 62, 65). This is not surprising since the strength of the mitogens is quite different. FBS, which contains multiple growth factors is likely able to stimulate more than one pathway that results in the initiation of cell proliferation. In contrast, both AngII and PGE_2 likely elicit a response through a single pathway. Furthermore, FBS is capable of stimulating a much larger proliferative response than AngII and PGE_2, presumably by stimulating a greater

percentage of the cell population (Figure 45, 50). The precursor analog of MIBG, MIBA, was also found unable to inhibit either RNA or DNA synthesis (Figure 64). What was interesting about this result is the implication that the decrease in RNA and DNA synthesis caused by MIBG was not due to inhibition of mitochondrial respiration. This conclusion is possible since it has been demonstrated that MIBA can inhibit mitochondrial respiration, although to a lesser extent than MIBG (Smets *et al.* 1988b; Van den Berg *et al.* 1997). Furthermore, the lack of inhibition of cell growth by MIBA indicates the importance of the guanidino group of MIBG and strengthens the premise that MIBG operates by inhibiting arg-mART by acting as a decoy substrate.

Neither MIBG or MIBA affected the basal cell number at a concentration of 20 μM and only MIBG was able to prevent the increase in cell number observed with FBS (2% v/v) treatment after 72 h treatment (Figure 65). This would suggest that MIBG is not cytotoxic to SMCs at this concentration for that period of time, contrasting markedly with H4IIE cells where cytotoxic effects on cell number were observed at this concentration (Figure 24). Interestingly, the MTT conversion assay also indicated that MIBG was not affecting the mitochondria of SMCs adversely (Figure 66). Photomicrographs of the cells after 72 h of treatment with MIBG or MIBA (over a large concentration range (0 to 500 μM)) also support the conclusion that MIBG is not cytotoxic to SMCs (Figure 67). Thus, SMCs, unlike H4IIE but more similar to L6 skeletal myoblasts, are more tolerant of MIBG treatment (MIBA is not as toxic either). This could be linked to a number of factors including: i) the number of mitochondria that are present within each cell type, ii) the transporters present in the cell membrane that influence uptake of MIBG, and iii) the origin of the cell type (i.e. epithelial vs. mesenchymal). Thus, MIBG may be functioning as a cytostatic agent, serving to remove SMCs from the cell cycle, rather than being cytotoxic. The work of Thyberg *et al.* (1995b) would confirm and support these findings,

since it was reported that MIBG (at twice the concentration used in this study) was able to reversibly inhibit cell proliferation. However, they also suggested that MIBG interferes with a process that occurs late in the cell cycle, since MIBG was effective even when added 8 h following treatment, and MIBG had no effect on the expression of early growth response genes such as c-*fos*, c-*jun* and c-*myc*.

In conclusion, these studies indicate that growth factors such as AngII and PGE_2 can induce arg-mART activity, and that MIBG, a known inhibitor of arg-mART (Loesberg *et al.* 1990b; Smets *et al.* 1990b) inhibits SMC growth. From these observations, the assumption can be made that MIBG is inhibiting SMC proliferation by preventing activation of an arg-mART. However, since the specific effects of MIBG toxicity are not clearly established, and appears to be dependent on cell type, a definitive link to ADP-ribosylation cannot been demonstrated. That MIBG inhibits SMC proliferation is not in doubt, however, the lack of a definitive mechanism for the inhibition of cell growth and proliferation is still troubling. In most cellular systems, other than suggesting that an ADP-ribosylation event may be involved, the exact spatial and temporal location at which MIBG may be working to inhibit cell proliferation has not been clarified and is presently not known. In an attempt to address this issue, the effect of MIBG on the activation of a variety of signaling molecules known to be involved in cell proliferative processes was determined.

7.4 Modulation of intracellular signaling pathways by MIBG

7.4.1 Background/rationale

Mitogenic stimulation is dependent on the activation of numerous molecules that transmit signals from a cell surface receptor to the nucleus of the cell. Signaling intermediates critical for cell proliferation include MAP kinase (Adam *et al.* 1995; Ahn *et*

al. 1992; Force & Bonventre 1998; Khalil & Morgan 1993; Klemke *et al.* 1997; Nelson *et al.* 1998), p21-Ras (Bos 1995) and PI3-kinase (Varticovski *et al.* 1994). The expression of early growth response genes is also essential for the initiation and maintenance of cell growth processes. Thus, since it has already been established that growth-stimulating agents such as PGE_2 can activate these signaling systems and that MIBG inhibits the proliferation of PGE_2-stimulated SMCs, the impact of MIBG on early growth signaling was investigated.

7.4.2 Specific Aims

1. To examine the effect of MIBG on MAP kinase activation.
2. To examine the effect of MIBG on p21-Ras activation.
3. To examine the effect of MIBG on PI3-kinase activation.
4. To examine the effect of MIBG on c-*fos* gene expression.

7.4.3 Experimental design

Primary cultures of quiescent porcine SMCs were pretreated with MIBG for 10 min prior to addition of PGE_2. SMCs were harvested for the evaluation of the specific signaling elements. An in gel MAP kinase activity assay was used to determine the effect of MIBG on MAP kinase activation. GTP binding to p21-Ras was measured to define the effect of MIBG on p21-Ras activation state. The effect of MIBG on PI3-kinase activation and formation of PIP_3 lipid intermediates was also assessed. As well, the effect of MIBG on c-*fos* gene expression was determined. Each of these investigations allows not only a prospective spatial and temporal placement for the inhibition by MIBG, but may also reveal a spatial and temporal placement for arg-mART reactions required for SMC growth and proliferation.

7.4.4 Results

7.4.4.1 Effect of MIBG on MAP kinase activation

As demonstrated in Figure 53, MAP kinase is activated by a variety of growth factors, including FBS and PGE_2. To determine if the cell growth inhibitory effect of MIBG is due to inhibition of MAP kinase activation, MIBG (50 μM) was added to SMCs 10 min prior to growth factor stimulation. It was observed that MIBG was not able to abrogate the MAP kinase response activated by PGE_2 (10^{-6} M) (Figure 68A). Densitometric analysis of a separate experiment confirmed the finding that MIBG did not inhibit the MAP kinase activation (Figure 68B). These data demonstrate that MIBG does not affect this critical cell growth pathway and further indicates that an arg-mART does not participate in the activation of MAP kinase. Similar results were obtained with H4IIE cells in chapter 5.

7.4.4.2 Effect of MIBG on p21-Ras activation

As demonstrated previously (Table 3), p21-Ras is not activated by PGE_2. However, the effect of MIBG on this process was still examined in case MIBG treatment would activate or potentiate p21-Ras activity. In other words, mART activation could function as a negative regulator of p21-Ras. Addition of MIBG (50 μM) 10 min prior to PGE_2 (10^{-6} M) addition revealed that MIBG did not influence p21-Ras stimulation (Table 3). These findings indicate that MIBG does not affect p21-Ras activity and that a mART does not serve as a negative regulator of this enzyme.

7.4.4.3 Effect of MIBG on PI3-kinase activation

As established in Figures 56 to 58, PI3-kinase is activated by PGE_2. Pretreatment of SMCs with MIBG (50 μM) for 10 min, did not inhibit PI3-kinase-dependent formation of PIP_3 stimulated by PGE_2 (10^{-6} M), as determined by an *in vivo* PI3-kinase assay (Figure 69A,B). These findings demonstrate that MIBG does not inhibit PI3-kinase

FIGURE 68: ***Effect of MIBG on Prostaglandin E_2-stimulated MAP Kinase Activation.*** (A) MAP kinase activity was measured by activity gel assay over 20 min after treatment with PGE_2 (10^{-6} M). Cells were pretreated with MIBG (50 μM) for 10 min prior to PGE_2 stimulation. Specific phosphorylation of myelin basic protein by $p42^{MAPK}$ and $p44^{MAPK}$ is shown. One of three independent experiments with different SMC isolations is presented, all of which exhibited the same response. (B) MAP kinase activity was measured by activity gel assay after 6 min of PGE_2 (10^{-6} M) stimulation. Cells were pretreated with MIBG (50 μM) 10 min prior to PGE_2 addition. Band intensities were determined by densitometry and the data plotted for the 42-kDa band. Data are representative of one of three independent experiments with different SMC isolations, all of which exhibited a similar response.

A

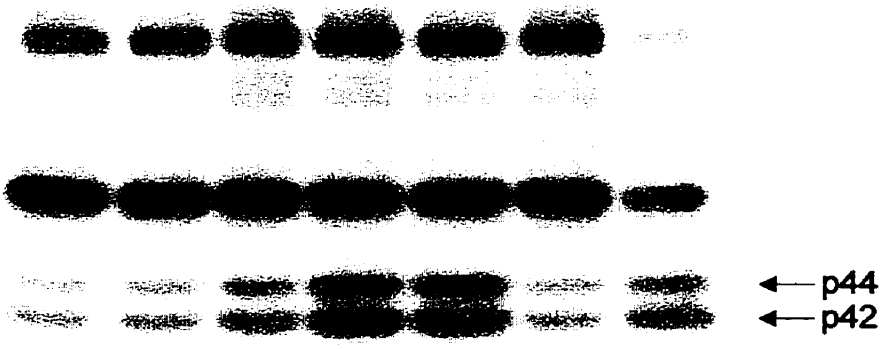

Time (mins):	0	30	2	5	10	20	5
PGE_2:	-	-	+	+	+	+	+
MIBG:	-	+	+	+	+	+	-

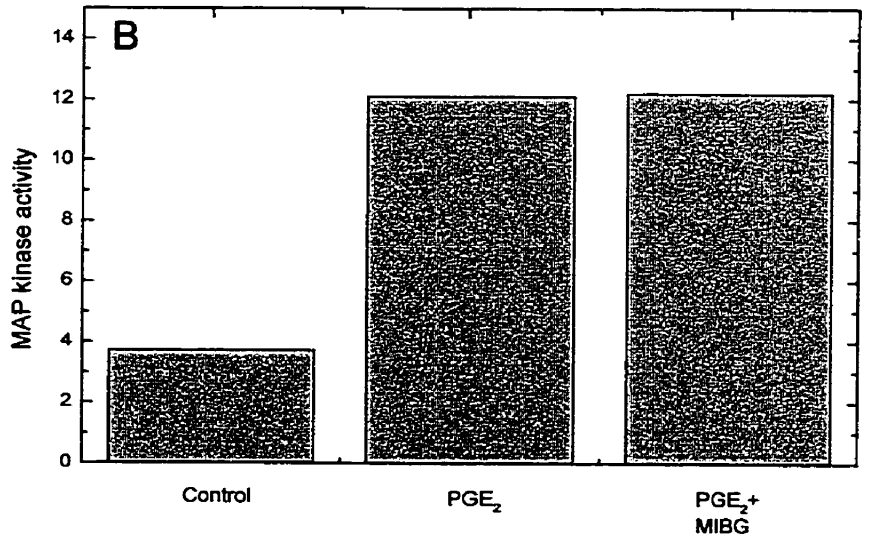

FIGURE 69: ***Effect of MIBG on PI3-Kinase Activation in Prostaglandin E_2-treated SMCs.***

Phosphate pools in quiescent SMCs were labelled with 200 μCi [^{32}P]orthophosphate for 4 h prior to treatment with MIBG (50 μM) for 10 min followed by addition of PGE_2 (10^{-6} M) or TxA_2 (10^{-7} M) for 15 min. Phosphoinositides were extracted from the cells and the phosphorylated forms of phosphoinositol were resolved by thin layer chromatography (TLC) as described in Materials and Methods (section 4.9.3). (A) A representative autoradiogram of a TLC plate is shown. PIP, PIP_2 and PIP_3 are indicated. These results were confirmed in two independent experiments. (B) Graphical representation of PIP_3 formation observed in (A) after densitometric analysis of the autoradiogram.

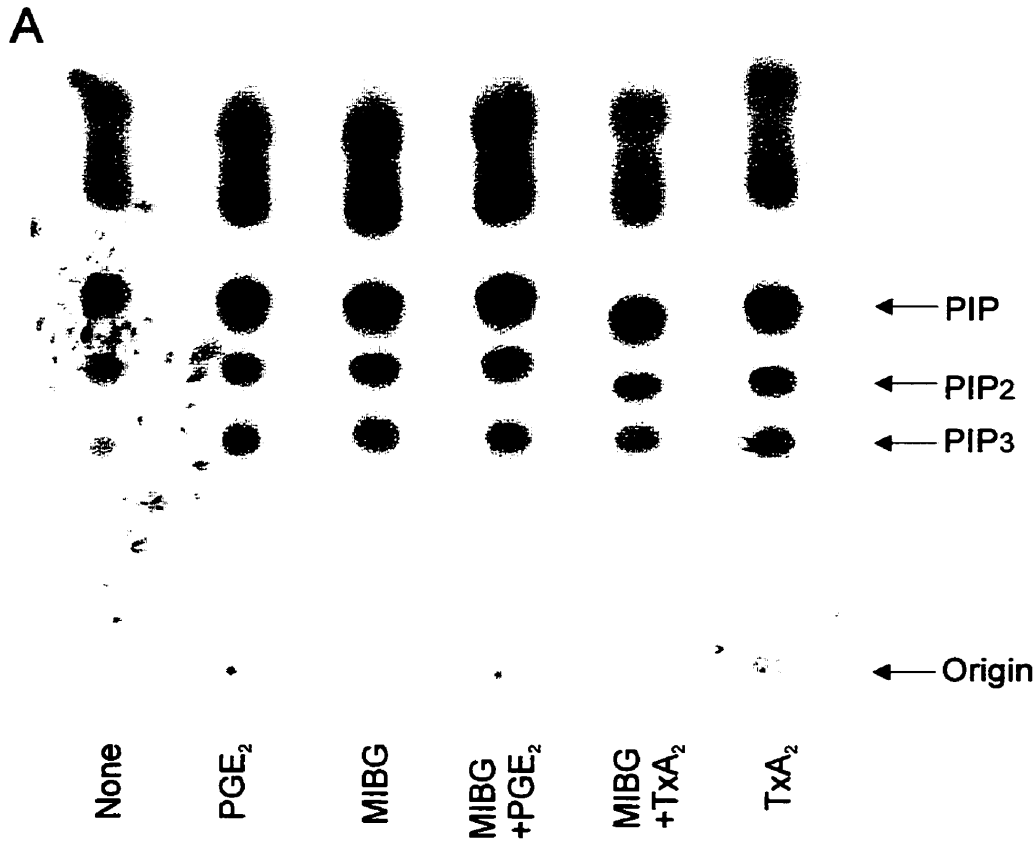
A
PIP
PIP2
PIP3
Origin
None
PGE2
MIBG
MIBG +PGE2
MIBG +TxA2
TxA2

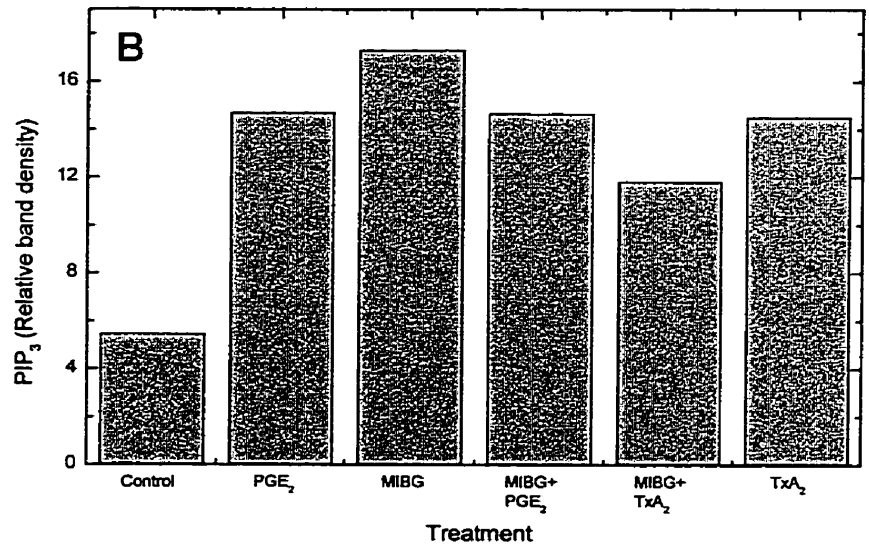
B
PIP3 (Relative band density)
0
4
8
12
16
Control
PGE2
MIBG
MIBG+ PGE2
MIBG+ TxA2
TxA2
Treatment

directly or any process leading to PI3-kinase activation and that a mART does not participate to regulate this signaling molecule.

7.4.4.4 Effect of MIBG on c-*fos* gene expression

As demonstrated in Figure 51, c-*fos* mRNA levels are transiently increased by treatment with PGE_2. Pretreatment of SMCs with MIBG (50 μM) for 10 min inhibited the increase in c-*fos* mRNA levels observed in response to PGE_2 (10^{-6} M) (Figure 70A). Densitometric analysis of a separate experiment confirmed the finding that MIBG treatment inhibited PGE_2-dependent c-*fos* gene expression (Figure 70B). This observation indicates that a step required for induction of c-*fos* gene transcription is sensitive to MIBG treatment and may involve regulation by a mART. Although the results presented in this section suggest that MIBG operates after MAP kinase, p21-Ras and PI3-kinase, but before the activation of c-*fos* gene expression, the results may also indicate that MIBG affects a parallel and independent pathway.

7.4.5 Discussion

The results of this section suggest that MIBG does not have an effect on signaling processes that lead to MAP kinase in SMCs (Figures 68, 69), similar to that which was observed with H4IIE cells in chapter 5. This would indicate that MIBG is not having an effect on either the PGE_2 receptor or the G protein to which it is coupled, and also not the downstream effectors that lead to MAP kinase. Activation of MAP kinase pathways by G protein-coupled receptors progresses through tyrosine phosphorylated intermediates (i.e. PI3-kinase) which subsequently activate MAP kinase through Ras-dependent or Ras-independent mechanisms (Arai & Escobedo 1996; de Vries-Smits *et al.* 1992; Egan *et al.* 1993; Hedin *et al.* 1999b; Seger & Krebs 1995; Thomas *et al.* 1992; Treisman 1995; Treisman 1996; Ueda *et al.* 1996; van Biesen *et al.* 1996; Zhang *et al.* 1993b). As

FIGURE 70: ***Effect of MIBG on Prostaglandin E_2-stimulated c-fos Gene Expression.***

(A) Quiescent SMCs were treated for 15 min with PGE_2 (10^{-6} M) subsequent to a 10 min pretreament with MIBG (50 μM). RNA was extracted and c-*fos* mRNA levels assessed by RT-PCR. Molecular mass markers (φX174 and DNA Marker VI) were used to confirm the size of the PCR products. One representative agarose gel is shown. These results were confirmed in three independent experiments using different SMC isolations. (B) Intensity of the c-*fos* bands was determined by scanning densitometry and the data shown relative to treatment.

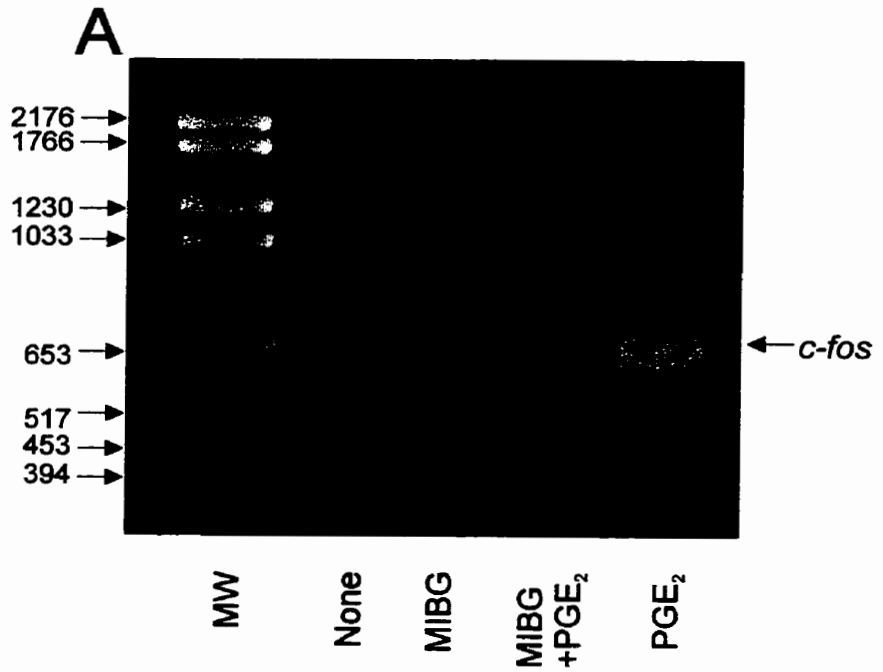
A
2176
1766
1230
1033
653
517
453
394
c-fos
MW
None
MIBG
MIBG +PGE2
PGE2

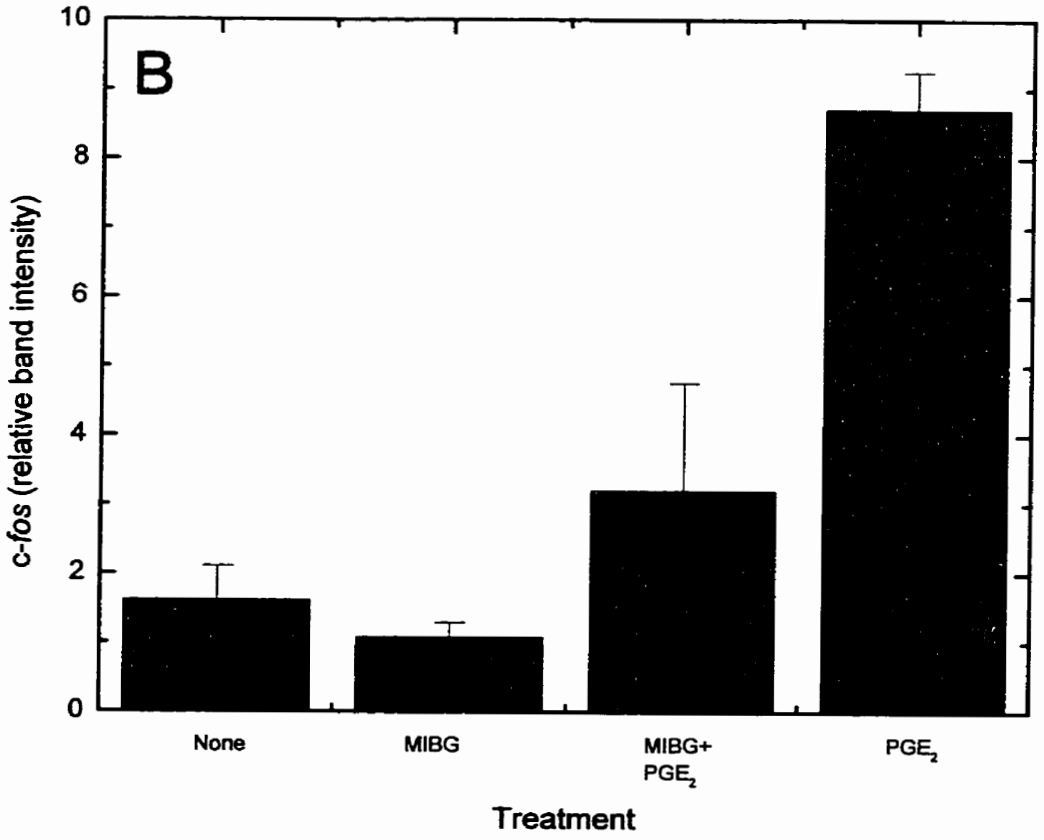
B
c-fos (relative band intensity)
0
2
4
6
8
10
None
MIBG
MIBG+ PGE2
PGE2
Treatment

discussed previously, PGE_2 does not activate Ras in porcine SMCs (Table 3), which would suggest that stimulation of the MAP kinase cascade by PGs occurs through a Ras-independent mechanism that is PI3-kinase-dependent. The intermediary molecule may thus be an isoform of PKC or, alternatively, the step is PKA-dependent (Takeda *et al.* 1999; Wan & Huang 1998). Although p21-Ras was not activated by PGE_2, it was still of interest to study the effect of MIBG on p21-Ras since recombinant Ras proteins have been found to be acceptors for mARTs in eucaryotic cells (Miwa & Sugimura 1990). MIBG treatment did not alter the GTP-binding status of Ras and confirms that PGE_2 modulates MAP kinase via a Ras-independent pathway (Table 3). Moreover, the lack of effect of MIBG indicates that the GTP-binding activity of p21-Ras is not negatively regulated by a mART activity.

When the activation of MAP kinase by PGE_2 was examined in the presence of MIBG treatment, it was found that MIBG did not affect the activation of MAP kinase by PGE_2 (Figure 68). MIBG also did not inhibit the production of PIP_3 by PGE_2-activated PI3-kinase (Figure 69). On the other hand, the induction of c-*fos* expression by PGE_2 was inhibited by MIBG treatment (Figure 70). This suggests that MIBG is working at a step subsequent to MAP kinase, since MAP kinase activates c-*fos* gene transcription directly by phosphorylating Elk-1 (Janknecht *et al.* 1993; Marais *et al.* 1993; Rao & Reddy 1994), and PI3-kinase activation is associated with MAP kinase activation (Della Rocca *et al.* 1997; Ferby *et al.* 1994; Force & Bonventre 1998; Hawes *et al.* 1996; Lopez-Ilasaca *et al.* 1997; Takeda *et al.* 1999). Interestingly, the c-*fos* results presented here contrast with those of Thyberg *et al.* (1995b) who reported that MIBG did not block expression of c-*fos*, c-*jun* or c-*myc* in rat aortic SMCs. This discrepancy can be explained by i) the use of different primary SMC culture models (i.e. rat vs. pig), ii) the addition of different growth

factors (i.e. newborn calf serum vs. PGE_2) and iii) the activation of alternative signaling pathways leading to c-*fos* gene transcription.

While MIBG may inhibit cytosolic arg-mARTs critical for signal transmission to the nucleus, inhibition of an ADP-ribosylation event within the nucleus cannot be excluded. From MAP kinase, the signal typically diverges. MAP kinase either translocates into the nucleus (Kim & Kahn 1997) or activates S6 kinase (Eldar-Finkelman *et al.* 1995; Sale *et al.* 1995; Terada *et al.* 1994). Within the nucleus, MAP kinase phosphorylates Elk-1, a transcription factor necessary for expression of the c-*fos* gene (Janknecht *et al.* 1993; Marais *et al.* 1993; Rao & Reddy 1994; Treisman *et al.* 1992). Thus, MIBG could inhibit the translocation of MAP kinase from the cytosol into the nucleus, although its activation and function are not suppressed within the cytosol. Preliminary Western blot evidence (data not shown; L. Yau, unpublished observations) would indicate that MIBG does not block the phosphorylation of Elk-1 in SMCs, and thus inhibition of c-*fos* gene expression does not occur via this route. The alternative is that MIBG is affecting S6 kinase (likely $p90^{RSK}$) and its ability to phosphorylate SRF, which can also modulate the expression of c-*fos* (Eldar-Finkelman *et al.* 1995; Sale *et al.* 1995; Terada *et al.* 1994).

Although an emphasis has been placed on known signaling mechanisms associated with MAP kinase in these experiments, the most important result is the obvious link between MIBG and c-*fos* gene expression. No other cell system has to this point been identified as a target for this inhibitor. But how is it possible that MIBG inhibits c-*fos* expression without affecting MAP kinase? The speculation in the previous paragraphs derives from an examination of the known signal transduction pathways coupling immediate early gene induction to mitogenic factors. However, several alternative, but significantly less well characterized, pathways exist. The c-*fos* gene

promoter, in addition to binding Elk-1 requires both CREB and SRF. The cAMP response element (CRE) located at (-56) may be the target for cAMP/PKA mediated signals. This idea is highly plausible since PGE_2 is thought to operate via this signal mechanism (see section 7.2). Alternatively, Rho-dependent phosphorylation of SRF activates c-*fos* gene trasncription via the serum response element (-300). This pathway may have the greatest relevance given the known association between Rho and ADP-ribosylation (Aktories 1997; Ehrengruber *et al.* 1995; Lerm *et al.* 2000; Maehama *et al.* 1994; Zhang *et al.* 1993a). Moreover, the transcription of c-*fos* has been shown to be regulated by both SRF and Elk-1 (Treisman *et al.* 1992). For these reasons, both CREB and SRF are now being studied to determine whether phosphorylation of these transcription factors is prevented by MIBG.

To summarize, the only signal step in the chain of events stimulated by PGE_2 and resulting in SMC growth that was inhibited by MIBG treatment was the expression of c-*fos*. A more detailed examination of the signaling pathways that might be linked to cellular growth and that may be affected by MIBG will need to carried out. Presently, the mode of action of MIBG still remains uncertain, although MIBG is a substrate of arg-mART and competes with physiological acceptors of this enzyme (Loesberg *et al.* 1990b; Smets *et al.* 1990b; Zolkiewska *et al.* 1994). Until a complete characterization of the substrates of these enzymes is available, the role of mono(ADP-ribosyl)ation in cell cycle control and regulation of cell proliferation will not be understood. However, it will now be possible to use c-*fos* gene expression as the endpoint to identify those cellular events that are sensitive to MIBG.

7.5 Effect of MIBG on SMC migration

7.5.1 Background/rationale

Cell migration has been extensively studied because it is known to occur during embryogenesis, wound healing, tumour metastasis and angiogenesis. Although complete details of cell migration are not well understood, cell migration is known to involve regulated attachment and detachment, cytoskeletal plasticity, contraction of non-muscle myosin and actin, and protein synthesis (Caterina & Devreotes 1991; Kelley *et al.* 1991; Madri *et al.* 1991). Many extracellular signals can stimulate migration, including physical forces (Ingber & Folkman 1989), vasoactive hormones (Bell & Madri 1989; Bell & Madri 1990), growth factors (Madri *et al.* 1991), ions, pH and pO_2 (Banai *et al.* 1990). Other factors that regulate SMC migration include plasma and platelets, hemodynamics, macrophages, SMCs and endothelial cells. Unfortunately, the intracellular signaling pathways involved in migration and directed cell movement are presently not clear. However, reorganization of the cytoskeleton and alterations in ECM contacts must occur, but how these events are coordinated is unknown (Stossel 1993).

Migration of cells plays a key role in the formation of a restenotic lesion post-vascular injury. Normal SMCs in the medial layer of the vessel wall undergo phenotypic modulation from the contractile state to a synthetic state after injury. This change in cell state renders the SMCs capable of directional movement in response to chemoattractant factors (i.e. PDGF, AngII, TGF-β, bFGF, etc.) and other environmental stimuli, and involves a marked change in cytoskeletal structure. The typical schema of events described for neointimal lesion formation in a rat carotid model involves a short burst of SMC proliferation, followed by migration of the cells from the media to the (neo)intima through breaks in the internal elastic lamina, with subsequent rounds of cell proliferation and ECM deposition (Casscells 1992; Schwartz *et al.* 1995a; Schwartz & Reidy 1996). In

other animal models of injury, the cellular events and timeline of progression may not be similar to that of the rat model, but still include both cellular migration from the media of the vessel wall into the (neo)intima and cellular proliferation with deposition of ECM (Schwartz 1994). Both cell migration and cell proliferation are equally important for neointimal formation, since restenosis can be prevented by inhibitors of either migration or cell proliferation (in many experimental systems) (Landzberg *et al.* 1997; Lefkovits & Topol 1997).

The progression of tumours is also characterized by cell proliferation (tumourigenicity) and cell migration (metastasis). Metastasis involves the movement of cancerous cells from one location to another and involves cellular migration. Many cancer therapies involve the use of compounds which not only halt the growth of a tumour but also retard the spreading of tumour cells. MIBG, a known inhibitor of arg-mART, used as both a radiolabelled and chemotherapeutic agent for the treatment of neuroendocrine tumours and neuroblastoma, inhibits both tumour growth and metastases of neuroblastoma type tumours (Hoefnagel *et al.* 1987; Hoefnagel *et al.* 1991; Kuin *et al.* 1999; Smets *et al.* 1988b; Taal *et al.* 1999; Taal *et al.* 1996; Zuetenhorst *et al.* 1999). Moreover, inhibitors of ARTs were found to inhibit the chemotaxis of human polymorphonuclear neutrophils (PMNs) and inhibition of the enzyme activity correlated closely with the inhibition of both chemotaxis and actin assembly (Allport *et al.* 1996a; Allport *et al.* 1996b). Interestingly, chemotactic activity in PMNs has been associated with ART1 (Kefalas *et al.* 1997; Kefalas *et al.* 1998), a GPI-linked cell surface enzyme also found in skeletal muscle and lymphocytes (Nemoto *et al.* 1996; Zolkiewska *et al.* 1992). In skeletal muscle, the substrate for the enzyme appears to be integrin α7 (Zolkiewska & Moss 1993), an adhesion receptor for laminin, whereas in T cells the substrate appears to be lymphocyte function-activated molecule 1 (LFA-1) (Nemoto *et al.*

1996). It may then be reasonable to assume that ADP-ribosylation of integrins on the surface of SMCs could perhaps trigger integrin signaling for cytoskeletal re-alignment or affect the adhesion of SMCs to the ECM. Saxty *et al.* (1998b) have already investigated the possibility that a mART activity might be found on SMCs. Using the A7r5 SMC cell line derived from embyronic rat thoracic aorta, they found that the chemotactic activity of A7r5 cells was independent of mART activity, even though a novel panel of mART inhibitors reduced the cell migration. Although a lack of cell surface mART may have been indicated, this study does not rule out the possibility that an intracellular mART is being activated during cell migration events, particularly since intracellular mARTs have already been shown to be associated with desmin filament rearrangement and the rearrangement of actin cytoskeletal components (Clancy *et al.* 1995; Huang *et al.* 1993; Okazaki & Moss 1996b; Terashima *et al.* 1992; Terashima *et al.* 1999; Terashima *et al.* 1995; Yuan *et al.* 1999; Zhou *et al.* 1996). As a result, it was of interest to determine if MIBG was capable of inhibiting SMC migration, an event that is associated with intimal lesion formation.

7.5.2 Specific aims

1. To assess the chemotactic action of AngII and PGE_2.
2. To determine the effect of MIBG on SMC migration.

7.5.3 Experimental design

Growing porcine SMCs were seeded into a Boyden chamber and migration through a membrane with 5 μM pores assessed with and without chemoattractant in the lower wells of the chamber. Inclusion of MIBG in the upper wells of the chamber was used to measure the effect of MIBG on SMC migration.

7.5.4 Results

7.5.4.1 Effect of PGE_2 and AngII on SMC migration

Several growth factors are known to stimulate SMC migration, including PDGF, interleukins and TNFα (Abedi *et al.* 1995; Abedi & Zachary 1995; Jang *et al.* 1993; Yue *et al.* 1994). AngII has also been shown to induce chemotaxis (Bell & Madri 1990; Dubey *et al.* 1995). It was therefore of interest to determine whether PGE_2 was also capable of stimulating SMC migration across a membrane in an artificial setting. Using the Boyden chamber method, it was observed that PGE_2 (10^{-6} M) was able to stimulate SMC migration (Figure 71A). Similarly, AngII (10^{-5} M) could direct SMC migration, as well as TxA_2 (10^{-7} M) and to a lesser extent PGI_2 (10^{-6} M) (Figure 71A). These data confirm that AngII is a chemoattractant factor for porcine coronary artery SMCs and also establish that PGE_2 is a chemoattractant for SMCs as are other prostanoids.

7.5.4.2 Effect of MIBG on AngII-mediated SMC migration

Since MIBG prevents the differentiation of L6 skeletal myoblasts, and inhibits cell growth and proliferation of both H4IIE hepatoma cells and SMCs, it was of interest to determine if MIBG would also affect SMC migration. Addition of MIBG (50 μM) to the upper wells of the Boyden chamber demonstrated that MIBG was capable of significantly decreasing the migratory response of SMCs to AngII (10^{-5} M), returning the levels to almost basal (Figure 71B). These data demonstrate that MIBG inhibits SMC migration.

7.5.5 Discussion

Migration and proliferation of SMCs are hallmark features of restenotic lesion formation (Landzberg *et al.* 1997; Schwartz *et al.* 1995a). Several reports in the literature have provided evidence that factors derived from platelets, injured endothelial cells and

FIGURE 71: ***Activation of Migration in SMCs by Angiotensin II and Prostaglandin E_2. Inhibition by MIBG.***

Growing SMCs were placed into a Boyden chamber and directional movement of SMCs through a 5 μm membrane towards a chemoattractant over 48 h monitored as described in section 4.5. SMCs on the underside of the membrane were fixed, stained and counted. (A) Chemoattractants placed into the lower chamber included angiotensin II (AngII) (10^{-5} M), PGE_2 (10^{-6} M), PGI_2 (10^{-6} M) or TxA_2 (10^{-7} M). (B) AngII (10^{-5} M) was placed into the lower chamber and MIBG (50 μM) in the upper chamber for the migration period (48 h). Data are presented as mean ± SE (n = 6). The graphs are representative of one of two independent experiments using different SMC isolations, both of which exhibited a similar response. Comparisons in (A) were made relative to untreated SMCs while comparisons in (B) were made relative to AngII treated SMCs with the Student's t-test (*, $p < 0.05$). (Data generated by Shawn Thomas, a B.Sc.Med summer student, and shown with his permission).

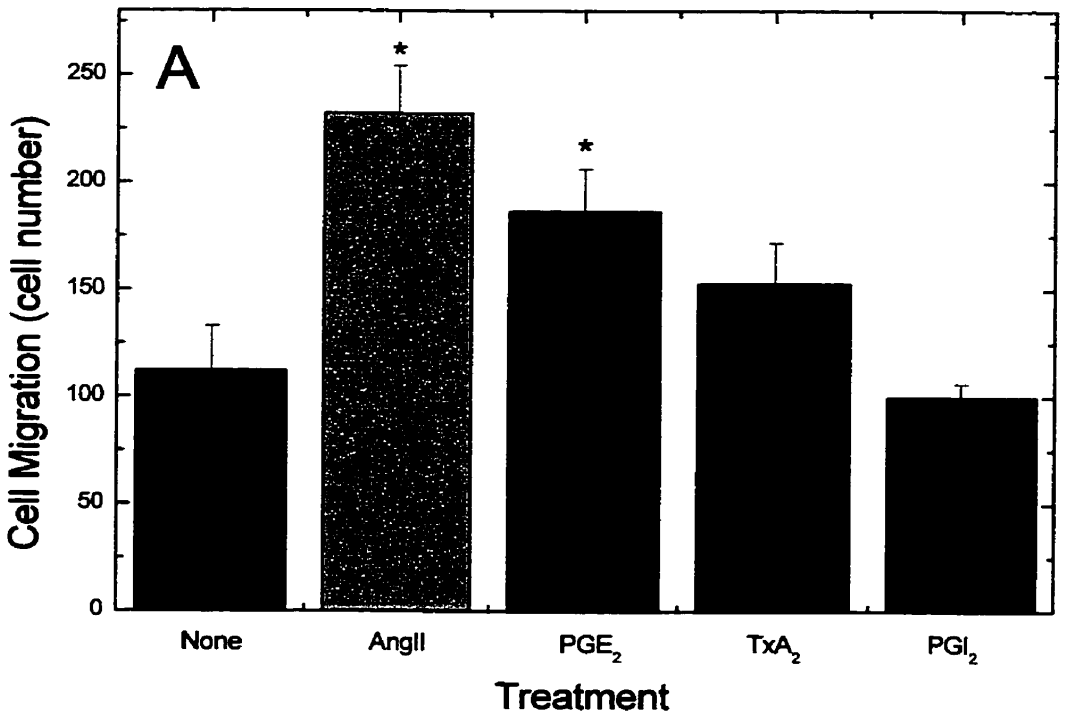
A
Cell Migration (cell number)
250
200
150
100
50
0
*
*
None
AngII
PGE2
TxA2
PGI2
Treatment

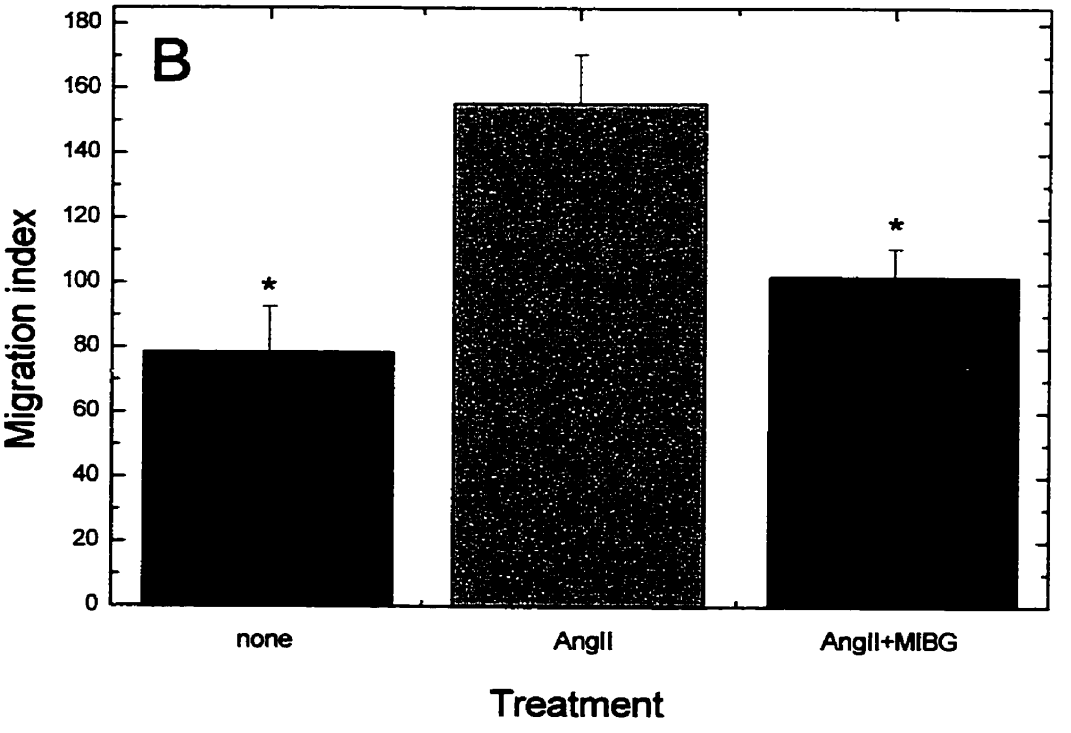
B
Migration index
180
160
140
120
100
80
60
40
20
0
*
*
none
AngII
AngII+MIBG
Treatment

SMCs are the primary products leading to both migration and proliferation of SMCs (Casscells 1992; Golino *et al.* 1997; Ross *et al.* 1986). Although the best characterized factors include PDGF, EGF, FGF, IL-1, IL-6 and TNFα, other agents, including thrombin and prostanoids such as TxA_2 and PGE_2, may also be involved (Hanasaki *et al.* 1990; Morinelli *et al.* 1994; Nagata *et al.* 1992).

In this study the ability of a peptide growth factor, AngII, and a nonpeptide growth factor, PGE_2 (as established in section 7.2), to promote SMC migration was studied using a Boyden chamber. AngII is already an established chemotactic factor for SMCs (Bell & Madri 1990; Dubey *et al.* 1995) and was used to determine the degree of chemotaxis induced by PGE_2. The ability of PGE_2 to cause migration was almost of the same magnitude as AngII (Figure 71A), suggesting a similar efficacy. In comparison to the proliferative response generated by these compounds (Figures 44, 45, 46), the results of this study would support the conclusion that AngII is a stronger chemotactic agent than PGE_2. Other prostanoids have previously been shown to have chemotactic abilities with respect to a variety of different cell types (Hofbauer *et al.* 2000; Nie *et al.* 2000). More recently, Ratti *et al.* (1998) indirectly demonstrated the importance of TxA_2 in promoting SMC migration and proliferation by reporting that picotamide, an anti-thromboxane agent, inhibited both the migration and proliferation of rat arterial myocytes. The ability of PGE_2 to promote migration of SMCs may be related to its ability to stimulate the proliferation of quiescent SMCs (section 7.2). Interestingly, PGE_2 has also been shown to decrease collagen synthesis, which may be a factor in SMC migration (Diaz *et al.* 1993; Holmes *et al.* 1997). Whether the breakdown of collagen promoted by PGE_2 is due to increases in MMP activity (i.e. MMP-9) remains to be determined.

MIBG treatment inhibited the migration of SMCs promoted by AngII (Figure 71B). Saxty *et al.* (1998b) had previously demonstrated that a panel of structurally

unrelated ADP-ribosylation inhibitors prevented chemotaxis in a rat thoracic aorta SMC cell line (A7r5). These inhibitors included Vitamin $K_{1/3}$, novobiocin, nicotinamide and small guanidine containing analogues of arginine such as agmatine (decarboxyl-arginine), arginine methylester (AME) and DEA-BAG (Banasik *et al.* 1992; Soman *et al.* 1986). Although all of the inhibitors were capable of inhibiting chemotaxis, and the efficacy of the panel of inhibitors suggested that it might be through inhibition of ART1 (a GPI-linked extracellular mART discovered by Zolkiewska and colleagues (Zolkiewska & Moss 1993; Zolkiewska *et al.* 1992)), it was concluded that these inhibitors could not operate by this mechanism since ART1 was not present on A7r5 SMCs (Saxty *et al.* 1998b). Rather, the authors agreed with the findings of Taguchi *et al.* (1993) that, similar to L-arginine, the inhibitory effects were likely due to an effect on nitric oxide generation instead of ADP-ribosylation. While it is possible that the SMCs used in this study do express ART1, MIBG may alternatively influence an intracellular ADP-ribosylation reaction. This assumption can be made based on the ability of AngII to increase an arg-mART activity in a previous section (section 7.3). Although enzyme activity was explored with respect to the capacity of AngII as a mitogen, a similar arg-mART reaction may be activated for the regulation of migration since both proliferation and migration are characteristic of the synthetic SMC phenotype. For example, MIBG may be inhibiting an ADP-ribosylation reaction involved in the assembly/disassembly of actin filaments (Clancy *et al.* 1995; Okazaki & Moss 1996b; Terashima *et al.* 1992; Terashima *et al.* 1999; Terashima *et al.* 1995). Actin is an important protein component of the cytoskeleton and is an important filamentous protein with respect to motility and contraction in SMCs (Elbaum *et al.* 1999; Takai *et al.* 1995; Taylor 1986). Alternatively, MIBG inhibits desmin assembly/disassembly (Huang *et al.* 1993; Yuan *et al.* 1999; Zhou *et al.* 1996) which can also affect the ability of the cell to migrate (and possibly even

proliferate) (Bernal & Stahel 1985; Li *et al.* 1997; Siegel *et al.* 1998). It also remains plausible that MIBG may affect the cytoskeletal rearrangements necessary for migration through key GTP-binding proteins such as Rho, Rac and cdc42.

Although a number of potential modes of action have been supplied, a cytotoxic effect of MIBG on the SMCs cannot be ruled out. Nevertheless, based on the response of SMCs in culture to MIBG seen in the previous section (section 7.3), it is unlikely that cytotoxicity is the mechanism of action on cell migration. Presently, the mechanism whereby MIBG inhibits SMC migration remains unknown and will the subject of future studies. Additional studies will include: i) actin and desmin assembly/disassembly and its regulation by arg-mART/MIBG in SMCs, ii) an examination of extracellular components that may be affected by MIBG, and iii) identification and characterization of the mART involved in SMC migration.

7.6 Summary

The studies summarized in this chapter cover the cell proliferative and migratory activities of SMCs, including the characterization of a novel stimulator of SMC proliferation and migration, PGE_2, and an examination of how MIBG might inhibit both of these cellular events. Furthermore, a mitogen-activated arg-mART activity associated with the microsomal fraction of SMCs was detected. While the mechanism of MIBG action was not fully clarified, the experiments that were described led to the identification of the c-*fos* gene as a target for this inhibitor. More mechanistic studies are now possible given this information. Moreover, the results of these studies, which indicate that MIBG can successfully and efficiently inhibit both the migration and proliferation of SMCs, two of the critical events in restenotic lesion formation, warrant further investigation of this compound in models of vascular injury and intimal lesion formation. The next chapter

describes the initial studies that were undertaken to examine the suitability of this compound for the treatment of restenosis.

8.0 Models of neointimal lesion formation

8.1 Introduction

Restenosis remains a significant problem following all types of revascularization procedures, including coronary angioplasty, occurring in 30 to 50% of cases (Badimon *et al.* 1995; Casterella & Teirstein 1999). Several factors contribute to the formation of an (neo)intimal lesion within injured coronary arteries, including thrombus formation, elastic artery recoil, migration and proliferation of SMCs, and vascular remodeling (Ellis & Muller 1992; Glagov 1994; Harker 1987; Lafont *et al.* 1995; Lau & Sigwart 1995; Liu *et al.* 1989; Mintz *et al.* 1996; Post *et al.* 1994; Schwartz *et al.* 1992a; Schwartz *et al.* 1995a; Schwartz & Reidy 1996; Steele *et al.* 1985; Wilentz *et al.* 1987). Although all of these factors contribute to lesion formation, the central mechanism appears to involve the SMC. For this reason, inhibition of SMC activation (i.e. migration and/or proliferation and/or deposition of ECM) could have a large impact on the pathogenesis on the morbidity of revascularization procedures. As a result, the behaviour of SMCs has been studied in a variety of systems *in vitro* and *in vivo*, and these cells have been the target of many studies and therapeutic treatments for the amelioration of restenosis (Andres 1998; Landzberg *et al.* 1997; Neville & Sidawy 1998; Nikol & Hofling 1995).

Many different types of animal models have been used for the study of restenosis post-angioplasty. Smaller animals (i.e. rats, rabbits and mice) have always been more popular and, as such, the pathogenesis and physiological relevance of injury in these models is better defined (Schwartz *et al.* 1995a). The popularity of these models is based on the fact that smaller animals are well characterized genetically, less expensive and more readily available. As well, they are easier to manipulate and, because they are smaller, the quantities of investigational new drugs required for *in vivo* screening are less (Handley 1995; Johnson *et al.* 1999). On the other hand, with the use of these smaller

animal models, especially for the testing of therapeutic compounds for the treatment of restenosis, the predictive value of the data is limited (Johnson *et al.* 1999). Likely this is the result of differences in pathophysiology and physiology of the animal models themselves (Schwartz 1994). Different portions of the vascular tree would also by employed, since in the rat, for example, the coronary arteries are too small.

Larger animals (i.e. pigs, dogs and primates), though less popular, have nevertheless been utilized for the pre-clinical evaluation of interventions to reduce restenosis. The disadvantages of the larger animal models are primarily the converse of the advantages of small animal models. These include greatly increased cost and limited distribution potential, less precise genetic characterization, paucity of transgenic models, more difficulty in manipulations and the requirement for larger quantities of investigational new drugs (Johnson *et al.* 1999; Schwartz 1994). However, the larger size of the animals allows for the use of instrumentation and evaluation of results much as would be done in humans. As well, in the case of pigs, there is a similarity of the coronary artery anatomy, and the histopathological characteristics of the proliferative response following deep coronary artery injury closely resemble that seen in humans (Schwartz *et al.* 1990; Steele *et al.* 1985). Thus, large animal models of restenosis, although less defined, have provided valuable insight into the progression of human disease. However, both the coronary vasculature and other vascular beds such as the femoral artery and carotid artery have been employed. Since there are significant differences in the responses of these vessels, interpretation of results from other vascular beds should be applied to the human coronaries with judicious care (Badimon *et al.* 1998; Pyles *et al.* 1997).

To this point, all studies in this thesis have employed cells in culture. It is evident from these experiments that MIBG is an agent that has potent anti-proliferative, anti-

migratory and anti-differentiation properties. Thus, MIBG might have application for the prevention of restenosis. Although an animal study appears warranted, an organ culture system was first employed to validate the effect of MIBG on neointimal formation.

A balloon injury similar to that which occurs during coronary angioplasty can be easily applied to the coronary vasculature of an *ex vivo* heart (Koo & Gotlieb 1992). Studies by Gotlieb and colleagues (Gotlieb & Boden 1984; Koo & Gotlieb 1989; Koo & Gotlieb 1991; Koo & Gotlieb 1992) and Wilson *et al.* (1999) have established that intimal proliferation occurs in coronary arteries in organ culture following medial distention by balloon inflation. Furthermore, with this model Wilson *et al.* (1999) demonstrated that the neointimal formation within the coronary artery segments can be inhibited by agents that alter the progression of restenosis.

The study that was conducted examined neointimal formation in the presence and absence of MIBG (0 to 50 μM) for 14 days. As reported by Wilson *et al.* (1999), a reduction in neointimal formation is indicated by a decrease in neointimal index, a ratio of intimal area to medial area (Figure 72). It was observed that MIBG reduced the neointimal index to basal levels at and above concentrations of 10 μM (Figure 73). Furthermore, there is no evidence of adverse effects upon histological examination (Figure 73A). Interestingly, migration may have a greater contribution to this model than cell proliferation (Wilson, Wong & Zahradka, unpublished observations). Regardless, these data clearly establish that MIBG has the potential to prevent restenosis. Extension to a live animal model was therefore initiated.

Based on the findings of the previous chapters and the success of MIBG to prevent intimal lesion formation in an organ culture model of restenosis, a specific hypothesis was proposed: *MIBG will reduce the extent of neointimal formation induced*

FIGURE 72: ***Organ Culture Model of Balloon Angioplasty.***

Porcine left anterior descending coronary arteries from *ex vivo* hearts were injured with a balloon catheter and placed into culture for 14 days according to Wilson *et al.* (1999). Control non-injured arteries were excised from weight-matched hearts and also placed into culture for 14 days. Segments were then fixed, embedded in resin and transected with an ultramicrotome. Lee's methylene blue stained sections were visualized under light microscopy. (A) Photomicrographs of control and balloon-injured segments are shown. Magnification: 11×. The different layers of the vasculature are indicated. (B) Quantitave analysis of neointimal thickening in control and injured vessels. Neointimal index = [neointimal area/medial area]. Data are presented as mean ± SE with the values for the control vessel set to 100%. Comparisons were made between non-injured and injured vessels using the Student's t-test (*, $p < 0.05$). One of three experiments is presented, all of which exhibited a similar response. For each experiment $n = 6$. (Data were generated by Jeff Werner, and are shown with his permission).

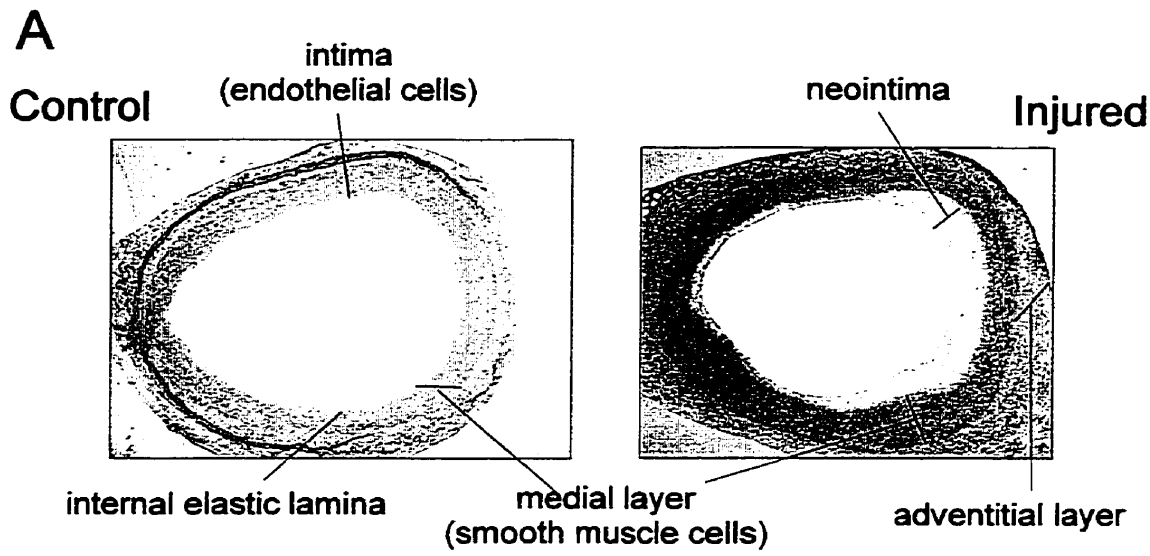
A
Control
intima
(endothelial cells)
neointima
Injured
internal elastic lamina
medial layer
(smooth muscle cells)
adventitial layer

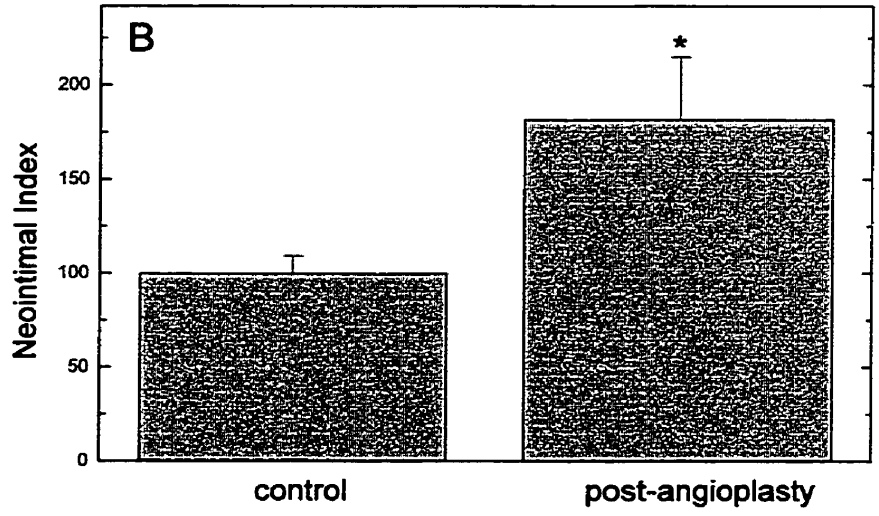
B
Neointimal Index
200
150
100
50
0
*
control
post-angioplasty

FIGURE 73: ***Effect of MIBG on Neointimal Formation after Balloon Angioplasty in an Organ Culture Model.***

Porcine left anterior descending coronary arteries from *ex vivo* hearts were injured with a balloon catheter and placed into culture for 14 days according to Wilson *et al.* (1999). Control non-injured arteries were excised from weight-matched hearts and also placed into culture for 14 days. Some balloon-injured segments were exposed to MIBG continuously over the 14 day period. Segments were then fixed, embedded in resin and transected with an ultramicrotome. Lee's methylene blue stained sections were visualized by light microscopy. (A) Photomicrographs of non-injured, control (control), balloon-injured (injured) and balloon-injured with MIBG (MIBG treated) are shown. Magnification: 15×. One of three experiments is presented, all of which exhibited a similar response. (B) Quantitative analysis of neointimal thickening in control, injured and MIBG-treated vessels. MIBG concentrations were varied in this experiment (10, 40 and 100 μM). Neointimal index = [neointimal area/medial area]. Data are presented as mean ± SE. Comparisons were made between non-injured and injured vessels (#, $p < 0.05$) and injured vessels and MIBG treated vessels (*, $p < 0.05$) with the Student's t-test. For each experiment $n = 6$. (Data were generated by Jeff Werner and are shown with his permission).

A

Control

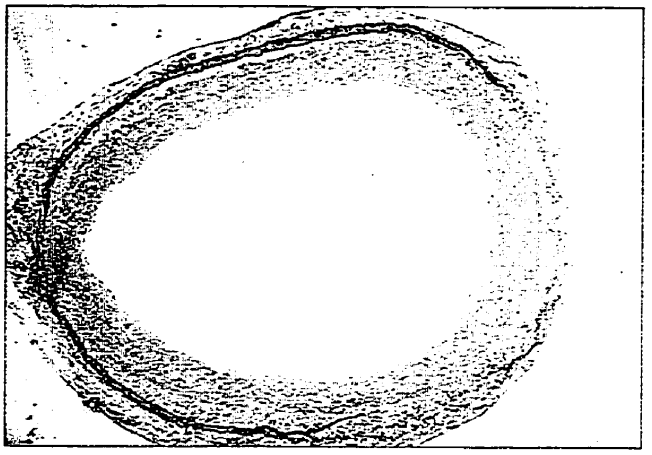

Injured

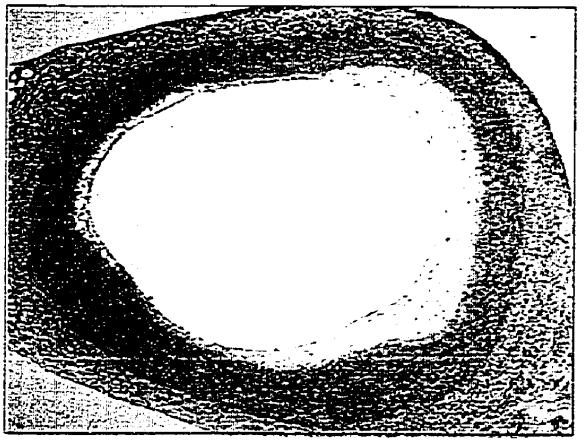

MIBG
treated

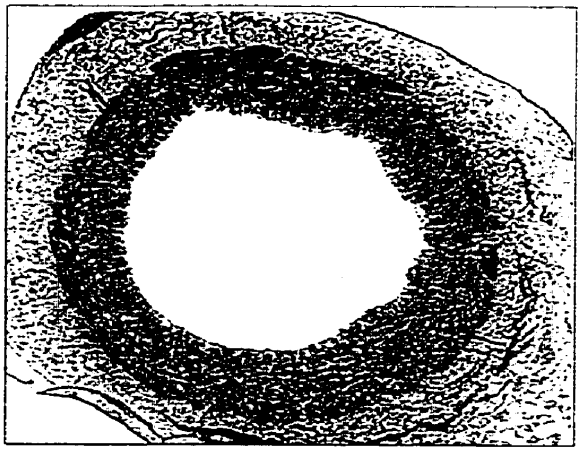

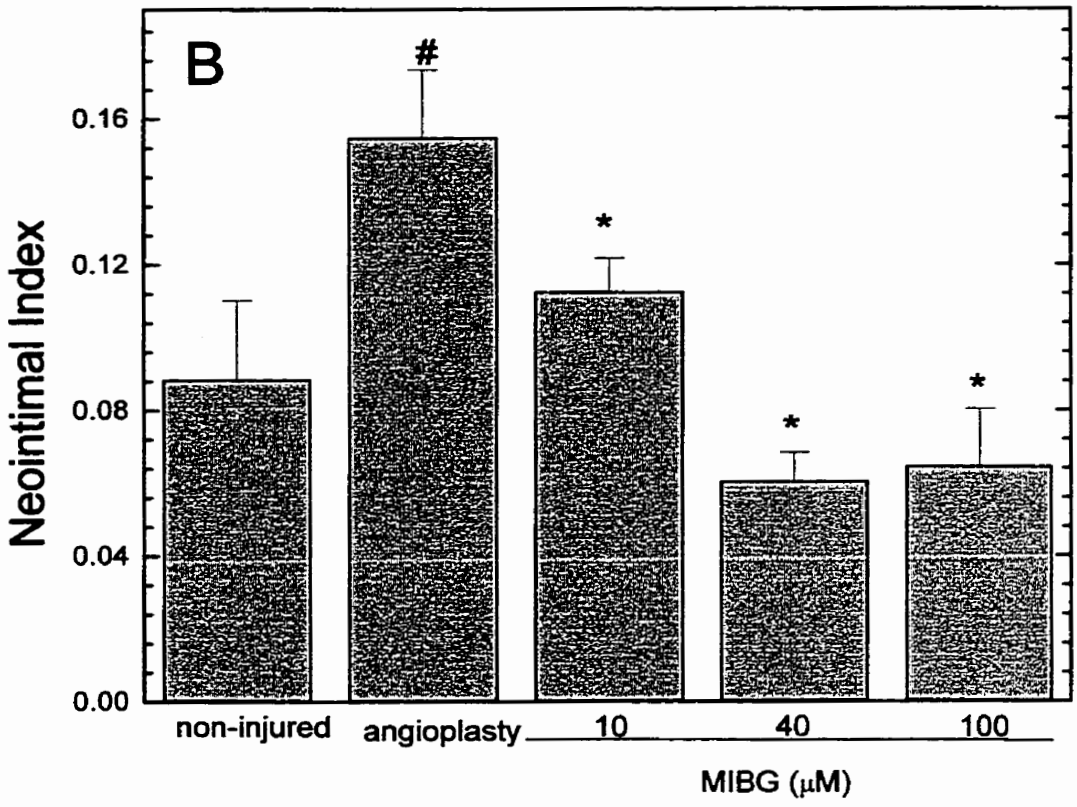
B
#
*
*
*
Neointimal Index
0.16
0.12
0.08
0.04
0.00
non-injured
angioplasty
10
40
100
MIBG (μM)

by balloon angioplasty when applied to the perivascular surface with a surgical fibrin glue (Tisseel).

8.2 *In vivo* porcine femoral angioplasty model of restenosis

8.2.1 Background/rationale

MIBG was tested for its ability to inhibit restenosis with an organ culture model of neointimal formation. With this system, MIBG was shown to be effective under conditions where injury and repair were simulated in an *ex vivo* culture environment. To extend these studies and provide experimental information that would eventually permit clinical application, a live animal model of balloon angioplasty was developed. The pig was chosen because of its greater similarity to humans (Ferrell *et al.* 1992; Johnson *et al.* 1999), while the femoral artery was selected for its accessibility. Although this particular vessel is not identical to the coronary arteries in structure and properties, both vessels nevertheless respond similarly to vascular injury and this permits an examination of events common to both peripheral and coronary vascular disease. Furthermore, Lamawansa *et al.* (1997 and 1999) and Yang *et al.* (1996) demonstrated that balloon injury of the porcine femoral artery results in the formation of a neointima. This particular pig model has a number of advantages: i) it is easy to produce a consistent injury, ii) it is accessible for angiography and IVUS (intravascular ultrasound), and iii) the response to injury is similar to human arteries (Ferrell *et al.* 1992).

8.2.2 Specific Aims

1. To establish the porcine femoral artery model of balloon injury as a viable experimental model for the study of restenosis.

2. To determine the effect of MIBG on neointimal lesion formation in this model.

8.2.3 Experimental Design

An *in vivo* model of balloon injury will be used to extend the findings generated using the organ culture model of balloon injury and restenosis. Porcine femoral arteries will be injured, and fibrin glue applied ± MIBG in a random, double-blind manner. The animals will be allowed to recover and the arteries will be harvested after 14 days. Each animal will serve as its own control (vessel ± MIBG), and each vessel will contain both positive and negative controls (± injury). Each femoral artery will be divided into four sections (i.e. proximal, balloon-injured, distal and arteriotomy). Each region is depicted on the angiogram presented in Figure 74. Vessels will be cut into segments and frozen in OCT for cryosectioning. Following staining with Lee's methylene blue, morphometric analysis will be used to calculate the neointimal index.

8.2.4 Results

8.2.4.1 Effect of MIBG on femoral artery balloon injury and restenosis

To define the response of the femoral artery to balloon injury, proximal segments of the vessel were compared to the balloon-injured region of the vessel. Balloon-injury resulted in a significant thickening of the intimal region (Figure 75B) compared to uninjured regions (Figure 75A) consistent with induction of a lesion. Treatment of the balloon-injured segment with MIBG significantly inhibited neointimal formation (Figure 75C). It was also interesting to note that the medial layer of injured segments (Figure 75B) had a more cellular and fibrotic pattern of staining compared to uninjured regions (Figure 75A), and injured regions treated with MIBG (Figure 75C). Moreover, in the

FIGURE 74: ***Angiogram of Porcine Femoral Artery Region.***

Porcine femoral arteries were subjected to balloon angioplasty *in vivo* and harvested after 14 days (see Materials and Methods section 4.2.4). Angiography was performed at the time of sacrifice (see Materials and Methods section 4.2.4.1). The four regions of the femoral artery analyzed in the experiment are identified: proximal region, balloon-injured region (site of angioplasty), distal region and arteriotomy site.

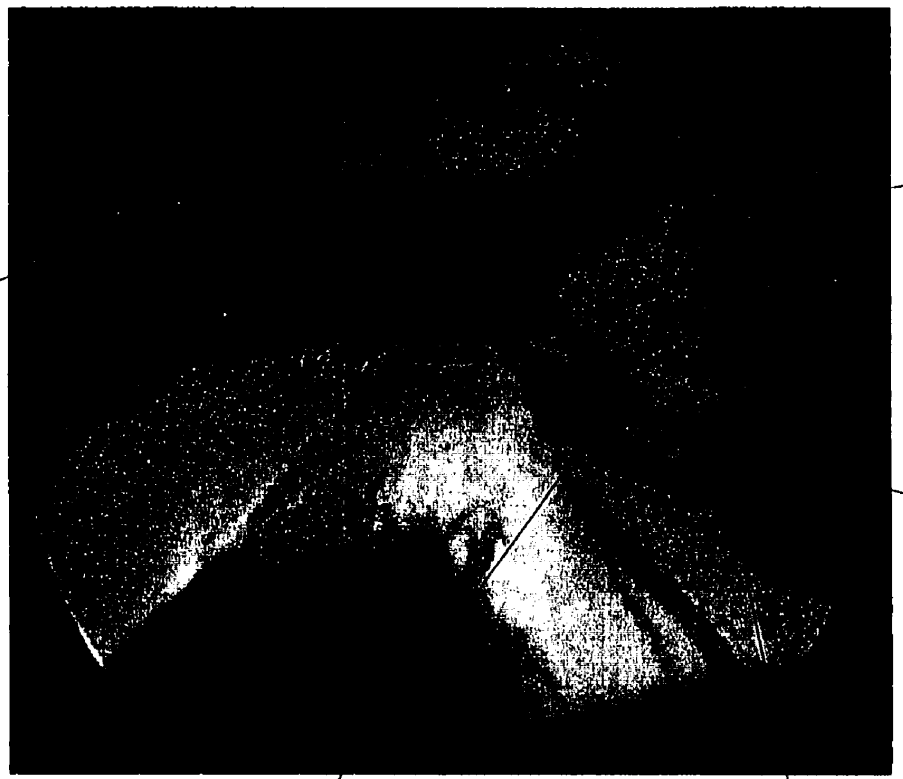
Site of
Angioplasty
Proximal
Region
Superficial
Femoral Artery
Distal Region
Arteriotomy

FIGURE 75: ***Porcine Femoral Artery Balloon-Injury Model. Effect of MIBG on Neointimal Formation.***

Porcine femoral arteries were injured with a balloon catheter *in vivo* and the vessels harvested after 14 days. Femoral arteries were divided into four regions: proximal (non-injured control), balloon (balloon-injured region), distal (region with possible endothelial denudation) and arteriotomy (cut site injury and site of entry for balloon). Each segment of femoral artery was overlayed with fibrin glue after the balloon-angioplasty procedure was completed. The fibrin glue contained either MIBG (25 mM) or no inhibitor. At the time of harvest, vessel regions were cut into two and each segment placed into OCT/Tissue Tek, flash frozen in a dry ice/ethanol bath and stored at -80°C. Segments were transected using a cryostat and sections stained with Lee's methylene blue after fixation. Photomicrographs were captured from (A) uninjured proximal region, (B) balloon-injured region, and (C) balloon-injured region with MIBG treatment. For each treatment condition n = 13. Magnification = 90×.

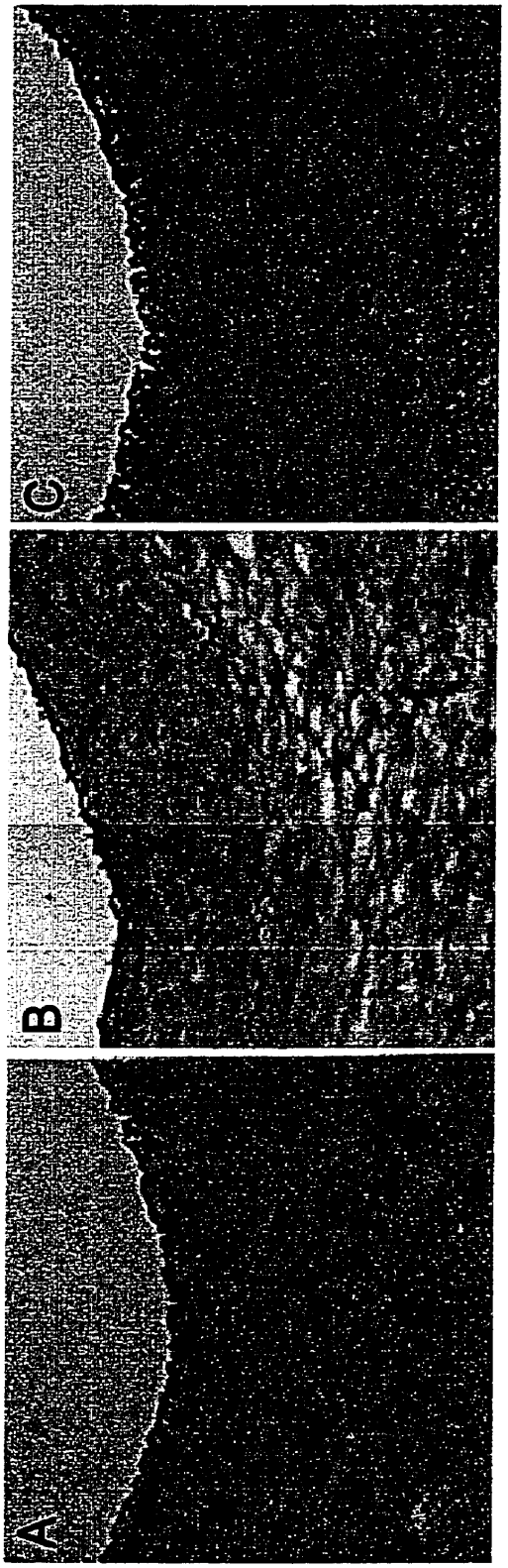
C
B
A

injured segment treated with MIBG, re-endothelialization appears to be occurring (Figure 75C) when compared to the injured segment without MIBG treatment (Figure 75B). This observation would need to be confirmed by conducting immunostaining experiments using antibodies for endothelial cell specific markers. These data suggest that MIBG is effective in preventing intimal lesion formation after arterial injury and that it will be an effective therapeutic option for the treatment of restenosis. The data also indicate that MIBG *in vivo* may be affecting not only the proliferation of SMCs, but perhaps also SMC migration, which supports the data presented in chapter 7.

A quantitative measure of neointimal formation revealed that MIBG treatment significantly decreased the neointimal index of the balloon injured region compared to the non-MIBG treated balloon injured region. (Figure 76). Moreover, in the distal and arteriotomy vessel segments, MIBG treatment was able to decrease the degree of neointimal formation observed (Figure 76) although statistically significant differences were not attained. The neointimal index was calculated for all 13 pigs that were in the experimental group, however, one pig was excluded from both the graphical and statistical analysis due to rupture of the femoral artery on one side during the angioplasty procedure and lack of balloon inflation on the other side. The decision to exclude this pig from the analysis was made at the time of the initial procedure. The efficacy of MIBG treatment for attenuating intimal lesion formation in the balloon injured region was confirmed by a match-paired t-test ($p = 0.009$) (data not shown) that compared the mean of the difference of the neointimal indices in MIBG treated and untreated balloon injured regions to zero. These data suggest that MIBG effectively inhibits restenosis. In addition, MIBG may influence vessel remodeling.

FIGURE 76: ***Quantitative Analysis of Vessel Sections from the Porcine Femoral Artery Injury Model.***

Quantitative analysis of whole vessel photomicrographs was used to determine neointimal thickening in all segments ± MIBG treatment (25 mM). Neointimal index = [neointimal area/medial area]. Data are presented as mean ± SE (n = 12). One animal was not included in the statistical analysis due to rupture of the vessels during balloon injury. Comparisons were made between untreated (balN) and treated (balM) balloon injured segments (*, $p < 0.05$) and injured untreated (balN, distN, artN) vs. proximal untreated (proxN) femoral artery segments (‡, $p < 0.05$). Column designations: proximal region = prox, balloon-injured region = bal, distal region = dist, arteriotomy site = art; untreated = N and MIBG-treated = M.

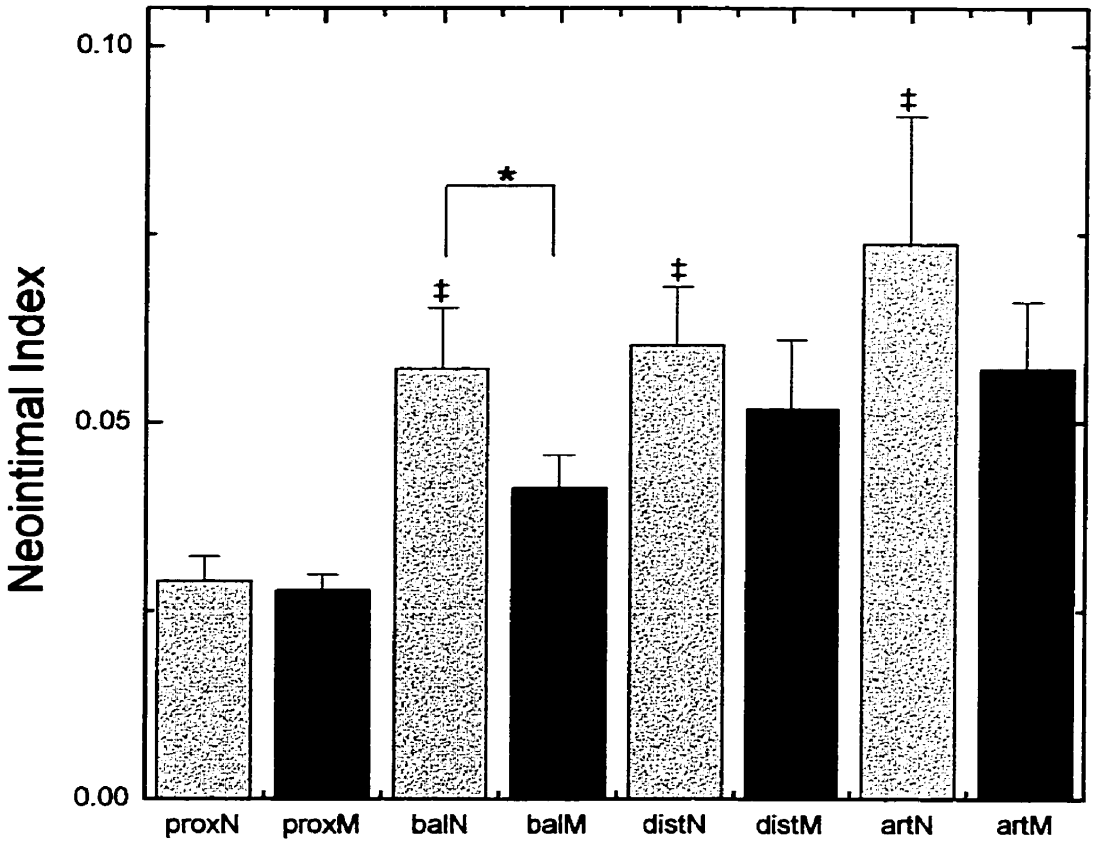
Neointimal Index
0.10
0.05
0.00
*
‡
‡
‡
‡
proxN
proxM
balN
balM
distN
distM
artN
artM

8.2.5 Discussion

Balloon injury of the porcine femoral artery resulted in a visible intimal thickening (Figure 75). It was noted that the medial layer had a more cellular and fibrous appearance than uninjured segments of the femoral artery, possibly indicating that SMCs from the medial layer had migrated to the lumen side and initiated the formation of the intimal lesion. Hypercellularity is also a hallmark of the wound healing response. Interestingly, the morphological appearance of the MIBG-treated segments was similar to that of the uninjured control segments, indicating that MIBG had indeed inhibited formation of the neointima. In the MIBG-treated segment, there appear to be cells that have partially re-colonized the lumen surface (Figure 75C). Although specific staining for endothelial cells (ECs) was not done, and is planned for the future, this may suggest that MIBG is promoting the re-endothelialization of the lumen surface and could potentially be one of the mechanisms by which MIBG inhibits neointimal formation. The endothelial layer has been shown to play an important role in maintaining the low rate of SMC proliferation and migration under normal conditions (Fishman *et al.* 1975).

In the balloon-injured segment, MIBG treatment significantly reduced the neointimal index compared to injured segments (Figure 76). MIBG also decreased the neointimal index in the distal and arteriotomy segments, although significance was not observed (Figure 76). This latter observation may indicate that MIBG is working in part by promoting positive remodeling of the vessel so that the lumen diameter is larger. Alternatively, MIBG may be reducing the sympathetically-mediated vasoconstriction that occurs following angioplasty (Gregorini *et al.* 1994; Gregorini *et al.* 1997). Neuronal release of NE is increased for up to 4 weeks following experimental angioplasty and persistent hypersensitivity to catecholamines is seen after angioplasty (Candipan *et al.* 1994). Considering the importance of elastic recoil to constrictive arterial remodeling and

thus restenosis (Ardissino *et al.* 1991; Candipan *et al.* 1994; Tesfamariam & Cohen 1988), an effect by MIBG on this process would provide additional benefits beyond those specific to cell migration and proliferation. Studies of the relationship between MIBG and vasoconstriction should be pursued in the future.

The latter finding from above may also suggest that MIBG is capable of reducing intimal lesion formation regardless of the type of vascular injury that is observed (Figure 76). The angioplasty segment is subjected to a stretch/crush injury, the distal segment is primarily an endothelial cell denudation injury and the arteriotomy site contains a cut site injury with suture. Regardless of injury type, if SMCs were activated to migrate and/or proliferate, the amount of intimal thickening seen at a given site would increase assuming that intimal hyperplasia has a substantial contribution to restenosis. If MIBG were capable of inhibiting either or both SMC migation and proliferation, which is shown in chapter 7, MIBG should effectively decrease the neointimal index.

MIBG was applied to the perivascular surface in Tisseel. Tisseel is a commercially available fibrin glue that is used routinely in the surgical suite. The biochemical reaction that produces the coagulum involves a reaction between thrombin and fibrinogen. This particular reaction has been capitalized upon to produce a natural, biodegradable adhesive that has since been applied for sustained drug delivery (Senderoff *et al.* 1991). Interestingly, due to the dependency of the reaction on conditions such as pH and ionic strength, the microstructure of the fibrin polymer can be manipulated to control the relative availability of encapsulated drug (Senderoff *et al.* 1991). In our experimental system, the only concerns associated with the use of Tisseel were the fact that thrombin has been shown to promote fibrosis and formation of neointima (Gallo *et al.* 1998; Maruyama *et al.* 1997; Pakala & Benedict 1999; Salvioni *et al.* 1998; Stouffer *et al.* 1996) and that fibrin degradation products can promote SMC migration and proliferation

(Naito *et al.* 2000). However, considering the results, MIBG apparently is sufficiently potent to override any negative effects that might be attributed to thrombin and/or fibrin.

Release of MIBG from its depot will lead to distribution within the adjacent region of the vessel. MIBG will then enter the cells. The mechanism of entry may involve either passive diffusion or a NE transporter based uptake and release system. Within neuroblastoma tumours, the latter mechanism leads to the redistribution of MIBG over a significant distance from its original point of application (Servidei *et al.* 1995; Smets *et al.* 1989; Weber *et al.* 1996). In this way, MIBG may be reaching the medial layer and affecting the migration and proliferation of SMCs. On the other hand, if the adventitia plays an important role in the formation of neointima (Li *et al.* 2000; Shi *et al.* 1996a; Shi *et al.* 1996b; Zalewski & Shi 1997), then placement of MIBG on the adventitial surface should prevent the migration of myofibroblasts to the luminal surface. Future studies will examine the distribution and localization of activity for MIBG in preventing neointimal thickening.

Direct application of MIBG to a vessel surface avoids the potential problems associated with systemic delivery (Taal *et al.* 1996). However, one of the unknown factors then becomes the actual concentration of MIBG that reaches the cells/tissue within the localized area. In these experiments, MIBG at a concentration of 25 mM was encapsulated within a 1.0 mL bolus of Tisseel, which was applied to each femoral artery. It is assumed that 25 mM would not be the concentration that the local tissues are exposed to after whole body and other local environmental considerations are factored in. Nevertheless, in any local application, the question as to the amount that reaches the systemic circulation is a concern. Although the concentration of MIBG encapsultated within the Tisseel (25 mM) was 3 orders of magnitude higher that than required in our cellular studies for efficacy (i.e. 20 to 50 μM), the equivalent dosage (25 mM) given

systemically would be 0.5 mg/kg or 8.9 μM. Use of MIBG as a pharmacological/chemotherapeutic agent for the suppression of tumour growth (Taal *et al.* 1999; Taal *et al.* 1996; Zuetenhorst *et al.* 1999) has demonstrated that a non-toxic single dose bolus in humans is approximately 15 mg/kg. Animal studies of higher dosage regimens (up to 60 mg/kg) have shown that renal function is compromised first (at 40 mg/kg) and is the primary cause of death (Kuin *et al.* 1999). In these studies, the apparent systemic dosage would be considerably less than the concentrations already employed by Taal and colleagues for treatment of carcinoids syndromes (15 mg/kg) (Taal *et al.* 1999; Taal *et al.* 1996; Zuetenhorst *et al.* 1999) and only 4 times higher than the concentrations of MIBG employed for scintillographic detection purposes (Hoefnagel *et al.* 1987). Further investigations will be required to determine the local effective concentration of MIBG after release from the Tisseel depot, and the length of time that MIBG remains in the depot and the time period over which it is released.

MIBG may have an additional effect on inflammation and/or thrombus formation. Jonsson *et al.* (1998) demonstrated that MIBG inhibits histamine receptor binding on endothelial cells and prevents histamine-induced inositol-triphosphate and prostacyclin production, and arachidonic acid release (Halldorsson *et al.* 1992). Histamine, prostanoids and arachidonic acid participate in activation of pathways for inflammatory responses (Bach 1982; Hedqvist *et al.* 2000; Vane & Botting 1987). MIBG may thus be affecting the progression of restenosis, in part, by inhibiting the inflammatory response. Moreover, Hauschildt *et al.* (1998) have demonstrated that MIBG can prevent the production of TNF-α and IL-6 at the protein and mRNA level in human monocytes. Thus, if MIBG is able to inhibit the production of proinflammatory cytokines by monocytes, the inflammatory response may be considerably reduced and thus any effects on SMCs decreased. This is highly relevant to restenosis since both TNF-α and

interleukins have been shown to stimulate migration of SMCs (Shawn Thomas, unpublished observations; Jang *et al.* 1993; Rectenwald *et al.* 2000; Yue *et al.* 1994), and the inflammatory response has been proposed to play a role in intimal lesion formation (Biasucci *et al.* 1999; Forrester *et al.* 1991; Nikol & Hofling 1995; Virmani & Farb 1999).

Longer term studies are now in progress to determine if the inhibitory effects of MIBG are sustainable beyond 14 days. A 45 day study period also more closely reflects the time over which patients develop restenosis when relative growth rates are factored in. Moreover, pathology specimens will enable an examination for adverse effects caused by MIBG with respect to cytotoxicity.

8.3 Summary

This final section of the thesis deals with the use of models of angioplasty and subsequent restenosis, both *in vitro* and *in vivo*, in order to assess the efficacy of MIBG as an inhibitor of intimal lesion formation. Both the organ culture model of restenosis and the *in vivo* femoral artery angioplasty model of restenosis demonstrated significant formation of neointima in the injured regions of the vasculature in comparison with non-injured segments. In both models, MIBG treatment was associated with a significant reduction in intimal lesion size, with a neointimal index (neointima/media ratio) approaching baseline values. These findings suggest that MIBG has potential for use in the treatment of restenosis post-angioplasty. Furthermore, Tisseel has been identified as an effective delivery vehicle. Although a mechanism for the action of MIBG is not yet known, based on findings in previous chapters of this thesis, it is speculated that MIBG is affecting an arg-mART that may be important for signaling pathways associated with proliferation and migration of SMCs. Future studies will be directed at proving the safety

and efficacy of MIBG in a porcine model with the goal of initiating clinical trials to test MIBG as a treatment for revascularization-induced restenosis.

9.0 Conclusions and Significance

Twenty years after the first successful PTCA procedure (and approximately 30 years after the first successful CABG procedure), restenosis remains a significant complication in the battle against CAD. To date, an effective form of therapy to neutralize the problem has not been found (Landzberg *et al.* 1997; Lefkovits & Topol 1997), although there are promising therapeutic interventions in the early stages of clinical testing (eg. probucol, tranilast and radioactive stents). The time-span covered by my research has seen many technical, technological, methodological and therapeutic advances implemented for the treatment of CAD and subsequent restenosis. However, the improvement in short-term and long-term outcomes has only been satisfactory. Whether this is due to the increased practice of coronary interventions in the face of lagging knowledge of the patho/biology of restenosis remains to be determined. Nevertheless, advances in our understanding of the biology of the complications resulting from interventional procedures, coupled with technical improvements, should help with the development of more rational and enduring strategies for the treatment of restenosis.

Over the past 20 years, much time and effort has been invested in both the experimental and clinical testing of compounds that target cell migration and cell proliferation, specific growth factor receptors, thrombus formation and the ensuing inflammatory process, and, more recently, ECM degradation. Mechanical strategies (i.e. stents) are now favoured in many treatment centres, however, upon comparison with more traditional interventional procedures such as balloon angioplasty, it is apparent that the rates of restenosis are equivalent. The advent of adenoviral vectors and improvements in anti-sense strategies coupled with the attractiveness and assumed specificity of gene therapy has led many researchers to evaluate this modality of treatment for restenosis. However, patient safety is still of major concern and long-term outcomes are not proven.

Interestingly, the uniform failure of clinical trials using systemic therapies to prevent restenosis and the arrival of gene therapy sparked a revolution in the field of drug delivery systems, since the ability to specifically target a region of vascular tissue was required. Intraluminal drug and gene delivery systems that could be coupled to the angioplasty catheter were developed in quick succession, as were technologies for polymeric-based, biodegradable perivascular application. An assessment of the success of these delivery systems coupled to pharmacological and gene therapies is still pending, although controversies about their use and utility have already been reviewed (Chorny *et al.* 2000). Nevertheless, the success of therapies applied in these manners will be dependent on drug and vehicle type, dosage, rates of release, length of sustained release, and ease of compliance and integration into the clinical setting.

Restenosis is a multi-factorial disease process with a very complex pathogenesis. The limited success that has been demonstrated with single modality therapy is likely due to the efficiency at which the body initiates and maintains the repair process (and the myriad of coordinated events that are involved therein), and the redundancy found in the many cellular responses and cellular signaling pathways that are involved. In addition, the differences in patient-to-patient response, and the differential contribution of neointimal thickening, remodeling, elastic recoil, etc., that varies on an individual basis, add layers of complexity to the treatment of restenosis that have yet to be accounted for. Our present understanding of the progression of arterial wound repair/intimal lesion formation is limited to the specific cellular processes (i.e. migration, proliferation and (de)-differentiation) that we can monitor as physical endpoints in our experimental systems. On the other hand, the interactions that occur between cells and the coordination of cellular events is still relatively unknown, as are many of the external, environmental and intracellular factors and signals.

The studies described within this thesis summarize the efforts to characterize components of three cellular processes that are critical to the development of restenotic lesions post-angioplasty, namely cell proliferation, cell migration and phenotypic plasticity (i.e. differentiation). The experimental culture systems that were utilized provided the capability to study distinct endpoints, the contribution of unique factors and discreet cellular responses, while the animal model that was developed provided a feasible system for relevant pharmacological testing. Using these resources, the work summarized by this thesis is the first to recognize the contribution of post-translational modification by arginine-dependent mono(ADP-ribosyl)transferases to cell proliferation, cell migration and differentiation. Furthermore, MIBG, an inhibitor of arginine-dependent ADP-ribosylation reactions (Loesberg *et al.* 1990b; Smets *et al.* 1990b), was identified as a potential therapeutic agent for the treatment of restenosis post-angioplasty.

MIBG was previously demonstrated to exhibit anti-proliferative activity and this property formed the basis for evaluating its applicability in the treatment of certain diseases such as cancer. Trials for cancer have been reported (Taal *et al.* 1999; Taal *et al.* 1996; Zuetenhorst *et al.* 1999) and the success rate is moderately good. Application to other related disease processes, however, has been overlooked. Restenosis is a multifactorial repair-based disease process that includes a cell proliferation component. Based on this reason alone, MIBG should successfully prevent restenosis. However, highly selective inhibitors of cell proliferation have proven unsuccessful in treating restenosis (Landzberg *et al.* 1997; Lefkovits & Topol 1997; Muller *et al.* 1991; Muller *et al.* 1992b). Nevertheless, we have shown that MIBG should still be able to prevent restenosis since MIBG is capable of inhibiting cell migration and differentiation in addition to cell proliferation. These multiple effects give MIBG an advantage over traditional pharmacological interventions that target a single cellular event (i.e.

proliferation or migration or differentiation). Thus, MIBG, and any compound with similar properties, should be suitable for the purpose of preventing vascular restenosis following injury regardless of cause (eg. angioplasty, vascular grafting, etc.).

How does MIBG influence all three cellular events and inhibit restenosis? The answer lies with the ability of MIBG to inhibit the activity of arginine-dependent mono(ADP-ribosyl)transferases. ADP-ribosylation reactions are activated in various cell types in response to a variety of stimuli, and the activation of these regulatory enzymes may be an important component of cell proliferation, cell differentiation and cell migration (Kharadia *et al.* 1992; Saxty *et al.* 1998a; Terashima *et al.* 1992; Thyberg *et al.* 1995b). Oddly enough, even after having been studied for over thirty years, the precise regulatory functions of these enzymes are not well known. What is intriguing though, is that ADP-ribosylation, much like phosphorylation, is reversible via the action of ADP-ribosyl-hydrolases (Moss *et al.* 1997). But how ADP-ribosylation exerts its regulatory effects remains a mystery. In large part, this uncertainty is a consequence of our lack of information regarding the targets of this modification. It is conceivable that ADP-ribosylation reactions operate through G proteins, which are not typically regulated by phosphorylation. Integration of ADP-ribosyltransferases as a regulatory component of cellular signaling pathways would add a further layer of control, and thereby permit more subtle coordination of cell functions. In accordance with this premise, dual regulation of bFGF by both phosphorylation and ADP-ribosylation has been demonstrated (Boulle *et al.* 1995; Feige & Baird 1989; Jones & Baird 1997; Vilgrain & Baird 1991; Vilgrain *et al.* 1993). Of particular interest is that fact that this family of enzymes appears to be closely linked to distinct cellular processes, namely proliferation, migration and differentiation (Kharadia *et al.* 1992; Saxty *et al.* 1998a; Terashima *et al.* 1992; Thyberg *et al.* 1995b), that are critical components of restenotic lesion formation (Bauters & Isner 1997; Davies

& Hagen 1994). Thus, MIBG, an inhibitor of arginine-dependent mono(ADP-ribosyl)ation reactions, would inhibit restenosis via its effect on multiple and independent targets. How ADP-ribosylation functions to regulate each of these distinct cellular processes (i.e. proliferation, migration and differentiation) remains to be determined and should be the subject of future studies.

While it is fine to discuss the individual events involved in the pathogenesis of restenosis post-angioplasty, neointimal formation is actually highly integrated and coordinated with other systemic and local processes in the whole animal, such as thrombus formation, vessel spasm/elastic recoil, inflammation, and remodeling (Biasucci *et al.* 1999; Califf *et al.* 1991; Glagov 1994; Liu *et al.* 1989). Whether MIBG also has an effect on these phenomena, however, remains to be determined. Based on its structure and reports in the literature, at least one possibility exists by which it may influence these processes independent of its effect via arg-mART. Since MIBG resembles NE and is taken into cells via the NE specific uptake-1, it may modulate adrenergic function, which has been shown to have detrimental effects towards elastic recoil and the development of restenosis (Candipan *et al.* 1994; Gregorini *et al.* 1994; Gregorini *et al.* 1997). MIBG may thus be able to decrease elastic recoil. In this way, the long-term ramifications for arterial remodeling may be improved, adding yet another beneficial feature to the restenosis fighting capacity of MIBG.

At the cellular level, MIBG does not appear to function by inhibiting traditional kinase cascade signaling pathways since the cellular intermediates normally associated with proliferation, migration and differentiation, specifically MAP kinase, PI3-kinase and p21-Ras (Coolican *et al.* 1997; Cowley *et al.* 1994; Klemke *et al.* 1997; Lopez-Ilasaca 1998; Marshall 1996; Pages *et al.* 1993; Poser *et al.* 2000; Pyles *et al.* 1997), are not affected by MIBG. Yet, MIBG is capable of interfering with agonist-dependent c-*fos*

mRNA expression. An alternate pathway for the regulation of c-*fos*, and its downstream effects, by MIBG has therefore been proposed. A model has been developed in which the traditional pathways that are initiated by growth factors and other stimuli diverge intracellularly, but converge at the level of the nucleus to regulate the transcription of early growth response genes (Figure 77). Since the induction of c-*fos* gene transcription requires the coordinate activation of several transcription factors including CREB, SRF and Elk-1 for ternary complex formation, a contribution by multiple intracellular pathways and intermediates is not implausible. Furthermore, the activation of at least one of these transcription factors (SRF) is regulated by a signaling pathway that is linked to the small GTP-binding protein Rho. Since the ADP-ribosylation of Rho has already been documented in the literature (Aktories 1997; Aktories & Wegner 1992; Lerm *et al.* 2000; Schmidt & Aktories 1998; Tsakiridis *et al.* 1998), MIBG could inhibit c-*fos* gene expression via this route, independent of MAP kinase.

The research summarized in this thesis presents evidence that MIBG will be a useful tool in the prevention of restenosis post-angioplasty. Further research will need to confirm not only the efficacy of this compound, but also to clarify the safety of this compound when directly applied to vascular tissues. Although extensive study of whole body toxicity has established the limits for systemic application, safety concerns for local delivery must be addressed before the compound can proceed to clinical trials. In addition, it will be of utmost importance to determine the mode of action of MIBG within cellular and experimental animal model systems, and to characterize the mode of distribution not only within a cell, but also as it pertains to local delivery. Thus, future experiments are recommended to proceed in a direction that will define not only the functions of MIBG, but will also provide new insight into the pathobiology of restenosis.

FIGURE 77: ***Model of Signal Intermediates Associated with c-fos Gene Induction by a Growth Stimulus or Injury.***

Targets for inhibitors of the traditional kinase cascade leading to c-*fos* gene transcription are shown. A plausible site for MIBG action in a parallel signaling pathway is presented.

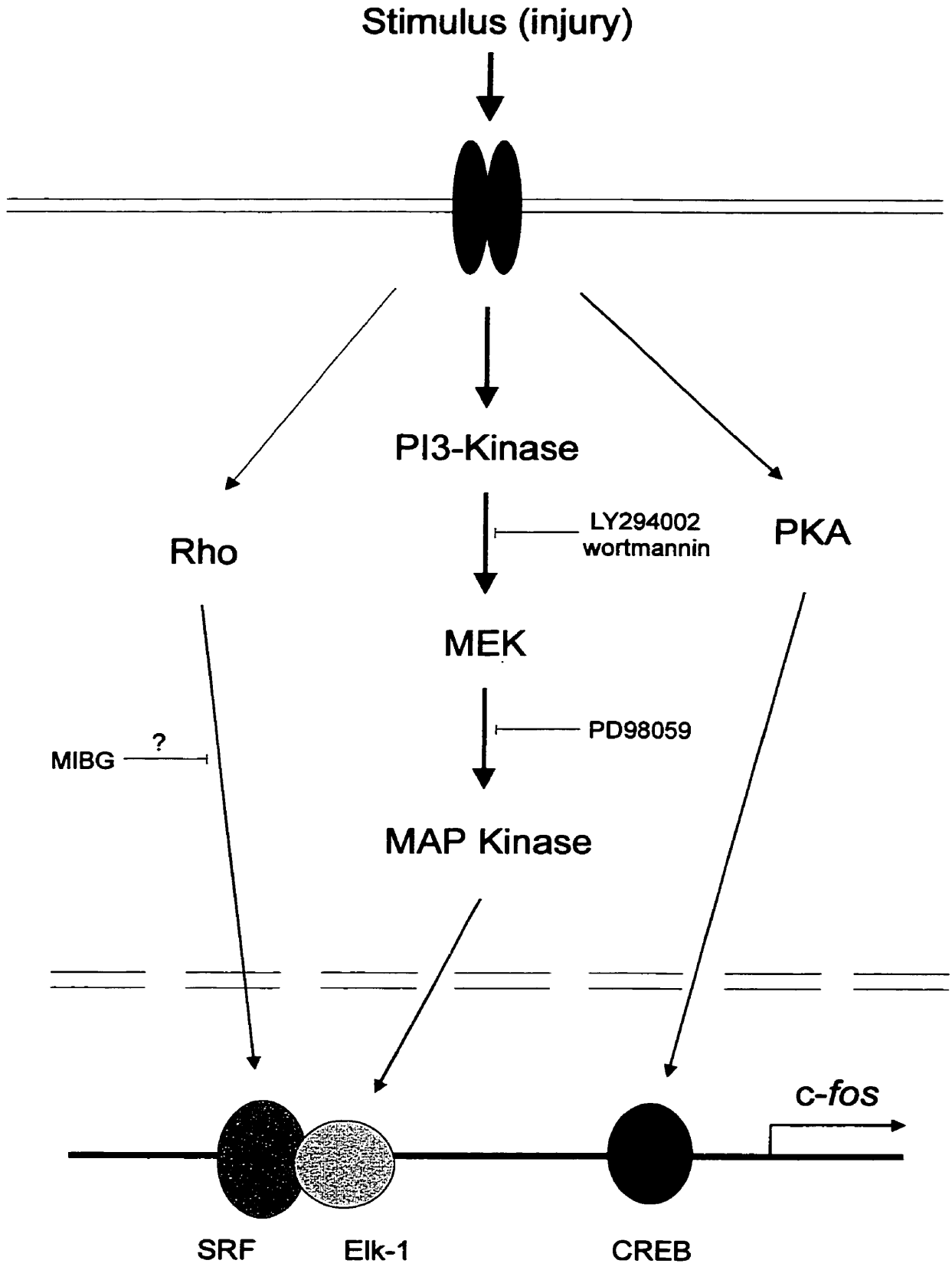
Stimulus (injury)
PI3-Kinase
LY294002
wortmannin
Rho
PKA
MEK
PD98059
MIBG
?
MAP Kinase
c-fos
SRF
Elk-1
CREB

Research efforts dealing with the problem or restenosis promise to bring new modalities of therapy to clinical trial before the end of the next decade. It is hoped that the novel compound described herein, MIBG, will be thoroughly investigated with respect to its clinical suitability so that patients undergoing revascularization procedures for CAD or other peripheral vascular disease could benefit from these findings. Regardless, in the end, it is hoped that the studies reported within this thesis will provide a broader perspective for understanding the complex biology of restenosis and the coordinated cellular repair process that it represents, and ultimately assist in the rational design of new compounds for the treatment of restenosis.

10.0 REFERENCES

Abedi, H., Dawes, K.E. & Zachary, I. (1995). Differential effects of platelet-derived growth factor BB on p125 focal adhesion kinase and paxillin tyrosine phosphorylation and on cell migration in rabbit aortic vascular smooth muscle cells and Swiss 3T3 fibroblasts. *J Biol Chem* **270**: 11367-76.

Abedi, H. & Zachary, I. (1995). Signalling mechanisms in the regulation of vascular cell migration. *Cardiovasc Res* **30**: 544-56.

Aboul-Ela, N., Jacobson, E.L. & Jacobson, M.K. (1988). Labeling methods for the study of poly- and mono(ADP-ribose) metabolism in cultured cells. *Anal Biochem* **174**: 239-50.

Adam, L.P., Franklin, M.T., Raff, G.J. & Hathaway, D.R. (1995). Activation of mitogen-activated protein kinase in porcine carotid arteries. *Circ Res* **76**: 183-90.

Adamietz, P. (1987). Poly(ADP-ribose) synthase is the major endogenous nonhistone acceptor for poly(ADP-ribose) in alkylated rat hepatoma cells. *Eur J Biochem* **169**: 365-72.

Adelman, A.G., Cohen, E.A., Kimball, B.P., Bonan, R., Ricci, D.R., Webb, J.G., Laramee, L., Barbeau, G., Traboulsi, M., Corbett, B.N. & et al. (1993). A comparison of directional atherectomy with balloon angioplasty for lesions of the left anterior descending coronary artery. *N Engl J Med* **329**: 228-33.

AHA, A.H.A. (1999). Economic Cost of Cardiovascular Disease. *American Heart Association*. www.americanheart,org/statistics.

Ahn, N.G., Seger, R., Bratlien, R.L. & Krebs, E.G. (1992). Growth factor-stimulated phosphorylation cascades: activation of growth factor-stimulated MAP kinase. *Ciba Found Symp* **164**: 113-26.

Akle, C.A., Wardle, D.G., Bomanji, J.B. & Talbot, I. (1997). mIBG diagnosis and therapy in smooth muscle tumours of the small bowel. *Eur J Nucl Med* **24**: 1196.

Aktories, K. (1994). Clostridial ADP-ribosylating toxins: effects on ATP and GTP-binding proteins. *Mol Cell Biochem* **138**: 167-76.

Aktories, K. (1997). Rho proteins: targets for bacterial toxins. *Trends Microbiol* **5**: 282-8.

Aktories, K. & Wegner, A. (1992). Mechanisms of the cytopathic action of actin-ADP-ribosylating toxins. *Mol Microbiol* **6**: 2905-8.

Alessi, D.R., Cuenda, A., Cohen, P., Dudley, D.T. & Saltiel, A.R. (1995). PD 098059 is a specific inhibitor of the activation of mitogen- activated protein kinase kinase in vitro and in vivo. *J Biol Chem* **270**: 27489-94.

Alexander, Schlant & Fuster. (1998). Hurst's The Heart. , McGraw-Hill, New York.

Alexander, R.W. & Gimbrone, M.A., Jr. (1976). Stimulation of prostaglandin E synthesis in cultured human umbilical vein smooth muscle cells. *Proc Natl Acad Sci U S A* **73**: 1617-20.

Ali, N. & Agrawal, D.K. (1994). Guanine nucleotide binding regulatory proteins: their characteristics and identification. *J Pharmacol Toxicol Methods* **32**: 187-96.

Allport, J.R., Donnelly, L.E., Hayes, B.P., Murray, S., Rendell, N.B., Ray, K.P. & MacDermot, J. (1996a). Reduction by inhibitors of mono(ADP-ribosyl)transferase of chemotaxis in human neutrophil leucocytes by inhibition of the assembly of filamentous actin. *Br J Pharmacol* **118**: 1111-8.

Allport, J.R., Donnelly, L.E., Kefalas, P., Lo, G., Nunn, A., Yadollahi-Farsani, M., Rendell, N.B., Murray, S., Taylor, G.W. & MacDermot, J. (1996b). A possible role for mono (ADP-ribosyl) transferase in the signalling pathway mediating neutrophil chemotaxis. *Br J Clin Pharmacol* **42**: 99-106.

Althaus, F.R. & Richter, C.H. (1987). ADP-ribosylation of proteins: Enzymology and biological significance. In: . Solioz, M. (eds.). Springer, Berlin. pp 1-237.

Alvarez-Gonzalez, R. & Jacobson, M.K. (1987). Characterization of polymers of adenosine diphosphate ribose generated in vitro and in vivo. *Biochemistry* **26**: 3218-24.

Alvarez-Gonzalez, R., Pacheco-Rodriguez, G. & Mendoza-Alvarez, H. (1994). Enzymology of ADP-ribose polymer synthesis. *Mol Cell Biochem* **138**: 33-7.

Ame, J.C., Rolli, V., Schreiber, V., Niedergang, C., Apiou, F., Decker, P., Muller, S., Hoger, T., Menissier-de Murcia, J. & de Murcia, G. (1999). PARP-2, A novel mammalian DNA damage-dependent poly(ADP-ribose) polymerase. *J Biol Chem* **274**: 17860-8.

Amstad, P.A., Krupitza, G. & Cerutti, P.A. (1992). Mechanism of c-fos induction by active oxygen. *Cancer Res* **52**: 3952-60.

Andersen, H.R., Maeng, M., Thorwest, M. & Falk, E. (1996). Remodeling rather than neointimal formation explains luminal narrowing after deep vessel wall injury: insights from a porcine coronary (re)stenosis model. *Circulation* **93**: 1716-24.

Andrawis, N.S., Ruley, E.H. & Abernethy, D.R. (1993). Angiotensin II regulates human vascular smooth muscle alpha-actin gene expression. *Biochem Biophys Res Commun* **196**: 962-8.

Andres, V. (1998). Control of vascular smooth muscle cell growth and its implication in atherosclerosis and restenosis. *Int J Mol Med* **2**: 81-9.

Arai, H. & Escobedo, J.A. (1996). Angiotensin II type 1 receptor signals through Raf-1 by a protein kinase C-dependent, Ras-independent mechanism. *Mol Pharmacol* **50**: 522-8.

Arcaro, A. & Wymann, M.P. (1993). Wortmannin is a potent phosphatidylinositol 3-kinase inhibitor: the role of phosphatidylinositol 3,4,5-trisphosphate in neutrophil responses. *Biochem J* **296**: 297-301.

Arciniegas, E., Ponce, L., Hartt, Y., Graterol, A. & Carlini, R.G. (2000). Intimal thickening involves transdifferentiation of embryonic endothelial cells. *Anat Rec* **258**: 47-57.

Ardissino, D., Barberis, P., De Servi, S., Merlini, P.A., Bramucci, E., Falcone, C. & Specchia, G. (1991). Abnormal coronary vasoconstriction as a predictor of restenosis after successful coronary angioplasty in patients with unstable angina pectoris. *N Engl J Med* **325**: 1053-7.

Arundel-Suto, C.M., Scavone, S.V., Turner, W.R., Suto, M.J. & Sebolt-Leopold, J.S. (1991). Effect of PD 128763, a new potent inhibitor of poly(ADP-ribose) polymerase, on X-ray-induced cellular recovery processes in Chinese hamster V79 cells. *Radiat Res* **126**: 367-71.

Asada, Y., Kisanuki, A., Hatakeyama, K., Takahama, S., Koyama, T., Kurozumi, S. & Sumiyoshi, A. (1994). Inhibitory effects of prostacyclin analogue, TFC-132, on aortic neointimal thickening in vivo and smooth muscle cell proliferation in vitro. *Prostaglandins Leukot Essent Fatty Acids* **51**: 245-8.

Asada, Y., Kisanuki, A., Tsuneyoshi, A., Marutsuka, K., Hatakeyama, K. & Sumiyoshi, A. (1996). Effects of inflation pressure of balloon catheter on vascular injuries and subsequent development of intimal hyperplasia in rabbit aorta. *Atherosclerosis* **121**: 45-53.

Babai, F., Musevi-Aghdam, J., Schurch, W., Royal, A. & Gabbiani, G. (1990). Coexpression of alpha-sarcomeric actin, alpha-smooth muscle actin and desmin during myogenesis in rat and mouse embryos I. Skeletal muscle. *Differentiation* **44**: 132-42.

Bach, M.K. (1982). Mediators of anaphylaxis and inflammation. *Annu Rev Microbiol* **36**: 371-413.

Badimon, J.J., Ortiz, A.F., Meyer, B., Mailhac, A., Fallon, J.T., Falk, E., Badimon, L., Chesebro, J.H. & Fuster, V. (1998). Different response to balloon angioplasty of carotid and coronary arteries: effects on acute platelet deposition and intimal thickening. *Atherosclerosis* **140**: 307-14.

Badimon, L., Alfon, J., Royo, T., Berrozpe, M., Martinez-Gonzalez, J., Vidal, F., Chesebro, J.H., Fuster, V. & Badimon, J.J. (1995). Cell biology of restenosis post-angioplasty. *Z Kardiol* **84**: 145-9.

Ball, E.H., Narindrasorasak, S. & Sanwal, B.D. (1979). The cyclic adenosine monophosphate phosphodiesterases of myoblasts, fibroblasts, and their somatic cell hybrids. *Can J Biochem* **57**: 1220-8.

Ball, E.H. & Sanwal, B.D. (1980). A synergistic effect of glucocorticoids and insulin on the differentiation of myoblasts. *J Cell Physiol* **102**: 27-36.

Ball, E.H., Seth, P.K. & Sanwal, B.D. (1980). Regulatory mechanisms involved in the control of cyclic adenosine 3':5'- monophosphate phosphodiesterases in myoblasts. *J Biol Chem* **255**: 2962-8.

Banai, S., Haggroth, L., Epstein, S.E. & Casscells, W. (1990). Influence of extracellular magnesium on capillary endothelial cell proliferation and migration. *Circ Res* **67**: 645-50.

Banasik, M., Komura, H., Shimoyama, M. & Ueda, K. (1992). Specific inhibitors of poly(ADP-ribose) synthetase and mono(ADP- ribosyl)transferase. *J Biol Chem* **267**: 1569-75.

Banasik, M. & Ueda, K. (1994). Inhibitors and activators of ADP-ribosylation reactions. *Mol Cell Biochem* **138**: 185-97.

Banskota, N.K., Taub, R., Zellner, K. & King, G.L. (1989). Insulin, insulin-like growth factor I and platelet-derived growth factor interact additively in the induction of the protooncogene c-myc and cellular proliferation in cultured bovine aortic smooth muscle cells. *Mol Endocrinol* **3**: 1183-90.

Barry, W.L., Wiegman, P.J., Gimple, L.W., Gertz, S.D., Powers, E.R., Owens, G.K. & Sarembock, I.J. (1997). A new single-injury model of balloon angioplasty in cholesterol-fed rabbits: beneficial effect of hirudin and comparison with double-injury model. *Lab Invest* **77**: 109-16.

Bar-Shavit, R., Benezra, M., Eldor, A., Hy-Am, E., Fenton, J.W.d., Wilner, G.D. & Vlodavsky, I. (1990). Thrombin immobilized to extracellular matrix is a potent mitogen for vascular smooth muscle cells: nonenzymatic mode of action. *Cell Regul* **1**: 453-63.

Baserga, R., Porcu, P., Rubini, M. & Sell, C. (1994). Cell cycle control by the IGF-1 receptor and its ligands. In: Current directions in insulin-like growth factor research. LeRoith, D. & Raizada, M.K. (eds.). Plenum Press, New York. pp 105-112.

Battistini, B., Chailler, P., D'Orleans-Juste, P., Briere, N. & Sirois, P. (1993). Growth regulatory properties of endothelins. *Peptides* **14**: 385-99.

Bauer, P.I., Buki, K.G., Hakam, A. & Kun, E. (1990). Macromolecular association of ADP-ribosyltransferase and its correlation with enzymic activity. *Biochem J* **270**: 17-26.

Bauters, C. & Isner, J.M. (1997). The biology of restenosis. *Prog Cardiovasc Dis* **40**: 107-16.

Beale, E., Andreone, T., Koch, S., Granner, M. & Granner, D. (1984). Insulin and glucagon regulate cytosolic phosphoenolpyruvate carboxykinase (GTP) mRNA in rat liver. *Diabetes* **33**: 328-32.

Bell, L. & Madri, J.A. (1989). Effect of platelet factors on migration of cultured bovine aortic endothelial and smooth muscle cells. *Circ Res* **65**: 1057-65.

Bell, L. & Madrū, J.A. (1990). Influence of the angiotensin system on endothelial and smooth muscle cell migration. *Am J Pathol* **137**: 7-12.

Beneke, R., Geisen, C., Zevnik, B., Bauch, T., Muller, W.U., Kupper, J.H. & Moroy, T. (2000). DNA excision repair and DNA damage-induced apoptosis are linked to Poly(ADP-ribosyl)ation but have different requirements for p53. *Mol Cell Biol* **20**: 6695-703.

Berger, N.A. (1985). Poly(ADP-ribose) in the cellular response to DNA damage. *Radiat Res* **101**: 4-15.

Berk, B.C. & Alexander, R.W. (1989). Vasoactive effects of growth factors. *Biochem Pharmacol* **38**: 219-25.

Bernal, S.D. & Stahel, R.A. (1985). Cytoskeleton-associated proteins: their role as cellular integrators in the neoplastic process. *Crit Rev Oncol Hematol* **3**: 191-204.

Bernstein, L.R., Antoniades, H. & Zetter, B.R. (1982). Migration of cultured vascular cells in response to plasma and platelet- derived factors. *J Cell Sci* **56**: 71-82.

Biasucci, L.M., Liuzzo, G., Buffon, A. & Maseri, A. (1999). The variable role of inflammation in acute coronary syndromes and in restenosis. *Semin Interv Cardiol* **4**: 105-10.

Birukov, K.G., Frid, M.G., Rogers, J.D., Shirinsky, V.P., Koteliansky, V.E., Campbell, J.H. & Campbell, G.R. (1993). Synthesis and expression of smooth muscle phenotype markers in primary culture of rabbit aortic smooth muscle cells: influence of seeding density and media and relation to cell contractility. *Exp Cell Res* **204**: 46-53.

Black, B.L. & Olson, E.N. (1998). Transcriptional control of muscle development by myocyte enhancer factor-2 (MEF2) proteins. *Annu Rev Cell Dev Biol* **14**: 167-96.

Blake, G.M., Lewington, V.J., Zivanovic, M.A. & Ackery, D.M. (1989). Glomerular filtration rate and the kinetics of 123I- metaiodobenzylguanidine. *Eur J Nucl Med* **15**: 618-23.

Blank, R.S. & Owens, G.K. (1990). Platelet-derived growth factor regulates actin isoform expression and growth state in cultured rat aortic smooth muscle cells. *J Cell Physiol* **142**: 635-42.

Blank, R.S., Swartz, E.A., Thompson, M.M., Olson, E.N. & Owens, G.K. (1995). A retinoic acid-induced clonal cell line derived from multipotential P19 embryonal carcinoma cells expresses smooth muscle characteristics. *Circ Res* **76**: 742-9.

Bobik, A. & Campbell, J.H. (1993). Vascular derived growth factors: cell biology, pathophysiology, and pharmacology. *Pharmacol Rev* **45**: 1-42.

Bobik, A., Grooms, A., Millar, J.A., Mitchell, A. & Grinpukel, S. (1990). Growth factor activity of endothelin on vascular smooth muscle. *Am J Physiol* **258**: C408-15.

Bochaton-Piallat, M.L., Gabbiani, F. & Gabbiani, G. (1994). Heterogeneity of rat aortic smooth muscle cell replication during development: correlation with replicative activity after experimental endothelial denudation in adults. *J Submicrosc Cytol Pathol* **26**: 1-8.

Bochaton-Piallat, M.L., Gabbiani, F., Ropraz, P. & Gabbiani, G. (1992). Cultured aortic smooth muscle cells from newborn and adult rats show distinct cytoskeletal features. *Differentiation* **49**: 175-85.

Bochaton-Piallat, M.L., Gabbiani, F., Ropraz, P. & Gabbiani, G. (1993). Age influences the replicative activity and the differentiation features of cultured rat aortic smooth muscle cell populations and clones. *Arterioscler Thromb* **13**: 1449-55.

Bochaton-Piallat, M.L., Ropraz, P., Gabbiani, F. & Gabbiani, G. (1996). Phenotypic heterogeneity of rat arterial smooth muscle cell clones. Implications for the development of experimental intimal thickening. *Arterioscler Thromb Vasc Biol* **16**: 815-20.

Bonin, P.D., Fici, G.J. & Singh, J.P. (1989). Interleukin-1 promotes proliferation of vascular smooth muscle cells in coordination with PDGF or a monocyte derived growth factor. *Exp Cell Res* **181**: 475-82.

Bonser, R.W., Thompson, N.T., Randall, R.W., Tateson, J.E., Spacey, G.D., Hodson, H.F. & Garland, L.G. (1991). Demethoxyviridin and wortmannin block phospholipase C and D activation in the human neutrophil. *Br J Pharmacol* **103**: 1237-41.

Bornfeldt, K.E., Campbell, J.S., Koyama, H., Argast, G.M., Leslie, C.C., Raines, E.W., Krebs, E.G. & Ross, R. (1997). The mitogen-activated protein kinase pathway can mediate growth inhibition and proliferation in smooth muscle cells. Dependence on the availability of downstream targets. *J Clin Invest* **100**: 875-85.

Bos, J.L. (1995). p21ras: an oncoprotein functioning in growth factor-induced signal transduction. *Eur J Cancer* **31A**: 1051-4.

Boulikas, T. (1988). At least 60 ADP-ribosylated variant histones are present in nuclei from dimethylsulfate-treated and untreated cells. *EMBO J* **7**: 57-67.

Boulikas, T. (1990). Poly(ADP-ribosylated) histones in chromatin replication. *J Biol Chem* **265**: 14638-47.

Boulle, N., Jones, E.M., Auguste, P. & Baird, A. (1995). Adenosine diphosphate ribosylation of fibroblast growth factor-2. *Mol Endocrinol* **9**: 767-75.

Bourcier, T., Dockter, M. & Hassid, A. (1995). Synergistic interaction of interleukin-1 beta and growth factors in primary cultures of rat aortic smooth muscle cells. *J Cell Physiol* **164**: 644-57.

Bowen-Pope, D.F. & Ross, R. (1982). Platelet-derived growth factor. II. Specific binding to cultured cells. *J Biol Chem* **257**: 5161-71.

Bowen-Pope, D.F., Ross, R. & Seifert, R.A. (1985). Locally acting growth factors for vascular smooth muscle cells: endogenous synthesis and release from platelets. *Circulation* **72**: 735-40.

Bowes, J., McDonald, M.C., Piper, J. & Thiemermann, C. (1999). Inhibitors of poly (ADP-ribose) synthetase protect rat cardiomyocytes against oxidant stress. *Cardiovasc Res* **41**: 126-34.

Bowes, J., Piper, J. & Thiemermann, C. (1998). Inhibitors of the activity of poly (ADP-ribose) synthetase reduce the cell death caused by hydrogen peroxide in human cardiac myoblasts. *Br J Pharmacol* **124**: 1760-6.

Brand-Saberi, B. & Christ, B. (1999). Genetic and epigenetic control of muscle development in vertebrates. *Cell Tissue Res* **296**: 199-212.

Bravo, R. (1990). Genes induced during the G0/G1 transition in mouse fibroblasts. *Semin Cancer Biol* **1**: 37-46.

Brizzi, M.F., Defilippi, P., Rosso, A., Venturino, M., Garbarino, G., Miyajima, A., Silengo, L., Tarone, G. & Pegoraro, L. (1999). Integrin-mediated adhesion of endothelial cells induces JAK2 and STAT5A activation: role in the control of c-fos gene expression. *Mol Biol Cell* **10**: 3463-71.

Brogan, W.C.d., Popma, J.J., Pichard, A.D., Satler, L.F., Kent, K.M., Mintz, G.S. & Leon, M.B. (1993). Rotational coronary atherectomy after unsuccessful coronary balloon angioplasty. *Am J Cardiol* **71**: 794-8.

Brown, C., Clark, L., Williams, L., Gallagher, S., Levesque, M. & Silva, J. (1996). Pearls for Practice: Coronary Restenosis. *Journal of the American Academy of Nurse Practitioners* **8**: 283-288.

Brune, B., Dimmeler, S., Molina y Vedia, L. & Lapetina, E.G. (1994). Nitric oxide: a signal for ADP-ribosylation of proteins. *Life Sci* **54**: 61-70.

Brune, B. & Lapetina, E.G. (1989). Activation of a cytosolic ADP-ribosyltransferase by nitric oxide- generating agents. *J Biol Chem* **264**: 8455-8.

Buchberger, A., Ragge, K. & Arnold, H.H. (1994). The myogenin gene is activated during myocyte differentiation by pre- existing, not newly synthesized transcription factor MEF-2. *J Biol Chem* **269**: 17289-96.

Bucher, M.L. & Swaffield, M.N. (1975). Regulation of hepatic regeneration in rats by synergistic action of insulin and glucagon. *Proc Natl Acad Sci U S A* **72**: 1157-60.

Burkart, V., Blaeser, K. & Kolb, H. (1999). Potent beta-cell protection in vitro by an isoquinolinone-derived PARP inhibitor. *Horm Metab Res* **31**: 641-4.

Burke, J.M. & Ross, R. (1979). Synthesis of connective tissue macromolecules by smooth muscle. *Int Rev Connect Tissue Res* **8**: 119-57.

Burkle, A., Muller, M., Wolf, I. & Kupper, J.H. (1994). Poly(ADP-ribose) polymerase activity in intact or permeabilized leukocytes from mammalian species of different longevity. *Mol Cell Biochem* **138**: 85-90.

Califf, R.M., Fortin, D.F., Frid, D.J., Harlan, W.R.d., Ohman, E.M., Bengtson, J.R., Nelson, C.L., Tcheng, J.E., Mark, D.B. & Stack, R.S. (1991). Restenosis after coronary angioplasty: an overview. *J Am Coll Cardiol* **17**: 2B-13B.

Campbell, J.H. & Campbell, G.R. (1997). The cell biology of atherosclerosis--new developments. *Aust N Z J Med* **27**: 497-500.

Campbell, J.H., Campbell, G.R., Kocher, O. & Gabbiani, G. (1987). Cell biology of smooth muscle in culture: implications for atherogenesis. *Int Angiol* **6**: 73-9.

Campbell, J.H., Kocher, O., Skalli, O., Gabbiani, G. & Campbell, G.R. (1989). Cytodifferentiation and expression of alpha-smooth muscle actin mRNA and protein during primary culture of aortic smooth muscle cells. Correlation with cell density and proliferative state. *Arteriosclerosis* **9**: 633-43.

Canada, H. (1995). Heart Disease and Stroke in Canada. *Health Canada*. www.hc-sc.gc/hpb/lcdc/bcrdd/hdsc97.

Candipan, R.C., Hsiun, P.T., Pratt, R. & Cooke, J.P. (1994). Vascular injury augments adrenergic neurotransmission. *Circulation* **89**: 777-84.

Carey, D.J. (1991). Control of growth and differentiation of vascular cells by extracellular matrix proteins. *Annu Rev Physiol* **53**: 161-77.

Carson, D.A., Seto, S., Wasson, D.B. & Carrera, C.J. (1986). DNA strand breaks, NAD metabolism, and programmed cell death. *Exp Cell Res* **164**: 273-81.

Carter, A.J., Laird, J.R., Farb, A., Kufs, W., Wortham, D.C. & Virmani, R. (1994). Morphologic characteristics of lesion formation and time course of smooth muscle cell proliferation in a porcine proliferative restenosis model. *J Am Coll Cardiol* **24**: 1398-405.

Casscells, W. (1992). Migration of smooth muscle and endothelial cells. Critical events in restenosis. *Circulation* **86**: 723-9.

Cassel, D. & Pfeuffer, T. (1978). Mechanism of cholera toxin action: covalent modification of the guanyl nucleotide-binding protein of the adenylate cyclase system. *Proc Natl Acad Sci U S A* **75**: 2669-73.

Casterella, P.J. & Teirstein, P.S. (1999). Prevention of coronary restenosis. *Cardiol Rev* 7: 219-31.

Catalioto, R.M., Renzetti, A.R., Criscuoli, M., Morbidelli, L. & Subissi, A. (1996). Role of calcium in angiotensin II-induced prostaglandin release and DNA synthesis in rat vascular smooth muscle cells. *J Cardiovasc Pharmacol* **27**: 195-200.

Caterina, M.J. & Devreotes, P.N. (1991). Molecular insights into eukaryotic chemotaxis. *FASEB J* **5**: 3078-85.

Cercek, B., Sharifi, B., Barath, P., Bailey, L. & Forrester, J.S. (1991). Growth factors in pathogenesis of coronary arterial restenosis. *Am J Cardiol* **68**: 24C-33C.

Cesarone, C.F., Scarabelli, L., Scovassi, A.I., Izzo, R., Menegazzi, M., Carcereri De Prati, A., Orunesu, M. & Bertazzoni, U. (1990). Changes in activity and mRNA levels of poly(ADP-ribose) polymerase during rat liver regeneration. *Biochim Biophys Acta* **1087**: 241-6.

Chamley, J.H., Campbell, G.R., McConnell, J.D. & Groschel-Stewart, U. (1977). Comparison of vascular smooth muscle cells from adult human, monkey and rabbit in primary culture and in subculture. *Cell Tissue Res* **177**: 503-22.

Chamley-Campbell, J., Campbell, G.R. & Ross, R. (1979). The smooth muscle cell in culture. *Physiol Rev* **59**: 1-61.

Chamley-Campbell, J.H., Campbell, G.R. & Ross, R. (1981). Phenotype-dependent response of cultured aortic smooth muscle to serum mitogens. *J Cell Biol* **89**: 379-83.

Chang, Y.C., Soman, G. & Graves, D.J. (1986). Identification of an enzymatic activity that hydrolyzes protein-bound ADP-ribose in skeletal muscle. *Biochem Biophys Res Commun* **139**: 932-9.

Chao, D., Severson, D.L., Zwiers, H. & Hollenberg, M.D. (1994). Radiolabelling of bovine myristoylated alanine-rich protein kinase C substrate (MARCKS) in an ADP-ribosylation reaction. *Biochem Cell Biol* **72**: 391-6.

Cheatham, B., Vlahos, C.J., Cheatham, L., Wang, L., Blenis, J. & Kahn, C.R. (1994). Phosphatidylinositol 3-kinase activation is required for insulin stimulation of pp70 S6 kinase, DNA synthesis, and glucose transporter translocation. *Mol Cell Biol* **14**: 4902-11.

Chen, Q., Kinch, M.S., Lin, T.H., Burridge, K. & Juliano, R.L. (1994). Integrin-mediated cell adhesion activates mitogen-activated protein kinases. *J Biol Chem* **269**: 26602-5.

Cheng, T.C., Wallace, M.C., Merlie, J.P. & Olson, E.N. (1993). Separable regulatory elements governing myogenin transcription in mouse embryogenesis. *Science* **261**: 215-8.

Choi, J., Costa, M.L., Mermelstein, C.S., Chagas, C., Holtzer, S. & Holtzer, H. (1990). MyoD converts primary dermal fibroblasts, chondroblasts, smooth muscle, and retinal pigmented epithelial cells into striated mononucleated myoblasts and multinucleated myotubes. *Proc Natl Acad Sci U S A* **87**: 7988-92.

Chorny, M., Fishbein, I. & Golomb, G. (2000). Drug delivery systems for the treatment of restenosis. *Crit Rev Ther Drug Carrier Syst* **17**: 249-84.

Chougule, P.B. (2000). Vascular radiation therapy to reduce coronary artery restenosis. *Surg Oncol Clin N Am* **9**: 577-84, x.

Christ, B., Nath, A., Bastian, H. & Jungermann, K. (1988). Regulation of the expression of the phosphoenolpyruvate carboxykinase gene in cultured rat hepatocytes by glucagon and insulin. *Eur J Biochem* **178**: 373-9.

Christen, T., Bochaton-Piallat, M.L., Neuville, P., Rensen, S., Redard, M., van Eys, G. & Gabbiani, G. (1999). Cultured porcine coronary artery smooth muscle cells. A new model with advanced differentiation. *Circ Res* **85**: 99-107.

Civen, M. & Knox, W.E. (1960). The specificity of tryptophan analogues as inducers, substrates, inhibitors and stabilizers of liver tryptophan pyrrolase. *J Biol Chem* **235**: 1716-1718.

Clancy, R., Leszczynska, J., Amin, A., Levartovsky, D. & Abramson, S.B. (1995). Nitric oxide stimulates ADP ribosylation of actin in association with the inhibition of actin polymerization in human neutrophils. *J Leukoc Biol* **58**: 196-202.

Clemmons, D.R. (1984). Interaction of circulating cell-derived and plasma growth factors in stimulating cultured smooth muscle cell replication. *J Cell Physiol* **121**: 425-30.

Clemmons, D.R. & Van Wyk, J.J. (1985). Evidence for a functional role of endogenously produced somatomedinlike peptides in the regulation of DNA synthesis in cultured human fibroblasts and porcine smooth muscle cells. *J Clin Invest* **75**: 1914-8.

Clowes, A.W., Clowes, M.M., Fingerle, J. & Reidy, M.A. (1989). Regulation of smooth muscle cell growth in injured artery. *J Cardiovasc Pharmacol* **14**: S12-15.

Clowes, A.W., Clowes, M.M., Kocher, O., Ropraz, P., Chaponnier, C. & Gabbiani, G. (1988). Arterial smooth muscle cells in vivo: relationship between actin isoform expression and mitogenesis and their modulation by heparin. *J Cell Biol* **107**: 1939-45.

Clowes, A.W. & Reidy, M.A. (1991). Prevention of stenosis after vascular reconstruction: pharmacologic control of intimal hyperplasia--a review. *J Vasc Surg* **13**: 885-91.

Clozel, J.P., Hess, P., Michael, C., Schietinger, K. & Baumgartner, H.R. (1991). Inhibition of converting enzyme and neointima formation after vascular injury in rabbits and guinea pigs. *Hypertension* **18**: II55-9.

Cohick, W.S. & Clemmons, D.R. (1993). The insulin-like growth factors. *Annu Rev Physiol* **55**: 131-53.

Coleman, R.A., Kennedy, I. & Sheldrick, R.L. (1987). New evidence with selective agonists and antagonists for the subclassification of PGE2-sensitive (EP) receptors. *Adv Prostaglandin Thromboxane Leukot Res* **17A**: 467-70.

Coleman, R.A., Smith, W.L. & Narumiya, S. (1994). International Union of Pharmacology classification of prostanoid receptors: properties, distribution, and structure of the receptors and their subtypes. *Pharmacol Rev* **46**: 205-29.

Collier, R.J. (1967). Effect of diphtheria toxin on protein synthesis: inactivation of one of the transfer factors. *J Mol Biol* **25**: 83-98.

Collier, R.J. (1975). Diphtheria toxin: mode of action and structure. *Bacteriol Rev* **39**: 54-85.

Combettes-Souverain, M. & Issad, T. (1998). Molecular basis of insulin action. *Diabetes Metab* **24**: 477-89.

Cook, S.J., Balmanno, K., Garner, A., Millar, T., Taverner, C. & Todd, D. (2000). Regulation of cell cycle re-entry by growth, survival and stress signalling pathways. *Biochem Soc Trans* **28**: 233-40.

Coolican, S.A., Samuel, D.S., Ewton, D.Z., McWade, F.J. & Florini, J.R. (1997). The mitogenic and myogenic actions of insulin-like growth factors utilize distinct signaling pathways. *J Biol Chem* **272**: 6653-62.

Corjay, M.H., Thompson, M.M., Lynch, K.R. & Owens, G.K. (1989). Differential effect of platelet-derived growth factor- versus serum- induced growth on smooth muscle alpha-actin and nonmuscle beta-actin mRNA expression in cultured rat aortic smooth muscle cells. *J Biol Chem* **264**: 10501-6.

Cornelissen, J., Van Kuilenburg, A.B., Voute, P.A. & Van Gennip, A.H. (1997a). The effect of the neuroblastoma-seeking agent meta-iodobenzylguanidine (MIBG) on NADH-driven superoxide formation and NADH-driven lipid peroxidation in beef heart submitochondrial particles. *Eur J Cancer* **33**: 421-4.

Cornelissen, J., Van Kuilenburg, A.B., Voute, P.A. & Van Gennip, A.H. (1997b). MIBG causes oxidative stress and up-regulation of anti-oxidant enzymes in the human neuroblastoma cell line SK-N-BE(2c). *Int J Cancer* **72**: 486-90.

Cornelissen, J., Wanders, R.J., Van den Bogert, C., Van Kuilenburg, A.B., Elzinga, L., Voute, P.A. & Van Gennip, A.H. (1995a). Meta-iodobenzylguanidine (MIBG) inhibits malate and succinate driven mitochondrial ATP synthesis in the human neuroblastoma cell line SK-N- BE(2c). *Eur J Cancer* **4**: 582-6.

Cornelissen, J., Wanders, R.J., Van Gennip, A.H., Van den Bogert, C., Voute, P.A. & Van Kuilenburg, A.B. (1995b). Meta-iodobenzylguanidine inhibits complex I and III of the respiratory chain in the human cell line Molt-4. *Biochem Pharmacol* **49**: 471-7.

Cornwell, D.G., Huttner, J.J., Milo, G.E., Panganamala, R.V., Sharma, H.M. & Geer, J.C. (1979). Polyunsaturated fatty acids, vitamin E, and the proliferation of aortic smooth muscle cells. *Lipids* **14**: 194-207.

Cornwell, T.L., Arnold, E., Boerth, N.J. & Lincoln, T.M. (1994). Inhibition of smooth muscle cell growth by nitric oxide and activation of cAMP-dependent protein kinase by cGMP. *Am J Physiol* **267**: C1405-13.

Corson, M.A. & Berk, B.C. (1993). Growth factors and the vessel wall. *Heart Dis Stroke* **2**: 166-70.

Cote, G., Tardif, J.C., Lesperance, J., Lambert, J., Bourassa, M., Bonan. R., Gosselin, G., Joyal, M., Tanguay, J.F., Nattel, S., Gallo, R. & Crepeau, J. (1999). Effects of probucol on vascular remodeling after coronary angioplasty. Multivitamins and Protocol Study Group. *Circulation* **99**: 30-5.

Cowley, S., Paterson, H., Kemp, P. & Marshall, C.J. (1994). Activation of MAP kinase kinase is necessary and sufficient for PC12 differentiation and for transformation of NIH 3T3 cells. *Cell* **77**: 841-52.

Creese, B.R. & Denborough, M.A. (1981). Sources of calcium for contraction of guinea-pig isolated tracheal smooth muscle. *Clin Exp Pharmacol Physiol* **8**: 175-82.

Creissen, D. & Shall, S. (1982). Regulation of DNA ligase activity by poly(ADP-ribose). *Nature* **296**: 271-2.

Cross, M.J., Stewart, A., Hodgkin, M.N., Kerr, D.J. & Wakelam, M.J. (1995). Wortmannin and its structural analogue demethoxyviridin inhibit stimulated phospholipase A2 activity in Swiss 3T3 cells. Wortmannin is not a specific inhibitor of phosphatidylinositol 3-kinase. *J Biol Chem* **270**: 25352-5.

Cserjesi, P., Lilly, B., Bryson, L., Wang, Y., Sassoon, D.A. & Olson, E.N. (1992). MHox: a mesodermally restricted homeodomain protein that binds an essential site in the muscle creatine kinase enhancer. *Development* **115**: 1087-101.

Czech, M.P. (1977). Molecular basis of insulin action. *Annu Rev Biochem* **46**: 359-84.

Czech, M.P. (1995). Molecular actions of insulin on glucose transport. *Annu Rev Nutr* **15**: 441-71.

Dalmau, M., Joaquin, M., Nakamura, T., Bartrons, R. & Gil, J. (1996). Nitric oxide inhibits DNA synthesis and induces activation of poly(ADP- ribose) polymerase in cultured rat hepatocytes. *Exp Cell Res* **228**: 14-8.

Dalsgaard, C.J., Hultgardh-Nilsson, A., Haegerstrand, A. & Nilsson, J. (1989). Neuropeptides as growth factors. Possible roles in human diseases. *Regul Pept* **25**: 1-9.

D'Amours, D., Desnoyers, S., D'Silva, I. & Poirier, G.G. (1999). Poly(ADP-ribosyl)ation reactions in the regulation of nuclear functions. *Biochem J* **342**: 249-68.

Dangas, G. & Fuster, V. (1996). Management of restenosis after coronary intervention. *Am Heart J* **132**: 428-36.

Dartsch, P.C., Voisard, R., Bauriedel, G., Hofling, B. & Betz, E. (1990a). Growth characteristics and cytoskeletal organization of cultured smooth muscle cells from human primary stenosing and restenosing lesions. *Arteriosclerosis* **10**: 62-75.

Dartsch, P.C., Weiss, H.D. & Betz, E. (1990b). Human vascular smooth muscle cells in culture: growth characteristics and protein pattern by use of serum-free media supplements. *Eur J Cell Biol* **51**: 285-94.

Davies, M.G. & Hagen, P.O. (1994). Pathobiology of intimal hyperplasia. *Br J Surg* **81**: 1254-69.

Davies, P.F. (1990). Coculture of endothelial and smooth muscle cells. In: Cell culture techniques in heart and vessel research. Piper, H.M. (eds.). Springer-Verlag, Berlin. pp 290-298.

Davies, P.F. & O'Connor, S.E. (1990). Methods of culturing vascular smooth muscle cells on microcarriers. In: Cell culture techniques in heart and vessel research. Piper, H.M. (eds.). Springer-Verlag, Berlin. pp 334-342.

Davis, R.L., Weintraub, H. & Lassar, A.B. (1987). Expression of a single transfected cDNA converts fibroblasts to myoblasts. *Cell* **51**: 987-1000.

de Crombrugghe, B., Lefebvre, V., Behringer, R.R., Bi, W., Murakami, S. & Huang, W. (2000). Transcriptional mechanisms of chondrocyte differentiation. *Matrix Biol* **19**: 389-94.

De Meyts, P., Wallach, B., Christoffersen, C.T., Urso, B., Gronskov, K., Latus, L.J., Yakushiji, F., Ilondo, M.M. & Shymko, R.M. (1994). The insulin-like growth factor-I receptor. Structure, ligand-binding mechanism and signal transduction. *Horm Res* **42**: 152-69.

de Murcia, G., Huletsky, A. & Poirier, G.G. (1988). Modulation of chromatin structure by poly(ADP-ribosyl)ation. *Biochem Cell Biol* **66**: 626-35.

de Murcia, G., Jongstra-Bilen, J., Ittel, M.E., Mandel, P. & Delain, E. (1983). Poly(ADP-ribose) polymerase auto-modification and interaction with DNA: electron microscopic visualization. *EMBO J* **2**: 543-8.

de Murcia, G., Schreiber, V., Molinete, M., Saulier, B., Poch, O., Masson, M., Niedergang, C. & Menissier de Murcia, J. (1994). Structure and function of poly(ADP-ribose) polymerase. *Mol Cell Biochem* **138**: 15-24.

de Murcia, J.M., Niedergang, C., Trucco, C., Ricoul, M., Dutrillaux, B., Mark, M., Oliver, F.J., Masson, M., Dierich, A., LeMeur, M., Walztinger, C., Chambon, P. & de Murcia, G. (1997). Requirement of poly(ADP-ribose) polymerase in recovery from DNA damage in mice and in cells. *Proc Natl Acad Sci U S A* **94**: 7303-7.

de Smet, B.J., Kuntz, R.E., van der Helm, Y.J., Pasterkamp, G., Borst, C. & Post, M.J. (1997). Relationship between plaque mass and neointimal hyperplasia after stent placement in Yucatan micropigs. *Radiology* **203**: 484-8.

de Vries-Smits, A.M., Burgering, B.M., Leevers, S.J., Marshall, C.J. & Bos, J.L. (1992). Involvement of p21ras in activation of extracellular signal-regulated kinase 2. *Nature* **357**: 602-4.

Delafontaine, P., Lou, H. & Alexander, R.W. (1991). Regulation of insulin-like growth factor I messenger RNA levels in vascular smooth muscle cells. *Hypertension* **18**: 742-7.

Della Rocca, G.J., van Biesen, T., Daaka, Y., Luttrell, D.K., Luttrell, L.M. & Lefkowitz, R.J. (1997). Ras-dependent mitogen-activated protein kinase activation by G protein- coupled receptors. Convergence of Gi- and Gq-mediated pathways on calcium/calmodulin, Pyk2, and Src kinase. *J Biol Chem* **272**: 19125-32.

DeLuca, C., Massaro, E.J. & Cohen, M.M. (1972). Biochemical and cytogenetic characterization of rat hepatoma cell lines in vitro. *Cancer Res* **32**: 2435-40.

Denizot, F. & Lang, R. (1986). Rapid colorimetric assay for cell growth and survival: Modifications to the tetrazolium dye procedure giving improved sensitivity and reliability. *J Immunol Methods* **89**: 271-77.

Desmet, W., Vrolix, M., De Scheerder, I., Van Lierde, J., Willems, J.L. & Piessens, J. (1994). Angiotensin-converting enzyme inhibition with fosinopril sodium in the prevention of restenosis after coronary angioplasty. *Circulation* **89**: 385-92.

Desnoyers, S., Shah, G.M., Brochu, G., Hoflack, J.C., Verreault, A. & Poirier, G.G. (1995). Biochemical properties and function of poly(ADP-ribose) glycohydrolase. *Biochimie* **77**: 433-8.

Devlin, B.H. & Konigsberg, I.R. (1983). Reentry into the cell cycle of differentiated skeletal myocytes. *Dev Biol* **95**: 175-92.

Di Cola, G., Cool, M.H. & Accili, D. (1997). Hypoglycemic effect of insulin-like growth factor-1 in mice lacking insulin receptors. *J Clin Invest* **99**: 2538-44.

Di Girolamo, M., Lupi, R., Silletta, M.G., Turacchio, S., Iurisci, C., Luini, A. & Corda, D. (1997). Modulatory role of GTP-binding proteins in the endogenous ADP-ribosylation of cytosolic proteins. *Adv Exp Med Biol* **419**: 343-7.

Di Salvo, J., Nelson, S.R. & Kaplan, N. (1997). Protein tyrosine phosphorylation in smooth muscle: a potential coupling mechanism between receptor activation and intracellular calcium. *Proc Soc Exp Biol Med* **214**: 285-301.

Dias, P., Dilling, M. & Houghton, P. (1994). The molecular basis of skeletal muscle differentiation. *Semin Diagn Pathol* **11**: 3-14.

Diaz, A., Munoz, E., Johnston, R., Korn, J.H. & Jimenez, S.A. (1993). Regulation of human lung fibroblast alpha 1(I) procollagen gene expression by tumor necrosis factor alpha, interleukin-1 beta, and prostaglandin E2. *J Biol Chem* **268**: 10364-71.

Dike, L.E. & Ingber, D.E. (1996). Integrin-dependent induction of early growth response genes in capillary endothelial cells. *J Cell Sci* **109**: 2855-63.

Domenighini, M. & Rappuoli, R. (1996). Three conserved consensus sequences identify the NAD-binding site of ADP-ribosylating enzymes, expressed by eukaryotes, bacteria and T-even bacteriophages. *Mol Microbiol* **21**: 667-74.

Donadoni, M.L., Gavezzotti, R., Borella, F., Di Giulio, A.M. & Gorio, A. (1995). Experimental diabetic neuropathy. Inhibition of protein mono-ADP- ribosylation prevents reduction of substance P axonal transport. *J Pharmacol Exp Ther* **274**: 570-6.

Donnelly, L.E., Boyd, R.S. & MacDermot, J. (1992). Gs alpha is a substrate for mono(ADP-ribosyl)transferase of NG108-15 cells. ADP-ribosylation regulates Gs alpha activity and abundance. *Biochem J* **288**: 331-6.

Dorland, W.A.N. (1988). *Dorland's illustrated medical dictionary*.W.B. Saunders, Philadelphia. xxxii, 1888.

Duband, J.L., Gimona, M., Scatena, M., Sartore, S. & Small, J.V. (1993). Calponin and SM 22 as differentiation markers of smooth muscle: spatiotemporal distribution during avian embryonic development. *Differentiation* **55**: 1-11.

Dubey, R.K., Jackson, E.K. & Luscher, T.F. (1995). Nitric oxide inhibits angiotensin II-induced migration of rat aortic smooth muscle cell. Role of cyclic-nucleotides and angiotensin1 receptors. *J Clin Invest* **96**: 141-9.

Dudley, D.T., Pang, L., Decker, S.J., Bridges, A.J. & Saltiel, A.R. (1995). A synthetic inhibitor of the mitogen-activated protein kinase cascade. *Proc Natl Acad Sci U S A* **92**: 7686-9.

Duman, R.S., Terwilliger, R.Z. & Nestler, E.J. (1991). Endogenous ADP-ribosylation in brain: initial characterization of substrate proteins. *J Neurochem* **57**: 2124-32.

Duncan, M.R., Rankin, P.R., King, R.L., Jacobson, M.K. & Dell'Orco, R.T. (1988). Stimulation of mono (ADP-ribosyl)ation by reduced extracellular calcium levels in human fibroblasts. *J Cell Physiol* **134**: 161-5.

Duprey, P. & Lesens, C. (1994). Control of skeletal muscle-specific transcription: involvement of paired homeodomain and MADS domain transcription factors. *Int J Dev Biol* **38**: 591-604.

Eber, B., Schumacher, M., Auer-Grumbach, P., Toplak, H. & Klein, W. (1992). Increased IgM-anticardiolipin antibodies in patients with restenosis after percutaneous transluminal coronary angioplasty. *Am J Cardiol* **69**: 1255-8.

Egan, S.E., Giddings, B.W., Brooks, M.W., Buday, L., Sizeland, A.M. & Weinberg, R.A. (1993). Association of Sos Ras exchange protein with Grb2 is implicated in tyrosine kinase signal transduction and transformation. *Nature* **363**: 45-51.

Ehrengruber, M.U., Boquet, P., Coates, T.D. & Deranleau, D.A. (1995). ADP-ribosylation of Rho enhances actin polymerization-coupled shape oscillations in human neutrophils. *FEBS Lett* **372**: 161-4.

Elbaum, M., Chausovsky, A., Levy, E.T., Shtutman, M. & Bershadsky, A.D. (1999). Microtubule involvement in regulating cell contractility and adhesion- dependent signalling: a possible mechanism for polarization of cell motility. *Biochem Soc Symp* **65**: 147-72.

Eldar-Finkelman, H., Seger, R., Vandenheede, J.R. & Krebs, E.G. (1995). Inactivation of glycogen synthase kinase-3 by epidermal growth factor is mediated by mitogen-activated protein kinase/p90 ribosomal protein S6 kinase signaling pathway in NIH/3T3 cells. *J Biol Chem* **270**: 987-90.

Ellis, S.G. & Muller, D.W. (1992). Arterial injury and the enigma of coronary restenosis [editorial; comment]. *J Am Coll Cardiol* **19**: 275-7.

Ellis, S.G., Savage, M., Fischman, D., Baim, D.S., Leon, M., Goldberg, S., Hirshfeld, J.W., Cleman, M.W., Teirstein, P.S., Walker, C. & et al. (1992). Restenosis after placement of Palmaz-Schatz stents in native coronary arteries. Initial results of a multicenter experience. *Circulation* **86**: 1836-44.

Evans, M.J. & Kovacs, C.J. (1977). Properties of the H-4-II-E tumor cell system. I. Growth and cell proliferation kinetics of an experimental hepatoma. *Cell Tissue Kinet* **10**: 233-43.

Fan, Y.Y., Ramos, K.S. & Chapkin, R.S. (1997). Dietary gamma-linolenic acid enhances mouse macrophage-derived prostaglandin E1 which inhibits vascular smooth muscle cell proliferation. *J Nutr* **127**: 1765-71.

Farzaneh, F., Zalin, R., Brill, D. & Shall, S. (1982). DNA strand breaks and ADP-ribosyl transferase activation during cell differentiation. *Nature* **300**: 362-6.

Favaloro, R.G. (1994). Current status of coronary artery bypass graft (CABG) surgery. *Semin Thorac Cardiovasc Surg* **6**: 67-71.

Faxon, D.P., Coats, W. & Currier, J. (1997). Remodeling of the coronary artery after vascular injury. *Prog Cardiovasc Dis* **40**: 129-40.

Feige, J.J. & Baird, A. (1989). Basic fibroblast growth factor is a substrate for protein phosphorylation and is phosphorylated by capillary endothelial cells in culture. *Proc Natl Acad Sci U S A* **86**: 3174-8.

Feigelson, P. & Greengard, O. (1961). a microsomal iron-porphyrin activator of rat liver tryptophan pyrrolase. *J Biol Chem* **236**: 153-157.

Ferby, I.M., Waga, I., Sakanaka, C., Kume, K. & Shimizu, T. (1994). Wortmannin inhibits mitogen-activated protein kinase activation induced by platelet-activating factor in guinea pig neutrophils. *J Biol Chem* **269**: 30485-8.

Ferguson, M.A. & Williams, A.F. (1988). Cell-surface anchoring of proteins via glycosyl-phosphatidylinositol structures. *Annu Rev Biochem* **57**: 285-320.

Fernandez-Alfonso, M.S., Martorana, P.A., Licka, I., van Even, P., Trobisch, D., Scholkens, B.A. & Paul, M. (1997). Early induction of angiotensin I-converting enzyme in rat carotid artery after balloon injury. *Hypertension* **30**: 272-7.

Ferrari, S., Molinari, S., Melchionna, R., Cusella-De Angelis, M.G., Battini, R., De Angelis, L., Kelly, R. & Cossu, G. (1997). Absence of MEF2 binding to the A/T-rich element in the muscle creatine kinase (MCK) enhancer correlates with lack of early expression of the MCK gene in embryonic mammalian muscle. *Cell Growth Differ* **8**: 23-34.

Ferrell, M., Fuster, V., Gold, H.K. & Chesebro, J.H. (1992). A dilemma for the 1990s. Choosing appropriate experimental animal model for the prevention of restenosis. *Circulation* **85**: 1630-1.

Ferro, A.M. & Olivera, B.M. (1984). Poly(ADP-ribosylation) of DNA topoisomerase I from calf thymus. *J Biol Chem* **259**: 547-54.

Field, M. (1976). Regulation of active ion transport in the small intestine. *Ciba Found Symp* **42**: 109-27.

Finking, G. & Hanke, H. (1997). Nikolaj Nikolajewitsch Anitschkow (1885-1964) established the cholesterol-fed rabbit as a model for atherosclerosis research. *Atherosclerosis* **135**: 1-7.

Fischell, T.A., Derby, G., Tse, T.M. & Stadius, M.L. (1988). Coronary artery vasoconstriction routinely occurs after percutaneous transluminal coronary angioplasty. A quantitative arteriographic analysis. *Circulation* **78**: 1323-34.

Fischman, D.L., Leon, M.B., Baim, D.S., Schatz, R.A., Savage, M.P., Penn, I., Detre, K., Veltri, L., Ricci, D., Nobuyoshi, M. & et al. (1994). A randomized comparison of coronary-stent placement and balloon angioplasty in the treatment of coronary artery disease. Stent Restenosis Study Investigators. *N Engl J Med* **331**: 496-501.

Fishman, J.A., Ryan, G.B. & Karnovsky, M.J. (1975). Endothelial regeneration in the rat carotid artery and the significance of endothelial denudation in the pathogenesis of myointimal thickening. *Lab Invest* **32**: 339-51.

Fletcher, L.M. & Tavare, J.M. (1999). Divergent signalling mechanisms involved in insulin-stimulated GLUT4 vesicle trafficking to the plasma membrane. *Biochem Soc Trans* **27**: 677-83.

Florio, C., Martin, J.G., Styhler, A. & Heisler, S. (1994). Antiproliferative effect of prostaglandin E2 in cultured guinea pig tracheal smooth muscle cells. *Am J Physiol* **266**: L131-7.

Force, T. & Bonventre, J.V. (1998). Growth factors and mitogen-activated protein kinases. *Hypertension* **31**: 152-61.

Forrester, J.S., Fishbein, M., Helfant, R. & Fagin, J. (1991). A paradigm for restenosis based on cell biology: clues for the development of new preventive therapies. *J Am Coll Cardiol* **17**: 758-69.

Franks, D.J., Plamondon, J. & Hamet, P. (1984). An increase in adenylate cyclase activity precedes DNA synthesis in cultured vascular smooth muscle cells. *J Cell Physiol* **119**: 41-5.

Frattali, A.L., Treadway, J.L. & Pessin, J.E. (1992). Transmembrane signaling by the human insulin receptor kinase. Relationship between intramolecular beta subunit trans- and cis- autophosphorylation and substrate kinase activation. *J Biol Chem* **267**: 19521-8.

Freemark, M., D'Ercole, A.J. & Handwerger, S. (1985). Somatomedin-C stimulates glycogen synthesis in fetal rat hepatocytes. *Endocrinology* **116**: 2578-82.

Frid, M.G., Moiseeva, E.P. & Stenmark, K.R. (1994). Multiple phenotypically distinct smooth muscle cell populations exist in the adult and developing bovine pulmonary arterial media in vivo. *Circ Res* **75**: 669-81.

Frishman, W.H., Chiu, R., Landzberg, B.R. & Weiss, M. (1998). Medical therapies for the prevention of restenosis after percutaneous coronary interventions. *Curr Probl Cardiol* **23**: 534-635.

Fritz, K.E., Jarmolych, J. & Daoud, A.S. (1970). Association of DNA synthesis and apparent dedifferentiation of aortic smooth muscle cells in vitro. *Exp Mol Pathol* **12**: 354-62.

Fujita, H., Okamoto, H. & Tsuyama, S. (1995). ADP-ribosylation in adrenal glands: purification and characterization of mono-ADP-ribosyltransferases and ADP-ribosylhydrolase affecting cytoskeletal actin. *Int J Biochem Cell Biol* **27**: 1065-78.

Fukuyama, J., Ichikawa, K., Hamano, S. & Shibata, N. (1996). Tranilast suppresses the vascular intimal hyperplasia after balloon injury in rabbits fed on a high-cholesterol diet. *Eur J Pharmacol* **318**: 327-32.

Furneaux, H.M. & Pearson, C.K. (1980). Intracellular NAD+ content and ADP-ribose polymerase activity of serum- stimulated baby hamster kidney fibroblasts. *J Cell Physiol* **105**: 401-7.

Furst, D.O., Osborn, M. & Weber, K. (1989). Myogenesis in the mouse embryo: differential onset of expression of myogenic proteins and the involvement of titin in myofibril assembly. *J Cell Biol* **109**: 517-27.

Fuster, V., Badimon, L., Badimon, J.J., Ip, J.H. & Chesebro, J.H. (1991). The porcine model for the understanding of thrombogenesis and atherogenesis. *Mayo Clin Proc* **66**: 818-31.

Gal, D., Rongione, A.J., Slovenkai, G.A., DeJesus, S.T., Lucas, A., Fields, C.D. & Isner, J.M. (1990). Atherosclerotic Yucatan microswine: an animal model with high-grade, fibrocalcific, nonfatty lesions suitable for testing catheter-based interventions. *Am Heart J* **119**: 291-300.

Galbut, D.L., Traad, E.A., Dorman, M.J., DeWitt, P.L., Larsen, P.B., Kurlansky, P.A., Button, J.H., Ally, J.M. & Gentsch, T.O. (1990). Seventeen-year experience with bilateral internal mammary artery grafts. *Ann Thorac Surg* **49**: 195-201.

Gallo, R., Padurean, A., Toschi, V., Bichler, J., Fallon, J.T., Chesebro, J.H., Fuster, V. & Badimon, J.J. (1998). Prolonged thrombin inhibition reduces restenosis after balloon angioplasty in porcine coronary arteries. *Circulation* **97**: 581-8.

Gasnier, B., Roisin, M.P., Scherman, D., Coornaert, S., Desplanches, G. & Henry, J.P. (1986). Uptake of meta-iodobenzylguanidine by bovine chromaffin granule membranes. *Mol Pharmacol* **29**: 275-80.

Gawler, D., Milligan, G., Spiegel, A.M., Unson, C.G. & Houslay, M.D. (1987). Abolition of the expression of inhibitory guanine nucleotide regulatory protein Gi activity in diabetes. *Nature* **327**: 229-32.

Gay, C.G. & Winkles, J.A. (1991). Interleukin 1 regulates heparin-binding growth factor 2 gene expression in vascular smooth muscle cells. *Proc Natl Acad Sci U S A* **88**: 296-300.

Gaze, M.N., Huxham, I.M., Mairs, R.J. & Barrett, A. (1991). Intracellular localization of metaiodobenzyl guanidine in human neuroblastoma cells by electron spectroscopic imaging. *Int J Cancer* **47**: 875-80.

Gershlick, A.H. & Baron, J. (1998). Dealing with in-stent restenosis. *Heart* **79**: 319-23.

Ghani, Q.P., Hussain, M.Z., Zhang, J. & Hunt, K.H. (1992). Control of procollagen gene transcription and prolyl hydroxylase activity by poly(ADP-ribose). In: ADP-ribosylation reactions. Poirier, g.G. & Moreau, P. (eds.). Springer-Verlag, New York. pp 211-217.

Giasson, E., Servant, M.J. & Meloche, S. (1997). Cyclic AMP-mediated inhibition of angiotensin II-induced protein synthesis is associated with suppression of tyrosine phosphorylation signaling in vascular smooth muscle cells. *J Biol Chem* **272**: 26879-86.

Gibbons, G.H. & Dzau, V.J. (1994). The emerging concept of vascular remodeling. *N Engl J Med* **330**: 1431-8.

Gierschik, P. (1992). ADP-ribosylation of signal-transducing guanine nucleotide-binding proteins by pertussis toxin. *Curr Top Microbiol Immunol* **175**: 69-96.

Gill, D.M. & Meren, R. (1978). ADP-ribosylation of membrane proteins catalyzed by cholera toxin: basis of the activation of adenylate cyclase. *Proc Natl Acad Sci U S A* **75**: 3050-4.

Gille, H., Sharrocks, A.D. & Shaw, P.E. (1992). Phosphorylation of transcription factor p62TCF by MAP kinase stimulates ternary complex formation at c-fos promoter. *Nature* **358**: 414-7.

Gimbrone, M.A., Jr. & Alexander, R.W. (1975). Angiotensin II stimulation of prostaglandin production in cultured human vascular endothelium. *Science* **189**: 219-20.

Gimbrone, M.A., Jr. & Cotran, R.S. (1975). Human vascular smooth muscle in culture. Growth and ultrastructure. *Lab Invest* **33**: 16-27.

Gire, V., Marshall, C. & Wynford-Thomas, D. (2000). PI-3-kinase is an essential anti-apoptotic effector in the proliferative response of primary human epithelial cells to mutant RAS. *Oncogene* **19**: 2269-76.

Gire, V., Marshall, C.J. & Wynford-Thomas, D. (1999). Activation of mitogen-activated protein kinase is necessary but not sufficient for proliferation of human thyroid epithelial cells induced by mutant Ras. *Oncogene* **18**: 4819-32.

Glagov, S. (1994). Intimal hyperplasia, vascular modeling, and the restenosis problem. *Circulation* **89**: 2888-91.

Glagov, S., Weisenberg, E., Zarins, C.K., Stankunavicius, R. & Kolettis, G.J. (1987). Compensatory enlargement of human atherosclerotic coronary arteries. *N Engl J Med* **316**: 1371-5.

Glowniak, J.V., Kilty, J.E., Amara, S.G., Hoffman, B.J. & Turner, F.E. (1993). Evaluation of metaiodobenzylguanidine uptake by the norepinephrine, dopamine and serotonin transporters. *J Nucl Med* **34**: 1140-6.

Glukhova, M.A., Frid, M.G. & Koteliansky, V.E. (1991). Phenotypic changes of human aortic smooth muscle cells during development and in the adult vessel. *Am J Physiol* **261**: 78-80.

Godeau, F., Belin, D. & Koide, S.S. (1984). Mono(adenosine diphosphate ribosyl) transferase in Xenopus tissues. Direct demonstration by a zymographic localization in sodium dodecyl sulfate--polyacrylamide gels. *Anal Biochem* **137**: 287-96.

Golino, P., Ambrosio, G., Ragni, M., Cirillo, P., Esposito, N., Willerson, J.T., Rothlein, R., Petrucci, L., Condorelli, M., Chiariello, M. & Buja, L.M. (1997). Inhibition of leucocyte and platelet adhesion reduces neointimal hyperplasia after arterial injury. *Thromb Haemost* **77**: 783-8.

Gordon, D., Mohai, L.G. & Schwartz, S.M. (1986). Induction of polyploidy in cultures of neonatal rat aortic smooth muscle cells. *Circ Res* **59**: 633-44.

Gordon, D., Reidy, M.A., Benditt, E.P. & Schwartz, S.M. (1990). Cell proliferation in human coronary arteries. *Proc Natl Acad Sci U S A* **87**: 4600-4.

Gorski, D.H., LePage, D.F., Patel, C.V., Copeland, N.G., Jenkins, N.A. & Walsh, K. (1993). Molecular cloning of a diverged homeobox gene that is rapidly down-regulated during the G0/G1 transition in vascular smooth muscle cells. *Mol Cell Biol* **13**: 3722-33.

Gospodarowicz, D., Hirabayashi, K., Giguere, L. & Tauber, J.P. (1981). Factors controlling the proliferative rate, final cell density, and life span of bovine vascular smooth muscle cells in culture. *J Cell Biol* **89**: 568-78.

Gotlieb & Havenith. (1991). Atherosclerosis lesions and pathogenesis. In: Cardiovascular pathology. Silver, M.D. (eds.). Churchill Livingstone, New York. pp 225-265.

Gotlieb, A.I. & Boden, P. (1984). Porcine aortic organ culture: a model to study the cellular response to vascular injury. *In Vitro* **20**: 535-42.

Grainger, D.J., Hesketh, T.R., Weissberg, P.L. & Metcalfe, J.C. (1992). Hexamethylenebisacetamide selectively inhibits the proliferation of human and rat vascular smooth-muscle cells. *Biochem J* **283**: 403-8.

Grainger, D.J., Witchell, C.M., Weissberg, P.L. & Metcalfe, J.C. (1994). Mitogens for adult rat aortic vascular smooth muscle cells in serum- free primary culture. *Cardiovasc Res* **28**: 1238-42.

Graves, D.J., Huiatt, T.W., Zhou, H., Huang, H.Y., Sernett, S.W., Robson, R.M. & McMahon, K.K. (1997). Regulatory role of arginine-specific mono(ADP-ribosyl)transferase in muscle cells. *Adv Exp Med Biol* **419**: 305-13.

Graves, J.D. & Krebs, E.G. (1999). Protein phosphorylation and signal transduction. *Pharmacol Ther* **82**: 111-21.

Graves, L.M., Bornfeldt, K.E., Raines, E.W., Potts, B.C., Macdonald, S.G., Ross, R. & Krebs, E.G. (1993). Protein kinase A antagonizes platelet-derived growth factor-induced signaling by mitogen-activated protein kinase in human arterial smooth muscle cells. *Proc Natl Acad Sci U S A* **90**: 10300-4.

Graves, L.M., Bornfeldt, K.E., Sidhu, J.S., Argast, G.M., Raines, E.W., Ross, R., Leslie, C.C. & Krebs, E.G. (1996). Platelet-derived growth factor stimulates protein kinase A through a mitogen-activated protein kinase-dependent pathway in human arterial smooth muscle cells. *J Biol Chem* **271**: 505-11.

Green, G.E. (1989). Use of internal thoracic artery for coronary artery grafting. *Circulation* **79**: I30-3.

Gregorini, L., Fajadet, J., Robert, G., Cassagneau, B., Bernis, M. & Marco, J. (1994). Coronary vasoconstriction after percutaneous transluminal coronary angioplasty is attenuated by antiadrenergic agents. *Circulation* **90**: 895-907.

Gregorini, L., Marco, J., Bernies, M., Cassagneau, B., Pomidossi, G., Anguissola, G.B. & Fajadet, J. (1997). The alpha-1 adrenergic blocking agent urapidil counteracts postrotational atherectomy "elastic recoil" where nitrates have failed. *Am J Cardiol* **79**: 1100-3.

Gressner, A.M. (1996). Transdifferentiation of hepatic stellate cells (Ito cells) to myofibroblasts: a key event in hepatic fibrogenesis. *Kidney Int Suppl* **54**: S39-45.

Gressner, A.M., Lahme, B. & Brenzel, A. (1995). Molecular dissection of the mitogenic effect of hepatocytes on cultured hepatic stellate cells. *Hepatology* **22**: 1507-18.

Grinstead, W.C., Rodgers, G.P., Mazur, W., French, B.A., Cromeens, D., Van Pelt, C., West, S.M. & Raizner, A.E. (1994). Comparison of three porcine restenosis models: the relative importance of hypercholesterolemia, endothelial abrasion, and stenting. *Coron Artery Dis* **5**: 425-34.

Grotendorst, G.R., Chang, T., Seppa, H.E., Kleinman, H.K. & Martin, G.R. (1982). Platelet-derived growth factor is a chemoattractant for vascular smooth muscle cells. *J Cell Physiol* **113**: 261-6.

Grotendorst, G.R., Seppa, H.E., Kleinman, H.K. & Martin, G.R. (1981). Attachment of smooth muscle cells to collagen and their migration toward platelet-derived growth factor. *Proc Natl Acad Sci U S A* **78**: 3669-72.

Grube, K. & Burkle, A. (1992). Poly(ADP-ribose) polymerase activity in mononuclear leukocytes of 13 mammalian species correlates with species-specific life span. *Proc Natl Acad Sci U S A* **89**: 11759-63.

Grundy, S.M. (1990). *Cholesterol and Atherosclerosis: Diagnosis and Treatment*.J.B. Lippincott Co., Philadelphia.

Gruntzig, A.R., Senning, A. & Siegenthaler, W.E. (1979). Nonoperative dilatation of coronary-artery stenosis: percutaneous transluminal coronary angioplasty. *N Engl J Med* **301**: 61-8.

Grunwald, J., Chobanian, A.V. & Haudenschild, C.C. (1987). Smooth muscle cell migration and proliferation: atherogenic mechanisms in hypertension. *Atherosclerosis* **67**: 215-21.

Guertner, C., Klepzig, H., Jr., Maul, F.D., Hartmann, A., Lelbach, S., Hellmann, A. & Hoer, G. (1993). Noradrenaline depletion in patients with coronary artery disease before and after percutaneous transluminal coronary angioplasty with iodine- 123 metaiodobenzylguanidine and single-photon emission tomography. *Eur J Nucl Med* **20**: 776-82.

Hadrava, V., Tremblay, J. & Hamet, P. (1989). Abnormalities in growth characteristics of aortic smooth muscle cells in spontaneously hypertensive rats. *Hypertension* **13**: 589-97.

Haggerty, D.F., Young, P.L., Buese, J.V. & Popjak, G. (1975). Effect of serum on phenylalanine hydroxylase levels in cultured hepatoma cells. *J Biol Chem* **250**: 8428-37.

Hahn, A.W., Resink, T.J., Bernhardt, J., Ferracin, F. & Buhler, F.R. (1991). Stimulation of autocrine platelet--derived growth factor AA-homodimer and transforming growth factor beta in vascular smooth muscle cells. *Biochem Biophys Res Commun* **178**: 1451-8.

Hahn, A.W., Resink, T.J., Scott-Burden, T., Powell, J., Dohi, Y. & Buhler, F.R. (1990). Stimulation of endothelin mRNA and secretion in rat vascular smooth muscle cells: a novel autocrine function. *Cell Regul* **1**: 649-59.

Hajjar, D.P. & Pomerantz, K.B. (1992). Signal transduction in atherosclerosis: integration of cytokines and the eicosanoid network. *FASEB J* **6**: 2933-41.

Hall, A. (1993). Ras-related proteins. *Curr Opin Cell Biol* **5**: 265-8.

Halldorsson, H., Bodvarsdottir, T., Kjeld, M. & Thorgeirsson, G. (1992). Role of ADP-ribosylation in endothelial signal transduction and prostacyclin production. *FEBS Lett* **314**: 322-6.

Hanasaki, K., Nakano, T. & Arita, H. (1990). Receptor-mediated mitogenic effect of thromboxane A2 in vascular smooth muscle cells. *Biochem Pharmacol* **40**: 2535-42.

Handley, D.A. (1995). Experimental therapeutics and clinical studies in (re)stenosis. *Micron* **26**: 51-68.

Hara, N., Mishima, K., Tsuchiya, M., Tanigawa, Y. & Shimoyama, M. (1987). Mono(ADP-ribosyl)ation of Ca2+-dependent ATPase in rabbit skeletal muscle sarcoplasmic reticulum and the effect of poly L-lysine. *Biochem Biophys Res Commun* **144**: 856-62.

Hara, S., Morishita, R., Tone, Y., Yokoyama, C., Inoue, H., Kaneda, Y., Ogihara, T. & Tanabe, T. (1995). Overexpression of prostacyclin synthase inhibits growth of vascular smooth muscle cells. *Biochem Biophys Res Commun* **216**: 862-7.

Hardcastle, J., Hardcastle, P.T. & Redfern, J.S. (1982). Morphine has no direct effect on PGE2-stimulated cyclic AMP production by rat isolated enterocytes. *J Pharm Pharmacol* **34**: 68.

Hardy, S., Kong, Y. & Konieczny, S.F. (1993). Fibroblast growth factor inhibits MRF4 activity independently of the phosphorylation status of a conserved threonine residue within the DNA- binding domain. *Mol Cell Biol* **13**: 5943-56.

Harker, L.A. (1987). Role of platelets and thrombosis in mechanisms of acute occlusion and restenosis after angioplasty. *Am J Cardiol* **60**: 20B-28B.

Hartikainen, J., Mustonen, J., Kuikka, J., Vanninen, E. & Kettunen, R. (1997). Cardiac sympathetic denervation in patients with coronary artery disease without previous myocardial infarction. *Am J Cardiol* **80**: 273-7.

Hassa, P.O. & Hottiger, M.O. (1999). A role of poly (ADP-ribose) polymerase in NF-kappaB transcriptional activation. *Biol Chem* **380**: 953-9.

Haudenschild, C.C. & Grunwald, J. (1985). Proliferative heterogeneity of vascular smooth muscle cells and its alteration by injury. *Exp Cell Res* **157**: 364-70.

Hauschildt, S., Ulmer, A.J., Flad, H.D., Heyden, T. & Heine, H. (1998). ADP-ribosylation: role in LPS-induced phosphorylation of two cytosolic proteins (p36/38) in monocytes. *Prog Clin Biol Res* **397**: 147-55.

Hautmann, M.B., Madsen, C.S., Mack, C.P. & Owens, G.K. (1998). Substitution of the degenerate smooth muscle (SM) alpha-actin CC(A/T- rich)6GG elements with c-fos serum response elements results in increased basal expression but relaxed SM cell specificity and reduced angiotensin II inducibility. *J Biol Chem* **273**: 8398-406.

Hautmann, M.B., Madsen, C.S. & Owens, G.K. (1997). A transforming growth factor beta (TGFbeta) control element drives TGFbeta-induced stimulation of smooth muscle alpha-actin gene expression in concert with two CArG elements. *J Biol Chem* **272**: 10948-56.

Hawes, B.E., Luttrell, L.M., van Biesen, T. & Lefkowitz, R.J. (1996). Phosphatidylinositol 3-kinase is an early intermediate in the G beta gamma-mediated mitogen-activated protein kinase signaling pathway. *J Biol Chem* **271**: 12133-6.

Hayaishi, O. & Ueda, K. (1977). Poly(ADP-ribose) and ADP-ribosylation of proteins. *Annu Rev Biochem* **46**: 95–116.

Hayashi, K., Nishio, E., Nakashima, K., Amioka, H., Kurokawa, J. & Kajiyama, G. (1992). Role of cholesterol-accumulating macrophages on vascular smooth muscle cell proliferation. *Clin Biochem* **25**: 345-9.

Heaton, J.H., Schilling, E.E., Gellehrter, T.D., Rechler, M.M., Spencer, C.J. & Nissley, S.P. (1980). Induction of tyrosine aminotransferase and amino acid transport in rat hepatoma cells by insulin and the insulin-like growth factor, multiplication-stimulating activity. Mediation by insulin and multiplication-stimulating activity receptors. *Biochim Biophys Acta* **632**: 192-203.

Hedin, K.E., Bell, M.P., Huntoon, C.J., Karnitz, L.M. & McKean, D.J. (1999a). Gi proteins use a novel beta gamma- and Ras-independent pathway to activate extracellular signal-regulated kinase and mobilize AP-1 transcription factors in Jurkat T lymphocytes. *J Biol Chem* **274**: 19992-20001.

Hedin, U., Roy, J., Tran, P.K., Lundmark, K. & Rahman, A. (1999b). Control of smooth muscle cell proliferation--the role of the basement membrane. *Thromb Haemost* **82** (Suppl 1): 23-6.

Hedqvist, P., Gautam, N. & Lindbom, L. (2000). Interactions between leukotrienes and other inflammatory mediators/modulators in the microvasculature. *Am J Respir Crit Care Med* **161**: S117-9.

Herity, N.A., Ward, M.R., Lo, S. & Yeung, A.C. (1999). Review: Clinical aspects of vascular remodeling. *J Cardiovasc Electrophysiol* **10**: 1016-24.

Hilz, H. (1997). ADP-ribose. A historical overview. *Adv Exp Med Biol* **419**: 15-24.

Hirata, Y., Takagi, Y., Fukuda, Y. & Marumo, F. (1989). Endothelin is a potent mitogen for rat vascular smooth muscle cells. *Atherosclerosis* **78**: 225-8.

Hoefnagel, C.A. (1994). Metaiodobenzylguanidine and somatostatin in oncology: role in the management of neural crest tumours. *Eur J Nucl Med* **21**: 561-81.

Hoefnagel, C.A., den Hartog Jager, F.C., Taal, B.G., Abeling, N.G. & Engelsman, E.E. (1987). The role of I-131-MIBG in the diagnosis and therapy of carcinoids. *Eur J Nucl Med* **13**: 187-91.

Hoefnagel, C.A., Schornagel, J. & Valdes Olmos, R.A. (1991). [131I]metaiodobenzylguanidine therapy of malignant pheochromocytoma: interference of medication. *J Nucl Biol Med* **35**: 308-12.

Hofbauer, R., Moser, D., Kaye, A.D., Knapp, S., Gmeiner, B., Kapiotis, S., Wagner, O. & Frass, M. (2000). Prostaglandin E(1) is able to increase migration of leukocytes through endothelial cell monolayers. *Microvasc Res* **59**: 354-60.

Hofstadter, F. (1995). [Pathology of wound healing]. *Chirurg* **66**: 174-81.

Holmes, D.R., Jr., Vlietstra, R.E., Smith, H.C., Vetrovec, G.W., Kent, K.M., Cowley, M.J., Faxon, D.P., Gruentzig, A.R., Kelsey, S.F., Detre, K.M. & et al. (1984). Restenosis after percutaneous transluminal coronary angioplasty (PTCA): a report from the PTCA Registry of the National Heart, Lung, and Blood Institute. *Am J Cardiol* **53**: 77C-81C.

Holmes, D.R., Wester, W., Thompson, R.W. & Reilly, J.M. (1997). Prostaglandin E2 synthesis and cyclooxygenase expression in abdominal aortic aneurysms. *J Vasc Surg* **25**: 810-5.

Holycross, B.J., Blank, R.S., Thompson, M.M., Peach, M.J. & Owens, G.K. (1992). Platelet-derived growth factor-BB-induced suppression of smooth muscle cell differentiation. *Circ Res* **71**: 1525-32.

Honjo, T., Nishizuka, Y. & Hayaishi, O. (1968). Diphtheria toxin-dependent adenosine diphosphate ribosylation of aminoacyl transferase II and inhibition of protein synthesis. *J Biol Chem* **243**: 3553-5.

Hoshi, H., Kan, M., Chen, J.K. & McKeehan, W.L. (1988). Comparative endocrinology-paracrinology-autocrinology of human adult large vessel endothelial and smooth muscle cells. *In Vitro Cell Dev Biol* **24**: 309-20.

Huang, H.Y., Graves, D.J., Robson, R.M. & Huiatt, T.W. (1993). ADP-ribosylation of the intermediate filament protein desmin and inhibition of desmin assembly in vitro by muscle ADP-ribosyltransferase. *Biochem Biophys Res Commun* **197**: 570-7.

Huang, H.Y., Zhou, H., Huiatt, T.W. & Graves, D.J. (1996). Target proteins for arginine-specific mono(ADP-ribosyl) transferase in membrane fractions from chick skeletal muscle cells. *Exp Cell Res* **226**: 147-53.

Huletsky, A., Niedergang, C., Frechette, A., Aubin, R., Gaudreau, A. & Poirier, G.G. (1985). Sequential ADP-ribosylation pattern of nucleosomal histones. ADP-ribosylation of nucleosomal histones. *Eur J Biochem* **146**: 277-85.

Hwang, D.L., Latus, L.J. & Lev-Ran, A. (1992). Effects of platelet-contained growth factors (PDGF, EGF, IGF-I, and TGF- beta) on DNA synthesis in porcine aortic smooth muscle cells in culture. *Exp Cell Res* **200**: 358-60.

Iavarone, A., Lasorella, A., Servidei, T., Riccardi, R. & Mastrangelo, R. (1993). Uptake and storage of m-iodobenzylguanidine are frequent neuronal functions of human neuroblastoma cell lines. *Cancer Res* **53**: 304-9.

Iglewski, W.J. (1994). Cellular ADP-ribosylation of elongation factor 2. *Mol Cell Biochem* **138**: 131-3.

Inagami, T. & Eguchi, S. (2000). Angiotensin II-mediated vascular smooth muscle cell growth signaling. *Braz J Med Biol Res* **33**: 619-24.

Ingber, D.E. & Folkman, J. (1989). How does extracellular matrix control capillary morphogenesis? *Cell* **58**: 803-5.

Ip, J.H., Fuster, V., Badimon, L., Badimon, J., Taubman, M.B. & Chesebro, J.H. (1990). Syndromes of accelerated atherosclerosis: role of vascular injury and smooth muscle cell proliferation. *J Am Coll Cardiol* **15**: 1667-87.

Isogaya, M., Yamada, N., Koike, H., Ueno, Y., Kumagai, H., Ochi, Y., Okazaki, S. & Nishio, S. (1995). Inhibition of restenosis by beraprost sodium (a prostaglandin I2 analogue) in the atherosclerotic rabbit artery after angioplasty. *J Cardiovasc Pharmacol* **25**: 947-52.

Itoh, H., Mukoyama, M., Pratt, R.E., Gibbons, G.H. & Dzau, V.J. (1993). Multiple autocrine growth factors modulate vascular smooth muscle cell growth response to angiotensin II. *J Clin Invest* **91**: 2268-74.

Iversen, L.L., Jarrott, B. & Simmonds, M.A. (1971). Differences in the uptake, storage and metabolism of (+)- and (-)- noradrenaline. *Br J Pharmacol* **43**: 845-55.

Ivert, T., Huttunen, K., Landou, C. & Bjork, V.O. (1988). Angiographic studies of internal mammary artery grafts 11 years after coronary artery bypass grafting. *J Thorac Cardiovasc Surg* **96**: 1-12.

Jackson, C.L. & Schwartz, S.M. (1992). Pharmacology of smooth muscle cell replication. *Hypertension* **20**: 713-36.

Jacobson, E.L., Cervantes-Laurean, D. & Jacobson, M.K. (1994). Glycation of proteins by ADP-ribose. *Mol Cell Biochem* **138**: 207-12.

Jacquemin, C., Thibout, H., Lambert, B. & Correze, C. (1986). Endogenous ADP-ribosylation of Gs subunit and autonomous regulation of adenylate cyclase. *Nature* **323**: 182-4.

Janakidevi, K., Fisher, M.A., Del Vecchio, P.J., Tiruppathi, C., Figge, J. & Malik, A.B. (1992). Endothelin-1 stimulates DNA synthesis and proliferation of pulmonary artery smooth muscle cells. *Am J Physiol* **263**: C1295-301.

Janat, M.F. & Liau, G. (1992). Transforming growth factor beta 1 is a powerful modulator of platelet- derived growth factor action in vascular smooth muscle cells. *J Cell Physiol* **150**: 232-42.

Jang, I.K., Lassila, R. & Fuster, V. (1993). Atherogenesis and inflammation. *Eur Heart J* **14** (Suppl K): 2-6.

Janknecht, R., Ernst, W.H., Pingoud, V. & Nordheim, A. (1993). Activation of ternary complex factor Elk-1 by MAP kinases. *EMBO J* **12**: 5097-104.

Jaques, S., Jr., Tobes, M.C. & Sisson, J.C. (1987). Sodium dependency of uptake of norepinephrine and m-iodobenzylguanidine into cultured human pheochromocytoma cells: evidence for uptake-one. *Cancer Res* **47**: 3920-8.

Jaques, S., Jr., Tobes, M.C., Sisson, J.C., Baker, J.A. & Wieland, D.M. (1984). Comparison of the sodium dependency of uptake of meta- Iodobenzylguanidine and norepinephrine into cultured bovine adrenomedullary cells. *Mol Pharmacol* **26**: 539-46.

Jarmolych, J., Daoud, A.S., Landau, J., Fritz, K.E. & McElvene, E. (1968). Aortic media explants. Cell proliferation and production of mucopolysaccharides, collagen, and elastic tissue. *Exp Mol Pathol* **9**: 171-88.

Johansson, M. (1999). A human poly(ADP-ribose) polymerase gene family (ADPRTL): cDNA cloning of two novel poly(ADP-ribose) polymerase homologues. *Genomics* **57**: 442-5.

Johnson, G.J., Griggs, T.R. & Badimon, L. (1999). The utility of animal models in the preclinical study of interventions to prevent human coronary artery restenosis: analysis and recommendations. On behalf of the Subcommittee on Animal, Cellular and Molecular Models of Thrombosis and Haemostasis of the Scientific and Standardization Committee of the International Society on Thrombosis and Haemostasis. *Thromb Haemost* **81**: 835-43.

Johnson, P.R., Armour, C.L., Carey, D. & Black, J.L. (1995). Heparin and PGE2 inhibit DNA synthesis in human airway smooth muscle cells in culture. *Am J Physiol* **269**: L514-9.

Jones, E.M. & Baird, A. (1997). Cell-surface ADP-ribosylation of fibroblast growth factor-2 by an arginine-specific ADP-ribosyltransferase. *Biochem J* **323**: 173-7.

Jonsson, O., Halldorsson, H., Kjeld, M. & Thorgeirsson, G. (1998). Inhibitory effects of meta-iodo-benzylguanidine (MIBG) on endothelial histamine receptor binding. *Biochim Biophys Acta* **1379**: 143-50.

Jumblatt, M.M. & Paterson, C.A. (1991). Prostaglandin E2 effects on corneal endothelial cyclic adenosine monophosphate synthesis and cell shape are mediated by a receptor of the EP2 subtype. *Invest Ophthalmol Vis Sci* **32**: 360-5.

Kadowaki, T., Tobe, K., Honda-Yamamoto, R., Tamemoto, H., Kaburagi, Y., Momomura, K., Ueki, K., Takahashi, Y., Yamauchi, T., Akanuma, Y. & Yazaki, Y. (1996). Signal transduction mechanism of insulin and insulin-like growth factor- 1. *Endocr J* **43** (Suppl): S33-41.

Kahn, B.B. (1996). Lilly lecture 1995. Glucose transport: pivotal step in insulin action. *Diabetes* **45**: 1644-54.

Kakuta, T., Currier, J.W., Haudenschild, C.C., Ryan, T.J. & Faxon, D.P. (1994). Differences in compensatory vessel enlargement, not intimal formation, account for restenosis after angioplasty in the hypercholesterolemic rabbit model. *Circulation* **89**: 2809-15.

Kallmeier, R.C., Somasundaram, C. & Babij, P. (1995). A novel smooth muscle-specific enhancer regulates transcription of the smooth muscle myosin heavy chain gene in vascular smooth muscle cells. *J Biol Chem* **270**: 30949-57.

Kameoka, M., Ota, K., Tetsuka, T., Tanaka, Y., Itaya, A., Okamoto, T. & Yoshihara, K. (2000). Evidence for regulation of NF-kappaB by poly(ADP-ribose) polymerase. *Biochem J* **346**: 641-9.

Kanagy, N.L., Charpie, J.R. & Webb, R.C. (1995). Nitric oxide regulation of ADP-ribosylation of G proteins in hypertension. *Med Hypotheses* **44**: 159-64.

Kapasi, A.A. & Singhal, P.C. (1999). Aging splenocyte and thymocyte apoptosis is associated with enhanced expression of p53, bax, and caspase-3. *Mol Cell Biol Res Commun* **1**: 78-81.

Kapeller, R. & Cantley, L.C. (1994). Phosphatidylinositol 3-kinase. *Bioessays* **16**: 565-76.

Karas, S.P., Gravanis, M.B., Santoian, E.C., Robinson, K.A., Anderberg, K.A. & King, S.B.d. (1992). Coronary intimal proliferation after balloon injury and stenting in swine: an animal model of restenosis. *J Am Coll Cardiol* **20**: 467-74.

Karin, M. (1996). The regulation of AP-1 activity by mitogen-activated protein kinases. *Philos Trans R Soc Lond B Biol Sci* **351**: 127-34.

Kasid, U.N., Halligan, B., Liu, L.F., Dritschilo, A. & Smulson, M. (1989). Poly(ADP-ribose)-mediated post-translational modification of chromatin- associated human topoisomerase I. Inhibitory effects on catalytic activity. *J Biol Chem* **264**: 18687-92.

Kastrati, A., Schomig, A., Dietz, R., Neumann, F.J. & Richardt, G. (1993). Time course of restenosis during the first year after emergency coronary stenting. *Circulation* **87**: 1498-505.

Kato, H., Faria, T.N., Stannard, B., Levy-Toledano, R., Taylor, S.I., Roberts, C.T., Jr. & LeRoith, D. (1993). Paradoxical biological effects of overexpressed insulin-like growth factor-1 receptors in Chinese hamster ovary cells. *J Cell Physiol* **156**: 145-52.

Katoh, Y. & Periasamy, M. (1996). Growth and differentiation of smooth muscle cells during vascular development. *Trends in Cardiovascular Medicine* **6**: 100-106.

Kaushal, S., Schneider, J.W., Nadal-Ginard, B. & Mahdavi, V. (1994). Activation of the myogenic lineage by MEF2A, a factor that induces and cooperates with MyoD. *Science* **266**: 1236-40.

Kawaichi, M., Ueda, K. & Hayaishi, O. (1981). Multiple autopoly(ADP-ribosyl)ation of rat liver poly(ADP-ribose) synthetase. Mode of modification and properties of automodified synthetase. *J Biol Chem* **256**: 9483-9.

Kefalas, P., Allport, J.R., Donnelly, L.E., Rendell, N.B., Murray, S., Taylor, G.W., Lo, G., Yadollahi-Farsani, M. & MacDermot, J. (1997). Arginine-specific mono(ADP-ribosyl)transferase activity in human neutrophil polymorphs. A possible link with the assembly of filamentous actin and chemotaxis. *Adv Exp Med Biol* **419**: 241-4.

Kefalas, P., Yadollahi-Farsani, M., Saxty, B.A. & MacDermot, J. (1998). Arginine-specific ADP-ribosyltransferase of human polymorphonuclear neutrophil

leucocytes: cDNA cloning and identification of a polymorphic site in the coding region. *Biochem Soc Trans* **26**: S81.

Kelley, C.A., Kawamoto, S., Conti, M.A. & Adelstein, R.S. (1991). Phosphorylation of vertebrate smooth muscle and nonmuscle myosin heavy chains in vitro and in intact cells. *J Cell Sci Suppl* **14**: 49-54.

Kelly, K.L. & Ruderman, N.B. (1993). Insulin-stimulated phosphatidylinositol 3-kinase. Association with a 185-kDa tyrosine-phosphorylated protein (IRS-1) and localization in a low density membrane vesicle. *J Biol Chem* **268**: 4391-8.

Kemp, P.R. & Metcalfe, J.C. (2000). Four isoforms of serum response factor that increase or inhibit smooth- muscle-specific promoter activity. *Biochem J* **345**: 445-51.

Kennedy, I., Coleman, R.A., Humphrey, P.P., Levy, G.P. & Lumley, P. (1982). Studies on the characterisation of prostanoid receptors: a proposed classification. *Prostaglandins* **24**: 667-89.

Khalil, R.A. & Morgan, K.G. (1993). PKC-mediated redistribution of mitogen-activated protein kinase during smooth muscle cell activation. *Am J Physiol* **265**: C406-11.

Kharadia, S.V., Huiatt, T.W., Huang, H.Y., Peterson, J.E. & Graves, D.J. (1992). Effect of an arginine-specific ADP-ribosyltransferase inhibitor on differentiation of embryonic chick skeletal muscle cells in culture. *Exp Cell Res* **201**: 33-42.

Kibbe, M.R., Billiar, T.R. & Tzeng, E. (2000). Gene therapy for restenosis. *Circ Res* **86**: 829-33.

Kiehlbauch, C.C., Aboul-Ela, N., Jacobson, E.L., Ringer, D.P. & Jacobson, M.K. (1993). High resolution fractionation and characterization of ADP-ribose polymers. *Anal Biochem* **208**: 26-34.

Kim, D.K., Zhang, L., Dzau, V.J. & Pratt, R.E. (1994). H19, a developmentally regulated gene, is reexpressed in rat vascular smooth muscle cells after injury. *J Clin Invest* **93**: 355-60.

Kim, S.J. & Kahn, C.R. (1997). Insulin regulation of mitogen-activated protein kinase kinase (MEK), mitogen-activated protein kinase and casein kinase in the cell nucleus: a possible role in the regulation of gene expression. *Biochem J* **323**: 621-7.

Kimball, B.P., Bui, S., Cohen, E.A., Carere, R.G. & Adelman, A.G. (1992). Comparison of acute elastic recoil after directional coronary atherectomy versus standard balloon angioplasty. *Am Heart J* **124**: 1459-66.

Kimes, B.W. & Brandt, B.L. (1976). Characterization of two putative smooth muscle cell lines from rat thoracic aorta. *Exp Cell Res* **98**: 349-66.

Kimura, T., Kaburagi, S., Tamura, T., Yokoi, H., Nakagawa, Y., Hamasaki, N., Nosaka, H., Nobuyoshi, M., Mintz, G.S., Popma, J.J. & Leon, M.B. (1997). Remodeling of human coronary arteries undergoing coronary angioplasty or atherectomy. *Circulation* **96**: 475-83.

Kimura, T., Miyauchi, K., Yamagami, S., Daida, H. & Yamaguchi, H. (1998). Local delivery infusion pressure is a key determinant of vascular damage and intimal thickening. *Jpn Circ J* **62**: 299-304.

King, S.B., 3rd, Williams, D.O., Chougule, P., Klein, J.L., Waksman, R., Hilstead, R., Macdonald, J., Anderberg, K. & Crocker, I.R. (1998). Endovascular beta-radiation to reduce restenosis after coronary balloon angioplasty: results of the beta energy restenosis trial (BERT). *Circulation* **97**: 2025-30.

Kirkland, J.B. (1991). Lipid peroxidation, protein thiol oxidation and DNA damage in hydrogen peroxide-induced injury to endothelial cells: role of activation of poly(ADP-ribose)polymerase. *Biochim Biophys Acta* **1092**: 319-25.

Kishi, K., Sasaki, T., Kuroda, S., Itoh, T. & Takai, Y. (1993). Regulation of cytoplasmic division of Xenopus embryo by rho p21 and its inhibitory GDP/GTP exchange protein (rho GDI). *J Cell Biol* **120**: 1187-95.

Kleczkowska, H.E. & Althaus, F.R. (1996). The role of poly(ADP-ribosyl)ation in the adaptive response. *Mutat Res* **358**: 215-21.

Klemke, R.L., Cai, S., Giannini, A.L., Gallagher, P.J., de Lanerolle, P. & Cheresh, D.A. (1997). Regulation of cell motility by mitogen-activated protein kinase. *J Cell Biol* **137**: 481-92 .

Kline, R.C., Swanson, D.P., Wieland, D.M., Thrall, J.H., Gross, M.D., Pitt, B. & Beierwaltes, W.H. (1981). Myocardial imaging in man with I-123 meta-iodobenzylguanidine. *J Nucl Med* **22**: 129-32.

Knebel, B., Kellner, S., Kotzka, J., Siemeister, G., Dreyer, M., Streicher, R., Schiller, M., Rudiger, H.W., Seemanova, E., Krone, W. & Muller-Wieland, D. (1997). Defects of insulin and IGF-1 action at receptor and postreceptor level in a patient with type A syndrome of insulin resistance. *Biochem Biophys Res Commun* **234**: 626-30.

Knox, W.E. (1951). Two mechanisms which increase in vivo the liver tryptophan peroxidase activity: Specific enzyme adaptation and stimulation of pituitary-adrenal system. *Brit J Exp Path* **32**: 462-469.

Knox, W.E., Auerbach, V.H. & Lin, E.C.C. (1956). Enzymatic and metabolic adaptations in animals. *Physiol Rev* **36**: 164-254.

Kocan, R.M., Moss, N.S. & Benditt, E.P. (1980). Human arterial wall cells and tissues in culture. *Methods Cell Biol*: 153-66.

Kocher, O., Gabbiani, F., Gabbiani, G., Reidy, M.A., Cokay, M.S., Peters, H. & Huttner, I. (1991). Phenotypic features of smooth muscle cells during the evolution of experimental carotid artery intimal thickening. Biochemical and morphologic studies. *Lab Invest* **65**: 459-70.

Kocher, O. & Gabbiani, G. (1986). Expression of actin mRNAs in rat aortic smooth muscle cells during development, experimental intimal thickening, and culture. *Differentiation* **32**: 245-51.

Kocher, O. & Madri, J.A. (1989). Modulation of actin mRNAs in cultured vascular cells by matrix components and TGF-beta 1. *In Vitro Cell Dev Biol* **25**: 424-34.

Koh, E., Morimoto, S., Jiang, B., Inoue, T., Nabata, T., Kitano, S., Yasuda, O., Fukuo, K. & Ogihara, T. (1993). Effects of beraprost sodium, a stable analogue of prostacyclin, on hyperplasia, hypertrophy and glycosaminoglycan synthesis of rat aortic smooth muscle cells. *Artery* **20**: 242-52.

Kolpakov, V., Gordon, D. & Kulik, T.J. (1995). Nitric oxide-generating compounds inhibit total protein and collagen synthesis in cultured vascular smooth muscle cells. *Circ Res* **76**: 305-9.

Komuro, I., Kurihara, H., Sugiyama, T., Yoshizumi, M., Takaku, F. & Yazaki, Y. (1988). Endothelin stimulates c-fos and c-myc expression and proliferation of vascular smooth muscle cells. *FEBS Lett* **238**: 249-52.

Koo, E.W. & Gotlieb, A.I. (1989). Endothelial stimulation of intimal cell proliferation in a porcine aortic organ culture. *Am J Pathol* **134**: 497-503.

Koo, E.W. & Gotlieb, A.I. (1991). Neointimal formation in the porcine aortic organ culture. I. Cellular dynamics over 1 month. *Lab Invest* **64**: 743-53.

Koo, E.W. & Gotlieb, A.I. (1992). The use of organ cultures to study vessel wall pathobiology. *Scanning Microsc* **6**: 827-34.

Koontz, J.W. (1984). The role of the insulin receptor in mediating the insulin-stimulated growth response in Reuber H-35 cells. *Mol Cell Biochem* **58**: 139-46.

Koopmann, C.F., Jr. (1995). Cutaneous wound healing. An overview. *Otolaryngol Clin North Am* **28**: 835-45.

Kovacs, C.J., Evans, M.J. & Hopkins, H.A. (1977). Properties of the H-4-II-E tumor cell system. II. In vitro characteristics of an experimental tumor cell line. *Cell Tissue Kinet* **10**: 245-54.

Kovala, T., Lorimer, I.A., Brickenden, A.M., Ball, E.H. & Sanwal, B.D. (1994). Protein kinase A regulation of cAMP phosphodiesterase expression in rat skeletal myoblasts. *J Biol Chem* **269**: 8680-5.

Kreimeyer, A., Wielckens, K., Adamietz, P. & Hilz, H. (1984). DNA repair-associated ADP-ribosylation in vivo. Modification of histone H1 differs from that of the principal acceptor proteins. *J Biol Chem* **259**: 890-6.

Krook, A., Moller, D.E., Dib, K. & O'Rahilly, S. (1996). Two naturally occurring mutant insulin receptors phosphorylate insulin receptor substrate-1 (IRS-1) but fail to mediate the biological effects of insulin. Evidence that IRS-1 phosphorylation is not sufficient for normal insulin action. *J Biol Chem* **271**: 7134-40.

Kudravi, S.A. & Reed, M.J. (2000). Aging, cancer, and wound healing. *In Vivo* **14**: 83-92.

Kuin, A., Aalders, M., van der Valk, M.A., Frey, A., Schmidt, H.H. & Smets, L.A. (1998). Renal toxicity of the neuron-blocking and mitochondriotropic agent m-iodobenzylguanidine. *Cancer Chemother Pharmacol* **42**: 37-45.

Kuin, A., Rutgers, M., van der Valk, M.A., Beijnen, J.H. & Smets, L.A. (1999). Bioavailability and toxicity after oral administration of m- iodobenzylguanidine (MIBG). *Br J Cancer* **79**: 802-6.

Kuin, A., Smets, L., Volk, T., Paans, A., Adams, G., Atema, A., Jahde, E., Maas, A., Rajewsky, M.F., Visser, G. & et al. (1994). Reduction of intratumoral pH by the mitochondrial inhibitor m-iodobenzylguanidine and moderate hyperglycemia. *Cancer Res* **54**: 3785-92.

Kumagai, N., Morii, N., Fujisawa, K., Nemoto, Y. & Narumiya, S. (1993). ADP-ribosylation of rho p21 inhibits lysophosphatidic acid-induced protein tyrosine phosphorylation and phosphatidylinositol 3-kinase activation in cultured Swiss 3T3 cells. *J Biol Chem* **268**: 24535-8.

Kuntz, R.E. & Baim, D.S. (1993). Defining coronary restenosis. Newer clinical and angiographic paradigms. *Circulation* **88**: 1310-23.

Kuntz, R.E. & Baim, D.S. (2000). Prevention of coronary restenosis : the evolving evidence base for radiation therapy. *Circulation* **101**: 2130-3.

Kuo, M.L., Chau, Y.P., Wang, J.H. & Shiah, S.G. (1996). Inhibitors of poly(ADP-ribose) polymerase block nitric oxide-induced apoptosis but not differentiation in human leukemia HL-60 cells. *Biochem Biophys Res Commun* **219**: 502-8.

Lafont, A., Guzman, L.A., Whitlow, P.L., Goormastic, M., Cornhill, J.F. & Chisolm, G.M. (1995). Restenosis after experimental angioplasty. Intimal, medial, and adventitial changes associated with constrictive remodeling. *Circ Res* **76**: 996-1002.

Lagueux, J., Shah, G.M., Menard, L., Thomassin, H., Duchaine, C., Hengartner, C. & Poirier, G.G. (1994). Poly(ADP-ribose) catabolism in mammalian cells. *Mol Cell Biochem* **138**: 45-52.

Lamawansa, M.D., Wysocki, S.J., House, A.K. & Norman, P.E. (1997). Morphometric changes seen in balloon-injured porcine iliac arteries: the influence of sympathectomy on intimal hyperplasia and remodelling. *Eur J Vasc Endovasc Surg* **13**: 43-7.

Lamawansa, M.D., Wysocki, S.J., House, A.K. & Norman, P.E. (1999). The changes seen in balloon-injured porcine femoral arteries following sympathectomy. *Cardiovasc Surg* **7**: 526-31.

Landzberg, B.R., Frishman, W.H. & Lerrick, K. (1997). Pathophysiology and pharmacological approaches for prevention of coronary artery restenosis following coronary artery balloon angioplasty and related procedures. *Prog Cardiovasc Dis* **39**: 361-98.

Lashford, L.S., Hancock, J.P. & Kemshead, J.T. (1991). Meta-iodobenzylguanidine (mIBG) uptake and storage in the human neuroblastoma cell line SK-N-BE(2C). *Int J Cancer* **47**: 105-9.

Laskey, W.K., Brady, S.T., Kussmaul, W.G., Waxler, A.R., Krol, J., Herrmann, H.C., Hirshfeld, J.W., Jr. & Sehgal, C. (1993). Intravascular ultrasonographic assessment of the results of coronary artery stenting. *Am Heart J* **125**: 1576-83.

Lassar, A. & Munsterberg, A. (1994). Wiring diagrams: regulatory circuits and the control of skeletal myogenesis. *Curr Opin Cell Biol* **6**: 432-42.

Lassar, A.B., Davis, R.L., Wright, W.E., Kadesch, T., Murre, C., Voronova, A., Baltimore, D. & Weintraub, H. (1991). Functional activity of myogenic HLH proteins requires hetero- oligomerization with E12/E47-like proteins in vivo. *Cell* **66**: 305-15.

Lassar, A.B., Skapek, S.X. & Novitch, B. (1994). Regulatory mechanisms that coordinate skeletal muscle differentiation and cell cycle withdrawal. *Curr Opin Cell Biol* **6**: 788-94.

Lau, K.W. & Sigwart, U. (1992). Novel coronary interventional devices: an update. *Am Heart J* **123**: 497-506.

Lau, K.W. & Sigwart, U. (1993). Angioplasty, stenting, atherectomy, and laser treatment after coronary artery bypass grafting. *Curr Opin Cardiol* **8**: 951-62.

Lau, K.-W. & Sigwart, U. (1995). Restenosis-an accelerated arteriopathy: pathophysiology, preventative strategies and research horizons. In: Molecular Interventions and Local Drug Delivery. Edelman, E.R. (eds.). W.B. Saunders Co. Ltd., London. pp 1-27.

Laughon, A. (1991). DNA binding specificity of homeodomains. *Biochemistry* **30**: 11357-67.

Lauris, V., Crettaz, M. & Kahn, C.R. (1986). Coordinate roles of insulin and glucose on the growth of hepatoma cells in culture. *Endocrinology* **118**: 2519-24.

Lautier, D., Lagueux, J., Thibodeau, J., Menard, L. & Poirier, G.G. (1993). Molecular and biochemical features of poly (ADP-ribose) metabolism. *Mol Cell Biochem* **122**: 171-93.

Law, R.E., Meehan, W.P., Xi, X.P., Graf, K., Wuthrich, D.A., Coats, W., Faxon, D. & Hsueh, W.A. (1996). Troglitazone inhibits vascular smooth muscle cell growth and intimal hyperplasia. *J Clin Invest* **98**: 1897-905.

Lawrence, M., Watson, L., Pettijohn, T., Doyle, T., Tasca, S.I. & Stoica, G. (1995). Immunohistochemical localization of proliferating cells, basic fibroblast growth factor and Fos protein following iliac artery balloon angioplasty in hypercholesterolemic rabbits. *In Vivo* **9**: 27-34.

Lawrence, R.A. & Jones, R.L. (1992). Investigation of the prostaglandin E (EP-) receptor subtype mediating relaxation of the rabbit jugular vein. *Br J Pharmacol* **105**: 817-24.

Lazar, D.F., Wiese, R.J., Brady, M.J., Mastick, C.C., Waters, S.B., Yamauchi, K., Pessin, J.E., Cuatrecasas, P. & Saltiel, A.R. (1995). Mitogen-activated protein kinase kinase inhibition does not block the stimulation of glucose utilization by insulin. *J Biol Chem* **270**: 20801-7.

Lazebnik, Y.A., Kaufmann, S.H., Desnoyers, S., Poirier, G.G. & Earnshaw, W.C. (1994). Cleavage of poly(ADP-ribose) polymerase by a proteinase with properties like ICE. *Nature* **371**: 346-7.

Ledford, B.E. & Leno, G.H. (1994). ADP-ribosylation of the molecular chaperone GRP78/BiP. *Mol Cell Biochem* **138**: 141-8.

Lee, D.J., Rosenfeldt, H. & Grinnell, F. (2000). Activation of ERK and p38 MAP kinases in human fibroblasts during collagen matrix contraction. *Exp Cell Res* **257**: 190-7.

Lee, N.D. (1956). The induced increase in the tryptophan peroxidase-oxidase activity of rat liver: Time studies. *J Biol Chem* **219**: 211-220.

Lefkovits, J. & Topol, E.J. (1997). Pharmacological approaches for the prevention of restenosis after percutaneous coronary intervention. *Prog Cardiovasc Dis* **40**: 141-58.

Lei, Z.Z. & Deng, Y.P. (1989). [The effect of prostaglandin E2 (PGE2) on growth, proliferation, morphology and protein synthesis of aortic smooth muscle cells (SMC) in vitro]. *Chung Hua Ping Li Hsueh Tsa Chih* **18**: 188-90.

Lemire, J.M., Covin, C.W., White, S., Giachelli, C.M. & Schwartz, S.M. (1994). Characterization of cloned aortic smooth muscle cells from young rats. *Am J Pathol* **144**: 1068-81.

Leno, G.H. & Ledford, B.E. (1989). ADP-ribosylation of the 78-kDa glucose-regulated protein during nutritional stress. *Eur J Biochem* **186**: 205-11.

Lerm, M., Schmidt, G. & Aktories, K. (2000). Bacterial protein toxins targeting rho GTPases. *FEMS Microbiol Lett* **188**: 1-6.

LeRoith, D., Werner, H., Beitner-Johnson, D. & Roberts, C.T., Jr. (1995). Molecular and cellular aspects of the insulin-like growth factor I receptor. *Endocr Rev* **16**: 143-63.

Leslie, J.B. & Watkins, W.D. (1985). Eicosanoids in the central nervous system. *J Neurosurg* **63**: 659-68.

Leverence, R.R., Beale, E.G. & Granner, D.K. (1988). 3-Aminobenzamide inhibits poly(ADP ribose) synthetase activity and induces phosphoenolpyruvate carboxykinase (GTP) in H4IIE hepatoma cells. *Arch Biochem Biophys* **260**: 667-73.

Levin, E.R. (1995). Endothelins. *N Engl J Med* **333**: 356-63.

Li, C. & Xu, Q. (2000). Mechanical stress-initiated signal transductions in vascular smooth muscle cells. *Cell Signal* **12**: 435-445.

Li, G., Chen, S.J., Oparil, S., Chen, Y.F. & Thompson, J.A. (2000). Direct in vivo evidence demonstrating neointimal migration of adventitial fibroblasts after balloon injury of rat carotid arteries. *Circulation* **101**: 1362-5.

Li, G., D'Souza-Schorey, C., Barbieri, M.A., Roberts, R.L., Klippel, A., Williams, L.T. & Stahl, P.D. (1995). Evidence for phosphatidylinositol 3-kinase as a regulator of endocytosis via activation of Rab5. *Proc Natl Acad Sci U S A* **92**: 10207-11.

Li, P.L., Chen, C.L., Bortell, R. & Campbell, W.B. (1999). 11,12-Epoxyeicosatrienoic acid stimulates endogenous mono-ADP- ribosylation in bovine coronary arterial smooth muscle. *Circ Res* **85**: 349-56.

Li, Z., Cheng, H., Lederer, W.J., Froehlich, J. & Lakatta, E.G. (1997). Enhanced proliferation and migration and altered cytoskeletal proteins in early passage smooth muscle cells from young and old rat aortic explants. *Exp Mol Pathol* **64**: 1-11.

Libby, P. & Hansson, G.K. (1991). Involvement of the immune system in human atherogenesis: current knowledge and unanswered questions. *Lab Invest* **64**: 5-15.

Libby, P., Ordovas, J.M., Birinyi, L.K., Auger, K.R. & Dinarello, C.A. (1986). Inducible interleukin-1 gene expression in human vascular smooth muscle cells. *J Clin Invest* **78**: 1432-8.

Libby, P. & Tanaka, H. (1997). The molecular bases of restenosis. *Prog Cardiovasc Dis* **40**: 97-106.

Libby, P., Warner, S.J. & Friedman, G.B. (1988). Interleukin 1: a mitogen for human vascular smooth muscle cells that induces the release of growth-inhibitory prostanoids. *J Clin Invest* **81**: 487-98.

Lim, L., Manser, E., Leung, T. & Hall, C. (1996). Regulation of phosphorylation pathways by p21 GTPases. The p21 Ras- related Rho subfamily and its role in phosphorylation signalling pathways. *Eur J Biochem* **242**: 171-85.

Lim, R.W., Zhu, C.Y. & Stringer, B. (1995). Differential regulation of primary response gene expression in skeletal muscle cells through multiple signal transduction pathways. *Biochim Biophys Acta* **1266**: 91-100.

Lin, L.L., Wartmann, M., Lin, A.Y., Knopf, J.L., Seth, A. & Davis, R.J. (1993). cPLA2 is phosphorylated and activated by MAP kinase. *Cell* **72**: 269-78.

Lin, Z., Lu, M.H., Schultheiss, T., Choi, J., Holtzer, S., DiLullo, C., Fischman, D.A. & Holtzer, H. (1994). Sequential appearance of muscle-specific proteins in myoblasts as a function of time after cell division: evidence for a conserved myoblast differentiation program in skeletal muscle. *Cell Motil Cytoskeleton* **29**: 1-19.

Lincoff, A.M., Topol, E.J. & Ellis, S.G. (1994). Local drug delivery for the prevention of restenosis. Fact, fancy, and future. *Circulation* **90**: 2070-84.

Lindahl, T., Satoh, M.S., Poirier, G.G. & Klungland, A. (1995). Post-translational modification of poly(ADP-ribose) polymerase induced by DNA strand breaks. *Trends Biochem Sci* **20**: 405-11.

Lindner, V., Lappi, D.A., Baird, A., Majack, R.A. & Reidy, M.A. (1991). Role of basic fibroblast growth factor in vascular lesion formation. *Circ Res* **68**: 106-13.

Lindner, V., Majack, R.A. & Reidy, M.A. (1990). Basic fibroblast growth factor stimulates endothelial regrowth and proliferation in denuded arteries. *J Clin Invest* **85**: 2004-8.

Lipton, B.H., Bensch, K.G. & Karasek, M.A. (1991). Microvessel endothelial cell transdifferentiation: phenotypic characterization. *Differentiation* **46**: 117-33.

Litvack, F., Eigler, N., Margolis, J., Rothbaum, D., Bresnahan, J.F., Holmes, D., Untereker, W., Leon, M., Kent, K., Pichard, A. & et al. (1994). Percutaneous excimer laser coronary angioplasty: results in the first consecutive 3,000 patients. The ELCA Investigators. *J Am Coll Cardiol* **23**: 323-9.

Liu, M.W., Roubin, G.S. & King, S.B.d. (1989). Restenosis after coronary angioplasty. Potential biologic determinants and role of intimal hyperplasia. *Circulation* **79**: 1374-87.

Livingstone, C., MacDonald, C., Willett, B. & Houslay, M.D. (1994). Analysis of the adenylate cyclase signalling system, and alterations induced by culture with insulin, in a novel SV40-DNA-immortalized hepatocyte cell line (P9 cells). *Biochem J* **300**: 835-42.

Lode, H.N., Bruchelt, G., Seitz, G., Gebhardt, S., Gekeler, V., Niethammer, D. & Beck, J. (1995). Reverse transcriptase-polymerase chain reaction (RT-PCR) analysis of monoamine transporters in neuroblastoma cell lines: correlations to meta-iodobenzylguanidine (MIBG) uptake and tyrosine hydroxylase gene expression. *Eur J Cancer* **4**: 586-90.

Loesberg, C., Van Rooij, H., Nooijen, W.J., Meijer, A.J. & Smets, L.A. (1990a). Impaired mitochondrial respiration and stimulated glycolysis by m-iodobenzylguanidine (MIBG). *Int J Cancer* **46**: 276-81.

Loesberg, C., van Rooij, H. & Smets, L.A. (1990b). Meta-iodobenzylguanidine (MIBG), a novel high-affinity substrate for cholera toxin that interferes with cellular mono(ADP-ribosylation). *Biochim Biophys Acta* **1037**: 92-9.

Loesberg, C., Van Rooji, H., Romijn, J.C. & Smets, L.A. (1991). Mitochondrial effects of the guanidino group-containing cytostatic drugs, m-iodobenzylguanidine and methylglyoxal bis (guanylhydrazone). *Biochem Pharmacol* **42**: 793-8.

Loesberg, C., van Wijk, R., Zandbergen, J., van Aken, W.G., van Mourik, J.A. & de Groot, P.G. (1985). Cell cycle-dependent inhibition of human vascular smooth muscle cell proliferation by prostaglandin E1. *Exp Cell Res* **160**: 117-25.

Lognonne, J.L. & Wahrmann, J.P. (1986). Spontaneous myoblast fusion is mediated by cell surface Ca2+-dependent protein kinase(s). *Exp Cell Res* **166**: 340-56.

Loop, F.D., Lytle, B.W., Cosgrove, D.M., Stewart, R.W., Goormastic, M., Williams, G.W., Golding, L.A., Gill, C.C., Taylor, P.C., Sheldon, W.C. & et al. (1986). Influence of the internal-mammary-artery graft on 10-year survival and other cardiac events. *N Engl J Med* **314**: 1-6.

Lopez-Ilasaca, M. (1998). Signaling from G-protein-coupled receptors to mitogen-activated protein (MAP)-kinase cascades. *Biochem Pharmacol* **56**: 269-77.

Lopez-Ilasaca, M., Crespo, P., Pellici, P.G., Gutkind, J.S. & Wetzker, R. (1997). Linkage of G protein-coupled receptors to the MAPK signaling pathway through PI 3-kinase gamma. *Science* **275**: 394-7.

Loppnow, H. & Libby, P. (1992). Functional significance of human vascular smooth muscle cell-derived interleukin 1 in paracrine and autocrine regulation pathways. *Exp Cell Res* **198**: 283-90.

Low, M.G. (1989). Glycosyl-phosphatidylinositol: a versatile anchor for cell surface proteins. *FASEB J* **3**: 1600-8.

Ludolph, D.C. & Konieczny, S.F. (1995). Transcription factor families: muscling in on the myogenic program. *FASEB J* **9**: 1595-604.

Lupi, R., Corda, D. & Di Girolamo, M. (2000). Endogenous ADP-ribosylation of the G protein beta subunit prevents the inhibition of type 1 adenylyl cyclase. *J Biol Chem* **275**: 9418-24.

Luttrell, L.M., van Biesen, T., Hawes, B.E., Koch, W.J., Krueger, K.M., Touhara, K. & Lefkowitz, R.J. (1997). G-protein-coupled receptors and their regulation: activation of the MAP kinase signaling pathway by G-protein-coupled receptors. *Adv Second Messenger Phosphoprotein Res* **31**: 263-77.

Luttrell, L.M., van Biesen, T., Hawes, B.E., Koch, W.J., Touhara, K. & Lefkowitz, R.J. (1995). G beta gamma subunits mediate mitogen-activated protein kinase activation by the tyrosine kinase insulin-like growth factor 1 receptor. *J Biol Chem* **270**: 16495-8.

Lydford, S.J., McKechnie, K.C. & Dougall, I.G. (1996). Pharmacological studies on prostanoid receptors in the rabbit isolated saphenous vein: a comparison with the rabbit isolated ear artery. *Br J Pharmacol* **117**: 13-20.

Lyon, R.T., Zarins, C.K., Lu, C.T., Yang, C.F. & Glagov, S. (1987). Vessel, plaque, and lumen morphology after transluminal balloon angioplasty. Quantitative study in distended human arteries. *Arteriosclerosis* 7: 306-14.

Lytle, B.W., Loop, F.D., Cosgrove, D.M., Ratliff, N.B., Easley, K. & Taylor, P.C. (1985). Long-term (5 to 12 years) serial studies of internal mammary artery and saphenous vein coronary bypass grafts. *J Thorac Cardiovasc Surg* **89**: 248-58.

Lytle, B.W., Loop, F.D., Cosgrove, D.M., Taylor, P.C., Goormastic, M., Peper, W., Gill, C.C., Golding, L.A. & Stewart, R.W. (1987). Fifteen hundred coronary reoperations. Results and determinants of early and late survival. *J Thorac Cardiovasc Surg* **93**: 847-59.

Madri, J.A., Bell, L., Marx, M., Merwin, J.R., Basson, C. & Prinz, C. (1991). Effects of soluble factors and extracellular matrix components on vascular cell behavior in vitro and in vivo: models of de- endothelialization and repair. *J Cell Biochem* **45**: 123-30.

Maehama, T., Sekine, N., Nishina, H., Takahashi, K. & Katada, T. (1994). Characterization of botulinum C3-catalyzed ADP-ribosylation of rho proteins and identification of mammalian C3-like ADP-ribosyltransferase. *Mol Cell Biochem* **138**: 135-40.

Majesky, M.W., Giachelli, C.M., Reidy, M.A. & Schwartz, S.M. (1992). Rat carotid neointimal smooth muscle cells reexpress a developmentally regulated mRNA phenotype during repair of arterial injury. *Circ Res* **71**: 759-68.

Malanga, M., Pleschke, J.M., Kleczkowska, H.E. & Althaus, F.R. (1998). Poly(ADP-ribose) binds to specific domains of p53 and alters its DNA binding functions. *J Biol Chem* **273**: 11839-43.

Malarkey, K., Chilvers, E.R., Lawson, M.F. & Plevin, R. (1995). Stimulation by endothelin-1 of mitogen-activated protein kinases and DNA synthesis in bovine tracheal smooth muscle cells. *Br J Pharmacol* **116**: 2267-73.

Malorni, W., Rivabene, R., Straface, E., Rainaldi, G., Monti, D., Salvioli, S., Cossarizza, A. & Franceschi, C. (1995). 3-Aminobenzamide protects cells from UV-B-induced apoptosis by acting on cytoskeleton and substrate adhesion. *Biochem Biophys Res Commun* **207**: 715-24.

Mangner, T.J., Tobes, M.C., Wieland, D.W., Sisson, J.C. & Shapiro, B. (1986). Metabolism of iodine-131 metaiodobenzylguanidine in patients with metastatic pheochromocytoma. *J Nucl Med* **27**: 37-44.

Mansour, S.J., Matten, W.T., Hermann, A.S., Candia, J.M., Rong, S., Fukasawa, K., Vande Woude, G.F. & Ahn, N.G. (1994). Transformation of mammalian cells by constitutively active MAP kinase kinase. *Science* **265**: 966-70.

Marais, R., Wynne, J. & Treisman, R. (1993). The SRF accessory protein Elk-1 contains a growth factor-regulated transcriptional activation domain. *Cell* **73**: 381-93.

Maresta, A., Balducelli, M., Cantini, L., Casari, A., Chioin, R., Fabbri, M., Fontanelli, A., Monici Preti, P.A., Repetto, S., De Servi, S. & et al. (1994). Trapidil (triazolopyrimidine), a platelet-derived growth factor antagonist, reduces restenosis after percutaneous transluminal coronary angioplasty. Results of the randomized, double-blind STARC study. Studio Trapidil versus Aspirin nella Restenosi Coronarica. *Circulation* **90**: 2710-5.

Margolis, J.R. & Mehta, S. (1992). Excimer laser coronary angioplasty. *Am J Cardiol* **69**: 3F-11F.

Marshall, C. (1999). How do small GTPase signal transduction pathways regulate cell cycle entry? *Curr Opin Cell Biol* **11**: 732-6.

Marshall, C.J. (1995). Specificity of receptor tyrosine kinase signaling: transient versus sustained extracellular signal-regulated kinase activation. *Cell* **80**: 179-85.

Marshall, C.J. (1996). Ras effectors. *Curr Opin Cell Biol* **8**: 197-204.

Maruta, H. & Burgess, A.W. (1994). Regulation of the Ras signalling network. *Bioessays* **16**: 489-96.

Maruyama, I., Shigeta, K., Miyahara, H., Nakajima, T., Shin, H., Ide, S. & Kitajima, I. (1997). Thrombin activates NF-kappa B through thrombin receptor and results in proliferation of vascular smooth muscle cells: role of thrombin in atherosclerosis and restenosis. *Ann N Y Acad Sci* **811**: 429-36.

Massague, J. & Czech, M.P. (1982). The subunit structures of two distinct receptors for insulin-like growth factors I and II and their relationship to the insulin receptor. *J Biol Chem* **257**: 5038-45.

Masutani, M., Suzuki, H., Kamada, N., Watanabe, M., Ueda, O., Nozaki, T., Jishage, K., Watanabe, T., Sugimoto, T., Nakagama, H., Ochiya, T. & Sugimura, T. (1999). Poly(ADP-ribose) polymerase gene disruption conferred mice resistant to streptozotocin-induced diabetes. *Proc Natl Acad Sci U S A* **96**: 2301-4.

Matsuyama, S. & Tsuyama, S. (1991). Mono-ADP-ribosylation in brain: purification and characterization of ADP-ribosyltransferases affecting actin from rat brain. *J Neurochem* **57**: 1380-7.

Mayo, M.L., Bringas, P., Jr., Santos, V., Shum, L. & Slavkin, H.C. (1992). Desmin expression during early mouse tongue morphogenesis. *Int J Dev Biol* **36**: 255-63.

McBride, W., Lange, R.A. & Hillis, L.D. (1988). Restenosis after successful coronary angioplasty. Pathophysiology and prevention. *N Engl J Med* **318**: 1734-7.

McClain, D.A., Maegawa, H., Thies, R.S. & Olefsky, J.M. (1990). Dissection of the growth versus metabolic effects of insulin and insulin-like growth factor-I in transfected cells expressing kinase- defective human insulin receptors. *J Biol Chem* **265**: 1678-82.

McDonald, L.J., Wainschel, L.A., Oppenheimer, N.J. & Moss, J. (1992). Amino acid-specific ADP-ribosylation: structural characterization and chemical differentiation of ADP-ribose-cysteine adducts formed nonenzymatically and in a pertussis toxin-catalyzed reaction. *Biochemistry* **31**: 11881-7.

McHugh, K.M. (1995). Molecular analysis of smooth muscle development in the mouse. *Dev Dyn* **204**: 278-90.

McKenna, K.T., McEniery, P.T., Maas, F., Aroney, C.N., Bett, J.H., Cameron, J., Holt, G. & Hossack, K.F. (1994). Percutaneous transluminal coronary angioplasty: clinical and quality of life outcomes one year later. *Aust N Z J Med* **24**: 15-21.

McKillop, I.H., Wu, Y., Cahill, P.A. & Sitzmann, J.V. (1998). Altered expression of inhibitory guanine nucleotide regulatory proteins (Gi-proteins) in experimental hepatocellular carcinoma. *J Cell Physiol* **175**: 295-304.

McNamara, C.A., Sarembock, I.J., Gimple, L.W., Fenton, J.W.d., Coughlin, S.R. & Owens, G.K. (1993). Thrombin stimulates proliferation of cultured rat aortic smooth muscle cells by a proteolytically activated receptor. *J Clin Invest* **91**: 94-8.

Meerkin, D., Bonan, R., Crocker, I.R., Arsenault, A., Chougule, P., Coen, V., Williams, D.O., Serruys, P. & King, S.B., 3rd. (1998). Efficacy of beta radiation in prevention of post-angioplasty restenosis. An interim report from the beta energy restenosis trial. *Herz* **23**: 356-61.

Mendoza-Alvarez, H. & Alvarez-Gonzalez, R. (1993). Poly(ADP-ribose) polymerase is a catalytic dimer and the automodification reaction is intermolecular. *J Biol Chem* **268**: 22575-80.

MERCATOR, S.G. (1992). Does the new angiotensin converting enzyme inhibitor cilazapril prevent restenosis after percutaneous transluminal coronary angioplasty? Results of the MERCATOR study: a multicenter, randomized, double-blind placebo-controlled trial. Multicenter European Research Trial with Cilazapril after Angioplasty to Prevent Transluminal Coronary Obstruction and Restenosis (MERCATOR) Study Group. *Circulation* **86**: 100-10.

Miano, J.M., Vlasic, N., Tota, R.R. & Stemerman, M.B. (1993). Localization of Fos and Jun proteins in rat aortic smooth muscle cells after vascular injury. *Am J Pathol* **142**: 715-24.

Mii, S., Ware, J.A., Mallette, S.A. & Kent, K.C. (1994). Effect of angiotensin II on human vascular smooth muscle cell growth. *J Surg Res* **57**: 174-8.

Milam, K.M. & Cleaver, J.E. (1984). Inhibitors of poly(adenosine diphosphate-ribose) synthesis: effect on other metabolic processes. *Science* **223**: 589-91.

Miles, K. & Wagner, M. (2000). Overexpression of nPKC theta is permissive for myogenic differentiation. *J Cell Biochem* **79**: 71-9.

Miller, D.A., Varthilingam, G.D., Borek, C. & Miller, O.J. (1972). The quinacine fluorescent and giemsa banding karyotype of the rat, Rattus norvegicus, and banded chromosome analyses of transformed and malignant rat liver cell lines. *Cancer Res* **32**: 2375.

Milligan, G. & Grassie, M.A. (1997). How do G-proteins stay at the plasma membrane? *Essays Biochem* **32**: 49-60.

Mintz, G.S., Hoffmann, R., Mehran, R., Pichard, A.D., Kent, K.M., Satler, L.F., Popma, J.J. & Leon, M.B. (1998). In-stent restenosis: the Washington Hospital Center experience. *Am J Cardiol* **81**: 7E-13E.

Mintz, G.S., Kent, K.M., Pichard, A.D., Satler, L.F., Popma, J.J. & Leon, M.B. (1997). Contribution of inadequate arterial remodeling to the development of focal coronary artery stenoses. An intravascular ultrasound study. *Circulation* **95**: 1791-8.

Mintz, G.S., Popma, J.J., Pichard, A.D., Kent, K.M., Satler, L.F., Wong, C., Hong, M.K., Kovach, J.A. & Leon, M.B. (1996). Arterial remodeling after coronary angioplasty: a serial intravascular ultrasound study. *Circulation* **94**: 35-43.

Miwa, M. & Sugimura, T. (1990). ADP-ribosylation and carcinogenesis. In: ADP-ribosylating toxin and G proteins: Insights into signal transduction. Moss, J. & Vaughan, M. (eds.). American Society of Microbiology, Washington. pp 543-560.

Mohn, K.L., Laz, T.M., Hsu, J.C., Melby, A.E., Bravo, R. & Taub, R. (1991). The immediate-early growth response in regenerating liver and insulin- stimulated H-35 cells: comparison with serum-stimulated 3T3 cells and identification of 41 novel immediate-early genes. *Mol Cell Biol* **11**: 381-90.

Molina y Vedia, L., Nolan, R.D. & Lapetina, E.G. (1989). The effect of iloprost on the ADP-ribosylation of Gs alpha (the alpha- subunit of Gs). *Biochem J* **261**: 841-5.

Molkentin, J.D., Li, L. & Olson, E.N. (1996). Phosphorylation of the MADS-Box transcription factor MEF2C enhances its DNA binding activity. *J Biol Chem* **271**: 17199-204.

Molkentin, J.D. & Olson, E.N. (1996a). Combinatorial control of muscle development by basic helix-loop-helix and MADS-box transcription factors. *Proc Natl Acad Sci U S A* **93**: 9366-73.

Molkentin, J.D. & Olson, E.N. (1996b). Defining the regulatory networks for muscle development. *Curr Opin Genet Dev* **6**: 445-53.

Montaldo, P.G., Carbone, R., Lanciotti, M., Ponzoni, M. & Cornaglia-Ferraris, P. (1991). In vitro pharmacology of metaiodobenzylguanidine uptake, storage and release in human neuroblastoma cells. *J Nucl Biol Med* **35**: 195-8.

Montaldo, P.G., Raffaghello, L., Guarnaccia, F., Pistoia, V., Garaventa, A. & Ponzoni, M. (1996). Increase of metaiodobenzylguanidine uptake and intracellular half-life during differentiation of human neuroblastoma cells. *Int J Cancer* **67**: 95-100.

Montaner, S., Perona, R., Saniger, L. & Lacal, J.C. (1999). Activation of serum response factor by RhoA is mediated by the nuclear factor-kappaB and C/EBP transcription factors. *J Biol Chem* **274**: 8506-15.

Morinelli, T.A., Zhang, L.M., Newman, W.H. & Meier, K.E. (1994). Thromboxane A2/prostaglandin H2-stimulated mitogenesis of coronary artery smooth muscle cells involves activation of mitogen-activated protein kinase and S6 kinase. *J Biol Chem* **269**: 5693-8.

Morisaki, N., Kanzaki, T., Motoyama, N., Saito, Y. & Yoshida, S. (1988). Cell cycle-dependent inhibition of DNA synthesis by prostaglandin I2 in cultured rabbit aortic smooth muscle cells. *Atherosclerosis* **71**: 165-71.

Morse, P.A., Gentry, G.A. & Potter, V.R. (1961). Pyrimidine metabolism in tissue culture cells derived from rat hepatomas. IV. Stationary cell cultures derived from minimal deviation hepatomas. *Cancer Res.*

Moss, J. (1987). Signal transduction by receptor-responsive guanyl nucleotide-binding proteins: modulation by bacterial toxin-catalyzed ADP-ribosylation. *Clin Res* **35**: 451-8.

Moss, J. & Stanley, S.J. (1981a). Amino acid-specific ADP-ribosylation. Identification of an arginine- dependent ADP-ribosyltransferase in rat liver. *J Biol Chem* **256**: 7830-3.

Moss, J. & Stanley, S.J. (1981b). Histone-dependent and histone-independent forms of an ADP- ribosyltransferase from human and turkey erythrocytes. *Proc Natl Acad Sci U S A* **78**: 4809-12.

Moss, J., Stanley, S.J., Nightingale, M.S., Murtagh, J.J., Jr., Monaco, L., Mishima, K., Chen, H.C., Williamson, K.C. & Tsai, S.C. (1992). Molecular and immunological characterization of ADP-ribosylarginine hydrolases. *J Biol Chem* **267**: 10481-8.

Moss, J., Stanley, S.J. & Watkins, P.A. (1980). Isolation and properties of an NAD- and guanidine-dependent ADP- ribosyltransferase from turkey erythrocytes. *J Biol Chem* **255**: 5838-40.

Moss, J., Tsai, S.C., Adamik, R., Chen, H.C. & Stanley, S.J. (1988). Purification and characterization of ADP-ribosylarginine hydrolase from turkey erythrocytes. *Biochemistry* **27**: 5819-23.

Moss, J. & Vaughan, M. (1977). Mechanism of action of choleragen. Evidence for ADP-ribosyltransferase activity with arginine as an acceptor. *J Biol Chem* **252**: 2455-7.

Moss, J. & Vaughan, M. (1988). ADP-ribosylation of guanyl nucleotide-binding regulatory proteins by bacterial toxins. *Adv Enzymol Relat Areas Mol Biol* **61**: 303-79.

Moss, J., Zolkiewska, A. & Okazaki, I. (1997). ADP-ribosylarginine hydrolases and ADP-ribosyltransferases. Partners in ADP-ribosylation cycles. *Adv Exp Med Biol* **419**: 25-33.

Mossman, T. (1983). Rapid colorimetric assay for cellular growth and survival: Application to proliferation and cytotoxicity assays. *J Immunol Methods* **65**: 55-63.

Mudra, H., Regar, E., Klauss, V., Werner, F., Henneke, K.H., Sbarouni, E. & Theisen, K. (1997). Serial follow-up after optimized ultrasound-guided deployment of Palmaz- Schatz stents. In-stent neointimal proliferation without significant reference segment response. *Circulation* **95**: 363-70.

Mueckler, M. (1994). Facilitative glucose transporters. *Eur J Biochem* **219**: 713-25.

Muller, D.W., Ellis, S.G. & Topol, E.J. (1991). Colchicine and antineoplastic therapy for the prevention of restenosis after percutaneous coronary interventions. *J Am Coll Cardiol* **17**: 126B-131B.

Muller, D.W., Ellis, S.G. & Topol, E.J. (1992a). Experimental models of coronary artery restenosis. *J Am Coll Cardiol* **19**: 418-32.

Muller, D.W., Topol, E.J., Abrams, G.D., Gallagher, K.P. & Ellis, S.G. (1992b). Intramural methotrexate therapy for the prevention of neointimal thickening after balloon angioplasty. *J Am Coll Cardiol* **20**: 460-6.

Murray, M.R. & Kopech, G. (1953). *A bibliography of the research in tissue culture.* Academic Press, Inc., New York.

Mutsaers, S.E., Bishop, J.E., McGrouther, G. & Laurent, G.J. (1997). Mechanisms of tissue repair: from wound healing to fibrosis. *Int J Biochem Cell Biol* **29**: 5-17.

Myers, M.G., Jr., Grammer, T.C., Wang, L.M., Sun, X.J., Pierce, J.H., Blenis, J. & White, M.F. (1994a). Insulin receptor substrate-1 mediates phosphatidylinositol 3'-kinase and p70S6k signaling during insulin, insulin-like growth factor-1, and interleukin-4 stimulation. *J Biol Chem* **269**: 28783-9.

Myers, M.G., Jr., Sun, X.J. & White, M.F. (1994b). The IRS-1 signaling system. *Trends Biochem Sci* **19**: 289-93.

Myers, M.G., Jr., Wang, L.M., Sun, X.J., Zhang, Y., Yenush, L., Schlessinger, J., Pierce, J.H. & White, M.F. (1994c). Role of IRS-1-GRB-2 complexes in insulin signaling. *Mol Cell Biol* **14**: 3577-87.

Myster, D.L. & Duronio, R.J. (2000). To differentiate or not to differentiate? *Curr Biol* **10**: R302-4.

Naftilan, A.J., Pratt, R.E. & Dzau, V.J. (1989). Induction of platelet-derived growth factor A-chain and c-myc gene expressions by angiotensin II in cultured rat vascular smooth muscle cells. *J Clin Invest* **83**: 1419-24.

Nagata, S., Kebo, D.K., Kunkel, S. & Glovsky, M.M. (1992). Effect of adenylate cyclase activators on C5a-induced human neutrophil aggregation, enzyme release and superoxide production. *Int Arch Allergy Immunol* **97**: 194-9.

Naidu, P.S., Ludolph, D.C., To, R.Q., Hinterberger, T.J. & Konieczny, S.F. (1995). Myogenin and MEF2 function synergistically to activate the MRF4 promoter during myogenesis. *Mol Cell Biol* **15**: 2707-18.

Naito, M., Stirk, C.M., Smith, E.B. & Thompson, W.D. (2000). Smooth muscle cell outgrowth stimulated by fibrin degradation products. The potential role of fibrin fragment E in restenosis and atherogenesis. *Thromb Res* **98**: 165-74.

Nakaki, T., Nakayama, M. & Kato, R. (1990). Inhibition by nitric oxide and nitric oxide-producing vasodilators of DNA synthesis in vascular smooth muscle cells. *Eur J Pharmacol* **189**: 347-53.

Nakata, T., Nagao, K., Tsuchihashi, K., Hashimoto, A., Tanaka, S. & Iimura, O. (1996). Regional cardiac sympathetic nerve dysfunction and the diagnostic efficacy of metaiodobenzylguanidine tomography in stable coronary artery disease. *Am J Cardiol* **78**: 292-7.

Narayanaswamy, M., Wright, K.C. & Kandarpa, K. (2000). Animal models for atherosclerosis, restenosis, and endovascular graft research. *J Vasc Interv Radiol* **11**: 5-17.

Negri, C., Donzelli, M., Bernardi, R., Rossi, L., Burkle, A. & Scovassi, A.I. (1997). Multiparametric staining to identify apoptotic human cells. *Exp Cell Res* **234**: 174-7.

Nelson, P.R., Yamamura, S., Mureebe, L., Itoh, H. & Kent, K.C. (1998). Smooth muscle cell migration and proliferation are mediated by distinct phases of activation of the intracellular messenger mitogen-activated protein kinase. *J Vasc Surg* **27**: 117-25.

Nemenoff, R.A., Winitz, S., Qian, N.X., Van Putten, V., Johnson, G.L. & Heasley, L.E. (1993). Phosphorylation and activation of a high molecular weight form of phospholipase A2 by p42 microtubule-associated protein 2 kinase and protein kinase C. *J Biol Chem* **268**: 1960-4.

Nemoto, E., Stohlman, S. & Dennert, G. (1996). Release of a glycosylphosphatidylinositol-anchored ADP- ribosyltransferase from cytotoxic T cells upon activation. *J Immunol* **156**: 85-92.

Neville, R.F. & Sidawy, A.N. (1998). Myointimal hyperplasia: basic science and clinical considerations. *Semin Vasc Surg* **11**: 142-8.

Newby, A.C. & George, S.J. (1993). Proposed roles for growth factors in mediating smooth muscle proliferation in vascular pathologies. *Cardiovasc Res* **27**: 1173-83.

Nguyen, H.T., Medford, R.M. & Nadal-Ginard, B. (1983). Reversibility of muscle differentiation in the absence of commitment: analysis of a myogenic cell line temperature-sensitive for commitment. *Cell* **34**: 281-93.

Nie, D., Lamberti, M., Zacharek, A., Li, L., Szekeres, K., Tang, K., Chen, Y. & Honn, K.V. (2000). Thromboxane A(2) regulation of endothelial cell migration, angiogenesis, and tumor metastasis. *Biochem Biophys Res Commun* **267**: 245-51.

Nikol, S. & Hofling, B. (1995). Regulation of smooth muscle cell proliferation and its possible role in preventing restenosis post-angioplasty. *Wien Klin Wochenschr* **107**: 379-89.

Nilsson, J. (1993). Cytokines and smooth muscle cells in atherosclerosis. *Cardiovasc Res* **27**: 1184-90.

Nilsson, J., Ksiazek, T., Heldin, C.H. & Thyberg, J. (1983). Demonstration of stimulatory effects of platelet-derived growth factor on cultivated rat arterial smooth muscle cells. Differences between cells from young and adult animals. *Exp Cell Res* **145**: 231-7.

Nilsson, J. & Olsson, A.G. (1984). Prostaglandin E1 inhibits DNA synthesis in arterial smooth muscle cells stimulated with platelet-derived growth factor. *Atherosclerosis* **53**: 77-82.

Nishiki, T., Narumiya, S., Morii, N., Yamamoto, M., Fujiwara, M., Kamata, Y., Sakaguchi, G. & Kozaki, S. (1990). ADP-ribosylation of the rho/rac proteins

induces growth inhibition, neurite outgrowth and acetylcholine esterase in cultured PC-12 cells. *Biochem Biophys Res Commun* **167**: 265-72.

Norgauer, J., Kownatzki, E., Seifert, R. & Aktories, K. (1988). Botulinum C2 toxin ADP-ribosylates actin and enhances O2- production and secretion but inhibits migration of activated human neutrophils. *J Clin Invest* **82**: 1376-82.

Novikoff, A.B. (1961). Enzyme localization in tumour cells. In: Cell physiology of neoplasia. Hsu, T.C. (eds.). Univ Texas Press, Austin. pp 219-268.

Obara, S., Mishima, K., Yamada, K., Taniguchi, M. & Shimoyama, M. (1989). DNA-regulated arginine-specific mono(ADP-ribosyl)ation and de-ADP-ribosylation of endogenous acceptor proteins in human neutrophils. *Biochem Biophys Res Commun* **163**: 452-7.

Obara, S., Yamada, K., Yoshimura, Y. & Shimoyama, M. (1991). Evidence for the endogenous GTP-dependent ADP-ribosylation of the alpha-subunit of the stimulatory guanyl-nucleotide-binding protein concomitant with an increase in basal adenylyl cyclase activity in chicken spleen cell membrane. *Eur J Biochem* **200**: 75-80.

O'Brien, E.R., Alpers, C.E., Stewart, D.K., Ferguson, M., Tran, N., Gordon, D., Benditt, E.P., Hinohara, T., Simpson, J.B. & Schwartz, S.M. (1993). Proliferation in primary and restenotic coronary atherectomy tissue. Implications for antiproliferative therapy. *Circ Res* **73**: 223-31.

O'Brien, E.R., Urieli-Shoval, S., Garvin, M.R., Stewart, D.K., Hinohara, T., Simpson, J.B., Benditt, E.P. & Schwartz, S.M. (2000). Replication in restenotic atherectomy tissue. *Atherosclerosis* **152**: 117-26.

O'Brien, T. & Simari, R.D. (2000). Gene therapy for atherosclerotic cardiovascular disease: a time for optimism and caution. *Mayo Clin Proc* **75**: 831-4.

Oei, S.L., Griesenbeck, J., Buchlow, G., Jorcke, D., Mayer-Kuckuk, P., Wons, T. & Ziegler, M. (1996). NAD+ analogs substituted in the purine base as substrates for poly(ADP- ribosyl) transferase. *FEBS Lett* **397**: 17-21.

Oesterle, S.N., Whitbourn, R., Fitzgerald, P.J., Yeung, A.C., Stertzer, S.H., Dake, M.D., Yock, P.G. & Virmani, R. (1998). The stent decade: 1987 to 1997. Stanford Stent Summit faculty. *Am Heart J* **136**: 578-99.

Ohnaka, K., Numaguchi, K., Yamakawa, T. & Inagami, T. (2000). Induction of cyclooxygenase-2 by angiotensin II in cultured rat vascular smooth muscle cells. *Hypertension* **35**: 68-75.

Okazaki, I.J. & Moss, J. (1996a). Mono-ADP-ribosylation: a reversible posttranslational modification of proteins. *Adv Pharmacol* **35**: 247-80.

Okazaki, I.J. & Moss, J. (1996b). Structure and function of eukaryotic mono-ADP-ribosyltransferases. *Rev Physiol Biochem Pharmacol* **129**: 51-104.

Okazaki, I.J. & Moss, J. (1998). Glycosylphosphatidylinositol-anchored and secretory isoforms of mono- ADP-ribosyltransferases. *J Biol Chem* **273**: 23617-20.

Okazaki, I.J. & Moss, J. (1999). Characterization of glycosylphosphatidylinositiol-anchored, secreted, and intracellular vertebrate mono-ADP-ribosyltransferases. *Annu Rev Nutr* **19**: 485-509.

Oliver, F.J., Menissier-de Murcia, J., Nacci, C., Decker, P., Andriantsitohaina, R., Muller, S., de la Rubia, G., Stoclet, J.C. & de Murcia, G. (1999). Resistance to endotoxic shock as a consequence of defective NF-kappaB activation in poly (ADP-ribose) polymerase-1 deficient mice. *EMBO J* **18**: 4446-54.

Olson, A.L. & Pessin, J.E. (1996). Structure, function, and regulation of the mammalian facilitative glucose transporter gene family. *Annu Rev Nutr* **16**: 235-56.

Olson, E.N., Perry, M. & Schulz, R.A. (1995). Regulation of muscle differentiation by the MEF2 family of MADS box transcription factors. *Dev Biol* **172**: 2-14.

Olson, M.F. & Marais, R. (2000). Ras protein signalling. *Semin Immunol* **12**: 63-73.

O'Neill, B.J. (2000). Clinical data: AVERT and QUO VADIS. *Can J Cardiol* **16** (Suppl E): 32E-35E.

Orlandi, A., Ehrlich, H.P., Ropraz, P., Spagnoli, L.G. & Gabbiani, G. (1994a). Rat aortic smooth muscle cells isolated from different layers and at different times after endothelial denudation show distinct biological features in vitro. *Arterioscler Thromb* **14**: 982-9.

Orlandi, A., Ropraz, P. & Gabbiani, G. (1994b). Proliferative activity and alpha-smooth muscle actin expression in cultured rat aortic smooth muscle cells are differently modulated by transforming growth factor-beta 1 and heparin. *Exp Cell Res* **214**: 528-36.

Owen, N.E. (1986). Effect of prostaglandin E1 on DNA synthesis in vascular smooth muscle cells. *Am J Physiol* **250**: C584-8.

Owens, G.K. (1989). Control of hypertrophic versus hyperplastic growth of vascular smooth muscle cells. *Am J Physiol* **257**: H1755-65.

Owens, G.K. (1995). Regulation of differentiation of vascular smooth muscle cells. *Physiol Rev* **75**: 487-517.

Owens, G.K. (1998). Molecular control of vascular smooth muscle cell differentiation. *Acta Physiol Scand* **164**: 623-35.

Owens, G.K., Vernon, S.M. & Madsen, C.S. (1996). Molecular regulation of smooth muscle cell differentiation. *J Hypertens Suppl* **14**: S55-64.

Owens, G.K. & Wise, G. (1997). Regulation of differentiation/maturation in vascular smooth muscle cells by hormones and growth factors. *Agents Actions Suppl* **48**: 3-24.

Pages, G., Lenormand, P., L'Allemain, G., Chambard, J.C., Meloche, S. & Pouyssegur, J. (1993). Mitogen-activated protein kinases p42mapk and p44mapk are required for fibroblast proliferation. *Proc Natl Acad Sci U S A* **90**: 8319-23.

Pakala, R. & Benedict, C. (1999). Synergy between thrombin and serotonin in inducing vascular smooth muscle cell proliferation. *J Lab Clin Med* **134**: 659-67.

Papkoff, J., Chen, R.H., Blenis, J. & Forsman, J. (1994). p42 mitogen-activated protein kinase and p90 ribosomal S6 kinase are selectively phosphorylated and activated during thrombin-induced platelet activation and aggregation. *Mol Cell Biol* **14**: 463-72.

Parrado, J., Bougria, M., Ayala, A. & Machado, A. (1999). Induced mono-(ADP)-ribosylation of rat liver cytosolic proteins by lipid peroxidant agents. *Free Radic Biol Med* **26**: 1079-84.

Pasricha, P.J., Hassoun, P.M., Teufel, E., Landman, M.J. & Fanburg, B.L. (1992). Prostaglandins E1 and E2 stimulate the proliferation of pulmonary artery smooth muscle cells. *Prostaglandins* **43**: 5-19.

Pasterkamp, G., Schoneveld, A.H., van Wolferen, W., Hillen, B., Clarijs, R.J., Haudenschild, C.C. & Borst, C. (1997). The impact of atherosclerotic arterial remodeling on percentage of luminal stenosis varies widely within the arterial system. A postmortem study. *Arterioscler Thromb Vasc Biol* **17**: 3057-63.

Patel, C.V., Gorski, D.H., LePage, D.F., Lincecum, J. & Walsh, K. (1992). Molecular cloning of a homeobox transcription factor from adult aortic smooth muscle. *J Biol Chem* **267**: 26085-90.

Paterson, H.F., Self, A.J., Garrett, M.D., Just, I., Aktories, K. & Hall, A. (1990). Microinjection of recombinant p21rho induces rapid changes in cell morphology. *J Cell Biol* **111**: 1001-7.

Pauletto, P., Chiavegato, A., Giuriato, L., Scatena, M., Faggin, E., Grisenti, A., Sarzani, R., Paci, M.V., Fulgeri, P.D., Rappelli, A. & et al. (1994). Hyperplastic growth of aortic smooth muscle cells in renovascular hypertensive rabbits is characterized by the expansion of an immature cell phenotype. *Circ Res* **74**: 774-88.

Payne, D.M., Rossomando, A.J., Martino, P., Erickson, A.K., Her, J.H., Shabanowitz, J., Hunt, D.F., Weber, M.J. & Sturgill, T.W. (1991). Identification of the regulatory phosphorylation sites in pp42/mitogen- activated protein kinase (MAP kinase). *EMBO J* **10**: 885-92.

Pero, R.W., Axelsson, B., Siemann, D., Chaplin, D. & Dougherty, G. (1999). Newly discovered anti-inflammatory properties of the benzamides and nicotinamides. *Mol Cell Biochem* **193**: 119-25.

Peterson, J.E., Larew, J.S. & Graves, D.J. (1990). Purification and partial characterization of arginine-specific ADP- ribosyltransferase from skeletal muscle microsomal membranes. *J Biol Chem* **265**: 17062-9.

Petritsch, C., Woscholski, R., Edelmann, H.M., Parker, P.J. & Ballou, L.M. (1995). Selective inhibition of p70 S6 kinase activation by phosphatidylinositol 3-kinase inhibitors. *Eur J Biochem* **230**: 431-8.

Pfeifle, B., Boeder, H. & Ditschuneit, H. (1987a). Interaction of receptors for insulin-like growth factor I, platelet- derived growth factor, and fibroblast growth factor in rat aortic cells. *Endocrinology* **120**: 2251-8.

Pfeifle, B., Hamann, H., Fussganger, R. & Ditschuneit, H. (1987b). Insulin as a growth regulator of arterial smooth muscle cells: effect of insulin of I.G.F.I. *Diabete Metab* **13**: 326-30.

Pfitzer, G. & Arner, A. (1998). Involvement of small GTPases in the regulation of smooth muscle contraction. *Acta Physiol Scand* **164**: 449-56.

Pieper, A.A., Verma, A., Zhang, J. & Snyder, S.H. (1999). Poly (ADP-ribose) polymerase, nitric oxide and cell death. *Trends Pharmacol Sci* **20**: 171-81.

Pietila, K., Moilanen, T. & Nikkari, T. (1980). Prostaglandins enhance the synthesis of glycosaminoglycans and inhibit the growth of rabbit aortic smooth muscle cells in culture. *Artery* 7: 509-18.

Piron, K.J. & McMahon, K.K. (1990). Localization and partial characterization of ADP-ribosylation products in hearts from adult and neonatal rats. *Biochem J* **270**: 591-7.

Pitot, H.C. (1959). Studies on the control of protein synthesis in normal and neoplastic rat liver, Ph.D. Dissertation. Tulane University, Tulane.

Pitot, H.C. (1962). Molecular pathogenesis of experimental liver cancer. *Fed Proc* **21**: 1124-1129.

Pitot, H.C., Peraino, C., Morse, P.A.J. & Potter, V.R. (1964). Hepatomas in tissue culture compared with adapting liver in vivo. *National Cancer Institute Monograph* **13**: 229-245.

Pleschke, J.M., Kleczkowska, H.E., Strohm, M. & Althaus, F.R. (2000). Poly(ADP-ribose) binds to specific domains in DNA checkpoint proteins. *J Biol Chem*.

Pomerantz, K.B. & Hajjar, D.P. (1989). Eicosanoids in regulation of arterial smooth muscle cell phenotype, proliferative capacity, and cholesterol metabolism. *Arteriosclerosis* **9**: 413-29.

Popoff, M.R. (1998). Interactions between bacterial toxins and intestinal cells. *Toxicon* **36**: 665-85.

Poser, S., Impey, S., Trinh, K., Xia, Z. & Storm, D.R. (2000). SRF-dependent gene expression is required for PI3-kinase-regulated cell proliferation. *EMBO J* **19**: 4955-4966.

Post, M.J., Borst, C. & Kuntz, R.E. (1994). The relative importance of arterial remodeling compared with intimal hyperplasia in lumen renarrowing after balloon angioplasty. A study in the normal rabbit and the hypercholesterolemic Yucatan micropig. *Circulation* **89**: 2816-21.

Post, M.J., de Smet, B.J., van der Helm, Y., Borst, C. & Kuntz, R.E. (1997). Arterial remodeling after balloon angioplasty or stenting in an atherosclerotic experimental model. *Circulation* **96**: 996-1003.

Potter, V.R., Watanabe, M., Becker, J.E. & Pitot, H.C. (1967). Hormonal effects on enzyme activities in tissue culture and in whole animals. *Adv Enzyme Regul* **5**: 303-16.

Powell, J.S., Muller, R.K. & Baumgartner, H.R. (1991). Suppression of the vascular response to injury: the role of angiotensin- converting enzyme inhibitors. *J Am Coll Cardiol* **17**: 137B-142B.

Powis, G., Bonjouklian, R., Berggren, M.M., Gallegos, A., Abraham, R., Ashendel, C., Zalkow, L., Matter, W.F., Dodge, J., Grindey, G. & et al. (1994). Wortmannin, a potent and selective inhibitor of phosphatidylinositol-3- kinase. *Cancer Res* **54**: 2419-23.

Prager, D. & Melmed, S. (1993). Insulin and insulin-like growth factor I receptors: are there functional distinctions? *Endocrinology* **132**: 1419-20.

Prvulovich, E.M., Stein, R.C., Bomanji, J.B., Ledermann, J.A., Taylor, I. & Ell, P.J. (1998). Iodine-131-MIBG therapy of a patient with carcinoid liver metastases. *J Nucl Med* **39**: 1743-5.

Purnell, M.R., Stone, P.R. & Whish, W.J. (1980). ADP-ribosylation of nuclear proteins. *Biochem Soc Trans* **8**: 215-27.

Pyles, J.M., March, K.L., Franklin, M., Mehdi, K., Wilensky, R.L. & Adam, L.P. (1997). Activation of MAP kinase in vivo follows balloon overstretch injury of porcine coronary and carotid arteries. *Circ Res* **81**: 904-10.

Quesada, P., d'Erme, M., Parise, G., Faraone-Mennella, M.R., Caiafa, P. & Farina, B. (1994). Nuclear matrix-associated poly(ADPribosyl)ation system in rat testis chromatin. *Exp Cell Res* **214**: 351-7.

Quesada, P., Tramontano, F., Faraone-Mennella, M.R. & Farina, B. (2000). The analysis of the poly(ADPR) polymerase mode of action in rat testis nuclear fractions defines a specific poly(ADP-ribosyl)ation system associated with the nuclear matrix. *Mol Cell Biochem* **205**: 91-9.

Raines, E.W., Bowen-Pope, D.F. & Ross, R. (1990). Platelet-derived growth factor. In: Handbook of Experimental Pharmacology. Sporn, M.B. & Roberts, A.B. (eds.). Springer-Verlag, Berlin. pp 173-262.

Raines, E.W., Dower, S.K. & Ross, R. (1989). Interleukin-1 mitogenic activity for fibroblasts and smooth muscle cells is due to PDGF-AA. *Science* **243**: 393-6.

Raines, E.W. & Ross, R. (1993). Smooth muscle cells and the pathogenesis of the lesions of atherosclerosis. *Br Heart J* **69**: S30-7.

Rakhit, S., Pyne, S. & Pyne, N.J. (2000). The platelet-derived growth factor receptor stimulation of p42/p44 mitogen-activated protein kinase in airway smooth muscle involves a G- protein-mediated tyrosine phosphorylation of Gab1. *Mol Pharmacol* **58**: 413-20.

Ramage, J.K., Catnach, S.M. & Williams, R. (1995). Overview: the management of metastatic carcinoid tumors. *Liver Transpl Surg* **1**: 107-10.

Rameh, L.E., Chen, C.S. & Cantley, L.C. (1995). Phosphatidylinositol (3,4,5)P3 interacts with SH2 domains and modulates PI 3-kinase association with tyrosine-phosphorylated proteins. *Cell* **83**: 821-30.

Rankin, P.W., Jacobson, E.L., Benjamin, R.C., Moss, J. & Jacobson, M.K. (1989). Quantitative studies of inhibitors of ADP-ribosylation in vitro and in vivo. *J Biol Chem* **264**: 4312-7.

Rao, V.N. & Reddy, E.S. (1994). elk-1 proteins interact with MAP kinases. *Oncogene* **9**: 1855-60.

Ratti, S., Quarato, P., Casagrande, C., Fumagalli, R. & Corsini, A. (1998). Picotamide, an antithromboxane agent, inhibits the migration and proliferation of arterial myocytes. *Eur J Pharmacol* **355**: 77-83.

Rectenwald, J.E., Moldawer, L.L., Huber, T.S., Seeger, J.M. & Ozaki, C.K. (2000). Direct evidence for cytokine involvement in neointimal hyperplasia. *Circulation* **102**: 1697-702.

Reel, J.R. & Kenney, F.T. (1968). "Superinduction" of tyrosine transaminase in hepatoma cell cultures: differential inhibition of synthesis and turnover by actionomycin D. *Proc Natl Acad Sci U S A* **61**: 200-6.

Regoli, D., D'Orleans-Juste, P., Rouissi, N. & Rhaleb, N.E. (1993). Vasoactive peptides and characterization of their receptors. *Regul Pept* **45**: 323-40.

Reimer, R., Heim, H.K., Muallem, R., Odes, H.S. & Sewing, K.F. (1992). Effects of EP-receptor subtype specific agonists and other prostanoids on adenylate cyclase activity of duodenal epithelial cells. *Prostaglandins* **44**: 485-93.

Reis, G.J., Pomerantz, R.M., Jenkins, R.D., Kuntz, R.E., Baim, D.S., Diver, D.J., Schnitt, S.J. & Safian, R.D. (1991). Laser balloon angioplasty: clinical, angiographic and histologic results. *J Am Coll Cardiol* **18**: 193-202.

Rensing, B.J., Hermans, W.R., Deckers, J.W., de Feyter, P.J., Tijssen, J.G. & Serruys, P.W. (1992). Lumen narrowing after percutaneous transluminal coronary balloon angioplasty follows a near gaussian distribution: a quantitative angiographic study in 1,445 successfully dilated lesions. *J Am Coll Cardiol* **19**: 939-45.

Reuber, M.D. (1961). A transplantable bile-secreting hepatocellular carcinoma in the rat. *J Natl Cancer Institute* **26**: 891-899.

Revtyak, G.E., Johnson, A.R. & Campbell, W.B. (1987). Prostaglandin synthesis in bovine coronary endothelial cells: comparison with other commonly studied endothelial cells. *Thromb Res* **48**: 671-83.

Richter, C. (1990). The prooxidant-induced and spontaneous mitochondrial calcium release: inhibition by meta-iodo-benzylguanidine (MIBG), a substrate for mono (ADP-ribosylation). *Free Radic Res Commun* **8**: 329-34.

Ridley, A.J. & Hall, A. (1992). The small GTP-binding protein rho regulates the assembly of focal adhesions and actin stress fibers in response to growth factors. *Cell* **70**: 389-99.

Ridley, A.J., Paterson, H.F., Johnston, C.L., Diekmann, D. & Hall, A. (1992). The small GTP-binding protein rac regulates growth factor-induced membrane ruffling. *Cell* **70**: 401-10.

Rivera, V.M. & Greenberg, M.E. (1990). Growth factor-induced gene expression: the ups and downs of c-fos regulation. *New Biol* **2**: 751-8.

Rizzo, M.A. & Romero, G. (1998). The role of G proteins in insulin signalling. *J Basic Clin Physiol Pharmacol* **9**: 167-95.

Robbins, D.J., Cheng, M., Zhen, E., Vanderbilt, C.A., Feig, L.A. & Cobb, M.H. (1992). Evidence for a Ras-dependent extracellular signal-regulated protein kinase (ERK) cascade. *Proc Natl Acad Sci U S A* **89**: 6924-8.

Rodbell, M. (1997). The complex regulation of receptor-coupled G-proteins. *Adv Enzyme Regul* **37**: 427-35.

Rosen, E.M., Goldberg, I.D., Shapiro, H.M., Zoller, L.C., Myrick, K.V., Levenson, S.E. & Halpin, P.A. (1985). Growth kinetics as a function of ploidy in diploid, tetraploid, and octaploid smooth muscle cells derived from the normal rat aorta. *J Cell Physiol* **125**: 512-20.

Rosenthal, D.S., Ding, R., Simbulan-Rosenthal, C.M., Vaillancourt, J.P., Nicholson, D.W. & Smulson, M. (1997). Intact cell evidence for the early synthesis, and subsequent late apopain-mediated suppression, of poly(ADP-ribose) during apoptosis. *Exp Cell Res* **232**: 313-21.

Ross, R. (1971). The smooth muscle cell. II. Growth of smooth muscle in culture and formation of elastic fibers. *J Cell Biol* **50**: 172-86.

Ross, R. (1993). The pathogenesis of atherosclerosis: a perspective for the 1990s. *Nature* **362**: 801-9.

Ross, R. (1995). Cell biology of atherosclerosis. *Annu Rev Physiol* **57**: 791-804.

Ross, R. & Fuster, V. (1996). The pathogenesis of atherosclerosis. In: Atherosclerosis and coronary artery disease. Fuster, V., Ross, R. & Topol, E.J. (eds.). Lippincott-Raven, Philadelphia. pp 441-460.

Ross, R., Glomset, J., Kariya, B. & Harker, L. (1974). A platelet-dependent serum factor that stimulates the proliferation of arterial smooth muscle cells in vitro. *Proc Natl Acad Sci U S A* **71**: 1207-10.

Ross, R., Nist, C., Kariya, B., Rivest, M.J., Raines, E. & Callis, J. (1978). Physiological quiescence in plasma-derived serum: influence of platelet- derived growth factor on cell growth in culture. *J Cell Physiol* **97**: 497-508.

Ross, R., Raines, E.W. & Bowen-Pope, D.F. (1986). The biology of platelet-derived growth factor. *Cell* **46**: 155-69.

Rudnicki, M.A., Schnegelsberg, P.N., Stead, R.H., Braun, T., Arnold, H.H. & Jaenisch, R. (1993). MyoD or Myf-5 is required for the formation of skeletal muscle. *Cell* **75**: 1351-9.

Rutgers, M., Tytgat, G.A., Verwijs-Janssen, M., Buitenhuis, C., Voute, P.A. & Smets, L.A. (1993). Uptake of the neuron-blocking agent meta-iodobenzylguanidine and serotonin by human platelets and neuro-adrenergic tumour cells. *Int J Cancer* **54**: 290-5.

Sabate, M., Serruys, P.W., van der Giessen, W.J., Ligthart, J.M., Coen, V.L., Kay, I.P., Gijzel, A.L., Wardeh, A.J., den Boer, A. & Levendag, P.C. (1999). Geometric vascular remodeling after balloon angioplasty and beta- radiation therapy: A three-dimensional intravascular ultrasound study. *Circulation* **100**: 1182-8.

Sachinidis, A., Flesch, M., Ko, Y., Schror, K., Bohm, M., Dusing, R. & Vetter, H. (1995). Thromboxane A2 and vascular smooth muscle cell proliferation. *Hypertension* **26**: 771-80.

Sadoshima, J., Qiu, Z., Morgan, J.P. & Izumo, S. (1995). Angiotensin II and other hypertrophic stimuli mediated by G protein- coupled receptors activate tyrosine kinase, mitogen-activated protein kinase, and 90-kD S6 kinase in cardiac myocytes. The critical role of Ca(2+)-dependent signaling. *Circ Res* **76**: 1-15.

Sale, E.M., Atkinson, P.G. & Sale, G.J. (1995). Requirement of MAP kinase for differentiation of fibroblasts to adipocytes, for insulin activation of p90 S6 kinase and for insulin or serum stimulation of DNA synthesis. *EMBO J* **14**: 674-84.

Saltis, J. & Bobik, A. (1992). Vascular smooth muscle growth in genetic hypertension: evidence for multiple abnormalities in growth regulatory pathways. *J Hypertens* **10**: 635-43.

Saltis, J., Thomas, A.C., Agrotis, A., Campbell, J.H., Campbell, G.R. & Bobik, A. (1995). Expression of growth factor receptors in arterial smooth muscle cells. Dependency on cell phenotype and serum factors. *Atherosclerosis* **118**: 77-87.

Salvioni, A., Galli, S., Marenzi, G., Lauri, G., Perego, G.B., Assanelli, E. & Guazzi, M.D. (1998). Thrombin activation and late restenosis after percutaneous transluminal coronary angioplasty. *Am Heart J* **135**: 503-9.

Sanchez-Margalet, V., Goldfine, I.D., Vlahos, C.J. & Sung, C.K. (1994). Role of phosphatidylinositol-3-kinase in insulin receptor signaling: studies with inhibitor, LY294002. *Biochem Biophys Res Commun* **204**: 446-52.

Sanchez-Margalet, V., Gonzalez-Yanes, C., Santos-Alvarez, J. & Najib, S. (1999). Insulin activates G alpha il,2 protein in rat hepatoma (HTC) cell membranes. *Cell Mol Life Sci* **55**: 142-7.

Sanz-Gonzalez, S.M., Poch, E., Perez-Roger, I., Diez-Juan, A., Ivorra, C. & Andres, V. (2000). Control of vascular smooth muscle cell growth by cyclin-dependent kinase inhibitory proteins and its implication in cardiovascular disease. *Front Biosci* **5**: D619-28.

Sartore, S., Franch, R., Roelofs, M. & Chiavegato, A. (1999). Molecular and cellular phenotypes and their regulation in smooth muscle. *Rev Physiol Biochem Pharmacol* **134**: 235-320.

Sartore, S., Scatena, M., Chiavegato, A., Faggin, E., Giuriato, L. & Pauletto, P. (1994). Myosin isoform expression in smooth muscle cells during physiological and pathological vascular remodeling. *J Vasc Res* **31**: 61-81.

Sasaoka, T., Ishiki, M., Sawa, T., Ishihara, H., Takata, Y., Imamura, T., Usui, I., Olefsky, J.M. & Kobayashi, M. (1996). Comparison of the insulin and insulin-like growth factor 1 mitogenic intracellular signaling pathways. *Endocrinology* **137**: 4427-34.

Sassoon, D.A. (1993). Myogenic regulatory factors: dissecting their role and regulation during vertebrate embryogenesis. *Dev Biol* **156**: 11-23.

Satoh, M.S. & Lindahl, T. (1992). Role of poly(ADP-ribose) formation in DNA repair. *Nature* **356**: 356-8.

Sawada, H., Kan, M. & McKeehan, W.L. (1990). Opposite effects of monokines (interleukin-1 and tumor necrosis factor) on proliferation and heparin-binding (fibroblast) growth factor binding to human aortic endothelial and smooth muscle cells. *In Vitro Cell Dev Biol* **26**: 213-6.

Saward, L. (2000). Both the AT1 and AT2 receptor subtypes mediate angiotensin II-stimulated growth in vascular smooth muscle cells, Doctor of Philosophy. University of Manitoba, Winnipeg.

Saward, L. & Zahradka, P. (1997a). Angiotensin II activates phosphatidylinositol 3-kinase in vascular smooth muscle cells. *Circ Res* **81**: 249-57.

Saward, L. & Zahradka, P. (1997b). Coronary artery smooth muscle in culture: migration of heterogeneous cell populations from vessel wall. *Mol Cell Biochem* **176**: 53-9.

Saxty, B., Yadollahi-Farsani, M., Kefalas, P., Paul, S. & MacDermot, J. (1998a). ADP-ribosyltransferase inhibitors and pseudo-substrates inhibit rat smooth muscle cell migration in vitro. *Biochem Soc Trans* **26**: S130.

Saxty, B.A. & van Heyningen, S. (1995). The purification of a cysteine-dependent NAD+ glycohydrolase activity from bovine erythrocytes and evidence that it exhibits a novel ADP- ribosyltransferase activity. *Biochem J* **310**: 931-7.

Saxty, B.A., Yadollahi-Farsani, M., Kefalas, P., Paul, S. & MacDermot, J. (1998b). Inhibition of chemotaxis in A7r5 rat smooth muscle cells by a novel panel of inhibitors. *Br J Pharmacol* **125**: 152-8.

Scaife, R.M., Wilson, L. & Purich, D.L. (1992). Microtubule protein ADP-ribosylation in vitro leads to assembly inhibition and rapid depolymerization. *Biochemistry* **31**: 310-6.

Schlondorff, D., DeCandido, S. & Satriano, J.A. (1987). Angiotensin II stimulates phospholipases C and A2 in cultured rat mesangial cells. *Am J Physiol* **253**: C113-20.

Schmidt, G. & Aktories, K. (1998). Bacterial cytotoxins target Rho GTPases. *Naturwissenschaften* **85**: 253-61.

Schnell, O., Muhr, D., Weiss, M., Dresel, S., Haslbeck, M. & Standl, E. (1996). Reduced myocardial 123I-metaiodobenzylguanidine uptake in newly diagnosed IDDM patients. *Diabetes* **45**: 801-5.

Schofer, J., Spielmann, R., Schuchert, A., Weber, K. & Schluter, M. (1988). Iodine-123 meta-iodobenzylguanidine scintigraphy: a noninvasive method to demonstrate myocardial adrenergic nervous system disintegrity in patients with idiopathic dilated cardiomyopathy. *J Am Coll Cardiol* **12**: 1252-8.

Schraufstatter, I.U., Hyslop, P.A., Hinshaw, D.B., Spragg, R.G., Sklar, L.A. & Cochrane, C.G. (1986). Hydrogen peroxide-induced injury of cells and its prevention by inhibitors of poly(ADP-ribose) polymerase. *Proc Natl Acad Sci U S A* **83**: 4908-12.

Schror, K. & Weber, A.A. (1997). Roles of vasodilatory prostaglandins in mitogenesis of vascular smooth muscle cells. *Agents Actions Suppl* **48**: 63-91.

Schubert, D., Harris, A.J., Devine, C.E. & Heinemann, S. (1974). Characterization of a unique muscle cell line. *J Cell Biol* **61**: 398-413.

Schulz, C., Herrmann, R.A., Beilharz, C., Pasquantonio, J. & Alt, E. (2000). Coronary stent symmetry and vascular injury determine experimental restenosis. *Heart* **83**: 462-7.

Schuman, E.M., Meffert, M.K., Schulman, H. & Madison, D.V. (1994). An ADP-ribosyltransferase as a potential target for nitric oxide action in hippocampal long-term potentiation. *Proc Natl Acad Sci U S A* **91**: 11958-62.

Schwartz, R.S. (1994). Neointima and arterial injury: dogs, rats, pigs, and more. *Lab Invest* **71**: 789-91.

Schwartz, R.S., Chu, A., Edwards, W.D., Srivatsa, S.S., Simari, R.D., Isner, J.M. & Holmes, D.R., Jr. (1996). A proliferation analysis of arterial neointimal hyperplasia: lessons for antiproliferative restenosis therapies. *Int J Cardiol* **53**: 71-80.

Schwartz, R.S., Edwards, W.D., Bailey, K.R., Camrud, A.R., Jorgenson, M.A. & Holmes, D.R., Jr. (1994). Differential neointimal response to coronary artery injury in pigs and dogs. Implications for restenosis models. *Arterioscler Thromb* **14**: 395-400.

Schwartz, R.S., Edwards, W.D., Huber, K.C., Antoniades, L.C., Bailey, K.R., Camrud, A.R., Jorgenson, M.A. & Holmes, D.R., Jr. (1993). Coronary restenosis: prospects for solution and new perspectives from a porcine model. *Mayo Clin Proc* **68**: 54-62.

Schwartz, R.S., Holmes, D.R., Jr. & Topol, E.J. (1992a). The restenosis paradigm revisited: an alternative proposal for cellular mechanisms. *J Am Coll Cardiol* **20**: 1284-93.

Schwartz, R.S., Huber, K.C., Murphy, J.G., Edwards, W.D., Camrud, A.R., Vlietstra, R.E. & Holmes, D.R. (1992b). Restenosis and the proportional neointimal response to coronary artery injury: results in a porcine model. *J Am Coll Cardiol* **19**: 267-74.

Schwartz, R.S., Murphy, J.G., Edwards, W.D., Camrud, A.R., Vliestra, R.E. & Holmes, D.R. (1990). Restenosis after balloon angioplasty. A practical proliferative model in porcine coronary arteries. *Circulation* **82**: 2190-200.

Schwartz, S.M. (1997). Smooth muscle migration in vascular development and pathogenesis. *Transpl Immunol* **5**: 255-60.

Schwartz, S.M., Campbell, G.R. & Campbell, J.H. (1986). Replication of smooth muscle cells in vascular disease. *Circ Res* **58**: 427-44.

Schwartz, S.M., deBlois, D. & O'Brien, E.R. (1995a). The intima. Soil for atherosclerosis and restenosis. *Circ Res* **77**: 445-65.

Schwartz, S.M., O'Brien, E.R., de Blois, D. & Giachelli, C.M. (1995b). Relevance of smooth muscle replication and development to vascular disease. In: The vascular smooth muscle cell: Molecular and biological responses to the extracellular matrix. Schwartz, S.M. & Mecham, R.P. (eds.). Academic Press Inc., San Diego. pp 81-140.

Schwartz, S.M. & Reidy, M.A. (1996). Restenosis: an assessment of factors important in arterial occlusion. In: Atherosclerosis and coronary artery disease. Fuster, V., Ross, R. & Topol, E.J. (eds.). Lippincott-Raven, Philadelphia. pp 701-714.

Schwartz, S.M., Reidy, M.A. & O'Brien, E.R. (1995c). Assessment of factors important in atherosclerotic occlusion and restenosis. *Thromb Haemost* **74**: 541-51.

Schwartz, S.M. & Ross, R. (1984). Cellular proliferation in atherosclerosis and hypertension. *Prog Cardiovasc Dis* **26**: 355-72.

Scott-Burden, T. & Vanhoutte, P.M. (1994). Regulation of smooth muscle cell growth by endothelium-derived factors. *Tex Heart Inst J* **21**: 91-7.

Scovassi, A.I., Denegri, M., Donzelli, M., Rossi, L., Bernardi, R., Mandarino, A., Frouin, I. & Negri, C. (1998). Poly(ADP-ribose) synthesis in cells undergoing apoptosis: an attempt to face death before PARP degradation. *Eur J Histochem* **42**: 251-8.

Scovassi, A.I. & Poirier, G.G. (1999). Poly(ADP-ribosylation) and apoptosis. *Mol Cell Biochem* **199**: 125-37.

Scrimgeour, A.G., Blakesley, V.A., Stannard, B.S. & LeRoith, D. (1997). Mitogen-activated protein kinase and phosphatidylinositol 3-kinase pathways are not sufficient for insulin-like growth factor I-induced mitogenesis and tumorigenesis. *Endocrinology* **138**: 2552-8.

See, J., Shell, W., Matthews, O., Canizales, C., Vargas, M., Giddings, J. & Cerrone, J. (1987). Prostaglandin E1 infusion after angioplasty in humans inhibits abrupt occlusion and early restenosis. *Adv Prostaglandin Thromboxane Leukot Res*: 266-70.

Seely, B.L., Reichart, D.R., Staubs, P.A., Jhun, B.H., Hsu, D., Maegawa, H., Milarski, K.L., Saltiel, A.R. & Olefsky, J.M. (1995). Localization of the insulin-like growth factor I receptor binding sites for the SH2 domain proteins p85, Syp, and GTPase activating protein. *J Biol Chem* **270**: 19151-7.

Seger, R. & Krebs, E.G. (1995). The MAPK signaling cascade. *FASEB J* **9**: 726-35.

Senderoff, R.I., Sheu, M.T. & Sokoloski, T.D. (1991). Fibrin based drug delivery systems. *J Parenter Sci Technol* **45**: 2-6.

Serruys, P.W., de Jaegere, P., Kiemeneij, F., Macaya, C., Rutsch, W., Heyndrickx, G., Emanuelsson, H., Marco, J., Legrand, V., Materne, P. & et al. (1994). A comparison of balloon-expandable-stent implantation with balloon angioplasty in patients with coronary artery disease. Benestent Study Group [see comments]. *N Engl J Med* **331**: 489-95.

Servant, M.J., Giasson, E. & Meloche, S. (1996). Inhibition of growth factor-induced protein synthesis by a selective MEK inhibitor in aortic smooth muscle cells. *J Biol Chem* **271**: 16047-52.

Servidei, T., Iavarone, A., Lasorella, A., Mastrangelo, S. & Riccardi, R. (1995). Release mechanisms of [125I]meta-iodobenzylguanidine in neuroblastoma cells: evidence of a carrier-mediated efflux. *Eur J Cancer* **4**: 591-5.

Seto, H., Shimizu, M., Nozawa, T., Yoshida, N., Inagaki, S., Kageyama, M. & Kakishita, M. (1996). Simultaneous assessment of regional adrenergic activity and perfusion with 123I-MIBG and 201Tl in congestive heart failure. *Nucl Med Commun* **17**: 225-30.

Seuwen, K., Lagarde, A. & Pouyssegur, J. (1988). Deregulation of hamster fibroblast proliferation by mutated ras oncogenes is not mediated by constitutive activation of phosphoinositide-specific phospholipase C. *EMBO J* **7**: 161-8.

Shall, S. (1994). The function of poly (ADP-ribosylation) in DNA breakage and rejoining. *Mol Cell Biochem* **138**: 71-5.

Shall, S. & de Murcia, G. (2000). Poly(ADP-ribose) polymerase-1: what have we learned from the deficient mouse model? *Mutat Res* **460**: 1-15.

Shanahan, C.M. & Weissberg, P.L. (1998). Smooth muscle cell heterogeneity: patterns of gene expression in vascular smooth muscle cells in vitro and in vivo. *Arterioscler Thromb Vasc Biol* **18**: 333-8.

Shanahan, C.M., Weissberg, P.L. & Metcalfe, J.C. (1993). Isolation of gene markers of differentiated and proliferating vascular smooth muscle cells. *Circ Res* **73**: 193-204.

Sharp, G.W. (1973). Action of cholera toxin on fluid and electrolyte movement in the small intestine. *Annu Rev Med* **24**: 19-23.

Shechter, M., Agranat, O., Har-Zahav, Y., Rath, S., Kaplinsky, E. & Rabinowitz, B. (1997). Prostaglandin E1 during angioplasty as preventative therapy for coronary restenosis. *Am J Ther* **4**: 395-400.

Shepherd, P.R., Reaves, B.J. & Davidson, H.W. (1996). Phosphoinositide 3-kinases and membrane traffic. *Trends Cell Biol* **6**: 92-97.

Sherris, D.A., Larrabee, W.F., Jr. & Murakami, C.S. (1995). Management of scar contractures, hypertrophic scars, and keloids. *Otolaryngol Clin North Am* **28**: 1057-68.

Shi, Y., Kornovski, B.S., Savani, R. & Turley, E.A. (1993). A rapid, multiwell colorimetric assay for chemotaxis. *J Immunol Methods* **164**: 149-54.

Shi, Y., O'Brien, J.E., Fard, A., Mannion, J.D., Wang, D. & Zalewski, A. (1996a). Adventitial myofibroblasts contribute to neointimal formation in injured porcine coronary arteries. *Circulation* **94**: 1655-64.

Shi, Y., Pieniek, M., Fard, A., O'Brien, J., Mannion, J.D. & Zalewski, A. (1996b). Adventitial remodeling after coronary arterial injury. *Circulation* **93**: 340-8.

Shieh, W.M., Ame, J.C., Wilson, M.V., Wang, Z.Q., Koh, D.W., Jacobson, M.K. & Jacobson, E.L. (1998). Poly(ADP-ribose) polymerase null mouse cells synthesize ADP-ribose polymers. *J Biol Chem* **273**: 30069-72.

Shirotani, M., Yui, Y., Hattori, R. & Kawai, C. (1991). U-61,431F, a stable prostacyclin analogue, inhibits the proliferation of bovine vascular smooth muscle cells with little antiproliferative effect on endothelial cells. *Prostaglandins* **41**: 97-110.

Shore, P. & Sharrocks, A.D. (1995). The MADS-box family of transcription factors. *Eur J Biochem* **229**: 1-13.

Short, J.H. & Darby, T.D. (1967). Sympathetic nervous system blocking agents. 3. Derivatives of benzylguanidine. *J Med Chem* **10**: 833-40.

Shulkin, B.L., Shapiro, B., Tobes, M.C., Shen, S.W., Wieland, D.M., Meyers, L.J., Lee, H.T., Petry, N.A., Sisson, J.C. & Beierwaltes, W.H. (1986). Iodine-123-4-amino-3-iodobenzylguanidine, a new sympathoadrenal imaging agent: comparison with iodine-123 metaiodobenzylguanidine. *J Nucl Med* **27**: 1138-42.

Siegel, G., Malmsten, M. & Klussendorf, D. (1998). Tumor cell locomotion and metastatic spread. *Microsc Res Tech* **43**: 276-82.

Siegel, J.A. (1997). Medical management of coronary artery disease revisited: the endothelial factor. *J S C Med Assoc* **93**: 333-5.

Siegel, R.J., Shah, P.K., Nathan, M., Rodriguez, L. & Shell, W.E. (1984). Prostaglandin E1 infusion in unstable angina: effects on anginal frequency and cardiac function. *Am Heart J* **108**: 863-8.

Simbulan, C.M., Suzuki, M., Izuta, S., Sakurai, T., Savoysky, E., Kojima, K., Miyahara, K., Shizuta, Y. & Yoshida, S. (1993). Poly(ADP-ribose) polymerase stimulates DNA polymerase alpha by physical association. *J Biol Chem* **268**: 93-9.

Simbulan-Rosenthal, C.M., Rosenthal, D.S., Boulares, A.H., Hickey, R.J., Malkas, L.H., Coll, J.M. & Smulson, M.E. (1998). Regulation of the expression or recruitment of components of the DNA synthesome by poly(ADP-ribose) polymerase. *Biochemistry* **37**: 9363-70.

Simbulan-Rosenthal, C.M., Rosenthal, D.S., Luo, R. & Smulson, M.E. (1999). Poly(ADP-ribosyl)ation of p53 during apoptosis in human osteosarcoma cells. *Cancer Res* **59**: 2190-4.

Sims, F.H. (1989). A comparison of structural features of the walls of coronary arteries from 10 different species. *Pathology* **21**: 115-24.

Sims, J.L., Sikorski, G.W., Catino, D.M., Berger, S.J. & Berger, N.A. (1982). Poly(adenosinediphosphoribose) polymerase inhibitors stimulate unscheduled deoxyribonucleic acid synthesis in normal human lymphocytes. *Biochemistry* **21**: 1813-21.

Singer, A.J. & Clark, R.A. (1999). Cutaneous wound healing. *N Engl J Med* **341**: 738-46.

Sisson, J.C., Wieland, D.M., Sherman, P., Mangner, T.J., Tobes, M.C. & Jacques, S., Jr. (1987). Metaiodobenzylguanidine as an index of the adrenergic nervous system integrity and function. *J Nucl Med* **28**: 1620-4.

Sjolund, M., Nilsson, J., Palmberg, L. & Thyberg, J. (1984). Phenotype modulation in primary cultures of arterial smooth-muscle cells. Dual effect of prostaglandin E1. *Differentiation* **27**: 158-62.

Skalli, O., Bloom, W.S., Ropraz, P., Azzarone, B. & Gabbiani, G. (1986). Cytoskeletal remodeling of rat aortic smooth muscle cells in vitro: relationships to culture conditions and analogies to in vivo situations. *J Submicrosc Cytol* **18**: 481-93.

Slosman, D.O., Morel, D.R., Mo Costabella, P.M. & Donath, A. (1988). Lung uptake of 131I-metaiodobenzylguanidine in sheep. An in vivo measurement of pulmonary metabolic function. *Eur J Nucl Med* **14**: 65-70.

Slosman, D.O., Pittet, N., Donath, A. & Polla, B.S. (1993). Fluorodeoxyglucose cell incorporation as an index of cell proliferation: evaluation of accuracy in cell culture. *Eur J Nucl Med* **20**: 1084-8.

Smets, L., Metwally, E.A., Knol, E. & Martens, M. (1988a). Potentiation of glucocorticoid-induced lysis in refractory and resistant leukemia cells by inhibitors of ADP-ribosylation. *Leuk Res* **12**: 737-43.

Smets, L.A., Bout, B. & Wisse, J. (1988b). Cytotoxic and antitumor effects of the norepinephrine analogue meta-iodo-benzylguanidine (MIBG). *Cancer Chemother Pharmacol* **21**: 9-13.

Smets, L.A., Janssen, M., Metwally, E. & Loesberg, C. (1990a). Extragranular storage of the neuron blocking agent meta-iodobenzylguanidine (MIBG) in human neuroblastoma cells. *Biochem Pharmacol* **39**: 1959-64.

Smets, L.A., Janssen, M., Rutgers, M., Ritzen, K. & Buttenhuis, C. (1991). Pharmacokinetics and intracellular distribution of the tumor-targeted radiopharmaceutical m-iodo-benzylguanidine in SK-N-SH neuroblastoma and PC-12 pheochromocytoma cells. *Int J Cancer* **48**: 609-15.

Smets, L.A., Loesberg, C., Janssen, M., Metwally, E.A. & Huiskamp, R. (1989). Active uptake and extravesicular storage of m-iodobenzylguanidine in human neuroblastoma SK-N-SH cells. *Cancer Res* **49**: 2941-4.

Smets, L.A., Loesberg, C., Janssen, M. & Van Rooij, H. (1990b). Intracellular inhibition of mono(ADP-ribosylation) by meta-iodobenzylguanidine: specificity, intracellular concentration and effects on glucocorticoid-mediated cell lysis. *Biochim Biophys Acta* **1054**: 49-55.

Smith, J.D., Bryant, S.R., Couper, L.L., Vary, C.P., Gotwals, P.J., Koteliansky, V.E. & Lindner, V. (1999). Soluble transforming growth factor-beta type II receptor inhibits negative remodeling, fibroblast transdifferentiation, and intimal lesion formation but not endothelial growth. *Circ Res* **84**: 1212-22.

Smith, K.P., Benjamin, R.C., Moss, J. & Jacobson, M.K. (1985). Identification of enzymatic activities which process protein bound mono(ADP-ribose). *Biochem Biophys Res Commun* **126**: 136-42.

Smith, R.C. & Walsh, K. (2000). Gene Therapy for Restenosis. *Curr Cardiol Rep* **2**: 13-23.

Smith, T.H., Block, N.E., Rhodes, S.J., Konieczny, S.F. & Miller, J.B. (1993). A unique pattern of expression of the four muscle regulatory factor proteins distinguishes somitic from embryonic, fetal and newborn mouse myogenic cells. *Development* **117**: 1125-33.

Smulson, M.E., Pang, D., Jung, M., Dimtchev, A., Chasovskikh, S., Spoonde, A., Simbulan-Rosenthal, C., Rosenthal, D., Yakovlev, A. & Dritschilo, A. (1998). Irreversible binding of poly(ADP)ribose polymerase cleavage product to DNA ends revealed by atomic force microscopy: possible role in apoptosis. *Cancer Res* **58**:3495-8.

Smulson, M.E. (1994). Poly(ADP-ribose) polymerase gene on chromosome 1q: early role in differentiation linked replication; gene on human chromosome 13q: marker of carcinogenesis. *Mol Cell Biochem* **138**: 77-84.

Snow, M.H. (1977a). Myogenic cell formation in regenerating rat skeletal muscle injured by mincing. I. A fine structural study. *Anat Rec* **188**: 181-99.

Snow, M.H. (1977b). Myogenic cell formation in regenerating rat skeletal muscle injured by mincing. II. An autoradiographic study. *Anat Rec* **188**: 201-17.

Sobue, K., Hayashi, K. & Nishida, W. (1998). Molecular mechanism of phenotypic modulation of smooth muscle cells. *Horm Res* **50**: 15-24.

Sobue, K., Hayashi, K. & Nishida, W. (1999). Expressional regulation of smooth muscle cell-specific genes in association with phenotypic modulation. *Mol Cell Biochem* **190**: 105-18.

Soltoff, S.P., Kaplan, D.R. & Cantley, L.C. (1993). Phosphatidylinositol 3-kinase. *Methods in Neurosciences* **18**: 100-112.

Solway, J., Seltzer, J., Samaha, F.F., Kim, S., Alger, L.E., Niu, Q., Morrisey, E.E., Ip, H.S. & Parmacek, M.S. (1995). Structure and expression of a smooth muscle cell-specific gene, SM22 alpha. *J Biol Chem* **270**: 13460-9.

Soman, G. & Graves, D.J. (1988). Endogenous ADP-ribosylation in skeletal muscle membranes. *Arch Biochem Biophys* **260**: 56-66.

Soman, G., Haregewoin, A., Hom, R.C. & Finberg, R.W. (1991). Guanidine group specific ADP-ribosyltransferase in murine cells. *Biochem Biophys Res Commun* **176**: 301-8.

Soman, G., Mickelson, J.R., Louis, C.F. & Graves, D.J. (1984a). NAD: guanidino group specific mono ADP-ribosyltransferase activity in skeletal muscle. *Biochem Biophys Res Commun* **120**: 973-80.

Soman, G., Narayanan, J., Martin, B.L. & Graves, D.J. (1986). Use of substituted (benzylidineamino)guanidines in the study of guanidino group specific ADP-ribosyltransferase. *Biochemistry* **25**: 4113-9.

Soman, G., Tomer, K.B. & Graves, D.J. (1983). Assay of mono ADP-ribosyltransferase activity by using guanylhydrazones. *Anal Biochem* **134**: 101-10.

Somlyo, A.P. & Somlyo, A.V. (1994a). Signal transduction and regulation in smooth muscle. *Nature* **372**: 231-6.

Somlyo, A.P. & Somlyo, A.V. (1994b). Smooth muscle: excitation-contraction coupling, contractile regulation, and the cross-bridge cycle. *Alcohol Clin Exp Res* **18**: 138-43.

Somsen, G.A., van Vlies, B., de Milliano, P.A., Borm, J.J., van Royen, E.A., Endert, E. & Lie, K.I. (1996). Increased myocardial [123I]-metaiodobenzylguanidine uptake after enalapril treatment in patients with chronic heart failure. *Heart* **76**: 218-22.

Sonnenburg, W.K. & Smith, W.L. (1988). Regulation of cyclic AMP metabolism in rabbit cortical collecting tubule cells by prostaglandins. *J Biol Chem* **263**: 6155-60.

Spahr, R. & Piper, H.M. (1990). Microcarrier cultures of endothelial cells. In: Cell culture techniques in heart and vessel research. Piper, H.M. (eds.). Springer-Verlag, Berlin. pp 220-229.

Spears, J.R., Reyes, V.P., Wynne, J., Fromm, B.S., Sinofsky, E.L., Andrus, S., Sinclair, I.N., Hopkins, B.E., Schwartz, L., Aldridge, H.E. & et al. (1990). Percutaneous coronary laser balloon angioplasty: initial results of a multicenter experience. *J Am Coll Cardiol* **16**: 293-303.

Speir, E., Modali, R., Huang, E.S., Leon, M.B., Shawl, F., Finkel, T. & Epstein, S.E. (1994). Potential role of human cytomegalovirus and p53 interaction in coronary restenosis. *Science* **265**: 391-4.

Spray, T.L. & Roberts, W.C. (1977). Morphologic observations in biologic conduits between aorta and coronary artery. *Cardiovasc Clin* **8**: 11-40.

Stary, H.C., Blankenhorn, D.H., Chandler, A.B., Glagov, S., Insull, W., Jr., Richardson, M., Rosenfeld, M.E., Schaffer, S.A., Schwartz, C.J., Wagner, W.D. & et al. (1992). A definition of the intima of human arteries and of its atherosclerosis-prone regions. A report from the Committee on Vascular Lesions of the Council on Arteriosclerosis, American Heart Association. *Circulation* **85**: 391-405.

Stary, H.C., Chandler, A.B., Dinsmore, R.E., Fuster, V., Glagov, S., Insull, W., Jr., Rosenfeld, M.E., Schwartz, C.J., Wagner, W.D. & Wissler, R.W. (1995). A definition of advanced types of atherosclerotic lesions and a histological classification of atherosclerosis. A report from the Committee on Vascular Lesions of the Council on Arteriosclerosis, American Heart Association. *Circulation* **92**: 1355-74.

Stary, H.C., Chandler, A.B., Glagov, S., Guyton, J.R., Insull, W., Jr., Rosenfeld, M.E., Schaffer, S.A., Schwartz, C.J., Wagner, W.D. & Wissler, R.W. (1994). A definition of initial, fatty streak, and intermediate lesions of atherosclerosis. A report from the Committee on Vascular Lesions of the Council on Arteriosclerosis, American Heart Association. *Circulation* **89**: 2462-78.

Stasia, M.J., Jouan, A., Bourmeyster, N., Boquet, P. & Vignais, P.V. (1991). ADP-ribosylation of a small size GTP-binding protein in bovine neutrophils by the C3 exoenzyme of Clostridium botulinum and effect on the cell motility. *Biochem Biophys Res Commun* **180**: 615-22.

Steele, P.M., Chesebro, J.H., Stanson, A.W., Holmes, D.R., Jr., Dewanjee, M.K., Badimon, L. & Fuster, V. (1985). Balloon angioplasty. Natural history of the pathophysiological response to injury in a pig model. *Circ Res* **57**: 105-12.

Stossel, T.P. (1993). On the crawling of animal cells. *Science* **260**: 1086-94.

Stouffer, G.A. & Owens, G.K. (1992). Angiotensin II-induced mitogenesis of spontaneously hypertensive rat- derived cultured smooth muscle cells is dependent on autocrine production of transforming growth factor-beta. *Circ Res* **70**: 820-8.

Stouffer, G.A., Schmedtje, J.F., Gulba, D., Huber, K., Bode, C., Aaron, J. & Runge, M.S. (1996). Restenosis following percutaneous revascularization--the potential role of thrombin and the thrombin receptor. *Ann Hematol* **73**: S39-41.

Stubberfield, C.R. & Cohen, G.M. (1988). NAD+ depletion and cytotoxicity in isolated hepatocytes. *Biochem Pharmacol* **37**: 3967-74.

Sturgill, T.W., Ray, L.B., Erikson, E. & Maller, J.L. (1988). Insulin-stimulated MAP-2 kinase phosphorylates and activates ribosomal protein S6 kinase II. *Nature* **334**: 715-8.

Sugden, P.H. & Clerk, A. (1997). Regulation of the ERK subgroup of MAP kinase cascades through G protein- coupled receptors. *Cell Signal* **9**: 337-51.

Suggs, W.D., Olson, S.C., Madnani, D., Patel, S., Veith, F.J. & Mandani, D. (1999). Antisense oligonucleotides to c-fos and c-jun inhibit intimal thickening in a rat vein graft model. *Surgery* **126**: 443-9.

Sun, X.J., Crimmins, D.L., Myers, M.G., Jr., Miralpeix, M. & White, M.F. (1993). Pleiotropic insulin signals are engaged by multisite phosphorylation of IRS-1. *Mol Cell Biol* **13**: 7418-28.

Sun, Y., Yamauchi, J., Kaziro, Y. & Itoh, H. (1999). Activation of c-fos promoter by Gbetagamma-mediated signaling: involvement of Rho and c-Jun N-terminal kinase. *J Biochem (Tokyo)* **125**: 515-21.

Sutherland, C., Waltner-Law, M., Gnudi, L., Kahn, B.B. & Granner, D.K. (1998). Activation of the ras mitogen-activated protein kinase-ribosomal protein kinase pathway is not required for the repression of phosphoenolpyruvate carboxykinase gene transcription by insulin. *J Biol Chem* **273**: 3198-204.

Szabo, C., Cuzzocrea, S., Zingarelli, B., O'Connor, M. & Salzman, A.L. (1997). Endothelial dysfunction in a rat model of endotoxic shock. Importance of the activation of poly (ADP-ribose) synthetase by peroxynitrite. *J Clin Invest* **100**: 723-35.

Taal, B.G., Hoefnagel, C., Boot, H., de Jong, D. & Rutgers, M. (1999). [Carcinoid tumors of the intestines: developments in the Netherlands for diagnosis and palliative treatment (published erratum appears in Ned Tijdschr Geneeskd 1999 Apr 3;143(14):768)]. *Ned Tijdschr Geneeskd* **143**: 445-51.

Taal, B.G., Hoefnagel, C.A., Valdes Olmos, R.A., Boot, H. & Beijnen, J.H. (1996). Palliative effect of metaiodobenzylguanidine in metastatic carcinoid tumors. *J Clin Oncol* **14**: 1829-38.

Taguchi, J., Abe, J., Okazaki, H., Takuwa, Y. & Kurokawa, K. (1993). L-arginine inhibits neointimal formation following balloon injury. *Life Sci* **53**: L387-92.

Takada, T., Iida, K. & Moss, J. (1995). Conservation of a common motif in enzymes catalyzing ADP-ribose transfer. Identification of domains in mammalian transferases. *J Biol Chem* **270**: 541-4.

Takada, T., Okazaki, I.J. & Moss, J. (1994). ADP-ribosylarginine hydrolases. *Mol Cell Biochem* **138**: 119-22.

Takai, Y., Sasaki, T., Tanaka, K. & Nakanishi, H. (1995). Rho as a regulator of the cytoskeleton. *Trends Biochem Sci* **20**: 227-31.

Takata, Y., Imamura, T., Haruta, T., Sasaoka, T., Morioka, H., Ishihara, H., Sawa, T., Usui, I., Ishiki, M. & Kobayashi, M. (1996). The dominant negative effect of a kinase-defective insulin receptor on insulin-like growth factor-I-stimulated signaling in Rat-1 fibroblasts. *Metabolism* **45**: 1474-82.

Takeda, H., Matozaki, T., Takada, T., Noguchi, T., Yamao, T., Tsuda, M., Ochi, F., Fukunaga, K., Inagaki, K. & Kasuga, M. (1999). PI 3-kinase gamma and protein kinase C-zeta mediate RAS-independent activation of MAP kinase by a Gi protein-coupled receptor. *EMBO J* **18**: 386-95.

Takeda, S., North, D.L., Diagana, T., Miyagoe, Y., Lakich, M.M. & Whalen, R.G. (1995). Myogenic regulatory factors can activate TATA-containing promoter elements via an E-box independent mechanism. *J Biol Chem* **270**: 15664-70.

Takeishi, Y., Atsumi, H., Fujiwara, S., Takahashi, K. & Tomoike, H. (1997). ACE inhibition reduces cardiac iodine-123-MIBG release in heart failure. *J Nucl Med* **38**: 1085-9.

Takishima, K., Griswold-Prenner, I., Ingebritsen, T. & Rosner, M.R. (1991). Epidermal growth factor (EGF) receptor T669 peptide kinase from 3T3-L1 cells is an EGF-stimulated "MAP" kinase. *Proc Natl Acad Sci U S A* **88**: 2520-4.

Tanaka, H., Sukhova, G.K., Swanson, S.J., Clinton, S.K., Ganz, P., Cybulsky, M.I. & Libby, P. (1993). Sustained activation of vascular cells and leukocytes in the rabbit aorta after balloon injury. *Circulation* **88**: 1788-803.

Tanaka, Y., Yoshihara, K., Itaya, A., Kamiya, T. & Koide, S.S. (1984). Mechanism of the inhibition of Ca2+, Mg2+-dependent endonuclease of bull seminal plasma induced by ADP-ribosylation. *J Biol Chem* **259**: 6579-85.

Tanigawa, Y., Tsuchiya, M., Imai, Y. & Shimoyama, M. (1984). ADP-ribosyltransferase from hen liver nuclei. Purification and characterization. *J Biol Chem* **259**: 2022-9.

Taniguchi, M., Tsuchiya, M. & Shimoyama, M. (1993). Comparison of acceptor protein specificities on the formation of ADP- ribose.acceptor adducts by arginine-specific ADP-ribosyltransferase from rabbit skeletal muscle sarcoplasmic reticulum with those of the enzyme from chicken peripheral polymorphonuclear cells. *Biochim Biophys Acta* **1161**: 265-71.

Taniguchi, T., Suzuki, S. & Shizuta, Y. (1985). Poly (ADP-ribosyl)ation of RNA polymerase II from wheat germ. *Biochem Biophys Res Commun* **127**: 526-32.

Tanizawa, A., Kubota, M., Hashimoto, H., Shimizu, T., Takimoto, T., Kitoh, T., Akiyama, Y. & Mikawa, H. (1989). VP-16-induced nucleotide pool changes and poly(ADP-ribose) synthesis: the role of VP-16 in interphase death. *Exp Cell Res* **185**: 237-46.

Tanuma, S. & Johnson, G.S. (1983). ADP-ribosylation of nonhistone high mobility group proteins in intact cells. *J Biol Chem* **258**: 4067-70.

Tanuma, S., Kawashima, K. & Endo, H. (1988). Eukaryotic mono(ADP-ribosyl)transferase that ADP-ribosylates GTP- binding regulatory Gi protein. *J Biol Chem* **263**: 5485-9.

Tanuma, S., Yagi, T. & Johnson, G.S. (1985). Endogenous ADP ribosylation of high mobility group proteins 1 and 2 and histone H1 following DNA damage in intact cells. *Arch Biochem Biophys* **237**: 38-42.

Taub, R., Roy, A., Dieter, R. & Koontz, J. (1987). Insulin as a growth factor in rat hepatoma cells. Stimulation of proto-oncogene expression. *J Biol Chem* **262**: 10893-7.

Taylor, E.W. (1986). Cell motility. *J Cell Sci Suppl* **4**: 89-102.

Tenaglia, A.N., Buller, C.E., Kisslo, K.B., Stack, R.S. & Davidson, C.J. (1992). Mechanisms of balloon angioplasty and directional coronary atherectomy as assessed by intracoronary ultrasound. *J Am Coll Cardiol* **20**: 685-91.

Terada, Y., Tomita, K., Homma, M.K., Nonoguchi, H., Yang, T., Yamada, T., Yuasa, Y., Krebs, E.G., Sasaki, S. & Marumo, F. (1994). Sequential activation of Raf-1 kinase, mitogen-activated protein (MAP) kinase kinase, MAP kinase, and S6 kinase by hyperosmolality in renal cells. *J Biol Chem* **269**: 31296-301.

Terashima, M., Mishima, K., Yamada, K., Tsuchiya, M., Wakutani, T. & Shimoyama, M. (1992). ADP-ribosylation of actins by arginine-specific ADP-ribosyltransferase purified from chicken heterophils. *Eur J Biochem* **204**: 305-11.

Terashima, M., Shimoyama, M. & Tsuchiya, M. (1999). Introduction of NAD decreases fMLP-induced actin polymerization in chicken polymorphonuclear leukocytes--the role of intracellular ADP- ribosylation of actin for cytoskeletal organization. *Biochem Mol Biol Int* **47**: 615-20.

Terashima, M., Yamamori, C. & Shimoyama, M. (1995). ADP-ribosylation of Arg28 and Arg206 on the actin molecule by chicken arginine-specific ADP-ribosyltransferase. *Eur J Biochem* **231**: 242-9.

Tesfamariam, B. & Cohen, R.A. (1988). Inhibition of adrenergic vasoconstriction by endothelial cell shear stress. *Circ Res* **63**: 720-5.

Thiemermann, C., Bowes, J., Myint, F.P. & Vane, J.R. (1997). Inhibition of the activity of poly(ADP ribose) synthetase reduces ischemia-reperfusion injury in the heart and skeletal muscle. *Proc Natl Acad Sci U S A* **94**: 679-83.

Thies, R.L. & Autor, A.P. (1991). Reactive oxygen injury to cultured pulmonary artery endothelial cells: mediation by poly(ADP-ribose) polymerase activation causing NAD depletion and altered energy balance. *Arch Biochem Biophys* **286**: 353-63.

Thomas, S.M., DeMarco, M., D'Arcangelo, G., Halegoua, S. & Brugge, J.S. (1992). Ras is essential for nerve growth factor- and phorbol ester-induced tyrosine phosphorylation of MAP kinases. *Cell* **68**: 1031-40.

Thomson, J.F. & Moss, E.M. (1955). Effect of adrenalectomy on tryptophan peroxidase, adenosine deaminase, and arginase content of regenerating rat liver. *Proc Soc Exp Biol Med* **89**: 230-233.

Thorens, B. (1992). Molecular and cellular physiology of GLUT-2, a high-Km facilitated diffusion glucose transporter. *Int Rev Cytol* **137**: 209-38.

Thorgeirsson, G., Robertson, A.L., Jr. & Cowan, D.H. (1979). Migration of human vascular endothelial and smooth muscle cells. *Lab Invest* **41**: 51-62.

Thyberg, J. (1996). Differentiated properties and proliferation of arterial smooth muscle cells in culture. *Int Rev Cytol* **169**: 183-265.

Thyberg, J. (1998). Phenotypic modulation of smooth muscle cells during formation of neointimal thickenings following vascular injury. *Histol Histopathol* **13**: 871-91.

Thyberg, J., Blomgren, K., Hedin, U. & Dryjski, M. (1995a). Phenotypic modulation of smooth muscle cells during the formation of neointimal thickenings in the rat carotid artery after balloon injury: an electron-microscopic and stercological study. *Cell Tissue Res* **281**: 421-33.

Thyberg, J., Blomgren, K., Roy, J., Tran, P.K. & Hedin, U. (1997). Phenotypic modulation of smooth muscle cells after arterial injury is associated with changes in the distribution of laminin and fibronectin. *J Histochem Cytochem* **45**: 837-46.

Thyberg, J., Hedin, U. & Bottger, B.A. (1990a). Attachment substrates for smooth muscle cells. In: Cell culture techniques in heart and vessel research. Piper, H.M. (eds.). Springer-Verlag, Berlin. pp 315-333.

Thyberg, J., Hedin, U., Sjolund, M., Palmberg, L. & Bottger, B.A. (1990b). Regulation of differentiated properties and proliferation of arterial smooth muscle cells. *Arteriosclerosis* **10**: 966-90.

Thyberg, J., Hultgardh-Nilsson, A. & Kallin, B. (1995b). Inhibitors of ADP-ribosylation suppress phenotypic modulation and proliferation of smooth muscle cells cultured from rat aorta. *Differentiation* **59**: 243-52.

Thyberg, J., Palmberg, L., Nilsson, J., Ksiazek, T. & Sjolund, M. (1983). Phenotype modulation in primary cultures of arterial smooth muscle cells. On the role of platelet-derived growth factor. *Differentiation* **25**: 156-67.

Tio, R.A., Isner, J.M. & Walsh, K. (1998). Gene therapy to prevent restenosis, the Boston experience. *Semin Interv Cardiol* **3**: 205-10.

Tobes, M.C., Jaques, S., Jr., Wieland, D.M. & Sisson, J.C. (1985). Effect of uptake-one inhibitors on the uptake of norepinephrine and metaiodobenzylguanidine. *J Nucl Med* **26**: 897-907.

Topol, E.J., Leya, F., Pinkerton, C.A., Whitlow, P.L., Hofling, B., Simonton, C.A., Masden, R.R., Serruys, P.W., Leon, M.B., Williams, D.O. & et al. (1993). A comparison of directional atherectomy with coronary angioplasty in patients with coronary artery disease. The CAVEAT Study Group. *N Engl J Med* **329**: 221-7.

Touhara, K., Hawes, B.E., van Biesen, T. & Lefkowitz, R.J. (1995). G protein beta gamma subunits stimulate phosphorylation of Shc adapter protein. *Proc Natl Acad Sci U S A* **92**: 9284-7.

Traverse, S., Gomez, N., Paterson, H., Marshall, C. & Cohen, P. (1992). Sustained activation of the mitogen-activated protein (MAP) kinase cascade may be required for differentiation of PC12 cells. Comparison of the effects of nerve growth factor and epidermal growth factor. *Biochem J* **288**: 351-5.

Treisman, R. (1995). Journey to the surface of the cell: Fos regulation and the SRE. *EMBO J* **14**: 4905-13.

Treisman, R. (1996). Regulation of transcription by MAP kinase cascades. *Curr Opin Cell Biol* **8**: 205-15.

Treisman, R., Marais, R. & Wynne, J. (1992). Spatial flexibility in ternary complexes between SRF and its accessory proteins. *EMBO J* **11**: 4631-40.

Trucco, C., Oliver, F.J., de Murcia, G. & Menissier-de Murcia, J. (1998). DNA repair defect in poly(ADP-ribose) polymerase-deficient cell lines. *Nucleic Acids Res* **26**: 2644-9.

Tsakiridis, T., Bergman, A., Somwar, R., Taha, C., Aktories, K., Cruz, T.F., Klip, A. & Downey, G.P. (1998). Actin filaments facilitate insulin activation of the src and collagen homologous/mitogen-activated protein kinase pathway leading to DNA synthesis and c-fos expression. *J Biol Chem* **273**: 28322-31.

Tsuchiya, M. & Shimoyama, M. (1994). Target protein for eucaryotic arginine-specific ADP-ribosyltransferase. *Mol Cell Biochem* **138**: 113-8.

Tuan, T.L. & Nichter, L.S. (1998). The molecular basis of keloid and hypertrophic scar formation. *Mol Med Today* **4**: 19-24.

Turpeinen, A.K., Vanninen, E., Kuikka, J.T. & Uusitupa, M.I. (1996). Demonstration of regional sympathetic denervation of the heart in diabetes. Comparison between patients with NIDDM and IDDM. *Diabetes Care* **19**: 1083-90.

Tytgat, G.A., Voute, P.A., Takeuchi, S., Miyoshi, I. & Rutgers, M. (1995). Meta-iodobenzylguanidine uptake in platelets, megakaryoblastic leukaemia cell lines MKPL-1 and CHRF-28-11 and erythroleukaemic cell line HEL. *Eur J Cancer* **4**: 603-6.

Ueda, K. & Hayaishi, O. (1985). ADP-ribosylation. *Annu Rev Biochem* **54**: 73-100.

Ueda, M., Becker, A.E., Tsukada, T., Numano, F. & Fujimoto, T. (1991). Fibrocellular tissue response after percutaneous transluminal coronary angioplasty. An immunocytochemical analysis of the cellular composition. *Circulation* **83**: 1327-32.

Ueda, Y., Hirai, S., Osada, S., Suzuki, A., Mizuno, K. & Ohno, S. (1996). Protein kinase C activates the MEK-ERK pathway in a manner independent of Ras and dependent on Raf. *J Biol Chem* **271**: 23512-9.

Uehara, T., Tokumitsu, Y. & Nomura, Y. (1999). Pertussis toxin-sensitive and insensitive intracellular signalling pathways in undifferentiated 3T3-L1 cells stimulated by insulin converge with phosphatidylinositol 3-kinase upstream of the Ras mitogen-activated protein kinase cascade. *Eur J Biochem* **259**: 801-8.

Uehara, Y., Ishimitsu, T., Kimura, K., Ishii, M., Ikeda, T. & Sugimoto, T. (1988). Regulatory effects of eicosanoids on thymidine uptake by vascular smooth muscle cells of rats. *Prostaglandins* **36**: 847-57.

Ui, M. & Katada, T. (1990). Bacterial toxins as probe for receptor-Gi coupling. *Adv Second Messenger Phosphoprotein Res* **24**: 63-9.

Umans, V.A., Hermans, W., Foley, D.P., Strikwerda, S., van den Brand, M., de Jaegere, P., de Feyter, P.J. & Serruys, P.W. (1993). Restenosis after directional coronary atherectomy and balloon angioplasty: comparative analysis based on matched lesions. *J Am Coll Cardiol* **21**: 1382-90.

Umemura, K., Watanabe, S., Kondo, K., Hashimoto, H. & Nakashima, M. (1997). Inhibitory effect of prostaglandin E1 on intimal thickening following photochemically induced endothelial injury in the rat femoral artery. *Atherosclerosis* **130**: 11-6.

Urioste, S.S., Arndt, K.A. & Dover, J.S. (1999). Keloids and hypertrophic scars: review and treatment strategies. *Semin Cutan Med Surg* **18** : 159-71.

Valdes Olmos, R.A., Hoefnagel, C.A. & van der Schoot, J.B. (1993). Nuclear medicine in the monitoring of organ function and the detection of injury related to cancer therapy. *Eur J Nucl Med* **20**: 515-46.

Valdez, M.R., Richardson, J.A., Klein, W.H. & Olson, E.N. (2000). Failure of Myf5 to support myogenic differentiation without myogenin, MyoD, and MRF4. *Dev Biol* **219**: 287-98.

Vallotton, M.B., Gerber-Wicht, C., Dolci, W. & Wuthrich, R.P. (1989). Interaction of vasopressin and angiotensin II in stimulation of prostacyclin synthesis in vascular smooth muscle cells. *Am J Physiol* **257**: E617-24.

van Biesen, T., Hawes, B.E., Luttrell, D.K., Krueger, K.M., Touhara, K., Porfiri, E., Sakaue, M., Luttrell, L.M. & Lefkowitz, R.J. (1995). Receptor-tyrosine-kinase- and G beta gamma-mediated MAP kinase activation by a common signalling pathway. *Nature* **376**: 781-4.

van Biesen, T., Hawes, B.E., Raymond, J.R., Luttrell, L. M., Koch, W.J. & Lefkowitz, R.J. (1996). G(o)-protein alpha-subunits activate mitogen-activated protein kinase via a novel protein kinase C-dependent mechanism. *J Biol Chem* **271**: 1266-9.

Van den Berg, J.D., Smets, L.A., Rutgers, M., Grummels, A., Fokkens, R., Jonkergouw, P. & van Rooij, H. (1997). Chemical characterization and comparative cellular effects of meta- iodobenzyl guanidine and benzyl guanidine. *Cancer Chemother Pharmacol* **40**: 131-7.

van Neck, J.W., Medina, J.J., Onnekink, C., Schwartz, S.M. & Bloemers, H.P. (1995). Expression of basic fibroblast growth factor and fibroblast growth factor receptor genes in cultured rat aortic smooth muscle cells. *Biochim Biophys Acta* **1261**: 210-4.

Van Putten, V., Li, X., Maselli, J. & Nemenoff, R.A. (1994). Regulation of smooth muscle alpha-actin promoter by vasopressin and platelet-derived growth factor in rat aortic vascular smooth muscle cells. *Circ Res* **75**: 1126-30.

vanderSpek, J., Cosenza, L., Woodworth, T., Nichols, J.C. & Murphy, J.R. (1994). Diphtheria toxin-related cytokine fusion proteins: elongation factor 2 as a target for the treatment of neoplastic disease. *Mol Cell Biochem* **138**: 151-6.

Vane, J. & Botting, R. (1987). Inflammation and the mechanism of action of anti-inflammatory drugs. *FASEB J* **1**: 89-96.

Varticovski, L., Harrison-Findik, D., Keeler, M.L. & Susa, M. (1994). Role of PI 3-kinase in mitogenesis. *Biochim Biophys Acta* **1226**: 1-11.

Venuti, J.M. & Cserjesi, P. (1996). Molecular embryology of skeletal myogenesis. *Curr Top Dev Biol* **34**: 169-206.

Vernon, S.M., Sarembock, I.J. & Owens, G.K. (1993). Thrombin-induced proliferation in cultured smooth muscle cells is not associated with downregulation of smooth muscle alpha-actin gene expression (Abstract). *Circulation* **86**: I-189.

Verspohl, E.J., Roth, R.A., Vigneri, R. & Goldfine, I.D. (1984). Dual regulation of glycogen metabolism by insulin and insulin-like growth factors in human hepatoma cells (HEP-G2). Analysis with an anti- receptor monoclonal antibody. *J Clin Invest* **74**: 1436-43.

Vilgrain, I. & Baird, A. (1991). Phosphorylation of basic fibroblast growth factor by a protein kinase associated with the outer surface of a target cell. *Mol Endocrinol* **5**: 1003-12.

Vilgrain, I., Gonzalez, A.M. & Baird, A. (1993). Phosphorylation of basic fibroblast growth factor (FGF-2) in the nuclei of SK-Hep-1 cells. *FEBS Lett* **331**: 228-32.

Villaschi, S., Nicosia, R.F. & Smith, M.R. (1994). Isolation of a morphologically and functionally distinct smooth muscle cell type from the intimal aspect of the normal rat aorta. Evidence for smooth muscle cell heterogeneity. *In Vitro Cell Dev Biol Anim* **30A**: 589-95.

Virmani, R. & Farb, A. (1999). Pathology of in-stent restenosis. *Curr Opin Lipidol* **10**: 499-506.

Vlahos, C.J., Matter, W.F., Hui, K.Y. & Brown, R.F. (1994). A specific inhibitor of phosphatidylinositol 3-kinase, 2-(4- morpholinyl)-8-phenyl-4H-1-benzopyran-4-one (LY294002). *J Biol Chem* **269**: 5241-8.

Voisard, R., von Eicken, J., Baur, R., Gschwend, J.E., Wenderoth, U., Kleinschmidt, K., Hombach, V. & Hoher, M. (1999). A human arterial organ culture model of postangioplasty restenosis: results up to 56 days after ballooning. *Atherosclerosis* **144**: 123-34.

Wafelman, A.R., Hoefnagel, C.A., Maes, R.A. & Beijnen, J.H. (1994a). Radioiodinated metaiodobenzylguanidine: a review of its biodistribution and pharmacokinetics, drug interactions, cytotoxicity and dosimetry. *Eur J Nucl Med* **21**: 545-59.

Wafelman, A.R., Konings, M.C., Hoefnagel, C.A., Maes, R.A. & Beijnen, J.H. (1994b). Synthesis, radiolabelling and stability of radioiodinated m- iodobenzylguanidine, a review. *Appl Radiat Isot* **45**: 997-107.

Wakabayashi, Y., Kurata, C., Mikami, T., Shouda, S., Okayama, K. & Tawarahara, K. (1997). Effects of cilazapril and verapamil on myocardial iodine-125-metaiodobenzylguanidine accumulation in cardiomyopathic BIO 53.58 hamsters. *J Nucl Med* **38**: 1540-5.

Waller, B.F. (1985). Coronary luminal shape and the arc of disease-free wall: morphologic observations and clinical relevance. *J Am Coll Cardiol* **6**: 1100-1.

Waller, B.F., Pinkerton, C.A., Orr, C.M., Slack, J.D., VanTassel, J.W. & Peters, T. (1991). Restenosis 1 to 24 months after clinically successful coronary balloon angioplasty: a necropsy study of 20 patients. *J Am Coll Cardiol* **17**: 58B-70B.

Walsh, K. (1997). Coordinate regulation of cell cycle and apoptosis during myogenesis. *Prog Cell Cycle Res* **3**: 53-8.

Wan, Y. & Huang, X.Y. (1998). Analysis of the Gs/mitogen-activated protein kinase pathway in mutant S49 cells. *J Biol Chem* **273**: 14533-7.

Wang, J., Nemoto, E. & Dennert, G. (1996). Regulation of CTL by ecto-nictinamide adenine dinucleotide (NAD) involves ADP-ribosylation of a p56lck-associated protein. *J Immunol* **156**: 2819-27.

Wang, Y., Falasca, M., Schlessinger, J., Malstrom, S., Tsichlis, P., Settleman, J., Hu, W., Lim, B. & Prywes, R. (1998). Activation of the c-fos serum response element by phosphatidyl inositol 3-kinase and rho pathways in HeLa cells. *Cell Growth Differ* **9**: 513-22.

Wang, Y., Simonson, M.S., Pouyssegur, J. & Dunn, M.J. (1992). Endothelin rapidly stimulates mitogen-activated protein kinase activity in rat mesangial cells. *Biochem J* **287**: 589-94.

Wang, Z.Q., Auer, B., Stingl, L., Berghammer, H., Haidacher, D., Schweiger, M. & Wagner, E.F. (1995). Mice lacking ADPRT and poly(ADP-ribosyl)ation develop normally but are susceptible to skin disease. *Genes Dev* **9**: 509-20.

Warner, S.J., Auger, K.R. & Libby, P. (1987). Human interleukin 1 induces interleukin 1 gene expression in human vascular smooth muscle cells. *J Exp Med* **165**: 1316-31.

Warner, S.J. & Libby, P. (1989). Human vascular smooth muscle cells. Target for and source of tumor necrosis factor. *J Immunol* **142**: 100-9.

Waters, S.B., Yamauchi, K. & Pessin, J.E. (1993). Functional expression of insulin receptor substrate-1 is required for insulin-stimulated mitogenic signaling. *J Biol Chem* **268**: 22231-4.

Watts, S.W. (1998). Activation of the mitogen-activated protein kinase pathway via the 5- HT2A receptor. *Ann N Y Acad Sci* **861**: 162-8.

Weber, H., Taylor, D.S. & Molloy, C.J. (1994a). Angiotensin II induces delayed mitogenesis and cellular proliferation in rat aortic smooth muscle cells. Correlation with the expression of specific endogenous growth factors and reversal by suramin. *J Clin Invest* **93**: 788-98.

Weber, H., Webb, M.L., Serafino, R., Taylor, D.S., Moreland, S., Norman, J. & Molloy, C.J. (1994b). Endothelin-1 and angiotensin-II stimulate delayed mitogenesis in cultured rat aortic smooth muscle cells: evidence for common signaling mechanisms. *Mol Endocrinol* **8**: 148-58.

Weber, W., Weber, J. & Senekowitsch-Schmidtke, R. (1996). Therapeutic effect of m-[131I]- and m-[125I]iodobenzylguanidine on neuroblastoma multicellular tumor spheroids of different sizes. *Cancer Res* **56**: 5428-34.

Weinstein, R., Stemerman, M.B. & Maciag, T. (1981). Hormonal requirements for growth of arterial smooth muscle cells in vitro: and endocrine approach to atherosclerosis. *Science* **212**: 818-20.

Weintraub, H., Dwarki, V.J., Verma, I., Davis, R., Hollenberg, S., Snider, L., Lassar, A. & Tapscott, S.J. (1991). Muscle-specific transcriptional activation by MyoD. *Genes Dev* **5**: 1377-86.

Weksler, B.B. (1987). Regulation of prostaglandin synthesis in human vascular cells. *Ann N Y Acad Sci* **509**: 142-8.

Wendling, W.W. & Harakal, C. (1991). Effects of prostaglandin F2 alpha and thromboxane A2 analogue on bovine cerebral arterial tone and calcium fluxes. *Stroke* **22**: 66-72.

Weng, B., Thompson, W.C., Kim, H.J., Levine, R.L. & Moss, J. (1999). Modification of the ADP-ribosyltransferase and NAD glycohydrolase activities of a mammalian transferase (ADP-ribosyltransferase 5) by auto-ADP-ribosylation. *J Biol Chem* **274**: 31797-803.

White, M.F. & Kahn, C.R. (1994). The insulin signaling system. *J Biol Chem* **269**: 1-4.

Wichter, T., Hindricks, G., Lerch, H., Bartenstein, P., Borggrefe, M., Schober, O. & Breithardt, G. (1994). Regional myocardial sympathetic dysinnervation in arrhythmogenic right ventricular cardiomyopathy. An analysis using 123I-meta-iodobenzylguanidine scintigraphy. *Circulation* **89**: 667-83.

Wick, M.J., Frank, D.W., Storey, D.G. & Iglewski, B.H. (1990). Structure, function, and regulation of Pseudomonas aeruginosa exotoxin A. *Annu Rev Microbiol* **44**: 335-63.

Wieland, D.M., Brown, L.E., Rogers, W.L., Worthington, K.C., Wu, J.L., Clinthorne, N.H., Otto, C.A., Swanson, D.P. & Beierwaltes, W.H. (1981). Myocardial imaging with a radioiodinated norepinephrine storage analog. *J Nucl Med* **22**: 22-31.

Wieland, D.M., Mangner, T.J., Inbasekaran, M.N., Brown, L.E. & Wu, J.L. (1984). Adrenal medulla imaging agents: a structure-distribution relationship study of radiolabeled aralkylguanidines. *J Med Chem* **27**: 149-55.

Wieland, D.M., Wu, J., Brown, L.E., Mangner, T.J., Swanson, D.P. & Beierwaltes, W.H. (1980). Radiolabeled adrenergi neuron-blocking agents: adrenomedullary imaging with [131I]iodobenzylguanidine. *J Nucl Med* **21**: 349-53.

Wilcox, J.N. (1993). Molecular biology: insight into the causes and prevention of restenosis after arterial intervention. *Am J Cardiol* **72**: 88E-95E.

Wilden, P.A., Siddle, K., Haring, E., Backer, J.M., White, M.F. & Kahn, C.R. (1992). The role of insulin receptor kinase domain autophosphorylation in receptor-mediated activities. Analysis with insulin and anti-receptor antibodies. *J Biol Chem* **267**: 13719-27.

Wilentz, J.R., Sanborn, T.A., Haudenschild, C.C., Valeri, C.R., Ryan, T.J. & Faxon, D.P. (1987). Platelet accumulation in experimental angioplasty: time course and relation to vascular injury. *Circulation* **75**: 636-42.

Willard, F.S. & Crouch, M.F. (2000). Nuclear and cytoskeletal translocation and localization of heterotrimeric G-proteins. *Immunol Cell Biol* **78**: 387-94.

Williamson, K.C. & Moss, J. (1990). Mono-ADP-ribosyltransferases and ADP-ribosylarginine hydrolases: a Mono-ADP-ribosylation cycle in animal cells. In: ADP-ribosylating toxins and G proteins: Insights into signal transduction. Moss, J. & Vaughan, M. (eds.). American Society for Microbiology, Washington, D.C. pp 493-510.

Wilson, D.P., Saward, L., Zahradka, P. & Cheung, P.K. (1999). Angiotensin II receptor antagonists prevent neointimal proliferation in a porcine coronary artery organ culture model. *Cardiovasc Res* **42**: 761-72.

Wintersberger, U. & Wintersberger, E. (1985). Poly ADP-ribosylation--a cellular emergency reaction? *FEBS Lett* **188**: 189-91.

Wohrley, J.D., Frid, M.G., Moiseeva, E.P., Orton, E.C., Belknap, J.K. & Stenmark, K.R. (1995). Hypoxia selectively induces proliferation in a specific subpopulation of smooth muscle cells in the bovine neonatal pulmonary arterial media. *J Clin Invest* **96**: 273-81.

Wong, M.W., Pisegna, M., Lu, M.F., Leibham, D. & Perry, M. (1994). Activation of Xenopus MyoD transcription by members of the MEF2 protein family. *Dev Biol* **166**: 683-95.

Wood, K.W., Sarnecki, C., Roberts, T.M. & Blenis, J. (1992). ras mediates nerve growth factor receptor modulation of three signal- transducing protein kinases: MAP kinase, Raf-1, and RSK. *Cell* **68**: 1041-50.

Woodgett, J.R. (1989). Early gene induction by growth factors. *Br Med Bull* **45**: 529-40.

Woolf, N. (1982). *Pathology of atherosclerosis.* Postgraduate pathology series. Butterworth Scientific, London. xv, 322.

Wren, F.E., Schor, A.M., Schor, S.L. & Grant, M.E. (1986). Modulation of smooth muscle cell behaviour by platelet-derived factors and the extracellular matrix. *J Cell Physiol* **127**: 297-302.

Wu, K.K. (1997). Prostacyclin and nitric oxide-related gene transfer in preventing arterial thrombosis and restenosis. *Agents Actions Suppl* **48**: 107-23.

Xu, Y.J., Yau, L., Yu, L.P., Elimban, V., Zahradka, P. & Dhalla, N.S. (1996). Stimulation of protein synthesis by phosphatidic acid in rat cardiomyocytes. *Biochem Pharmacol* **52**: 1735-40.

Yaffe, D. (1968). Retention of differentiation potentialities during prolonged cultivation of myogenic cells. *Proc Natl Acad Sci U S A* **61**: 477-83.

Yamakawa, T., Tanaka, S., Numaguchi, K., Yamakawa, Y., Motley, E.D., Ichihara, S. & Inagami, T. (2000). Involvement of Rho-kinase in angiotensin II-induced hypertrophy of rat vascular smooth muscle cells. *Hypertension* **35**: 313-8.

Yamamoto, K., Tsukidate, K. & Farber, J.L. (1993a). Differing effects of the inhibition of poly(ADP-ribose) polymerase on the course of oxidative cell injury in hepatocytes and fibroblasts. *Biochem Pharmacol* **46**: 483-91.

Yamamoto, M., Yamamoto, K. & Noumura, T. (1993b). Type I collagen promotes modulation of cultured rabbit arterial smooth muscle cells from a contractile to a synthetic phenotype. *Exp Cell Res* **204**: 121-9.

Yamashita, A., Sato, E., Yasuda, H., Kurokawa, T. & Ishibashi, S. (1991). Reduction of mono(ADP-ribosyl)ation of 20 kDa protein with maturation in rat testis: involvement of guanine nucleotides. *Biochim Biophys Acta* **1091**: 46-50.

Yang, Z.Y., Simari, R.D., Perkins, N.D., San, H., Gordon, D., Nabel, G.J. & Nabel, E.G. (1996). Role of the p21 cyclin-dependent kinase inhibitor in limiting intimal cell proliferation in response to arterial injury. *Proc Natl Acad Sci U S A* **93**: 7905-10.

Yano, H., Agatsuma, T., Nakanishi, S., Saitoh, Y., Fukui, Y., Nonomura, Y. & Matsuda, Y. (1995). Biochemical and pharmacological studies with KT7692 and LY294002 on the role of phosphatidylinositol 3-kinase in Fc epsilon RI-mediated signal transduction. *Biochem J* **312**: 145-50.

Yau, L., Elliot, T., Lalonde, C. & Zahradka, P. (1998). Repression of phosphoenolpyruvate carboxykinase gene activity by insulin is blocked by 3-aminobenzamide but not by PD128763, a selective inhibitor of poly(ADP-ribose) polymerase. *Eur J Biochem* **253**: 91-100.

Yau, L., Lukes, H., McDiarmid, H., Werner, J. & Zahradka, P. (1999). Insulin-like growth factor-I (IGF-I)-dependent activation of pp42/44 mitogen-activated protein kinase occurs independently of IGF-I receptor kinase activation and IRS-1 tyrosine phosphorylation. *Eur J Biochem* **266**: 1147-57.

Yau, L. & Zahradka, P. (1997). Immunodetection of activated mitogen-activated protein kinase in vascular tissues. *Mol Cell Biochem* **172**: 59-66.

Yokoi, H., Daida, H., Kuwabara, Y., Nishikawa, H., Takatsu, F., Tomihara, H., Nakata, Y., Kutsumi, Y., Ohshima, S., Nishiyama, S., Seki, A., Kato, K., Nishimura, S., Kanoh, T. & Yamaguchi, H. (1997). Effectiveness of an antioxidant in preventing restenosis after percutaneous transluminal coronary angioplasty: the Probucol Angioplasty Restenosis Trial. *J Am Coll Cardiol* **30**: 855-62.

Yoshida, S. & Simbulan, C.M. (1994). Interaction of poly(ADP-ribose)polymerase with DNA polymerase alpha. *Mol Cell Biochem* **138**: 39-44.

Yoshida, Y., Mitsumata, M., Yamane, T., Tomikawa, M. & Nishida, K. (1988). Morphology and increased growth rate of atherosclerotic intimal smooth- muscle cells. *Arch Pathol Lab Med* **112**: 987-96.

Yoshihara, K., Hashida, T., Yoshihara, H., Tanaka, Y. & Ohgushi, H. (1977). Enzyme-bound early product of purified poly(ADP-ribose) polymerase. *Biochem Biophys Res Commun* **78**: 1281-8.

Yuan, J., Huiatt, T.W., Liao, C.X., Robson, R.M. & Graves, D.J. (1999). The effects of mono-ADP-ribosylation on desmin assembly-disassembly. *Arch Biochem Biophys* **363**: 314-22.

Yue, T.L., Wang, X., Sung, C.P., Olson, B., McKenna, P.J., Gu, J.L. & Feuerstein, G.Z. (1994). Interleukin-8. A mitogen and chemoattractant for vascular smooth muscle cells. *Circ Res* **75**: 1-7.

Yun, K. & Wold, B. (1996). Skeletal muscle determination and differentiation: story of a core regulatory network and its context. *Curr Opin Cell Biol* **8**: 877-89.

Yutani C., Imakita, M., Ishibashi-Ueda, H., Tsukamoto, Y., Nishida, N. & Ikeda, Y. (1999). Coronary atherosclerosis and interventions: pathological sequences and restenosis. *Pathol Int* **49**: 273-90.

Zahradka, P. & Ebisuzaki, K. (1982). A shuttle mechanism for DNA-protein interactions. The regulation of poly(ADP-ribose) polymerase. *Eur J Biochem* **127**: 579-85.

Zahradka, P., Larson, D.E. & Sells, B.H. (1989). Post-transcriptional regulation of 5S rRNA synthesis following myoblast differentiation. *Eur J Biochem* **184**: 261-6.

Zahradka, P., Werner, J. & Yau, L. (1998). Expression and regulation of the insulin-like growth factor-1 receptor by growing and quiescent H4IIE hepatoma. *Biochim Biophys Acta* **1375**: 131-9.

Zahradka, P. & Yau, L. (1994). ADP-ribosylation and gene expression. *Mol Cell Biochem* **138**: 91-8.

Zalewski, A. & Shi, Y. (1997). Vascular myofibroblasts. Lessons from coronary repair and remodeling. *Arterioscler Thromb Vasc Biol* **17**: 417-22.

Zappelli, F., Willems, D., Osada, S., Ohno, S., Wetsel, W.C., Molinaro, M., Cossu, G. & Bouche, M. (1996). The inhibition of differentiation caused by TGFbeta in fetal myoblasts is dependent upon selective expression of PKCtheta: a possible molecular basis for myoblast diversification during limb histogenesis. *Dev Biol* **180**: 156-64.

Zavitz, K.H. & Zipursky, S.L. (1997). Controlling cell proliferation in differentiating tissues: genetic analysis of negative regulators of G1-->S-phase progression. *Curr Opin Cell Biol* **9**: 773-81.

Zeff, R.H., Kongtahworn, C., Iannone, L.A., Gordon, D.F., Brown, T.M., Phillips, S.J., Skinner, J.R. & Spector, M. (1988). Internal mammary artery versus saphenous vein graft to the left anterior descending coronary artery: prospective randomized study with 10-year follow-up. *Ann Thorac Surg* **45**: 533-6.

Zhang, J., King, W.G., Dillon, S., Hall, A., Feig, L. & Rittenhouse, S.E. (1993a). Activation of platelet phosphatidylinositide 3-kinase requires the small GTP-binding protein Rho. *J Biol Chem* **268**: 22251-4.

Zhang, J. & Snyder, S.H. (1992). Nitric oxide stimulates auto-ADP-ribosylation of glyceraldehyde-3- phosphate dehydrogenase. *Proc Natl Acad Sci U S A* **89**: 9382-5.

Zhang, X.F., Settleman, J., Kyriakis, J.M., Takeuchi-Suzuki, E., Elledge, S.J., Marshall, M.S., Bruder, J.T., Rapp, U.R. & Avruch, J. (1993b). Normal and oncogenic p21ras proteins bind to the amino-terminal regulatory domain of c-Raf-1. *Nature* **364**: 308-13.

Zhao, Y., Bjorbaek, C., Weremowicz, S., Morton, C.C. & Moller, D.E. (1995). RSK3 encodes a novel pp90rsk isoform with a unique N-terminal sequence: growth factor-stimulated kinase function and nuclear translocation. *Mol Cell Biol* **15**: 4353-63.

Zhou, H., Huiatt, T.W., Robson, R.M., Sernett, S.W. & Graves, D.J. (1996). Characterization of ADP-ribosylation sites on desmin and restoration of desmin intermediate filament assembly by de-ADP-ribosylation. *Arch Biochem Biophys* **334**: 214-22.

Zolkiewska, A. & Moss, J. (1993). Integrin alpha 7 as substrate for a glycosylphosphatidylinositol- anchored ADP-ribosyltransferase on the surface of skeletal muscle cells. *J Biol Chem* **268**: 25273-6.

Zolkiewska, A. & Moss, J. (1995). Processing of ADP-ribosylated integrin alpha 7 in skeletal muscle myotubes. *J Biol Chem* **270**: 9227-33.

Zolkiewska, A. & Moss, J. (1997). The alpha 7 integrin as a target protein for cell surface mono-ADP- ribosylation in muscle cells. *Adv Exp Med Biol* **419**: 297-303.

Zolkiewska, A., Nightingale, M.S. & Moss, J. (1992). Molecular characterization of NAD:arginine ADP-ribosyltransferase from rabbit skeletal muscle. *Proc Natl Acad Sci U S A* **89**: 11352-6.

Zolkiewska, A., Okazaki, I.J. & Moss, J. (1994). Vertebrate mono-ADP-ribosyltransferases. *Mol Cell Biochem* **138**: 107-12.

Zolkiewska, A., Thompson, W.C. & Moss, J. (1998). Interaction of integrin alpha 7 beta 1 in C2C12 myotubes and in solution with laminin. *Exp Cell Res* **240**: 86-94.

Zou, Y., Komuro, I., Yamazaki, T., Kudoh, S., Aikawa, R., Zhu, W., Shiojima, I., Hiroi, Y., Tobe, K., Kadowaki, T. & Yazaki, Y. (1998). Cell type-specific angiotensin II-evoked signal transduction pathways: critical roles of Gbetagamma subunit, Src family, and Ras in cardiac fibroblasts. *Circ Res* **82**: 337-45.

Zuetenhorst, H., Taal, B.G., Boot, H., Valdes Olmos, R. & Hoefnagel, C. (1999). Long-term palliation in metastatic carcinoid tumours with various applications of meta-iodobenzylguanidin (MIBG): pharmacological MIBG, 131I-labelled MIBG and the combination. *Eur J Gastroenterol Hepatol* **11**: 1157-64.